Methods in Molecular Biology 807

Springer Protocols

Richard O. Snyder
Philippe Moullier *Editors*

Adeno-Associated Virus

Methods and Protocols

Humana Press

METHODS IN MOLECULAR BIOLOGY™

Series Editor
John M. Walker
School of Life Sciences
University of Hertfordshire
Hatfield, Hertfordshire, AL10 9AB, UK

For further volumes:
http://www.springer.com/series/7651

Adeno-Associated Virus

Methods and Protocols

Edited by

Richard O. Snyder

University of Florida, Gainesville, FL, USA

Philippe Moullier

Unité INSERM 649, Nantes, France

Humana Press

Editors
Richard O. Snyder
University of Florida
Department of Molecular Genetics
and Microbiology
1600 SW Archer Road
Gainesville, FL 32610
USA
rsnyder@cerhb.ufl.edu

Philippe Moullier
CHU Hôtel Dieu
INSERM U649
Labo. Thérapie Génique
bd. Jean Monnet 30
44035 Nantes CX 1
Bâltiment Jean Monnet
France
moullier@ufl.edu

ISSN 1064-3745 e-ISSN 1940-6029
ISBN 978-1-61779-369-1 e-ISBN 978-1-61779-370-7
DOI 10.1007/978-1-61779-370-7
Springer New York Dordrecht Heidelberg London

Library of Congress Control Number: 2011939472

Printed on acid-free paper

Humana Press is part of Springer Science+Business Media (www.springer.com)

Preface

From a drug development perspective, gene transfer technology is relatively new and evolving at a rapid pace. Recombinant adeno-associated viral (rAAV) vectors have become more widely investigated and improved in their short history [1, 2]. Although wild-type AAV was studied for decades, the work of Xiao Xiao and R. Jude Samulski published in 1996 represents the first evidence that rAAV can be directly administered in situ resulting in efficient, remarkably tolerated, and long-term gene transfer in the mouse skeletal muscle following a single injection [3]. That year was also the year of the lentivirus vector capable of transducing resting neurons after intracerebral injection in the murine model [4]. Yet, 1996 was only 1 year after the Orkin and Motulsky report [5] emphasizing the need for better vectors. Today, progress in rAAV-mediated gene transfer is so robust that long-term, efficient, and regulatable transgene expression is reproducibly achieved in large animal models. For example, (1) the entire limb of hemophilia dogs and primates can be efficiently transduced resulting in long-term phenotypic correction [6, 7] and very recently in hemophilia B patients [8]; (2) rAAV administered once in nonhuman primate muscle shows sustained regulatable transgene expression for more than 5 years [9, 10]. Simultaneously, the discovery of new AAV serotypes [11] along with the ability to encapsidate either "self-complementing" or "single-stranded" vector DNA [12] has turned this vector system into an extremely powerful and versatile tool with preferential organ transduction patterns depending on the AAV capsid origin and/or the vector DNA used. Finally, considerable improvements have been made in the availability of clinical grade rAAV stocks [13] a critical issue, even though large-scale production remains problematic despite the existence of potentially powerful new biotechnological approaches (hybrid viruses such as herpes, baculovirus, and stable packaging cell lines). rAAV vectors and their use in gene transfer are multidisciplinary syntheses requiring the expertise of virologists, physical chemists, chemical engineers, geneticists, epigeneticists, physiologists, and immunologists as well as veterinarians, pharmacists, regulatory affairs specialists, manufacturers, analytical scientists, and medical doctors. The complexity of gene transfer agents in the context of their clinical use requires investigators to have an – or at least an appreciation of – the regulatory environment and constraints that affect vector design, manufacturing, preclinical testing, and clinical use, with an emphasis on patient protection. In this volume, we have invited experts in the field from the USA and Europe to contribute current knowledge from this multidimensional field relating to the biology of AAV, rAAV vector design, vector manufacturing and product testing, performance of rAAV vectors in major organs, rAAV-related immunological issues, design of animal and clinical studies, and clinical experience.

Gainesville, FL, USA — *Richard O. Snyder*
Nantes, France — *Philippe Moullier*

References

1. Hermonat, P. L., and Muzyczka, N. (1984) Use of adeno-associated virus as a mammalian DNA cloning vector: transduction of neomycin resistance into mammalian tissue culture cells, *Proc Natl Acad Sci USA* 81, 6466–6470.
2. Tratschin, J. D., West, M. H., Sandbank, T., and Carter, B. J. (1984) A human parvovirus, adeno-associated virus, as a eucaryotic vector: transient expression and encapsidation of the procaryotic gene for chloramphenicol acetyltransferase, *Mol Cell Biol* 4, 2072–2081.
3. Xiao, X., Li, J., and Samulski, R. J. (1996) Efficient long-term gene transfer into muscle tissue of immunocompetent mice by adeno-associated virus vector, *J Virol* 70, 8098–8108.
4. Naldini, L., Blomer, U., Gage, F. H., Trono, D., and Verma, I. M. (1996) Efficient transfer, integration, and sustained long-term expression of the transgene in adult rat brains injected with a lentiviral vector, *Proc Natl Acad Sci USA* 93, 11382–11388.
5. Orkin, S. H., and Motulsky, A. G. (1995) Report and Recommendations of the Panel to Assess the NIH Investment in Research on Gene Therapy.
6. Arruda, V. R., Stedman, H. H., Haurigot, V., Buchlis, G., Baila, S., Favaro, P., Chen, Y., Franck, H. G., Zhou, S., Wright, J. F., Couto, L. B., Jiang, H., Pierce, G. F., Bellinger, D. A., Mingozzi, F., Nichols, T. C., and High, K. A. (2010) Peripheral transvenular delivery of adeno-associated viral vectors to skeletal muscle as a novel therapy for hemophilia B, *Blood* 115, 4678–4688.
7. Toromanoff, A., Adjali, O., Larcher, T., Hill, M., Guigand, L., Chenuaud, P., Deschamps, J. Y., Gauthier, O., Blancho, G., Vanhove, B., Rolling, F., Cherel, Y., Moullier, P., Anegon, I., and Le Guiner, C. (2010) Lack of immunotoxicity after regional intravenous (RI) delivery of rAAV to nonhuman primate skeletal muscle, *Mol Ther* 18, 151–160.
8. Ponder, K. P. (2011) Hemophilia gene therapy: a holy grail found, *Mol Ther* 19, 427–428.
9. Rivera, V. M., Gao, G. P., Grant, R. L., Schnell, M. A., Zoltick, P. W., Rozamus, L. W., Clackson, T., and Wilson, J. M. (2005) Long-term pharmacologically regulated expression of erythropoietin in primates following AAV-mediated gene transfer, *Blood* 105, 1424–1430.
10. Penaud-Budloo, M., Le Guiner, C., Nowrouzi, A., Toromanoff, A., Cherel, Y., Chenuaud, P., Schmidt, M., von Kalle, C., Rolling, F., Moullier, P., and Snyder, R. O. (2008) Adeno-associated virus vector genomes persist as episomal chromatin in primate muscle, *J Virol* 82, 7875–7885.
11. Gao, G., Vandenberghe, L. H., Alvira, M. R., Lu, Y., Calcedo, R., Zhou, X., and Wilson, J. M. (2004) Clades of Adeno-associated viruses are widely disseminated in human tissues, *J Virol* 78, 6381–6388.
12. McCarty, D. M., Monahan, P. E., and Samulski, R. J. (2001) Self-complementary recombinant adeno-associated virus (scAAV) vectors promote efficient transduction independently of DNA synthesis, *Gene Ther* 8, 1248–1254.
13. Snyder, R. O., and Francis, J. (2005) Adeno-associated viral vectors for clinical gene transfer studies, *Curr Gene Ther* 5, 311–321.

Acknowledgments

We thank Victoria White and Czerne Reid for assistance with proofreading the chapters and coordinating with the authors.

Contents

Contributors

Oumeya Adjali • *Laboratoire de Thérapie Génique, INSERM UMR649, Université de Nantes, Nantes, France*

Mavis Agbandje-McKenna • *Department of Biochemistry and Molecular Biology, University of Florida, Gainesville, FL, USA*

Ignacio Anegon • *INSERM, Nantes, France*

Valder R. Arruda • *University of Pennsylvania School of Medicine, The Children's Hospital of Philadelphia, Philadelphia, PA, USA*

Patrick Aubourg • *UMR Inserm U745, Faculty of Pharmaceutical and Biological Sciences, University Paris Descartes-Sorbonne-Paris Cité, Paris, France*

Muriel Audit • *GenoSafe SAS, EVRY Cedex, France*

Jeffrey S. Bartlett • *Gene Therapy Center, The Research Institute at Nationwide Children's Hospital, Columbus, OH, USA; Department of Pediatrics, and Department of Molecular Virology, Immunology, and Medical Genetics, The Ohio State University Columbus, Columbus, OH, USA*

Raffi Bekeredjian • *Internal Medicine, University of Heidelberg, Heidelberg, Germany*

Mahajoub Bello-Roufai • *Center of Excellence for Regenerative Health Biotechnology, University of Florida, Alachua, FL, USA*

Jean Bennett • *Department of Ophthalmology, F.M. Kirby Center for Molecular Ophthalmology, Scheie Eye Institute, University of Pennsylvania, Philadelphia, PA, USA*

Lawrence T. Bish • *Department of Physiology, University of Pennsylvania School of Medicine, Philadelphia, PA, USA*

Véronique Blouin • *Laboratoire de Thérapie Génique, INSERM, Université de Nantes, Nantes, France*

Olivier Bockstael • *Hôpital Erasme, Université Libre de Bruxelles, Brussels, Belgium*

Chelsea M. Bolyard • *Gene Therapy Center, The Research Institute at Nationwide Children's Hospital, Columbus, OH, USA; Integrated Biomedical Sciences Graduate Program, School of Medicine, The Ohio State University, Columbus, OH, USA*

Nicole Brument • *INSERM UMR649, Institut de Recherche Thérapeutique - IRT1, Université de Nantes, Nantes, Cedex 01, France*

Hildegard Büning • *Department of Internal Medicine, University of Cologne, Cologne, Germany; Center for Molecular Medicine Cologne (ZMMK), University of Cologne, Cologne, Germany*

K. Reed Clark • *Center for Gene Therapy, The Research Institute at Nationwide Children's Hospital, Columbus, OH, USA*

Thomas J. Conlon • *Department of Pediatrics, University of Florida Powell Gene Therapy Center, Gainesville, FL, USA*

Therese Cronin • *Scheie Eye Institute, University of Pennsylvania, Philadelphia, PA, USA*

Olivier Danos • *INSERM U781, Hôpital Necker Enfants Malades and Universite Paris Descartes, Paris, France; University College London Cancer Institute, London, UK*
J. George Dickson • *School of Biological Sciences, Royal Holloway – University of London, London, UK*
Terence R. Flotte • *Department of Pediatrics, University of Massachusetts Medical School Gene Therapy Center, Worcester, MA, USA*
Kevin D. Foust • *The Research Institute at Nationwide Children's Hospital, Columbus, OH, USA*
Joyce D. Francis • *Center of Excellence for Regenerative Health Biotechnology, University of Florida, Alachua, FL, USA*
Achille Francois • *Laboratoire de Thérapie Génique, INSERM, Université de Nantes, Nantes, France*
Guangping Gao • *Gene Therapy Center, University of Massachusetts Medical School, Worcester, MA, USA*
John T. Gray • *Department of Hematology, St. Jude Children's Research Hospital, Memphis, TN, USA*
Michael Hallek • *Department of Internal Medicine, University of Cologne, Cologne, Germany; Center for Molecular Medicine Cologne (ZMMK), University of Cologne, Cologne, Germany*
Roland W. Herzog • *Division of Cellular and Molecular Therapy, University of Florida, Gainesville, FL, USA*
Katherine A. High • *Howard Hughes Medical Institute, Philadelphia, PA, USA; The Children's Hospital of Philadelphia, Philadelphia, PA, USA*
Brian Kaspar • *The Research Institute at Nationwide Children's Hospital, Columbus, OH, USA*
Jürgen Kleinschmidt • *German Cancer Research Center, Heidelberg, Germany*
Taeyoung Koo • *School of Biological Sciences, Royal Holloway – University of London, London, UK*
Caroline le Guiner • *INSERM UMR 649/GENETHON, Nantes, France*
Juan Li • *Division of Molecular Pharmaceutics, University of North Carolina at Chapel Hill, Chapel Hill, NC, USA*
R. Michael Linden • *King's College London School of Medicine, London, UK*
Ashley T. Martino • *Department of Pharmaceutical Sciences, St. John's University, Queens, NY, USA*
Daniel G. Miller • *Department of Pediatrics, University of Washington, Seattle, WA, USA*
Phillipe Moullier • *INSERM UMR 649/GENETHON/Molecular Genetics & Microbiology Department, University of Florida, Nantes, Cedex 01, France*
Christian Mueller • *Department of Pediatrics, University of Massachusetts Medical School, Worcester, MA, USA*
Oliver J. Müller • *Internal Medicine, University of Heidelberg, Heidelberg, Germany*
Magalie Penaud-Budloo • *INSERM UMR649, Institut de Recherche Thérapeutique, Université de Nantes, Nantes, France*

Chunping Qiao • *Division of Molecular Pharmaceutics, University of North Carolina at Chapel Hill, Chapel Hill, NC, USA*
Fabienne Rolling • *Laboratoire de Thérapie Génique, INSERM UMR649, Université de Nantes, Nantes, France*
Mark S. Sands • *Washington University School of Medicine, St. Louis, MO, USA*
Richard O. Snyder • *Department of Molecular Genetics and Microbiology, University of Florida College of Medicine, Gainesville, FL, USA; Center of Excellence for Regenerative Health Biotechnology, University of Florida, Alachua, FL, USA*
Knut Stieger • *Department of Ophthalmology, Justus-Liebig-University Giessen, Gissen, Germany*
H. Lee Sweeney • *Department of Physiology, University of Pennsylvania School of Medicine, Philadelphia, PA, USA*
Liliane Tenenbaum • *Hôpital Erasme, Université Libre de Bruxelles, Brussels, Belgium; Lausanne Hospital University, Lausanne, Switzerland*
Lijun Wang • *Center of Excellence for Regenerative Health Biotechnology, University of Florida, Alachua, FL, USA*
Matthew D. Weitzman • *Salk Institute, La Jolla, CA, USA*
Xiao Xiao • *Division of Molecular Pharmaceutics, University of North Carolina at Chapel Hill, Chapel Hill, NC, USA*
Li Zhong • *Gene Therapy Center, University of Massachusetts Medical School, Worcester, MA, USA*
Serge Zolotukhin • *Division of Cellular and Molecular Therapy, University of Florida, Gainesville, FL, USA*

Chapter 1

Adeno-Associated Virus Biology

Matthew D. Weitzman and R. Michael Linden

Abstract

Adeno-associated virus (AAV) was first discovered as a contaminant of adenovirus stocks in the 1960s. The development of recombinant AAV vectors (rAAV) was facilitated by early studies that generated infectious molecular clones, determined the sequence of the genome, and defined the genetic elements of the virus. The refinement of methods and protocols for the production and application of rAAV vectors has come from years of studies that explored the basic biology of this virus and its interaction with host cells. Interest in improving vector performance has in turn driven studies that have provided tremendous insights into the basic biology of the AAV lifecycle. In this chapter, we review the background on AAV biology and its exploitation for vectors and gene delivery.

Key words: AAV, rAAV, Adeno-associated virus, Recombinant AAV, Gene delivery, *Dependovirus*, Parvovirus

1. Introduction

1.1. Life Cycle

Adeno-associated viruses (AAVs) are helper-dependent members of the *Dependovirus* genus of the parvoviruses that have evolved to replicate under a diverse set of conditions (1). Productive AAV infection requires helper functions that can be supplied either by co-infecting helper viruses or by DNA damaging agents. Helper viruses shown to promote AAV replication include Adenovirus (Ad) and herpes simplex virus (HSV). In each case, the helper induces changes to the cellular environment that can serve to facilitate AAV gene expression and replication. Although ubiquitously prevalent in the human population, AAV has not been associated with any human disease. The success of AAV infection is determined by molecular interactions between the virus and its host cell at every step of the lifecycle. The AAVs are small viruses with

Richard O. Snyder and Philippe Moullier (eds.), *Adeno-Associated Virus: Methods and Protocols*,
Methods in Molecular Biology, vol. 807, DOI 10.1007/978-1-61779-370-7_1,

limited coding capacity, and they are therefore highly reliant on the cellular environment and machinery. In the absence of helper virus, AAV can establish a latent infection in many cell types, from which it can be rescued by subsequent helper virus infection. In the case of AAV2, latency is associated with targeted integration at a specific locus on human chromosome 19 and this requires the viral Rep protein (2–6).

1.2. Genome Structure

The most extensively studied serotype of AAV is type 2 (AAV2), which serves as a prototype for the AAV family. Since most experience with vectors has been obtained with AAV2, we will use information about this serotype to describe general features of AAVs. The AAV genome is a molecule of single-stranded DNA of approximately 4.7 kb. The plus and minus strands are packaged with equal efficiency into separate preformed particles. At either end of the genome are inverted terminal repeats (ITRs) that form T-shaped, base-paired hairpin structures, and contain *cis*-elements required for replication and packaging. Two genes (rep and cap) encode for four nonstructural proteins required for replication (Rep78, Rep68, Rep52, and Rep40) and three structural proteins that make up the capsid (VP1, VP2, and VP3). There are three viral promoters that are identified by their relative map position within the viral genome: p5, p19, and p40. Although the transcription profiles vary for different AAV serotypes (7), all transcripts of AAV2 contain a single intron. Unspliced RNAs encode Rep78 and Rep52, while Rep68 and Rep40 are encoded by spliced messages.

The virus can be rescued by transfection of molecular clones into mammalian cells together with Ad helper functions. The basis for the production of rAAV vectors is the fact that the rep and cap genes can be deleted from the viral genome and provided in trans. The viral genes can be replaced by a transgene with transcriptional control elements, resulting in a vector genome of approximately 4.5 kb flanked by the viral ITRs. Various approaches are employed for the production of rAAV vectors and many purification schemes have been developed, some of which are customized to specific serotypes (8). Purification protocols include ultracentrifugation through cesium chloride density gradients, the use of nonionic iodixanol gradients, and various forms of column chromatography.

Some of the inherent limitations of packaging genes into small rAAV genomes have been bypassed by elegant manipulation of the basic vector constructs. These include dual vectors that expand the rAAV packaging capacity (9) and self-complementary (scAAV) vectors that circumvent the requirement for dsDNA conversion (10). Dual vectors consist of two independent viruses that each carry a portion of the transgene cassette which is reconstituted following simultaneous co-infection. Examples of expanded capacity through dual vectors include *cis*-acting vectors in which regulatory elements are separated from the therapeutic gene (11), *trans*-splicing vectors in which exons in separate vectors are reconstituted through

splicing (12–16), and overlapping vectors that exploit homologous recombination (14). These vectors have the potential to double the capacity compared to a conventional single vector approach. The scAAV vectors can be made by reducing the construct size to approximately 2,500 bp, equivalent to half the size of the regular genome. Production of scAAV vectors can be promoted by deleting the terminal resolution site (TRS) sequence from one ITR such that dimeric genomes are generated (17–19). Upon uncoating, the scAAV vector genome can anneal rapidly to form a dsDNA hairpin molecule with a covalently closed ITR at one end, and two open-ended ITRs at the other end, mimicking a conventional rAAV vector genome. These scAAV vectors have a limited capacity for transgene load but in return offer efficient gene expression with a rapid onset of transduction compared to conventional vectors (10, 17–20).

1.3. Virion Structure

The AAV virion is an icosahedral nonenveloped particle with an encapsidated single-stranded DNA genome. The AAV2 virion is roughly 20 nm in diameter and is composed of 60 copies of the three capsid proteins VP1, VP2, and VP3 in a 1:1:10 ratio. The VP1 and VP2 proteins share the VP3 sequence and have additional residues at their N-termini. The N-terminus of VP1 has a conserved phospholipase A2 sequence that has been implicated in virus escape from endosomes and is crucial for infectivity (21). The VP2 protein is not essential for assembly or infection (22). The core of the VP3 protein consists of a conserved β-barrel motif composed of antiparallel β-sheets (23). This motif is found in other parvoviruses but the interstrand loops are variable, and it is these that determine receptor usage and serology. Structural information combined with genetic data has been important for understanding the molecular interactions of the virus particles. Structural images of several AAV capsids have been determined by X-ray crystallography and cryo-electron microscopy (23–26). There are extensive interactions between capsid subunits at the threefold axis where proteins come together to form three clusters of peaks on the surface topology of the virion (23).

1.4. AAV Serotypes and Variants

AAV serotypes were isolated as contaminants of adenovirus preparations from primates and other species (e.g., avian and bovine). AAV serotypes 2, 3, 5, and 6 were discovered from human cells, while AAV serotypes 1, 4, and 7–11 have nonhuman primate origins (27, 28). As testament to the high prevalence of AAV in humans and other primates, 108 new AAV isolates were identified and classified into various clades based on phylogenetic similarities of capsid sequences (27). The general organization of the parvovirus genome is conserved across the different serotypes, with a similar configuration of replication and structural genes, although there are some differences in transcription profiles (7). Comparing the capsid proteins of the various serotypes revealed 12 hypervariable surface regions, with most of the variability mapping to the threefold proximal peaks (29).

Vectors derived from naturally occurring AAV variants have demonstrated diverse tissue tropisms (30–32). Cross-packaging vectors that use the same vector genome in different capsids have allowed direct comparisons of different serotypes and have shown that the tropism can vary among different tissues in vivo (33–35). Comparisons between the structures of AAV capsids suggests that it is variation in surface topologies that determines the differences in cell surface attachment and receptor usage, intracellular trafficking pathways, and antigenicity between closely related serotypes (23–25). For example, the patches of residues used by AAV2 for heparan sulfate binding are absent from AAV5 and AAV8. Although much of the human population possesses antibodies to AAV capsids, the epitopes may vary between serotypes and not all neutralizing antibodies will cross-react (36).

The structural and functional knowledge obtained from natural AAV variants has enabled rational design of the capsid to improve specific properties (34, 37). The capsid proteins of different serotypes have been mixed to generate mosaic vectors (38), or recombined to generate chimeric virions (39, 40). Combinatorial libraries of capsid proteins have been generated by DNA shuffling and error-prone PCR and these enable directed evolution to isolate vectors with improved functionality (41–43). Targeted transduction and immune evasion have also been achieved through capsid manipulation by site-directed mutagenesis, peptide insertion, and chemical conjugation (44, 45).

1.5. Human AAV Infection

Despite the fact that AAVs have been studied for the past 50 years, little is known about the natural infection by this virus. This observation might be further surprising in light of the finding that approximately 80% of the population is seropositive for anti-AAV antibodies. These antibodies have been determined to be against serotypes 1, 2, 3, and 5. It has become apparent that approximately 60% of the population has neutralizing antibodies at age 10, which generally will persist into adulthood. However, together with the absence of any discernable pathology associated with AAV infection, our limited insights into the viral life cycle in vivo possibly underline the close link between the study of viruses cycles with disease. In this context, it has been noted that AAV might have evolved an ideal relationship with its human host. AAV is inherently replication-defective in normal, healthy cells. In the presence of conditions that can be described as adverse to the host (i.e., helper virus co- or super infection) AAV replicates to significant levels (100,000–1,000,000 copies per cell). A consequence is that cells affected by helper viruses (adenoviruses, herpes viruses, papilloma viruses) likely die as a result of AAV replication. Thus, it is reasonable to assume that AAV can indeed have a protective effect on its host.

In search of an in vivo life cycle, AAV particles have only been isolated in the context of acute adenovirus infections (46).

In addition, it has been proposed that AAV can be sexually transmitted (47, 48), possibly together with either herpes or papilloma viruses. It remains unclear, however, if the latent AAV infection that has been well studied in tissue culture, is in fact an essential component of the in vivo life style.

Our current understanding of effects by AAV infection on the host is limited to correlative studies. Consistent with a protective effect hypothesized above, epidemiological studies have suggested that while 85% of healthy women showed to be seropositive for AAV, in cervical cancer patients AAV antibodies could only be detected in 14% of the cases (49). Consistent with this observation is the finding that in healthy women the AAV titers were significantly higher than in women who had cervical cancer (50). More recently, this finding has been extended by the observation that individuals infected with HPV are less likely to develop cervical neoplasia when AAV is present, highlighting a potential protective effect (51). To date, none of these phenomena have been addressed mechanistically and only few hypotheses have been put forward that attempt to explain these findings.

In summary, very little is known about the life style of AAV in human hosts. In addition, an entire arm of the viral life cycle – the latent infection – which has extensively been studied in tissue culture, remains elusive in the context of the host.

1.6. A Brief History of Vectors

Knowledge of the basic biology of AAV and its interactions with the cell has helped to drive the development of rAAV vectors and has guided production and applications (52). The first vectors were generated in the 1980s by replacing the viral genes with a transgene and transfecting Ad-infected cells with this vector plasmid together with a complementing plasmid that provided Rep and Cap functions. rAAV genomes are packaged into virus particles which can be used to deliver the genome for transgene expression in target cells. The most commonly used protocol for the production of rAAV vectors involves transient transfection (53). Other strategies explored for the production of rAAV vectors include the use of producer cell lines, combining viral features into Ad-AAV hybrids (54), the use of herpesvirus systems (55), and production in insect cells using baculoviruses (56).

There are many settings where rAAV vectors have demonstrated efficient gene transduction in preclinical gene therapy studies (52) and have entered clinical trials (57, 58). Transduction efficiency varies depending on the target cell type and serotype capsid being utilized. A number of rate-limiting steps have been identified in the transduction process (59, 60). These hurdles include cytoplasmic trafficking to the nucleus, the rate of uncoating, vector genome instability, and conversion of the single-stranded DNA vector genome into a transcriptionally competent double-stranded DNA molecule.

2. Viral Replication

2.1. Entry and Trafficking

Much of our current knowledge of the AAV life cycle must be seen in the context of the extraordinary promiscuity of this virus. As learned mainly from recombinant viruses, taken together the serotypes of AAV can infect a wide range of tissue culture and a panoply of tissues. It is thus not surprising that some ambiguity remains with regard to viral entry and trafficking pathways. It is of note that, likely, each of the serotypes isolated to date might share, but more importantly, differ in a number of aspects of virus host interactions, including the use of specific receptors as well as particular trafficking pathways. Ultimately, only the in-depth characterization of each serotype will result in a meaningful understanding of the relevant host factors and pathways involved in AAV infection. An additional point of caution is provided by the limitation that most of the studies to date have been conducted with tissue culture-adapted viruses. It is thus possible, if not likely, that the adaptation process has selected for viral characteristics which cannot be assumed to be found in natural isolates. This point is supported by the finding that while tissue culture-adapted AAV2 readily binds heparin, isolates from human tonsils do not (61).

Arguably the first step in viral tropism is the attachment to the target cell. For the best-studied serotype (AAV2), heparan sulfate was first identified as the cellular docking partner (62). On the viral capsid, the docking site has been mapped to amino acids 585–588 with two relevant arginine residues at positions 585 and 588 (63, 64). Interestingly, these two residues are missing in the isolates from human tissue samples (61). In addition to heparan sulfate proteoglycans, fibroblast growth factor receptor 1 (FGFR1) has been shown to be bound by AAV2 and, in the context of recombinant viruses, its presence has been associated with enhanced transduction (65). An additional molecule identified to enhance AAV2 infection and transduction is the avb5 integrin, supporting a role in AAV2 binding and uptake (66). The interesting aspect of this finding is that the AAV2 capsid does not contain the RGD motif that typically binds to these molecules, suggesting that alternative viral binding sites are used for this interaction. In addition to HSPG attachment by AAV2, sialic acid have been identified as attachment moieties for AAV serotypes 4 and 5 (67, 68). Using an intriguing approach, Di Pasquale and colleagues identified platelet-derived growth factor receptor (PDGF-R) as the uptake receptor for AAV5 (69).

Despite the discovery of a number of attachment partners and protein receptors, to date little is known about the possible downstream effects of receptor binding. The question as to whether particular signaling pathways are involved in enhancing virus uptake and trafficking thus remains unanswered.

Subsequent to receptor binding AAV is thought to enter via clathrin-coated vescicles (70). Following the uptake, AAV2 has been observed in many different cellular compartments and it must be noted that it is still a matter of discussion whether – whatever pathway is followed – the intact virus ends up in the nucleus for uncoating (71, 72). Not unlike the complications experienced in the studies of a number of other viruses, the experimental setup generally used relies on the visualization of virus particles, thus making these approaches vulnerable to detection sensitivities. More importantly, wild-type viruses used in these experiments typically display a particle over infectivity ratio of approximately 10:1; recombinant viruses (required to perform functional studies) are in the range of 40 to 1. A consequence of this notion is the as yet unmet challenge to demonstrate that the visualized particles in trafficking studies indeed reflect the infectious virus rather than the noninfectious majority. Nevertheless, it has been demonstrated that AAV2 can be found in late endosomes as demonstrated by the use of drugs that block endosomal trafficking steps (70, 73, 74). It must be noted that these studies were performed in the absence of helper virus, thus modeling the initiation of the latent life cycle of AAV and the pathway likely to be relevant for gene therapy applications. However, it is reasonable to hypothesize that AAV trafficking follows the route of helper viruses (i.e., early endosome escape in the case of adenovirus) (75).

AAV replication initiates in the nucleus. However, it remains somewhat controversial how, and where, the DNA is released from the capsids. Nevertheless, it has been recognized that one of the rate-limiting steps in viral infection and vector transduction is the uncoating of the extraordinary stable AAV virion (70, 74, 76).

Overall, it has become apparent that many question remain with regard to trafficking of the virus from the cell surface ending up as functional DNA within the nucleus. A challenge will be the identification of relevant cells and tissues as well as the further characterization of the viral reagents used in the dissection of AAV uptake and trafficking pathways (77).

2.2. DNA Replication

The current model of the AAV replication can be divided into several steps. In the absence of helper virus factors limited expression of Rep 68/78 occurs, with three main consequences. AAV gene expression is then repressed (78); thus AAV DNA replication is inhibited and AAV DNA can be integrated into the host genome. Co-infection – or super infection of a latently infected cell – with a helper virus leads to rescue of the AAV genome and DNA replication (79).

In a simplifying attempt to summarize the data to date, the requirement for the productive replication of AAV can be divided into three steps: The single-strand genome of AAV must be extended into a double-strand template for transcription (of the *rep* gene)

(17, 80–84). It is not clear yet if Rep plays a significant role in this step. Subsequently *rep* genes are transcribed. This step appears to involve several levels of regulation. In general, co-infection with adenovirus activates the p5 (Rep68/78) promoter as well as the p19 (Rep52/40) promoter (78, 85–88). Analysis of a variety of mutations of the AAV genome has shown that Rep is involved in both, negative (in absence of helper effects) and positive regulation of transcription. Extensive DNA replication then occurs. Rep activities are essential for this step (89). Furthermore, the cell-free assays were able to demonstrate that bacterially expressed Rep68 is capable of mediating AAV DNA replication in an adenovirus-dependent manner in the presence of HeLa cell extracts (90–93).

The model of AAV DNA replication has been developed over the past few decades and has largely remained unchallenged. Key components of this model consist of the notion that the general mode consists of unidirectional strand-displacement replication (92, 94, 95). The AAV genome is flanked on either side by structural elements known as the inverted terminal repeats, or ITRs. The ITRs contain motifs that serve as the viral origin of replication, namely the Rep binding site (RBS) and TRS. The ITR's ability to self-anneal provides the basis for the model of AAV DNA replication. Through its self-complimentary sequence and the resulting secondary structure, the ITR provides a base-paired 3′ hydroxyl group for unidirectional DNA synthesis. This synthesis is believed to be mediated through the host replication machinery including polymerase d (90). However, it is likely that during replication, which is supported by herpes viruses, some components of the cellular replication machinery are replaced by those from the helper virus (96, 97). Once the AAV template has been copied, a remaining step is the terminal resolution, the replication of the ITR, which has self-annealed to form the initial replication primer. This end of the genome is faithfully replicated through the actions of the Rep protein, which specifically binds to the RBS motif (98) within the ITR and regenerates a 3′ hydroxyl end by exacting a site- and strand-specific nick at the TRS. This nick then provides the necessary 3′ hydroxyl group for the replication through the viral ITR. Rep endonuclease activity directed at the double-stranded TRS is indirectly ATP-dependent; Rep helicase activity is required to render the TRS site single-stranded and thus accessible to the nicking active site (99). This replication cycle can result in two possible products, a double-stranded full-length AAV genome and a single-stranded full-length AAV displacement product. It is as yet unknown whether these distinct replication products can serve as templates for distinct downstream activities. It is intriguing to speculate that while the single-stranded AAV genome might serve as a template for further replication, the double-stranded replication product would be directed to serve as a template for genome packaging.

2.3. Helper Functions

Productive AAV infection requires co-infection with helper viruses that provide functions that aid in AAV replication, including larger DNA viruses such as Ad and HSV. Genes from Ad that provide helper functions for AAV have been defined as E1a, E1b55K, E2a, and E4orf6, together with the viral associated RNA (VAI RNA). The E1a gene product activates other Ad promoters and also binds to YY1 to relieve repression for the AAV p5 promoter (100, 101). The product of the E2a gene is a single-strand DNA binding protein DBP that is found at AAV replication centers (102) and stimulates processivity of AAV replication in vitro (103). The E1b55K and E4orf6 proteins function together to promote AAV replication and second-strand synthesis (104, 105). The E1b55K/E4orf6 proteins function as an ubiquitin ligase, and degradation targets include the DNA repair proteins that make up the MRN complex, which limits rAAV transduction (106). The VA RNA stimulates expression of AAV proteins, possibly by preventing phosphorylation of the eIF2alpha translation factor (107). In general, the functions of Ad helper proteins are to enhance production of AAV proteins and to alter the cellular environment to promote AAV replication. In the context of this helper virus, it has been shown that cellular DNA polymerases perform AAV replication. High titer rAAV can be generated in the absence of helper virus by transfection of plasmids that provide the Ad helper genes (108).

In contrast to Ad, the helper proteins provided by HSV-1 were initially defined as a subset of HSV-1 replication proteins: the helicase/primase complex (UL5, UL8, and UL52) and the DNA binding protein ICP8 encoded by the UL29 gene (109). Although these minimal proteins are sufficient to replicate AAV (110), other HSV-1 proteins have been shown to enhance helper functions in combination with the replication proteins. These include the ICP0 transactivator that activates rep gene expression (111), and the ICP4 and ICP22 proteins that can augment activity (112). The HSV-1 DNA polymerase complex (the polymerase UL30 and its co-factor UL42) can also contribute to efficient AAV replication (112). In vitro studies have also shown that UL30 can replicate the AAV genome without the requirement for the helicase–primase complex (96).

AAV replication can also be stimulated in the absence of helper viruses by treatments that cause cellular and genotoxic stress (113). These agents include hydroxyurea, topoisomerase inhibitors, and UV irradiation. Exactly how these treatments create a favorable environment for AAV replication remains unclear. AAV replication has also been suggested to occur autonomously in certain cells, such as a skin raft model of keratinocyte differentiation (114).

2.4. Cellular Proteins

Cellular proteins that are involved in AAV replication have been identified by biochemical methods, genetic screens, and through the use of cell-based assays. AAV can replicate in cell extracts

(115, 116) and in vitro assays have enabled purification of host cell proteins involved in AAV DNA replication (117). Amplification of AAV DNA can be reconstituted in vitro with purified Rep proteins and the following cellular enzymes: DNA polymerase d, proliferating cell nuclear antigen (PCNA), replication factor C (RFC), and the minichromosome maintenance complex (MCM) (90). In vitro replication can also be enhanced by the addition of single-strand DNA binding proteins from the cell (RPA) and helper viruses (DBP of Ad and ICP8 of HSV) (103, 110).

Cellular proteins that bind to the viral Rep protein or directly to the terminal repeats may either be required for replication or may regulate aspects of the viral lifecycle. A recent proteomic analysis of multiprotein complexes that interact with Rep during productive infection with Ad helper virus identified 188 interacting proteins by tandem affinity purification (118). These factors included those involved in DNA replication, transcription, translation, protein degradation, and RNA splicing. How these host proteins regulate Rep functions or contribute to the AAV lifecycle is still unknown in many cases. Some of the known interactions that affect Rep functions include the importin alpha receptor that mediates nuclear import (119), the Sp1 factor that mediates transcriptional activation (120), the high mobility group protein 1 (HMG1) that stimulates Rep activities (121), and PKA/PrKX that may be involved in inhibition of adenovirus (122).

A number of cellular factors have been shown to regulate AAV through binding to the AAV ITR. The chaperone-associated protein FKBP52 is a single-stranded DNA binding protein that recognizes the D-sequence within the AAV ITR and has been suggested to block second-strand synthesis (83, 123). A one-hybrid screen designed to identify cellular proteins that recognize the Rep binding sequence within the AAV ITR found that the cellular zinc-finger protein ZF5 is a negative regulator of AAV2 replication (124). Other proteins have been shown to inhibit AAV transduction and replication, including human APOBEC3A (125), although the mechanisms of most are not yet known (126). The AAV ITRs are also recognized by cellular DNA repair proteins that process the viral genome to inhibit replication or recombine the termini (106, 127–130).

During infection there is temporal and spatial regulation of AAV DNA replication, capsid assembly, and genome packaging (102, 110, 131, 132). In a similar way to other viruses, AAV replication takes place at discrete sites within the nucleus. It has been suggested that one of the helper functions provided by proteins from HSV is to form a scaffold for the recruitment of cellular proteins (110). Rep proteins colocalize with viral DNA at viral replication centers (102). Cap proteins are seen transiently in nucleoli and they later accumulate with Rep in the nucleoplasm (131, 132).

2.5. Gene Expression and Transcriptional Regulation

The AAV genome is highly compact, with complex overlapping coding regions. The transcriptional profiles of a number of AAVs have been examined and allows them to be divided into three main groups that differ based on their use of internal polyadenylation sites (7). The transcription and regulation has been most extensively studied for the prototype AAV2 genome. Since the Rep proteins inhibit cell proliferation (133), AAV2 gene expression is tightly regulated through the repressive effects of cellular factors (100) and the viral Rep protein (134). The Rep proteins can mediate both activation and repression of AAV transcription (78, 85). In the absence of helper virus co-infection, the larger Rep proteins can suppress their own transcription through a binding element in the p5 promoter (78, 134). However, in the presence of Ad, Rep serves to activate all three promoters (78, 135) through direct binding to the viral DNA or through interactions with transcription factors such as Sp1 (120, 136). Inhibition of p5 can be relieved by the E1a transactivator of Ad (101) and the ICP0 protein of HSV (111). There is also evidence to suggest that the ITR can act as both an enhancer and an initiator for transcription (78, 137, 138), implying that it is recognized by cellular proteins that regulate transcription.

The ratios of the various Rep and Cap proteins is determined by the level of splicing, which is stimulated by helper virus co-infection (139). In the presence of helper proteins, the large Rep proteins increased the ratio of spliced to unspliced RNA. Rep enhancement of splicing is dependent on Rep binding to DNA but is independent from effects on transcriptional initiation (140). Further steps in processing of AAV RNAs are unclear. For example, it is not known how the unspliced messages are exported from the nucleus.

2.6. The Rep Proteins

A considerable number of studies indicate that the largest of the Rep proteins, Rep78/68, are required for virtually every step of the viral lifecycle. These include DNA replication (89, 141, 142), site-specific integration (4, 143, 144), rescue of integrated genomes (145, 146), and the regulation of both viral and cellular promoters (78, 85, 88, 120, 134, 142, 147–149). The smaller Rep proteins, Rep52 and -40, appear to be required for the accumulation and packaging of single-stranded genomes, thus explaining the prevalence of these transcripts during productive infection (139, 150, 151).

Consistent with their multifunctional role during the viral lifecycle, the products of the *rep* ORF, Rep78, -68, -52, and -40, possess a variety of biochemical activities. The three major functional domains are all present in the largest of the Rep proteins, Rep78. The Rep amino terminus possesses specific DNA binding and endonuclease activity (152, 153), the central domain bears motifs necessary for ATPase and helicase activity as well as the nuclear localization sequence, and the carboxy-terminal Zn-finger domain has been

implicated in interacting with a myriad of cellular factors. The remaining Rep isoforms, Rep68, -52, and -40, are a combination of these functional domains arising from alternative splicing schemes and differential promoter usage within the *rep* ORF. Notably, all four isoforms possess the helicase domain, with Rep40 representing the minimum AAV helicase. Overall, this central domain is the most highly conserved region among parvoviral nonstructural proteins. The AAV Rep helicase falls into the super family 3 (SF3) class, as do several other viral helicases including that of papillomoviruses, poliovirus, and simian virus 40 (SV40). Members of this family contain four highly conserved regions: motifs A, B (also known as Walker motifs A and B), and C essentially make up the core of the helicase active site consisting of an NTP-binding site, divalent metal cation coordination site, and sensor-1 site, respectively. Motif B′ is located between the Walker motifs and the C′ motif. Its role in catalysis was not yet known but the X-ray structures of members of the family solved recently imply a possible role in DNA interactions. A beginning toward understanding the molecular details and mechanism of Rep proteins during the viral life cycle has been the determination of the crystal structure of Rep40 (154, 155). The structure shows that Rep40 is structurally more similar to the AAA^+ class of cellular proteins than to DNA helicases from other superfamilies. Rep40 that contains the minimal helicase domain is bimodular with a small helical bundle at the N-terminus and a large α/β ATPase domain at the C-terminus. This domain has the classical topology of P loop ATPases, with a central β-sheet flanked by four helices on one side and two on the other. Comparison with the helicase domain of SV40-Tag points out important structural differences that might point to the unique the dynamic oligomeric nature of Rep proteins. Finally, the homology to papilloma virus E1, SV40 Tag and AAA^+ proteins in general have led to the suggestion that at least the larger Rep isoforms likely function as hexamers. However, recent cryo-electron microscopy studies revealed that Rep68 represents the only known helicase which forms bi-directional double-octameric rings when bound to a helicase substrate (156). This study further highlighted that the DNA substrate dictates the oligomeric form of Rep68, thus proposing a possible mechanism by which the multiple activities of this protein could be distinguished and/or regulated.

Finally, it must be noted that although a considerable number of biochemical studies have been conducted to characterize Rep, only little is known as yet with respect to the molecular mechanisms that are underlying the various biological functions of these unique proteins.

2.7. Genome Integration

To date, wild-type AAV remains the only known eukaryotic virus with the unique ability to integrate site-specifically into the human genome (146, 157). In this context it must be noted that all the

studies addressing this intriguing phenomenon have been conducted with cultured cells and no information is available about the significance of the latent arm of the AAV life cycle in the human host. However, recently the potential significance of the underlying mechanism to the development of targeted gene addition as a novel component of therapeutic gene delivery has been recognized and a number of approaches are under development that aim to apply aspects of wtAAV integration to clinically relevant disease models. Among those aspects are the unique characteristics of the human target site for integration as well as the seemingly sophisticated mechanism, which AAV has evolved in order to insert its genome into the human chromosome.

Site-specific integration was first documented by Kotin and colleagues, who identified viral-cellular junctions from numerous latently infected cell lines, and found that these junctions consistently mapped to one region on human chromosome 19 (3, 158, 159). Using an independent approach, Samulski and colleagues further confirmed this finding (6). The human target locus, termed *AAVS1*, was then isolated and the sequence was determined in order to assess potential characteristics of the cellular sequence that might account for the unusual integration site preference (2). In search for determinants of site-specific integration, the observation by Walsh and colleagues that recombinant viruses devoid of the rep gene did not show evidence of site-specific integration hinted at a role for AAV Rep in site-specific integration (160). More direct evidence was then provided by the observation that when provided *in trans* the large Rep proteins could restore *AAVS1* targeted integration (144, 161). A final and more mechanistic insight was provided when functional RBS and TRS motifs were identified within the human target sequence, suggesting that Rep played a key role in the initiation of site-specific integration (162, 163). Finally, it was demonstrated that in a functional integration assay using episomes carrying *AAVS1* fragments that the RBS-TRS motifs were necessary and sufficient for site-specific integration (143). Based on these findings and together with observations from cell-free integration assays, an initial model for the molecular mechanism of Rep-mediated site-specific integration was proposed (4). The core of this proposal was that AAV site-specific integration parallels AAV DNA replication. In a manner equivalent to the actions of Rep at the viral origin, it was proposed that Rep targets the AAV genome for integration at *AAVS1* by initiating replication at this chromosomal origin, i.e., specific DNA binding at the RBS followed by ATP-dependent endonuclease activity directed at the TRS. Once DNA replication is initiated, strand-switching between the chromosomal and proximal viral DNA template was thought to allow for the eventual incorporation of multiple copies of the AAV genome into the chromosomal locus. This model,

although consistent with the characteristics of the viral-cellular junctions and the organization of the integrated genomes remained hypothetical.

The potential utility of AAV-mediated targeted transgene integration relies on the safety of this viral approach. On the background of the observation that AAV is a nonpathogenic virus, it was somewhat counter-intuitive that the virus appeared to have evolved a mechanism to integrate its genome into a highly gene-rich genomic environment (164, 165), thus making insertional mutagenesis a near certainty. However, the discovery of the mouse ortholog of the human integration target sequence that closely resembled the genetic makeup of *AAVS1* (166) enabled studies to address possible functional consequences of Rep-mediated targeted integration. Henckaerts and colleagues used this system to establish a site-specific transgene integration assay in mouse embryonic stem cells. With this system, it became possible to address several questions. It became clear that targeted integration of a marker gene resulted in strong transgene expression, which persisted throughout in vitro differentiation of these cells into multiple lineages (167). In addition, when injected into blastocysts, the resulting animals demonstrated strong contribution by the site-specifically marked cells to all tissues in the absence of any discernable phenotypic effect throughout the lifetime of the animals. Taken together these experiments demonstrated that *AAVS1*-targeted gene addition could result in the safe genetic modification of relevant cells. These studies were further taken into human embryonic stem cells, where *AAVS1*-targeted maker gene expression aided in the identification of human cardiac progenitor cells that were able to functionally integrate into a mouse heart (168). Molecular characterization of integrants in numerous human and mouse cells then revealed a surprising aspect of the Rep-mediated integration mechanism. It was found that the initial integration mechanism needed to be amended by the finding that in all cases analyzed the mechanism involved a partial duplication of the target sequence, suggesting the intriguing possibility that AAV might have evolved a mechanism for targeted gene addition in the absence of functional perturbation of the disrupted target genes (167).

To date, we begin to understand numerous aspects of this unique viral mechanism. However, it is apparent that many questions remain unanswered. In particular, we do not yet know whether integration is at all a significant component of the viral life style in vivo. In addition, for the development of targeted gene addition in therapeutically relevant approaches (e.g., X-SCID treatment), many remaining questions need to be addressed, including the identification of safe delivery strategies for the Rep protein and – possibly more importantly – the efficiency of successful integration events.

3. Summary

3.1. Impact of Biology of Vector Development

It is apparent that our, albeit, partial understanding of the biology of AAV has greatly aided the development of AAV vectors. The isolation of a panoply of capsid variants from animals, e.g., has provided a large range of vector types with specific transduction characteristics. In addition, the determination of a number of capsid crystal structures has opened doors that will ultimately allow for the design of vectors with specific and exclusive tropism, to name just a few. On the other hand, it is also clear that many additional discoveries on the biology of AAV are needed in order to improve our current vectors. For example, to date it is unclear why recombinant viruses exhibit a several-fold lower infectivity than wild-type viruses. A further dissection of the requirements for genome packaging as well as the identification of pathways involved might result in vectors with considerably higher infectivity, thus allowing for the administration of much lower vector doses. Finally, a more comprehensive understanding of the integration mechanism could result in vectors for stem cell applications that could overcome the apparent concern for consequential insertional mutagenesis.

3.2. Impact of Vectors on AAV Biology

In addition to the basic biology driving the development of rAAV for gene delivery, vectors have also served as tools to study the cell biology of infection and have advanced our knowledge of the basic parvovirus biology. They have been useful in elucidating the early steps in virus infection, including receptor identification (69) and highlighting barriers to intracellular trafficking and uncoating (75, 76, 84, 169). Vectors have also been useful for examining the fate of viral genome during transduction in cell culture and in vivo models (170). These studies revealed that the majority of the vector genomes can persist as circular episomes of monomers or concatemers (5, 170, 171) and identified host DNA repair factors involved in processing AAV genomes (127–129, 172). It is likely that the dynamic relationship between understanding basic biology and developing vectors will continue, and advances in each area will propel the applications that are possible for gene therapy.

Acknowledgments

This article is an overview of AAV basic biology and is not an exhaustive review of the topic. We apologize for primary work not covered here either from lack of space or inadvertent oversight. Work on AAV in the Weitzman laboratory has been supported by NIH grants (AI067952, CA097093, AI051686, and AI074967)

and a Pioneer Developmental Chair from the Salk Institute. AAV work in the Linden laboratory was supported by NIH grants GM07390, 1GM071023, and GM075019, and by King's College London School of Medicine.

References

1. Berns, K. I., and Giraud, C. (1996) Biology of adeno-associated virus, *Curr Top Microbiol Immunol* ***218***, 1–23.
2. Kotin, R. M., Linden, R. M., and Berns, K. I. (1992) Characterization of a preferred site on human chromosome 19q for integration of adeno-associated virus DNA by non-homologous recombination, *EMBO J* ***11***, 5071–5078.
3. Kotin, R. M., Siniscalco, M., Samulski, R. J., Zhu, X. D., Hunter, L., Laughlin, C. A., McLaughlin, S., Muzyczka, N., Rocchi, M., and Berns, K. I. (1990) Site-specific integration by adeno-associated virus, *Proc Natl Acad Sci USA* ***87***, 2211–2215.
4. Linden, R. M., Winocour, E., and Berns, K. I. (1996) The recombination signals for adeno-associated virus site-specific integration, *Proc Natl Acad Sci USA* ***93***, 7966–7972.
5. McCarty, D. M., Young, S. M., Jr., and Samulski, R. J. (2004) Integration of adeno-associated virus (AAV) and recombinant AAV vectors, *Annu Rev Genet* ***38***, 819–845.
6. Samulski, R. J., Zhu, X., Xiao, X., Brook, J. D., Housman, D. E., Epstein, N., and Hunter, L. A. (1991) Targeted integration of adeno-associated virus (AAV) into human chromosome 19, *EMBO J* ***10***, 3941–3950.
7. Qiu, J., and Pintel, D. (2008) Processing of adeno-associated virus RNA, *Front Biosci* ***13***, 3101–3115.
8. Zolotukhin, S. (2005) Production of recombinant adeno-associated virus vectors, *Hum Gene Ther* ***16***, 551–557.
9. Ghosh, A., and Duan, D. (2007) Expanding adeno-associated viral vector capacity: a tale of two vectors, *Biotechnol Genet Eng Rev* ***24***, 165–177.
10. McCarty, D. M. (2008) Self-complementary AAV vectors; advances and applications, *Mol Ther* ***16***, 1648–1656.
11. Duan, D., Yue, Y., Yan, Z., and Engelhardt, J. F. (2000) A new dual-vector approach to enhance recombinant adeno-associated virus-mediated gene expression through intermolecular cis activation, *Nat Med* ***6***, 595–598.
12. Sun, L., Li, J., and Xiao, X. (2000) Overcoming adeno-associated virus vector size limitation through viral DNA heterodimerization, *Nat Med* ***6***, 599–602.
13. Nakai, H., Storm, T. A., and Kay, M. A. (2000) Increasing the size of rAAV-mediated expression cassettes in vivo by intermolecular joining of two complementary vectors, *Nat Biotechnol* ***18***, 527–532.
14. Duan, D., Yue, Y., and Engelhardt, J. F. (2001) Expanding AAV packaging capacity with trans-splicing or overlapping vectors: a quantitative comparison, *Mol Ther* ***4***, 383–391.
15. Yan, Z., Zhang, Y., Duan, D., and Engelhardt, J. F. (2000) Trans-splicing vectors expand the utility of adeno-associated virus for gene therapy, *Proc Natl Acad Sci USA* ***97***, 6716–6721.
16. Lai, L., Lin, K., Foulks, G., Ma, L., Xiao, X., and Chen, K. (2005) Highly efficient ex vivo gene delivery into human corneal endothelial cells by recombinant adeno-associated virus, *Curr Eye Res* ***30***, 213–219.
17. McCarty, D. M., Monahan, P. E., and Samulski, R. J. (2001) Self-complementary recombinant adeno-associated virus (scAAV) vectors promote efficient transduction independently of DNA synthesis, *Gene Ther* ***8***, 1248–1254.
18. McCarty, D. M., Fu, H., Monahan, P. E., Toulson, C. E., Naik, P., and Samulski, R. J. (2003) Adeno-associated virus terminal repeat (TR) mutant generates self-complementary vectors to overcome the rate-limiting step to transduction in vivo, *Gene Ther* ***10***, 2112–2118.
19. Wang, Z., Ma, H. I., Li, J., Sun, L., Zhang, J., and Xiao, X. (2003) Rapid and highly efficient transduction by double-stranded adeno-associated virus vectors in vitro and in vivo, *Gene Ther* ***10***, 2105–2111.
20. Wu, Z., Sun, J., Zhang, T., Yin, C., Yin, F., Van Dyke, T., Samulski, R. J., and Monahan, P. E. (2008) Optimization of self-complementary AAV vectors for liver-directed expression results in sustained correction of hemophilia B at low vector dose, *Mol Ther* ***16***, 280–289.
21. Girod, A., Wobus, C. E., Zadori, Z., Ried, M., Leike, K., Tijssen, P., Kleinschmidt, J. A., and Hallek, M. (2002) The VP1 capsid protein of adeno-associated virus type 2 is carrying a phospholipase A2 domain required for virus infectivity, *J Gen Virol* ***83***, 973–978.

22. Warrington, K. H., Jr., Gorbatyuk, O. S., Harrison, J. K., Opie, S. R., Zolotukhin, S., and Muzyczka, N. (2004) Adeno-associated virus type 2 VP2 capsid protein is nonessential and can tolerate large peptide insertions at its N terminus, *J Virol 78*, 6595–6609.
23. Xie, Q., Bu, W., Bhatia, S., Hare, J., Somasundaram, T., Azzi, A., and Chapman, M. S. (2002) The atomic structure of adeno-associated virus (AAV-2), a vector for human gene therapy, *Proc Natl Acad Sci USA 99*, 10405–10410.
24. Nam, H. J., Lane, M. D., Padron, E., Gurda, B., McKenna, R., Kohlbrenner, E., Aslanidi, G., Byrne, B., Muzyczka, N., Zolotukhin, S., and Agbandje-McKenna, M. (2007) Structure of adeno-associated virus serotype 8, a gene therapy vector, *J Virol 81*, 12260–12271.
25. Walters, R. W., Agbandje-McKenna, M., Bowman, V. D., Moninger, T. O., Olson, N. H., Seiler, M., Chiorini, J. A., Baker, T. S., and Zabner, J. (2004) Structure of adeno-associated virus serotype 5, *J Virol 78*, 3361–3371.
26. Padron, E., Bowman, V., Kaludov, N., Govindasamy, L., Levy, H., Nick, P., McKenna, R., Muzyczka, N., Chiorini, J. A., Baker, T. S., and Agbandje-McKenna, M. (2005) Structure of adeno-associated virus type 4, *J Virol 79*, 5047–5058.
27. Gao, G., Vandenberghe, L. H., Alvira, M. R., Lu, Y., Calcedo, R., Zhou, X., and Wilson, J. M. (2004) Clades of Adeno-associated viruses are widely disseminated in human tissues, *J Virol 78*, 6381–6388.
28. Gao, G. P., Alvira, M. R., Wang, L., Calcedo, R., Johnston, J., and Wilson, J. M. (2002) Novel adeno-associated viruses from rhesus monkeys as vectors for human gene therapy, *Proc Natl Acad Sci USA 99*, 11854–11859.
29. Gao, G., Alvira, M. R., Somanathan, S., Lu, Y., Vandenberghe, L. H., Rux, J. J., Calcedo, R., Sanmiguel, J., Abbas, Z., and Wilson, J. M. (2003) Adeno-associated viruses undergo substantial evolution in primates during natural infections, *Proc Natl Acad Sci USA 100*, 6081–6086.
30. Wu, Z., Asokan, A., and Samulski, R. J. (2006) Adeno-associated virus serotypes: vector toolkit for human gene therapy, *Mol Ther 14*, 316–327.
31. Gao, G., Vandenberghe, L. H., and Wilson, J. M. (2005) New recombinant serotypes of AAV vectors, *Curr Gene Ther 5*, 285–297.
32. Grimm, D., and Kay, M. A. (2003) From virus evolution to vector revolution: use of naturally occurring serotypes of adeno-associated virus (AAV) as novel vectors for human gene therapy, *Curr Gene Ther 3*, 281–304.
33. Rabinowitz, J. E., Rolling, F., Li, C., Conrath, H., Xiao, W., Xiao, X., and Samulski, R. J. (2002) Cross-packaging of a single adeno-associated virus (AAV) type 2 vector genome into multiple AAV serotypes enables transduction with broad specificity, *J Virol 76*, 791–801.
34. Wu, Z., Asokan, A., Grieger, J. C., Govindasamy, L., Agbandje-McKenna, M., and Samulski, R. J. (2006) Single amino acid changes can influence titer, heparin binding, and tissue tropism in different adeno-associated virus serotypes, *J Virol 80*, 11393–11397.
35. Wang, Z., Zhu, T., Qiao, C., Zhou, L., Wang, B., Zhang, J., Chen, C., Li, J., and Xiao, X. (2005) Adeno-associated virus serotype 8 efficiently delivers genes to muscle and heart, *Nat Biotechnol 23*, 321–328.
36. Peden, C. S., Burger, C., Muzyczka, N., and Mandel, R. J. (2004) Circulating anti-wild-type adeno-associated virus type 2 (AAV2) antibodies inhibit recombinant AAV2 (rAAV2)-mediated, but not rAAV5-mediated, gene transfer in the brain, *J Virol 78*, 6344–6359.
37. Vandenberghe, L. H., Wilson, J. M., and Gao, G. (2009) Tailoring the AAV vector capsid for gene therapy, *Gene Ther 16*, 311–319.
38. Rabinowitz, J. E., Bowles, D. E., Faust, S. M., Ledford, J. G., Cunningham, S. E., and Samulski, R. J. (2004) Cross-dressing the virion: the transcapsidation of adeno-associated virus serotypes functionally defines subgroups, *J Virol 78*, 4421–4432.
39. Hauck, B., Chen, L., and Xiao, W. (2003) Generation and characterization of chimeric recombinant AAV vectors, *Mol Ther 7*, 419–425.
40. Bowles, D. E., Rabinowitz, J. E., and Samulski, R. J. (2003) Marker rescue of adeno-associated virus (AAV) capsid mutants: a novel approach for chimeric AAV production, *J Virol 77*, 423–432.
41. Perabo, L., Endell, J., King, S., Lux, K., Goldnau, D., Hallek, M., and Buning, H. (2006) Combinatorial engineering of a gene therapy vector: directed evolution of adeno-associated virus, *J Gene Med 8*, 155–162.
42. Li, W., Asokan, A., Wu, Z., Van Dyke, T., DiPrimio, N., Johnson, J. S., Govindaswamy, L., Agbandje-McKenna, M., Leichtle, S., Redmond, D. E., Jr., McCown, T. J., Petermann, K. B., Sharpless, N. E., and Samulski, R. J. (2008) Engineering and selection of shuffled AAV genomes: a new strategy for producing targeted biological nanoparticles, *Mol Ther 16*, 1252–1260.
43. Maheshri, N., Koerber, J. T., Kaspar, B. K., and Schaffer, D. V. (2006) Directed evolution of

adeno-associated virus yields enhanced gene delivery vectors, *Nat Biotechnol* ***24***, 198–204.

44. Muzyczka, N., and Warrington, K. H., Jr. (2005) Custom adeno-associated virus capsids: the next generation of recombinant vectors with novel tropism, *Hum Gene Ther* ***16***, 408–416.
45. Buning, H., Perabo, L., Coutelle, O., Quadt-Humme, S., and Hallek, M. (2008) Recent developments in adeno-associated virus vector technology, *J Gene Med* ***10***, 717–733.
46. Blacklow, N. R., Hoggan, M. D., and Rowe, W. P. (1967) Isolation of adenovirus-associated viruses from man, *Proc Natl Acad Sci USA* ***58***, 1410–1415.
47. Han, L., Parmley, T. H., Keith, S., Kozlowski, K. J., Smith, L. J., and Hermonat, P. L. (1996) High prevalence of adeno-associated virus (AAV) type 2 rep DNA in cervical materials: AAV may be sexually transmitted, *Virus Genes* ***12***, 47–52.
48. Walz, C. M., Anisi, T. R., Schlehofer, J. R., Gissmann, L., Schneider, A., and Muller, M. (1998) Detection of infectious adeno-associated virus particles in human cervical biopsies, *Virology* ***247***, 97–105.
49. Mayor, H. D., Drake, S., Stahmann, J., and Mumford, D. M. (1976) Antibodies to adeno-associated satellite virus and herpes simplex in sera from cancer patients and normal adults, *Am J Obstet Gynecol* ***126***, 100–104.
50. Georg-Fries, B., Biederlack, S., Wolf, J., and zur Hausen, H. (1984) Analysis of proteins, helper dependence, and seroepidemiology of a new human parvovirus, *Virology* ***134***, 64–71.
51. Agorastos, T., Chrisafi, S., Lambropoulos, A. F., Mikos, T., Constandinides, T. C., Schlehofer, J. R., Schlehofer, B., Kotsis, A., and Bontis, J. N. (2008) Adeno-associated virus infection and cervical neoplasia: is there a protective role against human papillomavirus-related carcinogenesis?, *Eur J Cancer Prev* ***17***, 364–368.
52. Carter, B. J. (2004) Adeno-associated virus and the development of adeno-associated virus vectors: a historical perspective, *Mol Ther* ***10***, 981–989.
53. Wright, J. F. (2009) Transient transfection methods for clinical adeno-associated viral vector production, *Hum Gene Ther* ***20***, 698–706.
54. Zhang, H., Xie, J., Xie, Q., Wilson, J. M., and Gao, G. (2009) Adenovirus-adeno-associated virus hybrid for large-scale recombinant adeno-associated virus production, *Hum Gene Ther* ***20***, 922–929.
55. Clement, N., Knop, D. R., and Byrne, B. J. (2009) Large-scale adeno-associated viral vector production using a herpesvirus-based system enables manufacturing for clinical studies, *Hum Gene Ther* ***20***, 796–806.
56. Virag, T., Cecchini, S., and Kotin, R. M. (2009) Producing recombinant adeno-associated virus in foster cells: overcoming production limitations using a baculovirus-insect cell expression strategy, *Hum Gene Ther* ***20***, 807–817.
57. Carter, B. J. (2005) Adeno-associated virus vectors in clinical trials, *Hum Gene Ther* ***16***, 541–550.
58. Mueller, C., and Flotte, T. R. (2008) Clinical gene therapy using recombinant adeno-associated virus vectors, *Gene Ther* ***15***, 858–863.
59. Ding, W., Zhang, L., Yan, Z., and Engelhardt, J. F. (2005) Intracellular trafficking of adeno-associated viral vectors, *Gene Ther* ***12***, 873–880.
60. Srivastava, A. (2008) Adeno-associated virus-mediated gene transfer, *J Cell Biochem* ***105***, 17–24.
61. Chen, C. L., Jensen, R. L., Schnepp, B. C., Connell, M. J., Shell, R., Sferra, T. J., Bartlett, J. S., Clark, K. R., and Johnson, P. R. (2005) Molecular characterization of adeno-associated viruses infecting children, *J Virol* ***79***, 14781–14792.
62. Summerford, C., and Samulski, R. J. (1998) Membrane-associated heparan sulfate proteoglycan is a receptor for adeno-associated virus type 2 virions, *J Virol* ***72***, 1438–1445.
63. Kern, A., Schmidt, K., Leder, C., Muller, O. J., Wobus, C. E., Bettinger, K., Von der Lieth, C. W., King, J. A., and Kleinschmidt, J. A. (2003) Identification of a heparin-binding motif on adeno-associated virus type 2 capsids, *J Virol* ***77***, 11072–11081.
64. Opie, S. R., Warrington, K. H., Jr., Agbandje-McKenna, M., Zolotukhin, S., and Muzyczka, N. (2003) Identification of amino acid residues in the capsid proteins of adeno-associated virus type 2 that contribute to heparan sulfate proteoglycan binding, *J Virol* ***77***, 6995–7006.
65. Qing, K., Mah, C., Hansen, J., Zhou, S., Dwarki, V., and Srivastava, A. (1999) Human fibroblast growth factor receptor 1 is a co-receptor for infection by adeno-associated virus 2, *Nat Med* ***5***, 71–77.
66. Summerford, C., Bartlett, J. S., and Samulski, R. J. (1999) AlphaVbeta5 integrin: a co-receptor for adeno-associated virus type 2 infection, *Nat Med* ***5***, 78–82.
67. Kaludov, N., Brown, K. E., Walters, R. W., Zabner, J., and Chiorini, J. A. (2001) Adeno-associated virus serotype 4 (AAV4) and AAV5 both require sialic acid binding for hemagglutination and efficient transduction but differ

in sialic acid linkage specificity, *J Virol 75*, 6884–6893.

68. Walters, R. W., Yi, S. M., Keshavjee, S., Brown, K. E., Welsh, M. J., Chiorini, J. A., and Zabner, J. (2001) Binding of adeno-associated virus type 5 to 2,3-linked sialic acid is required for gene transfer, *J Biol Chem 276*, 20610–20616.
69. Di Pasquale, G., Davidson, B. L., Stein, C. S., Martins, I., Scudiero, D., Monks, A., and Chiorini, J. A. (2003) Identification of PDGFR as a receptor for AAV-5 transduction, *Nat Med 9*, 1306–1312.
70. Bartlett, J. S., Wilcher, R., and Samulski, R. J. (2000) Infectious entry pathway of adeno-associated virus and adeno-associated virus vectors, *J Virol 74*, 2777–2785.
71. Grieger, J. C., Snowdy, S., and Samulski, R. J. (2006) Separate basic region motifs within the adeno-associated virus capsid proteins are essential for infectivity and assembly, *J Virol 80*, 5199–5210.
72. Johnson, J. S., and Samulski, R. J. (2009) Enhancement of adeno-associated virus infection by mobilizing capsids into and out of the nucleolus, *J Virol 83*, 2632–2644.
73. Douar, A. M., Poulard, K., Stockholm, D., and Danos, O. (2001) Intracellular trafficking of adeno-associated virus vectors: routing to the late endosomal compartment and proteasome degradation, *J Virol 75*, 1824–1833.
74. Hansen, J., Qing, K., and Srivastava, A. (2001) Adeno-associated virus type 2-mediated gene transfer: altered endocytic processing enhances transduction efficiency in murine fibroblasts, *J Virol 75*, 4080–4090.
75. Xiao, W., Warrington, K. H., Jr., Hearing, P., Hughes, J., and Muzyczka, N. (2002) Adenovirus-facilitated nuclear translocation of adeno-associated virus type 2, *J Virol 76*, 11505–11517.
76. Thomas, C. E., Storm, T. A., Huang, Z., and Kay, M. A. (2004) Rapid uncoating of vector genomes is the key to efficient liver transduction with pseudotyped adeno-associated virus vectors, *J Virol 78*, 3110–3122.
77. Chiorini, J. A. (2006) Looking down the rabbit hole: understanding the binding, entry, and trafficking patterns of AAV particles in the cell, in *Parvoviruses* (Jonathan R. Kerr, S. F. C., Marshall E. Bloom, R. Michael Linden, Colin R. Parrish, Ed.), pp 168–170, Hodder Arnold, London.
78. Pereira, D. J., McCarty, D. M., and Muzyczka, N. (1997) The adeno-associated virus (AAV) Rep protein acts as both a repressor and an activator to regulate AAV transcription during a productive infection, *J Virol 71*, 1079–1088.
79. Berns, K. I., and Parrish, C. R. (2007) Parvoviridae, in *Fields Virology* (Knipe, D. M., and Howley, P. M., Eds.) 5th ed., pp 2437–2477, Lippincott Williams and Wilkins, Philadelphia, PA.
80. Ding, W., Yan, Z., Zak, R., Saavedra, M., Rodman, D. M., and Engelhardt, J. F. (2003) Second-strand genome conversion of adeno-associated virus type 2 (AAV-2) and AAV-5 is not rate limiting following apical infection of polarized human airway epithelia, *J Virol 77*, 7361–7366.
81. Ferrari, F. K., Samulski, T., Shenk, T., and Samulski, R. J. (1996) Second-strand synthesis is a rate-limiting step for efficient transduction by recombinant adeno-associated virus vectors, *J Virol 70*, 3227–3234.
82. Jayandharan, G. R., Zhong, L., Li, B., Kachniarz, B., and Srivastava, A. (2008) Strategies for improving the transduction efficiency of single-stranded adeno-associated virus vectors in vitro and in vivo, *Gene Ther 15*, 1287–1293.
83. Qing, K., Wang, X. S., Kube, D. M., Ponnazhagan, S., Bajpai, A., and Srivastava, A. (1997) Role of tyrosine phosphorylation of a cellular protein in adeno-associated virus 2-mediated transgene expression, *Proc Natl Acad Sci USA 94*, 10879–10884.
84. Zhong, L., Zhou, X., Li, Y., Qing, K., Xiao, X., Samulski, R. J., and Srivastava, A. (2008) Single-polarity recombinant adeno-associated virus 2 vector-mediated transgene expression in vitro and in vivo: mechanism of transduction, *Mol Ther 16*, 290–295.
85. Labow, M. A., Hermonat, P. L., and Berns, K. I. (1986) Positive and negative autoregulation of the adeno-associated virus type 2 genome, *J Virol 60*, 251–258.
86. Trempe, J. P., and Carter, B. J. (1988) Regulation of adeno-associated virus gene expression in 293 cells: control of mRNA abundance and translation, *J Virol 62*, 68–74.
87. Redemann, B. E., Mendelson, E., and Carter, B. J. (1989) Adeno-associated virus rep protein synthesis during productive infection, *J Virol 63*, 873–882.
88. Kyostio, S. R., Owens, R. A., Weitzman, M. D., Antoni, B. A., Chejanovsky, N., and Carter, B. J. (1994) Analysis of adeno-associated virus (AAV) wild-type and mutant Rep proteins for their abilities to negatively regulate AAV p5 and p19 mRNA levels, *J Virol 68*, 2947–2957.
89. Tratschin, J. D., Miller, I. L., and Carter, B. J. (1984) Genetic analysis of adeno-associated

virus: properties of deletion mutants constructed in vitro and evidence for an adeno-associated virus replication function, *J Virol* ***51***, 611–619.

90. Nash, K., Chen, W., and Muzyczka, N. (2008) Complete in vitro reconstitution of adeno-associated virus DNA replication requires the minichromosome maintenance complex proteins, *J Virol* ***82***, 1458–1464.
91. Ni, T. H., Zhou, X., McCarty, D. M., Zolotukhin, I., and Muzyczka, N. (1994) In vitro replication of adeno-associated virus DNA, *J Virol* ***68***, 1128–1138.
92. Ward, P. (2006) Replication of adeno-associated virus DNA, in *Parvoviruses* (Jonathan R. Kerr, S. F. C., Marshall E. Bloom, R. Michael Linden, Colin R. Parrish, Ed.), pp 189–211, Hodder Arnold, London.
93. Ward, P., and Berns, K. I. (1996) In vitro replication of adeno-associated virus DNA: enhancement by extracts from adenovirus-infected HeLa cells, *J Virol* ***70***, 4495–4501.
94. Senapathy, P., Tratschin, J. D., and Carter, B. J. (1984) Replication of adeno-associated virus DNA. Complementation of naturally occurring rep- mutants by a wild-type genome or an ori- mutant and correction of terminal palindrome deletions, *J Mol Biol* ***179***, 1–20.
95. Nahreini, P., and Srivastava, A. (1989) Rescue and replication of the adeno-associated virus 2 genome in mortal and immortal human cells, *Intervirology* ***30***, 74–85.
96. Ward, P., Falkenberg, M., Elias, P., Weitzman, M., and Linden, R. M. (2001) Rep-dependent initiation of adeno-associated virus type 2 DNA replication by a herpes simplex virus type 1 replication complex in a reconstituted system, *J Virol* ***75***, 10250–10258.
97. Slanina, H., Weger, S., Stow, N. D., Kuhrs, A., and Heilbronn, R. (2006) Role of the herpes simplex virus helicase-primase complex during adeno-associated virus DNA replication, *J Virol* ***80***, 5241–5250.
98. Owens, R. A., Weitzman, M. D., Kyostio, S. R., and Carter, B. J. (1993) Identification of a DNA-binding domain in the amino terminus of adeno-associated virus Rep proteins, *J Virol* ***67***, 997–1005.
99. Brister, J. R., and Muzyczka, N. (2000) Mechanism of Rep-Mediated Adeno-Associated Virus Origin Nicking., *J.Virology* ***74***, 7762–7771.
100. Shi, Y., Seto, E., Chang, L. S., and Shenk, T. (1991) Transcriptional repression by YY1, a human GLI-Kruppel-related protein, and relief of repression by adenovirus E1A protein, *Cell* ***67***, 377–388.
101. Chang, L. S., Shi, Y., and Shenk, T. (1989) Adeno-associated virus P5 promoter contains an adenovirus E1A-inducible element and a binding site for the major late transcription factor, *J Virol* ***63***, 3479–3488.
102. Weitzman, M. D., Fisher, K. J., and Wilson, J. M. (1996) Recruitment of wild-type and recombinant adeno-associated virus into adenovirus replication centers, *J Virol* ***70***, 1845–1854.
103. Ward, P., Dean, F. B., O'Donnell, M. E., and Berns, K. I. (1998) Role of the adenovirus DNA-binding protein in in vitro adeno-associated virus DNA replication, *J Virol* ***72***, 420–427.
104. Samulski, R. J., and Shenk, T. (1988) Adenovirus E1B 55-Mr polypeptide facilitates timely cytoplasmic accumulation of adeno-associated virus mRNAs, *J Virol* ***62***, 206–210.
105. Fisher, K. J., Gao, G. P., Weitzman, M. D., DeMatteo, R., Burda, J. F., and Wilson, J. M. (1996) Transduction with recombinant adeno-associated virus for gene therapy is limited by leading-strand synthesis, *J Virol* ***70***, 520–532.
106. Schwartz, R. A., Palacios, J. A., Cassell, G. D., Adam, S., Giacca, M., and Weitzman, M. D. (2007) The Mre11/Rad50/Nbs1 complex limits adeno-associated virus transduction and replication, *J Virol* ***81***, 12936–12945.
107. Nayak, R., and Pintel, D. J. (2007) Adeno-associated viruses can induce phosphorylation of eIF2alpha via PKR activation, which can be overcome by helper adenovirus type 5 virus-associated RNA, *J Virol* ***81***, 11908–11916.
108. Xiao, X., Li, J., and Samulski, R. J. (1998) Production of high-titer recombinant adeno-associated virus vectors in the absence of helper adenovirus, *J Virol* ***72***, 2224–2232.
109. Weindler, F. W., and Heilbronn, R. (1991) A subset of herpes simplex virus replication genes provides helper functions for productive adeno-associated virus replication, *J Virol* ***65***, 2476–2483.
110. Stracker, T. H., Cassell, G. D., Ward, P., Loo, Y. M., van Breukelen, B., Carrington-Lawrence, S. D., Hamatake, R. K., van der Vliet, P. C., Weller, S. K., Melendy, T., and Weitzman, M. D. (2004) The Rep protein of adeno-associated virus type 2 interacts with single-stranded DNA-binding proteins that enhance viral replication, *J Virol* ***78***, 441–453.
111. Geoffroy, M. C., Epstein, A. L., Toublanc, E., Moullier, P., and Salvetti, A. (2004) Herpes simplex virus type 1 ICP0 protein mediates activation of adeno-associated virus type 2 rep gene expression from a latent integrated form, *J Virol* ***78***, 10977–10986.

112. Alazard-Dany, N., Nicolas, A., Ploquin, A., Strasser, R., Greco, A., Epstein, A. L., Fraefel, C., and Salvetti, A. (2009) Definition of herpes simplex virus type 1 helper activities for adeno-associated virus early replication events, *PLoS Pathog* ***5***, e1000340.

113. Yalkinoglu, A. O., Heilbronn, R., Burkle, A., Schlehofer, J. R., and zur Hausen, H. (1988) DNA amplification of adeno-associated virus as a response to cellular genotoxic stress, *Cancer Res* ***48***, 3123–3129.

114. Meyers, C., Mane, M., Kokorina, N., Alam, S., and Hermonat, P. L. (2000) Ubiquitous human adeno-associated virus type 2 autonomously replicates in differentiating keratinocytes of a normal skin model, *Virology 272*, 338–346.

115. Ward, P., Urcelay, E., Kotin, R., Safer, B., and Berns, K. I. (1994) Adeno-associated virus DNA replication in vitro: activation by a maltose binding protein/Rep 68 fusion protein, *J Virol* ***68***, 6029–6037.

116. Ni, T. H., McDonald, W. F., Zolotukhin, I., Melendy, T., Waga, S., Stillman, B., and Muzyczka, N. (1998) Cellular proteins required for adeno-associated virus DNA replication in the absence of adenovirus coinfection, *J Virol 72*, 2777–2787.

117. Nash, K., Chen, W., McDonald, W. F., Zhou, X., and Muzyczka, N. (2007) Purification of host cell enzymes involved in adeno-associated virus DNA replication, *J Virol* ***81***, 5777–5787.

118. Nash, K., Chen, W., Salganik, M., and Muzyczka, N. (2009) Identification of cellular proteins that interact with the adeno-associated virus rep protein, *J Virol* ***83***, 454–469.

119. Cassell, G. D., and Weitzman, M. D. (2004) Characterization of a nuclear localization signal in the C-terminus of the adeno-associated virus Rep68/78 proteins, *Virology* ***327***, 206–214.

120. Pereira, D. J., and Muzyczka, N. (1997) The adeno-associated virus type 2 p40 promoter requires a proximal Sp1 interaction and a p19 CArG-like element to facilitate Rep transactivation, *J Virol 71*, 4300–4309.

121. Costello, E., Saudan, P., Winocour, E., Pizer, L., and Beard, P. (1997) High mobility group chromosomal protein 1 binds to the adeno-associated virus replication protein (Rep) and promotes Rep-mediated site-specific cleavage of DNA, ATPase activity and transcriptional repression, *EMBO J* ***16***, 5943–5954.

122. Di Pasquale, G., and Chiorini, J.A. (2003) PKA/PrKX activity is a modulator of AAV/adenovirus interaction., *EMBO J 22*, 1716–1724.

123. Qing, K., Hansen, J., Weigel-Kelley, K. A., Tan, M., Zhou, S., and Srivastava, A. (2001) Adeno-associated virus type 2-mediated gene transfer: role of cellular FKBP52 protein in transgene expression, *J Virol 75*, 8968–8976.

124. Cathomen, T., Stracker, T. H., Gilbert, L. B., and Weitzman, M. D. (2001) A genetic screen identifies a cellular regulator of adeno-associated virus, *Proc Natl Acad Sci USA* ***98***, 14991–14996.

125. Chen, H., Lilley, C. E., Yu, Q., Lee, D. V., Chou, J., Narvaiza, I., Landau, N. R., and Weitzman, M. D. (2006) APOBEC3A is a potent inhibitor of adeno-associated virus and retrotransposons, *Curr Biol* ***16***, 480–485.

126. Konig, R., Zhou, Y., Elleder, D., Diamond, T. L., Bonamy, G. M., Irelan, J. T., Chiang, C. Y., Tu, B. P., De Jesus, P. D., Lilley, C. E., Seidel, S., Opaluch, A. M., Caldwell, J. S., Weitzman, M. D., Kuhen, K. L., Bandyopadhyay, S., Ideker, T., Orth, A. P., Miraglia, L. J., Bushman, F. D., Young, J. A., and Chanda, S. K. (2008) Global analysis of host-pathogen interactions that regulate early-stage HIV-1 replication, *Cell* ***135***, 49–60.

127. Choi, V. W., McCarty, D. M., and Samulski, R. J. (2006) Host cell DNA repair pathways in adeno-associated viral genome processing, *J Virol* ***80***, 10346–10356.

128. Zentilin, L., Marcello, A., and Giacca, M. (2001) Involvement of cellular double-stranded DNA break binding proteins in processing of the recombinant adeno-associated virus genome, *J Virol 75*, 12279–12287.

129. Cervelli, T., Palacios, J. A., Zentilin, L., Mano, M., Schwartz, R. A., Weitzman, M. D., and Giacca, M. (2008) Processing of recombinant AAV genomes occurs in specific nuclear structures that overlap with foci of DNA-damage-response proteins, *J Cell Sci* ***121***, 349–357.

130. Schwartz, R. A., Carson, C. T., Schuberth, C., and Weitzman, M. D. (2009) Adeno-associated virus replication induces a DNA damage response coordinated by DNA-dependent protein kinase, *J Virol* ***83***, 6269–6278.

131. Wistuba, A., Kern, A., Weger, S., Grimm, D., and Kleinschmidt, J. A. (1997) Subcellular compartmentalization of adeno-associated virus type 2 assembly, *J Virol 71*, 1341–1352.

132. Hunter, L. A., and Samulski, R. J. (1992) Colocalization of adeno-associated virus Rep and capsid proteins in the nuclei of infected cells, *J Virol* ***66***, 317–324.

133. Yang, Q., Chen, F., and Trempe, J. P. (1994) Characterization of cell lines that inducibly express the adeno-associated virus Rep proteins, *J Virol* ***68***, 4847–4856.

134. Kyostio, S. R., Wonderling, R. S., and Owens, R. A. (1995) Negative regulation of the adeno-associated virus (AAV) P5 promoter involves both the P5 rep binding site and the consensus ATP-binding motif of the AAV Rep68 protein, *J Virol* ***69***, 6787–6796.

135. Lackner, D. F., and Muzyczka, N. (2002) Studies of the mechanism of transactivation of the adeno-associated virus p19 promoter by Rep protein, *J Virol* ***76***, 8225–8235.

136. Pereira, D. J., and Muzyczka, N. (1997) The cellular transcription factor SP1 and an unknown cellular protein are required to mediate Rep protein activation of the adeno-associated virus p19 promoter, *J Virol* ***71***, 1747–1756.

137. Haberman, R. P., McCown, T. J., and Samulski, R. J. (2000) Novel transcriptional regulatory signals in the adeno-associated virus terminal repeat A/D junction element, *J Virol* ***74***, 8732–8739.

138. Flotte, T. R., Afione, S. A., Solow, R., Drumm, M. L., Markakis, D., Guggino, W. B., Zeitlin, P. L., and Carter, B. J. (1993) Expression of the cystic fibrosis transmembrane conductance regulator from a novel adeno-associated virus promoter, *J Biol Chem* ***268***, 3781–3790.

139. Mouw, M. B., and Pintel, D. J. (2000) Adeno-associated virus RNAs appear in a temporal order and their splicing is stimulated during coinfection with adenovirus, *J Virol* ***74***, 9878–9888.

140. Qiu, J., and Pintel, D. J. (2002) The adeno-associated virus type 2 Rep protein regulates RNA processing via interaction with the transcription template, *Mol Cell Biol* ***22***, 3639–3652.

141. Hermonat, P. L., Labow, M. A., Wright, R., Berns, K. I., and Muzyczka, N. (1984) Genetics of adeno-associated virus: isolation and preliminary characterization of adeno-associated virus type 2 mutants, *J Virol* ***51***, 329–339.

142. Holscher, C., Kleinschmidt, J. A., and Burkle, A. (1995) High-level expression of adeno-associated virus (AAV) Rep78 or Rep68 protein is sufficient for infectious-particle formation by a rep-negative AAV mutant, *J Virol* ***69***, 6880–6885.

143. Linden, R. M., Ward, P., Giraud, C., Winocour, E., and Berns, K. I. (1996) Site-specific integration by adeno-associated virus, *Proc Natl Acad Sci USA* ***93***, 11288–11294.

144. Surosky, R. T., Urabe, M., Godwin, S. G., McQuiston, S. A., Kurtzman, G. J., Ozawa, K., and Natsoulis, G. (1997) Adeno-associated virus Rep proteins target DNA sequences to a unique locus in the human genome, *J Virol* ***71***, 7951–7959.

145. Wang, X. S., Ponnazhagan, S., and Srivastava, A. (1995) Rescue and replication signals of the adeno-associated virus 2 genome, *J Mol Biol* ***250***, 573–580.

146. Berns, K. I., and Linden, R. M. (1995) The cryptic life style of adeno-associated virus, *Bioessays* ***17***, 237–245.

147. Hermonat, P. L. (1994) Down-regulation of the human c-fos and c-myc proto-oncogene promoters by adeno-associated virus Rep78, *Cancer Lett* ***81***, 129–136.

148. Labow, M. A., Graf, L. H., Jr., and Berns, K. I. (1987) Adeno-associated virus gene expression inhibits cellular transformation by heterologous genes, *Mol Cell Biol 7*, 1320–1325.

149. McCarty, D. M., Christensen, M., and Muzyczka, N. (1991) Sequences required for coordinate induction of adeno-associated virus p19 and p40 promoters by Rep protein, *J Virol* ***65***, 2936–2945.

150. Chejanovsky, N., and Carter, B. J. (1989) Mutagenesis of an AUG codon in the adeno-associated virus rep gene: effects on viral DNA replication, *Virology* ***173***, 120–128.

151. King, J. A., Dubielzig, R., Grimm, D., Kleinschmidt, J. A. (2001) DNA helicase-mediated packaging of adeno-associated virus type 2 genomes into preformed capsids, *EMBO J* ***20***, 3282–3291.

152. Hickman, A. B., Ronning, D. R., Kotin, R. M., and Dyda, F. (2002) Structural unity among viral origin binding proteins: crystal structure of the nuclease domain of adeno-associated virus Rep, *Mol Cell* ***10***, 327–337.

153. Im, D. S., and Muzyczka, N. (1990) The AAV origin binding protein Rep68 is an ATP-dependent site-specific endonuclease with DNA helicase activity., *Cell* ***61***, 447–457.

154. James, J. A., Escalante, C.R., Yoon-Robarts, M., Edwards, T.A., Linden, R.M., and Aggarwal, A.K. (2003) Crystal Structure of the SF3 Helicase from Adeno-Associated Virus Type 2, *Structure* ***11***, 1025–1035.

155. James, J. A., Aggarwal, A. K., Linden, R. M., and Escalante, C. R. (2004) Structure of adeno-associated virus type 2 Rep40-ADP complex: insight into nucleotide recognition and catalysis by superfamily 3 helicases, *Proc Natl Acad Sci USA* ***101***, 12455–12460.

156. Mansilla-Soto, J., Yoon-Robarts, M., Rice, W. J., Arya, S., Escalante, C. R., and Linden, R. M. (2009) DNA structure modulates the oligomerization properties of the AAV initiator protein Rep68, *PLoS Pathog* ***5***, e1000513.

157. Dutheil, N., and Linden, R. M. (2006) Site-specific integration by adeno-associated virus,

in *Parvoviruses* (Jonathan R. Kerr, S. F. C., Marshall E. Bloom, R. Michael Linden, Colin R. Parrish, Ed.), pp 213–237, Hodder Arnold, London.

158. Kotin, R. M., and Berns, K. I. (1989) Organization of adeno-associated virus DNA in latently infected Detroit 6 cells, *Virology **170***, 460–467.
159. Kotin, R. M., Menninger, J. C., Ward, D. C., and Berns, K. I. (1991) Mapping and direct visualization of a region-specific viral DNA integration site on chromosome 19q13-qter, *Genomics **10***, 831–834.
160. Walsh, C. E., Liu, J. M., Xiao, X., Young, N. S., Nienhuis, A. W., and Samulski, R. J. (1992) Regulated high level expression of a human gamma-globin gene introduced into erythroid cells by an adeno-associated virus vector, *Proc Natl Acad Sci USA **89***, 7257–7261.
161. Balague, C., Kalla, M., and Zhang, W. W. (1997) Adeno-associated virus Rep78 protein and terminal repeats enhance integration of DNA sequences into the cellular genome, *J Virol **71***, 3299–3306.
162. Urcelay, E., Ward, P. Wiener, M., Safer, B. and Kotin, R.M. (1995) Asymmetric replication in vitro from a human sequence element is dependent on adeno-associated virus Rep proteins., *J.Virology **69***, 2038–2046.
163. Weitzman, M. D., Kyostio, S. R., Kotin, R. M., and Owens, R. A. (1994) Adeno-associated virus (AAV) Rep proteins mediate complex formation between AAV DNA and its integration site in human DNA, *Proc Natl Acad Sci USA **91***, 5808–5812.
164. Dutheil, N., Henckaerts, E., Kohlbrenner, E., and Linden, R. M. (2009) Transcriptional Analysis of the Adeno-Associated Virus Integration Site, *J Virol.*
165. Dutheil, N., Shi, F., Dupressoir, T., and Linden, R. M. (2000) Adeno-associated virus site-specifically integrates into a muscle-specific DNA region, *Proc Natl Acad Sci USA **97***, 4862–4866.
166. Dutheil, N., Yoon-Robarts, M., Ward, P., Henckaerts, E., Skrabanek, L., Berns, K. I., Campagne, F., and Linden, R. M. (2004) Characterization of the mouse adeno-associated virus AAVS1 ortholog, *J Virol **78***, 8917–8921.
167. Henckaerts, E., Dutheil, N., Zeltner, N., Kattman, S., Kohlbrenner, E., Ward, P., Clement, N., Rebollo, P., Kennedy, M., Keller, G. M., and Linden, R. M. (2009) Site-specific integration of adeno-associated virus involves partial duplication of the target locus, *Proc Natl Acad Sci USA **106***, 7571–7576.
168. Yang, L., Soonpaa, M. H., Adler, E. D., Roepke, T. K., Kattman, S. J., Kennedy, M., Henckaerts, E., Bonham, K., Abbott, G. W., Linden, R. M., Field, L. J., and Keller, G. M. (2008) Human cardiovascular progenitor cells develop from a KDR+ embryonic-stem-cell-derived population, *Nature **453***, 524–528.
169. Wang, J., Xie, J., Lu, H., Chen, L., Hauck, B., Samulski, R. J., and Xiao, W. (2007) Existence of transient functional double-stranded DNA intermediates during recombinant AAV transduction, *Proc Natl Acad Sci USA **104***, 13104–13109.
170. Schultz, B. R., and Chamberlain, J. S. (2008) Recombinant adeno-associated virus transduction and integration, *Mol Ther **16***, 1189–1199.
171. Duan, D., Sharma, P., Yang, J., Yue, Y., Dudus, L., Zhang, Y., Fisher, K. J., and Engelhardt, J. F. (1998) Circular intermediates of recombinant adeno-associated virus have defined structural characteristics responsible for long-term episomal persistence in muscle tissue, *J Virol 72*, 8568–8577.
172. Inagaki, K., Ma, C., Storm, T. A., Kay, M. A., and Nakai, H. (2007) The role of DNA-PKcs and artemis in opening viral DNA hairpin termini in various tissues in mice, *J Virol **81***, 11304–11321.

Chapter 2

Design and Construction of Functional AAV Vectors

John T. Gray and Serge Zolotukhin

Abstract

Using the basic principles of molecular biology and laboratory techniques presented in this chapter, researchers should be able to create a wide variety of AAV vectors for both clinical and basic research applications. Basic vector design concepts are covered for both protein coding gene expression and small non-coding RNA gene expression cassettes. AAV plasmid vector backbones (available via AddGene) are described, along with critical sequence details for a variety of modular expression components that can be inserted as needed for specific applications. Protocols are provided for assembling the various DNA components into AAV vector plasmids in *Escherichia coli*, as well as for transferring these vector sequences into baculovirus genomes for large-scale production of AAV in the insect cell production system.

Key words: AAV, Vector plasmid, Vector performance, Transfection, Molecular cloning, Baculovirus, Vector design

1. Introduction

1.1. Basics of Vector Design

The construction of viral vectors is an exercise in compromise, as there is always some limitation as to the length and type of sequence that can be delivered, and any number of functional elements that could in theory improve the behavior of the vector. It is the goal of this chapter to provide tools and instruction to begin this process with a limited set of such elements, but it remains to the investigator to complete the effort by carefully evaluating the actual performance of the vector in therapeutically or experimentally relevant target cells and, if necessary, revisiting the construction process to correct deficiencies observed.

The basic design of an AAV vector is relatively simple, in that it consists of an appropriately sized expression cassette flanked by inverted terminal repeats (ITRs), which mediate the replication

Richard O. Snyder and Philippe Moullier (eds.), *Adeno-Associated Virus: Methods and Protocols*,
Methods in Molecular Biology, vol. 807, DOI 10.1007/978-1-61779-370-7_2,

and packaging of the vector genome by the AAV replication protein Rep and associated factors in vector producer cells. This chapter attempts to provide specific methodological details to enable an investigator to utilize standard molecular cloning techniques to assemble a functional AAV vector plasmid for use in the transient transfection system in HEK293 cells, which will suffice for many preliminary evaluations of vector performance. For those vectors slated for larger scale applications (as in large animal models or human clinical trials), we additionally provide instructions for moving existing AAV cassettes into a baculovirus genome for production in the insect cell system. A key aspect of our approach to this chapter is that we attempt to provide specific sequence details about many commonly used components of vector cassettes, to enable more specific design using either fully synthetic methods or PCR amplification from commonly available sources.

Beyond the requirements for optimal genome size and the presence of AAV ITRs, AAV vector designs are only limited by whatever functions can be conferred on a 4–5-kbp segment of DNA. We will provide below a basic introduction for two of the most common types of vectors, first for standard expression of a protein coding gene and second for the expression of non-coding RNAs to generate siRNA for targeted gene knockdown. There are other powerful vector designs beyond the scope of this chapter, but which may also be useful to the reader. In this book, Chapter 13 describes the use of AAV vectors for targeted homologous recombination, which requires the insertion of homology arms in the vector flanking the segment to be inserted into a cell genome. Another powerful technology utilizes the expression of non-coding RNA designed to interact with the cellular splicing machinery and mutant mRNA to induce "exon-skipping," which in the case of certain muscular dystrophy mutations can restore functionality to the resulting translated protein (1). Likewise, expression of ribozymes within non-coding RNA transcripts can be used to target mRNA for degradation (2).

Finally, should a vector prove to be clinically efficacious, commercialization may be affected by relevant intellectual property, which can be found by thorough review of patent databases and/or consultation with intellectual property professionals.

1.2. Protein-Coding Expression Design Concepts

A diagram of a basic expression cassette is presented in Fig. 1. Expression of protein coding mRNA begins with the initiation of transcription by RNA Polymerase II at promoter sequences, which dictate the location and orientation of transcription. Enhancer sequences, which function in a more position- and orientation-independent manner, can be located either upstream or downstream of the promoter, and modulate both the strength and tissue specificity of the promoter. Although in many cases a single contiguous fragment from a naturally derived sequence will provide

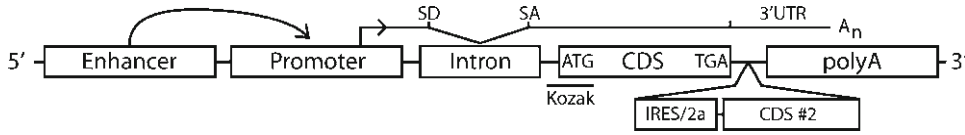

Fig. 1. Schematic diagram of a basic protein coding expression cassette. Basic components of a vector expression cassette are indicated. *SD* splice donor, *SA* splice acceptor, *CDS* coding sequence. See text for additional explanations.

both functions, in some cases chimeric promoters are constructed using separate enhancers and promoters positioned in a variety of arrangements. The selection of the promoter you wish to use in your vector depends upon the spatial and temporal control necessary for your application, the level of expression desired and the amount of space available. Although we provide information in the Subheading 3 for a few more commonly used promoters, the choices available are very broad should an investigator wish to explore more deeply. Chapters 5–9 of this book discuss tissue-specific vectors in detail, and a recent review (3) describes several regulatable promoters that have been engineered for inducible gene expression using small molecules.

Introns are frequently inserted downstream of promoters to capitalize on the fact that the splicing process facilitates mRNA export and increases steady state levels of mRNA in the cytoplasm. As the presence of a translational termination codon upstream of an intron splice junction is a trigger for initiation of the nonsense mediated mRNA degradation (NMD) pathway (4), introns should be located upstream of the end of any protein coding sequence. When transmitting very large coding sequences, one should also consider that the increase in gene expression provided by an intron may very well be negated by significant reductions in vector yield caused by exceeding the packaging capacity of the AAV system, and in those cases an intronless construct may be the best option.

In order to achieve optimal translation efficiency, the coding sequence must be positioned such that the ATG initiator codon is the first ATG of the spliced message. The use of optimal Kozak sequences just upstream of the ATG significantly improves translation initiation efficiency and ensures that ribosomal scanning of the vector-encoded mRNA does not lead to translation of aberrant products lacking N-terminal amino acids (5). Although the most important element of this consensus is a purine at the –3 position, the small size of the full optimal sequence (CCACCATG) enables easy incorporation into any construct coding sequence generated synthetically or by PCR.

Additional enhancement of gene expression can be provided by a process called "codon optimization," which involves the construction of a cDNA with alternate codons chosen to facilitate robust gene expression while still encoding the same amino acid sequence. The concept behind this technique is that though there

are multiple triplet codons that can encode for a single amino acid, it is often the case that the best expression is achieved when amino acids are coded by the codons most commonly found in highly expressed genes. Codon usage is naturally biased to favor a subset of codons in different species and also in highly expressed genes. Although these biases can originate via a variety of mechanisms (6), it has been shown that "optimal" codons can enhance translational efficiency by utilizing the most abundant charged tRNAs in the cell (7). Codon optimization can be performed by commercial gene synthesis companies, which have in many cases developed algorithms for automated selection of the codons in a gene and have convenient online ordering forms. The cost can depend upon the length of the gene being synthesized, and range from $0.39 to $2 per base pair. It should be noted, however, that the potential for introduction of sequences that negatively affect gene expression is also a risk with this process, and it is difficult to predict which sequences will have such an effect. For example, it has been shown that the sequences coding for protein domain boundaries are more likely to be coded by "translationally slow" codons (8), providing support for the hypothesis that slower translation at domain boundaries enhances fitness by allowing each domain to fold co-translationally in distinct temporal phases (9). Codon-optimized genes should therefore be tested carefully to confirm that the resulting protein product is not improperly folded.

Although in most cases fully spliced cDNAs are used in vectors to preserve space, in some cases coding sequences in vectors are interrupted with introns, such that splicing allows regeneration of an intact open reading frame. One example of this application is the use of native intronic sequences from the first intron of the human Factor IX gene, which allowed incorporation of the endogenous tissue-specific enhancers present in those sequences (10). Other applications include the insertion of regulatable polyA cassettes in an intron to allow regulation of complete expression (11) and the splitting of large coding sequences between two vectors genomes, which can, after head-to-tail joining in vivo, transcribe through both genomes to generate transcripts longer than 5 kb and which are spliced to yield an intact coding sequence (12).

Although clinical vectors almost invariably exclude them, additional exogenous peptides are often fused or co-expressed with the primary gene of interest for research and pre-clinical applications. Epitope tags are small and allow the use of commonly available antibody reagents to quantitate expression in cell lysates from tissues transduced with the vector. Signal peptides, when not encoded by the natural cDNA sequences, can be inserted at the N-terminus of an open reading frame to direct proteins to be secreted from the cell. Co-transmission of a second, separate coding sequence has numerous research and clinical applications, most commonly in allowing the co-expression of fluorescent marking

proteins to track cells transduced with the vector. This can be achieved using internal ribosome entry sites (IRES), or more recently by using specialized "2A peptide" sequences, which, when translated, cause a failure in peptidyl bond formation between the two coding open reading frames, resulting in efficient co-expression of two separate proteins in an approximately 1:1 ratio (13).

Sequences downstream of the translational stop codon form the 3′ untranslated regions (3′ UTR) of a transcript. Recent discoveries of the mechanisms of action for non-coding RNAs have illuminated the importance of these sequences as mediators of micro-RNA (miRNA) binding and regulation of both RNA stability and translation (14). For some genes such as Factor IX, sequences in the 3′ UTR facilitate optimal expression of vector-derived transcripts (10), whereas in other genes omission of endogenous 3′ UTR sequences can prevent unwanted degradation (15). In another creative application of these natural interactions, insertion of multiple miRNA target site sequences rendered expression of an otherwise ubiquitously expressed transcript specific to non-hematopoietic tissues, enhancing evasion of immunological consequences of expression in those tissues (16).

1.3. Noncoding RNA Expression Design Concepts

Small 21–25-nucleotide (nt) long RNA fragments in cells have been shown to be powerful modulators of mRNA translation and stability, and are increasingly utilized for experimental and therapeutic purposes. These short, interfering RNAs (siRNAs) act via their assembly into an RNA-Induced Silencing Complex (RISC), wherein the RNA fragment provides specificity via base complementarity to allow the RISC to target mRNAs for degradation or translation inhibition, depending upon the degree of complementarity between the two RNAs. Construction of an expression vector to generate siRNAs in vivo has largely been accomplished using two strategies, short hairpin RNAs (shRNAs) (17) and microRNA mimics (18, 19). Although shRNA cassettes can be more potent than miRNA mimics (20), miRNA mimics have been shown to have reduced toxicity (21).

The structure of these two types of non-coding RNA expression cassettes are presented in Fig. 2, along with an illustration of the different processing steps leading to the loading of the RISC with the siRNA. Transcription of an shRNA cassette (Fig. 2a) is typically mediated by RNA Polymerase III to generate a hairpin free of additional nucleotides beyond the hairpin ends. This hairpin exits the nucleus where it is processed by the cytoplasmic enzyme Dicer, which cleaves the loop sequence and allows the resulting RNA fragment to be loaded onto the RISC (17). MicroRNA mimics (Fig. 2b), on the other hand, can be generated using RNA Pol II, typically by inserting an extended RNA sequence derived from a naturally occurring primary miRNA transcript into either an intron or the 3′ UTR of a pre-existing protein coding

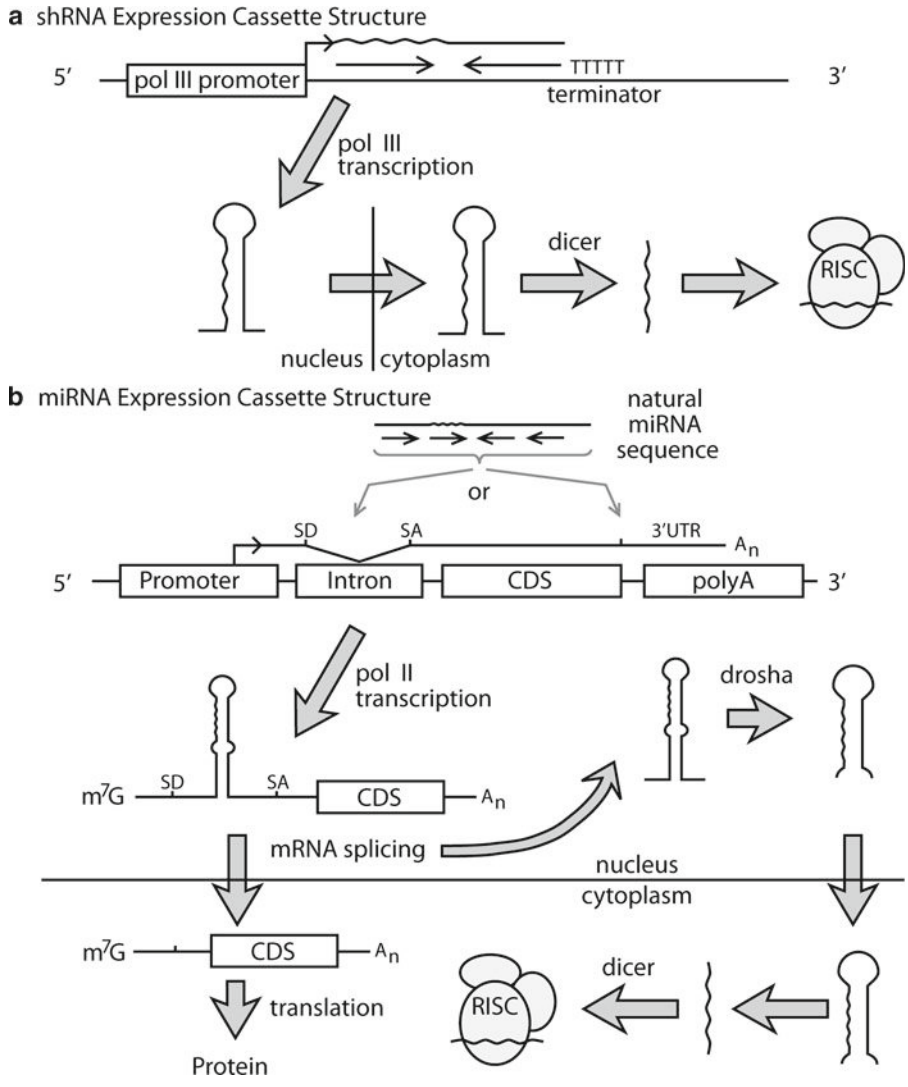

Fig. 2. Schematic diagram of two forms of non-coding RNA expression cassettes. Expression of siRNA for targeted knockdown of gene expression. *Wavy lines* indicate portion of primary RNA transcript that will be incorporated into the RISC. *Thin black arrows* indicate complementary arms of a hairpin. (**a**) Pol III promoter-driven expression of short hairpin RNAs (shRNAs). (**b**) Pol II-driven expression cassette for simultaneous expression of protein coding RNA and miRNA mimics.

expression cassette. The specific 21–22-nt RNA targeting sequence and its complement are grafted into the primary miRNA fragment native sequence in place of the miRNA sequence. The natural flanking sequences are recognized by the nuclear enzyme Drosha, which acts upstream of Dicer during miRNA biogenesis by cleaving the extended hairpin at bulged nucleotides distal of the loop. Hairpins processed in this way appear to be more efficiently transported to the cytoplasm and processed by the Dicer enzyme, apparently leading to reduced toxicity (21). Additionally, miRNA mimics

provide the added benefit that a wide range of well-characterized RNA Pol II promoters and expression components can be used, including regulated and tissue specific promoters (19). Additionally, some naturally occurring miRNA primary transcripts are processed to yield multiple miRNAs, which can be utilized to engineer a single vector encoded transcript that generates multiple miRNA mimics (22).

1.4. Special Considerations for Constructing Baculoviruses Containing AAV Vector Genomes

Although a baculovirus vector-mediated manufacture of rAAV in insect Sf9 cells is a scale-up method of choice, it is not usually recommended for a routine production of research vectors used for the initial screening at titers of 10^{12}–10^{13} DNase Resistant Particles (drp). Initially, rAAV vectors can be made by transient transfection at small scale to evaluate performance in rodents (23). Once the transgene expression cassette is optimized and the most efficient serotype is determined, the next step usually involves production of high titer vector stocks for pre-clinical studies in a large-animal model. At this stage, it might be worth investing effort in construction of the baculovirus expression vector (BEV) carrying rAAV cassette. The latter could be combined with the existent and published (24–26) Rep-, and VP-expressing helpers in a full complement set required for rAAV production.

Currently, there are three comparable systems to provide *rep* and *cap* helper functions in Sf9 cells. The first one is a modified BEV expressing both Rep and VP (26). A similar system expressing Rep and VP from two separate BEVs had been described by Chen (25). Yet another system utilizes stable insect cell lines expressing inducible Rep and VP upon infection with BEV-rAAV (24). Regardless of the approach, constructing rAAV-carrying BEV is a prerequisite step and it is described below in detail.

BEVs are prepared using Invitrogen's Bac-to-Bac system. The system utilizes a bacmid, an intermediate shuttle plasmid vector of 143 kbp incorporating complete BV genome, as well as Km^R gene and bacterial *ori*. It also contains a Tn7 attachment site engineered in-frame within a *lacZ* α peptide sequence. The rAAV cassette is first cloned into a Bac-to-Bac plasmid, flanked by Tn7R and Tn7L sequences. This is then transformed into the *Escerichia coli* DH10BAC that contains the bacmid, and a helper plasmid encoding the transposase. The rAAV cassette is transposed on to the bacmid and selected by growth in the presence of gentamicin, kanamycin and tetracycline. The parental bacmid encodes the LacZ α peptide which complements with the chromosomal β peptide to form a fully functional β-galactosidase which cleaves X-gal and produces blue colonies. The transposed cassette disrupts the *lacZ* α gene, and thus recombinant bacmid clones are white. Bacmid DNA is prepared from the putative recombinant clones, and the transposition is confirmed by PCR or Hirt DNA analysis. The recombinant bacmid is transfected into Sf9 cells, and several days later infectious BEV is harvested from the medium.

2. Materials

2.1. Construction of AAV Vector Plasmids Suitable for Transient Transfection of 293 Cells

1. AAV vector plasmid backbone: Although many plasmids are available from academic and commercial sources, the specific sites provided in this chapter are selected for pAAV-GFP and pscAAV-GFP, which have been deposited to AddGene (AddGene.org/John_T_Gray) and linked to this article (Fig. 3). pAAV-GFP contains two intact ITRs flanking a

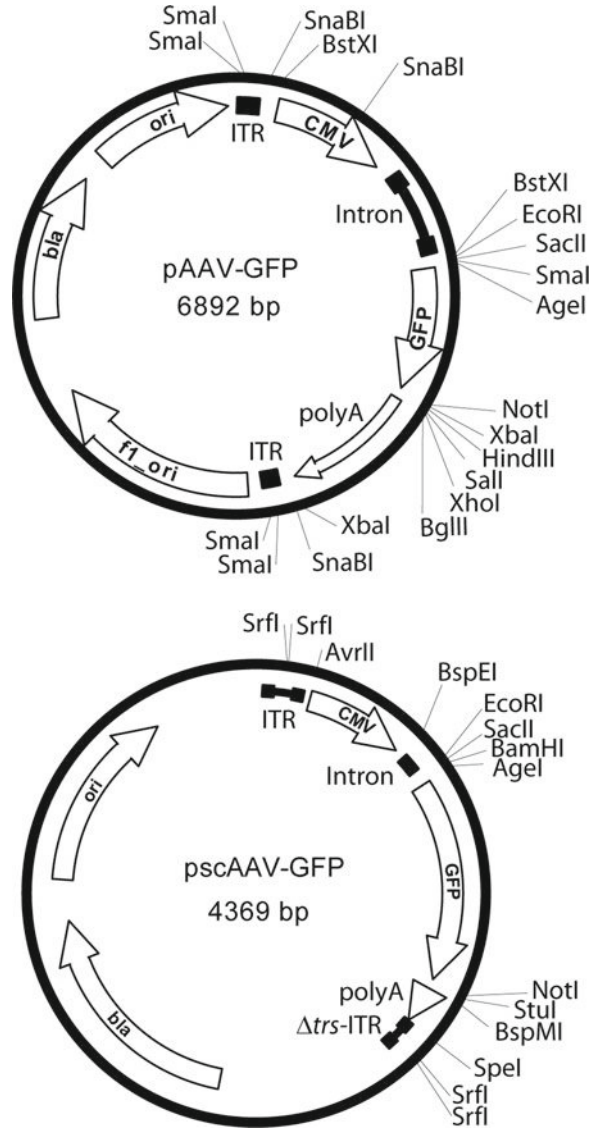

Fig. 3. Maps of single-stranded and Δ*trs* AAV vectors available from AddGene, showing relevant features and restriction sites. Additional details on the structure of these plasmids can be downloaded from the AddGene records linked to this article.

Table 1
Useful restriction enzyme sites in AddGene AAV vectors

	Vector plasmid			
	pAAV-GFP		pscAAV-GFP	
Component to be replaced	5′ Enzymes	3′ Enzymes	5′ Enzymes	3′ Enzymes
GFP	*Eco*RI, *Sac*II, and *Age*I	*Not*I, *Hin*dIII, *Sal*I, *Xho*I, and *Bgl*II	*Eco*RI, *Sac*II, *Bam*HI and *Age*I	*Not*I, *Stu*I, and *Bsp*MI (*Xho*I compatible)
CMV promoter (with intron)	*Bst*XI	*Bst*XI, *Eco*RI, *Sac*II, and *Age*I	*Avr*II	*Eco*RI
PolyA sequence	*Xba*I	*Xba*I	*Not*I, *Stu*I, and *Bsp*MI	*Spe*I
Entire expression cassette	*Sna*BI	*Sna*BI	*Avr*II	*Spe*I

GFP expression cassette, which allows for production of single stranded AAV vectors. In pscAAV-GFP, the right ITR contains a terminal resolution site mutation (Δ*trs*), which prevents Rep-mediated nicking and forces packaging of dimer or self-complementary genomes. Pay strict attention to the integrity of the vector ITRs in your plasmid preparations (see Note 1). The restriction enzyme combinations used to replace individual components of the expression cassette in these plasmids are outlined in Table 1. Modular expression cassette components: Table 2 provides a brief list of *cis*-acting vector sequence components that can be assembled into an AAV vector expression cassette.

2. PCR cloning kit, provided by commercial vendor (pGEM-T-Easy, Promega, Topo, Invitrogen, etc.).
3. Restriction endonucleases, high fidelity PCR enzymes and kits (Pfu Turbo, Stratagene, Santa Clara, CA or Phusion, NEB, Beverly, MA or the like), transformation competent *E. coli* (SURE strain, Stratagene), and standard molecular cloning equipment.
4. Sterile 50% glycerol, in water, for freezing *E. coli* stocks (use at a final glycerol concentration of 25%).

2.2. Construction of Transfer and Bacmid Plasmid Vectors

1. SURE *E. coli* electrocompetent cells (Stratagene).
2. Bac-to-Bac Baculovirus Expression System and pFastBacDual vector (Invitrogen, Carlsbad, CA). All reagents required for the construction of transfer and bacmid vector are listed in the kit.

Table 2
Useful sequence elements for constructing AAV vector expression cassettes

Name	Length	Accession	Sequence	Comments
CMV immediate early promoter/ enhancer	42	X03922	CCATTGCATACGTTGTATC CATATCATAATATG… CGGGACCGATCCAGCCTCC	Strong expression in a wide range of tissues. Enhancer portion (first 454 bp) can be used with heterologous promoters. Shorter versions remove up to 321 bp from 5′ end, and 47 bp from the 3′ end, but have not been directly compared with the full length form
Murine PGK promoter	513	M18735	AATTCTACCGGGTAGGGGAGGCG… CATCTCCGGGCCTTTCGACCT	Mild but consistent expression in a wide variety of cell types
Human EF1α promoter	1,169	HUMEF1a	CGTGAGGCTCCGGTGCCC… TTTTTCTTCCATTTCAG GTGTCGTGAA	Strong, consistent expression in a wide range of tissues. This fragment includes the first intron (positions 237–1,159), which enhances expression but is often removed to create a 'short' version
Human ApoE hepatic control region (HCR)	192	HSU32510	CCCTAAAATGGGCAAACATTGCA… GCGTGGTTTAGGTAG TGTGAGAGGG	Strong liver-specific enhancer. Used with human α-1-antitrypsin promoter in 'LP1′ liver specific promoter (38)
Human α-1-antitrypsin promoter	256	HUMA1ATP	AATGACTCCTTTCGGTAAG TGCAGTG…CACCACTGACCTGGG ACAGTGAATC	Liver-specific promoter. Used with ApoE HCR in 'LP1′ liver-specific promoter (38)
Rat Synapsin promoter	1,108	RATSYN1A	GGGTTTTGGCTACGTCCAGAGC… ACCGACCCACTGCCCCTTGT	Neuron-specific promoter (39, 40)
Human muscle creatine kinase enhancer (MCK)	206	AF188002	CCACTACGGGTCTAGGCTGCCC… AAAAATAACCCTGTCCCTGG TGGATC	Muscle-specific enhancer, used in combination with MCK promoter fragment (41)
Human MCK promoter	366	AF188002	CAATCAAGGCTGTGGGGGACTG… GGCTGCCCCCGGGTCAC	Muscle-specific promoter, used in combination with MCK enhancer (41)

RNaseP H1 fragment RNA polymerase III promoter	221	NC_00014.8 Range 20811229.. 20811569	GAATTCGAACGCTGACGTC ATCA… GGAATCTTATAAGTTCTGTATGAG ACCAC	Promoter used for the expression of short, hairpin RNAs for targeted knockdown of genes, as used in the pSUPER vectors (17). Insert hairpin followed by 'TTTTT' (for pol III termination) downstream of this sequence. For hairpin design algorithms, see http://www.ambion.com
Human β-globin intron, RsaI deleted	547	GQ370762	GATCCTGAGAACTTCAGGGTGAGT CTATGG…GGCCCATCACTTTGG CAAAGAATT	Large, but provides significantly enhanced expression in many cell types. RsaI digestion of native human genomic sequence removes an internal 374 bp fragment to generate this 547 bp element
SV40 intron	93	J02400	CTCTAAGGTAAATATAAAATTTTT AAGTGTATAATGTGTTAAACTAC TGATTCTAATTGTTTCTCTCTTTTAG ATTCCAACCTTTGGAACTGA	This very short sequence has been modified to enhance similarity to consensus splice site signals
Internal ribosome entry site (IRES) from ECMV	556	NC_001479	CCCCCCCCCTAACGTTACTGG… CGTGGTTTTCCTTTGAAAAACACGAT	Used for creating bicistronic vectors by placing this sequence between two coding sequences. For optimal translation of the downstream ORF, position ATG within 10 bp of the end of this sequence
Porcine teschovirus-1 2A peptide	57	AJ011380	GCCACGAACTTCTCTCTGTTAAA GCAAGCAGGAGACGTGGAAGAAA ACCCCGGTCCC	This sequence must be fused in frame between two open reading frames, with no intervening stop codons, to allow efficient cotranslation of two coding sequences (13)
SV40 late polyadenylation sequence	133	J02400	TGCTTTATTTGTGAAATTTGT GATGCTATTGCTTTATTTGTAAC CATTATAAGCTGCAATAAACAAGTT AACAACAACAATTGCAT TCATTTTATGTTTCAGGTTCAG GGGGAGGTGTGGGAGGTTTTTTAAA	Compact, relatively strong polyadenylation sequence

(continued)

Table 2 (continued)

Name	Length	Accession	Sequence	Comments
Bovine growth hormone polyadenylation sequence	225	M57764	CTGTGCCTTCTAGTTGCCAGCCA…GGGATGCGGTGGGCTCTATGG	Very strong polyadenylation sequence
Human β-globin polyadenylation sequence	760	GQ370762	AATTCACCCCACCAGTGCAGGC…TGCCTCCCCCACTCACAGTGAC	Very strong longer polyadenylation sequence
Human miR-30a primary microRNA sequence fragment	324	Human Chr. 6, 72113127-72113449	TGTTTGAATGAGGCTTCAGTACTT TACAGAA…CAAAGCTGAAT TAAAATGGTATAAATTAAATCACTTT	This primary miRNA transcript sequence is processed to generate the miR-30a microRNA. Substitution of nts 129–154 (left arm) and 170–193 (right arm) with your targeting sequence and its complement can lead to efficient loading of the inserted sequence into the RISC (18)

Each element in the table is provided with a GenBank accession number and sequence tags to uniquely identify the sequence that can be used, along with either the entire sequence for short segments, or the beginning and end sequence for longer sequences (>100 bp), separated by an ellipsis. The length of the beginning and end sequences of longer sequence entries were chosen such that oligonucleotide primers of the provided sequence and length will have a melting temperature of >60°C, to facilitate the design of PCR primers with enzyme sites chosen for compatibility with the above or other plasmid backbones

3. PCR primers: pUC/M13 forward or reverse primer (New England Biolabs, Beverly, MA) and a vector insert specific primer.
4. A real-time quantitative SYBRgreen PCR mixture (e.g., iQ SYBR Green Supermix, Bio-Rad, Hercules, CA), or RT² Real-Time™ SYBR Green PCR master mix (SuperArray Bioscience Corporation, Frederick, MD).

2.3. Generation of Primary BEV Stocks

1. Sf9 insect cells (Invitrogen).
2. Sf9 cell culture medium (e.g., Sf-900 II SFM (1×) liquid, Invitrogen).
3. Reagents suitable for transfection of insect cells. For example: cationic liposomes (Cellfectin – Invitrogen, ESCORT – Sigma-Aldrich, St. Louis, MO, *Tfx*™ – Promega, Madison, WI, FectoFly™ – Polyplus-Transfection Inc., New York, NY); polyethyleneimine/PEI (ExGen 500 – Fermentas, Glen Burnie, MD); or calcium phosphate (Baculovirus Expression Vector System – BD Biosciences, San Jose, CA). Any one of these reagents could be utilized to transfect cells with bacmid DNA following manufacturer's protocol.
4. Rep78/68-expressing BEV, such as Bac-Rep (27) or similar.
5. DNA Clean & Concentrator™-5 Kit (Zymo Research, Orange, CA).
6. Reagents for standard agarose gel electrophoresis.

2.4. Expansion, Validation, and Titration of Plaque Purified BEV Stocks

1. Sf9 insect cells (Invitrogen).
2. Sf9 cell culture medium (e.g., Sf-900 II SFM (1×) liquid, Invitrogen).
3. Alkaline PEG 200 solution, pH 13.5 (28).
4. PCR primers: Bac-F: 5′-CCGTAACGGACCTCGTACTT-3′; Bac-R: 5′-CCGTTGGGATTTGTGGTAAC-3′.
5. A real-time quantitative SYBRgreen PCR mixture (e.g., iQ SYBR Green Supermix, Bio-Rad), or RT² Real-Time™ SYBR Green PCR master mix (SuperArray Bioscience Corporation).

3. Methods

3.1. Construction of AAV Vector Plasmids Suitable for Transient Transfection of 293 Cells

1. Design the expression cassette and the assembly process. In the simplest form, this can be the ligation of your cDNA into one of the plasmids shown in Fig. 1. after removing GFP (e.g., with *Eco*RI and *Not*I digestion). However, by using a modular design strategy, it is straightforward to generate a small library of fragments that can be combined in multiple configurations

to create a series of vectors with alternative genes and regulatory elements. For considerations of AAV vector size constraints and clinical AAV vector backbones see Notes 2 and 3, respectively.

2. Using a high fidelity polymerase (such as *Pfu* Turbo, Stratagene or Phusion, New England Biolabs), PCR amplify the individual components using primers containing the necessary restriction enzyme sites and ligate them each into a PCR cloning plasmid (see Note 4). Alternatively, using the sequences provided in Table 2 and the referenced GenBank record, one can order the entire sequence to be commercially synthesized and provided cloned in a plasmid (see Note 5).
3. Fully sequence the component fragment plasmids. These plasmids should be saved and over time become part of a valuable library for future constructions (á la, the BioBricks™ model (29)).
4. Purify the fragments from parental plasmids after restriction digestion, ligate them together, and transform *E. coli* (see Note 1).
5. Screen small scale plasmid preparations for structural integrity.
   (a) After your small scale *E. coli* culture has grown overnight, save a small frozen glycerol stock of your cells prior to purifying the plasmid DNA from the remaining culture. Leaving bacterial cells at 4°C for extended periods increases the likelihood that the ITRs will be deleted (see Note 1).
   (b) In addition to whatever digestions are necessary to confirm proper assembly of the fragments in the ligation, always screen your plasmid preparations with an appropriate enzyme to monitor for ITR deletion, such as SmaI or SrfI (see Note 1).
6. Using the frozen cell stock for the individual clone that meets all screening criteria, prepare a large-scale plasmid preparation by re-streaking the frozen cells to obtain fresh, individual colonies and inoculating a single colony into a larger culture.
7. After the large-scale culture has grown to late log phase, and prior to lysing the cells for DNA purification, remove another aliquot of culture liquid to prepare several 0.5–1.0 ml glycerol aliquots for long-term storage. If the purified DNA from this culture proves to be significantly free of ITR-deleted plasmid, then all future plasmid preparations should be generated from this validated stock to reduce the risk of re-introducing ITR deletions.

3.2. Construction of Transfer and Bacmid Plasmid Vectors

1. First, modify Invitrogen's pFastBacDual plasmid by StuI and XhoI double digest, blunting with Klenow, and religation. This step deletes both *p10* and *polh* promoters, which are not

required for rAAV cassette rescue. The truncated polylinker contains 12 unique restriction sites that could be utilized to insert your recombinant AAV vector genomes.

2. Transfer each AAV vector genome into the plasmid created in Subheading 3.2 (step 1), including both ITRs flanking the expression cassette. Again, pay strict attention to the integrity of your ITRs (see Note 1).
3. Transform *E. coli* DH10BAC electrocompetent cells with the pFastBacDual-derived vector plasmid containing your AAV vector genome. Incubate plates at 37°C for at least 24 h followed by overnight incubation at RT. The extended time is required for colonies to grow and to develop light blue color. Clones containing recombinant transposed bacmids are white and usually slightly bigger in size. Pick 6–8 white colonies, expand in 2 ml LB cultures, and purify the bacmid DNA for further screening.
4. At this stage, candidate bacmids can be optionally screened by PCR to confirm the presence of the vector genome. Using one primer in the backbone (either pUC/M13 forward or reverse primers) and one primer in your vector cassette, PCR amplify each bacmid preparation to confirm successful introduction of the vector genome. Although the ITR inhibits the PCR and can lead to amplification of truncated products, it can still be a useful tool to exclude recombinants that do not contain a vector genome. The integrity of the AAV ITRs is screened at a later step by testing replicative fitness.

3.3. Generation of Primary BEV Stocks

1. Transfect Sf9 cells with bacmid DNA samples using any one of the reagents described in Subheading 2.2 (item 2) following manufacturer's protocol (see Note 6). The supernatant (4 ml from 60 mm cell culture dish) harvested at day 5 post-transfection contains BEV-rAAV stock, albeit at a lower titer of 10^7–10^8 pfu/ml. Multiple bacmids for each recombinant vector are typically transfected separately to allow screening of the resulting BEV for replicative fitness.
2. Each supernatant can at this point be screened for replicative fitness in an in vivo AAV genome replication assay. This allows the best stock of BEV to be used in the plaque purification, and can reduce the number of plaques that must be similarly screened.
   (a) To do this assay, add 0.5 ml of each supernatant to 60-mm dish with Sf9 cells plated at ~75% confluence. Knowing the precise titers and multiplicity of infection (MOI) is not important for this step as long as all BEV stocks derived from the individual transfected bacmid DNAs are treated the same way. To rescue rAAV cassette, co-infect cells with

Rep78/68-expressing BEV, such as Bac-Rep (27) or similar vector at MOI of 5.

(b) Forty-eight hour postinfection, isolate Hirt DNA according to the following procedure (modified from ref. 30). Harvest cells in the culture media from each of the dishes, transfer into 15-ml conical tubes and pellet by centrifugation at 1,000 × *g* for 5 min. Resuspend cell pellets in 1 ml PBS, transfer into Eppendorf tubes, centrifuge at 5,000 × *g* for 5 min, and discard the supernatants. Resuspend cell pellets in 250 µl 50 mM Tris–HCl, pH 7.5, 10 mM EDTA containing 100 µg/ml RNase A and lyse by the addition of 250 µl 1.2% SDS. Gently mix the suspension by inverting the tube several times and then incubate at RT for 5 min. Precipitate cellular debris and chromosomal DNA by the addition of 350 µl solution containing 3 M CsCl, 1 M potassium acetate and 0.67 M acetic acid. Immediately, gently mix the tubes and place them on ice for 15 min. After centrifugation for 15 min at 14,000 × *g*, load the supernatants onto a silica-based matrix spin column, such as those supplied with DNA Clean & Concentrator™-5 Kit (D4004, Zymo Research). Wash the column twice with the wash buffer (supplied in a kit) and elute the DNA in 20 µl H_2O. Utilizing spin columns greatly facilitates the DNA purification while reducing the sample-to-sample yield variability.

(c) Load half of the DNA sample (10 µl) onto 1.2% agarose TAE gel containing 10 µg/ml EtBr and separate the DNA during 1.5 h electrophoresis. The pattern of UV light-visualized bands should display a major band corresponding to rAAV-cassette double-stranded monomer, as well as several bands corresponding to higher order concatemers, a replication intermediate (Fig. 4). Comparing all DNA samples on the gel allows identifying one or two clones with higher yield of replicating AAV vector genomic DNA. These clones presumably contain BEV-rAAVs with higher content of intact ITRs.

3. Perform plaque purification using the best supernatant. Assuming that the starting titer of the original, bacmid-derived BEV-rAAV is 10^8 pfu/ml, use tenfold serial dilutions to derive a plate with no more than ten isolated plaques (see Note 7).

3.4. Expansion, Validation, and Titration of Plaque Purified BEV Stocks

1. Pick 3–4 well isolated plaques (called P0) and expand them by serial infection of naïve Sf9 cells. Optimally this is achieved by titrating each amplification supernatant so as to determine the quantity of supernatant necessary to achieve 0.1 MOI during

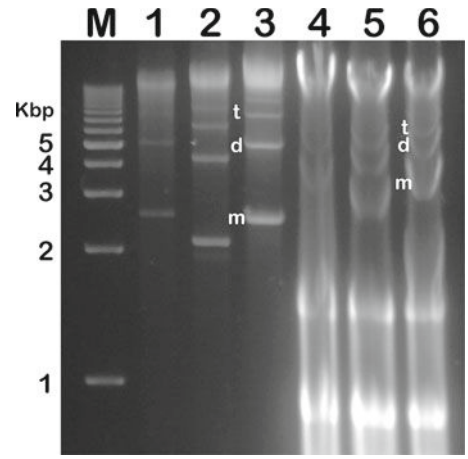

Fig. 4. Agarose gel analysis of replicating rAAV DNA isolated using modified Hirt procedure. *Lane M* contains 1-kbp DNA ladder. *Lanes 1* and *4*, *2* and *5*, *3* and *6* contain same rAAV expression cassettes but purified using modified Hirt protocol (*lanes 1–3*) or standard Hirt protocol (*lanes 4–6*). Letters "*m,*" "*d,*" and "*t*" indicate rAAV mono-, di-, and trimer replicating forms, respectively. Because of the excessive contaminating RNA and DNA in *lanes 4–6*, the mobility of rAAV forms is abnormally retarded. *Lanes 2* and *5* contain a smaller size self-complementary (sc) rAAV cassette.

each phase of expansion. As plaque assay is impractical at such steps, a quick quantitative PCR assay is described below. Alternatively, one can simply dilute each supernatant 1:100 into a naïve Sf9 culture for each amplification.

2. To perform a quick QPCR assay to estimate a relative plaque forming unit (pfu) titer, use this adaptation of an alkaline PEG-based method for direct PCR (28). Briefly, add 5 µl of baculovirus stock to 95 µl of alkaline PEG solution. After vortexing, incubate the sample at room temperature for 15 min and then dilute fivefold by adding 0.4 ml H_2O. Use 5 µl of this diluted mixture directly in QPCR 25 µl reaction mixture containing 12.5 µl SybrGreenER and 1.5 µl of 5 µM universal BEV Bac-F and Bac-R primers each (see Note 8).
3. Early in the amplification process (P1 or P2), perform an assay of the AAV vector genome replicative fitness, as described in Subheading 3.3 (step 2). Select the best replicator for the master seed virus stock for future expansions.
4. Propagate and expand the selected plaque purified clone by inoculating fresh Sf9 cells at an MOI of 0.1 (see Note 9). The large-scale production and purification of the insect cell-derived rAAV vectors are not covered in this chapter. Follow the detailed procedures described elsewhere (26, 31–36).

4. Notes

1. AAV vector plasmids are notorious for the instability and frequent deletion of the ITRs when propagated in *E. coli*. For this reason it is important to carefully confirm the integrity of every preparation used for vector construction. Even the best plasmid preparations contain significant quantities (5–15%) of DNA containing small deletions in the ITR, which during cloning procedures can be randomly selected and amplified. The ITRs have such strong secondary structure they cannot be sequenced with standard automated protocols, and so integrity of the ITRs is typically monitored by restriction enzyme analysis sufficient to identify small deletions (20 bp). Most commonly this is achieved with digestion with *Sma*I or *Srf*I, which cut twice within an unstable portion of the ITR, although an ideal strategy must also consider the ability of the resulting fragments to be separated and accurately sized on gels (Fig. 5). As long as this type of careful screening technique and optimal microbiological practice is maintained, then significant modifications to standard molecular cloning techniques are not absolutely necessary. Once a validated, frozen glycerol stock of *E. coli* is archived, subsequent preparations of plasmids from those stocks rarely contain high levels of deleted DNA, in

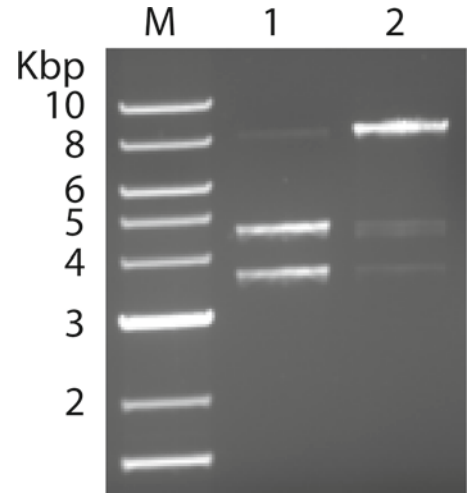

Fig. 5. Agarose gel analysis of SrfI digested AAV vector plasmid DNA. A complete digestion product would be expected to generate two bands for each plasmid, with sizes of 3.7 and 4.7 kbp. *Lane 1*, AAV vector plasmid preparation with minimal ITR deletion, cut with SrfI. Note that this successful preparation still appears as a partial digestion, with an 8.4 kbp, singly cut plasmid band visible at ~5% of total. *Lane 2*, an ITR deleted preparation with the proportions reversed, and ~5% of the DNA digested at both ITRs.

contrast to frequent deletions observed when screening fresh transformants. Because of these stability issues, most investigators utilize a recombination deficient strain, such as SURE for AAV vector plasmid propagation and cloning.

2. AAV vector genomes cannot significantly exceed 5 kb without dramatically reducing yield. For single-stranded vectors, the size of the resulting genome can easily be measured as the length of the sequence between and including the ITRs. For double stranded genomes, the Δ*trs* ITR becomes a central hairpin in the middle of a dimer genome, and so the total length of the vector in the plasmid, including the ITRs, should be less than 2.4 kbp.
3. For clinical applications, additional modifications to the vector backbone plasmid are desired. Substitution of kanamycin resistance for ampicillin allows preparation of the plasmid without allergenic β-lactam antibiotics. Additionally, the backbone sequences of plasmids can occasionally be incorporated into vector particles by virtue of their proximity to the AAV ITR. Insertion of large fragments of stuffer DNA into the backbone can reduce this phenomenon (37).
4. In many cases PCR products can be ligated directly to plasmid backbone fragments after digestion with restriction enzymes; however, the efficiency is significantly reduced, often precluding successful assembly of more than two fragments at a time. Preliminary subcloning and sequencing is slower, but provides an easily archived reagent and allows for the most efficient ligation reaction.
5. The advent of lower cost gene synthesis services provides yet another avenue from PCR for getting your gene of interest into a vector. This also has the advantage of allowing the modification of coding sequences to "optimize" expression or other properties for the particular application you are interested in. The instability and strong secondary structure of AAV ITRs makes direct synthesis of whole vectors by this method much more challenging, and for that reason most investigators, even if they are synthesizing the gene and or regulatory elements, will subsequently ligate those elements into a plasmid backbone for large-scale DNA propagation necessary for vector production.
6. The efficiency of Sf9 cell transfection can be assessed using a plasmid with GFP reporter gene driven by baculovirus promoter, such as immediate early OpIE2 in pIZ/V5-His vector (Invitrogen). This reporter has to be constructed in advance using conventional cloning techniques. Late promoters, such as *polh* or *p10* in pFastBacDual cloning vector are not functional in Sf9 cells even if cells are infected with baculovirus.

These late promoters require *cis*-acting viral enhancer elements (homologous region, *hr*) to be fully activated.

7. For a plaque assay, it is important to plate Sf9 cells at no higher than 40–50% confluence at the time of infection. At higher densities, plaques are smaller in size, harder to visualize, and yield fewer viruses. The other important consideration is the quality of the BEV-rAAV. To improve the virus stability during propagation, it is critical to infect cells at low MOI of about 0.1. Most of the virus harvested in a plaque derives from the second round infection around the cell infected at time zero. At high initial seeding density cells grow confluent by the time of secondary infection and, thus, only few nearby cells are infected at significantly higher than optimal MOIs. This results in smaller plaques, lower yields, and higher ratios of re-arranged, ITR-less progeny virus, which, by the fourth passage, becomes the prevalent species.
8. The BEV sample is assayed side by side with a serially diluted reference standard, a BEV of a known titer. Universal BEV primers sequences are the following: Bac-F: 5′-CCGTAAC GGACCTCGTACTT-3′; Bac-R: 5′-CCGTTGGGATTTGTGG TAAC-3′. The amplified sequence is part of AcMNPV gene *Ac-IE-01*, locus tag – *ACNVgp142*, a putative early gene trans-activator; the size of the amplified DNA fragment is 103 bp. The sensitivity of RT PCT titering method is as low as 10^5 pfu/ml. One can use either universal BEV primers or transgene-specific primers. When using the latter, a shuttle plasmid with the cloned transgene is utilized to generate a serially diluted reference standard. Prior to PCR analysis, plasmid DNA should be linearized by a single-cutter restriction enzyme, phenol/chloroform purified, and stored at 1 μg/μl frozen. Serial dilution DNA standards are prepared at the time of the RT PCR experiment, preferentially after handling experimental samples. Titers derived by this method are identical to the titers obtained using standard plaque assay.
9. Using the Baculovirus system, one should expect to produce at least 10^{14} drp rAAV from 1 L Sf9 cells culture. This would require about 50 ml of BEV helper stock of a relatively low titer of 2×10^8 pfu/ml. If BEV harvested from the plaque designated as “passage zero” (P0), then propagating BEV exponentially to passage two (P2) will generate as much as 4–5 L of the BEV stock. BEV helpers were shown to be stable up to P5, thus generating sufficient amount of BEV does not constitute a serious technical challenge. Titration of viral stocks harvested at P1 through P3 is recommended to propagate the vector at the known MOI of 0.1. Once the BEV stock is produced, it could be stored for extended periods of time (up to a year) at 4°C. Adding FBS to 1% increases long-term stability

of the stored stock. Over time, the infectious titer of the stock is reduced necessitating re-titration assays. Because titers drop due to viral particle aggregation, the RT PCR assay described above might not be appropriate due to potential overestimation of the infectious titer. Instead, a regular plaque assay, although more laborious, will generate the up-to-date infectious titer information.

References

1. Goyenvalle, A., Vulin, A., Fougerousse, F., Leturcq, F., Kaplan, J. C., Garcia, L., and Danos, O. (2004) Rescue of dystrophic muscle through U7 snRNA-mediated exon skipping, *Science* ***306***, 1796–1799.
2. Bertrand, E., Castanotto, D., Zhou, C., Carbonnelle, C., Lee, N. S., Good, P., Chatterjee, S., Grange, T., Pictet, R., Kohn, D., Engelke, D., and Rossi, J. J. (1997) The expression cassette determines the functional activity of ribozymes in mammalian cells by controlling their intracellular localization, *RNA* ***3***, 75–88.
3. Goverdhana, S., Puntel, M., Xiong, W., Zirger, J. M., Barcia, C., Curtin, J. F., Soffer, E. B., Mondkar, S., King, G. D., Hu, J., Sciascia, S. A., Candolfi, M., Greengold, D. S., Lowenstein, P. R., and Castro, M. G. (2005) Regulatable gene expression systems for gene therapy applications: Progress and future challenges, *Mol. Ther.* ***12***, 189–211.
4. Akimitsu, N. (2008) Messenger RNA Surveillance Systems Monitoring Proper Translation Termination, *J. Biochem. (Tokyo)* ***143***, 1–8.
5. Kozak, M. (1986) Point mutations define a sequence flanking the AUG initiator codon that modulates translation by eukaryotic ribosomes, *Cell* ***44***, 283–292.
6. Hershberg, R., and Petrov, D. A. (2008) Selection on Codon Bias, *Annu. Rev. Genet.* ***42***, 287–299.
7. Sorensen, M. A., Kurland, C. G., and Pedersen, S. (1989) Codon usage determines translation rate in Escherichia-coli, *J. Mol. Biol.* ***207***, 365–377.
8. Thanaraj, T. A., and Argos, P. (1996) Ribosome-mediated translational pause and protein domain organization, *Protein Sci.* ***5***, 1594–1612.
9. Purvis, I. J., Bettany, A. J. E., Santiago, T. C., Coggins, J. R., Duncan, K., Eason, R., and Brown, A. J. P. (1987) The efficiency of folding of some proteins is increased by controlled rates of translation in vivo. A hypothesis, *J. Mol. Biol.* ***193***, 413–417.
10. Miao, C. H., Ohashi, K., Patijn, G. A., Meuse, L., Ye, X., Thompson, A. R., and Kay, M. A. (2000) Inclusion of the hepatic locus control region, an intron, and untranslated region increases and stabilizes hepatic factor IX gene expression in vivo but not in vitro, *Mol.Ther.* ***1***, 522–532.
11. Qiao, C., Wang, B., Zhu, X., Li, J., and Xiao, X. (2002) A novel gene expression control system and its use in stable, high-titer 293 cell-based adeno-associated virus packaging cell lines, *J. Virol.* ***76***, 13015–13027.
12. Chao, H. J., Sun, L. W., Bruce, A., Xiao, X., and Walsh, C. E. (2002) Expression of human factor VIII by splicing between dimerized AAV vectors, *Mol. Ther.* ***5***, 716–722.
13. Szymczak, A. L., Workman, C. J., Wang, Y., Vignali, K. M., Dilioglou, S., Vanin, E. F., and Vignali, D. A. (2004) Correction of multi-gene deficiency in vivo using a single 'self-cleaving' 2A peptide-based retroviral vector, *Nat. Biotechnol.* ***22***, 589–594.
14. Bartel, D. P. (2009) MicroRNAs: Target Recognition and Regulatory Functions, *Cell* ***136***, 215–233.
15. Murray, E. L., and Schoenberg, D. R. (2007) A plus U-rich instability elements differentially activate 5 –3 and 3 –5 mRNA decay, *Mol. Cell. Biol.* ***27***, 2791–2799.
16. Brown, B. D., Venneri, M. A., Zingale, A., Sergi, L. S., and Naldini, L. (2006) Endogenous microRNA regulation suppresses transgene expression in hematopoietic lineages and enables stable gene transfer, *Nat. Med.* ***12***, 585–591.
17. Brummelkamp, T. R., Bernards, R., and Agami, R. (2002) A system for stable expression of short interfering RNAs in mammalian cells, *Science* ***296***, 550–553.
18. Silva, J. M., Li, M. Z., Chang, K., Ge, W., Golding, M. C., Rickles, R. J., Siolas, D., Hu, G., Paddison, P. J., Schlabach, M. R., Sheth, N., Bradshaw, J., Burchard, J., Kulkarni, A., Cavet, G., Sachidanandam, R., McCombie, W. R., Cleary, M. A., Elledge, S. J., and Hannon, G. J.

(2005) Second-generation shRNA libraries covering the mouse and human genomes, *Nat. Genet. **37***, 1281–1288.

19. Stegmeier, F., Hu, G., Rickles, R. J., Hannon, G. J., and Elledge, S. J. (2005) A lentiviral microRNA-based system for single-copy polymerase II-regulated RNA interference in mammalian cells, *Proc. Natl. Acad. Sci. U.S.A. **102***, 13212–13217.
20. Boudreau, R. L., Monteys, A. M., and Davidson, B. L. (2008) Minimizing variables among hairpin-based RNAi vectors reveals the potency of shRNAs, *Rna-a Publication of the Rna Society **14***, 1834–1844.
21. Boudreau, R. L., Martins, I., and Davidson, B. L. (2009) Artificial MicroRNAs as siRNA Shuttles: Improved Safety as Compared to shRNAs In vitro and In vivo, *Mol. Ther. **17***, 169–175.
22. Liu, Y. P., Haasnoot, J., ter Brake, O., Berkhout, B., and Konstantinova, P. (2008) Inhibition of HIV-1 by multiple siRNAs expressed from a single microRNA polycistron, *Nucleic Acids Res. **36***, 2811–2824.
23. Xiao, X., Li, J., and Samulski, R. J. (1998) Production of high-titer recombinant adeno-associated virus vectors in the absence of helper adenovirus, *The Journal of Virology 72*, 2224–2232.
24. Aslanidi, G., Lamb, K., and Zolotukhin, S. (2009) An inducible system for highly efficient production of recombinant adeno-associated virus (rAAV) vectors in insect Sf9 cells, *Proc. Natl. Acad. Sci. U.S.A. **106***, 5059–5064.
25. Chen, H. (2008) Intron splicing-mediated expression of AAV Rep and Cap genes and production of AAV vectors in insect cells, *Mol. Ther. **16***, 924–930.
26. Smith, R. H., Levy, J. R., and Kotin, R. M. (2009) A Simplified Baculovirus-AAV Expression Vector System Coupled With One-step Affinity Purification Yields High-titer rAAV Stocks From Insect Cells, *Mol. Ther. **17***, 1888–96.
27. Urabe, M., Ding, C., and Kotin, R. M. (2002) Insect cells as a factory to produce adeno-associated virus type 2 vectors, *Hum. Gene Ther. **13***, 1935–1943.
28. Chomczynski, P., and Rymaszewski, M. (2006) Alkaline polyethylene glycol-based method for direct PCR from bacteria, eukaryotic tissue samples, and whole blood, *Biotechniques **40***, 454, 456, 458.
29. Shetty, R. P., Endy, D., and Knight, T. F., Jr. (2008) Engineering BioBrick vectors from BioBrick parts, *J. Biol. Eng. 2*, 5.
30. Arad, U. (1998) Modified Hirt procedure for rapid purification of extrachromosomal DNA from mammalian cells, *Biotechniques **24***, 760–762.
31. Cecchini, S., Negrete, A., and Kotin, R. M. (2008) Toward exascale production of recombinant adeno-associated virus for gene transfer applications, *Gene Ther. **15***, 823–830.
32. Negrete, A., and Kotin, R. M. (2007) Production of recombinant adeno-associated vectors using two bioreactor configurations at different scales, *J. Virol. Methods **145***, 155–161.
33. Negrete, A., and Kotin, R. M. (2008) Large-scale production of recombinant adeno-associated viral vectors, *Methods Mol. Biol. **433***, 79–96.
34. Negrete, A., and Kotin, R. M. (2008) Strategies for manufacturing recombinant adeno-associated virus vectors for gene therapy applications exploiting baculovirus technology, *Brief. Funct. Genomic. Proteomic. 7*, 303–311.
35. Negrete, A., Yang, L. C., Mendez, A. F., Levy, J. R., and Kotin, R. M. (2007) Economized large-scale production of high yield of rAAV for gene therapy applications exploiting baculovirus expression system, *J. Gene Med. **9***, 938–948.
36. Aucoin, M. G., Perrier, M., and Kamen, A. A. (2008) Critical assessment of current adeno-associated viral vector production and quantification methods, *Biotechnol Adv **26***, 73–88.
37. Cao, L., Liu, Y. H., During, M. J., and Xiao, W. D. (2000) High-titer, wild-type free recombinant adeno-associated virus vector production using intron-containing helper plasmids, *J. Virol. **74***, 11456–11463.
38. Nathwani, A. C., Gray, J. T., Ng, C. Y., Zhou, J., Spence, Y., Waddington, S. N., Tuddenham, E. G., Kemball-Cook, G., McIntosh, J., Boon-Spijker, M., Mertens, K., and Davidoff, A. M. (2006) Self-complementary adeno-associated virus vectors containing a novel liver-specific human factor IX expression cassette enable highly efficient transduction of murine and nonhuman primate liver, *Blood. **107***, 2653–2661.
39. Hoesche, C., Sauerwald, A., Veh, R. W., Krippl, B., and Kilimann, M. W. (1993) The 5′-flanking region of the rat synapsin-I gene directs neuron-specific and developmentally-regulated reporter gene-expression in transgenic mice, *J. Biol. Chem. **268***, 26494–26502.
40. Thiel, G., Greengard, P., and Sudhof, T. C. (1991) Characterization of tissue-specific transcription by the human synapsin-I gene promoter, *Proc. Natl. Acad. Sci. U.S.A. **88***, 3431–3435.
41. Shield, M. A., Haugen, H. S., Clegg, C. H., and Hauschka, S. D. (1996) E-box sites and a proximal regulatory region of the muscle creatine kinase gene differentially regulate expression in diverse skeletal muscles and cardiac muscle of transgenic mice, *Mol. Cell. Biol. **16***, 5058–5068.

Chapter 3

AAV Capsid Structure and Cell Interactions

Mavis Agbandje-McKenna and Jürgen Kleinschmidt

Abstract

The Adeno-associated viruses (AAVs) are not associated with any diseases, and their ability to package non-genomic DNA and to transduce different cell/tissue populations has generated significant interest in understanding their basic biology in efforts to improve their utilization for corrective gene delivery. This includes their capsid structure, cellular tropism and interactions for entry, uncoating, replication, DNA packaging, capsid assembly, and antibody neutralization. The human and nonhuman primate AAVs are clustered into serologically distinct genetic clade and serotype groups, which have distinct cellular/tissue tropisms and transduction efficiencies. These properties are highly dependent upon the AAV capsid amino acid sequence, their capsid structure, and their interactions with host cell factors, including cell surface receptors, co-receptors, signaling molecules, proteins involved in host DNA replication, and host-derived antibodies. This chapter reviews the current structural information on AAV capsids and the capsid viral protein regions playing a role in the cellular interactions conferring an infective phenotype, which are then used to annotate the functional regions of the capsid. Based on the current data, the indication is that the AAVs, like other members of the *Parvoviridae* and other ssDNA viruses that form a $T=1$ capsid, have evolved a multifunctional capsid with conserved core regions as is required for efficient capsid trafficking, capsid assembly, and genome packaging. Disparate surface loop structures confer differential receptor recognition and are involved in antibody recognition. The role of structural regions in capsid uncoating remains to be elucidated.

Key words: AAV capsid structure, Glycan receptor recognition, Internalization, Endosomal trafficking, Uncoating, Genome replication, Capsid assembly, Antibody response

1. Introduction

Twelve distinct human and nonhuman primate AAV serotypes (AAV1–12) have been sequenced to date, and numerous recombinant AAVs have been identified in primate and human tissues through PCR studies (1–5). These viruses are classified into eight genetic groups, clades A–F and clonal isolates AAV4 and AAV5, based on

Richard O. Snyder and Philippe Moullier (eds.), *Adeno-Associated Virus: Methods and Protocols*,
Methods in Molecular Biology, vol. 807, DOI 10.1007/978-1-61779-370-7_3, © Springer Science+Business Media, LLC 2011

antigenic reactivity and sequence comparisons (1). The representative members of these groups are AAV1–AAV9, with AAV1 and AAV6 belonging to the same clade A because of their high sequence similarity and antigenic cross-reactivity (1). The representative members share ~60–99% sequence identity, with AAV4 and AAV5 being the most different from each other and from the other members (1).

The 4.7-kb single-stranded (ss) DNA AAV viral genome has two open reading frames (ORF), *rep* and *cap*. The *rep* ORF codes for four overlapping proteins required for replication and DNA packaging. The *cap* ORF encodes three capsid viral proteins (VPs) from two alternately spliced mRNAs. One of these mRNAs contains the entire *cap* ORF and encodes VP1. The other mRNA encodes for VP2, from an alternate start codon (ACG), and VP3 from a conventional downstream ATG. AAV capsids are assembled as a $T=1$ icosahedral particle (~260 Å in diameter) from a total of 60 copies of VP1, VP2, and VP3, in a predicted ratio of 1:1:8/10 (6). VP3 is a 61-kDa protein that constitutes 90% of the capsid's protein content. The less abundant capsid proteins, VP1 (87 kDa) and VP2 (73 kDa), share the same C terminal amino acid (aa) sequence with VP3 but have additional N terminal sequences. The only essential cis active sequences in AAV genomes are the 145-bp terminal repeats (ITRs), which function as origins for DNA replication, packaging sequences, and integration sites (7–10). Recombinant AAV vectors (rAAV) to be used for gene corrective gene delivery applications are generated by retaining the ITRs and replacing the internal wild type (wt) AAV coding sequences with therapeutic genes (7, 11, 12).

1.1. AAV Life Cycle, the Need for a Multifunctional Capsid VP

As is the case for other DNA packaging viruses, the parvovirus capsid, with its packaged ssDNA genome, has to traverse two cellular barriers during infection, the plasma and nuclear membranes, for replication in the cell nucleus. The parvovirus VPs that assemble the capsid are capable of performing the wide variety of structural and biological functions required during the viral life cycle. In addition, the capsid is a metastable entity, being capable of structural transitions to deploy essential functions for navigating the cell to and from the nucleus, while apparently keeping its infectious genome protected.

The initial capsid VP functions include host cell surface receptor recognition, endosomal entry and trafficking, cytoplasmic processing, and nuclear entry. Once inside the nucleus, uncoating to release the packaged genome occurs, followed by genome replication, message transcription and protein translation, nuclear import of VPs for assembly into capsids, viral genomic encapsidation, and nuclear export. Furthermore, the capsid is the target of both T-cell and B-cell host-mediated immune responses as discussed in Chapter 11. In addition, pseudotyping studies in which

the AAV2 ITRs are used as packaging signals for encapsidation of the same transgene into rAAVs of different serotypes have shown that transduction efficiencies in different tissues are dictated by the capsid sequence (e.g. (1, 13–17)) as discussed in Chapter 4. Thus identifying the aa sequences enabling the VP functions has been an important aspect of studies aimed at understanding the basic biology of the AAVs.

The relatively small ssDNA genome size for the parvoviruses has allowed the use of genetic manipulation to identify functional aas/regions of the VPs/capsid. For the AAVs these studies show that the viruses have evolved to utilize the unique N-terminal region of VP1 (VP1u) for a phospholipase A_2 (PLA_2) function required for endosomal escape during infection, N-terminal aas common to VP1 and VP2 for nuclear entry, and aa stretches within the common VP region for receptor attachment, tropism and transduction efficiency, capsid assembly, DNA packaging, and host antibody recognition. AAV2 is the best genetically characterized AAV serotype. The role and aas/regions of the AAV2 capsid VPs and assembled capsid involved in the cellular interactions that dictated successful infection will be discussed following a review of the structural information available for the various AAV serotypes.

1.2. AAV Capsid Structure

Towards correlating the VP/capsid function of the AAVs during cellular infection with structural features, effort has been extended to determine the structure of the representative members of the AAV antigenic clade and clonal isolate groups using X-ray crystallography and/or cryo-electron microscopy (cryo-EM) and image reconstruction. Preliminary characterization of crystals or structure determinations have been reported for AAV1–AAV9 ((18–36) and unpublished data). In the structures determined, only the C-terminal overlapping VP aa residues (~520 aas) have been observed (Fig. 1). This is also the case for all other parvovirus structures determined to date (6). For example, in the crystal structures of AAV2, AAV4, and AAV8 aa residues 217–735, 216–734, and 220–737 (VP1 numbering as will be used throughout this chapter) are ordered, respectively. The unique VP1 N-terminal region (VP1u) (138 aas), the N-terminal aas of VP2 that overlaps with VP1 (65 aas), and the first ~15 residues of VP3, have been disordered (24–26, 30, 31, 34). These "disordered" N-terminal sequences are reported to be located inside the capsid (33, 37) consistent with the location of the first N-terminal residue observed in crystal structures (24–26). Interestingly, cryo-EM studies of empty AAV2 capsids identified density "globules" located inside the capsid at the icosahedral twofold axis that have been interpreted as the N-terminal regions of VP1 and VP2 (33). These globules were absent in reconstructions of empty capsids in which VP1, VP2 or VP1and VP2 were deleted ((33), unpublished data). They were also not detected in fractions that contained only full

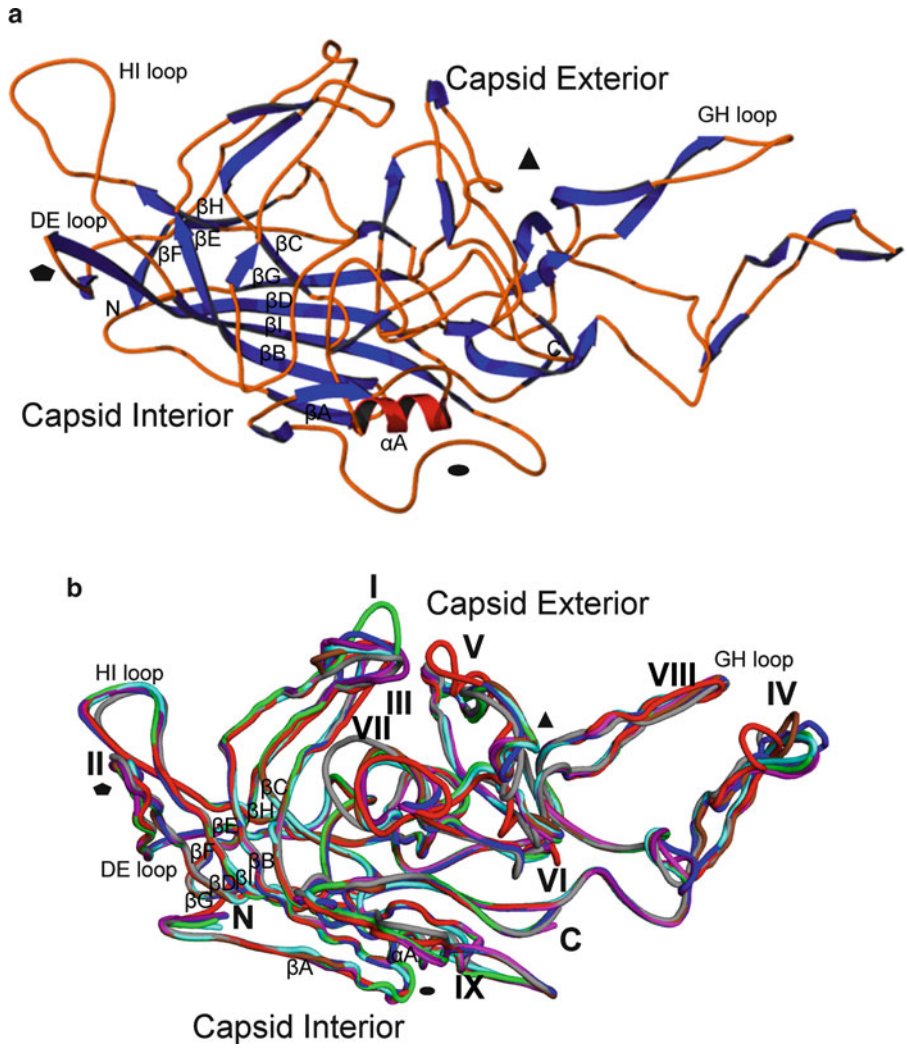

Fig. 1. The AAV VP structure. (**a**) Ribbon diagram of the AAV2 VP3 (PDB ID # 1LP3) showing β-strands (*in blue*), the conserved αA (*in red*), and the loops connecting the strands (*in orange*). The strands of the core eight-stranded β-barrel are labeled along with βA, the DE loop (between β-strands βD and βE), the HI loop (between β-strands βH and βI), and the GH loop (between β-strands βG and βH). The N- and C-termini of the ordered overlapping VP3 region are labeled. The approximate icosahedral two-, three-, and fivefold axes are depicted by the *filled oval*, *triangle*, and *pentagon*, respectively. The capsid interior and exterior are also indicated. (**b**) Superimposition of the crystal structures of AAV1 (*magenta*), AAV2 (*blue*), AAV4 (*red*), AAV5 (*gray*), AAV6 (*pink*), AAV7 (*cyan*), AAV8 (*green*), and AAV9 (*brown*). Common variable regions (labeled I-IX), the N- and C-termini, and the interior and exterior capsid regions are labeled. The approximate icosahedral two-, three-, and fivefold axes are depicted by the *filled oval*, *triangle*, and *pentagon*, respectively.

capsids and in AAV1 empty capsids (38). The lack of N-terminal VP sequence ordering in the high-resolution structures is likely due to the low copy numbers of VP1 and VP2 in the capsids (mentioned above) and to the possibility that the N-termini of VP1, VP2, and VP3 adopt different conformations inside the capsid, which is incompatible with the icosahedral symmetry assumed during structure determination.

The topology of the structurally ordered common VP region (hereafter referred to as VP3 since this protein is the most abundant in the capsid) is highly conserved between the AAV serotypes and among members of other parvovirus genera, even for members that are only ~20% or less identical at the aa sequence level, such as AAV2 and B19 (39). It consists of a core eight-stranded (βB-βI, named from the N to the C-terminus of the VP3 structure) antiparallel β-barrel motif that forms the contiguous capsid shell and an α-helix (αA), which are conserved in all parvovirus structures determined to date (Fig. 1a) (6). There is an additional β-strand, βA, at the N-terminal region of the VP3, which forms antiparallel interactions with βB and is also conserved in all the AAV and parvovirus structures (Fig. 1a). Loop insertions between the β-barrel strands, which also contain small stretches of β-strand structure, form the majority (~70%) of the VP3 topology (Fig. 1a). The loops are named for the strands they connect; for example, the DE loop is located between β-strands βD and βE. The largest of the connecting loops is the GH loop between βG and βH and contains ~230 aas and encompasses variable regions (VR) IV to VIII (Fig. 1b), while the smallest, the FG loop, is only 2–3 aas in length.

The 60 copies of the VP monomers assemble the $T=1$ icosahedral capsid via two-, three-, and fivefold symmetry-related interactions (Fig. 2a–c). These interactions create the characteristic features of the AAV capsids, depressions at the twofold axes, protrusions surrounding a depression at the threefold axes, and cylindrical channels at the fivefold axes surrounded by a depression (Fig. 2d–f). A conserved loop at the C-termini of the VP (e.g. residues 696–704 in AAV2), located after βI, invade neighboring VP monomers to form the majority of the icosahedral twofold symmetry-related interactions and is located between this depression and that surrounding the icosahedral fivefold axis (Fig. 2a). The conserved αA helix is also involved in the twofold interactions and forms the wall of the depression (Fig. 2a). The twofold interactions are the least extensive between the VP monomers, being only one polypeptide chain thick, making this capsid region the thinnest with the smallest buried surface area of the three interacting symmetry interfaces (24). The interactions between icosahedral threefold related VP monomers are the most extensive and involve aa residues in the BC, EF, and GH loops (Fig. 2b). The GH loops interdigitate to form the spike-like protrusions offset from the icosahedral threefold axes (Fig. 2d–f). The HI loop forms most of the interactions between icosahedral fivefold symmetry-related VP3 monomers (Fig. 2c). The loop is positioned above the β-strands of adjacent VP3 monomers and forms the floor of the conserved depression that surrounds the channel at the axis (Fig. 2c). The remaining fivefold interactions are formed by regions of the βBIDG sheet and ordered N-terminal residues in adjacent monomers. The cylindrical

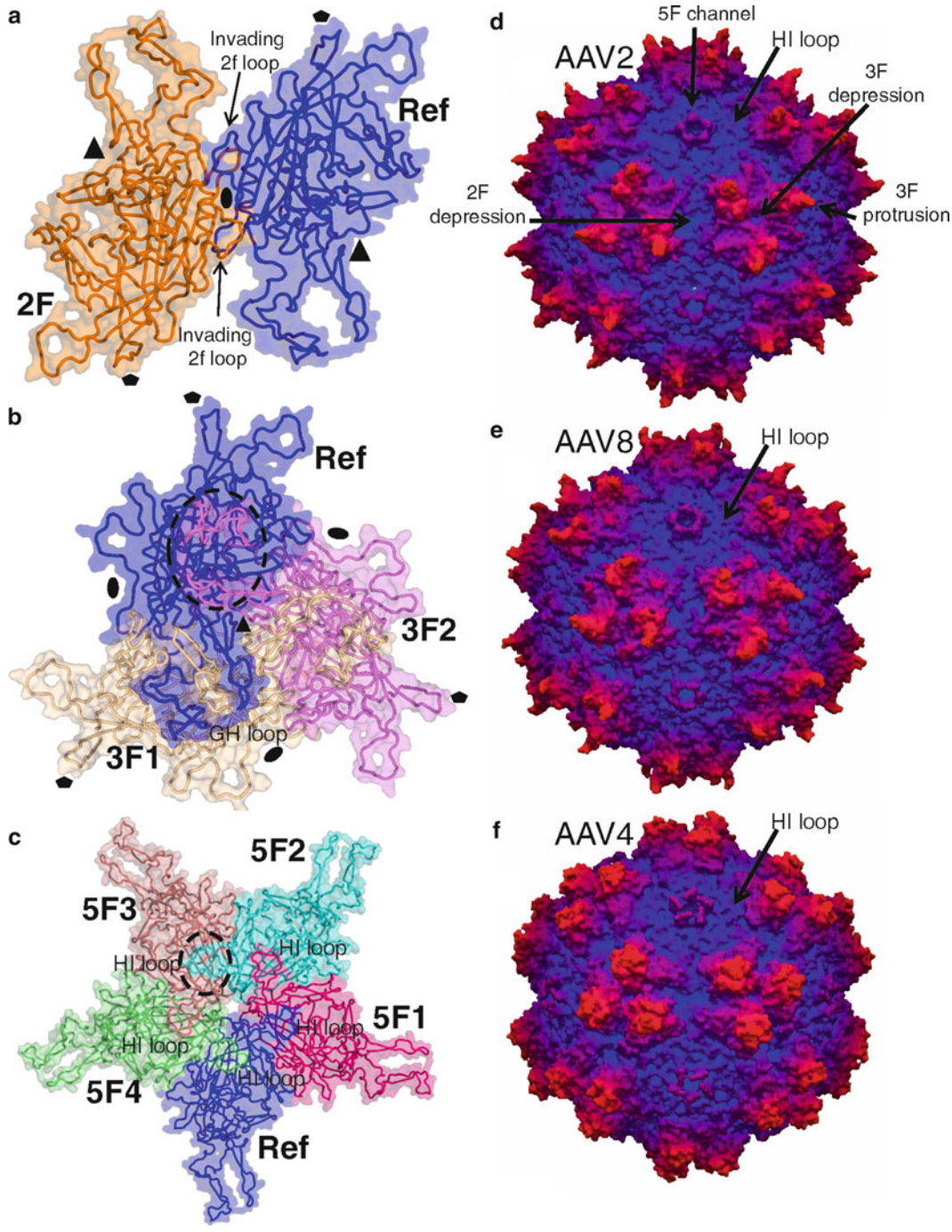

Fig. 2. The AAV capsid structure. (**a**–**c**) Coil diagrams of AAV2 VP3s in a transparent surface rendering showing icosahedral symmetry-related two-, three-, and fivefold interactions, respectively. The reference (*Ref in blue*), twofold (2F *in orange*), threefold (3F1 and 3F2 in *magenta and wheat*) and fivefold (5F1 to 5F4 *in red*, *cyan*, *brown*, and *green*) related monomers are labeled. In (**a**) the loops, which invade the symmetry-related monomer at the twofold axis are labeled. In (**b**) the interdigitation of the Ref and a threefold (3F2) symmetry-related monomer forming one of the three protrusions, which surround the threefold axis is highlighted by a *dashed circle*. In (**c**) the loop between βH and βI that invades neighboring fivefold symmetry-related monomer is highlighted by a *dashed circle* (for 5F2 on top of the 5F3 monomer) and is labeled on all five monomers.

channel at the fivefold axis is formed by the DE loop, which is a β-ribbon that creates a surface turret (Figs. 1a, b and 2c–f). This channel connects the inside and outside of the capsid. As noted above, the first structurally ordered N-terminal residue observed for the AAVs (as is also the case for other parvoviruses) is located inside the capsid at the base of this channel, consistent with suggestions that this is the site for externalization of N-terminal sequences for the PLA2 and NLS function for VP1. Exposure of the phospholipase activity on the capsid surface is required for parvovirus infectivity as discussed below (37, 40–46).

Comparison of the atomic models for the available AAV structures ((24–26) and unpublished data) shows that the core β-barrel motif (βB-βI labeled in Fig. 1a) and αA (shown in red in the ribbon diagram in Fig. 1a) are highly conserved (Fig. 1b), as has been observed for the autonomous parvovirus capsids (reviewed in refs. 6, 47). The N-terminal residues, βA strand, and βBIDG sheet form the interior surface of the capsid, while the loops inserted between the β-strands form the capsid surface (Fig. 1a, b) (48). These loops are variable in conformation between the AAVs (Fig. 1b) as has been observed for the autonomous parvovirus capsids (reviewed in ref. 47). The AAV surface loop differences were designated I–IX based on the comparison of AAV2 and AAV4; the two most structurally different serotypes (compare the blue and red coil structures in Fig. 1b) (24). The observed structural difference between these two serotypes is consistent with their sequence divergence (~65% sequence identity) (1). The variable surface loops are formed by the differing amino acids. AAV2 and AAV8, which share a high sequence identity (83%) between them, differ in just three of these variable regions, I, II, and IV (25). The AAV variable loops become clustered, from icosahedral symmetry-related monomers, to form the "wall" between the depressions surrounding the icosahedral two- and fivefold axes, the "shoulder" and top of the three protrusions that surround the threefold axes, and the top of the channel at the fivefold axes. The clustered loops create the differences in surface topology observed between the AAV capsids (examples for AAV2, AAV4 and AAV8 shown in Fig. 2d–f). Variable regions I, III, VII, and IX are located between the depressions surrounding the two- and fivefold axes and results in differences in the thickness and width of this wall between these two axes in the example viruses shown in Fig. 2d–f. AAV4's rounder protrusions surrounding the

Fig. 2. (continued) (**d–f**) Depth-cued surface representation of the AAV2, AAV8, and AAV4 capsid crystal structures, respectively, viewed down the icosahedral twofold axis. The regions of the capsid surface at the lowest radial distance from the capsid center are *in blue*; those at the furthest distance are *in red*. The approximate positions of a twofold (2F) depression, threefold (3F) protrusion and depression, a fivefold (5F) channel and an HI loop on the floor of the depression surrounding the 5F axis is indicated in (**d**). An HI loop position is also indicated in (**e**) and (**f**). The approximate icosahedral two, three, and fivefold axes are depicted as in Fig. 1.

threefold axis compared to the more pointed structures in AAV2 and AAV8 is due to conformational differences in variable regions IV, V, VI, and VIII (Fig. 2d, f). The differences at variable regions IV, V, and VI are more pronounced in AAV4 compared to the other serotype structures determined to date (red coil in Fig. 1b). The difference at variable region II (top of the DE loop) creates the structural difference at the top of the cylindrical channel observed in AAV2 and AAV4 (Fig. 2d, f, respectively).

The available capsid structures for AAV serotypes AAV1–AAV9 can be divided into two general topologies with respect to the protrusions that surround the icosahedral threefold axes. AAV1–AAV3b, AAV6–AAV8 have pointed "finger-like" protrusions, while AAV4, AAV5, and AAV9 have "rounder" protrusions surrounding the icosahedral threefold axis of symmetry (examples for AAV2, AAV4, and AAV8 shown in Fig. 2d–f). Sequence alignments and 3D homologous model building (data not shown) suggest that AAV3, AAV10, and AAV12 will fall into the first structural class, while AAV11 will be more like the structures with the rounder protrusions. Interestingly, sequence alignments predicted that AAV9 should fall into the first structural class although its surface topology was more similar to the structures in the second class. Significantly, surface topologies alone do not determine the receptor binding or transduction phenotypes for the AAVs, since viruses within each structure class appear to require specific recognition of different surface receptors for transduction and they have different transduction efficiencies in the same tissues (1). Thus the aa sequence composition and structural topology of these surface loops must encode several important functions, including tissue tropism (including receptor recognition for internalization and cellular trafficking), transduction efficiency, and the antigenic responses directed against the capsid (Table 1).

1.3. AAV Cell Binding and Entry

Like most other viruses, attachment to a cell surface receptor is an essential first step of parvovirus infection. Conventionally, it is believed that after binding to a primary receptor, interaction with a co-receptor leads to virus internalization of AAV via endocytosis. A list of receptors that have been proposed to be used by the AAVs for cell entry is shown in Table 2.

1.3.1. Recognition–Glycan Receptor Interaction

Cell transduction phenotypes for members of the AAVs have been shown to be due to the ability of their capsids to use different cell surface glycans for cell binding. Heparan sulfate proteoglycan (HSPG), the first receptor identified for an AAV virus (49), functions primarily to attach the AAV2 and AAV3 serotypes to the cell surface. AAV1, which is ~83% identical to AAV2, binds both α2–3 and α2–6-N-linked sialic acid, not heparan sulfate (HS) (16, 50, 51). AAV4 and AAV5 that are ~60% identical to each other, and ~65% to AAV2, also bind sialic acid, although AAV4 binds α2–3 O-linked

Table 1
Variable regions on the AAV capsid structure and annotated functions

VR	Function	References
I	Transduction[a]/A20 & IVIG neutralization	(65, 67, 191)
II	Transduction[a]	(65)
III	Transduction[a], A20/MAb neutralization	(65, 67, 191)
IV	Transduction[a]/HS/MAb & IVIG neutralization	(65, 67)
V	Transduction/HB/HS/ & IVIG neutralization	(64–67)
VI	Transduction/HB/HS/& MAb & IVIG neutralization	(64–67)
VII	A20/HS/MAb & IVIG Neutralization	(65)
VIII	Transduction/HB/SIA/HS/ MAb/IVIG neutralization	(64–66)
IX	Transduction/HB/A20, HS & IVIG neutralization	(65, 67, 191)

HB heparin binding, *SIA* sialic acid binding, *HS* human sera, *IVIG* intravenous immunoglobulin
[a]Transduction inhibition not due to Hep-phenotype

Table 2
Glycan receptors and co-receptors for AAVs

	Receptors/co-receptors	References
AAV1	α2–3/α2–6 N linked SA	(16, 50, 51)
AAV2	HSPG, FGFR1, HGFR, integrins, 37/67 kDa LamR	(49, 69–73)
AAV3	HSPG, 37/67 kDa LamR	(49, 71)
AAV4	α2–3 O linked SA	(52, 53)
AAV5	α2–3 N linked SA, PDGFR	(52–54)
AAV6	HSPG, α2–3/α2–6 N linked SA	(51, 55)
AAV7	Not determined	
AAV8	37/67 kDa LamR	(71)
AAV9	Galactose, 37/67 kDa LamR	(56, 57, 71)

sialic acids, while AAV5 binds α2–3 N-linked sialic acids ((52, 53) and unpublished data). Platelet-derived growth factor receptor (PDGFR) is the sialylated protein mediating AAV5 infection (54). AAV6, a tissue culture adapted recombinant between AAV1 and AAV2, binds both HS and sialic acid (51, 55). The nature of the glycosylation (if any) required for cellular transduction by AAV7 and AAV8 has not been determined. For AAV9 galactose has been identified as a cell surface glycan mediating cellular entry and transduction (56, 57). Thus the representative members of the primate AAV clades fall into three broad groups with respect to the cell surface glycans recognition for cellular transduction: those that bind HS (AAV2, AAV3, and AAV6), those that bind sialic acid (AAV1, AAV4, AAV5, and AAV6), and AAV9 that binds galactose plus those for which there are no data (AAV7 and AAV8).

Despite the high structural homology between parvovirus capsids, different regions, configured only on assembled capsids, are used for receptor attachment by different parvoviruses (47, 58). The depression at the icosahedral twofold axis is used by MVM (59), the wall between the two- and fivefold depressions by CPV (60–62), and the depression at the threefold axis by B19 (63).

Studies aimed at deciphering AAV tissue tropism and transduction properties have utilized mutagenesis, cell binding, and transduction assays, mainly on AAV2, to identify individual capsid protein aa sequences that play a central role in cellular recognition (64–67). Mutagenesis studies identified the aas responsible for AAV2's heparin-binding phenotype as R484, R487, K532, R585, and R588, with R585 and R588 being the most critical for this interaction (64, 66). It is noteworthy that several natural isolates of AAV2, in which the aa at positions 585 and 588 are not arginines; do not bind HS (68).

The availability of the high-resolution 3D structure for AAV2 (26) enabled the visualization of the AAV2 HS binding site on the capsid, with residues being contributed from symmetry-related VP monomers at the wall of the protrusions surrounding the icosahedral threefold axes and in the valley that runs from the two- to threefold axis (Fig. 3a). More recently, cryo-EM and image reconstruction studies of AAV2 complexed with either an HS oligosaccharide or an HSPG have been used to structurally verify this binding site on the AAV2 capsid (27, 32). In both studies, HS density was shown proximal to the basic residues at the threefold protrusion. In the Levy et al. study, (32) additional structural rearrangements were observed at the twofold and fivefold axes compared to the wtAAV2 no-HS reconstruction, which were postulated to be capsid transitions necessary for subsequent steps in the AAV life cycle, such as the opening of the fivefold pore for PLA2 activity. However, these additional structural rearrangements were not reported by O'Donell et al. (27).

Using X-ray crystallography followed by mutagenesis, the AAV5 binding site for sialic acid has also been mapped to the

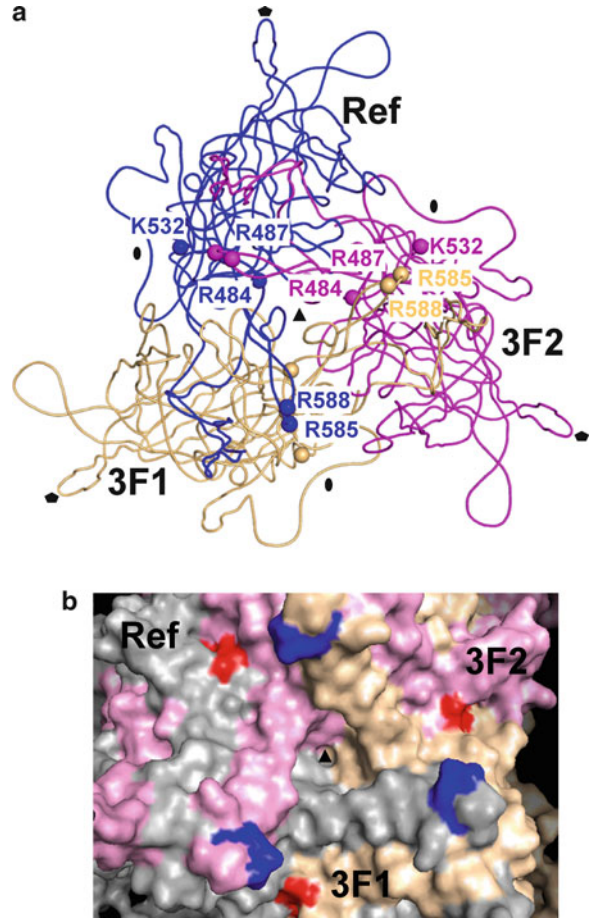

Fig. 3. The receptor attachment regions on AAV2. (**a**) A trimer of the AAV2 VP3 (coil representation, viewed down the icosahedral threefold axis and colored *in blue* (Ref), *magenta* (3F2), and *wheat* (3F1)) showing the location of the heparan sulfate binding site residues (R484, R487, K532, R585, and R588) as small spheres at the interface between each two 3-fold related monomers (labeled according to the monomer color, *pink and wheat*). R487 is hidden behind R585 and R588 in this top down view of the threefold axis. (**b**) Close-up view (down the threefold axis) of a solid surface representation of a trimer of AAV2 VP3 (*colored in gray* (Ref), *pink* (3F2), and *wheat* (3F1)) showing the position of R585 and R588 (*shaded in blue*) and the proposed 511-NGR-513 integrin recognition motif (*in red*). The approximate icosahedral two, three, and fivefold axes are indicated as in Fig. 1.

icosahedral threefold axes (unpublished results). In addition, mutagenesis, transduction studies, 3D model building, and the crystal structures of these viruses locates the AAV1/AAV6 difference that results in their differential HS recognition to capsid regions proximate to the AAV2 HS binding site (36, 52). These observations suggest that there may be a common capsid site for binding the glycan receptor in all of the AAV serotypes and differences in aa sequence and structural topology at this common site dictates glycan specificity in recognition.

1.3.2. Internalization–Co-receptor Interaction

Potential co-receptors involved in internalization of AAV2 include integrin αVβ5, integrin α5β1, fibroblast growth factor receptor 1 (FGFR1), hepatocyte growth factor receptor, and 37/67-kDa laminin receptor (69–73). FGFR1 is also reported to function in the internalization of AAV3 and laminin receptor is reported to mediate cell entry by AAV3 as well as AAV8 and AAV9 (69–71). The only other AAV serotype for which a protein receptor has been reported is AAV5 for which platelet-derived growth factor receptor has been shown to mediate cellular recognition and transduction (54). Thus this discussion of AAV co-receptor interaction for internalization will be mostly focused on AAV2.

Most AAVs enter the cell via clathrin-coated vesicles in a dynamin-dependent process (74–76). For AAV5, caveolar uptake into caveosome-like organelles has also been observed (77). Single particle real-time tracking suggests that AAV2 uptake into HeLa cells occurs within the range of 100 ms after multiple repeated contacts with the cell membrane (78). However, endocytosis might also be slow and rate limiting in other cell types (79). For AAV2, inhibition of αVβ5 integrin prevents endocytosis (80). However, the involvement of αVβ5 integrin in AAV2 infection has also been questioned by others (81). Binding to cell surface receptors triggers intracellular signaling pathways such as Rac1 activation, which leads to subsequent activation of the phosphoinositol-3-kinase pathway (80). Activation of Rac1 seems to be necessary to initiate endocytosis of AAV2. The phosphoinsititol-3-kinase pathway has been suggested to influence movement of AAV2 particles to the nucleus in endocytotic vesicles. The entry site on polarized cells also has an influence on the infection outcome. AAV2 vectors transduce polarized human airway epithelia more efficiently from the basolateral surface than from the apical site (79).

There are some indications for specific AAV2 VP3 sequences that interact with co-receptors. For binding to α5β1 integrin an NGR motif comprising aas 511–513 of AAV2 has been identified (73). This sequence motif is present in most AAV serotypes, except in AAV4, AAV5, and AAV11 (73). It is partially surface-exposed and located close to the base of the threefold protrusions, across a valley from AAV2's HS binding site (Fig. 3b). Mutation of this site has only a moderate effect on cell binding but blocks cell entry. The NGR motif overlaps with a surface-exposed capsid domain, called "dead zone," where site-directed mutations can lead to a greater than 1,000-fold decrease in transduction in vitro that is not due to a defect in HS binding (65). The dead zone consists of 18 adjacent aa positions, localized in the capsid region between the depressions at the icosahedral two- and fivefold axes, close to the base of the protrusions that surround the threefold axis. It contains aas contributed from the variable VP regions (discussed above) that are clustered from symmetry-related monomers. The overlap of the NGR motif with the dead zone and the proximity of this

motif to the HS binding site suggest that binding to HS might promote binding of potential cellular co-receptor proteins to this domain. Structural rearrangements of the capsid following HS binding observed by Levy et al. (32) were observed in this capsid region close to the NGR motif and were postulated as possible transitions that further exposure its residue to enable contact with a co-receptor. In the Lochrie et al. study (65) a dimeric heparin/bFGF/FGFR1 complex was modelled into the dead zone. However, structural studies of the AAV2-co-receptor complexes as well as binding and interaction studies will be required to determine whether this domain is involved in co-receptor binding and cell entry and the specific aas, which mediate the interactions.

1.4. Endosomal Trafficking and Release

Endosomal trafficking of AAV to the nuclear area is slow and a rate-limiting process in a number of cell types (82–84). AAV capsids could be co-localized with markers of early endosomes, late endosomes, recycling endosomes, and lysosomes (75, 85, 86). However, it is difficult to determine which compartment is most relevant for infection and which is part of a dead-end pathway. Particle-to-infectivity ratios of 100–1,000 indicate that only a small fraction of the applied viruses leads to successful infection or gene transduction. AAV2 and AAV5, the best characterized serotypes with respect to endosomal trafficking, accumulate in perinuclear vesicles, presumably recycling endosomes and AAV5 may then also enter the trans-golgi network (76). Biochemical fractionation suggests that rAAV2 moves to the late endosomal (or even the lysosomal) compartment (87, 88). However, other studies reported that AAV2 escapes from early endosomes (75, 89) suggesting that processing in later compartments is not required for successful gene transduction. These differences are not only cell-type dependent but also dose dependent (85). At low multiplicity of infection (MOI), AAV2 capsids are primarily found in Rab7-positive late endosomes of HeLa cells, whereas at high multiplicities they localize in Rab11-positive vesicles (85). The Rab11 pathway seems to provide more efficient transduction with AAV2 compared with the Rab7 pathway.

Inhibition of endosomal acidification by bafilomycin A or NH_4Cl blocks infection with AAV2 (75, 83, 87, 90). This indicates the requirement of acid-dependent host factors for endosomal processing, although cell-type specific differences have also been observed (90). Interactions of capsid proteins of AAV2 and AAV8 with endosomal proteases cathepsin B and L have been shown by the yeast two hybrid system (91). The activity of these endosomal proteases have a significant influence on the efficiency of AAV gene transduction (91) probably by selective cleavage of capsid proteins for further uncoating steps. The VP protein interaction domains or the protease cleavage sites on the capsids are not known.

AAV exits from the endosomal compartment before it travels to the nucleus (43). A phospholipase A2 (PLA2) domain located

on the VP1u of all AAV types (46) likely plays a crucial role in this step. This has originally been shown in studies with the minute virus of mice (MVM) and canine parvovirus (CPV) and confirmed for AAV2 (42, 92, 93). PLA2-inactivating point mutations result in low levels of gene transduction, although the mutant viruses accumulate in a typical perinuclear pattern (45). The VP1u containing PLA2 domain is proposed to be buried inside the capsid of AAVs and is not observed in the structures determined to date due to low occupancy in the capsid (6). Genetic data suggest that VP1u might be exposed through channels at the fivefold axes of symmetry (37). Consistently, some weak electron density has been observed within the fivefold channel of DNA containing CPV, MVM, and AAV8 into which a glycine sequence, conserved in most parvoviruses and common to all the capsid VPs could be fitted (25, 95–97). In addition, molecular modelling has shown that an extended polypeptide sequence can be accommodated in the channel at the fivefold axis (33). However, the capsid structure with exposed VP1 N-termini has not been solved experimentally, to date.

Several exchanges of channel forming aas that block exposure of the PLA2 domain and strongly decrease infectivity suggested a connection between exposure of the PLA domain through the channels at the fivefold axes and infectivity (37). However, exchange of the conserved leucine 336 at the base of the channel (inside) may not only affect externalization of VP1/VP2 N-termini but in addition influence other structural features required for infection (98). Mutation of a conserved phenylalanine 661 to glycine in the HI loop, which forms the floor of the depression surrounding the channel (Fig. 2c, as discussed above), prevented externalization of VP1u in vitro and led to a tenfold reduction in infectivity (99). This suggests a connection between HI loop and channel opening in VP1u exposure. It is possible that the HI loop mutation prevents or alters its movement to open up the channel following HS binding as proposed based on the structure of the AAV2-HS complex (32). Importantly, exposure of VP1u occurs also during AAV infection in vivo, most likely in the endosomal compartment (43). Bafilomycin and chloroquine treatment inhibited VP1/VP2 externalization indicating that endosomal acidification is involved in PLA2 activation (75, 87). However, in vitro acidification of capsids to pH 5.5 did not lead to externalization of N-terminal capsid protein sequences (unpublished data). Thus, it remains unclear how PLA2 externalization is triggered and by which mechanism PLA2 permits escape from the endosomal vesicles.

1.5. Cytoplasmic Processing and Nuclear Entry

Before AAV enters the nucleus, after endosomal/lysosomal escape, further processing has to occur in the cytoplasm. This processing requires modification of the capsid structure within the endosome, because native viruses microinjected into the cytoplasm do not enter the nucleus and do not lead to productive infection in presence

of adenovirus coinfection (43). Ongoing structural studies under pH conditions that mimic the environment encountered in the endocytic pathway suggest capsid transitions that reorganize surface aas (unpublished data); however, the exact nature of the modification remains to be elucidated.

Treatment of cells with proteasome inhibitors significantly increases gene transduction with AAV2, AAV5, AAV7, and AAV8 (79, 87, 100–104). This has been interpreted to result from reduced degradation of capsids in the cytoplasm since increased gene transduction is associated with increased nuclear accumulation of viral genomes. The effect of proteasome inhibitors shows cell-type specificity (90, 103). Interestingly, they also had a differential effect on gene transduction of polarized human airway epithelia when the vectors were applied from the apical site versus the basolateral site. Gene transduction from the apical surface was strongly stimulated, while the basolateral infection pathway was not significantly affected (101). Capsids immunoprecipitated with capsid-specific antibodies show a reaction with ubiquitin antibodies in western blotting indicating ubiquitination of capsids within infected cells (105–107). Inhibition of EGFR-PTK signaling leads to decreased ubiquitination of AAV2 capsids suggesting that protein phosphorylation precedes ubiquitination and proteasomal degradation of capsids (105). Consequently, mutation of capsid surface tyrosines, proposed to be phosphorylation sites, reduced VP protein ubiquitination and enhanced nuclear transport of vectors and gene transduction (106, 107). Treatment of cells with proteasome inhibitors may not only influence processes in the cytoplasm but also in the nucleus.

Movement of AAV in the cytoplasm to the nucleus can possibly be directed along the cytoskeleton and facilitated by ATP-dependent motor proteins, although Brownian diffusion has also been observed (78). Interaction of AAV capsids with microtubule-associated proteins has been reported (108, 109). Treatment of cells with microtubule- or microfilament-directed drugs showed various effects on infection or gene transduction. In some cases they had no effect; while in others they prevented trafficking of viral particles to the nucleus (78, 80, 110). However, there was no discrimination as to whether the drugs affected viral transport within vesicles or after release into the cytoplasm. Modification of an AAV2 capsid with a dynein light chain binding peptide at positions 583 and 587 (on the threefold protrusions) increased viral transduction suggesting that AAV is able to use dynein for efficient cytoplasmic movement to the nucleus (111).

Little is known about the process that allows translocation of AAV across the nuclear membranes. Proteasome inhibitors (79, 87, 100, 102, 106, 107, 112) and adenovirus have been described to increase nuclear accumulation of AAV. The VP1/VP2 N-termini contain three basic sequence motifs (here abbreviated as (BC) for

basic clusters), which resemble classical nuclear localization signals (NLS). Mutation of each of these sequences dramatically reduced AAV infectivity (43, 67), while in another report mutation of BC1 and BC2 had only a moderate effect (113). Cytoplasmic injection of VP1/VP2 N-terminus specific antibodies, which recognize epitopes close to these motifs, inhibited infection showing that these domains are accessible on the capsid surface in the cytoplasm (43). Exchange of BC3 aas inhibited transfer of encapsulated DNA into the nucleus and this defect could be reversed by a CPV-derived NLS supporting the interpretation that BC3 acts as an NLS for nuclear transport of the capsids (113). Isolated BC3 peptides, however, did not show nuclear transport activity when coupled to a reporter protein, in contrast to peptides of BC1 and BC2, which showed NLS activity (43). Microinjection of virions into the cytoplasm with or without exposed N-termini did not lead to detectable nuclear transport of viruses, whereas standard nuclear proteins show efficient and fast nuclear accumulation in such an assay. This indicates that the process is at least very inefficient and may require additional processing of capsids in the endosome (43) as already mentioned. Furthermore, in vitro experiments suggest that nuclear uptake of capsids may not occur by transport through the nuclear pore-complex, but through an as yet unidentified pathway (89, 114). For MVM, perforation of the nuclear membrane has been observed upon microinjection of the virus into Xenopus Oocytes (115). This has later also been confirmed by infection of mouse fibroblasts suggesting that the nuclear import mechanism might involve disruption of the nuclear envelope and import through the resulting holes (116). Whether AAV follows an analogous pathway for nuclear entry has not been shown.

1.6. Nuclear Events

1.6.1. Uncoating

AAV uncoating is a slow process (117–120). The detection of AAV capsids in the nucleus (75, 80, 89) suggested that it occurs in the nucleus. Microinjection of different antibodies, which react with capsids and not with disassembled capsid proteins, into the nucleus prevented infection with AAV2 providing functional evidence for uncoating in the nucleus (43). Also antibodies directed against the exposed VP1/VP2 N-termini inhibited infection, whereas an antibody reacting with the C-terminus of the capsid proteins, which is not accessible on intact capsids, had no effect. However, another report suggests that uncoating may occur before or during nuclear entry (121). AAV genomes could be detected by fluorescent in situ hybridization in the nucleus without detectable amounts of capsids, while the majority of genomes remained in a peri-nuclear area in co-localization with capsids. This observation was interpreted in favor of uncoating before or during nuclear entry (121). The assumption for this interpretation is that genomes and capsids were detected with the same sensitivity. In vitro capsid disassembly has been reported with a nuclear but not with a cytoplasmic extract of

liver cells (118), suggesting a need for nuclear factors. However, it is also conceivable that genome release occurs without capsid disassembly.

Parvoviruses are able to release their genome in vitro after treatment with heat or urea from intact capsids (122–124). Upon heat treatment of AAV virus particles at 65°C a species could be detected (by sedimentation analysis), which had lost its genomes (37). Electron microscopic analysis of such preparations showed freshly released AAV genomes associated with intact capsids (unpublished data). Attempts to analyze DNA release in vivo indicated a high stability of the virions in cells and excluded an extensive genome release during viral entry (43, 94). Only 10–20% of viral input DNA became nuclease sensitive during infection (43). The process/mechanism of DNA release in vivo is also not yet known. It is possible that the exposed VP1/VP2 N-termini detected in the nucleus (43) play a role in the uncoating reaction. The VP1/VP2 N termini contain a conserved binding motif for CDK2/CyclinA kinase (94). This is the same sequence that has been suggested to function also as a nuclear localization signal for AAV2 (113). It has been proposed that interaction of CDK2/cyclinA kinase with this motif may lead to phosphorylation of the AAV capsid during infection. Inhibition of CDK2 kinase enhanced gene transduction of AAV8 and AAV2; however, mutation of the sequence motif significantly reduced infectivity of AAV2 (43, 67), maybe due to overlapping functions in the infection process. Further investigation is required to clarify the role of this sequence element in AAV infection and gene transduction.

A crucial step following genome release is the conversion of the ssDNA AAV genome into a double strand (ds) form, a prerequisite for gene expression (118, 125–132). Whether ssDNA conversion is associated with the genome release is not known. However, it could be advantageous given the high instability of free ssDNA. Circularisation, concatemerization (133, 134) and integration (135) are further key steps following ssDNA conversion that characterize gene transduction and the fate of transduced cells.

There have been several reports that processing of AAV genomes in the nucleus takes place in specific nuclear structures that overlap with the localization of DNA-damage-response proteins (136–138). Whether capsids also localize to these areas has not been analyzed. In a recent report capsids were observed to become localized to the nucleoli of infected cells (139). These virus capsids were found to retain infectivity upon isolation from nucleoli and reinfection, suggesting that they did not release their genomes in the nucleoli. Treatment with proteasome inhibitors increased nucleolar accumulation whereas hydroxyurea mobilized viruses into the nucleoplasm. However, both treatments stimulated transduction. Also siRNA mediated knock down of nucleolin and nucleophosmin both stimulated gene transduction, although they

had opposite effects on nucleolar localization of the virus capsids. These results were interpreted with the assumption of two different intra-nuclear trafficking pathways. Nothing is known about capsid structures involved in any of these intra-nuclear processes.

1.6.2. Genome Replication

AAV DNA is replicated by an ssDNA displacement mechanism and involves the formation of monomer and dimer duplex replication intermediates (RFm and RFd) (140). The ITRs act as origins of replication and are the only *cis*-acting elements required for AAV DNA replication and encapsidation (8–10). Rep proteins Rep78 and Rep68 bind to the ITRs (141–145), catalyse the resolution of closed termini by their site-specific endonuclease and helicase activities and reinitiate replication (146–148). The large Rep proteins (Rep78 or Rep68), DNA polymerase δ, RFC, PCNA, and the minichromosome maintenance complex are the minimal protein complexes required in *trans* for AAV DNA replication in vitro (149). DNA replication is stimulated by cellular- or helper virus-derived ssDNA binding proteins (150–152). Capsids and capsid proteins do not play a role in the formation of RFm and RFd DNA; however, accumulation of displaced ssDNA depends on the presence of capsids (153). This is also reflected at the cellular level by the detection of Rep protein expression in co-localization with AAV DNA early in infection when no VP expression is detectable (154). At later stages in infection when DNA becomes encapsidated, Rep proteins, VPs, and AAV DNA co-localize in clusters within the nucleus (154–156). It seems that capsids sequester ssDNA to protect it from degradation, because ssDNA could not be detected in extracts of cells transfected with a packaging mutant (AAV2-R432A), which is capable of capsid formation but not ssDNA encapsidation (157). It is not known whether or not ssDNA encapsidation depends on DNA replication. Addition of aphidicolin to an in vitro encapsidation reaction prevented the formation of packaged AAV particles suggesting that packaging of AAV DNA was dependent on active DNA replication (158). Furthermore, in pulse chase experiments, hydroxyl urea inhibited DNA encapsidation when the drug was included in the labeling period (159) supporting a dependence on replication. However, addition of hydroxyurea after the labeling step did not prevent packaging. This later result suggests that packaging can occur from a pool of replicated DNA under conditions in which replication is inhibited.

1.6.3. Capsid Assembly

Based on pulse chase experiments Myers and Carter established the pathway of AAV assembly by showing that free VPs rapidly assemble into empty capsids into which viral ssDNA is inserted in a slow process, which lasts several hours (159). There is mounting evidence that capsid assembly occurs in the nucleus. Capsids are first detected in nucleoli of productively infected cells (154). At later stages of infection they are detected throughout the nucleus and co-localize with Rep proteins and DNA in subnuclear

clusters (154–156). Capsids assembled in the absence of Rep proteins remain mainly associated with nucleoli, while co-expression of Rep proteins leads to mobilization of capsids into other parts of the nucleus (154). Two nucleolar proteins – nucleolin and nucleophosmin – have been found to be associated with AAV capsids or VPs (81, 160). Interestingly, Rep68 also interacts with nucleophosmin and transiently co-localizes with nucleophosmin and capsids at the border of nucleoli (160). Interaction sites of these proteins with capsids are not known and a functional role in the capsid assembly process has not been described. Newly synthesized capsid proteins VP1 and VP2 accumulate efficiently in the nucleus, whereas VP3 stays to some extent in the cytoplasm (154, 161). N-terminal deletions of VP2 suggested a nuclear localization signal between aas 166 and 171 comprising the sequence PAKKRL. However, this sequence was not sufficient to transport a heterologous protein into the nucleus (43). Since capsid assembly depends on the concentration of expressed VPs (154), their nuclear accumulation might not only provide interaction with nuclear factors that facilitate the assembly reaction but might also increase their local concentration.

Biochemical fractionation experiments showed that VPs oligomerize in the cytoplasm, but do not form capsids (162). Using sedimentation experiments in sucrose density gradients, in the low molecular weight range, a small fraction of monomers could be separated from a 10 to 15S fraction containing all three capsid proteins, which is compatible with a transient pool of VP trimers or pentamers (162). In the nucleus the vast majority of VPs is assembled into capsids sedimenting between 60S and 110S. Besides the soluble pools of capsids and VP proteins an insoluble pool of VPs and capsids exists in the nucleus for which nothing is known concerning its contribution to the assembly reaction (162).

Controversial observations have been published regarding the requirement of the different VPs VP1, VP2, and VP3 for capsid formation. Initially it was reported that VP3 alone, partially located in the cytoplasm, is not able to form capsids (161, 163). When, however, VP3 was fused with a nuclear localization signal it accumulated in the nucleus and capsid assembly could be detected (164), suggesting that VP3 contains sufficient information for virus-like-particle assembly. In addition, two groups reported formation of VP3 only capsids using *cap* gene constructs in which expression of VP1 and VP2 was abolished (165, 166).

This controversy has more recently been resolved by the discovery of an assembly activating protein expressed from an alternative open reading frame of the cap gene, initiated upstream of the VP3 coding sequence (167).

The first insertional mutagenesis study on the AAV2 cap gene described seven mutants, which were negative for production of capsids protecting the viral genome (166). These were located at approximate amino acid (aa) positions 52, 182, 397, 453, 617, and

618 (VP1 numbering) (166). However, due to the fact that capsid formation and DNA packaging were not distinguished in this study it is difficult to assign the phenotype of the mutations to one of the two processes. Since this study, there have been several reports of site-directed mutations, which have abrogated capsid assembly (Fig. 4a, Table 3). These include charge to alanine scanning mutants at aas stretches 228–232, 235–239, 285–289, 291–295, 307–311, 607–611, 681–683, 689–693 (67); mutations at aas 309, 310, and 312 (113); and mutations at aas 322, 322/323/324 (37). A number of insertion mutations in the VP1/VP2 N-termini (not observed in the AAV2 crystal structure), as well as at aas 224, 323, 339, 375, 441, 454, 472, 480, 526, 553, 562, 590, 638, 664, 682, and 735 within the ordered VP3 sequence have also been reported to result in no capsid phenotypes (67, 190).

The aas mutations which play a role in capsid assembly and are ordered in the available crystal structure of AAV2 span the entire VP3 common sequence but most of them are clustered on the assembled capsid structure, (1) at VP:VP monomer interfaces and involved in symmetry-related interactions, (2) located close to the fivefold channel, or (3) located in essential secondary structure elements, such as βD and βI (Fig. 4a, Table 3). The block in the assembly pathway by these mutants have not been determined, but clustering at symmetry-related interfaces suggests the inhibition of the aa interactions necessary to generate the building block(s) required for capsid assembly (e.g. monomer interface mutations) or they may result in protein folding problems (e.g. mutations in secondary structure elements).

1.6.4. Genome Packaging

Packaging of ssDNA generated by strand displacement DNA synthesis into preformed empty capsids is a slow reaction (159). By density gradient centrifugation assembly intermediates containing partially encapsulated DNA associated with capsids can be detected (159, 168). The only necessary *cis* acting element for genome encapsidation is the ITR (7). Since this element is also required as origin for DNA replication it has been difficult to define a separate packaging signal. Several reports suggest that the D element within the ITR (or part of it) acts as a packaging signal (169–172). Determination of the efficiency of packaging with respect to the genome size showed that encapsidation of AAV (vector) genomes between 4.1 and 4.9 kb was optimal (173). Packaging efficiencies of genomes over 5.2 kb were strongly reduced and packaging was suboptimal below 4.1 kb. The observation that genomes of less than half of the wild-type genome size were packaged with two copies per virion suggested that AAV packaging follows a "head full" mechanism. Several studies reported packaging of oversized genomes (of 5.6–8.9 kb) into different AAV serotype capsids (174–176). Using DNA sequences of different length and multiple AAV serotypes, three recent reports showed that the

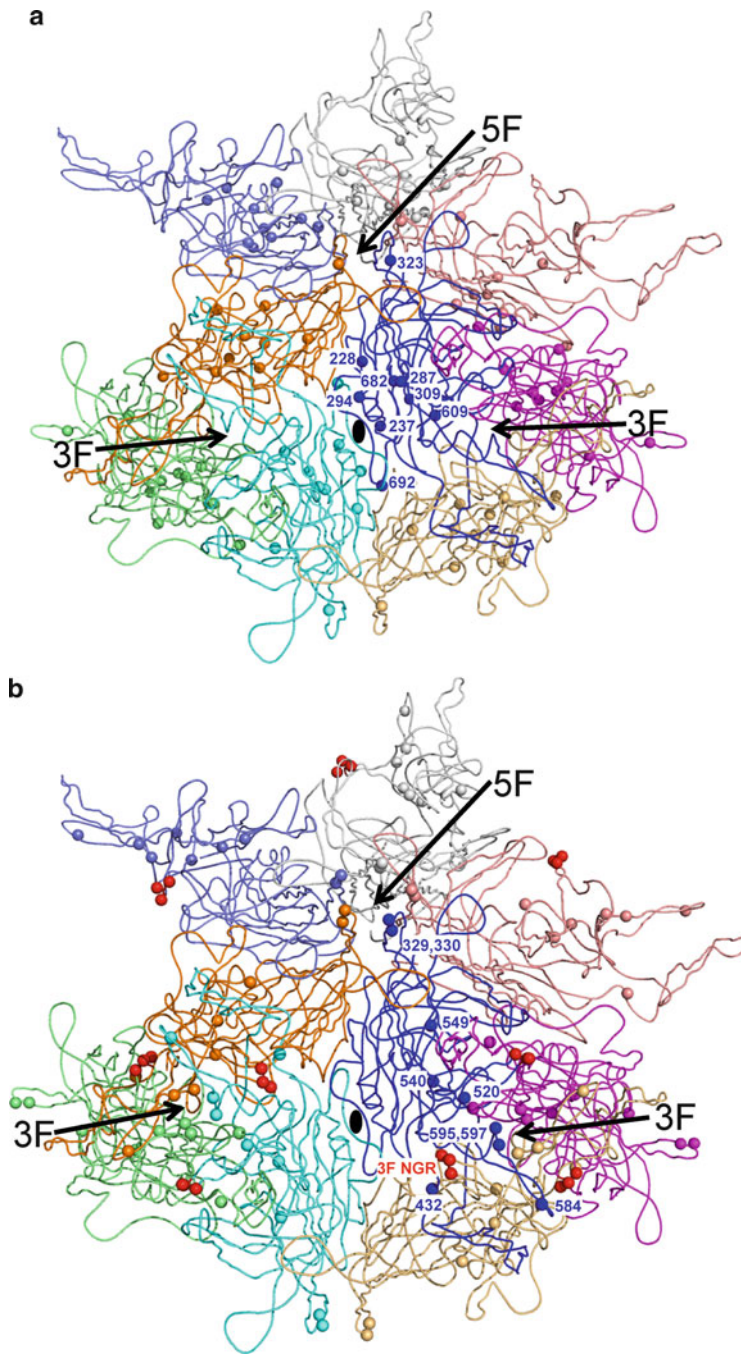

Fig. 4. Capsid location of assembly and genome packaging determinants. (**a**) A coil representation of a 9mer of AAV2 VP3 monomers (in different colors with the reference monomer *in blue*, and positioned as in Figs. 2a and 3a) viewed down the icosahedral twofold axis and showing the location of amino acids positions (either single site change, insertion site, or in the middle of a stretch of amino acids mutated, see Table 3 for stretches), which led to a no-capsid phenotype as small spheres colored the same as the contributing monomer. The residues on the reference monomer are labeled. The no-capsid mutations are located at secondary structure elements or VP:VP interfaces (see Table 3). (**b**) A coil representation a 9mer of AAV2 VP3 monomers (colored and viewed as in (**a**)) showing the location of amino acids which when mutated led to a no-packaging phenotype (see Table 4). Other than residues 329 and 330 on the DE loop, the remaining mutant amino acids are clustered around the threefold axes. The approximate two (2F), three (3F), and fivefold (5F) axes are indicated by arrows and labeled.

Table 3
Location of capsid assembly mutants on the AAV2 capsid structure

AA #	VP/capsid location	References
228–232	βA strand, 5F interaction	(67)
235–239	Wall of 2F axis, close to αA	(67)
285–289	βC strand	(67)
291–295	αA	(67)
307–312	Interior surface, βD Strand	(67, 113
322–324	DE loop, 5F interaction	(37, 168)
607–611	Buried, strand region, close to 3Faxis	(67)
681–683	βI strand, interior capsid surface,	(67)
689–693	Buried, 2F interface	(67)

physical packaging size of AAV genomes is limited to approximately 5 kb (177–179). The apparent packaging of oversized genomes was shown to be due to partial packaging of fragments of the larger DNA which at high multiplicities of infection could reassemble in the host cells and lead to a low level expression of the full length transgene.

Co-localization of AAV DNA, capsids, and Rep proteins in nuclear foci at some stage of virus reproduction suggests that genome replication and encapsidation are coordinated (154–156). Provision of the *cap* gene in *trans* – as required for packaging of recombinant genomes – does not efficiently support encapsidation, suggesting a link between *cap* expression in *cis* and encapsidation (180). This is also reflected in a lower genome-to-particle ratio of recombinant vectors compared to wt viruses generated by transient transfection (181–184). The molecular basis for this observation has not been elucidated. Immunoprecipitation experiments demonstrated interactions of Rep proteins with capsids during genome packaging (162, 168). Part of the capsid-associated Rep protein is covalently linked to the 5′ end of replicated DNA and can be released by DNAse treatment (185). But also a DNA-independent interaction of Rep proteins with empty capsids as well as specific Rep–Rep interactions were demonstrated (186). Since the large Rep proteins bind specifically to the ITRs, it was proposed that Rep proteins mediate the attachment of the ssDNA AAV genome to the capsid in order to initiate the packaging reaction (186). This hypothesis is supported by the observation that the small Rep proteins, Rep52 and Rep40, are required for DNA encapsidation (187), and that the helicase function of these proteins is needed to

completely insert capsid-associated DNA genomes into capsids (188). Mutation of the DNA-binding aas of Rep40 results in a significant packaging defect (189). Genome encapsidation is suggested to proceed in a preferred 3′ to 5′ direction and the helicase activity of the small (and possibly the large) Rep proteins, present in encapsidation complexes, are proposed to drive translocation of full length ssDNA into procapsids (188).

The Rep protein domains involved in Rep–Cap interactions were mapped to aas 322–482 comprising the Rep ATPase/helicase domain (186). A panel of mutants with aa exchanges at the fivefold channel of the AAV2 capsid showed reduced genome packaging and reduced Rep–capsid binding (157). Mutations of two threonines at the rim of the channel (T329A/T330A) at the fivefold axes (Fig. 4b, Table 4) strongly reduced Rep–capsid interactions. This suggests that highly conserved AAV VP aas at this capsid region are (directly or indirectly) involved in rep–capsid interaction (157). However, the portal through which AAV ssDNA genomes are inserted into capsids has not been determined at the structural level. Another packaging mutant (R432A) (67) located closer to the threefold axis, distant from the channel and not surface exposed in the assembled wild type capsid structure (Fig. 4b) showed increased Rep binding to the capsid (157). In the wild type AAV2 crystal structure, the side-chain of R432 is involved in interactions with the main chain of a surface loop, VR I (Fig. 1b), from a threefold symmetry-related monomer. The change to alanine would disrupt this interaction and is likely to result in a structural change on the capsid surface. Thus the observed increase in Rep interaction suggests that the anticipated structural change on the capsid in the mutant alters capsid–Rep interactions. Further studies are required to characterize the increased Rep binding properties of this mutant. A further hot spot of packaging deficient mutants was observed at positions 520, 540, and 549 (190). These amino acids line the wall/base of the threefold protrusions (Fig. 4b, Table 4). Also close to the base of the threefold protrusions, conversion of the NGR motif (aa 511–513) (Fig. 4b, Table 4) to RGD produces empty capsids (73). This motif, discussed earlier in association with co-receptor binding, is located close to aa 432 discussed above (Fig. 4b). Another cluster of packaging deficient insertion mutations was observed at aas 584, 595, and 597 (190). However, the packaging defect observed at position 584 depended on the sequence of the inserted peptide indicating a rather indirect effect on the packaging process. Mapping of the residues onto the crystal structure of AAV2 shows them mostly located at or close to the threefold axis with the exception of 329 and 330. Thus while all these mutants have not been further analyzed with respect to the molecular basis of the packaging defect, the involvement of the threefold residues suggests a direct or indirect role for this capsid region in capsid–Rep interactions during this process.

Table 4
Location of genome packaging mutants on the AAV2 capsid structure

AA #	VP/capsid location	References
329, 330	DE loop, top of 5F pore	(157)
432	Buried, base of 3F protrusion, GH loop	(67)
511–513	Surface, close to 3F axis	(73)
520	Buried, base of 3F protrusion	(168)
540	Buried, base of 3F protrusion	(168)
549	Surface, base of 3F protrusion, close to 5F symmetry-related HI loop	(168)
584	Surface, 3F axis side of 3F protrusion	(168)
595	3F interface	(168)
597	Surface, at 3F axis inside depression	(168)

1.7. AAV Capsid Interactions with the Host Immune System

The AAV capsid is susceptible to both T-cell and B-cell mediated host antibody responses as discussed in Chapter 11. Several studies have shown that pre-existing immunity to AAV can limit effective gene transfer most likely due to antibody mediated neutralization of incoming vectors (e.g. (191, 192)). These pre-existing host immune responses, in addition to those that could arise following vector administration thus represent a major obstacle to the use of the AAVs as effective gene delivery systems. Thus, in efforts to understand the antigenic structure of the AAV capsid, attention has been directed at characterizing AAV interactions with antibodies. AAV2 is the best antigenically characterized serotype using antibodies generated in mouse (154, 193), although some mouse antibodies have also been generated against other serotypes, including AAV1, AAV4–AAV6 (194), and AAV8 and AAV9 (unpublished data). In AAV2, three linear epitopes (A1, A69, and B1) and four conformational epitopes (A20, C24-B, C37-B, and D3) have been reported by Wobus et al. (193) based on peptide mapping, although the residues for the C24-B site have not been identified. In addition, Moskalenko et al. (192) were able to identify VP peptides capable of blocking capsid binding by human serum samples.

The linear AAV2 A1 antibody recognizes VP1 only (aa 123–131), while A69 recognizes a peptide in the VP1/VP2 common region (aa 169–184), and B1 recognizes all three capsid proteins via an epitope at their C-termini (aa 726–733) (193). The B1 antibody is non-neutralizing. The A1 and A69 antibodies cannot neutralize infection when applied extracellularly because their

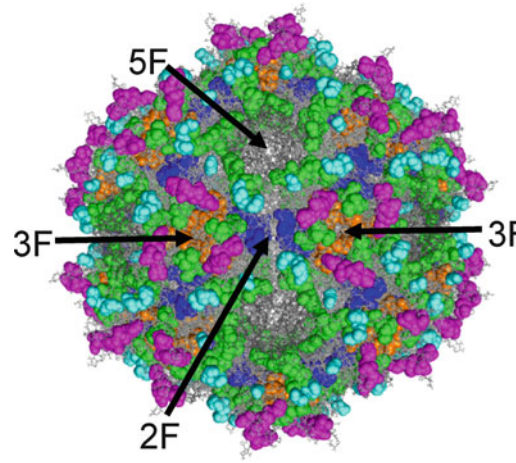

Fig. 5. Antigenic structure of the AAV2 capsid. A stick representation of the AAV2 capsid (assembled from 60 VP3 monomers) *in gray* viewed down the icosahedral twofold axis with the amino acids for different antigenic epitopes depicted as colored spheres: A20 is in *green and cyan*, C37-B is in *magenta*, D3 is in *orange*, and B1 is *in blue*. The approximate two, three, and fivefold axes are indicated as in Fig. 4.

N-terminal epitopes are inside the capsid, but are neutralizing when injected into the cytoplasm or the nucleus, consistent with the externalization of these regions during AAV trafficking (43). The A1 and A69 epitopes are not ordered in the available crystal structure of AAV2 and the B1 epitope is located close to the icosahedral twofold axis of the capsid but is partially buried (Fig. 5, blue spheres), consistent with its recognition of only denatured VPs. The A1 antibody was reported to cross-react with serotypes AAV1–AAV6, the A69 antibody cross-reacts weakly with AAV1, AAV3, and AAV6, and B1 cross-reacts with most of the AAV serotypes except AAV4 and newly isolated AAV4-like viruses. These reactivities are consistent with sequence homology between these viruses in the epitopes, with the similarity between AAV4 and AAV5 with each other and the other representative members of the AAV antigenic clades (1).

The Wobus et al. AAV2 antibodies, which recognize conformational epitopes, have been reported to utilize different mechanisms for virus neutralization (193). The C24-B and C37-B antibodies elicit neutralization by inhibiting virus attachment to its HS receptor, A20 antibody functions at a post attachment step, and D3 is non-neutralizing. The conformation antibodies recognize regions on the capsid surface loops clustered at the icosahedral threefold axes, the protrusions that surround them or close to the protrusions (Fig. 5), consistent with the important roles of these regions in the infection pathway as already described. The A20 antibody, which is widely used for verifying the presence of assembled AAV2 capsids and only cross-reacts with AAV3,

was originally reported to recognize aas 272–281, 369–378, and 566–575 (Fig. 5, green spheres) (193). Further mutagenesis of individual AAV2 surface aas in a study aimed at characterizing its antigenic structure identified additional aas 263, 264, 384, 385, 548, and 708, as forming part of the A20 footprint (Fig. 5, cyan spheres) (65). The A20 epitope thus contains amino acids from four different regions of the VP3 sequence that are clustered together on the capsid surface ridge between the two-, three-, and fivefold axes in the AAV2 capsid structure, at or close the VR I, III, VII, and IX. The peptide mapped footprint also extends under the HI loop, which lines the floor of the depression surrounding the fivefold axis (Fig. 5, green spheres). The Lochrie et al. study also identified residues in VR I and IV to IX as playing a role in AAV2 binding and recognition by pooled human sera and intravenous immunoglobulin G (65). This footprint as well as that recognized by A20 overlaps with the transduction dead zone proposed to be involved co-receptor recognition by Lochrie et al. (65). Thus the A20 antibody, pooled sera, and immunoglobulin G may potentially be blocking co-receptor or some other interaction and inhibiting subsequent steps required for trafficking and capsid uncoating. This possibility requires further investigation. The C37-B antibody specifically recognizes only AAV2 (193). Its epitope contains aas 493–502 and 602–610, which are located in VR V and close to VR VIII containing the critical AAV2 HS binding residues R585 and R588 (Fig. 5, magenta spheres). Thus, the HS binding inhibition neutralizing mechanism for this antibody is consistent with the structural location of its epitope. The D3 antibody cross-reacts with AAV1, AAV3, and AAV5, but not AAV4, consistent with the conservation of its epitope residues, aas 474–483, in the former AAV serotypes. These residues are located at the threefold axis (Fig. 5, orange spheres) close to VR V and other structural differences between AAV2 and AAV4, which surround the threefold protrusions, consistent with its lack of AAV4 recognition. The D3 epitope is mostly buried below surface loops (Fig. 5), which may explain the non-neutralizing phenotype of the antibody.

The AAV2 peptides reported to inhibit binding by neutralizing bodies by Moskalenko et al. (192) include six stretches of amino acids located in the common VP3 sequence and do not overlap with the amino acids regions mapped for the Wobus et al. antibodies. These peptides contain aas 241–260, 305–356, 401–420, 443–460, 473–484, and 697–716, which are structurally located in strand βB, strands βD-βE, strands βF-βG, VR IV, strand region of GH loop, and VR IX, respectively, of the VP3 crystal structure. The b-strand amino acids are not surface accessible on the assembled capsid suggesting that antibodies recognized by peptides from this region were generated against degraded capsid VPs. The 443–460 and 697–716, located in VR IV and IX, respectively, may be

capable of interacting with antibodies generated against capsid given their surface exposure.

The next phase of the characterization of the antigenic structures of the AAVs, with respect to antibody recognition, is utilizing structural biology combined with mutagenesis and biochemical approaches. These studies are confirming the epitopes identified by peptide mapping and site-directed mutagenesis, identifying sites for newly generated antibodies, such as the ADK series (194) and providing information on dominant antigenic regions of the capsid (unpublished results). The anticipation is that such studies will provide a better understanding of capsid regions, which are targets for pre-existing host immune responses to be engineered to circumvent these interactions and improve vector efficacy.

2. Materials

2.1. Structure Determination AAV Virus-Like Particles by X-Ray Crystallography and Cryo-Electron Microscopy

1. Bac-to-Bac expression system (Invitrogen, Calsbad, CA).
2. pFastBac™ donor plasmid (Invitrogen, Calsbad, CA).
3. Control plasmid (pFastBac™-Gus or pFastBac™ HT-CAT) (Invitrogen, Calsbad, CA).
4. MAX Efficiency® DH10Bac™ competent cells CellFECTIN® reagent (Invitrogen, Calsbad, CA).
5. JM109 cells (Promega, Madison, WI).
6. CellFECTIN® reagent (Invitrogen, Calsbad, CA).
7. Restriction enzymes (New England Biolabs, Ipswich, MA).
8. T4 DNA ligase (New England Biolabs, Ipswich, MA).
9. Calf Intestinal Alkaline Phosphotase (New England Biolabs, Ipswich, MA).
10. Fetal Bovine Serum (FBS) (Gibco/Invitrogen, Calsbad, CA).
11. *E. coli* competent cells (Invitrogen, Calsbad, CA).
12. Antibiotics (Ampicillin, Gentamicin, Kanamycin, Antimycotic, tetracycline).
13. Antibiotic and Antimycotic (Sigma, St. Louis, MO).
14. Bluo-gal (Invitrogen, Calsbad, CA).
15. IPTG (Sigma, St. Louis, MO).
16. RNAse A.
17. LB Medium (Sigma, St. Louis, MO).
18. S.O.C Medium (Invitrogen, Calsbad, CA).
19. Sf-900 11 Medium and Sf-900 II Medium 1.3× (Gibco/Invitrogen, Calsbad, CA).
20. Grace's Medium (Sigma, St. Louis, MO).

21. Six-well tissue culture plates.
22. Sea plaque agarose (Lonza, Rockland, ME).
23. Neutral Red (Sigma, St. Louis, MO).
24. Chemicals – Tris buffer, EDTA, NaCl, $MgCl_2$, sucrose, glycerol, agarose, Triton X-100, potassium acetate, NaN_3, HEPES buffer, NaOH, sodium dodecyl sulfate (SDS), isopropanol, ethanol, polyethylene glycol (PEG).
25. PBS (2.71 mM Na_2HPO_4, 1.54 mM KH_2PO_4 and 155.17 mM NaCl).
26. Benzonase (Merck KGaA, Darmstadt, Germany).
27. Amicon Ultra filters (Millipore Corporation, Billerica, MA).
28. VDX 24-well Limbro plates, siliconized cover slips, imersion oil, cryo-loops, cryo vials (Hampton Research, Aliso Viejo, CA).
29. Liquid Nitrogen (local suppliers).
30. Continuous carbon or Quantifoil Holey carbon grids (Electron Microscopy Sciences, Hatfield, PA).

2.2. Subcellular Localization of AAV Virus/Vector Particles During Infection

1. Hela cells (ATCC, CCL_2), cultured at 37°C and 5% CO_2 in Dulbeccos modified Eagle's medium (DMEM) implemented with 10% heat-inactivated calf serum, 100 U/ml penicillin, 10 μg/ml streptomycin, and 2 mM L-glutamin.
2. Poly-lysin for coating of cover slips (Sigma-Aldrich, Deissenhofen, Germany).
3. Glass cover slips (Langenbrink, Emmendingen, Germany) or from any other supplier.
4. Iodixanol = OptiPrep (Axis-Shield PoC, Oslo, Norway).
5. PBS (18.4 mM Na_2HPO_4, 10.9 mM KH_2PO_4, 125 mM NaCl).
6. Para-formaldehyde (Merk, Darmstadt, Germany).
7. Ammoniumchloride (NH_4Cl) (Merk, Darmstadt, Germany).
8. Triton X-100 (Serva, Heidelberg, Germany).
9. Lamin-B antibody (Santa Cruz Biotechnology, Santa Cruz, California, USA).
10. Bovine serum albumin (Sigma-Aldrich, Deissenhofen, Germany).
11. Fluorescence labeled antibodies (Molecular Probes, Invitrogen, Eugene, Oregon, USA).
12. PermaFluor (Labvision, Fremont, California, USA); alternatively Prolong antifade Gold with DAPI (4′, 6′-diamidino-2phenylindole) (Molecular Probes, Invitrogen, Eugene, Oregon, USA).

3. Methods

3.1. Structure Determination of AAV Virus-Like Particles by X-Ray Crystallography and Cryo-Electron Microscopy

Cloning of recombinant donor plasmid (pFastBac) with AAV cap gene

1. Digest 1 μg of pFastBac with two restriction enzymes from the multiple cloning site in a 50-μL total volume, one enzyme should generate a sticky end and the other enzyme should create a blunt end. (If one enzyme is used, dephosphorylate after digestion using Calf Intestinal Alkaline Phosphotase).
2. Digest 1 μg of the plasmid containing the AAV cap gene with two compatible (or the same as above) restriction enzymes in a 50-μl total volume.
3. Ligate the pFastBac and the cap gene fragments with 1 μl DNA ligase and 1 μl DNA ligase buffer and supplement with water to a final volume of 10 μl.
4. Transform 50 μL competent JM109 cells with 1 μl of ligation mixture to create the recombinant bacmid.
5. Screen the recombinant donor bacmid on gentamicin agar plate and their proper orientation determined by restriction enzyme analysis or by sequencing.

Transposition of DH10 Bac *E. coli* cells

1. Add 5 ng of recombinant donor bacmid to 100 μl of DH10Bac cells in a pre-chilled 15-ml round-bottom polypropylene tube.
2. Gently mix cells and DNA mixture, then incubate on ice for 30 min.
3. Heat shock cell and DNA mixture at 42°C for 45 s then immediately transfer to ice and chill for 2 min.
4. Add 900 μL of S.O.C medium to the newly transformed cells and shake for 4 h at 225 rpm.
5. Serially dilute the transformation mix using S.O.C. (10^{-1}, 10^{-2}, etc) and plate 100 μL of each dilution plated on Luria broth (LB) agar plates containing 50 μg/ml kanamycin, 7 μg/ml gentamicin, 100 μg/ml bluo-gal, and 40 μg/ml IPTG (bluo-gal plates).
6. Incubate the plates for 48 h at 37°C and pick white colonies and re-streak on fresh bluo-gal plates and incubate overnight at 37°C.
7. Use clones picked to inoculate 1 ml LB medium containing 50 μg/ml kanamycin, 7 μg/ml gentamicin with a shaking speed of 250 rpm for 24 h at 37°C. Confirm the clone by restriction digests.

8. Harvest cells in a 1.5 ml microcentrifuge tube by centrifugation for 1 min at 14,000 × *g*.
9. Aspirate supernatant and resuspend cells in 0.3 ml of resuspension buffer (15 mM Tris-HCl pH 8.0; 10 mM EDTA, 100 μg/ml RNase A), mix gently with 0.3 ml of lysis buffer (0.2 M NaOH, 1% SDS), and incubate for 5 min RT.
10. Slowly add 0.3 ml of neutralizing reagent (3 M Potassium acetate pH 5.5) to the contents of the tube and incubate for 10 min. A white fluffy precipitate will form, centrifuge for 10 min at 14,000 × *g*.
11. Collect supernatant and mix with equal volume of isopropanol. Incubate on ice for 10 min. Centrifuge at 14,000 × *g* for 15 min RT.
12. Aspirate supernatant and wash pellet with 0.5 ml of 75% ethanol and centrifuge at 14,000 × *g* for 5 min RT.
13. Air dry pellet and resuspend in 40 μl of Tris–EDTA, pH 8.0, and analyze by agarose gel electrophoresis.

Transfection of sf9 cells

1. Add 1 μg of purified recombinant bacmid DNA to 100 μl unsupplemented Grace's medium and then add to a mixture of cellfectin (6 μl) and unsupplemented Grace's media (100 μl).
2. Incubate the mixture for 45 min RT, and add to six-well tissue culture plates containing 0.5×10^6 Sf9 cells and 0.8 ml of unsupplemented Grace's medium.
3. Allow the cells to incubate for 5 h at RT and then remove the DNA:Cellfectin mix.
4. Add 2 ml of Sf9 medium to the cells and allow to incubate for 72 h. When harvested, this 2 ml of media contains the recombinant bacmids and the sample represents the P1 viral stock.

Baculovirus P1–P3 amplification

1. Infect 10 ml of Sf9 cell suspension at 2×10^6 cells/ml with the P1 stock, at an MOI of 0.1.
2. Incubate the inoculated cells at 27°C for 72 h.
3. Harvest the cells to generate the P2 stock (supernatant).
4. Repeat this procedure to generate infection is repeated to generate 50 ml of a P3 stock, which is used for expression of the VP.

Baculovirus titration: plaque assay

1. Plate a six-well tissue culture dish with 2×10^6 cells in each well and incubate for 1 h.
2. Prepare dilutions of your virus in Sf9 media (10^{-1}, 10^{-2}, 10^{-3}, 10^{-4}, 10^{-5}, 10^{-6}, 10^{-7}, 10^{-8}).

3. At the end of the incubation aspirate the media leaving the cells attached to the plate and add 200 µl of each dilution (10^{-1}, 10^{-2}, 10^{-3}, 10^{-4}, 10^{-5}, 10^{-6}, 10^{-7}, 10^{-8}) of virus.
4. Swirl and flip each plate five times to ensure that cells do not dry out.
5. Incubate plates for 1 h, swirl and flip every 10 min.
6. Aspirate virus from the plates and add 6 ml agar solution (20.5 ml Sf-900 II 1.3× media, 1.65 ml FBS, 0.165 ml Antibiotic and Antimycotic, and 10 ml 4% agar).
7. Allow agar solution to harden (15 min) then add 2 ml of 1× Sf9 media and incubate 72 h at 27°C.
8. Aspirate the medium, add 2 ml of 1:14 neutral red in 1× PBS for 2 h, and leave in the dark O/N RT.
9. Count plaques and calculate titer in the form of pfu/ml, for subsequent infection of Sf9 cells for producing AAV VLPs.

Production and purification of AAV VLPs

1. Infect Sf9 cells grown in Erlenmeyer flasks at 27°C using Sf-900 II medium with a titered recombinant baculovirus stock at a MOI of 5.0 plaque-forming units (PFU) per cell.
2. Harvest the cells at ~72 h post-infection (pi) and spin down at 1,090 × *g*.
3. Resuspend cell pellet in lysis buffer (50 mM Tris–HCl, pH 8.0, 100 mM NaCl, 10 mM $MgCl_2$, 0.2% Triton X-100) at a final concentration of ~1×10^7 cells/ml.
4. Release the VLPs from the cells by three cycles of rapid freeze–thaw in lysis buffer, with the addition of Benzonase (Merck KGaA, Germany) after the second cycle.
5. Clarify the sample by centrifugation at 12,100 × *g* for 15 min at 4°C, discard any resulting pellet.
6. Create a 20% (w/v) sucrose cushion (in 25 mM Tris–HCl pH 8.0, 0.3% Triton X-100, 100 mM NaCl; buffer A) by layering the sucrose solution at the bottom of a sucrose gradient tube containing the clarified cell lysate.
7. Pellet the cell lysate through the 20% sucrose cushion by ultra-centrifugation at 149,000 × *g* for 3 h at 4°C.
8. Quickly discard the supernatant after the spin and resuspend the pellet O/N in ~1 ml of buffer A (with 1 mM EDTA added) at 4°C.
9. Subject the resuspended sample to multiple low-speed spins at 3,000 × *g* to remove insoluble material, as required.
10. Load the clarified supernatant onto a sucrose-step gradient [5–40% (w/v)], prepared by layering ~1.5 ml of sucrose (at 5% percentage steps) into a Beckman ultraclear tube, beginning with the 40% and ending with the 5% fraction at the top.

11. Spin the gradient at 154,693 × *g* for 3 h at 4°C. Extract a visible blue VLP band (illuminated by a light source, and generally located in the 20% sucrose layer) with a needle attached to a syringe.
12. Dialyze the extracted band into 50 mM Tris–HCl pH 8.0, 15 mM NaCl at 4°C to remove sucrose.
13. Check the purity and integrity of the VLPs using SDS–PAGE and negative-stain electron microscopy (EM), respectively. The EM visualization requires specialist microscopy instrumentation. If the sample is not ~95% pure, it has to be re-banded on a second sucrose gradient.
14. Buffer exchange the purified sample into the desired buffer (for example, for AAV1 the buffer is 100 mM HEPES–NaOH pH 7.3, 50 mM $MgCl_2$, 0.03% NaN_3, and 25% glycerol) at 5,000 × *g* using 10-kDa molecular-weight cutoff Amicon Ultra filters and concentrated to a final concentration of ~10 mg/ml for X-ray crystallographic studies or into the same buffer without the glycerol for cryo-EM studies.

Crystallization and structure determination by X-ray crystallography

1. Screen for crystallization conditions using the hanging drop vapor diffusion method with VDX 24-well Limbro plates and siliconized cover slips: Grease the top of the each well of the Limbro plate with immersion oil and put 1.0 ml of reservoir (precipitant) solution (e.g. 100 mM HEPES-NAOH pH 7.3, 50 mM MgCL2, 0.03% NaN3, and 25% glycerol, 1.0 M NaCl, 5% PEG 6K for AAV1) into each well. Apply 2-5 ul of the virus sample to the cover slip, mix with 2-5 ul of the reservoir solution, and suspend over the 1.0 ml of the reservoir solution in the well of the Limbro plate. Store at RT. Can screen a range of NaCl and PEG conditions.
2. Manually select crystals obtained at RT with a cryo-loop and flash-cool to −173°C in a liquid-nitrogen stream prior to data collection. Note: Additional cryo-protectant solution is not necessary if the crystals are grown in the presence of 25% glycerol (as was done for example of AAV1 given above). If crystals were grown without cryo-protectant, this has to be added before freezing. If data collection is not done immediately or if the crystals are to be transported, the frozen crystal is stored in a cryo-vial filled with liquid nitrogen and stored in a liquid nitrogen dewar.
3. X-ray diffraction data collection: This requires specialist instrumentation, which is not available in most laboratories. For the AAV VLPs, X-ray diffraction images are collected at synchrotron sources, such as the Advanced Photon Source (APS), Argonne National Laboratory on beamline 22-ID with a wavelength of 1.0 Å using a MAR300 CCD detector. A crystal-to-detector distance of 400 mm is used to record 0.3° oscillation images with an exposure time of 5 s per image.

4. Observed diffraction intensities (a diffraction pattern collected in the images) are indexed, integrated, scaled, and merged using the HKL-2000 suite of programs. This program provides information on the space group in which the VLPs are crystallized. A file containing indexed reflections, their intensities (amplitudes), and the error associated with each measured reflection is the output from HKL2000 and is used for subsequent steps in the structure determination procedure.
5. The structure is determined by a procedure referred to as molecular replacement, which uses phase information from a known structure, and involves the determination of the orientation and position of the viral capsid in the crystal unit cell. These experimental methods require specialist training in X-ray crystallography.
6. Based on the space group of AAV1 (as an example), R32, a model consisting of ten AAV4 VP3 alanine chains is used as a search model for molecular replacement phasing in the CCP4 program AMoRe. This program calculates a cross-rotation function between the search model (in this case AAV4) and the unknown data (AAV1) and a translation function, which provides angular information for rotating the search model (e.g. AAV4) into the orientation of the unknown AAV data and positioning it in the crystal unit cell, respectively.
7. The molecular replacement procedure is followed by refinement of the model, with respect to the observed data (structure factors) using the program CNS, and then alternating cycles of map calculation for manual rebuilding of the model for a better fit into the density, using the program Coot, and further refinement (in CNS), constraint by non-crystallographic symmetry (NCS, icosahedral symmetry) operators.
8. The X-ray crystallographic structure determination is complete when there is no further improvement in the refinement statistics, which compares the model to the observed structure factor data.

Vitrification and structure determination by cryo-electron microscopy and image reconstruction

1. Vitrify 3.5–5 μl of sample with an automated or manual plunge freezing device either on grids with Quantifoil Holey carbon films or on grids with continuous carbon films.
2. Examine the sample at −193°C on cryo-electron microscope, such as an FEI Tecnai G² Polara electron microscope, at an accelerating voltage of 200 keV and a nominal magnification of 59,000×. This instrumentation is only available in specialist labs, and the AAV VLP studies have been done in collaboration with Dr. Timothy Baker, UCSD.

3. Record images with a Gatan Ultrascan 4000 CCD camera at a step size of 1.883 Å/pixel.
4. Record the images with an objective lens under focus value of 1.25–3.0 μm. The total electron dose on each image is generally in the range of ~24–28 $e^-/Å^2$.
5. Save the CCD images in a Gatan DM3 format and later convert to the tiff format for analysis.
6. Extract each particle image from the micrograph using the RobEM software package (http://cryoEM.ucsd.edu/programs.shtm). This package is also used to normalize the micrographs as well as estimate their defocus levels.
7. Generate a starting model at ~30 Å resolution from ~150 particle images for the structure determination using a random-model computation procedure.
8. Use this starting model to initiate full orientation and origin determinations and refinement of the entire set of particle images using the current version of AUTO3DEM. Corrections to compensate for the effects of phase reversals in the contrast-transfer functions of the images are performed followed by a reconstruction of a 3D map from the selected particle images.
9. Make an estimate of the resolution of the reconstruction (resolution ranges of 10–15 Å have been obtained for the AAVs) using a 0.5 threshold of the Fourier Shell Correlation (FSC0.5) criterion.
10. Determine the handedness of the map by comparison of the surface features with those of other AAV structures determined by X-ray crystallography.
11. Build a pseudo-atomic model into the cryo-EM reconstructed density map, based on sequence comparison of the serotype under study with available AAV structures, and dock the model into the density map for interpretation of the internal and surface features of the capsid.

3.2. Subcellular Localization of AAV Virus/Vector Particles During Infection

1. Seed HeLa cells (6×10^4/well) in 24-well plates containing (optionally poly-L-lysin coated) 10-mm glass cover slips.
2. After 24 h, incubate the cells for 45 min at 4°C with 5×10^5 viral (or vector) particles (iodixanol step gradient purified)/cell (equivalent to approximately 5×10^4 genome containing particles/cell) in serum-free medium. Thereafter wash the cells three times in cold medium and continue incubation in complete medium at 37°C. Alternatively, infect cells at 37°C without the cell binding step at 4°C.

Table 5
Available monoclonal anti-AAV capsid[a] antibodies suitable for immunofluorescence analysis

Antibody	AAV serotype	References
ADK1a, ADK1b	AAV1	(194)
A20, C24, C37	AAV2	(154, 193)
A20, C24	AAV3	(154, 193)
ADK4	AAV4	(194)
ADK5a, ADK5b, C24	AAV5	(193, 194)
ADK1a, ADK1b, ADK6	AAV6	(194, unpublished)
ADK8, ADK8/9	AAV8	unpublished
ADK9, (ADK8/9)	AAV8	unpublished

[a]Although these antibodies detect AAV capsids (e.g. during capsid formation), only A20 has so far been used for localization of AAV particles during infection

3. At desired time points post infection, wash the cells three times with PBS and fix them with 2% para-formaldehyde (PFA) for 15 min at room temperature.
4. Quench non-reacted PFA by two incubations with 50 mM NH_4Cl for 5 min, then permeabilize cell membranes with 0.2% Triton X-100 in PBS for 10 min.
5. Following three washes with PBS, incubate the cells with primary antibodies directed against AAV capsids (Table 5) and optionally with an antibody that visualizes cellular structures, for example the nucleus (e.g. Lamin B) overnight at 4°C at appropriate dilutions in PBS containing 1% bovine serum albumin.
6. The following day, wash cells three times with PBS and incubate for 1 h with secondary antibodies (e.g. chicken anti-mouse Alexa 594 to react with AAV capsid antibodies and chicken anti-goat Alexa 488 to react with antibodies directed against cellular structures) at dilutions recommended by the manufacturer.
7. After further six washes in PBS, mount cover slips cell side down on glass slides with Permafluor or Prolong antifade Gold with DAPI.
8. Take confocal images of 0.3 μm optical sections with a laser scanning microscope (e.g. Zeiss LSM 510 META). Images can further be processed using a deconvolution module (e.g. of the Zeiss software) and Adobe Photoshop.

4. Notes

The AAV capsid is built on a simple design, a $T=1$ icosahedral capsid, assembled from essentially 60 copies of a single VP sequence, with a fraction of these containing conserved unique regions functionalized for specific activities, such as the ~5 copies of the VP1u with its PLA2 domain. While many aspects of the AAV–cellular host interactions require further study, there is a wealth of information that show that the AAV VPs assemble a multifunctional capsid that is capable of engaging in the myriad of cellular interactions required for successful host infection. The requirement for high fidelity of capsid assembly is evident in the conserved structural core of the AAV serotype capsid and the detrimental effect of mutations at monomer–monomer interfaces and secondary structure elements (Figs. 1 and 4a). The requirement for genome packaging efficiency has also been encoded on surface amino acids, which likely contact the Rep-packing machinery (Fig. 4b). The need to occupy a specific host cellular niche is satisfied by the evolution of variable loops conferring the individual capsid surface topologies, which together with sequence differences, have been reported to play essential roles in cellular receptor recognition and determination of transduction efficiency in different host cells (Table 1). These variable loops are also targets of the host immune antibody response (Table 1) and as such have the potential to be artificially evolved to escape recognition in vector development.

This chapter has mostly focused on sequence and structural annotation of AAV2 VP/capsid function because this serotype is the best characterized in terms of basic biology. Significantly, the availability of a structural library for most of the other representative members of AAV antigenic clades now provides a platform for similar annotations of the other serotypes as basic biology information related to their cellular infection pathway becomes available.

The final section provides a rudimentary description of the approaches used for structural analysis and a protocol for subcellular localization of AAV particles during infection. The reader is directed to the references in the preceding sections for more detail.

Acknowledgments

The authors would like to thank Lakshmanan Govindasamy and Brittney L. Gurda for help in generating Figures 1–5, Antonette Bennett for providing information on baculovirus expression of AAV VLPs, and Britta Gerlach and Bettina Böttcher for providing unpublished data. NIH project R01 GM082946 to MA-M is also acknowledged for support.

References

1. Gao, G., Vandenberghe, L. H., Alvira, M. R., Lu, Y., Calcedo, R., Zhou, X., and Wilson, J. M. (2004) Clades of Adeno-associated viruses are widely disseminated in human tissues, *J Virol* ***78***, 6381–6388.
2. Gao, G. P., Alvira, M. R., Wang, L., Calcedo, R., Johnston, J., and Wilson, J. M. (2002) Novel adeno-associated viruses from rhesus monkeys as vectors for human gene therapy, *Proc Natl Acad Sci USA* ***99***, 11854–11859.
3. Mori, S., Wang, L., Takeuchi, T., and Kanda, T. (2004) Two novel adeno-associated viruses from cynomolgus monkey: pseudotyping characterization of capsid protein, *Virology* ***330***, 375–383.
4. Schmidt, M., Govindasamy, L., Afione, S., Kaludov, N., Agbandje-McKenna, M., and Chiorini, J. A. (2008) Molecular characterization of the heparin-dependent transduction domain on the capsid of a novel adeno-associated virus isolate, AAV(VR-942), *J Virol* ***82***, 8911–8916.
5. Schmidt, M., Voutetakis, A., Afione, S., Zheng, C., Mandikian, D., and Chiorini, J. A. (2008) Adeno-associated virus type 12 (AAV12): a novel AAV serotype with sialic acid- and heparan sulfate proteoglycan-independent transduction activity, *J Virol* ***82***, 1399–1406.
6. Chapman, M. S., and Agbandje-McKenna, M. (2006) Atomic structure if viral particles., in *Parvoviruses* (Kerr, J. R., Cotmore, S. F., Bloom, M. E., Linden, R. M., and Parrish, C. R., Eds.), pp 107–123, Edward Aenold Ltd. New York, New York.
7. McLaughlin, S. K., Collis, P., Hermonat, P. L., and Muzyczka, N. (1988) Adeno-associated virus general transduction vectors: analysis of proviral structures, *J Virol* ***62***, 1963–1973.
8. Samulski, R. J., Srivastava, A., Berns, K. I., and Muzyczka, N. (1983) Rescue of adeno-associated virus from recombinant plasmids: gene correction within the terminal repeats of AAV, *Cell* ***33***, 135–143.
9. Senapathy, P., Tratschin, J. D., and Carter, B. J. (1984) Replication of adeno-associated virus DNA. Complementation of naturally occurring rep-mutants by a wild-type genome or an ori-mutant and correction of terminal palindrome deletions, *J Mol Biol* ***179***, 1–20.
10. Samulski, R. J., Chang, L.-S., and Shenk, T. (1987) A recombinant plasmid from which an infectious adeno-associated virus genome can be excised in vitro and its use to study viral replication, *J Virol* ***61***, 3096–3101.
11. Hermonat, P. L., and Muzyczka, N. (1984) Use of adeno-associated virus as a mammalian DNA cloning vector: transduction of neomycin resistance into mammalian tissue culture cells, *Proc Natl Acad Sci USA* ***81***, 6466–6470.
12. Samulski, R. J., Sally, M., and Muzyczka, N. (1988) Adeno-associated viral vectors., in *Cold Spring Harbor*, Cold Spring Harbor Laboraory Press, NY., Cold Spring Harbor.
13. Hauck, B., Chen, L., and Xiao, W. (2003) Generation and characterization of chimeric recombinant AAV vectors, *Mol Ther 7*, 419–425.
14. Hauck, B., and Xiao, W. (2003) Characterization of tissue tropism determinants of adeno-associated virus type 1, *J Virol 77*, 2768–2774.
15. Hildinger, M., Auricchio, A., Gao, G., Wang, L., Chirmule, N., and Wilson, J. M. (2001) Hybrid vectors based on adeno-associated virus serotypes 2 and 5 for muscle-directed gene transfer, *J Virol 75*, 6199–6203.
16. Rabinowitz, J. E., Rolling, F., Li, C., Conrath, H., Xiao, W., Xiao, X., and Samulski, R. J. (2002) Cross-packaging of a single adeno-associated virus (AAV) type 2 vector genome into multiple AAV serotypes enables transduction with broad specificity, *J Virol 76*, 791–801.
17. Rabinowitz, J. E., Bowles, D. E., Faust, S. M., Ledford, J. G., Cunningham, S. E., and Samulski, R. J. (2004) Cross-dressing the virion: the transcapsidation of adeno-associated virus serotypes functionally defines subgroups, *J Virol 78*, 4421–4432.
18. DiMattia, M., Govindasamy, L., Levy, H. C., Gurda-Whitaker, B., Kalina, A., Kohlbrenner, E., Chiorini, J. A., McKenna, R., Muzyczka, N., Zolotukhin, S., and Agbandje-McKenna, M. (2005) Production, purification, crystallization and preliminary X-ray structural studies of adeno-associated virus serotype 5, *Acta Crystallogr Sect F Struct Biol Cryst Commun* ***61***, 917–921.
19. Kaludov, N., Padron, E., Govindasamy, L., McKenna, R., Chiorini, J. A., and Agbandje-McKenna, M. (2003) Production, purification and preliminary X-ray crystallographic studies of adeno-associated virus serotype 4, *Virology* ***306***, 1–6.
20. Mitchell, M., Nam, H. J., Carter, A., McCall, A., Rence, C., Bennett, A., Gurda, B., McKenna, R., Porter, M., Sakai, Y., Byrne, B. J., Muzyczka, N., Aslanidi, G., Zolotukhin, S., and Agbandje-McKenna, M. (2009) Production, purification and preliminary X-ray crystallographic studies of adeno-associated virus

serotype 9, *Acta Crystallogr Sect F Struct Biol Cryst Commun* ***65***, 715–718.

21. Miller, E. B., Gurda-Whitaker, B., Govindasamy, L., McKenna, R., Zolotukhin, S., Muzyczka, N., and Agbandje-McKenna, M. (2006) Production, purification and preliminary X-ray crystallographic studies of adeno-associated virus serotype 1, *Acta Crystallogr Sect F Struct Biol Cryst Commun* ***62***, 1271–1274.
22. Quesada, O., Gurda, B., Govindasamy, L., McKenna, R., Kohlbrenner, E., Aslanidi, G., Zolotukhin, S., Muzyczka, N., and Agbandje-McKenna, M. (2007) Production, purification and preliminary X-ray crystallographic studies of adeno-associated virus serotype 7, *Acta Crystallogr Sect F Struct Biol Cryst Commun* ***63***, 1073–1076.
23. Lane, M. D., Nam, H. J., Padron, E., Gurda-Whitaker, B., Kohlbrenner, E., Aslanidi, G., Byrne, B., McKenna, R., Muzyczka, N., Zolotukhin, S., and Agbandje-McKenna, M. (2005) Production, purification, crystallization and preliminary X-ray analysis of adeno-associated virus serotype 8, *Acta Crystallogr Sect F Struct Biol Cryst Commun* ***61***, 558–561.
24. Govindasamy, L., Padron, E., McKenna, R., Muzyczka, N., Kaludov, N., Chiorini, J. A., and Agbandje-McKenna, M. (2006) Structurally mapping the diverse phenotype of adeno-associated virus serotype 4, *J Virol* ***80***, 11556–11570.
25. Nam, H. J., Lane, M. D., Padron, E., Gurda, B., McKenna, R., Kohlbrenner, E., Aslanidi, G., Byrne, B., Muzyczka, N., Zolotukhin, S., and Agbandje-McKenna, M. (2007) Structure of adeno-associated virus serotype 8, a gene therapy vector, *J Virol* ***81***, 12260–12271.
26. Xie, Q., Bu, W., Bhatia, S., Hare, J., Somasundaram, T., Azzi, A., and Chapman, M. S. (2002) The atomic structure of adeno-associated virus (AAV-2), a vector for human gene therapy, *Proc Natl Acad Sci U S A* ***99***, 10405–10410.
27. O'Donnell, J., Taylor, K. A., and Chapman, M. S. (2009) Adeno-associated virus-2 and its primary cellular receptor – Cryo-EM structure of a heparin complex, *Virology* ***385***, 434–443.
28. Lerch, T. F., Xie, Q., Ongley, H. M., Hare, J., and Chapman, M. S. (2009) Twinned crystals of adeno-associated virus serotype 3b prove suitable for structural studies, *Acta Crystallogr Sect F Struct Biol Cryst Commun* ***65***, 177–183.
29. Xie, Q., Ongley, H. M., Hare, J., and Chapman, M. S. (2008) Crystallization and preliminary X-ray structural studies of adeno-associated virus serotype 6, *Acta Crystallogr Sect F Struct Biol Cryst Commun* ***64***, 1074–1078.
30. Padron, E., Bowman, V., Kaludov, N., Govindasamy, L., Levy, H., Nick, P., McKenna, R., Muzyczka, N., Chiorini, J. A., Baker, T. S., and Agbandje-McKenna, M. (2005) Structure of adeno-associated virus type 4, *J Virol* ***79***, 5047–5058.
31. Walters, R. W., Agbandje-McKenna, M., Bowman, V. D., Moninger, T. O., Olson, N. H., Seiler, M., Chiorini, J. A., Baker, T. S., and Zabner, J. (2004) Structure of adeno-associated virus serotype 5, *J Virol* ***78***, 3361–3371.
32. Levy, H. C., Bowman, V. D., Govindasamy, L., McKenna, R., Nash, K., Warrington, K., Chen, W., Muzyczka, N., Yan, X., Baker, T. S., and Agbandje-McKenna, M. (2009) Heparin binding induces conformational changes in Adeno-associated virus serotype 2, *J Struct Biol* ***165***, 146–156.
33. Kronenberg, S., Bottcher, B., von der Lieth, C. W., Bleker, S., and Kleinschmidt, J. A. (2005) A conformational change in the adeno-associated virus type 2 capsid leads to the exposure of hidden VP1 N termini, *J Virol* ***79***, 5296–5303.
34. Kronenberg, S., Kleinschmidt, J. A., and Bottcher, B. (2001) Electron cryo-microscopy and image reconstruction of adeno-associated virus type 2 empty capsids, *EMBO Rep* ***2***, 997–1002.
35. Lerch, T. F., Xie, Q., and Chapman, M. S. (2010) The structure of adeno-associated virus serotype 3B (AAV-3B): insights into receptor binding and immune evasion, *Virology*, *403*, 26–36.
36. Robert, N. G., Govindasamy, L., Gurda, B. L., McKenna, R., Kozyreva, O. G., Samulski, R. J., Parent, K. N., Baker, T. S., and Agbandje-McKenna, M. (2010) Structural Characterization of the Dual Glycan Binding Adeno-Associated Virus Serotype 6, *J Virol.* *84*, 12945–12957.
37. Bleker, S., Sonntag, F., and Kleinschmidt, J. A. (2005) Mutational analysis of narrow pores at the fivefold symmetry axes of adeno-associated virus type 2 capsids reveals a dual role in genome packaging and activation of phospholipase A2 activity, *J Virol* ***79***, 2528–2540.
38. Gerlach, B., Kleinschmidt, J. A., Böttcher, B. (2011) Conformational changes in adeno-associated virus type 1 induced by genome packaging, *JMB*, *409*(3), 427–438 and unpublished results.
39. Kaufmann, B., Simpson, A. A., and Rossmann, M. G. (2004) The structure of human parvovirus B19, *Proc Natl Acad Sci USA* ***101***, 11628–11633.

40. Farr, G. A., Cotmore, S. F., and Tattersall, P. (2006) VP2 cleavage and the leucine ring at the base of the fivefold cylinder control pH-dependent externalization of both the VP1 N terminus and the genome of minute virus of mice, *J Virol* ***80***, 161–171.
41. Farr, G. A., and Tattersall, P. (2004) A conserved leucine that constricts the pore through the capsid fivefold cylinder plays a central role in parvoviral infection, *Virology* ***323***, 243–256.
42. Farr, G. A., Zhang, L. G., and Tattersall, P. (2005) Parvoviral virions deploy a capsid-tethered lipolytic enzyme to breach the endosomal membrane during cell entry, *Proc Natl Acad Sci U S A* ***102***, 17148–17153.
43. Sonntag, F., Bleker, S., Leuchs, B., Fischer, R., and Kleinschmidt, J. A. (2006) Adeno-associated virus type 2 capsids with externalized VP1/VP2 trafficking domains are generated prior to passage through the cytoplasm and are maintained until uncoating occurs in the nucleus, *J Virol* ***80***, 11040–11054.
44. Mani, B., Baltzer, C., Valle, N., Almendral, J. M., Kempf, C., and Ros, C. (2006) Low pH-dependent endosomal processing of the incoming parvovirus minute virus of mice virion leads to externalization of the VP1 N-terminal sequence (N-VP1), N-VP2 cleavage, and uncoating of the full-length genome, *J Virol* ***80***, 1015–1024.
45. Girod, A., Wobus, C. E., Zadori, Z., Ried, M., Leike, K., Tijssen, P., Kleinschmidt, J. A., and Hallek, M. (2002) The VP1 capsid protein of adeno-associated virus type 2 is carrying a phospholipase A2 domain required for virus infectivity, *J Gen Virol* ***83***, 973–978.
46. Zadori, Z., Szelei, J., Lacoste, M. C., Li, Y., Gariepy, S., Raymond, P., Allaire, M., Nabi, I. R., and Tijssen, P. (2001) A viral phospholipase A2 is required for parvovirus infectivity, *Dev Cell* ***1***, 291–302.
47. Kontou, M., Govindasamy, L., Nam, H. J., Bryant, N., Llamas-Saiz, A. L., Foces-Foces, C., Hernando, E., Rubio, M. P., McKenna, R., Almendral, J. M., and Agbandje-McKenna, M. (2005) Structural determinants of tissue tropism and in vivo pathogenicity for the parvovirus minute virus of mice, *J Virol 79*, 10931–10943.
48. Bennett, A., McKenna, R., and Agbandje-McKenna, M. (2008) A comparative analysis of the structural architecture of ssDNA viruses, *Computational and Mathematical Methods in Medicine* ***Vol. 9***, 183–196.
49. Summerford, C., and Samulski, R. J. (1998) Membrane-associated heparan sulfate proteoglycan is a receptor for adeno-associated virus type 2 virions, *J Virol 72*, 1438–1445.
50. Chen, S., Kapturczak, M., Loiler, S. A., Zolotukhin, S., Glushakova, O. Y., Madsen, K. M., Samulski, R. J., Hauswirth, W. W., Campbell-Thompson, M., Berns, K. I., Flotte, T. R., Atkinson, M. A., Tisher, C. C., and Agarwal, A. (2005) Efficient transduction of vascular endothelial cells with recombinant adeno-associated virus serotype 1 and 5 vectors, *Hum Gene Ther* ***16***, 235–247.
51. Wu, Z., Miller, E., Agbandje-McKenna, M., and Samulski, R. J. (2006) Alpha2,3 and alpha2,6 N-linked sialic acids facilitate efficient binding and transduction by adeno-associated virus types 1 and 6, *J Virol* ***80***, 9093–9103.
52. Kaludov, N., Brown, K. E., Walters, R. W., Zabner, J., and Chiorini, J. A. (2001) Adeno-associated virus serotype 4 (AAV4) and AAV5 both require sialic acid binding for hemagglutination and efficient transduction but differ in sialic acid linkage specificity, *J Virol 75*, 6884–6893.
53. Walters, R. W., Yi, S. M., Keshavjee, S., Brown, K. E., Welsh, M. J., Chiorini, J. A., and Zabner, J. (2001) Binding of adeno-associated virus type 5 to 2,3-linked sialic acid is required for gene transfer, *J Biol Chem* ***276***, 20610–20616.
54. Di Pasquale, G., Davidson, B. L., Stein, C. S., Martins, I., Scudiero, D., Monks, A., and Chiorini, J. A. (2003) Identification of PDGFR as a receptor for AAV-5 transduction, *Nat Med* ***9***, 1306–1312.
55. Wu, Z., Asokan, A., Grieger, J. C., Govindasamy, L., Agbandje-McKenna, M., and Samulski, R. J. (2006) Single amino acid changes can influence titer, heparin binding, and tissue tropism in different adeno-associated virus serotypes, *J Virol* ***80***, 11393–11397.
56. Shen, S., Brown, S. M., Randell, S. H., Asokan, A. Terminal N-Linked Galactose Is the Primary Receptor for Adeno-associated Virus 9. *J Biological Chemistry*, *286*, 13532–13540.
57. Bell, C. L., Vandenberghe, L. H., Bell, P., Limberis, M. P., Gao, G.-P., Vliet, K. V., Agbandje-McKenna, M., and Wilson, J. M. (2011) The AAV9 receptor and its modification to improve in vivo lung gene transfer in mice, *J Clin Invest*, *121*(6), 2427–2435.
58. Agbandje-McKenna, M., and Chapman, M. S. (2006) Correlating structure with function in the viral capsid, in *Parvoviruses* (Kerr, J. R., Cotmore, S. F., Bloom, M. E., Linden, R. M.,

and Parrish, C. R., Eds.), Edward Arnold, New York, New York.

59. Lopez-Bueno, A., Rubio, M. P., Bryant, N., McKenna, R., Agbandje-McKenna, M., and Almendral, J. M. (2006) Host-selected amino acid changes at the sialic acid binding pocket of the parvovirus capsid modulate cell binding affinity and determine virulence, *J Virol* ***80***, 1563–1573.
60. Govindasamy, L., Hueffer, K., Parrish, C. R., and Agbandje-McKenna, M. (2003) Structures of host range-controlling regions of the capsids of canine and feline parvoviruses and mutants, *J Virol 77*, 12211–12221.
61. Hueffer, K., Govindasamy, L., Agbandje-McKenna, M., and Parrish, C. R. (2003) Combinations of two capsid regions controlling canine host range determine canine transferrin receptor binding by canine and feline parvoviruses, *J Virol 77*, 10099–10105.
62. Hafenstein, S., Palermo, L. M., Kostyuchenko, V. A., Xiao, C., Morais, M. C., Nelson, C. D., Bowman, V. D., Battisti, A. J., Chipman, P. R., Parrish, C. R., and Rossmann, M. G. (2007) Asymmetric binding of transferrin receptor to parvovirus capsids, *Proc Natl Acad Sci U S A* ***104***, 6585–6589.
63. Chipman, P. R., Agbandje-McKenna, M., Kajigaya, S., Brown, K. E., Young, N. S., Baker, T. S., and Rossmann, M. G. (1996) Cryo-electron microscopy studies of empty capsids of human parvovirus B19 complexed with its cellular receptor, *Proc Natl Acad Sci U S A* ***93***, 7502–7506.
64. Kern, A., Schmidt, K., Leder, C., Muller, O. J., Wobus, C. E., Bettinger, K., Von der Lieth, C. W., King, J. A., and Kleinschmidt, J. A. (2003) Identification of a heparin-binding motif on adeno-associated virus type 2 capsids, *J Virol 77*, 11072–11081.
65. Lochrie, M. A., Tatsuno, G. P., Christie, B., McDonnell, J. W., Zhou, S., Surosky, R., Pierce, G. F., and Colosi, P. (2006) Mutations on the external surfaces of adeno-associated virus type 2 capsids that affect transduction and neutralization, *J Virol* ***80***, 821–834.
66. Opie, S. R., Warrington, K. H., Jr., Agbandje-McKenna, M., Zolotukhin, S., and Muzyczka, N. (2003) Identification of amino acid residues in the capsid proteins of adeno-associated virus type 2 that contribute to heparan sulfate proteoglycan binding, *J Virol 77*, 6995–7006.
67. Wu, P., Xiao, W., Conlon, T., Hughes, J., Agbandje-McKenna, M., Ferkol, T., Flotte, T., and Muzyczka, N. (2000) Mutational analysis of the adeno-associated virus type 2 (AAV2) capsid gene and construction of AAV2 vectors with altered tropism, *J Virol 74*, 8635–8647.
68. Chen, C. L., Jensen, R. L., Schnepp, B. C., Connell, M. J., Shell, R., Sferra, T. J., Bartlett, J. S., Clark, K. R., and Johnson, P. R. (2005) Molecular characterization of adeno-associated viruses infecting children, *J Virol 79*, 14781–14792.
69. Qing, K., Mah, C., Hansen, J., Zhou, S., Dwarki, V., and Srivastava, A. (1999) Human fibroblast growth factor receptor 1 is a co-receptor for infection by adeno-associated virus 2, *Nat Med* ***5***, 71–77.
70. Kashiwakura, Y., Tamayose, K., Iwabuchi, K., Hirai, Y., Shimada, T., Matsumoto, K., Nakamura, T., Watanabe, M., Oshimi, K., and Daida, H. (2005) Hepatocyte growth factor receptor is a coreceptor for adeno-associated virus type 2 infection, *J Virol 79*, 609–614.
71. Akache, B., Grimm, D., Pandey, K., Yant, S. R., Xu, H., and Kay, M. A. (2006) The 37/67-kilodalton laminin receptor is a receptor for adeno-associated virus serotypes 8, 2, 3, and 9, *J Virol* ***80***, 9831–9836.
72. Summerford, C., Bartlett, J. S., and Samulski, R. J. (1999) AlphaVbeta5 integrin: a co-receptor for adeno-associated virus type 2 infection, *Nat Med* ***5***, 78–82.
73. Asokan, A., Hamra, J. B., Govindasamy, L., Agbandje-McKenna, M., and Samulski, R. J. (2006) Adeno-associated virus type 2 contains an integrin alpha5beta1 binding domain essential for viral cell entry, *J Virol* ***80***, 8961–8969.
74. Duan, D., Li, Q., Kao, A. W., Yue, Y., Pessin, J. E., and Engelhardt, J. F. (1999) Dynamin is required for recombinant adeno-associated virus type 2 infection, *J Virol 73*, 10371–10376.
75. Bartlett, J. S., Wilcher, R., and Samulski, R. J. (2000) Infectious entry pathway of adeno-associated virus and adeno-associated virus vectors, *J Virol 74*, 2777–2785.
76. Bantel-Schaal, U., Hub, B., and Kartenbeck, J. (2002) Endocytosis of adeno-associated virus type 5 leads to accumulation of virus particles in the Golgi compartment, *J Virol 76*, 2340–2349.
77. Bantel-Schaal, U., Braspenning-Wesch, I., and Kartenbeck, J. (2009) Adeno-associated virus type 5 exploits two different entry pathways in human embryo fibroblasts, *J Gen Virol* ***90***, 317–322.
78. Seisenberger, G., Ried, M. U., Endress, T., Buning, H., Hallek, M., and Brauchle, C. (2001) Real-time single-molecule imaging of

the infection pathway of an adeno-associated virus, *Science* ***294***, 1929–1932.

79. Duan, D., Yue, Y., Yan, Z., Yang, J., and Engelhardt, J. F. (2000) Endosomal processing limits gene transfer to polarized airway epithelia by adeno-associated virus, *J Clin Invest* ***105***, 1573–1587.
80. Sanlioglu, S., Benson, P. K., Yang, J., Atkinson, E. M., Reynolds, T., and Engelhardt, J. F. (2000) Endocytosis and nuclear trafficking of adeno-associated virus type 2 are controlled by rac1 and phosphatidylinositol-3 kinase activation, *J Virol* ***74***, 9184–9196.
81. Qiu, J., and Brown, K. E. (1999) A 110-kDa nuclear shuttle protein, nucleolin, specifically binds to adeno-associated virus type 2 (AAV-2) capsid, *Virology* ***257***, 373–382.
82. Hansen, J., Qing, K., Kwon, H. J., Mah, C., and Srivastava, A. (2000) Impaired intracellular trafficking of adeno-associated virus type 2 vectors limits efficient transduction of murine fibroblasts, *J Virol* ***74***, 992–996.
83. Hansen, J., Qing, K., and Srivastava, A. (2001) Adeno-associated virus type 2-mediated gene transfer: altered endocytic processing enhances transduction efficiency in murine fibroblasts, *J Virol* ***75***, 4080–4090.
84. Hauck, B., Zhao, W., High, K., and Xiao, W. (2004) Intracellular viral processing, not single-stranded DNA accumulation, is crucial for recombinant adeno-associated virus transduction, *J Virol* ***78***, 13678–13686.
85. Ding, W., Zhang, L. N., Yeaman, C., and Engelhardt, J. F. (2006) rAAV2 traffics through both the late and the recycling endosomes in a dose-dependent fashion, *Mol Ther* ***13***, 671–682.
86. Ding, W., Zhang, L., Yan, Z., and Engelhardt, J. F. (2005) Intracellular trafficking of adeno-associated viral vectors, *Gene Ther* ***12***, 873–880.
87. Douar, A. M., Poulard, K., Stockholm, D., and Danos, O. (2001) Intracellular trafficking of adeno-associated virus vectors: routing to the late endosomal compartment and proteasome degradation, *J Virol* ***75***, 1824–1833.
88. Hansen, J., Qing, K., and Srivastava, A. (2001) Adeno-associated virus type 2-mediated gene transfer: altered endocytic processing enhances transduction efficiency in murine fibroblasts, *J Virol* ***75***, 4080–4090.
89. Xiao, W., Warrington, K. H., Jr., Hearing, P., Hughes, J., and Muzyczka, N. (2002) Adenovirus-facilitated nuclear translocation of adeno-associated virus type 2, *J Virol* ***76***, 11505–11517.
90. Pajusola, K., Gruchala, M., Joch, H., Luscher, T. F., Yla-Herttuala, S., and Bueler, H. (2002) Cell-type-specific characteristics modulate the transduction efficiency of adeno-associated virus type 2 and restrain infection of endothelial cells, *J Virol* ***76***, 11530–11540.
91. Akache, B., Grimm, D., Shen, X., Fuess, S., Yant, S. R., Glazer, D. S., Park, J., and Kay, M. A. (2007) A two-hybrid screen identifies cathepsins B and L as uncoating factors for adeno-associated virus 2 and 8, *Mol Ther* ***15***, 330–339.
92. Suikkanen, S., Antila, M., Jaatinen, A., Vihinen-Ranta, M., and Vuento, M. (2003) Release of canine parvovirus from endocytic vesicles, *Virology* ***316***, 267–280.
93. Stahnke, S., Lux, K., Uhrig, S., Kreppel, F., Hösel, M., Coutelle, O., Ogris, M., Hallek, M., and Büning, H. (2011) Intrinsic phospholipase A2 activity of adeno-associated virus is involved in endosomal escape of incoming particles, *Virology* ***409***, 77–83. Epub 2010 Oct 25.
94. Murphy, S. L., Bhagwat, A., Edmonson, S., Zhou, S., and High, K. A. (2008) High-throughput screening and biophysical interrogation of hepatotropic AAV, *Mol Ther* ***16***, 1960–1967.
95. Agbandje-McKenna, M., Llamas-Saiz, A. L., Wang, F., Tattersall, P., and Rossmann, M. G. (1998) Functional implications of the structure of the murine parvovirus, minute virus of mice, *Structure* ***6***, 1369–1381.
96. Tsao, J., Chapman, M. S., Agbandje, M., Keller, W., Smith, K., Wu, H., Luo, M., Smith, T. J., Rossmann, M. G., Compans, R. W., and et al. (1991) The three-dimensional structure of canine parvovirus and its functional implications, *Science* ***251***, 1456–1464.
97. Xie, Q., and Chapman, M. S. (1996) Canine parvovirus capsid structure, analyzed at 2.9 A resolution, *J Mol Biol* ***264***, 497–520.
98. Grieger, J. C., Johnson, J. S., Gurda-Whitaker, B., Agbandje-McKenna, M., and Samulski, R. J. (2007) Surface-exposed adeno-associated virus Vp1-NLS capsid fusion protein rescues infectivity of noninfectious wild-type Vp2/Vp3 and Vp3-only capsids but not that of fivefold pore mutant virions, *J Virol* ***81***, 7833–7843.
99. DiPrimio, N., Asokan, A., Govindasamy, L., Agbandje-McKenna, M., and Samulski, R. J. (2008) Surface loop dynamics in adeno-associated virus capsid assembly, *J Virol* ***82***, 5178–5189.
100. Yan, Z., Zak, R., Luxton, G. W., Ritchie, T. C., Bantel-Schaal, U., and Engelhardt, J. F.

(2002) Ubiquitination of both adeno-associated virus type 2 and 5 capsid proteins affects the transduction efficiency of recombinant vectors, *J Virol* ***76***, 2043–2053.

101. Ding, W., Yan, Z., Zak, R., Saavedra, M., Rodman, D. M., and Engelhardt, J. F. (2003) Second-strand genome conversion of adeno-associated virus type 2 (AAV-2) and AAV-5 is not rate limiting following apical infection of polarized human airway epithelia, *J Virol 77*, 7361–7366.
102. Yan, Z., Zak, R., Zhang, Y., Ding, W., Godwin, S., Munson, K., Peluso, R., and Engelhardt, J. F. (2004) Distinct classes of proteasome-modulating agents cooperatively augment recombinant adeno-associated virus type 2 and type 5-mediated transduction from the apical surfaces of human airway epithelia, *J Virol* ***78***, 2863–2874.
103. Denby, L., Nicklin, S. A., and Baker, A. H. (2005) Adeno-associated virus (AAV)-7 and -8 poorly transduce vascular endothelial cells and are sensitive to proteasomal degradation, *Gene Ther* ***12***, 1534–1538.
104. Jennings, K., Miyamae, T., Traister, R., Marinov, A., Katakura, S., Sowders, D., Trapnell, B., Wilson, J. M., Gao, G., and Hirsch, R. (2005) Proteasome inhibition enhances AAV-mediated transgene expression in human synoviocytes in vitro and in vivo, *Mol Ther* ***11***, 600–607.
105. Zhong, L., Zhao, W., Wu, J., Li, B., Zolotukhin, S., Govindasamy, L., Agbandje-McKenna, M., and Srivastava, A. (2007) A dual role of EGFR protein tyrosine kinase signaling in ubiquitination of AAV2 capsids and viral second-strand DNA synthesis, *Mol Ther* ***15***, 1323–1330.
106. Zhong, L., Li, B., Mah, C. S., Govindasamy, L., Agbandje-McKenna, M., Cooper, M., Herzog, R. W., Zolotukhin, I., Warrington, K. H., Jr., Weigel-Van Aken, K. A., Hobbs, J. A., Zolotukhin, S., Muzyczka, N., and Srivastava, A. (2008) Next generation of adeno-associated virus 2 vectors: point mutations in tyrosines lead to high-efficiency transduction at lower doses, *Proc Natl Acad Sci U S A* ***105***, 7827–7832.
107. Zhong, L., Li, B., Jayandharan, G., Mah, C. S., Govindasamy, L., Agbandje-McKenna, M., Herzog, R. W., Weigel-Van Aken, K. A., Hobbs, J. A., Zolotukhin, S., Muzyczka, N., and Srivastava, A. (2008) Tyrosine-phosphorylation of AAV2 vectors and its consequences on viral intracellular trafficking and transgene expression, *Virology* ***381***, 194–202.
108. Kelkar, S., De, B. P., Gao, G., Wilson, J. M., Crystal, R. G., and Leopold, P. L. (2006) A common mechanism for cytoplasmic dynein-dependent microtubule binding shared among adeno-associated virus and adenovirus serotypes, *J Virol* ***80***, 7781–7785.
109. Zhao, W., Zhong, L., Wu, J., Chen, L., Qing, K., Weigel-Kelley, K. A., Larsen, S. H., Shou, W., Warrington, K. H., Jr., and Srivastava, A. (2006) Role of cellular FKBP52 protein in intracellular trafficking of recombinant adeno-associated virus 2 vectors, *Virology* ***353***, 283–293.
110. Hirosue, S., Senn, K., Clement, N., Nonnenmacher, M., Gigout, L., Linden, R. M., and Weber, T. (2007) Effect of inhibition of dynein function and microtubule-altering drugs on AAV2 transduction, *Virology* ***367***, 10–18.
111. Xu, J., Ma, C., Bass, C., and Terwilliger, E. F. (2005) A combination of mutations enhances the neurotropism of AAV-2, *Virology* ***341***, 203–214.
112. Xiao, W., Warrington, K. H., Jr., Hearing, P., Hughes, J., and Muzyczka, N. (2002) Adenovirus-facilitated nuclear translocation of adeno-associated virus type 2, *J Virol* ***76***, 11505–11517.
113. Grieger, J. C., Snowdy, S., and Samulski, R. J. (2006) Separate basic region motifs within the adeno-associated virus capsid proteins are essential for infectivity and assembly, *J Virol* ***80***, 5199–5210.
114. Hansen, J., Qing, K., and Srivastava, A. (2001) Infection of purified nuclei by adeno-associated virus 2, *Mol Ther* ***4***, 289–296.
115. Cohen, S., and Pante, N. (2005) Pushing the envelope: microinjection of Minute virus of mice into Xenopus oocytes causes damage to the nuclear envelope, *J Gen Virol* ***86***, 3243–3252.
116. Cohen, S., Behzad, A. R., Carroll, J. B., and Pante, N. (2006) Parvoviral nuclear import: bypassing the host nuclear-transport machinery, *J Gen Virol 87*, 3209–3213.
117. Sipo, I., Fechner, H., Pinkert, S., Suckau, L., Wang, X., Weger, S., and Poller, W. (2007) Differential internalization and nuclear uncoating of self-complementary adeno-associated virus pseudotype vectors as determinants of cardiac cell transduction, *Gene Ther* ***14***, 1319–1329.
118. Thomas, C. E., Storm, T. A., Huang, Z., and Kay, M. A. (2004) Rapid uncoating of vector genomes is the key to efficient liver transduction with pseudotyped adeno-associated virus vectors, *J Virol 78*, 3110–3122.
119. Zhong, L., Li, W., Yang, Z., Qing, K., Tan, M., Hansen, J., Li, Y., Chen, L., Chan, R. J., Bischof, D., Maina, N., Weigel-Kelley, K. A.,

Zhao, W., Larsen, S. H., Yoder, M. C., Shou, W., and Srivastava, A. (2004) Impaired nuclear transport and uncoating limit recombinant adeno-associated virus 2 vector-mediated transduction of primary murine hematopoietic cells, *Hum Gene Ther* ***15***, 1207–1218.

120. Stieger, K., Schroeder, J., Provost, N., Mendes-Madeira, A., Belbellaa, B., Le Meur, G., Weber, M., Deschamps, J. Y., Lorenz, B., Moullier, P., and Rolling, F. (2009) Detection of intact rAAV particles up to 6 years after successful gene transfer in the retina of dogs and primates, *Mol Ther* ***17***, 516–523.
121. Lux, K., Goerlitz, N., Schlemminger, S., Perabo, L., Goldnau, D., Endell, J., Leike, K., Kofler, D. M., Finke, S., Hallek, M., and Buning, H. (2005) Green fluorescent protein-tagged adeno-associated virus particles allow the study of cytosolic and nuclear trafficking, *J Virol* ***79***, 11776–11787.
122. Cotmore, S. F., D'Abramo A, M., Jr., Ticknor, C. M., and Tattersall, P. (1999) Controlled conformational transitions in the MVM virion expose the VP1 N-terminus and viral genome without particle disassembly, *Virology* ***254***, 169–181.
123. Ros, C., Baltzer, C., Mani, B., and Kempf, C. (2006) Parvovirus uncoating in vitro reveals a mechanism of DNA release without capsid disassembly and striking differences in encapsidated DNA stability, *Virology* ***345***, 137–147.
124. Vihinen-Ranta, M., Wang, D., Weichert, W. S., and Parrish, C. R. (2002) The VP1 N-terminal sequence of canine parvovirus affects nuclear transport of capsids and efficient cell infection, *J Virol* ***76***, 1884–1891.
125. Ferrari, F. K., Samulski, T., Shenk, T., and Samulski, R. J. (1996) Second-strand synthesis is a rate-limiting step for efficient transduction by recombinant adeno-associated virus vectors, *J Virol* ***70***, 3227–3234.
126. Fisher, K. J., Gao, G., Weitzman, M. D., DeMatteo, R., Burda, J., and Wilson, J. M. (1996) Transduction with recombinant adeno-associated virus for gene therapy is limited by leading-strand synthesis, *J. Virol.* ***70***, 520–532.
127. Zhong, L., Zhou, X., Li, Y., Qing, K., Xiao, X., Samulski, R. J., and Srivastava, A. (2008) Single-polarity recombinant adeno-associated virus 2 vector-mediated transgene expression in vitro and in vivo: mechanism of transduction, *Mol Ther* ***16***, 290–295.
128. Zhou, X., Zeng, X., Fan, Z., Li, C., McCown, T., Samulski, R. J., and Xiao, X. (2008) Adeno-associated virus of a single-polarity DNA genome is capable of transduction in vivo, *Mol Ther* ***16***, 494–499.
129. Qing, K., Hansen, J., Weigel-Kelley, K. A., Tan, M., Zhou, S., and Srivastava, A. (2001) Adeno-associated virus type 2-mediated gene transfer: role of cellular fkbp52 protein in transgene expression, *J Virol* ***75***, 8968–8976.
130 Qing, K., Khuntirat, B., Mah, C., Kube, D. M., Wang, X. S., Ponnazhagan, S., Zhou, S., Dwarki, V. J., Yoder, M. C., and Srivastava, A. (1998) Adeno-associated virus type 2-mediated gene transfer: correlation of tyrosine phosphorylation of the cellular single-stranded D sequence-binding protein with transgene expression in human cells in vitro and murine tissues in vivo, *J Virol* ***72***, 1593–1599.
131. Qing, K., Wang, X. S., Kube, D. M., Ponnazhagan, S., Bajpai, A., and Srivastava, A. (1997) Role of tyrosine phosphorylation of a cellular protein in adeno-associated virus 2-mediated transgene expression, *Proc Natl Acad Sci U S A* ***94***, 10879–10884.
132. Qing, K., Li, W., Zhong, L., Tan, M., Hansen, J., Weigel-Kelley, K. A., Chen, L., Yoder, M. C., and Srivastava, A. (2003) Adeno-associated virus type 2-mediated gene transfer: role of cellular T-cell protein tyrosine phosphatase in transgene expression in established cell lines in vitro and transgenic mice in vivo, *J Virol* ***77***, 2741–2746.
133. Nakai, H., Storm, T. A., Fuess, S., and Kay, M. A. (2003) Pathways of removal of free DNA vector ends in normal and DNA-PKcs-deficient SCID mouse hepatocytes transduced with rAAV vectors, *Hum Gene Ther* ***14***, 871–881.
134. Yue, Y., and Duan, D. (2003) Double strand interaction is the predominant pathway for intermolecular recombination of adeno-associated viral genomes, *Virology* ***313***, 1–7.
135. McCarty, D. M., Young, S. M., Jr., and Samulski, R. J. (2004) Integration of adeno-associated virus (AAV) and recombinant AAV vectors, *Annu Rev Genet* ***38***, 819–845.
136. Cervelli, T., Palacios, J. A., Zentilin, L., Mano, M., Schwartz, R. A., Weitzman, M. D., and Giacca, M. (2008) Processing of recombinant AAV genomes occurs in specific nuclear structures that overlap with foci of DNA-damage-response proteins, *J Cell Sci* ***121***, 349–357.
137. Schwartz, R. A., Palacios, J. A., Cassell, G. D., Adam, S., Giacca, M., and Weitzman, M. D. (2007) The Mre11/Rad50/Nbs1 complex limits adeno-associated virus transduction and replication, *J Virol* ***81***, 12936–12945.
138. Jurvansuu, J., Raj, K., Stasiak, A., and Beard, P. (2005) Viral transport of DNA damage that mimics a stalled replication fork, *J Virol* ***79***, 569–580.

139. Johnson, J. S., and Samulski, R. J. (2009) Enhancement of adeno-associated virus infection by mobilizing capsids into and out of the nucleolus, *J Virol* ***83***, 2632–2644.

140. Knipe, D. M., and Howley, P. M. H. (2001) *Fields Viroloy*, Lippincott Williams&Wilkins, Philadelphia, USA.

141. Chiorini, J. A., Wiener, S. M., Owens, R. A., Kyostio, S. R., Kotin, R. M., and Safer, B. (1994) Sequence requirements for stable binding and function of Rep68 on the adeno-associated virus type 2 inverted terminal repeats, *J Virol* ***68***, 7448–7457.

142. McCarty, D. M., Pereira, D. J., Zolotukhin, I., Zhou, X., Ryan, J. H., and Muzyczka, N. (1994) Identification of linear DNA sequences that specifically bind the adeno-associated virus Rep protein, *J Virol* ***68***, 4988–4997.

143. Owens, R. A., Weitzman, M. D., Kyostio, S. R., and Carter, B. J. (1993) Identification of a DNA-binding domain in the amino terminus of adeno-associated virus Rep proteins, *J Virol* ***67***, 997–1005.

144. Snyder, R. O., Im, D. S., Ni, T., Xiao, X., Samulski, R. J., and Muzyczka, N. (1993) Features of the adeno-associated virus origin involved in substrate recognition by the viral Rep protein, *J Virol* ***67***, 6096–6104.

145. Ryan, J. H., Zolotukhin, S., and Muzyczka, N. (1996) Sequence requirements for binding of Rep68 to the adeno-associated virus terminal repeats, *J Virol* ***70***, 1542–1553.

146. Snyder, R. O., Samulski, R. J., and Muzyczka, N. (1990) In vitro resolution of covalently joined AAV chromosome ends, *Cell* ***60***, 105–113.

147. Im, D. S., and Muzyczka, N. (1990) The AAV origin binding protein Rep68 is an ATP-dependent site-specific endonuclease with DNA helicase activity, *Cell* ***61***, 447–457.

148. Zhou, X., Zolotukhin, I., Im, D. S., and Muzyczka, N. (1999) Biochemical characterization of adeno-associated virus rep68 DNA helicase and ATPase activities, *J Virol* ***73***, 1580–1590.

149. Nash, K., Chen, W., and Muzyczka, N. (2008) Complete in vitro reconstitution of adeno-associated virus DNA replication requires the minichromosome maintenance complex proteins, *J Virol* ***82***, 1458–1464.

150. Ni, T. H., McDonald, W. F., Zolotukhin, I., Melendy, T., Waga, S., Stillman, B., and Muzyczka, N. (1998) Cellular proteins required for adeno-associated virus DNA replication in the absence of adenovirus coinfection, *J Virol* ***72***, 2777–2787.

151. Ward, P., Dean, F. B., O'Donnell, M. E., and Berns, K. I. (1998) Role of the adenovirus DNA-binding protein in in vitro adeno-associated virus DNA replication, *J Virol* ***72***, 420–427.

152. Stracker, T. H., Cassell, G. D., Ward, P., Loo, Y. M., van Breukelen, B., Carrington-Lawrence, S. D., Hamatake, R. K., van der Vliet, P. C., Weller, S. K., Melendy, T., and Weitzman, M. D. (2004) The Rep protein of adeno-associated virus type 2 interacts with single-stranded DNA-binding proteins that enhance viral replication, *J Virol* ***78***, 441–453.

153. Myers, M. W., and Carter, B. J. (1981) Adeno-associated virus replication. The effect of L-canavanine or a helper virus mutation on accumulation of viral capsids and progeny single-stranded DNA, *J Biol Chem* ***256***, 567–570.

154. Wistuba, A., Kern, A., Weger, S., Grimm, D., and Kleinschmidt, J. A. (1997) Subcellular compartmentalization of adeno-associated virus type 2 assembly, *J Virol* ***71***, 1341–1352.

155. Weitzman, M. D., Fisher, K. J., and Wilson, J. M. (1996) Recruitment of wild-type and recombinant adeno-associated virus into adenovirus replication centers, *J Virol* ***70***, 1845–1854.

156. Hunter, L. A., and Samulski, R. J. (1992) Colocalization of adeno-associated virus Rep and capsid proteins in the nuclei of infected cells, *J Virol* ***66***, 317–324.

157. Bleker, S., Pawlita, M., and Kleinschmidt, J. A. (2006) Impact of capsid conformation and Rep-capsid interactions on adeno-associated virus type 2 genome packaging, *J Virol* ***80***, 810–820.

158. Zhou, X., and Muzyczka, N. (1998) In vitro packaging of adeno-associated virus DNA, *J Virol* ***72***, 3241–3247.

159. Myers, M. W., and Carter, B. J. (1980) Assembly of adeno-associated virus, *Virology* ***102***, 71–82.

160. Bevington, J. M., Needham, P. G., Verrill, K. C., Collaco, R. F., Basrur, V., and Trempe, J. P. (2007) Adeno-associated virus interactions with B23/Nucleophosmin: identification of sub-nucleolar virion regions, *Virology* ***357***, 102–113.

161. Ruffing, M., Zentgraf, H., and Kleinschmidt, J. A. (1992) Assembly of viruslike particles by recombinant structural proteins of adeno-associated virus type 2 in insect cells, *J Virol* ***66***, 6922–6930.

162. Wistuba, A., Weger, S., Kern, A., and Kleinschmidt, J. A. (1995) Intermediates of adeno-associated virus type 2 assembly: iden-

tification of soluble complexes containing Rep and Cap proteins, *J Virol* ***69***, 5311–5319.

163. Steinbach, S., Wistuba, A., Bock, T., and Kleinschmidt, J. A. (1997) Assembly of adeno-associated virus type 2 capsids in vitro, *J Gen Virol* ***78 (Pt 6)***, 1453–1462.
164. Hoque, M., Ishizu, K., Matsumoto, A., Han, S. I., Arisaka, F., Takayama, M., Suzuki, K., Kato, K., Kanda, T., Watanabe, H., and Handa, H. (1999) Nuclear transport of the major capsid protein is essential for adeno-associated virus capsid formation, *J Virol* ***73***, 7912–7915.
165. Warrington, K. H., Jr., Gorbatyuk, O. S., Harrison, J. K., Opie, S. R., Zolotukhin, S., and Muzyczka, N. (2004) Adeno-associated virus type 2 VP2 capsid protein is nonessential and can tolerate large peptide insertions at its N terminus, *J Virol* ***78***, 6595–6609.
166. Rabinowitz, J. E., Xiao, W., and Samulski, R. J. (1999) Insertional mutagenesis of AAV2 capsid and the production of recombinant virus, *Virology* ***265***, 274–285.
167. Sonntag et al (2010) *PNAS 107*, 10220–10225.
168. Prasad, K. M., and Trempe, J. P. (1995) The adeno-associated virus Rep78 protein is covalently linked to viral DNA in a preformed virion, *Virology* ***214***, 360–370.
169. Wang, X. S., Ponnazhagan, S., and Srivastava, A. (1996) Rescue and replication of adeno-associated virus type 2 as well as vector DNA sequences from recombinant plasmids containing deletions in the viral inverted terminal repeats: selective encapsidation of viral genomes in progeny virions, *J Virol* ***70***, 1668–1677.
170. Wang, X. S., Qing, K., Ponnazhagan, S., and Srivastava, A. (1997) Adeno-associated virus type 2 DNA replication in vivo: mutation analyses of the D sequence in viral inverted terminal repeats, *J Virol* ***71***, 3077–3082.
171. Srivastava, A., Wang, X.-S., Ponnazhagan, S., Zhou, S. Z., and Yoder, M. C. (1996) Adeno-associated Virus 2-Mediated Transduction and Erythroid Lineage-Specific Expression in Human Hematopoietic Progenitor Cells, in *Adeno-Associated Virus (AAV) Vectors in Gene Therapy* (Berns, K. I., and Giraud, C., Eds.), pp 93–117, Springer, Berlin Heidelberg New York.
172. Xiao, X., Xiao, W., Li, J., and Samulski, R. J. (1997) A novel 165-base-pair terminal repeat sequence is the sole cis requirement for the adeno-associated virus life cycle, *J Virol* ***71***, 941–948.
173. Dong, J. Y., Fan, P. D., and Frizzell, R. A. (1996) Quantitative analysis of the packaging capacity of recombinant adeno-associated virus, *Hum Gene Ther 7*, 2101–2112.
174. Hermonat, P. L., Quirk, J. G., Bishop, B. M., and Han, L. (1997) The packaging capacity of adeno-associated virus (AAV) and the potential for wild-type-plus AAV gene therapy vectors, *FEBS Lett* ***407***, 78–84.
175. Grieger, J. C., and Samulski, R. J. (2005) Packaging capacity of adeno-associated virus serotypes: impact of larger genomes on infectivity and postentry steps, *J Virol* ***79***, 9933–9944.
176. Allocca, M., Doria, M., Petrillo, M., Colella, P., Garcia-Hoyos, M., Gibbs, D., Kim, S. R., Maguire, A., Rex, T. S., Di Vicino, U., Cutillo, L., Sparrow, J. R., Williams, D. S., Bennett, J., and Auricchio, A. (2008) Serotype-dependent packaging of large genes in adeno-associated viral vectors results in effective gene delivery in mice, *J Clin Invest* ***118***, 1955–1964.
177. Lai, Y., Yue, Y., and Duan, D. Evidence for the failure of adeno-associated virus serotype 5 to package a viral genome > or = 8.2 kb, *Mol Ther* ***18***, 75–79.
178. Dong, B., Nakai, H., and Xiao, W. Characterization of genome integrity for oversized recombinant AAV vector, *Mol Ther* ***18***, 87–92.
179. Wu, Z., Yang, H., and Colosi, P. Effect of genome size on AAV vector packaging, *Mol Ther* ***18***, 80–86.
180. Ward, P., Clement, N., and Linden, R. M. (2007) cis effects in adeno-associated virus type 2 replication, *J Virol* ***81***, 9976–9989.
181. Grimm, D., Kern, A., Pawlita, M., Ferrari, F., Samulski, R., and Kleinschmidt, J. (1999) Titration of AAV-2 particles via a novel capsid ELISA: packaging of genomes can limit production of recombinant AAV-2, *Gene Ther* ***6***, 1322–1330.
182. Drittanti, L., Jenny, C., Poulard, K., Samba, A., Manceau, P., Soria, N., Vincent, N., Danos, O., and Vega, M. (2001) Optimised helper virus-free production of high-quality adeno-associated virus vectors, *J Gene Med* ***3***, 59–71.
183. Sommer, J. M., Smith, P. H., Parthasarathy, S., Isaacs, J., Vijay, S., Kieran, J., Powell, S. K., McClelland, A., and Wright, J. F. (2003) Quantification of adeno-associated virus particles and empty capsids by optical density measurement, *Mol Ther 7*, 122–128.
184. Park, J. Y., Lim, B. P., Lee, K., Kim, Y. G., and Jo, E. C. (2006) Scalable production of

adeno-associated virus type 2 vectors via suspension transfection, *Biotechnol Bioeng* ***94***, 416–430.

185. Prasad, K. M., Zhou, C., and Trempe, J. P. (1997) Characterization of the Rep78/adeno-associated virus complex, *Virology* ***229***, 183–192.
186. Dubielzig, R., King, J. A., Weger, S., Kern, A., and Kleinschmidt, J. A. (1999) Adeno-associated virus type 2 protein interactions: formation of pre-encapsidation complexes, *J Virol* ***73***, 8989–8998.
187. Chejanovsky, N., and Carter, B. J. (1989) Mutagenesis of an AUG codon in the adeno-associated virus rep gene: effects on viral DNA replication, *Virology* ***173***, 120–128.
188. King, J. A., Dubielzig, R., Grimm, D., and Kleinschmidt, J. A. (2001) DNA helicase-mediated packaging of adeno-associated virus type 2 genomes into preformed capsids, *Embo J* ***20***, 3282–3291.
189. Yoon-Robarts, M., Blouin, A. G., Bleker, S., Kleinschmidt, J. A., Aggarwal, A. K., Escalante, C. R., and Linden, R. M. (2004) Residues within the B' motif are critical for DNA binding by the superfamily 3 helicase Rep40 of adeno-associated virus type 2, *J Biol Chem* ***279***, 50472–50481.
190. Shi, W., Arnold, G. S., and Bartlett, J. S. (2001) Insertional mutagenesis of the adeno-associated virus type 2 (AAV2) capsid gene and generation of AAV2 vectors targeted to alternative cell-surface receptors, *Hum Gene Ther* ***12***, 1697–1711.
191. Zaiss and Muruve (2008) Immunity to adeno-associated virus vectors in animals and humans: a continued challenge. *Gene Therapy* ***15***, 808–16.
192. Moskalenko, M., Chen, L., van Roey, M., Donahue, B. A., Snyder, R. O., McArthur, J. G., and Patel, S. D. (2000) Epitope mapping of human anti-adeno-associated virus type 2 neutralizing antibodies: implications for gene therapy and virus structure, *J Virol* ***74***, 1761–1766.
193. Wobus, C. E., Hugle-Dorr, B., Girod, A., Petersen, G., Hallek, M., and Kleinschmidt, J. A. (2000) Monoclonal antibodies against the adeno-associated virus type 2 (AAV-2) capsid: epitope mapping and identification of capsid domains involved in AAV-2-cell interaction and neutralization of AAV-2 infection, *J Virol* ***74***, 9281–9293.
194. Kuck, D., Kern, A., and Kleinschmidt, J. A. (2007) Development of AAV serotype-specific ELISAs using novel monoclonal antibodies, *J Virol Methods* ***140***, 17–24.

Chapter 4

Exploiting Natural Diversity of AAV for the Design of Vectors with Novel Properties

Guangping Gao, Li Zhong, and Olivier Danos

Abstract

Twelve AAV serotypes have been described so far in human and nonhuman primate (NHP) populations while surprisingly high diversity of AAV sequences is detected in tissue biopsies. The analysis of these novel AAV sequences has indicated a rapid evolution of the viral genome both by accumulation of mutations and recombination. This chapter describes how this rich resource of naturally evolved sequences is used to derive gene transfer vectors with a wide array of activities depending on the nature of the cap gene used in the packaging system. AAV2-based recombinant genomes have been packaged in dozens of different capsid types, resulting in a wide array of "pseudotyped vectors" that constitute a rich resource for the development of gene therapy clinical trials. We describe a polymerase chain reaction-based molecular rescue method for novel AAV isolation that uses primers designed to recognize the highly conserved regions in known AAV isolates and generate amplicons across the hypervariable regions of novel AAV genomes present in the analyzed sample.

Key words: AAV, AAV2, Molecular rescue, Pseudotyped vector, AAV isolation, Amplicon

1. Introduction

1.1. Natural Diversity of AAVs: Molecular Basis of AAV Diversity

AAV was originally isolated as a contaminant of adenovirus preparations before it was characterized in humans (1). Data on the natural history of AAV infection in human populations have only been obtained recently, and many aspects of the virus–host interactions remain obscure (2–4). Twelve AAV serotypes have been characterized in human and nonhuman primate (NHP) populations. In addition, AAV sequences can be isolated from tissue biopsies by polymerase chain reaction (PCR), as further detailed in this chapter (5–8) or Rolling Circle Amplification (3). These approaches have revealed a surprisingly high diversity of AAV species in infected individuals

Richard O. Snyder and Philippe Moullier (eds.), *Adeno-Associated Virus: Methods and Protocols*,
Methods in Molecular Biology, vol. 807, DOI 10.1007/978-1-61779-370-7_4,

and have led to the definition of over a hundred new "serotypes" whose cross-neutralizing properties were only retrospectively analyzed.

Experimental infection of NHPs result in rapid genome variations and recombination and in the generation of diversity comparable to that observed with RNA viruses (5). High mutation rates have indeed been documented with single-stranded DNA viruses including parvoviruses (9). In addition, recombination hot spots have been identified on the AAV genome, suggesting that this is also an important drive of diversity (2, 5, 6, 10, 11). Most variations in AAV populations accumulate in the cap gene which encodes the three virion structural proteins, VP1, VP2, and VP3. Amino acid variation observed in AAV populations or between serotypes occurs in VP3, the basic capsomer domain shared by the three proteins that assemble into a 60-subunit icosahedron. Changes accumulate in 12 hypervariable regions encoding solvent-exposed loops that form protuberances on the capsid surface and interact with receptor molecules at the cell surface. On some of the AAV serotypes (AAV2, AAV3), a complex motif on VP3 creates a pocket for interaction with heparan sulfate proteoglycan (12, 13) that allows docking of the virion at the cell surface before interaction with a secondary receptor and internalization. Many amino acid positions on VP3 are highly constrained by the capsid structure and therefore invariant (14).

VP1 and VP2 have additional N-terminal domains with essential functions for virion entry and intracellular trafficking. The VP1 unique region contains a conserved phospholipase A2 catalytic site whose activity is required for releasing the particle from the endosome. Basic amino acid sequences common to VP1 and VP2 are needed for efficient nuclear targeting (15).

The VP1/VP2 unique region displays less variability because a different evolutionary pressure is applied on this part of the molecule. Interestingly, most of the recombination events in the cap gene result in reassortments of VP1/VP2 with VP3 (11). Such reassortments are also observed when novel AAV cap genes are selected from complex libraries resulting from in vitro evolution experiments (16, 17). Thus, the natural diversity of the multifunctional cap gene is driven by a high mutation rate that allows for efficient receptor switch or escape from the host immune response. Recombination provides a means to retain the VP1/VP2 domains that cannot afford high levels of changes.

1.2. Serological Properties of AAV Variants

By definition, a new AAV serotype is a novel isolate that does not efficiently cross-react with neutralizing sera against other existing AAVs. The activity of neutralizing antibodies (NAbs) against AAV is measured in assays where serum dilutions are tested for their capacity to inhibit virus or vector activity on cultured cells. The NAb titer is given by the dilution where 50% of cell transduction or infection is inhibited (5, 18, 19). Preexisting NAbs to AAVs are

highly prevalent in human and NHP populations (5, 19–23). Seropositivity to AAV2 is the highest among humans in all regions in the world followed by AAV1, ranging from 30 to 80% (19, 21). In contrast, the antibodies to NHP-derived AAV7 and AAV8 are found in only 1–11% of subjects, while NAbs against Rhesus macaque-derived AAVrh32.33 are remarkably absent (19). As a consequence, these NHP-derived AAVs have an important potential for developing vectors that would overcome a preexisting immunity to the highly prevalent serotypes in patients treated with gene therapy.

In contrast to human populations, seropositivity to AAV2 is rarely detected in mice and NHPs. NAbs to AAV2 persist for over 1 year after vector administration in these species and then decline, without compromising the efficacy of vector readministration (22). On the other hand, NHP-derived AAVs including AAV1, 4, 7, 8, 9, 10, 11, and 12 are widespread in the NHP population and this high prevalence of preexisting NAbs could affect the performances of vectors made from these serotypes in a way that would not predict the human situation (5, 18, 23). These issues must be taken into account when designing preclinical or toxicology studies in NHPs.

Serological cross-reactivities exist between AAV serotypes, but they cannot be predicted from the degree of phylogenetic relationship. AAV6 is almost identical to AAV1 in terms of phylogeny, and as expected, this results in a high serological cross-reactivity (6). In contrast, although the structure of AAV5 is different from AAV1, there is an unanticipated serological reactivity between the two (6). AAV12 is highly resistant to neutralization by circulating antibodies from human serum and is serologically distinct from both AAV4 and AAV2, despite its high sequence homology with AAV4 (24).

Several in vivo gene transfer studies have indicated that preexisting NAbs to a given AAV serotype do not affect transduction efficiency by another serotype (25–27). Yet cross-reactivity was observed in studies where AAV1-mediated transduction of murine liver was decreased by about 20-fold after treatment with a first AAV2 vectors (10). In a recent clinical trial using an AAV1-α-1 antitrypsin vector, NAbs to AAV1 were detected although transgene expression was sustained for at least 1 year. Interestingly, some subjects in this trial unexpectedly developed high titer NAbs to distinct AAV serotypes such as AAV7, 8, and 32.33 (28). This challenges the notion that using a different serotype in a second injection would always overcome the humoral response to the first vector.

1.3. Vectorology

The natural or artificially evolved diversity of AAV cap genes has considerably expanded the versatility and utility of AAV vectors. Importantly, the ITR and rep genes from AAV2 can be kept constant while cap genes from different serotypes or isolates are used to derive “pseudotyped” vectors that only differ by the nature of their

capsid (29–31). A pseudotype with an AAV2-based vector genome packaged in a capsid from serotype X is designated as AAV2/X. Pseudotyped vectors can be produced according to all established methods including plasmid DNA transfection (32), stable producer cell lines, infection with recombinant herpes simplex (33), or baculovirus (34). Chimerical virions with a capsid composed of a mixture of capsomers of different origin can also be obtained, and they display unique properties (35, 36). In most cases, swapping cap genes does not affect packaging and virion production efficiency, with the possible exception of AAV2/5 pseudotypes for which a higher packaging capacity of up to 9 kb has been reported (37). However, this observation has been challenged by the fact that mostly deleted genomes with only one ITR are detected in the virions, suggesting that recombination between deleted genomes rather than packaging of larger genomes takes place (38, 39). Pseudotyping is also compatible with enhancing modifications of AAV vectors such as "self-complementary genomes" (40) or mutations of surface exposed tyrosines whose phosphorylation triggers proteosomal degradation (41). Vectors with ITRs from AAV5 have been constructed in order to reduce the risk of mobilization of an AAV2 ITR-based recombinant genome following an AAV2 infection. Given the prevalence of AAV2 in human populations, such vectors may represent safer alternatives for clinical applications (42).

1.4. Properties and Performances of Pseudotyped AAV Vectors for Gene Transfer In Vivo: Differential Transduction Efficiencies and Biodistribution

For a given application and target cell, many possible pseudotyped vectors are available. Most clinical trials to date have been conducted with the AAV2 serotype, but others, including AAV1, AAV5, AAV8, and AAVrh10 are now in use. Because of their different surface properties, these new vectors inevitably present novel biodistribution and toxicology profiles (43, 44).

Studies have reported that AAV1 and AAV6 could efficiently transduce muscle (27, 45), AAV5 resulted in higher transduction efficiencies and broader distributions in the brain (46, 47), AAV8 is very efficient in liver (7), muscle, and heart (48), and AAV9 can outperform other AAV serotypes in muscle and heart (49). In addition, tissue tropism and transduction efficiency of AAV vectors in vivo are also significantly influenced by the routes of administration.

The intravenous (IV) delivery of AAV vectors led to systemic transgene expression in vivo. AAV1–9 mediated transgene expression, tropism, and biodistribution in mice after tail vein injection have been thoroughly evaluated (43, 44, 50). The onset of expression of AAV1, 6, 7, 8, and 9 is earliest, followed by AAV4 and 5 then AAV2 and 3. This could reflect the fact that different pseudotype vectors enter the cell and deliver their payload in the nucleus using various intracellular routes. In terms of efficiency of transgene expression, AAV2, 3, 4, and 5 are in the low-expression group, AAV1, 6, and 8 are in the medium-expression group, and AAV7 and 9 are in the high-expression group (44). Overall, transduction

efficiency can be ranked as: AAV9 > AAV8 = AAVrh.10 > AAV7 > AAV6 > AAV1 > AAV5 > AAV2 > AAV3. Different AAV serotypes show different targeting patterns and tissue tropisms after IV administration. The most commonly transduced organ after IV injection is the liver (44, 51–54). AAV2 mainly transduces the liver and the transgene level is 26–30 times greater than the levels in skeletal muscle and the heart (44). High vector genome copy numbers have been observed in the liver following tail vein injection of AAV8 and 9 into mice (55). Injections via the portal vein are more efficient for AAV delivery to the liver (56, 57). However, some studies have documented that AAV8-mediated liver transgene expression is independent of the route of IV administration (58, 59). Gender significantly influences AAV-mediated liver transgene expression after IV vector delivery, with higher levels of expression observed in male compared with female mice (43, 50, 60). The skeletal muscles and the heart are also efficiently targeted by AAV vectors after peripheral vein injection (44, 48, 56, 61). Not only can AAV9 efficiently transduce skeletal muscles in mice (62), it can also lead to robust and sustained whole-body skeletal muscle transduction in neonatal dogs in the absence of pharmacological intervention or immune suppression after IV delivery (61). The heart is also efficiently transduced by AAV serotypes 4, 6, 7, 8, and 9 after tail vein injection in mice, in which AAV9 leads to the highest transgene expression and the most vector genomes in the heart (44, 63–66).

Intraperitoneal (IP) delivery of AAV vectors also leads to systemic gene transfer (48, 67, 68). AAV1, 2, 5, 6, 7, and 8-mediated short- and long-term transgene expression were compared after intraperitoneal injection of vectors in neonatal mice. Overall, AAV8 is the most efficient vector to cross the blood vessel barrier, leading to systemic gene transfer in skeletal and cardiac muscles. Transgene expression is detected as early as 3 days post-IP injection and sustained to adulthood throughout the vast majority of the muscle. In contrast, IP injections did not result in detectable transgene expression in brain, spleen, gonads, intestine, and blood vessels smooth muscle (48). In adult mice, IP delivery of AAV vectors can result in efficient transduction of islets and exocrine acinar cells of the pancreatic, with AAV8 being again the most efficient (69).

AAV vectors have spurred new interest in gene transfer to the respiratory epithelium, a long sought after the goal of gene therapy. While early studies in rabbits had shown a good level of transduction using AAV2 (70), AAV5, 8, and 9 are now considered better options. A recent comparative study indicates that AAV8 leads to the highest transduction levels followed by AAV9 and AAV5 in the murine lung using either intratracheal or noninvasive intranasal delivery methods (71).

1.5. Translational Studies: From Mouse to Human Clinical Trials

As outlined above, the transduction efficiency and tissue tropism of AAV serotypes vary significantly in vivo, depending on species and route of administration. Yet, to develop safe and efficient AAV vectors for human gene therapy, it is a regulatory requirement to evaluate their performances and toxicity in both small and large animal models. Table 1 summarizes translational studies performed with AAV vectors in small and large preclinical animal models for the development of human clinical trials. Sustained transgene expression has been observed in brain, heart, kidney, liver, retina, lung, and spleen following systemic vascular delivery by AAV vectors in mice (44, 51, 63, 72–75). In dogs, AAV1- and AAV2-mediated factor IX gene transfer in the liver or muscle resulted in long-term correction of the hemophilia B phenotype (76–78). AAV6, 8, and 9 have been used for long-term factor VIII gene expression in the liver of hemophilia A dogs without antibody formation or other toxicities and cured the disease (79, 80). Although AAV2 vectors led to stable liver transgene expression in cynomolgus macaques, efficiency of gene transfer with AAV7 and 8 vectors was higher (40, 81). AAV8 stands out as the vector of choice for muscle transduction in large animals, outperforming serotypes 1 and 2 (82–84). Percutaneous transendocardial delivery of AAV6 vectors achieves global cardiac gene transfer in dogs, which is superior to serotypes AAV8 and 9 (85). Successful transduction of NHP neurons by AAV vectors is established, with AAV1 and AAV5 performing much better than AAV2 (86–90). Successful transduction of NHP retina by AAV2 and AAV5 vectors have provided strong support for the treatment of retinal degenerative retinopathies diseases, such as Leber congenital amaurosis (91–94).

Overall, AAV vectors have been used successfully in a variety of in vivo gene transfer studies in preclinical animal models and achieved long-term therapeutic effect without notable toxicity, which may predict a positive outcome for future clinical trials. However, in a recent gene therapy trial using AAV2 vector, two patients with severe hemophilia B developed a vector dose-dependent transaminitis that limited the duration of hepatocyte-derived hF.IX expression to less than 8 weeks. This was due to a $CD8^+$ T-cell response to the injected capsid that eliminated AAV2-transduced hepatocytes, a phenomenon that was not predicted from preclinical studies in murine and canine models (95–97). This case raises the question of whether animal models are reliable predictors in the context of human gene therapy clinical trials using AAV vectors. On the other hand, recent AAV2 vector-mediated clinical gene transfer in Leber's congenital amaurosis have shown remarkable efficacy (98–100), consistent with the preclinical studies in animal models.

Table 1
AAV vectors have been characterized in vertical translation studies from animal preclinical models to human clinical trials

Serotype	Target: Tissue/organ	Preclinical study in small animal models	Preclinical study in large animal models	Clinical studies
AAV1 (nonhuman primates)	Heart	Mouse (103), rat (104)	Cat (107), NHP (88)	Heart failure (115)
	Liver	Mouse (43)	Pig (108), sheep (109)	
	Lung	Mouse (105)	Ferret, pig (110), NHP (111)	
	Muscle	Mouse (106)	Rabbit (112), cat (113), dog (78), NHP (114)	A1ATD (28), LGMD2D (116), LPLD (117)
AAV2 (humans)	Brain	Mouse (118), rat (119)	Cat (107), NHP (86–88)	Alzheimer (137), Batten (138), Canavan (139), Parkinson (140) LCA (98–100)
	Eye	Mouse (120), rat (121)	Dog (130), NHP (91, 93, 94)	
	Heart	Mouse (103), hamsters (122), rat (123)	Pig (131)	Inflammatory arthritis (72)
	Joint	Mouse (124), rat (125)	Rabbit (132), horse (133)	Hemophilia B (95)
	Liver	Mouse (51, 53), rat (126)	Dog (134), NHP (40)	CF (141)
	Lung	Mouse (127)	Rabbit (135), NHP (136)	A1ATD (142), hemophilia B (143)
	Muscle	Mouse (128), rat (129)	Dog (76, 77), NHP (114)	
AAV4 (nonhuman primates)	Eye	Rat (144)	Dog (144), NHP (144)	
AAV5 (humans)	Brain	Mouse (145), rat (119)	NHP (88–90)	
	Eye	Mouse (120), rat (146)	NHP (92)	
	Joint	Mouse (147), rat (148)		
	Liver	Mouse (149)	NHP (152)	
	Lung	Mouse (150), rat (151)	NHP (111)	

(continued)

Table 1 (continued)

Serotype	Target: Tissue/organ	Preclinical study in small animal models	Preclinical study in large animal models	Clinical studies
AAV6 (humans)	Heart	Mouse (153), rat (104)	Dog (85)	
	Liver	Mouse (79)	Dog (79)	
	Muscle	Mouse (154)	Dog (155)	
AAV7 (nonhuman primates)	Liver	Mouse (156)	NHP (40, 81)	
AAV8 (nonhuman primates)	Brain	Mouse (157), rat (158)		
	Heart	Mouse (48), hamster (48)		
	Liver	Mouse (7)	Dog (79, 80), NHP (57, 81)	Hemophilia B (160)
	Muscle	Mouse (48), hamster (48)	Dog (82, 83), NHP (84)	
	Pancreas	Mouse (69), rat (159)		
AAV9 (humans)	Brain	Mouse (161), rat (162)	Cat (165)	
	Heart	Mouse (55, 63), rat (163)	Dog (85)	
	Liver	Mouse (44, 55, 80)	Dog (80)	
	Lung	Mouse (164)		
	Muscle	Mouse (62)		
AAVrh10 (nonhuman primates)	Brain	Mouse (166), rat (166)		
	Lung	Mouse (167)		
AAV12 (nonhuman primates)	Muscle	Mouse (24)		
	Salivary lands	Mouse (24)		

A1ATD a-1 antitrypsin deficiency, *DMD* Duchenne muscular dystrophy, *LCA* Leber congenital amaurosis, *LGMD2D* limb-girdle muscular dystrophy type 2D, CF cystic fibrosis, *LPLD* lipoprotein lipase deficiency, *NHP* nonhuman primate

1.6. Isolation, Characterization, and Vector Development of New AAV Serotypes and Natural Variants by PCR-Based Method

In early 2000, several molecular methods were developed on the basis of the latency of AAV infection in attempts to isolate AAV proviral sequences from animal tissues where AAV proviral genomes persisted latently. To date, three molecular methods have been employed for recovery of proviral AAV sequences from tissue DNAs, namely, PCR, rolling circle linear amplification (RCLA), and transfection and rescue of infectious AAVs in 293 cells from the noncutter endonuclease-treated total tissue DNAs. It was the application of those molecular rescue methods that remarkably accelerated the discovery of a rapidly expanding diverse family of natural AAV serotypes and variants (101, 102). In this section, we primarily focus on the PCR-based molecular rescue which was the most widely used, sensitive and effective method for AAV isolation (102). Briefly, this method uses the PCR primers that anneal to the highly conserved regions in previously characterized early AAV isolates to amplify across the hypervariable regions of unknown AAV genomes for isolation and characterization of novel sequences (101).

2. Materials

2.1. PCR-Based Method for Novel AAV Discovery

2.1.1. Preparation of Tissue DNA

1. QIAamp Tissue DNA mini Kit (Qiagen, Valencia, CA).
2. Disposable Scalpels (Fisher, Pittsburg, PA).
3. TissueLyser (Qiagen, Valencia, CA).
4. Stainless steel beads, 5 mm (Qiagen, Valencia, CA).
5. Proteinase K 20 mg/ml stock (Qiagen, Valencia, CA).
6. RNaseA (Qiagen, Valencia, CA).

2.1.2. PCR Reagents

1. Platinum PCR SuperMix High Fidelity (InVitrogen, Carlsbad, CA).
2. Nuclease-free water (Qiagen, Valencia, CA).
3. Primers of choices in 10 μM concentration.

2.1.3. Agarose Gel Electrophoresis and Topo-Cloning

1. 1–1.2% of agarose gel (Fisher, Pittsburg, PA).
2. 1× TAE buffer (Fisher, Pittsburg, PA).
3. Top TA cloning kit for sequencing (InVitrogen, Carlsbad, CA).
4. QIAprep Spin Miniprep kit (Qiagen, Valencia, CA).

2.2. Vectorology of Novel AAV Serotypes

2.2.1. Molecular Cloning

1. Appropriate restriction endonucleases and corresponding buffers.
2. Alkaline phosphatase, Calf intestinal (CIP) (New England BioLab, Ipswich, MA).
3. T4 DNA Ligase (New England BioLab, Ipswich, MA).

4. QIAquick gel extraction kit (Qiagen, Valencia, CA).
5. MAX Efficiency DH5α Competent cell (InVitrogen, Carlsbad, CA).

2.2.2. Test for rAAV Production

1. HEK293 cells (ATCC, Manassas, VA).
2. Lipofectamin transfection reagent (InVitrogen, Carlsbad, CA).
3. E1-deleted helper adenovirus.

3. Methods

3.1. PCR-Based Method for Novel AAV Discovery

The isolation of novel AAVs can be accomplished by simple PCR technology provided the appropriate primers are available. *cap* sequences of different AAVs are naturally segregated into 12 hypervariable regions which are distinct from each other but interspersed with conserved regions (5). This kind of molecular structure allows us to design PCR primers that are annealed to the conserved regions and can amplify across the hypervariable regions for molecular retrieval of novel *cap* sequences.

As an initial attempt for detecting and isolating AAV sequences, one can start with the "signature PCR" method (7). This was developed by aligning the genomic *cap* sequences of AAV serotypes 1–6 and some avian AAVs for analysis and PCR primer selection. A set of primers that target the conserved regions of AAV genomes and flank a region of divergence were used to generate a 255 bp amplicon by PCR amplification of primate tissue DNAs. This highly sensitive method of retrieving a short fragment of AAV cap sequences is called "signature PCR" because the 250 bp PCR fragment spans a hypervariable region. Signature PCR is very useful and reliable for high-throughput screening and identification of endogenous AAVs that are present in primate tissues. Sequencing or restriction analysis of this PCR product with a panel of selected restriction enzymes allows to easily determine whether the retrieved AAV sequence is novel and worth to isolate the extended proviral sequences (7).

To isolate full-length *cap* sequences, two different strategies can be exploited. With the first one, one can generate two overlapping PCR amplicons using primers in the conserved regions and then fuse them into a full-length *cap* gene sequence (7). The second strategy is to directly amplify a 3.1 kb region spanning 3′ of *rep* (about 800 bp) and the entire *cap* gene sequence. The primers used for the full-length *cap* gene amplification are located in a highly conserved sequence of *rep* and an untranslated region in the 3′ end of AAV genomes (5, 6).

A potential limitation of the PCR-based method for rescue of proviral sequences is possible sequence artifacts of the PCR

(see Notes 1–4). To rule out PCR artifacts such as PCR-mediated gene splicing by overlap extension between different partial DNA templates with homologous sequences or by possible recombination events in bacteria, extensive analyses have been performed. Results of those experiments confirmed that sequence variation captured by the molecular rescue method indeed reflected the natural diversity of primate AAVs (5).

3.1.1. Design of PCR Primers

Perform sequence alignment of the *cap* genes from different AAV serotypes and variants using ClustalX and identify the conserved regions for primer design. For selection of conserved oligonucleotide sequences of your choice, make sure that the first 3–5 nucleotides at the 3′ end of each primers are perfectly matched with those in most of AAV *cap* sequences. Alternatively, the following pairs of conserved primers have proven to work effectively for isolating over 120 novel AAV sequences and should be considered for your applications. (1) For signature PCR with an amplicon size of approximately 250 bp, use AV19s 5′AGGT AATGCCTCAGGAAATTGGCATT3′ as the 5′ primer and AV18as 5′GAATCCCCAGTTGTTGTTGATGAGTC3′ as the 3′ primer; (2) To amplify the entire cap sequence and a part of rep sequence by two separate but overlapping amplicons (an 1.7 kb upstream fragment spanning 800 bp of *rep* and 700 bp of *cap* gene and an 1.5 kb downstream fragment of *cap* gene), use AV1ns 5′GCTGCGTCAACTGGACCAATGAGAAC3′ as the 5′ primer, AV18as 5′GAATCCCCAGTTGTTGTTGATGAGTC3′ as the 3′ primer for the 1.7 kb fragment, and AV19s 5′AGGTAATGCCTC AGGAAATTGGCATT3′ as the 5′ primer, AV2cas 5′CGCAGAGAC CAAAGTTCAACTGAAACGA3′ as the 3′ primer for the 1.5 kb fragment; (3) To amplify the entire *cap* gene and a portion of rep gene as one 3.1 kb fragment, use AV1ns 5′GCTGCGTCAACTGGA CCAATGAGAAC3′ as 5′ primer and AV2cas 5′ CGCAGAGACC AAAGTTCAACTGAAACGA3′ as the 3′ primer.

3.1.2. Extraction of Total Cellular DNA from Tissue Samples

1. For NHP tissues, apply for local IACUC approval for tissue collection from NHP animals.
2. For collection of human tissues from either surgical procedures or postmortem examination or organ donors, seek the approval of IRB protocols by local Institutional Review Board.
3. Ideally, each tissue sample should be dissected with a single disposable scalpel and snap-frozen in individual sterilized container.
4. For tissue DNA extraction, prepare work space in a Biosafety Level II Tissue Culture Hood first by UV irradiating all surfaces for 15 min, wiping all surfaces with Lysol first and then with 70% ethanol (see Notes 2 and 3).

5. Take the frozen tissues out of freezer and keep the tissues on dry ice.
6. Place one 5 mm steel bead in each of the labeled sterile 2 ml microfuge tubes.
7. Thaw no more than three tissues at a time in the hood at room temperature.
8. Quickly cut about 25 mg each of the partially thawed tissues and place in the correspondingly labeled tubes.
9. Immediately return the remaining tissues to dry ice and then freezer.
10. Repeat for remaining tissue samples.
11. Pulse spin (30 s, max speed) down all samples in a microcentrifuge such that tissues are at the bottom of the tubes.
12. To each sample, add 180 µl Buffer ATL from the QIAamp Tissue DNA mini Kit and homogenize tissues in Qiagen *Tissue Lyser* (20 s at frequency 30) and pulse spin (30 s, max speed) all samples again.
13. Perform tissue DNA extraction, following the user manual of the QIAamp Tissue DNA mini Kit.
14. Finally, dilute each DNA samples to a concentration of 50 ng/µl in nuclease-free water and store at 4°C.

3.1.3. Performance of PCR

1. Prepare work space in a BSL II hood as described above (see Notes 2 and 3).
2. Thaw 1× High Fidelity Platinum PCR SuperMix on ice.
3. For each 20 µl PCR, use 18 µl of 1× SuperMix, 0.6 = µl each of primers (10 µM) and 1 µl of DNA template.
4. To prepare PCR master mix containing both 1× SuperMix and primers, count the total numbers (n) of tissue DNA samples and prepare the PCR master mix in a 1.5 ml sterile Eppendorf tube according to the following formula:

1× SperMix	18 µl × n + 4
10 µM forward PCR primer	0.6 µl × n + 4
10 µM reverse PCR primer	0.6 µl × n + 4
Total	19.2 µl × n + 4

5. Mix the PCR master mix by repeated pipetting up and down.
6. Label 0.2 ml micro-PCR tubes and add 19.2 µl PCR master mix to each tube.
7. Add 1 µl of nuclease-free water to the first PCR tube as the no template control and close the tube.

8. Subsequently, add 1 μl of one tissue DNA (50 ng/μl) into a PCR tube, mix by pipetting, and close the tube immediately after mixing.
9. Repeat for other tissue samples.
10. Finally, add 10 ng of pAAVrep2/cap2 plasmid (10 ng/μl) to the positive control PCR tube on the regular laboratory bench and load the PCR tubes onto a PCR device.
11. Generally speaking, PCR runs with the following conditions should result in satisfactory outcomes (see Note 5).
    (a) For signature PCR, 1 min at 97°C, followed by 35–42 cycles (optimization may be required) of 15 s at 97°C, 10 s at 60°C, 45 s at 68–72°C (optimization may be required) and ended with a 10 min extension at 68–72°C (optimization may be required).
    (b) To retrieve large cap fragments, 1 min at 97°C, followed by 35–45 cycles (optimization may be required) of 15 s at 97°C, 10 s at 55–60°C (optimization may be required), 2–4 min at 68–72°C (optimization may be required), and ended with a 10 min extension at 68–72°C (optimization may be required). However, depending on the quality/integrity of template DNA, conservativeness of the novel AAV sequences in the primer regions and abundance of AAV proviral DNA in the tissue, more extensive optimization for PCR conditions may be required in some cases.

3.1.4. Examination of PCR Product

At the end of PCR, take 5 μl each reaction from PCR tubes and load onto a 1 (large cap PCR fragment)–1.2% (signature PCR fragment) of agarose gel to perform gel electrophoresis in 1× TAE buffer and examine the results of PCR rescue of AAV sequences from tissue samples.

3.1.5. Cloning of PCR Fragment and Sequence Characterization

Perform Topo-cloning following manufacturer's instruction. Identify the PCR-insert containing clones by *Eco*RI digestions by agarose gel electrophoresis as described in Subheading 3.1.4. For each PCR fragment, analyze at least six clones by sequencing. For sequence characterization, align the newly isolated VP1 sequences with those of known AAV serotypes/variants available from GeneBank using ClustalX and further analyze with the Vector NTI software package (Informax, Inc, Bethesda, MD, USA).

3.2. Vectorology of Novel AAV Serotypes

AAV2 is the first AAV serotype that was engineered as a gene transfer vehicle, but further clinical development of AAV2 vector has been limited by its poor transduction efficiency, restricted tissue tropism, and highly prevalent serology in humans. An effective strategy that has emerged in recent years for expanding the utility of AAV vector is to transcapsidate recombinant AAV2 genomes with the

capsids from different AAV species (7, 10, 31). Briefly, the *cap* gene fragment in the AAV2 vector packaging plasmid that consists of AAV2 *rep* and AAV2 *cap* genes is replaced with the cap fragments from PCR clones of novel AAVs to form chimerical packaging plasmids. AAV2 Rep protein expressed from these chimerical constructs enables efficient rescue and replication rAAV genomes flanked with AAV2 ITRs, whereas packaging of rAAV genomes with other AAV capsids confers the viral vectors with novel biological properties. Nevertheless, one of the challenges in creating such chimerical packaging plasmids is to identify convenient and generic restriction sites for molecular fusion between AAV2 *rep* and novel AAV *cap* genes.

To date, depending on the sequence homology in the beginning of VP1 between AAV2 and the AAV of interest, several cloning strategies have been exploited to create chimerical plasmids. In AAV2 and some other AAV serotypes, a *Swa*I site conveniently exists in the intronic region of the *cap* gene, approximately 10 bp upstream of VP1 start codon, and can be used for creating the chimerical clones. In addition, extensive analyses of 3.1 kb novel AAV PCR clones reveal that there are two or three *Xho*I restriction sites conveniently located in the beginning of the *VP1* gene. Particularly, the first *Xho*I site is at 25 bp after the ATG start codon of VP1, which seems to be highly conserved within many VP1 sequences. The other one or two *Xho*I sites are located approximately 200 bp downstream of the first *Xho*I site. Thus, if the first 9 or 10 amino acids between AAV2 VP1 and that of incoming AAV serotypes are identical, novel AAV *cap* gene sequence can be fused with the first 28 bp of AAV2 *cap* through an *Xho*I partial digestion to generate chimeric packaging plasmids.

The next step in the novel AAV vector development is to test the functionality of chimerical packaging plasmids for the production of rAAVs. The chimerical packaging plasmids can be co-transfected into 293 cells with a vector plasmid carrying recombinant AAV2 genome with a reporter gene, and adenovirus helper plasmid to produce transcapsidated AAV vectors. Infectious viral vector generated from the co-transfection can be examined by infecting 293 cells with crude viral lysate in the presence of adenovirus helper.

3.2.1. Creation of Chimerical Packaging Plasmid

1. Analyze both pAAVrep2/cap2 recipient plasmid and novel AAV PCR-Topo clones to identify appropriate cloning sites (see Note 6).
2. For the novel AAV clones with *Swa*I site, perform the standard molecular cloning procedures to generate chimeric packaging plasmids.
3. For the novel AAV clones with multiple *Xho*I sites, carry out *Xho*I partial digestion at 37°C for 55 min by using 1 μl of 1:32 diluted *Xho*I per two micrograms of plasmid DNA.

4. Stop the digestion by heat-inactivation at 80°C for 20 min.
5. Proceed with other standard molecular cloning steps to generate chimeric packaging plasmids.

3.2.2. Evaluation of Novel Packaging Plasmid for rAAV Production (see Note 7)

1. One day prior to transfection, seed 293 cells in a 24-well plate with 1 ml of 2×10^5 cells/ml per well.
2. At the time of transfection, use 0.2 μg each of pAAV2CMVEGFP, pAd helper plasmid, and test chimeric packaging plasmid to co-transfect each well of 293 cells by Lipofectamin as instructed by manufacturer.
3. Depending on phylogenetic classification of each novel capsid to be tested, use corresponding serotypes of packaging plasmids (e.g., pAAVrep2/cap2, pAAVrep2/cap8, etc.) for co-transfection as the positive control.
4. Change the medium for each well of the transfected cells with 1 ml fresh growth medium (DMEM supplemented with 10% FBS and 1% Pen/Strip) next day.
5. Seventy-two hours after transfection, scrap cells off and harvest the entire cell suspension from each well individually in sterile Eppendorf tubes for three rounds of freeze–thaw in dry ice–ethanol and 37°C water baths, respectively.
6. Spin down the tubes at 14,000 rpm for 10 min to collect the entire 1 ml of supernatant from each sample as crude lysate.
7. Seed 293 cells in another set of 24-well plates as described in step 1.
8. Next day, infect each well of cells with 200 viral particles of helper adenovirus first, followed by infecting two well each of 293 cells with 30 and 300 μl of supernatant from each test production.
9. Thirty-six to forty-eight hours postinfection, examine EGFP transduction of each well under a UV-light microscope to compare rAAV productivity of each test packaging plasmid with that of the corresponding control packaging plasmid.

4. Notes

1. Environmental contamination and false-positive PCR.
   Recovery of endogenous AAVs from primate tissues requires highly sensitive PCR method. Thus, even minor contamination in the processes of tissue DNA preparation and PCR set up with AAV viruses that are aerosol and prevalent in natural environment and/or AAV plasmids in laboratory settings will

spawn false-positive results and skew novel AAV discovery. The following extraordinary precautions should be taken to minimize environmental and operator contaminations.

2. Space separation. If possible, designate a room and set up the work space away from the main laboratory area where AAV production and AAV cloning work are performed. Carry out all work in a BSL II hood.
3. Decontamination. Before and after each use of the work space, UV irradiates the hood, tube racks, and pipettors for 15 min first, followed by surface cleaning with Lysol and then 70% ethanol.
4. Physical prevention. Always keep all reagent vials and sample tubes closed until they need to be opened. Always use barrier pipette tips for reagent and sample transfer. Always wear preventive clothing (if possible disposable laboratory coat, gloves, mask, cap, sleeve covers, etc.) in the designate work area.
5. PCR conditions. It is very difficult to come up a universal PCR condition for isolating different novel AAVs from different tissue DNA samples. The following factors should be considered in optimization of PCR conditions: (1) quality and concentration of tissue DNAs, (2) primer design and selection for some distantly related viruses, (3) annealing and extension temperatures and extension time. In general, start with more stringent temperature and 1 min extension time per kilobase of the amplicon.
6. Creation of chimerical packaging plasmids. Most of times, restriction patterns of the cap fragment in the recipient plasmid and newly creative chimerical packaging plasmids are quite similar. Extreme precaution should be taken to identify new packaging plasmid by careful restriction mapping. Sequencing analysis may be required for confirmation.
7. Evaluation of chimerical packaging plasmids for rAAV production. The sharp contrast in in vitro and in vivo transduction between AAV2 and other novel AAV serotypes-based vector is well known. AAV2 vector is the best transducer in vitro but works poorly in vivo. Although vectors based on novel serotypes such as AAVs7, 8, and 9 demonstrate strong tissue tropisms and high efficiency of transduction in vivo, they work poorly in in vitro transduction. When evaluating the novel packaging plasmids in vitro, one probably should disregard those packaging plasmids that produce no rAAVs at all, but should consider those poor producers for at least one test for large-scale production.

References

1. Blacklow, N. R., Hoggan, M. D., and Rowe, W. P. (1967) Isolation of adenovirus-associated viruses from man, *Proc Natl Acad Sci USA* ***58***, 1410–1415.
2. Chen, C.-L., Jensen, R. L., Schnepp, B. C., Connell, M. J., Shell, R., Sferra, T. J., Bartlett, J. S., Clark, K. R., and Johnson, P. R. (2005) Molecular Characterization of Adeno-Associated Viruses Infecting Children, *J Virol 79*, 14781–14792.
3. Schnepp, B. C., Jensen, R. L., Chen, C. L., Johnson, P. R., and Clark, K. R. (2005) Characterization of adeno-associated virus genomes isolated from human tissues, *J Virol 79*, 14793–14803.
4. Schnepp, B. C., Jensen, R. L., Clark, K. R., and Johnson, P. R. (2009) Infectious molecular clones of adeno-associated virus isolated directly from human tissues, *J Virol 83*, 1456–1464.
5. Gao, G., Alvira, M. R., Somanathan, S., Lu, Y., Vandenberghe, L. H., Rux, J. J., Calcedo, R., Sanmiguel, J., Abbas, Z., and Wilson, J. M. (2003) Adeno-associated viruses undergo substantial evolution in primates during natural infections, *Proc Natl Acad Sci USA* ***100***, 6081–6086.
6. Gao, G., Vandenberghe, L. H., Alvira, M. R., Lu, Y., Calcedo, R., Zhou, X., and Wilson, J. M. (2004) Clades of Adeno-Associated Viruses Are Widely Disseminated in Human Tissues, *J Virol 78*, 6381–6388.
7. Gao, G. P., Alvira, M. R., Wang, L., Calcedo, R., Johnston, J., and Wilson, J. M. (2002) Novel adeno-associated viruses from rhesus monkeys as vectors for human gene therapy, *Proc Natl Acad Sci USA 99*, 11854–11859.
8. Gao, G., Vandenberghe, L. H., and Wilson, J. M. (2005) New recombinant serotypes of AAV vectors, *Curr Gene Ther 5*, 285–297.
9. Duffy, S., Shackelton, L. A., and Holmes, E. C. (2008) Rates of evolutionary change in viruses: patterns and determinants, *Nat Rev Genet 9*, 267–276.
10. Xiao, W., Chirmule, N., Berta, S. C., McCullough, B., Gao, G., and Wilson, J. M. (1999) Gene Therapy Vectors Based on Adeno-Associated Virus Type 1, *J Virol 73*, 3994–4003.
11. Takeuchi, Y., Myers, R., and Danos, O. (2008) Recombination and population mosaic of a multifunctional viral gene, adeno-associated virus cap, *PLoS ONE 3*, e1634.
12. Opie, S. R., Warrington, K. H., Jr., Agbandje-McKenna, M., Zolotukhin, S., and Muzyczka, N. (2003) Identification of amino acid residues in the capsid proteins of adeno-associated virus type 2 that contribute to heparan sulfate proteoglycan binding, *J Virol 77*, 6995–7006.
13. Levy, H. C., Bowman, V. D., Govindasamy, L., McKenna, R., Nash, K., Warrington, K., Chen, W., Muzyczka, N., Yan, X., Baker, T. S., and Agbandje-McKenna, M. (2009) Heparin binding induces conformational changes in Adeno-associated virus serotype 2, *J Struct Biol* ***165***, 146–156.
14. Vandenberghe, L. H., Breous, E., Nam, H. J., Gao, G., Xiao, R., Sandhu, A., Johnston, J., Debyser, Z., Agbandje-McKenna, M., and Wilson, J. M. (2009) Naturally occurring singleton residues in AAV capsid impact vector performance and illustrate structural constraints, *Gene Ther* ***16***, 1416–1428.
15. Grieger, J. C., Snowdy, S., and Samulski, R. J. (2006) Separate Basic Region Motifs within the Adeno-Associated Virus Capsid Proteins Are Essential for Infectivity and Assembly, *J Virol* ***80***, 5199–5210.
16. Excoffon, K. J., Koerber, J. T., Dickey, D. D., Murtha, M., Keshavjee, S., Kaspar, B. K., Zabner, J., and Schaffer, D. V. (2009) Directed evolution of adeno-associated virus to an infectious respiratory virus, *Proc Natl Acad Sci USA* ***106***, 3865–3870.
17. Ward, P., and Walsh, C. E. (2009) Chimeric AAV Cap sequences alter gene transduction, *Virology* ***386***, 237–248.
18. Wang, L., Calcedo, R., Wang, H., Bell, P., Grant, R., Vandenberghe, L. H., Sanmiguel, J., Morizono, H., Batshaw, M. L., and Wilson, J. M. (2009) The Pleiotropic Effects of Natural AAV Infections on Liver-directed Gene Transfer in Macaques, *Mol Ther* ***18***, 126–134.
19. Calcedo, R., Vandenberghe, L. H., Gao, G., Lin, J., and Wilson, J. M. (2009) Worldwide epidemiology of neutralizing antibodies to adeno-associated viruses, *J Infect Dis* ***199***, 381–390.
20. Pattison, J. (1988) *Parvovirus and human disease*. CRC Press, Boca Raton.
21. Halbert, C. L., Miller, A. D., McNamara, S., Emerson, J., Gibson, R. L., Ramsey, B., and Aitken, M. L. (2006) Prevalence of neutralizing antibodies against adeno-associated virus (AAV) types 2, 5, and 6 in cystic fibrosis and normal populations: Implications for gene therapy using AAV vectors, *Hum Gene Ther 17*, 440–447.
22. Chirmule, N., Xiao, W., Truneh, A., Schnell, M. A., Hughes, J. V., Zoltick, P., and Wilson,

J. M. (2000) Humoral immunity to adeno-associated virus type 2 vectors following administration to murine and nonhuman primate muscle, *J Virol* ***74***, 2420–2425.

23. Mori, S., Takeuchi, T., Enomoto, Y., Kondo, K., Sato, K., Ono, F., Sata, T., and Kanda, T. (2008) Tissue distribution of cynomolgus adeno-associated viruses AAV10, AAV11, and AAVcy.7 in naturally infected monkeys, *Arch Virol* ***153***, 375–380.
24. Schmidt, M., Voutetakis, A., Afione, S., Zheng, C., Mandikian, D., and Chiorini, J. A. (2008) Adeno-associated virus type 12 (AAV12): a novel AAV serotype with sialic acid- and heparan sulfate proteoglycan-independent transduction activity, *J Virol* ***82***, 1399–1406.
25. Halbert, C. L., Rutledge, E. A., Allen, J. M., Russell, D. W., and Miller, A. D. (2000) Repeat transduction in the mouse lung by using adeno-associated virus vectors with different serotypes, *J Virol* ***74***, 1524–1532.
26. Peden, C. S., Burger, C., Muzyczka, N., and Mandel, R. J. (2004) Circulating anti-wild-type adeno-associated virus type 2 (AAV2) antibodies inhibit recombinant AAV2 (rAAV2)-mediated, but not rAAV5-mediated, gene transfer in the brain, *J Virol* ***78***, 6344–6359.
27. Riviere, C., Danos, O., and Douar, A. M. (2006) Long-term expression and repeated administration of AAV type 1, 2 and 5 vectors in skeletal muscle of immunocompetent adult mice, *Gene Ther 13*, 1300–1308.
28. Brantly, M. L., Chulay, J. D., Wang, L., Mueller, C., Humphries, M., Spencer, L. T., Rouhani, F., Conlon, T. J., Calcedo, R., Betts, M. R., Spencer, C., Byrne, B. J., Wilson, J. M., and Flotte, T. R. (2009) Sustained transgene expression despite T lymphocyte responses in a clinical trial of rAAV1-AAT gene therapy, *Proc Natl Acad Sci USA* ***106***, 16363–16368.
29. Rabinowitz, J. E., Rolling, F., Li, C., Conrath, H., Xiao, W., Xiao, X., and Samulski, R. J. (2002) Cross-packaging of a single adeno-associated virus (AAV) type 2 vector genome into multiple AAV serotypes enables transduction with broad specificity, *J Virol* ***76***, 791–801.
30. Wu, Z., Asokan, A., and Samulski, R. J. (2006) Adeno-associated virus serotypes: vector toolkit for human gene therapy, *Mol Ther 14*, 316–327.
31. Van Vliet, K. M., Blouin, V., Brument, N., Agbandje-McKenna, M., and Snyder, R. O. (2008) The role of the adeno-associated virus capsid in gene transfer, *Methods Mol Biol 437*, 51–91.
32. Wright, J. F. (2009) Transient Transfection Methods for Clinical Adeno-Associated Viral Vector Production, *Hum Gene Ther* ***20***, 698–706.
33. Kang, W., Wang, L., Harrell, H., Liu, J., Thomas, D. L., Mayfield, T. L., Scotti, M. M., Ye, G. J., Veres, G., and Knop, D. R. (2009) An efficient rHSV-based complementation system for the production of multiple rAAV vector serotypes, *Gene Ther* ***16***, 229–239.
34. Smith, R. H., Levy, J. R., and Kotin, R. M. (2009) A simplified baculovirus-AAV expression vector system coupled with one-step affinity purification yields high-titer rAAV stocks from insect cells, *Mol Ther 17*, 1888–1896.
35. Rabinowitz, J. E., Bowles, D. E., Faust, S. M., Ledford, J. G., Cunningham, S. E., and Samulski, R. J. (2004) Cross-dressing the virion: the transcapsidation of adeno-associated virus serotypes functionally defines subgroups, *J Virol* ***78***, 4421–4432.
36. Kohlbrenner, E., Aslanidi, G., Nash, K., Shklyaev, S., Campbell-Thompson, M., Byrne, B. J., Snyder, R. O., Muzyczka, N., Warrington, K. H., Jr., and Zolotukhin, S. (2005) Successful production of pseudotyped rAAV vectors using a modified baculovirus expression system, *Mol Ther* ***12***, 1217–1225.
37. Allocca, M., Doria, M., Petrillo, M., Colella, P., Garcia-Hoyos, M., Gibbs, D., Kim, S. R., Maguire, A., Rex, T. S., Di Vicino, U., Cutillo, L., Sparrow, J. R., Williams, D. S., Bennett, J., and Auricchio, A. (2008) Serotype-dependent packaging of large genes in adeno-associated viral vectors results in effective gene delivery in mice, *J Clin Invest* ***118***, 1955–1964.
38. Lai, Y., Yue, Y., and Duan, D. (2010) Evidence for the Failure of Adeno-associated Virus Serotype 5 to Package a Viral Genome >/= 8.2 kb, *Mol Ther 18*, 75–79.
39. Dong, B., Nakai, H., and Xiao, W. (2009) Characterization of Genome Integrity for Oversized Recombinant AAV Vector, *Mol Ther 18*, 87–92.
40. Gao, G. P., Lu, Y., Sun, X., Johnston, J., Calcedo, R., Grant, R., and Wilson, J. M. (2006) High-level transgene expression in nonhuman primate liver with novel adeno-associated virus serotypes containing self-complementary genomes, *J Virol* ***80***, 6192–6194.
41. Zhong, L., Li, B., Mah, C. S., Govindasamy, L., Agbandje-McKenna, M., Cooper, M., Herzog, R. W., Zolotukhin, I., Warrington, K. H., Jr., Weigel-Van Aken, K. A., Hobbs, J. A., Zolotukhin, S., Muzyczka, N., and Srivastava, A. (2008) Next generation of adeno-associated virus 2 vectors: point mutations in tyrosines lead to high-efficiency

transduction at lower doses, *Proc Natl Acad Sci USA 105*, 7827–7832.

42. Hewitt, F. C., Li, C., Gray, S. J., Cockrell, S., Washburn, M., and Samulski, R. J. (2009) Reducing the risk of adeno-associated virus (AAV) vector mobilization with AAV type 5 vectors, *J Virol **83***, 3919–3929.
43. Paneda, A., Vanrell, L., Mauleon, I., Crettaz, J. S., Berraondo, P., Timmermans, E. J., Beattie, S. G., Twisk, J., van Deventer, S., Prieto, J., Fontanellas, A., Rodriguez-Pena, M. S., and Gonzalez-Aseguinolaza, G. (2009) Effect of adeno-associated virus serotype and genomic structure on liver transduction and biodistribution in mice of both genders, *Hum Gene Ther **20***, 908–917.
44. Zincarelli, C., Soltys, S., Rengo, G., and Rabinowitz, J. E. (2008) Analysis of AAV serotypes 1–9 mediated gene expression and tropism in mice after systemic injection, *Mol Ther **16***, 1073–1080.
45. Hauck, B., and Xiao, W. (2003) Characterization of tissue tropism determinants of adeno-associated virus type 1, *J Virol 77*, 2768–2774.
46. Davidson, B. L., Stein, C. S., Heth, J. A., Martins, I., Kotin, R. M., Derksen, T. A., Zabner, J., Ghodsi, A., and Chiorini, J. A. (2000) Recombinant adeno-associated virus type 2, 4, and 5 vectors: transduction of variant cell types and regions in the mammalian central nervous system, *Proc Natl Acad Sci USA 97*, 3428–3432.
47. Lin, D., Fantz, C. R., Levy, B., Rafi, M. A., Vogler, C., Wenger, D. A., and Sands, M. S. (2005) AAV2/5 vector expressing galactocerebrosidase ameliorates CNS disease in the murine model of globoid-cell leukodystrophy more efficiently than AAV2, *Mol Ther **12***, 422–430.
48. Wang, Z., Zhu, T., Qiao, C., Zhou, L., Wang, B., Zhang, J., Chen, C., Li, J., and Xiao, X. (2005) Adeno-associated virus serotype 8 efficiently delivers genes to muscle and heart, *Nat Biotechnol **23***, 321–328.
49. Mitchell, M., Nam, H. J., Carter, A., McCall, A., Rence, C., Bennett, A., Gurda, B., McKenna, R., Porter, M., Sakai, Y., Byrne, B. J., Muzyczka, N., Aslanidi, G., Zolotukhin, S., and Agbandje-McKenna, M. (2009) Production, purification and preliminary X-ray crystallographic studies of adeno-associated virus serotype 9, *Acta Crystallogr Sect F Struct Biol Cryst Commun **65***, 715–718.
50. Nathwani, A. C., Cochrane, M., McIntosh, J., Ng, C. Y., Zhou, J., Gray, J. T., and Davidoff, A. M. (2009) Enhancing transduction of the liver by adeno-associated viral vectors, *Gene Ther **16***, 60–69.
51. Ponnazhagan, S., Mukherjee, P., Yoder, M. C., Wang, X. S., Zhou, S. Z., Kaplan, J., Wadsworth, S., and Srivastava, A. (1997) Adeno-associated virus 2-mediated gene transfer in vivo: organ-tropism and expression of transduced sequences in mice, *Gene **190***, 203–210.
52. Koeberl, D. D., Alexander, I. E., Halbert, C. L., Russell, D. W., and Miller, A. D. (1997) Persistent expression of human clotting factor IX from mouse liver after intravenous injection of adeno-associated virus vectors, *Proc Natl Acad Sci USA **94***, 1426–1431.
53. Snyder, R. O., Miao, C. H., Patijn, G. A., Spratt, S. K., Danos, O., Nagy, D., Gown, A. M., Winther, B., Meuse, L., Cohen, L. K., Thompson, A. R., and Kay, M. A. (1997) Persistent and therapeutic concentrations of human factor IX in mice after hepatic gene transfer of recombinant AAV vectors, *Nat Genet **16***, 270–276.
54. Harding, T. C., Koprivnikar, K. E., Tu, G. H., Zayek, N., Lew, S., Subramanian, A., Sivakumaran, A., Frey, D., Ho, K., VanRoey, M. J., Nichols, T. C., Bellinger, D. A., Yendluri, S., Waugh, J., McArthur, J., Veres, G., and Donahue, B. A. (2004) Intravenous administration of an AAV-2 vector for the expression of factor IX in mice and a dog model of hemophilia B, *Gene Ther **11***, 204–213.
55. Inagaki, K., Fuess, S., Storm, T. A., Gibson, G. A., McTiernan, C. F., Kay, M. A., and Nakai, H. (2006) Robust systemic transduction with AAV9 vectors in mice: efficient global cardiac gene transfer superior to that of AAV8, *Mol Ther **14***, 45–53.
56. Gregorevic, P., Blankinship, M. J., Allen, J. M., Crawford, R. W., Meuse, L., Miller, D. G., Russell, D. W., and Chamberlain, J. S. (2004) Systemic delivery of genes to striated muscles using adeno-associated viral vectors, *Nat Med **10***, 828–834.
57. Nathwani, A. C., Gray, J. T., McIntosh, J., Ng, C. Y., Zhou, J., Spence, Y., Cochrane, M., Gray, E., Tuddenham, E. G., and Davidoff, A. M. (2007) Safe and efficient transduction of the liver after peripheral vein infusion of self-complementary AAV vector results in stable therapeutic expression of human FIX in nonhuman primates, *Blood **109***, 1414–1421.
58. Nakai, H., Wu, X., Fuess, S., Storm, T. A., Munroe, D., Montini, E., Burgess, S. M., Grompe, M., and Kay, M. A. (2005) Large-scale molecular characterization of adeno-associated

virus vector integration in mouse liver, *J Virol* ***79***, 3606–3614.

59. Sarkar, R., Tetreault, R., Gao, G., Wang, L., Bell, P., Chandler, R., Wilson, J. M., and Kazazian, H. H., Jr. (2004) Total correction of hemophilia A mice with canine FVIII using an AAV 8 serotype, *Blood* ***103***, 1253–1260.
60. Davidoff, A. M., Ng, C. Y., Zhou, J., Spence, Y., and Nathwani, A. C. (2003) Sex significantly influences transduction of murine liver by recombinant adeno-associated viral vectors through an androgen-dependent pathway, *Blood* ***102***, 480–488.
61. Yue, Y., Ghosh, A., Long, C., Bostick, B., Smith, B. F., Kornegay, J. N., and Duan, D. (2008) A single intravenous injection of adeno-associated virus serotype-9 leads to whole body skeletal muscle transduction in dogs, *Mol Ther* ***16***, 1944–1952.
62. Pacak, C. A., Sakai, Y., Thattaliyath, B. D., Mah, C. S., and Byrne, B. J. (2008) Tissue specific promoters improve specificity of AAV9 mediated transgene expression following intra-vascular gene delivery in neonatal mice, *Genet Vaccines Ther* ***6***, 13.
63. Pacak, C. A., Mah, C. S., Thattaliyath, B. D., Conlon, T. J., Lewis, M. A., Cloutier, D. E., Zolotukhin, I., Tarantal, A. F., and Byrne, B. J. (2006) Recombinant adeno-associated virus serotype 9 leads to preferential cardiac transduction in vivo, *Circ Res* ***99***, e3-9.
64. Fechner, H., Sipo, I., Westermann, D., Pinkert, S., Wang, X., Suckau, L., Kurreck, J., Zeichhardt, H., Muller, O., Vetter, R., Erdmann, V., Tschope, C., and Poller, W. (2008) Cardiac-targeted RNA interference mediated by an AAV9 vector improves cardiac function in coxsackievirus B3 cardiomyopathy, *J Mol Med* ***86***, 987–997.
65. Bostick, B., Yue, Y., Lai, Y., Long, C., Li, D., and Dongsheng, D. (2008) AAV-9 microdystrophin gene therapy ameliorates electrocardiographic abnormalities in mdx mice, *Hum Gene Ther 19, 851-856.*
66. Goehringer, C., Rutschow, D., Bauer, R., Schinkel, S., Weichenhan, D., Bekeredjian, R., Straub, V., Kleinschmidt, J. A., Katus, H. A., and Muller, O. J. (2009) Prevention of cardiomyopathy in delta-sarcoglycan knockout mice after systemic transfer of targeted adeno-associated viral vectors, *Cardiovasc Res* ***82***, 404–410.
67. Ogura, T., Mizukami, H., Mimuro, J., Madoiwa, S., Okada, T., Matsushita, T., Urabe, M., Kume, A., Hamada, H., Yoshikawa, H., Sakata, Y., and Ozawa, K. (2006) Utility of intraperitoneal administration as a route of AAV serotype 5 vector-mediated neonatal gene transfer, *J Gene Med* ***8***, 990–997.
68. Foust, K. D., Poirier, A., Pacak, C. A., Mandel, R. J., and Flotte, T. R. (2008) Neonatal intraperitoneal or intravenous injections of recombinant adeno-associated virus type 8 transduce dorsal root ganglia and lower motor neurons, *Hum Gene Ther* ***19***, 61–70.
69. Wang, Z., Zhu, T., Rehman, K. K., Bertera, S., Zhang, J., Chen, C., Papworth, G., Watkins, S., Trucco, M., Robbins, P. D., Li, J., and Xiao, X. (2006) Widespread and stable pancreatic gene transfer by adeno-associated virus vectors via different routes, *Diabetes* ***55***, 875–884.
70. Halbert, C. L., Standaert, T. A., Aitken, M. L., Alexander, I. E., Russell, D. W., and Miller, A. D. (1997) Transduction by adeno-associated virus vectors in the rabbit airway: efficiency, persistence, and readministration, *J Virol 71*, 5932–5941.
71. Liqun Wang, R., McLaughlin, T., Cossette, T., Tang, Q., Foust, K., Campbell-Thompson, M., Martino, A., Cruz, P., Loiler, S., Mueller, C., and Flotte, T. R. (2009) Recombinant AAV serotype and capsid mutant comparison for pulmonary gene transfer of alpha-1-antitrypsin using invasive and noninvasive delivery, *Mol Ther 17*, 81–87.
72. Mease, P. J., Hobbs, K., Chalmers, A., El-Gabalawy, H., Bookman, A., Keystone, E., Furst, D. E., Anklesaria, P., and Heald, A. E. (2009) Local delivery of a recombinant adenoassociated vector containing a tumour necrosis factor alpha antagonist gene in inflammatory arthritis: a phase 1 dose-escalation safety and tolerability study, *Ann Rheum Dis* ***68***, 1247–1254.
73. Ghosh, A., Allamarvdasht, M., Pan, C. J., Sun, M. S., Mansfield, B. C., Byrne, B. J., and Chou, J. Y. (2006) Long-term correction of murine glycogen storage disease type Ia by recombinant adeno-associated virus-1-mediated gene transfer, *Gene Ther* ***13***, 321–329.
74. Bostick, B., Ghosh, A., Yue, Y., Long, C., and Duan, D. (2007) Systemic AAV-9 transduction in mice is influenced by animal age but not by the route of administration, *Gene Ther* ***14***, 1605–1609.
75. Daly, T. M., Okuyama, T., Vogler, C., Haskins, M. E., Muzyczka, N., and Sands, M. S. (1999) Neonatal intramuscular injection with recombinant adeno-associated virus results in prolonged beta-glucuronidase expression in situ and correction of liver pathology in mucopolysaccharidosis type VII mice, *Hum Gene Ther* ***10***, 85–94.
76. Niemeyer, G. P., Herzog, R. W., Mount, J., Arruda, V. R., Tillson, D. M., Hathcock, J.,

van Ginkel, F. W., High, K. A., and Lothrop, C. D., Jr. (2009) Long-term correction of inhibitor-prone hemophilia B dogs treated with liver-directed AAV2-mediated factor IX gene therapy, *Blood* ***113***, 797–806.

77. Herzog, R. W., Yang, E. Y., Couto, L. B., Hagstrom, J. N., Elwell, D., Fields, P. A., Burton, M., Bellinger, D. A., Read, M. S., Brinkhous, K. M., Podsakoff, G. M., Nichols, T. C., Kurtzman, G. J., and High, K. A. (1999) Long-term correction of canine hemophilia B by gene transfer of blood coagulation factor IX mediated by adeno-associated viral vector, *Nat Med* ***5***, 56–63.
78. Arruda, V. R., Schuettrumpf, J., Herzog, R. W., Nichols, T. C., Robinson, N., Lotfi, Y., Mingozzi, F., Xiao, W., Couto, L. B., and High, K. A. (2004) Safety and efficacy of factor IX gene transfer to skeletal muscle in murine and canine hemophilia B models by adeno-associated viral vector serotype 1, *Blood* ***103***, 85–92.
79. Jiang, H., Lillicrap, D., Patarroyo-White, S., Liu, T., Qian, X., Scallan, C. D., Powell, S., Keller, T., McMurray, M., Labelle, A., Nagy, D., Vargas, J. A., Zhou, S., Couto, L. B., and Pierce, G. F. (2006) Multiyear therapeutic benefit of AAV serotypes 2, 6, and 8 delivering factor VIII to hemophilia A mice and dogs, *Blood* ***108***, 107–115.
80. Sarkar, R., Mucci, M., Addya, S., Tetreault, R., Bellinger, D. A., Nichols, T. C., and Kazazian, H. H., Jr. (2006) Long-term efficacy of adeno-associated virus serotypes 8 and 9 in hemophilia a dogs and mice, *Hum Gene Ther* ***17***, 427–439.
81. Gao, G., Lu, Y., Calcedo, R., Grant, R. L., Bell, P., Wang, L., Figueredo, J., Lock, M., and Wilson, J. M. (2006) Biology of AAV serotype vectors in liver-directed gene transfer to nonhuman primates, *Mol Ther* ***13***, 77–87.
82. Qiao, C., Li, J., Zheng, H., Bogan, J., Yuan, Z., Zhang, C., Bogan, D., Kornegay, J., and Xiao, X. (2009) Hydrodynamic limb vein injection of adeno-associated virus serotype 8 vector carrying canine myostatin propeptide gene into normal dogs enhances muscle growth, *Hum Gene Ther 20*, 1–10.
83. Ohshima, S., Shin, J. H., Yuasa, K., Nishiyama, A., Kira, J., Okada, T., and Takeda, S. (2009) Transduction efficiency and immune response associated with the administration of AAV8 vector into dog skeletal muscle, *Mol Ther* ***17***, 73–80.
84. Rodino-Klapac, L. R., Montgomery, C. L., Bremer, W. G., Shontz, K. M., Malik, V., Davis, N., Sprinkle, S., Campbell, K. J., Sahenk, Z., Clark, K. R., Walker, C. M., Mendell, J. R., and Chicoine, L. G. (2010) Persistent expression of FLAG-tagged micro dystrophin in nonhuman primates following intramuscular and vascular delivery, *Mol Ther* ***18***, 109–117.
85. Bish, L. T., Sleeper, M. M., Brainard, B., Cole, S., Russell, N., Withnall, E., Arndt, J., Reynolds, C., Davison, E., Sanmiguel, J., Wu, D., Gao, G., Wilson, J. M., and Sweeney, H. L. (2008) Percutaneous transendocardial delivery of self-complementary adeno-associated virus 6 achieves global cardiac gene transfer in canines, *Mol Ther* ***16***, 1953–1959.
86. During, M. J., Samulski, R. J., Elsworth, J. D., Kaplitt, M. G., Leone, P., Xiao, X., Li, J., Freese, A., Taylor, J. R., Roth, R. H., Sladek, J. R., Jr., O'Malley, K. L., and Redmond, D. E., Jr. (1998) In vivo expression of therapeutic human genes for dopamine production in the caudates of MPTP-treated monkeys using an AAV vector, *Gene Ther* ***5***, 820–827.
87. Bankiewicz, K. S., Forsayeth, J., Eberling, J. L., Sanchez-Pernaute, R., Pivirotto, P., Bringas, J., Herscovitch, P., Carson, R. E., Eckelman, W., Reutter, B., and Cunningham, J. (2006) Long-term clinical improvement in MPTP-lesioned primates after gene therapy with AAV-hAADC, *Mol Ther* ***20***, 350–360.
88. Ciron, C., Cressant, A., Roux, F., Raoul, S., Cherel, Y., Hantraye, P., Deglon, N., Schwartz, B., Barkats, M., Heard, J. M., Tardieu, M., Moullier, P., and Colle, M. A. (2009) Human alpha-iduronidase gene transfer mediated by adeno-associated virus types 1, 2, and 5 in the brain of nonhuman primates: vector diffusion and biodistribution, *Hum Gene Ther 20*, 350–360.
89. Eslamboli, A., Romero-Ramos, M., Burger, C., Bjorklund, T., Muzyczka, N., Mandel, R. J., Baker, H., Ridley, R. M., and Kirik, D. (2007) Long-term consequences of human alpha-synuclein overexpression in the primate ventral midbrain, *Brain* ***130***, 799–815.
90. Colle, M. A., Piguet, F., Bertrand, L., Raoul, S., Bieche, I., Dubreil, L., Sloothaak, D., Bouquet, C., Moullier, P., Aubourg, P., Cherel, Y., Cartier, N., and Sevin, C. (2010) Efficient intracerebral delivery of AAV5 vector encoding human ARSA in non-human primate, *Hum Mol Genet* ***19***, 147–158.
91. Bennett, J., Maguire, A. M., Cideciyan, A. V., Schnell, M., Glover, E., Anand, V., Aleman, T. S., Chirmule, N., Gupta, A. R., Huang, Y., Gao, G. P., Nyberg, W. C., Tazelaar, J., Hughes, J., Wilson, J. M., and Jacobson, S. G. (1999) Stable transgene expression in rod photoreceptors after recombinant adeno-associated virus-mediated gene transfer to monkey retina, *Proc Natl Acad Sci USA* ***96***, 9920–9925.

92. Lotery, A. J., Yang, G. S., Mullins, R. F., Russell, S. R., Schmidt, M., Stone, E. M., Lindbloom, J. D., Chiorini, J. A., Kotin, R. M., and Davidson, B. L. (2003) Adeno-associated virus type 5: transduction efficiency and cell-type specificity in the primate retina, *Hum Gene Ther* ***14***, 1663–1671.

93. Jacobson, S. G., Boye, S. L., Aleman, T. S., Conlon, T. J., Zeiss, C. J., Roman, A. J., Cideciyan, A. V., Schwartz, S. B., Komaromy, A. M., Doobrajh, M., Cheung, A. Y., Sumaroka, A., Pearce-Kelling, S. E., Aguirre, G. D., Kaushal, S., Maguire, A. M., Flotte, T. R., and Hauswirth, W. W. (2006) Safety in nonhuman primates of ocular AAV2-RPE65, a candidate treatment for blindness in Leber congenital amaurosis, *Hum Gene Ther* ***17***, 845–858.

94. Stieger, K., Schroeder, J., Provost, N., Mendes-Madeira, A., Belbellaa, B., Le Meur, G., Weber, M., Deschamps, J. Y., Lorenz, B., Moullier, P., and Rolling, F. (2009) Detection of intact rAAV particles up to 6 years after successful gene transfer in the retina of dogs and primates, *Mol Ther* ***17***, 516–523.

95. Manno, C. S., Pierce, G. F., Arruda, V. R., Glader, B., Ragni, M., Rasko, J. J., Ozelo, M. C., Hoots, K., Blatt, P., Konkle, B., Dake, M., Kaye, R., Razavi, M., Zajko, A., Zehnder, J., Rustagi, P. K., Nakai, H., Chew, A., Leonard, D., Wright, J. F., Lessard, R. R., Sommer, J. M., Tigges, M., Sabatino, D., Luk, A., Jiang, H., Mingozzi, F., Couto, L., Ertl, H. C., High, K. A., and Kay, M. A. (2006) Successful transduction of liver in hemophilia by AAV-Factor IX and limitations imposed by the host immune response, *Nat Med* ***12***, 342–347.

96. Mingozzi, F., Maus, M. V., Hui, D. J., Sabatino, D. E., Murphy, S. L., Rasko, J. E., Ragni, M. V., Manno, C. S., Sommer, J., Jiang, H., Pierce, G. F., Ertl, H. C., and High, K. A. (2007) CD8(+) T-cell responses to adeno-associated virus capsid in humans, *Nat Med* ***13***, 419–422.

97. Herzog, R. W. (2007) Immune responses to AAV capsid: are mice not humans after all? *Mol Ther* ***15***, 649–650.

98. Bainbridge, J. W., Smith, A. J., Barker, S. S., Robbie, S., Henderson, R., Balaggan, K., Viswanathan, A., Holder, G. E., Stockman, A., Tyler, N., Petersen-Jones, S., Bhattacharya, S. S., Thrasher, A. J., Fitzke, F. W., Carter, B. J., Rubin, G. S., Moore, A. T., and Ali, R. R. (2008) Effect of gene therapy on visual function in Leber's congenital amaurosis, *N Engl J Med* ***358***, 2231–2239.

99. Maguire, A. M., Simonelli, F., Pierce, E. A., Pugh, E. N., Jr., Mingozzi, F., Bennicelli, J., Banfi, S., Marshall, K. A., Testa, F., Surace, E. M., Rossi, S., Lyubarsky, A., Arruda, V. R., Konkle, B., Stone, E., Sun, J., Jacobs, J., Dell'Osso, L., Hertle, R., Ma, J. X., Redmond, T. M., Zhu, X., Hauck, B., Zelenaia, O., Shindler, K. S., Maguire, M. G., Wright, J. F., Volpe, N. J., McDonnell, J. W., Auricchio, A., High, K. A., and Bennett, J. (2008) Safety and efficacy of gene transfer for Leber's congenital amaurosis, *N Engl J Med* ***358***, 2240–2248.

100. Hauswirth, W. W., Aleman, T. S., Kaushal, S., Cideciyan, A. V., Schwartz, S. B., Wang, L., Conlon, T. J., Boye, S. L., Flotte, T. R., Byrne, B. J., and Jacobson, S. G. (2008) Treatment of leber congenital amaurosis due to RPE65 mutations by ocular subretinal injection of adeno-associated virus gene vector: short-term results of a phase I trial, *Hum Gene Ther* ***19***, 979–990.

101. Gao, G., Vandenberghe, L. H., and Wilson, J. M. (2005) New recombinant serotypes of AAV vectors, *Curr Gene Ther* ***5***, 285–297.

102. Vandenberghe, L. H., Wilson, J. M., and Gao, G. (2009) Tailoring the AAV vector capsid for gene therapy, *Gene Ther* ***16***, 311–319.

103. Du, L., Kido, M., Lee, D. V., Rabinowitz, J. E., Samulski, R. J., Jamieson, S. W., Weitzman, M. D., and Thistlethwaite, P. A. (2004) Differential myocardial gene delivery by recombinant serotype-specific adeno-associated viral vectors, *Mol Ther* ***10***, 604–608.

104. Palomeque, J., Chemaly, E. R., Colosi, P., Wellman, J. A., Zhou, S., Del Monte, F., and Hajjar, R. J. (2007) Efficiency of eight different AAV serotypes in transducing rat myocardium in vivo, *Gene Ther* ***14***, 989–997.

105. Yan, Z., Lei-Butters, D. C., Liu, X., Zhang, Y., Zhang, L., Luo, M., Zak, R., and Engelhardt, J. F. (2006) Unique biologic properties of recombinant AAV1 transduction in polarized human airway epithelia, *J Biol Chem* ***281***, 29684–29692.

106. Lorain, S., Gross, D. A., Goyenvalle, A., Danos, O., Davoust, J., and Garcia, L. (2008) Transient immunomodulation allows repeated injections of AAV1 and correction of muscular dystrophy in multiple muscles, *Mol Ther* ***16***, 541–547.

107. Vite, C. H., Passini, M. A., Haskins, M. E., and Wolfe, J. H. (2003) Adeno-associated virus vector-mediated transduction in the cat brain, *Gene Ther* ***10***, 1874–1881.

108. Kawase, Y., Ly, H. Q., Prunier, F., Lebeche, D., Shi, Y., Jin, H., Hadri, L., Yoneyama, R., Hoshino, K., Takewa, Y., Sakata, S., Peluso, R., Zsebo, K., Gwathmey, J. K., Tardif, J. C., Tanguay, J. F., and Hajjar, R. J. (2008) Reversal of cardiac dysfunction after long-term expression of SERCA2a by gene transfer

in a pre-clinical model of heart failure, *J Am Coll Cardiol* ***51***, 1112–1119.

109. Byrne, M. J., Power, J. M., Preovolos, A., Mariani, J. A., Hajjar, R. J., and Kaye, D. M. (2008) Recirculating cardiac delivery of AAV2/1SERCA2a improves myocardial function in an experimental model of heart failure in large animals, *Gene Ther* ***15***, 1550–1557.
110. Liu, X., Luo, M., Guo, C., Yan, Z., Wang, Y., and Engelhardt, J. F. (2007) Comparative biology of rAAV transduction in ferret, pig and human airway epithelia, *Gene Ther* ***14***, 1543–1548.
111. Flotte, T. R., Fischer, A. C., Goetzmann, J., Mueller, C., Cebotaru, L., Yan, Z., Wang, L., Wilson, J. M., Guggino, W. B., and Engelhardt, J. F. (2010) Dual reporter comparative indexing of rAAV pseudotyped vectors in chimpanzee airway, *Mol Ther* ***18***, 594–600.
112. Flotte, T. R., Conlon, T. J., Poirier, A., Campbell-Thompson, M., and Byrne, B. J. (2007) Preclinical characterization of a recombinant adeno-associated virus type 1-pseudotyped vector demonstrates dose-dependent injection site inflammation and dissemination of vector genomes to distant sites, *Hum Gene Ther* ***18***, 245–256.
113. Ross, C. J., Twisk, J., Bakker, A. C., Miao, F., Verbart, D., Rip, J., Godbey, T., Dijkhuizen, P., Hermens, W. T., Kastelein, J. J., Kuivenhoven, J. A., Meulenberg, J. M., and Hayden, M. R. (2006) Correction of feline lipoprotein lipase deficiency with adeno-associated virus serotype 1-mediated gene transfer of the lipoprotein lipase S447X beneficial mutation, *Hum Gene Ther* ***17***, 487–499.
114. Rivera, V. M., Gao, G. P., Grant, R. L., Schnell, M. A., Zoltick, P. W., Rozamus, L. W., Clackson, T., and Wilson, J. M. (2005) Long-term pharmacologically regulated expression of erythropoietin in primates following AAV-mediated gene transfer, *Blood* ***105***, 1424–1430.
115. Jaski, B. E., Jessup, M. L., Mancini, D. M., Cappola, T. P., Pauly, D. F., Greenberg, B., Borow, K., Dittrich, H., Zsebo, K. M., and Hajjar, R. J. (2009) Calcium upregulation by percutaneous administration of gene therapy in cardiac disease (CUPID Trial), a first-in-human phase 1/2 clinical trial, *J Card Fail* ***15***, 171–181.
116. Mendell, J. R., Rodino-Klapac, L. R., Rosales-Quintero, X., Kota, J., Coley, B. D., Galloway, G., Craenen, J. M., Lewis, S., Malik, V., Shilling, C., Byrne, B. J., Conlon, T., Campbell, K. J., Bremer, W. G., Viollet, L., Walker, C. M., Sahenk, Z., and Clark, K. R. (2009) Limb-girdle muscular dystrophy type 2D gene therapy restores alpha-sarcoglycan and associated proteins, *Ann Neurol* ***66***, 290–297.
117. Stroes, E. S., Nierman, M. C., Meulenberg, J. J., Franssen, R., Twisk, J., Henny, C. P., Maas, M. M., Zwinderman, A. H., Ross, C., Aronica, E., High, K. A., Levi, M. M., Hayden, M. R., Kastelein, J. J., and Kuivenhoven, J. A. (2008) Intramuscular administration of AAV1-lipoprotein lipase S447X lowers triglycerides in lipoprotein lipase-deficient patients, *Arterioscler Thromb Vasc Biol* ***28***, 2303–2304.
118. Griffey, M. A., Wozniak, D., Wong, M., Bible, E., Johnson, K., Rothman, S. M., Wentz, A. E., Cooper, J. D., and Sands, M. S. (2006) CNS-directed AAV2-mediated gene therapy ameliorates functional deficits in a murine model of infantile neuronal ceroid lipofuscinosis, *Mol Ther* ***13***, 538–547.
119. Burger, C., Gorbatyuk, O. S., Velardo, M. J., Peden, C. S., Williams, P., Zolotukhin, S., Reier, P. J., Mandel, R. J., and Muzyczka, N. (2004) Recombinant AAV viral vectors pseudotyped with viral capsids from serotypes 1, 2, and 5 display differential efficiency and cell tropism after delivery to different regions of the central nervous system, *Mol Ther* ***10***, 302–317.
120. Yang, G. S., Schmidt, M., Yan, Z., Lindbloom, J. D., Harding, T. C., Donahue, B. A., Engelhardt, J. F., Kotin, R., and Davidson, B. L. (2002) Virus-mediated transduction of murine retina with adeno-associated virus: effects of viral capsid and genome size, *J Virol* ***76***, 7651–7660.
121. Glushakova, L. G., Timmers, A. M., Pang, J., Teusner, J. T., and Hauswirth, W. W. (2006) Human blue-opsin promoter preferentially targets reporter gene expression to rat s-cone photoreceptors, *Invest Ophthalmol Vis Sci* ***47***, 3505–3513.
122. Li, J., Wang, D., Qian, S., Chen, Z., Zhu, T., and Xiao, X. (2003) Efficient and long-term intracardiac gene transfer in delta-sarcoglycan-deficiency hamster by adeno-associated virus-2 vectors, *Gene Ther* ***10***, 1807–1813.
123. Tuuminen, R., Nykanen, A. I., Krebs, R., Soronen, J., Pajusola, K., Keranen, M. A., Koskinen, P. K., Alitalo, K., and Lemstrom, K. B. (2009) PDGF-A, -C, and -D but not PDGF-B increase TGF-beta1 and chronic rejection in rat cardiac allografts, *Arterioscler Thromb Vasc Biol* ***29***, 691–698.
124. Takahashi, H., Kato, K., Miyake, K., Hirai, Y., Yoshino, S., and Shimada, T. (2005) Adeno-associated virus vector-mediated anti-angiogenic gene therapy for collagen-induced arthritis in mice, *Clin Exp Rheumatol* ***23***, 455–461.

125. Dai, J., and Rabie, A. B. (2007) Direct AAV-mediated gene delivery to the temporomandibular joint, *Front Biosci* **12**, 2212–2220.

126. Wheeler, M. D., Kono, H., Rusyn, I., Arteel, G. E., McCarty, D., Samulski, R. J., and Thurman, R. G. (2000) Chronic ethanol increases adeno-associated viral transgene expression in rat liver via oxidant and NFkappaB-dependent mechanisms, *Hepatology* **32**, 1050–1059.

127. Halbert, C. L., and Miller, A. D. (2004) AAV-mediated gene transfer to mouse lungs, *Methods Mol Biol* **246**, 201–212.

128. Yoshimura, M., Sakamoto, M., Ikemoto, M., Mochizuki, Y., Yuasa, K., Miyagoe-Suzuki, Y., and Takeda, S. (2004) AAV vector-mediated microdystrophin expression in a relatively small percentage of mdx myofibers improved the mdx phenotype, *Mol Ther* **10**, 821–828.

129. Zaratiegui, M., Castilla-Cortazar, I., Garcia, M., Quiroga, J., Prieto, J., and Novo, F. J. (2002) IGF1 gene transfer into skeletal muscle using recombinant adeno-associated virus in a rat model of liver cirrhosis, *J Physiol Biochem* **58**, 169–176.

130. Acland, G. M., Aguirre, G. D., Ray, J., Zhang, Q., Aleman, T. S., Cideciyan, A. V., Pearce-Kelling, S. E., Anand, V., Zeng, Y., Maguire, A. M., Jacobson, S. G., Hauswirth, W. W., and Bennett, J. (2001) Gene therapy restores vision in a canine model of childhood blindness, *Nat Genet* **28**, 92–95.

131. Kaplitt, M. G., Xiao, X., Samulski, R. J., Li, J., Ojamaa, K., Klein, I. L., Makimura, H., Kaplitt, M. J., Strumpf, R. K., and Diethrich, E. B. (1996) Long-term gene transfer in porcine myocardium after coronary infusion of an adeno-associated virus vector, *Ann Thorac Surg* **62**, 1669–1676.

132. Ulrich-Vinther, M., Duch, M. R., Soballe, K., O'Keefe, R. J., Schwarz, E. M., and Pedersen, F. S. (2004) In vivo gene delivery to articular chondrocytes mediated by an adeno-associated virus vector, *J Orthop Res* **22**, 726–734.

133. Goodrich, L. R., Choi, V. W., Carbone, B. A., McIlwraith, C. W., and Samulski, R. J. (2009) Ex Vivo Serotype-Specific Transduction of Equine Joint Tissue by Self-Complementary Adeno-Associated Viral Vectors, *Hum Gene Ther* **20**, 1697–1702.

134. Mount, J. D., Herzog, R. W., Tillson, D. M., Goodman, S. A., Robinson, N., McCleland, M. L., Bellinger, D., Nichols, T. C., Arruda, V. R., Lothrop, C. D., Jr., and High, K. A. (2002) Sustained phenotypic correction of hemophilia B dogs with a factor IX null mutation by liver-directed gene therapy, *Blood* **99**, 2670–2676.

135. Rubenstein, R. C., McVeigh, U., Flotte, T. R., Guggino, W. B., and Zeitlin, P. L. (1997) CFTR gene transduction in neonatal rabbits using an adeno-associated virus (AAV) vector, *Gene Ther* **4**, 384–392.

136. Conrad, C. K., Allen, S. S., Afione, S. A., Reynolds, T. C., Beck, S. E., Fee-Maki, M., Barrazza-Ortiz, X., Adams, R., Askin, F. B., Carter, B. J., Guggino, W. B., and Flotte, T. R. (1996) Safety of single-dose administration of an adeno-associated virus (AAV)-CFTR vector in the primate lung, *Gene Ther* **3**, 658–668.

137. Tuszynski, M. H., Thal, L., Pay, M., Salmon, D. P., U, H. S., Bakay, R., Patel, P., Blesch, A., Vahlsing, H. L., Ho, G., Tong, G., Potkin, S. G., Fallon, J., Hansen, L., Mufson, E. J., Kordower, J. H., Gall, C., and Conner, J. (2005) A phase 1 clinical trial of nerve growth factor gene therapy for Alzheimer disease, *Nat Med* **11**, 551–555.

138. Worgall, S., Sondhi, D., Hackett, N. R., Kosofsky, B., Kekatpure, M. V., Neyzi, N., Dyke, J. P., Ballon, D., Heier, L., Greenwald, B. M., Christos, P., Mazumdar, M., Souweidane, M. M., Kaplitt, M. G., and Crystal, R. G. (2008) Treatment of late infantile neuronal ceroid lipofuscinosis by CNS administration of a serotype 2 adeno-associated virus expressing CLN2 cDNA, *Hum Gene Ther* **19**, 463–474.

139. Janson, C., McPhee, S., Bilaniuk, L., Haselgrove, J., Testaiuti, M., Freese, A., Wang, D. J., Shera, D., Hurh, P., Rupin, J., Saslow, E., Goldfarb, O., Goldberg, M., Larijani, G., Sharrar, W., Liouterman, L., Camp, A., Kolodny, E., Samulski, J., and Leone, P. (2002) Clinical protocol. Gene therapy of Canavan disease: AAV-2 vector for neurosurgical delivery of aspartoacylase gene (ASPA) to the human brain, *Hum Gene Ther* **13**, 1391–1412.

140. Kaplitt, M. G., Feigin, A., Tang, C., Fitzsimons, H. L., Mattis, P., Lawlor, P. A., Bland, R. J., Young, D., Strybing, K., Eidelberg, D., and During, M. J. (2007) Safety and tolerability of gene therapy with an adeno-associated virus (AAV) borne GAD gene for Parkinson's disease: an open label, phase I trial, *Lancet* **369**, 2097–2105.

141. Wagner, J. A., Nepomuceno, I. B., Messner, A. H., Moran, M. L., Batson, E. P., Dimiceli, S., Brown, B. W., Desch, J. K., Norbash, A. M., Conrad, C. K., Guggino, W. B., Flotte, T. R., Wine, J. J., Carter, B. J., Reynolds, T. C., Moss, R. B., and Gardner, P. (2002) A phase II, double-blind, randomized, placebo-controlled clinical trial of tgAAVCF using maxillary sinus delivery in patients with cystic

fibrosis with antrostomies, *Hum Gene Ther* ***13***, 1349–1359.

142. Flotte, T. R., Brantly, M. L., Spencer, L. T., Byrne, B. J., Spencer, C. T., Baker, D. J., and Humphries, M. (2004) Phase I trial of intramuscular injection of a recombinant adeno-associated virus alpha 1-antitrypsin (rAAV2-CB-hAAT) gene vector to AAT-deficient adults, *Hum Gene Ther* ***15***, 93–128.
143. Kay, M. A., Manno, C. S., Ragni, M. V., Larson, P. J., Couto, L. B., McClelland, A., Glader, B., Chew, A. J., Tai, S. J., Herzog, R. W., Arruda, V., Johnson, F., Scallan, C., Skarsgard, E., Flake, A. W., and High, K. A. (2000) Evidence for gene transfer and expression of factor IX in haemophilia B patients treated with an AAV vector, *Nat Genet* ***24***, 257–261.
144. Weber, M., Rabinowitz, J., Provost, N., Conrath, H., Folliot, S., Briot, D., Cherel, Y., Chenuaud, P., Samulski, J., Moullier, P., and Rolling, F. (2003) Recombinant adeno-associated virus serotype 4 mediates unique and exclusive long-term transduction of retinal pigmented epithelium in rat, dog, and nonhuman primate after subretinal delivery, *Mol Ther 7*, 774–781.
145. Alisky, J. M., Hughes, S. M., Sauter, S. L., Jolly, D., Dubensky, T. W., Jr., Staber, P. D., Chiorini, J. A., and Davidson, B. L. (2000) Transduction of murine cerebellar neurons with recombinant FIV and AAV5 vectors, *Neuroreport* ***11***, 2669–2673.
146. Gorbatyuk, M., Justilien, V., Liu, J., Hauswirth, W. W., and Lewin, A. S. (2007) Preservation of photoreceptor morphology and function in P23H rats using an allele independent ribozyme, *Experimental eye research* ***84***, 44–52.
147. Apparailly, F., Khoury, M., Vervoordeldonk, M. J., Adriaansen, J., Gicquel, E., Perez, N., Riviere, C., Louis-Plence, P., Noel, D., Danos, O., Douar, A. M., Tak, P. P., and Jorgensen, C. (2005) Adeno-associated virus pseudotype 5 vector improves gene transfer in arthritic joints, *Hum Gene Ther* ***16***, 426–434.
148. Adriaansen, J., Khoury, M., de Cortie, C. J., Fallaux, F. J., Bigey, P., Scherman, D., Gould, D. J., Chernajovsky, Y., Apparailly, F., Jorgensen, C., Vervoordeldonk, M. J., and Tak, P. P. (2007) Reduction of arthritis following intra-articular administration of an adeno-associated virus serotype 5 expressing a disease-inducible TNF-blocking agent, *Ann Rheum Dis* ***66***, 1143–1150.
149. Kitajima, K., Marchadier, D. H., Burstein, H., and Rader, D. J. (2006) Persistent liver expression of murine apoA-l using vectors based on adeno-associated viral vectors serotypes 5 and 1, *Atherosclerosis* ***186***, 65–73.
150. De, B., Heguy, A., Leopold, P. L., Wasif, N., Korst, R. J., Hackett, N. R., and Crystal, R. G. (2004) Intrapleural administration of a serotype 5 adeno-associated virus coding for alpha1-antitrypsin mediates persistent, high lung and serum levels of alpha1-antitrypsin, *Mol Ther* ***10***, 1003–1010.
151. Sandalon, Z., Bruckheimer, E. M., Lustig, K. H., Rogers, L. C., Peluso, R. W., and Burstein, H. (2004) Secretion of a TNFR:Fc fusion protein following pulmonary administration of pseudotyped adeno-associated virus vectors, *J Virol* ***78***, 12355–12365.
152. Nathwani, A. C., Gray, J. T., Ng, C. Y., Zhou, J., Spence, Y., Waddington, S. N., Tuddenham, E. G., Kemball-Cook, G., McIntosh, J., Boon-Spijker, M., Mertens, K., and Davidoff, A. M. (2006) Self-complementary adeno-associated virus vectors containing a novel liver-specific human factor IX expression cassette enable highly efficient transduction of murine and nonhuman primate liver, *Blood* ***107***, 2653–2661.
153. Towne, C., Raoul, C., Schneider, B. L., and Aebischer, P. (2008) Systemic AAV6 delivery mediating RNA interference against SOD1: neuromuscular transduction does not alter disease progression in fALS mice, *Mol Ther* ***16***, 1018–1025.
154. Sun, B., Zhang, H., Franco, L. M., Brown, T., Bird, A., Schneider, A., and Koeberl, D. D. (2005) Correction of glycogen storage disease type II by an adeno-associated virus vector containing a muscle-specific promoter, *Mol Ther* ***11***, 889–898.
155. Wang, Z., Allen, J. M., Riddell, S. R., Gregorevic, P., Storb, R., Tapscott, S. J., Chamberlain, J. S., and Kuhr, C. S. (2007) Immunity to adeno-associated virus-mediated gene transfer in a random-bred canine model of Duchenne muscular dystrophy, *Hum Gene Ther* ***18***, 18–26.
156. Moscioni, D., Morizono, H., McCarter, R. J., Stern, A., Cabrera-Luque, J., Hoang, A., Sanmiguel, J., Wu, D., Bell, P., Gao, G. P., Raper, S. E., Wilson, J. M., and Batshaw, M. L. (2006) Long-term correction of ammonia metabolism and prolonged survival in ornithine transcarbamylase-deficient mice following liver-directed treatment with adeno-associated viral vectors, *Mol Ther* ***14***, 25–33.
157. Broekman, M. L., Comer, L. A., Hyman, B. T., and Sena-Esteves, M. (2006) Adeno-associated virus vectors serotyped with AAV8 capsid are more efficient than AAV-1 or -2 serotypes for widespread gene delivery to the neonatal mouse brain, *Neuroscience* ***138***, 501–510.

158. Lawlor, P. A., Bland, R. J., Mouravlev, A., Young, D., and During, M. J. (2009) Efficient gene delivery and selective transduction of glial cells in the mammalian brain by AAV serotypes isolated from nonhuman primates, *Mol Ther* ***17***, 1692–1702.

159. Craig, A. T., Gavrilova, O., Dwyer, N. K., Jou, W., Pack, S., Liu, E., Pechhold, K., Schmidt, M., McAlister, V. J., Chiorini, J. A., Blanchette-Mackie, E. J., Harlan, D. M., and Owens, R. A. (2009) Transduction of rat pancreatic islets with pseudotyped adeno-associated virus vectors, *Virol J* ***6***, 61.

160. Nienhuis, A. W. (2007) Discussion of human gene transfer protocol 0707–864: an open-label dose-escalation study of a selfcomplementary adeno-associated viral vector (scAAV2/8-LPlhFIXco) for gene therapy of hemophilia B, *RAC NIH http://www4.od.nih.gov/oba/rac/meetings/Dec2007/final_RAC_agenda_dec07.pdf*.

161. Foust, K. D., Nurre, E., Montgomery, C. L., Hernandez, A., Chan, C. M., and Kaspar, B. K. (2009) Intravascular AAV9 preferentially targets neonatal neurons and adult astrocytes, *Nat Biotechnol* ***27***, 59–65.

162. Xue, Y. Q., Ma, B. F., Zhao, L. R., Tatom, J. B., Li, B., Jiang, L. X., Klein, R. L., and Duan, W. M. (2010) AAV9-mediated erythropoietin gene delivery into the brain protects nigral dopaminergic neurons in a rat model of Parkinson's disease, *Gene Ther* ***17***, 83–94.

163. Bish, L. T., Morine, K., Sleeper, M. M., Sanmiguel, J., Wu, D., Gao, G., Wilson, J. M., and Sweeney, H. L. (2008) Adeno-associated virus (AAV) serotype 9 provides global cardiac gene transfer superior to AAV1, AAV6, AAV7, and AAV8 in the mouse and rat, *Hum Gene Ther* ***19***, 1359–1368.

164. Limberis, M. P., and Wilson, J. M. (2006) Adeno-associated virus serotype 9 vectors transduce murine alveolar and nasal epithelia and can be readministered, *Proc Natl Acad Sci USA* ***103***, 12993–12998.

165. Duque, S., Joussemet, B., Riviere, C., Marais, T., Dubreil, L., Douar, A. M., Fyfe, J., Moullier, P., Colle, M. A., and Barkats, M. (2009) Intravenous administration of self-complementary AAV9 enables transgene delivery to adult motor neurons, *Mol Ther* ***17***, 1187–1196.

166. Klein, R. L., Dayton, R. D., Tatom, J. B., Henderson, K. M., and Henning, P. P. (2008) AAV8, 9, Rh10, Rh43 vector gene transfer in the rat brain: effects of serotype, promoter and purification method, *Mol Ther* ***16***, 89–96.

167. De, B. P., Heguy, A., Hackett, N. R., Ferris, B., Leopold, P. L., Lee, J., Pierre, L., Gao, G., Wilson, J. M., and Crystal, R. G. (2006) High levels of persistent expression of alpha1-antitrypsin mediated by the nonhuman primate serotype rh.10 adeno-associated virus despite preexisting immunity to common human adeno-associated viruses, *Mol Ther* ***13***, 67–76.

Chapter 5

Gene Therapy in Skeletal Muscle Mediated by Adeno-Associated Virus Vectors

Chunping Qiao, Taeyoung Koo, Juan Li, Xiao Xiao, and J. George Dickson

Abstract

Adeno-associated virus (AAV) is the most promising gene delivery vehicle for muscle-directed gene therapy. AAV's natural tropism to muscle cells, long-term persistent transgene expression, multiple serotypes, as well as its minimal immune response have made AAV vectors well suited for muscle-directed gene therapy. AAV vector-mediated gene delivery to augment muscle structural proteins, such as dystrophin and sarcoglycans, offers great hope for muscular dystrophy patients. In addition, muscle can be used as a therapeutic platform for AAV vectors to express nonmuscle secretory/regulatory pathway proteins for diabetes, atherosclerosis, hemophilia, cancer, etc. AAV vector can be delivered into both skeletal muscle and cardiac muscle by means of local, regional, and systemic administrations. Successful animal studies have led to several noteworthy clinical trials involving muscle-directed gene therapy. In this chapter, we describe the basic methodology that is currently utilized in the area of AAV-mediated muscle-directed gene therapy. These methods include vector delivery route, vector dosage, detection of transgene expression by immunostaining and western blot, determination of vector copy numbers and quantification of mRNA expression, as well as potential immune responses involved in AAV delivery. Technical details and tips leading to successful experimentation are also discussed.

Key words: Muscle-directed gene therapy, Adeno-associated virus, Vector-mediated gene delivery, Dystrophin, Sarcoglycans, Muscular dystrophy, Transgene expression, Vector dosage

1. Introduction

Adeno-associated virus (AAV)-mediated genetic compensation via delivery of genes into the muscle for various diseases is one of the most promising gene transfer strategies. It has potential for long-term gene transduction in both dividing (myoblasts) and nondividing (myotubes and cardiomyocytes) muscle cells and stabilizing or halting disease progression by the delivery of therapeutic genes.

Richard O. Snyder and Philippe Moullier (eds.), *Adeno-Associated Virus: Methods and Protocols*,
Methods in Molecular Biology, vol. 807, DOI 10.1007/978-1-61779-370-7_5,

AAV vectors can efficiently transduce muscle cells not only by local muscle injection (1), but also, notably, by intravenous systemic delivery of a few robust AAV serotypes such as AAV8 (2, 3) and AAV9 (4). The tropism of various AAV vector serotypes for differentiated postmitotic muscle tissues can be very high, reaching >90%. Certain serotypes of AAV vectors, such as AAV1 (5–7), AAV6 (8), AAV7 (9), AAV8 (3), and AAV9 (10, 11) achieve efficient transduction of the skeletal muscle that is significantly higher than AAV2 vectors.

Muscular dystrophies are hereditary, degenerative disorders of skeletal or voluntary muscle that result from defects in genes that encode a diverse group of proteins (12). Currently, there is no efficacious treatment for any form of muscular dystrophy. Thus, there is an urgent need to search for novel therapeutics. Duchenne muscular dystrophy (DMD) is a severe X-linked recessive disorder caused by recessive mutations in the dystrophin gene. A major limitation on AAV-mediated DMD gene therapy is the limited packaging size of 4.5 kb, which precludes large genes such as the 14 kb dystrophin cDNA (13). There are two existing strategies to solve this problem. One is to split the large gene and package it into two AAV vectors (dual vectors). After delivering those two vectors in vivo, the gene will be restored either by homologous recombination through the AAV terminal repeats followed by mRNA (14–16) or protein trans-splicing (17). The other strategy is to create miniature versions of dystrophin genes ideal for AAV packaging while maintaining functional domains (18–21). The latter strategy has been utilized in a clinical trial. In addition to DMD, several groups have initiated AAV-mediated gene therapy for Limb Girdle Muscular Dystrophies (LGMD) (22–27) and congenital muscular dystrophy (28) with impressive success in small-animal models.

In addition to being a direct therapeutic target, muscle – the largest organ in the body – has long been sought as a therapeutic platform to express nonmuscle secretory/regulatory pathway proteins. For example, delivery of AAV vectors encoding apolipoprotein E or erythropoietin to muscle can be utilized for atherosclerosis (29, 30). Similarly, delivery of AAV vectors encoding coagulation factors to muscle can be utilized for hemophilia (31).

The successful animal studies of AAV-mediated gene therapy in muscle have led to several noteworthy clinical trials. A phase I clinical safety trial involving local intramuscular injection of AAV2 vectors to transfer a coagulation Factor (FIX) in human patients with hemophilia B has been completed (31). Phase I trials for α1-antitrypsin (AAT) gene therapy and AAT deficiency-related lung disease have been performed using rAAV2 and rAAV1 vectors, respectively (32, 33). Functional microdystrophin gene transfer in DMD patients via intramuscular injection is currently in progress. AAV1-mediated alpha-sarcoglycan gene therapy via intramuscular injection for LGMD is also in progress.

A major impediment to the use of AAV-mediated gene delivery to muscle in clinical applications is the immune response against the vector and transgene product. It has been recently reported that AAV1 capsid-specific CD4+ and CD8+ T-cell immune response was observed, subsequent to intramuscular injection of AAV1 for lipoprotein lipase (LPL)-deficiency in a clinical trial (34). This immune response has never been encountered in small-animal models, but has been observed in random-bred wild-type and muscular dystrophy dogs (35, 36). These new challenges call for improvement of targeted gene delivery, tissue-specific therapeutic gene expression, immune modulation, new vector development, and large-scale production technologies. In this chapter, we focus mainly on the basic methods that are utilized in AAV-mediated gene therapy to muscle.

2. Materials

2.1. Intramuscular Delivery of AAV in Mice

1. Anesthetic solution: Hypnorm and Hypnovel mixture in sterile distilled water in 1:1:2 proportions (Roche, Welwyn Garden City, UK).
2. 28- and 30-Gauge needles and syringe (BD, San Jose, CA).
3. AAV vectors (50 µl of solution in physiological saline ranging from 5×10^8 vector genomes (vg) total to 5×10^{10} vg).
4. Sterile saline solution (0.9% NaCl) or PBS.
5. CO_2 and CO_2 chamber for sacrificing mice.

2.2. Intravenous Systemic Delivery of AAV in Neonatal and Adult Mice

1. Lamp fixture and infrared heat lamp (Zoo Med Laboratories, Inc. San Luis Obispo, CA).
2. Mouse restrainer.
3. 30 G × ½ in. PrecisionGlide Needle (BD, San Jose, CA).

2.3. Hydrodynamic Limb Vein Injection of AAV in Dogs

1. Syringe pump (Model PHD 2000; Harvard Instruments, Holliston, MA).
2. Rubber tourniquet, catheter, and a syringe pump are needed for dog limb perfusion.

2.4. Immunofluorescent and Immunohistochemical Staining

1. OCT embedding medium (Raymond A Lamb-laboratories, Waltham, MA).
2. DakoCytomation pen (DakoCytomation, Glostrup, Denmark).
3. Mouse on Mouse (M.O.M) kit (Vector Labs, Burlingame, CA).

4. Blocking solution for Immunofluorescent (IF) staining: 10% horse serum in PBS.
5. Antibody dilution buffer: 2% horse serum in PBS.
6. Avidin/Biotin blocking kit (Vector Labs, Burlingame, CA).
7. DAB substrate kit (Vector Labs, Burlingame, CA).
8. DPX mountant (BDH, VWR International Ltd, Leicestershire, UK).
9. Mounting medium with DAPI (Vector Labs, Burlingame, CA).
10. PBS-T: 1×PBS with 0.05% (v/v) Tween.
11. Positively charged or APES (aminopropyltriethoxysilane) coated glass slides (VWR International Ltd, Leicestershire, UK).

2.5. Hematoxylin and Eosin Staining

1. Eosin Y (BD, San Jose, CA).
2. Hematoxylin (Sigma, St. Louis, MO).

2.6. Muscle Western Blotting

1. Homogenization buffer: 75 mM Tris–HCl, pH 6.8, 4% SDS, 0.1% bromophenol blue, 20% glycerol, and 1% β-mercapto-ethanol or DTT to a final concentration of 100 mM.
2. BCA protein assay kit (Bio-Rad laboratories, Hercules, CA).
3. TissueLyser system (Qiagen, Valencia, CA).
4. 4× NUPAGE sample buffer (Invitrogen, Carlsbad, CA).
5. NuPAGE 4–12% Bis-Tris (Invitrogen, Carlsbad, CA 92008) and 3–8% Tris–Acetate (Invitrogen, Carlsbad, CA 92008) polyacrylamide gels.
6. NuPAGE antioxidant (Invitrogen, Carlsbad, CA).
7. NuPAGE MES SDS 20× (Invitrogen, Carlsbad, CA) and Tris–Acetate SDS 20× (Invitrogen, Carlsbad, CA) running buffers.
8. NuPAGE Transfer Buffer (Invitrogen, Carlsbad, CA).
9. ECL Western blotting detection reagents (Amersham Biosciences, Pittsburgh, PA).
10. Hybond-ECL Nitrocellulose Membranes (Amersham Biosciences, Pittsburgh, PA).
11. Hyperfilm ECL, high-performance chemiluminescence film (Amersham Biosciences, Pittsburgh, PA).
12. TBS-T: 1×TBS (10 mM Tris–HCl, pH 8.0, 150 mM NaCl) with 0.1% (v/v) Tween.
13. Coomassie staining solution: 0.25% (w/v) Coomassie blue R250, 45% methanol, 10% (v/v) glacial acetic acid in water.
14. Destaining solution: 45% (v/v) methanol, 10% (v/v) glacial acetic acid.

15. Stripping buffer: 75 mM Tris–HCl at pH 6.8, 100 mM DTT, 2% SDS (w/v).
16. Blocking buffer: 5% milk powder, 0.1% Tween-20.

2.7. Titration of AAV Vectors with Quantitative PCR

1. Real-time PCR machine.
2. Real-time PCR reagent (see Note 1).
3. Primer express software (Applied Biosystems, Foster city, CA).
4. Primers and probe.
5. Optical quality sealing film (Applied Biosystems, Foster city, CA).

2.8. q-PCR for Examination of Vector Distribution in Muscle Tissues

1. Total DNA extraction kits (QIAGEN, UK).
2. DNeasy Blood and Tissue kit (QIAGEN, Valencia, CA).

2.9. q-PCR for Measurement of mRNA Expression

1. Trizol reagent for RNA extraction (Invitrogen, Carlsbad, CA).
2. Gusb (glucuronidase, beta) (Applied Biosystems, Foster City, CA).
3. High-Capacity cDNA Reverse Transcription Kit with RNase inhibitor (Applied Biosystems, Foster City, CA).

2.10. Immunology

1. Anti-mouse CD4 and CD8 (BD Biosciences, San Jose, CA).
2. Rat anticanine CD4 and CD8 IgGs (Serotec, Oxford, UK).
3. Cy™3 conjugated goat anti-mouse IgG and goat anti-rat IgG (Jackson ImmunoResearch, West Grove, PA, USA).
4. Alexa Fluor 488 Goat anti-mouse IgG (Molecular probes, Eugene, OR).
5. Mounting medium with DAPI (Vector Laboratories, Burlingame, CA).
6. Blocking solution for IF staining: 10% horse serum in PBS.
7. Antibody dilution buffer: 2% horse serum in PBS.

3. Methods

3.1. Intramuscular Delivery of AAV in Mice

1. Prepare an anesthetic solution freshly.
2. Weigh and sedate a mouse (C57BL/10 strain). A dosage of 3–5 μl anesthetic per gram body weight is calculated (e.g., ~100 μl of anesthetic/5–6 week old mouse (~20 g) is sufficient to anesthetize for more than 1 h).
3. Perform intraperitoneal injections using a gauge 27 needle, and further procedures are delayed until animals have fully lost their foot pinch reflexes.

4. Shave a small area on the mouse muscle, such as tibialis anterior (TA) muscle.
5. Extend the limb with the TA muscle facing forward.
6. Insert a 30-gauge needle perpendicularly in the middle of the TA muscle and the AAV solution is injected in 2–3 s. A successful injection is indicated by muscle contraction resulting in raising reflex of the foot.
7. Place animals on heating pad during recovery and monitored hourly for 4 h and then daily for the remainder of the experiment.
8. Sacrifice animals 3–4 weeks postinjection (or longer) using CO_2 chamber and remove muscles from each treated mouse. Arrange muscles on individual cork-board blocks and embedded in OCT embedding medium.
9. Snap-freeze muscles in isopentane chilled with liquid nitrogen for 5–10 s to avoid ice crystal mediated damage, and very quickly transfer to liquid nitrogen.
10. Store the blocked muscles at −80°C for subsequent analysis.
11. For RNA and protein purification, slice the muscles longitudinally with a scalpel. Wrap each part in foil and snap freeze it in liquid nitrogen. Subsequent storage is at −80°C.

3.2. Intravenous Systemic Delivery of AAV in Neonatal and Adult Mice

1. Warm the wild-type adult mice under an infrared heat lamp (100–160 W) for 5–10 min to dilate the tail vein (see Note 2).
2. Prepare the desired dilution of the AAV in sterile saline solution or PBS. Hold mouse in a restrainer throughout without anesthesia, and administer the appropriate dose (ranging from 1×10^{12} up to 1×10^{14} vg/kg) via the tail vein using a 29-gauge needle.
3. Sacrifice the mice according to the specific experimental design after systemic delivery (see Note 3). The AAV9 or AAV8 vector usually will display good gene expression in cardiac muscle and skeletal muscle in 3–4 weeks.
4. Collect the lower limb muscles of TA, extensor digitorum longus (EDL), and soleus, and block them for cryosectioning. In addition, block the heart and diaphragm for cryosectioning. Muscles can be divided into several pieces and blocked.
5. Neonatal delivery (see Note 4): There are two commonly used methods to achieve systemic delivery of AAV vector to neonatal mice: facial (superficial temporal) vein delivery (37), which is technically challenging, and intraperitoneal injection (3, 28). In facial vein injection, cool the mouse on ice so that it will not move vigorously during injection. One person holds the neonatal mouse and exposes the temporal vein, while a second

person performs the injection with a 1 ml or 0.5 ml insulin syringe and 30 G × ½ in. needles and an injection volume up to 50 μl. For intraperitoneal injection, deliver AAV vector (50–100 μl volume containing 1×10^{10} up to 1×10^{11} vg) into the intraperitoneal cavity (see Note 5).

3.3. Hydrodynamic Limb Vein Injection of AAV in Dogs

1. Sedate adult dogs by intramuscular (IM) administration of atropine sulfate (0.04 mg/kg) and butorphanol tartrate (0.4 mg/kg), then maintained with 1–2% Sevoflurane.
2. Monitor all vital closely throughout the procedure. Shave the limbs to be injected scrub them with betadine and 70% isopropyl alcohol.
3. Insert a catheter into the saphenous vein and secure it with tape.
4. For pelvic limb injection, wrap a rubber tourniquet tightly around the proximal limb at the level of the inguinal area. For thoracic injection, place the catheter in the cephalic vein and the wrap tourniquet tightly around the proximal limb in the axillary space.
5. Dilute appropriate amount of AAV vector (ranging from 1×10^{12} vg/kg body weight to 1×10^{14} vg/kg) in PBS buffer or saline. Calculate the volume of PBS buffer or saline according to body weight (10–20 ml/kg). The injection speed is 1 ml/s for both limbs and is controlled by a syringe pump. The total occlusion time is 10 min from the beginning of injection (38).

3.4. Immunofluorescent and Immunohistochemical Staining

1. Cut up sections of 8–10 μm thickness to several levels through the length of the muscles from blocks (e.g., each level 200 μm apart) using a Cryostat and place sections on positively charged or APES (aminopropyltriethoxysilane) coated glass slides.
2. Air dry the slides for 20 min after which they are stained according to the steps below, or transferred to −80°C chambers for future use.
3. If they are frozen, remove the muscle cryosection slides from storage at −80°C and leave at room temperature (RT) for 30 min to air dry.
4. Smudge the periphery of each slide with a hydrophobic pen (DakoCytomation) to keep the solutions on sections when applying the reagents.
5. Fixation (see Note 6): Fix the sections in cold acetone at −20°C and allow them to air dry at RT for 30 min.
6. Wash the sections three times for 3 min with PBS-T.
7. For immunohistochemical (IHC) staining: Block the endogenous biotin present in the Avidin/Biotin blocking kit. Incubate

sections with each solution for 15 min each and wash three times for 3 min with PBS-T.

8. Blocking: For monoclonal antibody utilized in mouse muscles, the Mouse on Mouse (M.O.M) kit must be used. This kit is specifically designed to reduce the background staining often encountered when using mouse monoclonal antibodies on mouse tissue sections. The high sensitivity reported for this technique is due to the very strong blocking at the beginning of the staining and the biotin-avidin system. Incubate muscle sections with diluted blocking serum for 1 h to reduce nonspecific binding (two drops of blocking serum in 2.5 ml of PBS for mouse antibody). For polyclonal antibody utilized in mouse muscle, incubate muscle sections with blocking buffer.
9. First antibody incubation: Dilute the monoclonal antibody in M.O.M diluent solution (600 μl of protein concentrate in 7.5 ml of PBS), and dilute the polyclonal antibody in antibody dilution buffer. Incubate the first antibody at RT for 1 h or overnight at 4°C.
10. Wash the slides three times for 3 min with PBS-T.
11. Secondary antibody incubation: For IF staining, dilute the fluorescence-labeled secondary antibody in antibody dilution buffer at certain ratio suggested by the manufacture's protocol. For IHC staining, dilute the secondary antimonoclonal antibody conjugated with biotinylated peroxidase in M.O.M diluent solution and incubated at RT for 10 min. Dilute secondary antipolyclonal antibody conjugated with biotinylated peroxidase in antibody dilution buffer and incubate at RT for 1 h.
12. The sections are washed three times for 3 min with PBS-T.
13. Detection for IHC staining:
    (a) Add the avidin-enzyme complex (ABC) and incubate for 5 min. It binds to the biotinylated secondary antibody.
    (b) Wash the sections three times for 3 min with PBS-T.
    (c) Signals are visualized using the hydrogen peroxide activated DAB substrate kit for peroxidise.
    (d) Watch the slides under the microscope until the staining is developed. Overexposure of samples to reagents at this stage can result in a heavy background.
    (e) Wash the sections in running tap water for 5 min to stop the reaction of DAB substrate.
    (f) Incubate the sections in 100% ethanol three times for 1 min.
    (g) Incubate the sections in Xylene for 10 min and mount in DPX mountant. Keep the slides at RT. The signal is visualized under the standard light microscope (Fig. 1).

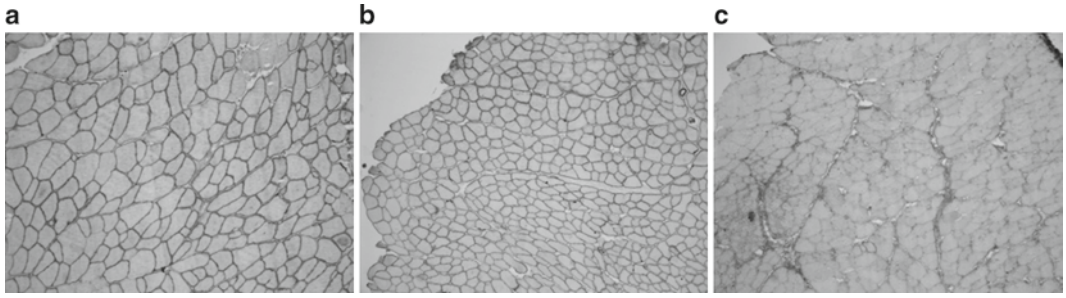

Fig. 1. Immunohistochemical (IHC) staining of dystrophin positive fibers using AAV-mediated gene augmentation in *mdx* mice. (**a**) TA muscles of *mdx* mice were injected with AAV2/9-microdystrophin and tissues were harvested after 2 months of injection. The cryosectioned slides were subjected to IHC staining with antidystrophin antibody Manex 1011C antibody (1:100). Biotin-labeled anti-mouse IgG antibody was used as a secondary antibody. The signal was visualized with a DAB substrate and mounted using DPX mountant. (**b**) C57BL/10 and (**c**) *mdx* mice were used as a positive and negative control, respectively. The signals were observed using a Leica light microscope.

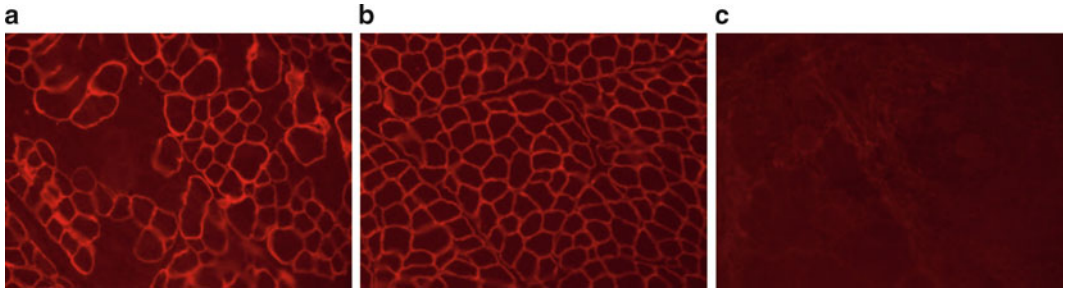

Fig. 2. Immunofluorescent (IF) labeling of dystrophin using AAV-mediated gene augmentation in skeletal muscle of Canine X-linked muscular dystrophic dog (*CXMD*). (**a**) TA muscles of *CXMD* dogs were injected with AAV2/8-microdystrophin and after 2 months tissues were harvested, cryosectioned, and evaluated for microdystrophin expression by IF using NCL-dys1 antibody (1:100). The signal was visualized using an Alexa 568-conjugated anti-mouse IgG (1:1000) and mounted using a mount medium. (**b**) Wild-type and (**c**) *CXMD* muscle were used as a positive and negative control, respectively. Fluorescent signals were observed using a Leica fluorescent microscope.

14. Detection for IF staining:
    (a) Counterstain the sections with DAPI (4′, 6-diamidino-2′-phenylindole, dihydrochloride) to display nuclei. Mount the sections with mounting medium. Keep the slides at 4°C without light exposure.
    (b) Review the results under fluorescent microscope as shown in Fig. 2.

3.5. Hematoxylin and Eosin Staining (Fig. 3)

1. Remove muscle cryosections from storage at −80°C and leave them at RT for 30 min to air dry.
2. Fix the tissue in 95% ethanol with 3% acetic acid for 30 s.
3. Wash the slide in running tap water to remove OCT.
4. Immerse sections in hematoxylin solution for 5–15 min.

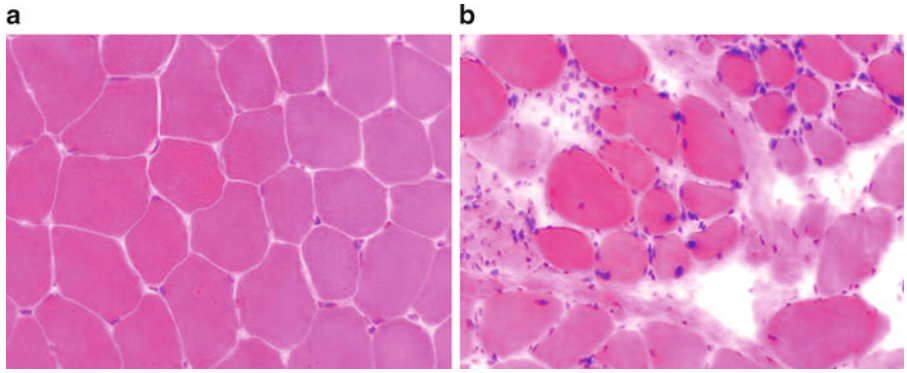

Fig. 3. Example of muscle histology by H&E staining. (**a**) Normal dog muscle shows even size/diameter distribution of muscle fibers with peripheral nuclei. (**b**) Muscular dystrophic muscle was characterized by uneven muscle fiber sizes, central nucleation, and mononuclear cell infiltration. Nuclei shows *blue-purple color* using hematoxylin and cytoplasm for *bright pink* color using eosin.

5. Check signal of the nuclei microscopically.
6. Rinse the slide under running tap water for 5 min.
7. Immerse in 1% (w/v) aqueous solution of eosin for 30 s to 2 min for counter staining, and rinsed gently.
8. Perform dehydration in progressively higher concentration solutions of ethanol (starting from 75%, then 95%, up to 100%), followed by a dip in Xylene for 10 min.
9. Mount hematoxylin and eosin (H&E) stained sections in DPX mountant.

3.6. Muscle Western Blotting

1. Preparation of protein samples: Dissect muscle tissue samples from animals and flash frozen in liquid nitrogen. When performing experiments, remove muscles from storage at −80°C and store on dry ice to prevent thawing.
   (a) Add 300 µl of homogenization buffer to each muscle in a 1.5 ml Eppendorf tube with a Tungsten Carbide Bead (3 mm) and homogenization is carried out using the TissueLyser system by agitating at 20 Hz until a uniform homogenate is obtained.
   (b) Transfer the homogenate to a new 1.5 ml tube and pass three times through a 25 G needle to shear the DNA. Centrifuge the homogenate for 5 min at 4000×*g* at 4°C to remove any large debris. Keep the samples at −80°C.
2. Assay of protein concentration where appropriate: Calculate the protein concentration from a standard curve, using a series of BSA standards of known concentration. Dilute Samples to an appropriate concentration to include 5% β-mercapto-ethanol

and 10^{-3}% bromophenol blue. Boil 1–10 μg amounts of protein in sample buffer for 5 min before being separated. A cocktail of protease inhibitors is often added to the sample buffer.

3. Running of SDS-PAGE gel:
   (a) Denature samples by heating at 100°C for 5 min.
   (b) Load 20–60 μg of denatured sample protein into each lane of the gel and run electrophoreses through a 3–8% polyacrylamide Tris–Acetate gel or 4–8% Bis-Tris gels.
   (c) Run Gels at 150 V for approximately 1 h using X-Cell SureLock Mini-Cell equipment with NOVEX® Tris–Acetate SDS Running buffer with 500 μl NuPage Antioxidant.
4. Coomassie blue staining of protein gels to visualize the total protein loaded (optional): If this step is desired, two identical gels have to be run. One gel is for staining, and the other one is for blotting. After electrophoresis, the gel is transferred to a clean container.
   (a) Soak SDS-polyacrylamide gels, containing separated proteins, in approximately 100 ml of Coomassie staining solution for 1 h, resulting in visualization of the band (s) of interest.
   (b) Destaining of the gel is performed by successive incubations in a destaining solution until the bands become visible.
5. Protein transfer: Blot proteins onto Hybond™ ECL™ nitrocellulose membranes using the NOVEX® X-Cell II blotting apparatus with the transfer buffer with 10% (v/v) methanol and 1 ml NuPage Antioxidant for 1.5 h at 24 V. Wash the membrane once with TBS-T.
6. Blocking: Block nonspecific binding in blocking buffer for 1 h at RT or overnight in cold room (4°C) with gentle agitation.
7. Primary antibody incubation: Hybridize the nitrocellulose blots with a primary antibody and incubate for 1 h at RT. Dilute all antibody solutions in blocking buffer.
8. Wash the membranes three times in TBS-T for 10 min while being shaken.
9. Perform secondary antibody incubation with an HRP-conjugated secondary antibody for 1 h, followed by a washing step as described in step 7.
10. Addition of substrate: Expose the membrane to the western blotting ECL chemiluminescent detection system for 1 min and develop the film in dark room in order to visualize the antibody reactions.

11. Stripping Nitrocellulose Membranes (optional): To re-probe with alternative antibodies or to reduce background signal, the nitrocellulose membrane can be stripped after ECL development.
    (a) Wash the membrane in TBS-T to remove any traces of ECL reagents then place it in stripping buffer at RT with gentle agitation for 1 h.
    (b) Wash the blot briefly in TBS-T to remove any traces of stripping buffer. The blot is then ready for blocking step preparation for the alternative antibody incubation.

3.7. Titration of AAV Vectors with Quantitative PCR

There are three basic methods for AAV titration. One is quantification of physical AAV particles via ELISA (enzyme-linked immunosorbent assay) based on an antibody that selectively recognizes assembled AAV capsids (39). The big disadvantage of the ELISA method is that the empty AAV particles are also detected. It is also costly compared with other methods. The most reliable and traditional method for AAV titration is dot (or slot) blotting. However, this method is quite time-consuming as it usually takes 2 days to finish a single assay. The third method for AAV titration is quantitative PCR (q-PCR), which is discussed in depth in the following protocols. q-PCR is easy to perform and it takes much less time to obtain the virus titer than with dot blot. Reproducibility and contamination are major concerns for q-PCR, so precautions need to be taken by setting up a negative control well and duplicate or triplicate samples to obtain consistent results.

q-PCR is used to measure the quantity of a PCR product. It is the method of choice to quantitatively measure starting amounts of DNA, cDNA, or RNA. In the gene therapy field, this method is usually used for titration of AAV viral vector, vector distribution study, and measurement of mRNA expression.

1. Preparation of viral DNA template:
    (a) Mix 5 µl virus sample, 193 µl DMEM (or virus suspension buffer), and 2 µl DNase I (5 U/µl). It is best to use a virus of a known titer as a reference.
    (b) Incubate samples at 37°C for 1 h to digest the DNA impurities outside the viral shell.
    (c) Inactivate the DNase I by boiling 10–15 min. This also pops open the viral particles and releases the viral DNA.
    (d) Dilute the virus digestion mixture times (10 + 990 µl H_2O).
    (e) Take 5 µl of diluted sample for q-PCR.
2. Preparation of plasmid standard and standard calculation:
    (a) Calculate the mass of a single plasmid molecule. $m = (n) \times (1.096 \times 10^{-21}\ \text{g/bp})$, m = mass, n = plasmid size.

For example, the plasmid size of pdx11-LacZ is 7863 bp, and its mass of a single plasmid molecule would be $m = 7,863 \times 1.096 \times 10^{-21} = 8.42 \times 10^{-18}$ g.

(b) Calculate the mass of plasmid containing the copy numbers of interest. For example, the mass of 1×10^{11} copies of pdx11-LacZ $= 8.42 \times 10^{-18} \times 10^{11} = 8.42 \times 10^{-7}$ g $= 8.42 \times 10^{-1}$ μg $= 0.842$ μg.

(c) Calculate the concentration of plasmid DNA needed to achieve the copy number of interest. We usually dilute our plasmid stock to 0.1 μg/μl. For pdx11-LacZ, take 8.42 μl of 0.1 μg/μl plasmid (1×10^{11} copies) and put it in 991.58 μl of DNase- and RNase-free TE, the concentration would be 1×10^{8} copies/μl.

(d) Perform a serial dilution of the plasmid. We usually do tenfold dilution with TE buffer (pH 8.0) starting from 10^{8} copies/μl. We will have 10^{7} copies/μl, 10^{6} copies/μl, 10^{5} copies/μl, and 10^{4} copies/μl. Then the standards will be ready for q-PCR.

3. Preparation of primers and probe: Design primers and minor groove binder (MGB) probe with Primer Express Software provided by Applied Biosystems. If SYBR green detection is used, there is no need to design a probe (see Note 7). Make 10× stock of primers and probes. For probe-based detection system, the 10× stock primer concentration is 9 μM, and the working primer concentration is 900 nM. The 10× stock probe concentration is 2.5 μM, and the working primer concentration is 250 nM.

4. Making the reaction mixture (see Note 8): If using the AmpliTaq gold polymerase instead of the master mix (from ABI), the reactions are the following:

10× PCR buffer:	5 μl
25 mM $MgCl_2$:	4 μl
25 mM dNTPs:	0.5 μl
Primer 1 (10×):	5 μl
Primer 2 (10×):	5 μl
CMV probes (10×):	5 μl
ROX:	0.8 μl
Taq polymerase:	0.3 μl
H_2O:	19.4 μl
	45 μl

If master mix (2×) is utilized, only additional primers and probes are needed to add into reaction mixture together with the master mix (containing enzymes, buffers, dNTPs, and Rox).

5. PCR sample addition: Transfer 45 μl aliquots of the reaction mixture into a 96-well thin-wall PCR plate. Add 5 μl of the DNA template (standards or the unknown sample) into a reaction mixture. Cover the plate with a piece of optical quality sealing film and briefly spun to remove bubbles.
6. Setting PCR conditions: The PCR conditions (2 cycle PCR) will be: 95°C for 10 min to denature the DNA and activate hot-start enzyme followed by 40 cycles of 95°C for 15 s and 60°C for 1 min. If you did your viral DNA sample dilution according to the protocol suggested (40 times dilution first, then 100 times dilution, total 4,000-fold), multiple the number by 4,000. This will be your final titer per 5 μl of virus.

3.8. q-PCR for Examination of Vector Distribution in Muscle Tissues

1. DNA extraction: AAV vector can remain in episomal form or integrate into chromosome after delivering AAV vector into muscle tissue. Therefore, we should extract total DNA from the muscle tissue (see Note 9). Complete tissue digestion and addition of RNase A to degrade RNA are critical to achieving high quality of DNA. It is not necessary to run the extracted DNA in agarose gel, but it will help in determining the quality of DNA. For example, any RNA contamination or DNA degradation during the purification process will be evident. Absolute quantification of real-time PCR will be utilized to determine vector distribution. In addition to designing primers and probe based on the delivered vector, the primers and probe against endogenous control also need to be considered. In our laboratory, we have developed primers and probe based on the mouse glucagon gene as our endogenous control. The sequences are listed in the following as references: Taqman mouse glucagon probe: FAM–cag caa agg aat tca–MGB; Glucagon-Real-F (mouse): AAG GGA CCT TTA CCA GTG ATG TG; Glucagon-real-R(mouse): ACT TAC TCT CGC CTT CCT CGG.
2. Setting up q-PCR and data analysis: Similar to the virus titration method, we need to have plasmid standards for both vector and endogenous controls. Therefore, we need to set up two rows of standards in one plate: one row for the vector standards and one row for the endogenous control plasmid standards (Fig. 4). For each unknown sample, we will have two reactions: one for the vector and one for endogenous control. For the data analysis, the copy numbers for vector and copy numbers for the corresponding endogenous control will be calculated separately. The copy number of delivered vector in a specific tissue per diploid cell = (vector copy number/endogenous control) × 2.

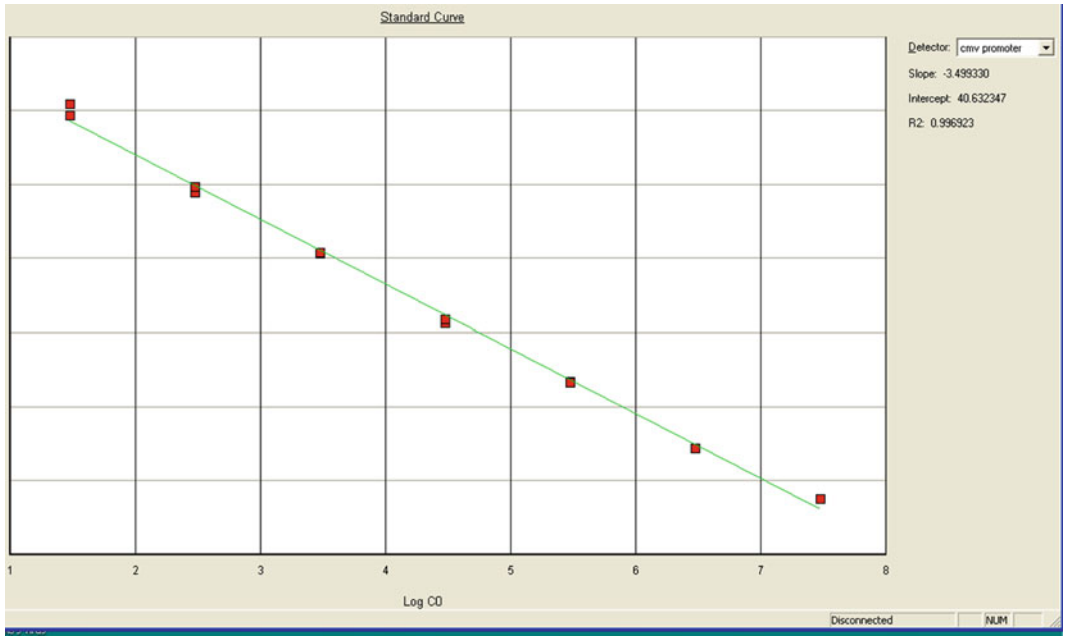

Fig. 4. Example of a DNA quantity standard curve. To note, R^2 equal to or greater than 0.98 represents a good PCR and reliable standard. Here R^2 equals 0.996923.

3.9. q-PCR for Measurement of mRNA Expression

Relative quantification will be utilized for the detection of mRNA expression which differs from virus titration and vector copy number studies. For relative quantification, there is no standards involved. However, the endogenous mRNA control for normalization should be considered.

1. Extraction of total RNA from different tissues: Trizol reagent is utilized to extract total RNA. The manufacturer's protocol must be strictly followed. DNA contamination in the RNA prep is a big concern when the Trizol is utilized.
2. cDNA synthesis: Similar to regular reverse transcription PCR, cDNA will be synthesized utilizing cDNA synthesis kit. In our laboratory, we use the High-Capacity cDNA Reverse Transcription Kit with RNase inhibitor. The cDNA should be frozen in −20°C for short-term and long-term storage.
3. Design of primers and probe: The primers and probe against the mRNA and endogenous control of interest will be designed. The ideal primers and probe should detect the template from only cDNA, but not the contaminated DNA. If there is an intron (to be spliced out in mRNA) in the studied AAV vector, the probe should be designed flanking intron/exon junctions. By using this strategy, the q-PCR machine can only detect signal from spliced mRNA after reverse transcription, but not the vector genomic DNA with intron. If there is no intron

splicing sites or exon junction sequences are not suitable for probe, there are some other strategies can be used to avoid DNA contamination in the RNA prep. RNase-free DNase can be used to digest the extracted RNA. For cDNA synthesis, a contamination control tube is set up by withholding reverse transcriptase. The purpose of this step is to avoid cDNA synthesis. In addition, for q-PCR, set up a control well with the sample derived from no reverse transcriptase tube, and set up the other control well with water as a sample. By taking these steps, we should be able to distinguish how much contamination we got from the system, and how much vector DNA contamination we obtained from the RNA prep. If there is still a significant amount of DNA contamination in the RNA prep after DNase treatment, a different RNA preparation method should be used to remove DNA contamination. For endogenous mRNA control, we utilized beta glucuronidase (Gusb).

4. Setting up relative qPCRs and data analysis: For each sample, two reactions will be set up: one is for the gene of interest and the other one is for the endogenous control. Similar to the absolute quantification, it is better to duplicate or triplicate each sample. Since relative quantification is a relative comparison of the PCR signal between several groups (40), there is no need to set up standards. After running, the data will be loaded into the relative quantification analysis software, and results will be displayed automatically. During analysis, one sample (not a negative control) will be set as a calibrator, and the results will show relative fold difference of each sample compared with the calibrator (Fig. 5).

3.10. Immunology

The immune response against AAV vector and transgene product is the main hurdle in large animal study and clinical trials involving AAV-mediated muscle-directed gene therapy. Many factors affect immune reactions of AAV vectors in vivo. These factors include species, AAV serotypes, delivery route, vector dosage, promoters, and specific transgene. In general, AAV is considered less immunogenic in small rodents, and the immune reaction against transgene (41) and capsid (35) became apparent in large animals and in human patients. The immunity profiles of different AAV serotypes are different. Systemic delivery of AAV vector can induce immunotolerance (42, 43). Therefore, it is less likely to trigger strong immunity against transgene than intramuscular delivery. Utilization of small vector doses, tissue-specific promoter, and endogenous transgene are less likely to induce immune reaction in mice (44, 45). In this section, we describe only the simple immunofluorescent staining protocol for CD4 and CD8 to examine mature T-cell infiltration in AAV-transduced muscle.

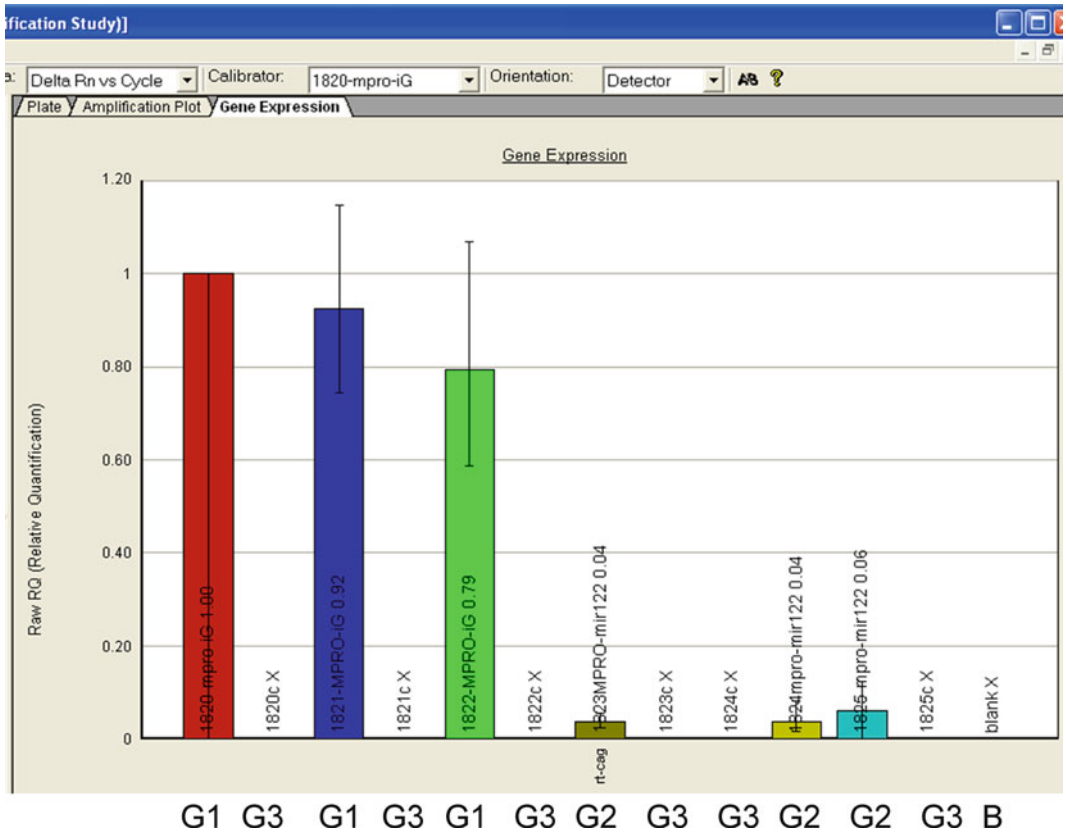

Fig. 5. An example of relative quantification analysis. The target mRNA was myostatin propeptide, and the endogenous control we utilized was mouse GusB (glucuronidase, beta). Results shown are from three groups of mice. Group 1 (G1) has high expression of myostatin propeptide; group 2 has low expression of myostatin propeptide; group 3 is mock control. B is blank well with no sample addition.

1. Tissue fixation: Cryosection the snap-frozen muscles tissues at 8 μm thickness and fix the tissue with ice-cold acetone for 10 min.
2. Blocking: Wash the fixed slide in PBS three times, then block it with blocking buffer (see Note 10).
3. First antibody incubation: For mouse tissue, use the monoclonal antibody anti-mouse CD4 and CD8. For dog tissue, use the rat anticanine CD4 and CD8 IgGs. Dilute all antibodies with antibody dilution buffer at 1:100 of ratio for use. Incubate the first antibody for 1 h at RT followed by three washes of 1× PBS.
4. Second antibody incubation: Two different fluorophore-labeled secondary antibodies used in the laboratory are: Red fluorescence (Cy™3 conjugated goat anti-mouse IgG and goat anti-rat IgG) and green fluorescence (Alexa Fluor 488 Goat anti-mouse IgG). Dilute all secondary antibodies in antibody

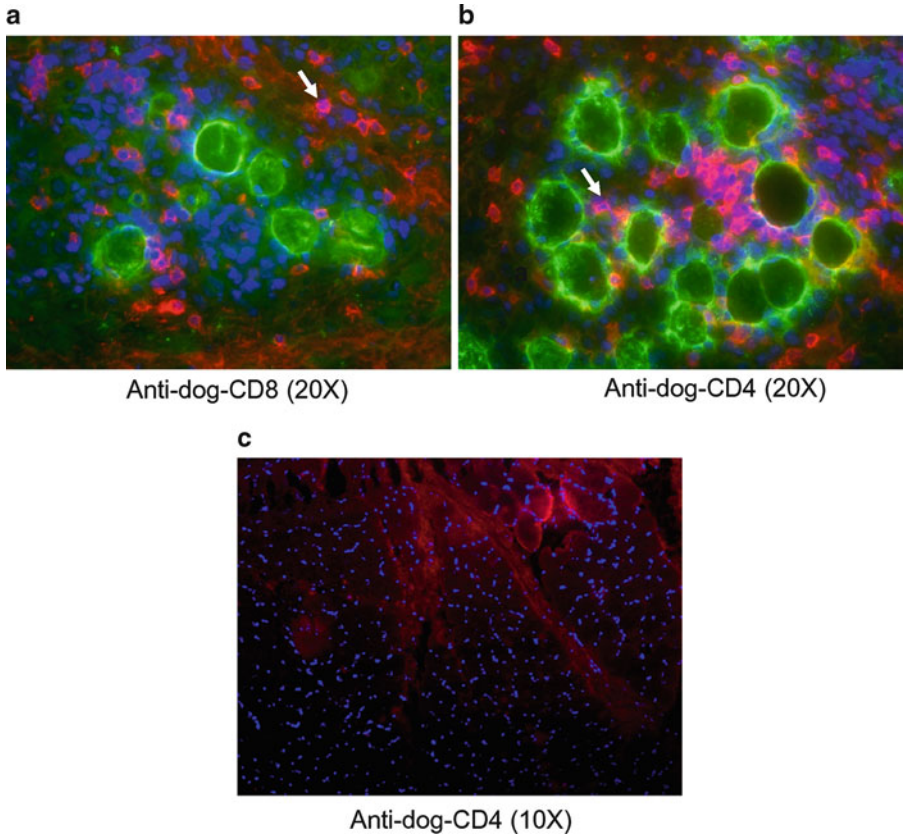

Fig. 6. Immunofluorescent staining of CD4 (*red*) and CD8 (*red*) positive T-cells and GFP-positive (*green*) myofibers in dog muscle. Panels (**a**) and (**b**) are from normal dog muscles injected with AAV2-CMV-GFP vector intramuscularly and panel (**c**) is from normal dog control muscle. The slides were counter-stained with DAPI to show the cell nuclei (*blue*).

dilution buffer. Incubate the secondary antibodies for 1 h followed by three washes with 1× PBS.

5. Counterstaining with DAPI to display nuclei: Counterstain the sections with DAPI followed by one time of wash with PBS. Mount the sections with mounting medium.
6. Reviewing results under the fluorescent microscope: Examples are shown in Fig. 6. Red indicates CD4 or CD8 positive, blue indicates nuclei, and green indicates transgene expression. CD4 or CD8 positive cells are blue nucleus surrounded by a circle of red fluorescence (arrow head).

4. Notes

1. Varies depending on the detection system of real-time PCR machine used. For example, we use 7,300 real-time PCR system (Applied Biosystems) in our laboratory. For CYBR green

detection system, the SYBR Green PCR master Mix (Applied Systems) is required. For probe-based detection system, AmpliTaq Gold master mix (Applied Biosystems) is required. Even without master mix, the regular Taq polymerase can also be used for real-time PCR.

2. From personal experience, we find *mdx* mice are sensitive to heat generated from heat lamp. Unlike wild-type mice, the *mdx* mice are more prone to death under the heat of infrared lamp even without any experimental procedure. We prefer to use warm water to dilate the tail vein for vector delivery. For muscular dystrophic mice such as *mdx* mice, dipping the mouse tail into warm water is sufficient to dilate the vein. *Mdx* mice are very sensitive to whole-body heating, which can be fatal.
3. The delivered gene usually starts to express from 3 to 7 days postvector delivery, and it will reach a peak expression in about 3–4 weeks. The gene expression will be persistent in muscle and heart in normal mouse, but diminish in tissues undergoing rapid cell division, such as neonatal liver. It is noteworthy that the muscular dystrophic muscle will undergo degeneration and regeneration. Hence the gene expression in those muscles will not be persistent if the fundamental defect is not corrected.
4. The easiest approach to achieve systemic delivery of AAV vector to the whole-body muscle is through neonatal delivery. There are several advantages to this method. First, because the size of a neonatal mouse is small, a relatively small amount of vector dose is required if we calculate the utilized dosage according to mouse weight. Second, higher transgene expression will be achieved in muscle and heart via neonatal delivery than the adult gene transfer. This is partly due to the increased vascular permeability of neonatal mice. Third, selective retention of vector DNA in muscle and heart cells will be achieved after systemic gene delivery in neonatal mice. Despite the fact that AAV (such as AAV8) is highly effective in transducing liver cells, the vector DNA is rapidly degraded during liver growth and cell division. In fact, vector DNA persists in tissues that undergo minimal cell division, such as heart and muscle (3).
5. A trick of the intraperitoneal injection procedure is to enter the needle into intraperitoneal cavity through quadriceps muscle. This prevents the vector from leaking out through the needle entrance.
6. To detect structure proteins, such as dystrophin, with immunofluorescent staining in muscle tissue, we usually do not fix the tissue. Blocking solution will be directly added to the slide after air dry. Polyclonal antibodies are raised in rabbits and nonmouse species are highly preferred over mouse monoclonal antibodies, which require M.O.M. blocking.

7. For q-PCR, probe-based detection is usually more specific and easier to perform, but cyber green-based detection is less expensive. It requires primers that do not generate nonspecific PCR products, which would give rise to false readings. For cyber green detection, the primer quality and concentration is very critical. 200 nM working primer concentrations are generally used.
   Primers and probes are usually designed against either the polyA or promoter region of the AAV vector plasmid. The advantage of this design is that one set of primers and probe can be utilized for multiple vectors.
8. The components of q-PCR are slightly different if using different real-time PCR machines. For example, if the Applied Biosystems Real-time PCR machine is used, the Rox (internal reference dye) should be added to the reaction mixture. The analysis software will automatically search for Rox as internal control. If the Bio-Rad real-time PCR machine is used, there is no need to add Rox dye.
9. To prepare DNA for q-PCR, avoiding contamination is a key. Making aliquots of reagents and using filter tips will be helpful. The appropriate sample size should be used. Too much sample will actually decrease DNA yield.
10. For mouse CD4 and CD8 staining, incubation of the slides in 1% Triton X-100 (in PBS) for 10 min before blocking will improve the specificity.

References

1. Xiao, X., Li, J., and Samulski, R. J. (1996) Efficient long-term gene transfer into muscle tissue of immunocompetent mice by adeno-associated virus vector, *J Virol* ***70***, 8098–8108.
2. Gao, G. P., Alvira, M. R., Wang, L., Calcedo, R., Johnston, J., and Wilson, J. M. (2002) Novel adeno-associated viruses from rhesus monkeys as vectors for human gene therapy, *Proc Natl Acad Sci U S A* ***99***, 11854–11859.
3. Wang, Z., Zhu, T., Qiao, C., Zhou, L., Wang, B., Zhang, J., Chen, C., Li, J., and Xiao, X. (2005) Adeno-associated virus serotype 8 efficiently delivers genes to muscle and heart, *Nat Biotechnol* ***23***, 321–328.
4. Inagaki, K., Fuess, S., Storm, T. A., Gibson, G. A., McTiernan, C. F., Kay, M. A., and Nakai, H. (2006) Robust systemic transduction with AAV9 vectors in mice: efficient global cardiac gene transfer superior to that of AAV8, *Mol Ther* ***14***, 45–53.
5. Hauck, B., and Xiao, W. (2003) Characterization of tissue tropism determinants of adeno-associated virus type 1, *J Virol 77*, 2768–2774.
6. Hauck, B., Xu, R. R., Xie, J., Wu, W., Ding, Q., Sipler, M., Wang, H., Chen, L., Wright, J. F., and Xiao, W. (2006) Efficient AAV1-AAV2 hybrid vector for gene therapy of hemophilia, *Hum Gene Ther* ***17***, 46–54.
7. Riviere, C., Danos, O., and Douar, A. M. (2006) Long-term expression and repeated administration of AAV type 1, 2 and 5 vectors in skeletal muscle of immunocompetent adult mice, *Gene Ther* ***13***, 1300–1308.
8. Blankinship, M. J., Gregorevic, P., Allen, J. M., Harper, S. Q., Harper, H., Halbert, C. L., Miller, D. A., and Chamberlain, J. S. (2004) Efficient transduction of skeletal muscle using vectors based on adeno-associated virus serotype 6, *Mol Ther* ***10***, 671–678.
9. Louboutin, J. P., Wang, L., and Wilson, J. M. (2005) Gene transfer into skeletal muscle using novel AAV serotypes, *J Gene Med 7*, 442–451.
10. Bish, L. T., Morine, K., Sleeper, M. M., Sanmiguel, J., Wu, D., Gao, G., Wilson, J. M., and Sweeney, H. L. (2008) Adeno-associated virus (AAV) serotype 9 provides global cardiac

gene transfer superior to AAV1, AAV6, AAV7, and AAV8 in the mouse and rat, *Hum Gene Ther* ***19***, 1359–1368.

11. Yue, Y., Ghosh, A., Long, C., Bostick, B., Smith, B. F., Kornegay, J. N., and Duan, D. (2008) A single intravenous injection of adeno-associated virus serotype-9 leads to whole body skeletal muscle transduction in dogs, *Mol Ther* ***16***, 1944–1952.
12. Emery, A. E. (2002) The muscular dystrophies, *Lancet* ***359***, 687–695.
13. Athanasopoulos, T., Graham, I. R., Foster, H., and Dickson, G. (2004) Recombinant adeno-associated viral (rAAV) vectors as therapeutic tools for Duchenne muscular dystrophy (DMD), *Gene Ther* ***11 Suppl 1***, S109-121.
14. Sun, L., Li, J., and Xiao, X. (2000) Overcoming adeno-associated virus vector size limitation through viral DNA heterodimerization, *Nat Med* ***6***, 599–602.
15. Chao, H., Sun, L., Bruce, A., Xiao, X., and Walsh, C. E. (2002) Expression of Human Factor VIII by Splicing between Dimerized AAV Vectors, *Mol Ther* ***5***, 716–722.
16. Duan, D., Yue, Y., Yan, Z., and Engelhardt, J. F. (2000) A new dual-vector approach to enhance recombinant adeno-associated virus-mediated gene expression through intermolecular cis activation, *Nat Med* ***6***, 595–598.
17. Li, J., Sun, W., Wang, B., Xiao, X., and Liu, X. Q. (2008) Protein trans-splicing as a means for viral vector-mediated in vivo gene therapy, *Hum Gene Ther* ***19***, 958–964.
18. Wang, B., Li, J., and Xiao, X. (2000) Adeno-associated virus vector carrying human minidystrophin genes effectively ameliorates muscular dystrophy in mdx mouse model, *Proc Natl Acad Sci U S A* ***97***, 13714–13719.
19. Harper, S. Q., Hauser, M. A., DelloRusso, C., Duan, D., Crawford, R. W., Phelps, S. F., Harper, H. A., Robinson, A. S., Engelhardt, J. F., Brooks, S. V., and Chamberlain, J. S. (2002) Modular flexibility of dystrophin: implications for gene therapy of Duchenne muscular dystrophy, *Nat Med* ***8***, 253–261.
20. Foster, H., Sharp, P. S., Athanasopoulos, T., Trollet, C., Graham, I. R., Foster, K., Wells, D. J., and Dickson, G. (2008) Codon and mRNA sequence optimization of microdystrophin transgenes improves expression and physiological outcome in dystrophic mdx mice following AAV2/8 gene transfer, *Mol Ther* ***16***, 1825–1832.
21. Fabb, S. A., Wells, D. J., Serpente, P., and Dickson, G. (2002) Adeno-associated virus vector gene transfer and sarcolemmal expression of a 144 kDa micro-dystrophin effectively restores the dystrophin-associated protein complex and inhibits myofibre degeneration in nude/mdx mice, *Hum Mol Genet* ***11***, 733–741.
22. Li, J., Dressman, D., Tsao, Y. P., Sakamoto, A., Hoffman, E. P., and Xiao, X. (1999) rAAV vector-mediated sarcogylcan gene transfer in a hamster model for limb girdle muscular dystrophy, *Gene Ther* ***6***, 74–82.
23. Xiao, X., Li, J., Tsao, Y. P., Dressman, D., Hoffman, E. P., and Watchko, J. F. (2000) Full functional rescue of a complete muscle (TA) in dystrophic hamsters by adeno-associated virus vector-directed gene therapy, *J Virol* ***74***, 1436–1442.
24. Kawada, T., Nakazawa, M., Nakauchi, S., Yamazaki, K., Shimamoto, R., Urabe, M., Nakata, J., Hemmi, C., Masui, F., Nakajima, T., Suzuki, J., Monahan, J., Sato, H., Masaki, T., Ozawa, K., and Toyo-Oka, T. (2002) Rescue of hereditary form of dilated cardiomyopathy by rAAV-mediated somatic gene therapy: amelioration of morphological findings, sarcolemmal permeability, cardiac performances, and the prognosis of TO-2 hamsters, *Proc Natl Acad Sci U S A* ***99***, 901–906.
25. Li, J., Wang, D., Qian, S., Chen, Z., Zhu, T., and Xiao, X. (2003) Efficient and long-term intracardiac gene transfer in delta-sarcoglycan-deficiency hamster by adeno-associated virus-2 vectors, *Gene Ther* ***10***, 1807–1813.
26. Cordier, L., Hack, A. A., Scott, M. O., Barton-Davis, E. R., Gao, G., Wilson, J. M., McNally, E. M., and Sweeney, H. L. (2000) Rescue of skeletal muscles of gamma-sarcoglycan-deficient mice with adeno-associated virus-mediated gene transfer, *Mol Ther* ***1***, 119–129.
27. Dressman, D., Araishi, K., Imamura, M., Sasaoka, T., Liu, L. A., Engvall, E., and Hoffman, E. P. (2002) Delivery of alpha- and beta-sarcoglycan by recombinant adeno-associated virus: efficient rescue of muscle, but differential toxicity, *Hum Gene Ther* ***13***, 1631–1646.
28. Qiao, C., Li, J., Zhu, T., Draviam, R., Watkins, S., Ye, X., Chen, C., Li, J., and Xiao, X. (2005) Amelioration of laminin-alpha2-deficient congenital muscular dystrophy by somatic gene transfer of miniagrin, *Proc Natl Acad Sci U S A* ***102***, 11999–12004.
29. Harris, J. D., Schepelmann, S., Athanasopoulos, T., Graham, I. R., Stannard, A. K., Mohri, Z., Hill, V., Hassall, D. G., Owen, J. S., and Dickson, G. (2002) Inhibition of atherosclerosis in apolipoprotein-E-deficient mice following muscle transduction with adeno-associated virus vectors encoding human apolipoprotein-E, *Gene Ther* ***9***, 21–29.

30. Osman, E., Evans, V., Graham, I. R., Athanasopoulos, T., McIntosh, J., Nathwani, A. C., Simons, J. P., Dickson, G., and Owen, J. S. (2009) Preliminary evaluation of a self-complementary AAV2/8 vector for hepatic gene transfer of human apoE3 to inhibit atherosclerotic lesion development in apoE-deficient mice, *Atherosclerosis* ***204***, 121–126.
31. Kay, M. A., Manno, C. S., Ragni, M. V., Larson, P. J., Couto, L. B., McClelland, A., Glader, B., Chew, A. J., Tai, S. J., Herzog, R. W., Arruda, V., Johnson, F., Scallan, C., Skarsgard, E., Flake, A. W., and High, K. A. (2000) Evidence for gene transfer and expression of factor IX in haemophilia B patients treated with an AAV vector, *Nat Genet* ***24***, 257–261.
32. Brantly, M. L., Chulay, J. D., Wang, L., Mueller, C., Humphries, M., Spencer, L. T., Rouhani, F., Conlon, T. J., Calcedo, R., Betts, M. R., Spencer, C., Byrne, B. J., Wilson, J. M., and Flotte, T. R. (2009) Sustained transgene expression despite T lymphocyte responses in a clinical trial of rAAV1-AAT gene therapy, *Proc Natl Acad Sci U S A* ***106***, 16363–16368.
33. Brantly, M. L., Spencer, L. T., Humphries, M., Conlon, T. J., Spencer, C. T., Poirier, A., Garlington, W., Baker, D., Song, S., Berns, K. I., Muzyczka, N., Snyder, R. O., Byrne, B. J., and Flotte, T. R. (2006) Phase I trial of intramuscular injection of a recombinant adeno-associated virus serotype 2 alphal-antitrypsin (AAT) vector in AAT-deficient adults, *Hum Gene Ther* ***17***, 1177–1186.
34. Mingozzi, F., Meulenberg, J. J., Hui, D. J., Basner-Tschakarjan, E., Hasbrouck, N. C., Edmonson, S. A., Hutnick, N. A., Betts, M. R., Kastelein, J. J., Stroes, E. S., and High, K. A. (2009) AAV-1-mediated gene transfer to skeletal muscle in humans results in dose-dependent activation of capsid-specific T cells, *Blood* ***114***, 2077–2086.
35. Wang, Z., Allen, J. M., Riddell, S. R., Gregorevic, P., Storb, R., Tapscott, S. J., Chamberlain, J. S., and Kuhr, C. S. (2007) Immunity to adeno-associated virus-mediated gene transfer in a random-bred canine model of Duchenne muscular dystrophy, *Hum Gene Ther* ***18***, 18–26.
36. Wang, Z., Kuhr, C. S., Allen, J. M., Blankinship, M., Gregorevic, P., Chamberlain, J. S., Tapscott, S. J., and Storb, R. (2007) Sustained AAV-mediated dystrophin expression in a canine model of Duchenne muscular dystrophy with a brief course of immunosuppression, *Mol Ther* ***15***, 1160–1166.
37. Foust, K. D., Nurre, E., Montgomery, C. L., Hernandez, A., Chan, C. M., and Kaspar, B. K. (2009) Intravascular AAV9 preferentially targets neonatal neurons and adult astrocytes, *Nat Biotechnol* ***27***, 59–65.
38. Qiao, C., Li, J., Zheng, H., Bogan, J., Li, J., Yuan, Z., Zhang, C., Bogan, D., Kornegay, J., and Xiao, X. (2009) Hydrodynamic limb vein injection of adeno-associated virus serotype 8 vector carrying canine myostatin propeptide gene into normal dogs enhances muscle growth, *Hum Gene Ther* ***20***, 1–10.
39. Grimm, D., Kern, A., Pawlita, M., Ferrari, F., Samulski, R., and Kleinschmidt, J. (1999) Titration of AAV-2 particles via a novel capsid ELISA: packaging of genomes can limit production of recombinant AAV-2, *Gene Ther* ***6***, 1322–1330.
40. Livak, K. J., and Schmittgen, T. D. (2001) Analysis of relative gene expression data using real-time quantitative PCR and the 2(–Delta Delta C(T)) Method, *Methods (San Diego, Calif)* ***25***, 402–408.
41. Manno, C. S., Chew, A. J., Hutchison, S., Larson, P. J., Herzog, R. W., Arruda, V. R., Tai, S. J., Ragni, M. V., Thompson, A., Ozelo, M., Couto, L. B., Leonard, D. G., Johnson, F. A., McClelland, A., Scallan, C., Skarsgard, E., Flake, A. W., Kay, M. A., High, K. A., and Glader, B. (2003) AAV-mediated factor IX gene transfer to skeletal muscle in patients with severe hemophilia B, *Blood* ***101***, 2963–2972.
42. Cao, O., Dobrzynski, E., Wang, L., Nayak, S., Mingle, B., Terhorst, C., and Herzog, R. W. (2007) Induction and role of regulatory CD4+CD25+ T cells in tolerance to the transgene product following hepatic in vivo gene transfer, *Blood* ***110***, 1132–1140.
43. Martino, A. T., Nayak, S., Hoffman, B. E., Cooper, M., Liao, G., Markusic, D. M., Byrne, B. J., Terhorst, C., and Herzog, R. W. (2009) Tolerance induction to cytoplasmic beta-galactosidase by hepatic AAV gene transfer: implications for antigen presentation and immunotoxicity, *PloS one* ***4***, e6376.
44. Qiao, C., Li, J., Jiang, J., Zhu, X., Wang, B., Li, J., and Xiao, X. (2008) Myostatin Propeptide Gene Delivery by Adeno-Associated Virus Serotype 8 Vectors Enhances Muscle Growth and Ameliorates Dystrophic Phenotypes in mdx Mice, *Hum Gene Ther* ***19***, 241–254.
45. Foster, K., Graham, I. R., Otto, A., Foster, H., Trollet, C., Yaworsky, P. J., Walsh, F. S., Bickham, D., Curtin, N. A., Kawar, S. L., Patel, K., and Dickson, G. (2009) Adeno-associated virus-8-mediated intravenous transfer of myostatin propeptide leads to systemic functional improvements of slow but not fast muscle, *Rejuvenation research* ***12***, 85–94.

Chapter 6

AAV-Mediated Liver-Directed Gene Therapy

Mark S. Sands

Abstract

The liver is directly or indirectly involved in many essential processes and is affected by numerous inherited diseases. Therefore, many inherited diseases could be effectively treated by targeting the liver using gene transfer approaches. The challenges associated with liver-directed gene therapy are efficient targeting of hepatocytes, stability of the vector genome, and persistent high level expression. Many of these obstacles can be overcome with adeno-associated viral (AAV) gene transfer vectors. The first AAV gene transfer vector developed for in vivo use was based on the AAV2 serotype. AAV2 has a broad tropism and transduces many cell types, including hepatocytes, relatively efficiently in vivo. The capsid protein confers the serological profile and at least 12 primate AAV serotypes have already been characterized. Importantly, pseudotyping a recombinant AAV vector with different capsid proteins can dramatically alter the tropism. Both AAV8 and AAV9 have higher affinities for hepatocytes when compared to AAV2. In particular, AAV8 can transduce three- to fourfold more hepatocytes and deliver three- to fourfold more genomes per transduced cell when compared to AAV2. Depending on the dose, AAV8 can transduce up to 90–95% of hepatocytes in the mouse liver following intraportal vein injection. Interestingly, comparable levels of transduction can be achieved following intravenous injection. Direct intraparenchymal injection of an AAV vector also mediates relatively high level long term expression. Additional specificity can be conferred by using liver-specific promoters in conjunction with AAV8 capsid proteins. In addition to treating primary hepatocyte defects, immune reactions to transgene products can be minimized by circumventing the fixed tissue macrophages of the liver, Kupffer cells, and limiting expression to hepatocytes. The ability to target hepatocytes by virtue of the AAV serotype and the use of liver-specific promoters allows investigators to test novel therapeutic approaches and answer basic clinical and biological questions.

Key words: Adeno-associated virus, Gene therapy, Liver, Hepatocytes, Inherited metabolic disease

1. Introduction

The liver performs a myriad of tasks that are essential to the maintenance and proper function of nearly every organ system (1). An enormous number of proteins are synthesized and metabolized in the liver. These include both intracellular and secreted proteins.

Richard O. Snyder and Philippe Moullier (eds.), *Adeno-Associated Virus: Methods and Protocols*,
Methods in Molecular Biology, vol. 807, DOI 10.1007/978-1-61779-370-7_6, © Springer Science+Business Media, LLC 2011

Intracellular and integral membrane proteins are responsible for carbohydrate utilization and storage. The liver is also a major site of lipid metabolism. Many secreted proteins are synthesized in the liver. The major serum protein component, albumin, is synthesized in the liver. In addition, most of the circulating clotting factors, α_1-antitrypsin, ceruloplasmin, and a host of other secreted proteins are produced in the liver. The liver plays an important role in detoxifying naturally occurring metabolites such as ammonia and bilirubin. Drugs and environmental agents are also detoxified, conjugated, and excreted by the liver.

The enormous number of complex tasks performed by the liver are controlled by proteins (enzymes, integral membrane proteins, signaling molecules, secreted proteins, etc.); all of which are susceptible to mutations in their respective genes. Mutations in any of the genes encoding the proteins involved in these processes typically lead directly to disease or a predisposition to disease. The diseases can range from defects in carbohydrate metabolism, lipid metabolism, bleeding disorders, increased vulnerability to drugs and environmental toxins, and cognitive deficits, just to name a few. Given the vast number of functions the liver carries out and its importance for general health, it is clear that it is an important therapeutic target. The ability to stably and efficiently introduce functional expression cassettes into hepatocytes that can compensate for primary liver defects would be a powerful therapeutic tool. The well developed secretory machinery of the liver could also be exploited in order to express and secrete proteins that are not normally produced in the liver. For example, clotting factor VIII or Von Willebrand factor, which are normally produced and secreted from endothelial cells could potentially be expressed and secreted from the liver. Finally, many of the complex interactions and pathways in the liver are not fully understood. Expressing specific transgenes in the livers of intact animals could be an effective method to test various hypotheses and better understand basic mechanisms.

The ability to stably introduce functional genes that mediate persistent high level expression into the liver had been a major challenge. The development of gene transfer vectors based on adeno-associated virus (AAV) overcame many of these obstacles. The first AAV-based gene transfer vector was described by Hermonat and Muzyczka (1984) and utilized the AAV2 serotype (2). However, the first generation vectors were difficult to make and purify in quantities sufficient for in vivo use, even in murine models. Once the technical challenges associated with larger scale production were overcome (3, 4), it quickly became clear that AAV2-based vectors had a relatively broad tropism and mediated persistent high level expression in vivo. Early studies showed that AAV2 appeared to have the greatest tropism for liver and skeletal muscle (5–7). Intravenous injection of an AAV2-based gene transfer vector in mice resulted in transduction of most tissues with the

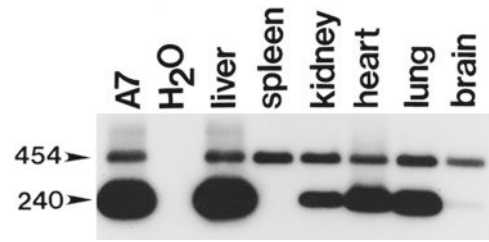

Fig. 1. Transduced viral cDNA persists in most tissues for at least 1 year. Tissues from 1-year-old mice were analyzed for the presence of viral cDNA using primers, which amplify a 240-bp band from human cDNA and a 454-bp band from the endogenous murine GUSB gene. A murine fibroblast line (A7) that has been transduced with a single retroviral copy of the human GUSB cDNA is shown as a positive control. Persistence of AAV-transduced human GUSB cDNA is seen in most tissues at 1 year. The spleen, however, shows no indication of persistent viral transduction at this late time-point. The Southern blot shows the PCR products from a single mouse and is representative of the pattern observed in three separate mice 1 year after injection. Reproduced from Gene Therapy, 2001, with permission from Nature Publishing Group.

exception of those rich in hematopoietic-derived cells (6–8). Importantly, the AAV genome persisted in most tissues, including the liver, for at least 1 year (Fig. 1) and continued to mediate high level expression (8).

These studies were encouraging and represented a major technical advance towards effective in vivo gene therapy. As the field progressed it became clear that the AAV2-based genome was quite versatile and could be efficiently packaged with other AAV capsid proteins. Changing the serotype dramatically affected the tropism. For example, serotypes 1, 5, and 4 were more efficient than AAV2 at transducing cells in the murine central nervous system (9, 10). Likewise, the liver is also more susceptible to transduction by vectors pseudotyped with specific AAV capsid proteins. Although AAV2-based vectors transduced the liver more efficiently than other tissues, serotypes 8 and 9 had an even greater affinity for the liver (11–13). Portal vein injection of a vector pseudotyped with the AAV8 capsid protein resulted in dramatically increased liver transduction compared to vectors pseudotyped with AAV1, AAV2, AAV5, or AAV7 capsid proteins (Table 1) (11). Interestingly, comparable levels of liver transduction were observed with an AAV8 vector regardless of whether it was delivered by intraportal vein injection or by intravenous (tail vein) injection (Fig. 2) (12). It was also demonstrated in the same study that, depending on the dose, greater than 95% of hepatocytes could be transduced with a single injection of an AAV8-pseudotyped vector. The discovery of different AAV capsid proteins and the demonstration that pseudotyped vectors have dramatically different tropisms represent an elegant and effective approach to tissue-specific gene therapy.

Table 1
Real-time PCR analysis for abundance of AAV vectors in nu/nu mouse liver after injection of 1×10^{11} genome copies of vector. A set of probe and primers targeting the SV40 poly(A) region of the vector genome was used for TagMan PCR. Values shown are means of three individual animals with standard deviations. The animals were sacrificed at day 56 to harvest liver tissues for DNA extraction. Reproduced from the Proceedings of the National Academy of Sciences of the United States of America, 2002, with permission from the National Academy of Sciences of the United States of America

AAV vectors/dose	Genome copies per cell
AAV2/1Alb*A1AT*	0.6 ± 0.36
AAV2Alb*A1AT*	0.003 ± 0.001
AAV2/5Alb*A1AT*	0.83 ± 0.64
AAV2/7Alb*A1AT*	2.2 ± 1.7
AAV2/8Alb*A1AT*	18 ± 11

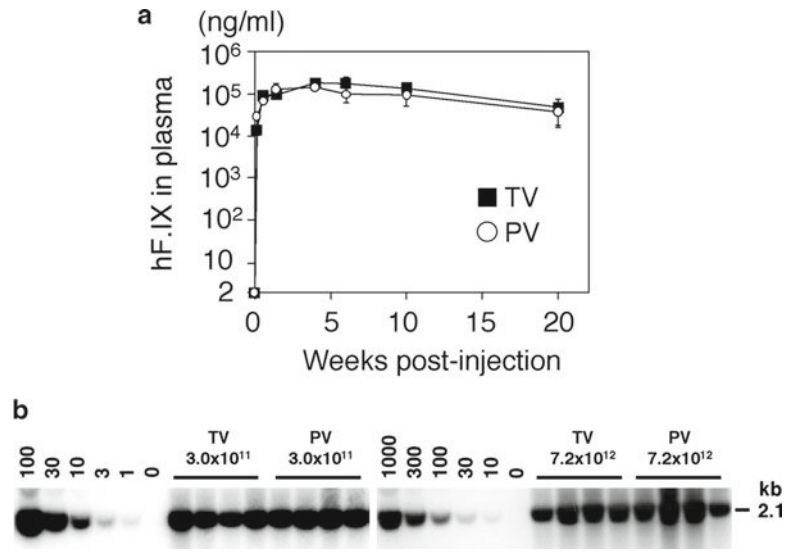

Fig. 2. Comparison of efficiency of rAAV8-mediated liver transduction between tail vein and portal vein injections. (**a**) Plasma human coagulation factor IX (hF.IX) levels after tail vein (TV) or portal vein (PV) injection of AAV8-hF.IX16 into male C57BL/6 mice. Robust human coagulation factor IX expression with no lag phase was observed with both routes. Expression peaked 4 weeks after injection, followed by a substantial (≈75%) decline. *Vertical bars* indicate standard deviations. (**b**) Vector genome copy numbers (ds-vg/dge) in

Although the tropism of AAV-based gene transfer vectors can be shifted towards a specific cell type or tissue by using different capsid proteins, the specificity is not absolute. More restricted expression can be achieved by combining a particular AAV capsid protein with a tissue- or cell-specific promoter. This has particular significance for liver-directed gene therapy. Fixed tissue macrophages in the liver known as Kupffer cells, can act as antigen presenting cells. Expression of foreign proteins in Kupffer cells can elicit an immune response and effectively eliminate any therapeutic effect by developing antibodies to the protein or eliminating the transduced cells through a cytotoxic T cell-mediated mechanism. It has been shown that limiting expression of a foreign transgene to hepatocytes using an AAV8-pseudotyped vector in combination with a hepatocyte-specific promoter dramatically decreases the immune response (14, 15). In fact, recent reports show that liver-specific gene transfer can effectively "tolerize" a mouse model of human disease (16, 17). In one case, the "tolerized" animals can subsequently be treated with intravenous recombinant protein without developing antibodies or lethal hypersensitivity reactions (18).

The thoughtful use of specific AAV capsid proteins is an effective method to enhance liver-specific expression. However, there is an equally effective, if less elegant, means of accomplishing the same goal. It has been shown that direct injection of an AAV2 vector into the liver parenchyma results in relatively widespread transduction throughout the liver (19). This approach mediates persistent expression that is sufficient to reduce the disease burden in several tissues in a murine model of lysosomal storage disease. Although this approach allows some infectious particles to be disseminated through the vasculature and transduce other tissues, the liver remains the predominant target.

An important advantage of AAV gene transfer vectors for human gene therapy applications is that they are believed to persist primarily as extrachromosomal episomes (20, 21). This would effectively eliminate insertional mutagenesis which, in certain circumstances, can lead to serious adverse events when using stably integrating vectors (22, 23). However, several independent studies have shown that rearranged portions of recombinant AAV vectors can stably integrate into the host genome (24, 25). Although there

Fig. 2. (continued) livers transduced with AAV8-EF1α-nlslacZ via tail vein or portal vein injection at 3.0×10^{11} or 7.2×10^{12} vg/mouse. Total liver DNA was extracted 6 weeks post injection, and 10 μg of DNA was analyzed by Southern blot with BglI digestion and a 2.1-kb *lacZ* probe (BglI-BglI fragment). The *left and right blots* were analyzed separately with a different series of vector copy number standards. The double-stranded vector copy number standards (0 to 100 and 0 to 1,000 ds-vg/dge) were prepared by adding the corresponding amount of plasmid, pAAV-EF1α-nlslacZ, to 10 μg of liver DNA extracted from a naïve mouse. *Each lane* represents an individual mouse. Routes of administration and vector doses are indicated above the lanes. Reprinted with permission of the American Society of Microbiology (12).

have been no reports of toxicity in most in vivo pre-clinical experiments or in clinical trials, there has been one report of AAV integration being associated with hepatocellular carcinoma (HCC) (26). Toxicity was first observed in a pre-clinical experiment where effective long-term (≥1 year) disease correction was achieved in mice with a lysosomal storage disorder following systemic delivery of an AAV vector during the neonatal period (8, 27). At 18 months of age the AAV-treated animals still appeared healthy; however, three out of five of the remaining animals had HCC (27). It seemed unlikely that over-expression of the transgene product (β-glucuronidase, GUSB) was the cause of the toxicity since several transgenic lines expressing as much as 1,000-fold higher than normal levels of GUSB showed no evidence of toxicity (28). The initial observation of toxicity following systemic neonatal AAV-mediated gene therapy was reproduced in a larger study where 30–50% of both affected and normal animals developed HCC (26). A thorough molecular analysis of four independent tumors from different animals revealed that a portion of the AAV vector had integrated within a 6-kilobase region near the distal end of mouse chromosome 12. This integration event disrupted the expression of an adjacent micro-RNA-rich region. Interestingly, there have been two additional reports in different disease models using different transgenes of hepatic tumor formation following AAV-mediated gene therapy (29, 30). However, detailed analysis of the proviral structures was not performed in those studies. It remains unclear whether these observations are species- or tissue-specific. Alternatively, these observations could be dependent on the developmental stage at which the vector is delivered (neonatal) or the underlying disease state of the liver. Clearly, the frequency and mechanisms of these observations need to be more precisely elucidated in order for informed risk-vs-benefit determinations to be made.

Progress towards effective liver-directed gene therapy as well as a better understanding of the underlying pathogenesis of primary liver defects will be greatly accelerated by the ability to efficiently and stably transfer functional genes to the livers of intact animal models of disease. The advent of recombinant AAV vectors, the ability to enhance delivery to the liver through pseudotyping with different AAV capsid proteins, and the effective use of liver-specific promoters provides an opportunity to accomplish these goals. Several methods for delivering gene transfer vectors to the livers of murine models of disease are outlined below.

2. Materials

2.1. Liver-Directed Gene Delivery

1. 1-cc Tuberculin syringes.
2. 30-G needles.
3. 3× illuminated desktop magnifying glass.

4. Anesthetic cocktail: 20 mg/ml Ketamine (Fort Dodge Animal Health, Fort Dodge, IA), .375 mg/ml Xylazine (AGRI Laboratories, St. Joseph, MO), (100 μl Anesthetic cocktail/25 g mouse).
5. Sterile surgical supplies (scalpel, scissors, forceps, sponges, etc.).
6. Absorbable gelatin sponge (Ethicon, Somerville, NJ).
7. 4–0 polyester suture (Ethicon, Somerville, NJ).
8. Topical disinfectant: 70% ethanol.
9. Povidone: topical iodine prep pad (Triad Disposables, Brookfield, WI).
10. Mouse restrainer.

2.2. Biochemical, Histological, and Molecular Analyses

1. Microhematocrit capillary tubes.
2. Tissue fixative: 10% neutral-buffered formalin (Sigma, St. Louis, MO).
3. Standard molecular biology equipment (microcentrifuge, microcentrifuge tubes, micropipettors, agarose gel electrophoresis, transfer membranes, etc.).
4. DNA isolation kit.
5. Standard PCR Thermocycler or Real-Time PCR Thermocycler.

3. Methods

As mentioned above, liver-directed gene delivery with an AAV vector can be accomplished by several methods. Conceptually, the easiest methods involve the injection of vector into the liver either through the portal vein or directly into the liver parenchyma. Unfortunately, both methods are relatively invasive and require some surgical skill (see below). A more elegant approach involves pseudotyping the viral vector with an AAV capsid that enhances liver tropism, and incorporating a liver-specific promoter into the expression cassette. Liver-directed gene transfer using a liver-specific vector/promoter combination can be accomplished with a simple intravenous injection. This eliminates the need to become proficient in surgical techniques. There are numerous liver-specific expression cassettes, and infectious AAV vector stocks pseudotyped with a variety of capsid proteins can be obtained on a fee-for-service basis from several core laboratories. These techniques are beyond the scope of this chapter and will be discussed elsewhere. The techniques outlined below are intended for use in rodent (rat and mouse) models. The reader should seek assistance from an experienced veterinarian if similar experiments are to be carried out in larger (canine, primate, etc.) animal models.

3.1. Liver-Directed Gene Delivery

Intraportal vein injection, direct intraparenchymal liver injection and intravenous injection techniques have been described in detail elsewhere. Therefore, the methods outlined below represent basic guides for these approaches. The reader is encouraged to seek experienced collaborators to assist with the techniques, in particular the survival surgery techniques.

3.1.1. Intraportal Vein Injection (see Ref. 31)

1. Place adult mice under surgical anesthesia by intraperitoneal injection of anesthetic cocktail. Surgical anesthesia is confirmed when the animal is unresponsive when the toe is pinched and the blinking reflex is no longer present.
2. Prepare the abdomen prior to surgery by washing with topical disinfectant followed by Povidone. Establish a sterile field over the abdomen.
3. Make a 2–3-cm long midline incision in the abdomen starting 2–3 mm below the xyphiod process.
4. Eviscerate the intestines and reflect them to the left to expose the portal vein (see Note 1).
5. Introduce a 30-G needle directly into the portal vein.
6. Inject 0.2 ml of viral suspension uniformly and slowly over a period of 1 min.
7. Keep the needle in place for approximately 10–20 s after the injection.
8. Remove the needle and gently press a small piece of absorbable sponge over the insertion point to prevent bleeding.
9. Close the abdomen with two layers (muscle and skin) of running 4–0 polyester suture.
10. Place the animal under a heating lamp until it has recovered and then house singly until the wound is completely healed.

3.1.2. Intraparenchymal Liver Injection (see Ref. 19)

1. Up to 200 μl of total injectate can be delivered to the adult mouse liver in four to five separate injection sites (40–50 μl/site).
2. Place adult mice under surgical anesthesia by intraperitoneal injection of anesthetic cocktail. Surgical anesthesia is confirmed when the animal is unresponsive when the toe is pinched and the blinking reflex is no longer present.
3. Prepare the abdomen for surgery by washing with topical disinfectant followed by Povidone. Establish a sterile field over the abdomen.
4. Make a 2–3-cm long midline incision in the abdomen starting 2–3 mm below the xyphiod process in order to expose the liver.
5. Inject viral suspension directly into the liver parenchyma through a 30-G needle affixed to a tuberculin syringe.

6. Inject the suspension slowly with intermittent pressure (see Note 2).
7. Remove the needle and stop the bleeding by gentle pressure with a sterile cotton sponge.
8. Choose a new site and repeat the procedure.
9. Close the abdomen with two layers (muscle and skin) of running 4–0 polyester suture.
10. Place the animal under a heating lamp until it has recovered and then house singly until the wound is completely healed.

3.1.3. Adult I.V. Injection

1. Up to 300–400 μl of injectate can be delivered intravenously to an adult mouse by this route.
2. Place a mouse in a standard mouse restrainer such that the injector has free access to the entire length of tail.
3. The most accessible veins in the mouse tail are on the lateral sides of the tail. The vein on the dorsal aspect of the mouse tail is difficult to routinely inject. The vessel on the ventral aspect of the tail is an artery and should never be injected.
4. Insert a 30-G needle affixed to a 1-cc tuberculin syringe into one of the lateral veins at a site as distal as possible on the tail. Choose a distal site so that if the first attempt is unsuccessful, the injector can simply choose another more proximal injection site (see Note 3).
5. Slowly inject the viral suspension once the needle is in place (see Note 4).
6. Remove the needle once the injection is complete and apply pressure to the site until bleeding stops.
7. Return the mouse to its cage immediately after the injection.

3.1.4. Neonatal I.V. Injection (see Ref. 32)

1. Up to 100 μl of viral suspension can be delivered to a neonatal mouse by this technique.
2. This procedure is most easily accomplished with two people; one restraining the animal and the other injecting.
3. Neonatal mice can be injected by this route between 1 and 4 days of life. It becomes increasingly difficult to visualize the vein beyond the first 4 days of life.
4. Place neonatal mice on a dry towel at 4°C for several minutes prior to injection to minimize their movement and reduce trauma.
5. One person gently immobilizes the forelimbs and holds the head such that the lateral aspect is facing up. This exposes the superficial temporal vein that extends from behind the eye into the neck.
6. Position the mouse under the 3× illuminated magnifying glass.

7. The other person inserts the 30-G needle affixed to a 1-cc tuberculin syringe under the skin next to the vein. The approach should be from the head towards the neck.
8. Move the needle over the vein and advance slowly into the vein until the bevel is obscured by blood. This indicates that the needle is in the vessel (see Note 5).
9. Do not advance further.
10. Inject the viral suspension slowly (see Note 6).
11. Once the injection is complete, remove the needle and apply gentle pressure to the vein. Bleeding typically stops within 2–3 min.
12. Place the mouse under a heating lamp before returning to the female.
13. If the injection is unsuccessful, allow the mouse to recover for 5–10 min and then attempt a second injection on the other side.

3.2. Liver-Specific Analyses

Two important and disease-independent considerations when evaluating liver-directed gene transfer are the presence of the transgene and toxicity. Determining the presence of a specific transgene in liver tissue can be accomplished by several standard molecular biology methods. However, the exact methods and conditions will vary depending on the transgene used. Therefore, the methods will be discussed in general terms. Although the techniques for toxicity determinations are standard, it is inefficient for most small independent research laboratories to incorporate those technologies into their laboratory. Therefore, the assays necessary for an initial determination of toxicity will be outlined and examples (not an exhaustive list) of representative service providers will be listed. If toxicity is suspected after an initial screen, the investigator is encouraged to seek expert (Pathologist, etc.) advice to determine the appropriate course of action to better understand the findings.

3.2.1. Southern Blot (see Ref. 33)

1. Isolate high molecular weight genomic DNA or lower molecular weight "Hirt" DNA from liver tissue by standard techniques.
2. Digest the DNA to completion with appropriate restriction endonucleases (see Note 7).
3. Separate the restriction fragments by agarose gel electrophoresis (see Note 8).
4. Transfer the DNA fragments by passive diffusion or by electrotransfer to a charged synthetic membrane.
5. Prepare a suitable radiolabeled or fluorescently labeled DNA fragment, being mindful of where the restriction sites are located.

6. Equilibrate the membrane containing the bound DNA fragments in buffer, probe with the labeled DNA fragment, then wash extensively to remove any unbound DNA probe.
7. Visualize the labeled membrane (blot) by exposure to film or by an alternate imaging system.
8. Incorporate known molecular weight markers or an internal standard in order to: (1) identify the position of the transgene, (2) estimate the copy number of the transgene, and (3) estimate the number of unique integration sites of the transgene.

3.2.2. Standard PCR (see Ref. 33)

Real-Time (RTPCR) or Quantitative (QPCR) PCR is perhaps the easiest and most reliable method to quantify the amount of transgenes in the liver of animals following viral-mediated gene transfer. However, this requires specialized equipment that may be beyond the capabilities of small independent laboratories. Alternate, less expensive PCR-based methods have been established that allow investigators to detect the presence and estimate the level of gene transfer. These methods are briefly outlined below:

1. Isolate total DNA from liver tissue samples by standard techniques.
2. Design single-stranded DNA primers that are complementary to either the transgene or the expression cassette within the gene transfer vector.
3. PCR primers can be developed for several purposes. A single pair of primers can be devised that will detect the presence of the transgene or expression cassette. This is useful when using a transgene that does not naturally exist in the host genome [bacterial β-galactosidase, green fluorescent protein (GFP), etc.]. When amplifying a therapeutic transgene that has a corresponding full length endogenous gene, an internal control can be incorporated into this type of analysis. A single set of primers that amplifies both the transgene (usually a cDNA) and the corresponding full length gene within the host genome can be devised (see Fig. 1). Regions of the cDNA that have exact, or nearly exact sequence homology to the host gene but are separated by one or more introns are required for this analysis. Typically, the PCR products from the transgene and the full length gene should differ by 50 to several hundred base pairs in length in order to easily separate the two fragments by gel electrophoresis. Alternatively, a second set of PCR primers can be developed that amplifies a PCR product of distinct size from a different host gene. This type of analysis can be used to simultaneously detect any transgene and an independent host gene.
4. Perform PCR on the total DNA isolated from liver (the exact PCR protocol will vary depending on the transgene and primer configurations).

5. Separate the PCR products by gel electrophoresis. Visualize the PCR products by ethidium-bromide fluorescence or by Southern blot analysis (see above).
6. The ability to simultaneously amplify a distinct sized PCR product using either a single set of primers or two sets of primers allows the investigator to estimate the amount of the transgene relative to a known host gene (see Note 9).

3.2.3. Real-Time or Quantitative PCR (see Ref. 33)

1. Isolate total DNA from liver tissue samples by standard techniques.
2. Synthesize PCR primers specific for the transgene. PCR primers used for QPCR typically amplify a fragment less than 100 bp in length.
3. Determine the PCR protocol (annealing time, extension time, etc.) empirically in test runs using standard techniques. Perform the amplification using either a fluorescently labeled probe or fluorescently labeled nucleotides.
4. PCR products are detected and quantified by two methods: (1) Synthesize a fluorescently labeled primer that binds a region of DNA between the two original primers. As the internal primer is incorporated into the PCR products, the fluorescent label is liberated and detected by the Real-Time PCR instrument. This is a method that indirectly measures the amplification of the product. However, this method provides additional specificity since all three primers must bind their respective sites in order for the fluorescent probe to be liberated. (2) Use fluorescently labeled nucleotides that will be incorporated into the amplified product. This method provides a direct measure of the amount of amplified product and is typically more versatile since a gene-specific fluorescently labeled primer is not required. However, this method may not be as specific since it only requires two primers to faithfully bind their respective complementary sequences. Any off-target amplification cannot be distinguished from the desired PCR product.
5. Perform the quantitative PCR reaction and compare to a known internal standard. In the case of transgene copy number the standard is typically a single copy gene [e.g. glyceraldehydes-3-phosphate dehydrogenase (GAPDH)]. When quantifying mRNA levels by QPCR, the internal standard is typically an mRNA from a house-keeping gene such as β-actin or GAPDH. However, care must be taken when quantifying mRNA since the levels of certain housekeeping genes can change depending on the disease state or the transgene that is expressed.

3.2.4. Liver Toxicity

An important consideration for the development of liver-directed gene therapy is safety. Toxic effects of gene transfer to the liver can be determined in animal models of disease either indirectly

(serum chemistry) or directly (histology). The advantage of determining changes in liver enzymes by serum chemistry is that this can be performed repeatedly in the same animal using survival techniques. In contrast, performing histology to directly determine liver toxicity typically involves sacrificing the animal, this is especially true for small (rodent) animal models of disease. In most cases, a thorough evaluation of toxicity involves both serial serum chemistry analyses and histology at a terminal time point.

3.2.5. Serum Chemistries

1. Anesthetize animals (see above) prior to blood collection to minimize unnecessary stress.
2. Collect blood from the lateral saphenous vein, which proceeds dorsally then laterally over the tarsal joint.
3. Shave the lateral aspect of the hind leg to expose the skin. Cleanse the area with a topical disinfectant.
4. Knick the vein with a sterile scalpel.
5. Collect up to 150 μl of blood into either a heparinized or non-heparinized microhematocrit capillary tube, depending on whether plasma or serum is needed, respectively. Apply gentle pressure until bleeding is stopped (see Note 10).
6. Alternatively, blood can be obtained from the tail.
7. Cleanse the tail thoroughly with topical disinfectant and cut 2–3 mm of the tail tip off with sharp sterile scissors.
8. Collect up to 150 μl of blood from the tail tip. Apply gentle pressure to stop the bleeding (see Note 11).
9. The most common serum enzymes that serve as indicators of liver damage are: Serum Glutamic-Oxaloacetic Transaminase (SGOT or AST), Serum Glutamic-Pyruvic Transaminase (SGPT or ALT), Alkaline Phosphatase (ALP), Gamma-Glutamyl Transpeptidase (GGT), Lactic Acid Dehydrogenase (LDH), and Bilirubin (see Note 12).

3.2.6. Histology

1. An initial histological screen for liver toxicity can be performed by staining fixed tissue with Hematoxylin and Eosin (H&E).
2. Sacrifice animals by anesthetic overdose or by CO_2 asphyxiation.
3. Make a midline abdominal incision to expose the liver.
4. Remove a piece of liver ranging from several mm^3 to 1 cm^3 from one of the liver lobes and place in 1–5 ml of tissue fixative for at least 48 h.
5. Dehydrate the piece of liver and embed in paraffin for sectioning. The sections are then stained with H&E and evaluated by a pathologist with experience examining rodent tissue (see Note 13).
6. Specialized histological analyses (e.g. electron microscopy, immunohistochemistry, etc.) may be warranted if abnormalities

are detected on the H&E-stained sections. The most appropriate analysis can be determined after discussions with an experienced pathologist and is beyond the scope of this review.

4. Notes

1. The portal vein is a relatively large vein that originates in the intestines and drains directly into the liver. The anterior lobes of the liver may have to be lifted in order to see the vein. The intestines are kept moist during the procedure by covering them with sterile gauze soaked in sterile saline.
2. The injection site is monitored during the injection through a surgical stereoscope to ensure that there is no hemorrhage or extravasation. If either of these situations occurs, the needle is removed, the bleeding stopped with gentle pressure, and a new site is injected.
3. If the injector experiences difficulty with this approach, keep in mind the lateral veins are extremely superficial. Some degree of vasodilation can be achieved if the tail is gently heated with warm water.
4. If the injector has difficulty depressing the plunger due to increased pressure, it is likely that the needle is not in the vein. In that case remove the needle and choose a new site.
5. The skin is translucent at this age and the bevel of the needle can easily be seen through the skin.
6. Typically the vein distal to the injection site will blanch if the injection is successful. If the needle is not in the vein, an easily visible bulge will immediately form with as little as 10 μl injected subcutaneously.
7. Restriction sites within the transgene or expression cassette will liberate the entire transgene or internal fragments of the transgene. A single restriction site within the transgene or expression cassette will liberate transgene/genomic junction fragments from integrated proviral forms.
8. The appropriate agarose concentration will depend on the expected size of the fragments. In general, low concentration gels will be used to identify large junction fragments and higher agarose concentrations will be used to identify internal fragments of known size.
9. Numerous controls must be run with this type of analysis to determine the appropriate PCR protocol, the relative rates of amplification from the primers, and the relative affinity of the probes for the PCR products if Southern blot analysis is to be performed.

10. This procedure can be performed once every 2 weeks without altering normal hematologic parameters.
11. Unlike blood collection from the saphenous vein, blood collection from the tail tip can only be performed one or two times. One advantage of collecting blood from the tail tip is that DNA can be isolated from the piece of tissue for genotyping.
12. Elevations or reductions in these circulating enzymes are *non-specific* indicators of liver disease or damage. If the levels of these enzymes deviate from normal, a liver specialist should be consulted so more specific liver tests can be performed. It is not cost-effective for most independent research laboratories to establish these techniques in their laboratories. There are numerous contract laboratories that will perform these assays on a fee-for-service basis [National Toxicology Program, Department of Health and Human Services (http://ntp.niehs.nih.gov/index.cfm?objectid=070C9D76-D1D1-84FD-998ECE4408785E21), Quest Diagnostics, Madison, NJ (http://www.questdiagnostics.com)]. Finally, it is critical for the investigator to provide serum from normal control animals since the standards and normal values used by contract laboratories are typically human specific.
13. Normal control animals will aid in this evaluation. As with serum chemistry analyses, it is inefficient for most independent laboratories to bring this expertise into the laboratory. There are numerous laboratories that will perform histology on a fee-for-service basis [e.g. HistoTox Labs, Boulder, CO, (http://www.histotoxlabs.com), Wax-it, Vancouver, CA, (http://www.waxitinc.com)].

References

1. Cecil Textbook of Medicine, 22nd edition (2004), Saunders, Philadelphia, PA. Goldman, L and Ausiello, D, eds.
2. Hermonat, P. L., and Muzyczka, N. (1984) Use of adeno-associated virus as a mammalian DNA cloning vector: Transduction of neomycin resistance into mammalian tissue culture cells *Proc Natl Acad Sci* **81**, 6466–6470.
3. Grimm, D., Kern, A., Rittner, K., and Kleinschmidt, J. A. (1998) Novel tools for production and purification of recombinant adeno-associated virus vectors *Hum Gene Ther* **9**, 2745–2460.
4. Zolotukhin, S., Byrne, B. J., Mason, E., Zolotukhin, I., Potter, M., Chesnut, K., Summerford, C., Samulski, R. J., and Muzyzcka, N. (1999) Recombinant adeno-associated virus purification using novel methods improves infectious titer and yield *Gene Ther* **6**, 973–985.
5. Xiao, X., Li, J., and Samulski, R. J. (1996) Efficient long-term gene transfer into muscle tissue of immunocompetent mice by adeno-associated virus vector *J Virol* **70**, 8098–8108.
6. Ponnazhagan, S., Mukherjee, P., Yoder, M. C., Wang, X. S., Zhou, S. Z., Kaplan, J., Wadsworth, S., and Srivastava, A. (1997) Adeno-associated virus 2-mediated gene transfer in vivo: Organ-tropism and expression of transduced sequences in mice *Gene* **190**, 203–210.
7. Daly, T. M., Vogler, C., Levy, B., Haskins, M. E., and Sands, M. S. (1999) Intravenous injection of recombinant AAV into neonatal mice with mucopolysaccharidosis type VII results in persistent β-glucuronidase expression and widespread reduction of lysosomal storage *Proc Natl Acad Sci* **96**, 2296–2300.
8. Daly, T. M., Ohlemiller, K. K., Roberts, M. S., Vogler, C. A., and Sands, M. S. (2001)

Prevention of systemic clinical disease in MPS VII mice following AAV-mediated neonatal gene transfer *Gene Ther* **8**, 1291–1298.

9. Davidson, B. L., Stein, C. S., Heth, J. A., Martins, I., Kotin, R. M., Derksen, T. A., Zabner, J., Ghodsi, A., and Chiorini, J. A. (2000) Recombinant adeno-associated virus type 2, 4, and 5 vectors: Transduction of variant cell types and regions in the mammalian central nervous system Proc Natl Acad Sci 97, 3428–3432.
10. Burger, C., Gorbatyuk, O. S., Velardo, M. J., Peden, C. S., Williams, P., Zolotukhin, S., Reier, P. J., Mandel, R. J., and Muzyczka, N. (2004) Recombinant AAV viral vectors pseudotyped with viral capsids from serotypes 1, 2, and 5 display differential efficiency and cell tropism after delivery to different regions of the central nervous system *Mol Ther* **10**, 302–317.
11. Gao, G. P., Alvira, M. R., Wang, L., Calcedo, R., Johnston, J., and Wilson, J. M. (2002) Novel adeno-associated viruses from rhesus monkeys as vectors for human gene therapy *Proc Natl Acad Sci* **99**, 11854–11859.
12. Nakai, H., Fuess, S., Storm, T. A., Muramatsu, S., Nara, Y., and Kay, M. A. (2005) Unrestricted hepatocyte transduction with adeno-associated virus serotype 8 vectors in mice *J Virol* **79**, 214–224.
13. Inagaki, K., Fuess, S., Storm, T. A., Gibson, G. A., McTiernan, C. F., Kay, M. A., and Nakai, H. (2006) Robust systemic transduction with AAV9 vectors in mice: Efficient global cardiac gene transfer superior to that of AAV8 *Mol Ther* **14**, 45–53.
14. Wang, L., Nichols, T. C., Read, M. S., Bellinger, D. A., and Verma, I. M. (2000) Sustained expression of therapeutic levels of factor IX in hemophilia B dogs by AAV-mediated gene therapy in liver *Mol Ther* **1**, 154–158.
15. Franco, L. M., Sun, B., Yang, X., Bird, A., Zhang, H., Schneider, A., Brown, T., Young, S. P., Clay, T. M., Amalfitano, A., Chen, Y. T., and Koeberl, D. D. (2005) Evasion of immune responses to introduced human acid alpha-glucosidase by liver-restricted expression in glycogen storage disease type II *Mol Ther* **12**, 876–884.
16. Cooper, M., Nayak, S., Hoffman, B. E., Terhorst, C., Cao, O., and Herzog, R. W. (2009) Improved induction of immune tolerance to factor IX by hepatic AAV8 gene transfer *Hum Gene Ther* **20**, 767–776.
17. Ishiwata, A., Mimuro, J., Mizukami, H., Kashiwakura, Y., Takano, K., Ohmori, T., Madoiwa, S., and Ozawa, Sakata, Y. (2009) Liver-restricted expression of the canine factor VIII gene facilitates prevention of inhibitor formation in factor VIII-deficient mice *J Gene Med* **11**, 1020–1029.
18. Sun, B., Kulis, M. D., Young, S. P., Hobeika, A. C., Li, S., Bird, A., Zhang, H., Li, Y., Clay, T. M., Burks, W., Kishnani, P. S., and Koeberl, D. D. (2010) Immunomodulatory gene therapy prevents antibody formation and lethal hypersensitivity reactions in murine Pompe disease *Mol Ther* **18**, 353–360.
19. Sferra, T. J., Backstrom, K., Wang, C., Rennard, R., Miller, M., and Hu, Y. (2004) Widespread correction of lysosomal storage following intrahepatic injection of a recombinant adeno-associated virus in the adult MPS VII mouse *Mol Ther* **10**, 478–490.
20. Duan, D., Sharma, P., Yang, J., Yue, Y., Dudas, L., Zhang, Y., Fisher, K. J., and Engelhardt, J. F. (1998) Circular intermediates of recombinant adeno-associated virus have defined structural characteristics responsible for long-term episomal persistence in muscle tissue *J Virol* **72**, 8568–8577.
21. Nakai, H., Yant, S. R., Storm, T. A., Fuess, S., Meuse, L., and Kay, M. A. (2001) Extra chromosomal recombinant adeno-associated virus vector genomes are primarily responsible for stable liver transduction in vivo *J Virol* **75**, 6969–6976.
22. Hacein-Bey-Abina, S., Von Kolle, C., Schmidt, M., McCormack, M. P., Wulffrat, N., Leboulch, P., Lim, A., Osborne, C. S., Pawliuk, R., Morillon, E., Sorensen, R., Forster, A., Fraser, P., Cohen, J. I., de Saint Basile, G., Alexander, I., Wintergerst, U., Freborg, T., Aurias, A., Stoppa-Lyonnet, D., Romana, S., Radford-Weiss, I., Gross, F., Valensi, F., Delabesse, E., Macintyre, E., Sigaux, F., Soulier, J., Leiva, L. E., Wissler, M., Prinz, C., Rabbitts, T. H., Le Deist, F., Fischer, A., and Cavazzana-Calvo, M. (2003) LMO2-associated clonal T cell proliferation in two patients after gene therapy for SCID-X1 *Science* **302**, 415–419.
23. Stein, S., Ott, M. G., Schultze-Strasser, S., Jauch, A., Burwinkel, B., Kinner, A., Schmidt, M., Kramer, A., Schwable, J., Glimm, H., Koehl, U., Preiss, C., Ball, C., Martin, H., Gohring, G., Schwarzwaelder, K., Hofmann, W. K., Karakaya, K., Tchatchou, S., Yang, R., Reinecke, P., Kuhlcke, K., Schlegelberger, B., Thrasher, A. J., Hoelzer, D., Seger, R., von Kalle, C., and Grez, M. (2010) Genomic instability and myelodysplasia with monosomy 7 consequent to EVI1 activation after gene therapy for chronic granulomatous disease *Nat Med* **16**, 198–205.
24. Nakai, H., Wu, X., Fuess, S., Storm, T. A., Munroe, D., Montini, E., Burgess, S. M., Grompe, M., and Kay, M. A. (2005) Lareg-scale

molecular characterization of adeno-associated virus vector integration in mouse liver *J Virol* **79**, 3606–3614.

25. Miller, D. G., Trobridge, G. G., Petek, L. M., Jacobs, M. A., Kaul, R., and Russell, D. W. (2005) Large-scale analysis of adeno-associated virus vector integration sites in normal human cells *J Virol* **79**, 11434–11442.
26. Donsante, A., Miller, D. G., Li, Y., Vogler, C., Brundt, E. M., Russell, D. W., and Sands, M. S. AAV vector integration sites in mouse hepatocellular carcinoma *Science* **317**, 477.
27. Donsante, A., Vogler, C., Muzyczka, N., Crawford, J. M., Barker, J., Flotte, T., Campbell-Thompson, M., Daly, T., and Sands, M. S. (2001) Observed incidence of tumorigenesis in long-term rodent studies of rAAV vectors *Gene Ther* **8**, 1343–1346.
28. Vogler, C., Galvin, N., Levy, B., Grubb, J., Jiang, J., Zhou, X. Y., and Sly, W. S. (2003) Transgene produces massive overexpression of human β-glucuronidase in mice, lysosomal storage of enzyme, and strain-dependent tumors *Proc Natl Acad Sci* **100**, 2669–2673.
29. Embury, J. E., Charron, C. C., Poirier, A. E., Zori, A., Carmichael, R., Flotte, T. R., and Laipis, P. J. (2006) Long term portal vein administration of AAV-WPRE vector results in increased incidence of neoplastic disease and hepatic pathology *Mol Ther* **13**, S83.
30. Bell, P., Moscioni, D., McCarter, R. J., Wu, D., Gao, G., Hoang, A., Sanmiguel, J. C., Sun, X., Wivel, N. A., Raper, S. E., Furth, E. E., Batshaw, M. L., and Wilson, J. M. (2006) Analysis of tumors arising in male B6C3F1 mice with and without AAV vector delivery to liver *Mol Ther* **14**, 34–44.
31. Cai, S. R., Garbow, J. R., Culverhouse, R., Church, R. D., Zhang, W., Shannon, W. D., and McLeod, H. L. (2005) A mouse model for developing treatment for secondary liver tumors *Int J Oncol* **27**, 113–120.
32. Sands, M. S., and Barker, J. E. (1999) Percutaneous intravenous injection into neonatal mice *Lab Animal Sci* **49**, 328–331.
33. Molecular Cloning: A laboratory manual, 3rd edition, (2001) Cold Spring Harbor Laboratory Press, Cold Spring Harbor, NY, Sambrook, J., Russell, D., eds.

Chapter 7

Recombinant AAV Delivery to the Central Nervous System

Olivier Bockstael, Kevin D. Foust, Brian Kaspar, and Liliane Tenenbaum

Abstract

Recombinant AAV-mediated gene delivery to the CNS can be performed either by direct delivery at the target site or from the periphery, using intramuscular injections and retrograde transport along motor neuron projections or intravenous injections and blood–brain barrier crossing.

In this chapter, we describe:

1. Methods for recombinant virus administration, including stereotactic surgery, intramuscular, and intravenous administration.
2. Methods to evaluate the number and biodistribution of brain and spinal cord cells expressing the transgene by immunohistochemisty as well as the amount of transgene product by ELISA in the target region.
3. Methods to characterize the cellular specificity of transgene expression by double immunofluorescence.
4. Methods to quantify the amounts of viral DNA as well as of transgene mRNA by quantitative PCR and RT-PCR, respectively.

Key words: Stereotaxy, Intravenous injection, Retrograde transport, Immunohistochemistry, Confocal microscopy, GFP, GDNF, Quantitative PCR, mRNA, Hirt DNA

1. Introduction

Applications for AAV vector gene delivery to the central nervous system (CNS) include a wide range of neurological disorders and CNS trauma as well as local transgenesis for disease modeling. Gene therapy strategies are being tested for correction of enzymatic deficiencies in lysosomal storage diseases (1–5), providing neurotrophic support in neurodegenerative diseases (6–9), modulating neurotransmission (10, 11), compensatory replacement of lost neurotransmitters (12, 13), delivering siRNA for the correction of autosomal dominant mutations (14, 15), and delivering of anti-inflammatory cytokines (16).

Richard O. Snyder and Philippe Moullier (eds.), *Adeno-Associated Virus: Methods and Protocols*,
Methods in Molecular Biology, vol. 807, DOI 10.1007/978-1-61779-370-7_7,

The temporal, regional pattern as well as the cellular specificity of AAV-mediated transgene expression in the brain is usually not homogenous and largely dependent on the capsid serotype, transcriptional elements, and site of delivery.

The properties of the viral preparation (purity, titer) as well as the technique of delivery, e.g., convection-enhanced delivery (17), delivery of co-factors such as heparin (18) or mannitol (19), might have a high impact on the transduction pattern.

The CNS is made up of many different cell types, including neuron and glial cells. There are many types of neurons varying in morphology, size and function. Glial cells include astrocytes, oligodendrocytes, and microglia. The method to evaluate transgene expression as well as the nature of the transgene product (intracellular, secreted, transported) might also influence the results. Histological stainings such as immunohistochemistry or simple or double immunofluorescence constitute the method of choice to characterize the biodistribution of transgene expression but are of limited usefulness for quantification of transduction efficiency. The amount of transgene expression is rather evaluated by bulk measures on brain extracts such as ELISA or RT-qPCR. Finally, the vector can be delivered either directly in the brain or in the periphery, i.e., intramuscularly or intravenously, resulting in different transduction patterns. This chapter focuses on methods to achieve CNS delivery by AAV vectors using conventional approaches routinely used in neuroscience research. Thanks to stereotaxy, regions of the brain can be reached by needles directed from outside using a stereotaxic instrument. Various atlases prepared from brains of adult male or female rats and mice are available (20, 21). The coordinates are taken from a reference point on the skull, the most commonly used being the bregma which is the point of intersection between mid-saggital coronal sutures. Minimally invasive techniques should be used to avoid immune and inflammatory reactions which can provoke the rejection of transduced cells (22, 23) (see Note 1).

Recently we, and others, (24–26) demonstrated that a new AAV serotype, type 9, crosses the blood–brain barrier (BBB) when intravenously injected in mice, cats, and nonhuman primates. Data in rats have yet to be published. The efficiency of crossing is dose dependent, and the types of cells targeted are dependent on the animal age. Administration in neonate animals results in primarily neuronal transduction, whereas injection into adults infects mostly glial cells. The utilization of self-complementary AAV (scAAV9) genomes greatly enhances the number of cells transduced. We will describe the procedure for neonate mouse temporal vein and adult tail vein injections.

We and others (27–30) have identified that AAV vectors can be retrogradely transported from the muscle to spinal cord motor neuron. In brief, axonal projections from motor neurons take up

virus and transport the virus back to the cell body in a retrograde fashion where the motor neuron then produces the therapeutic transgene product. It is important to note that efficiencies vary for each serotype tested, with reports of AAV1 as more efficient at retrograde transport properties to motor neurons.

2. Materials

2.1. Direct Intracerebral rAAV Delivery by Stereotaxy

1. Class 2 laboratory equipped with a class 2 biosafety cabinet (vertical laminar flow with HEPA filters) or dual access animal containment workstation (equipped with a vertical laminar vertical flow and ULPA filters; for example: ESCO VIVA VDA-4A1, Analis, Namur, Belgium) (see Note 2).
2. Masks and gloves.
3. Biohazardous containers (to be incinerated).
4. 0.1 M NaOH.
5. Individual ventilation cages (Allentown, France).
6. Stereotaxic apparatus (Kopf Model 900 Small Animal Stereotaxic Instrument, Tujunga, California or Stoelting 51600 Lab Standard stereotaxic instrument, Dublin, Ireland).
7. Mouse adaptor (Stoelting).
8. Drill (Fine Science Tools, Heidelberg, Germany).
9. Microdrill Trephines (Fine Science Tools).
10. Programmable injector (microprocessor-controlled infusion pump equipped with a ultra Micropump III, World Precision Instruments, Sarasota, FL, USA).
11. Ten-microliter Hamilton syringe connected to a blunt-end 40 mm-long 30G needle (Hamilton, 701SN Pst3).
12. Light source such as a fiber optic lamp with movable arms.
13. Viral suspension diluted in DPBS (with Ca^{2+} and Mg^{2+}, BioWittaker, Lonza) at the desired titer (usually between 10^{11} and 10^{12} viral genomes per milliliter, titers are matched if several viruses are used in the same experiment) and kept on ice during the whole stereotaxic procedure.
14. Anesthetics: ketamine (Ketalar 50 mg/ml, Pfizer), xylasine (Rompun 2%, Bayer).
15. Carbomerum (2 mg/ml; Vidisic, Tramedico, Sint-Niklaas, Belgium).
16. Surgery instruments: knife, forceps, etc.
17. Cotton buds.

2.2. Intravenous Injection of AAV9

2.2.1. Neonate Temporal Vein Injection

1. Mice 1–2 days old.
2. Bed of wet ice.
3. Dissecting microscope.
4. Light source at an oblique angle such as a fiber optic lamp with movable arms.
5. 3/10 cc insulin syringe with half in 30 G needle, one per animal.
6. scAAV9 solution at $\geq 1 \times 10^{11}$ viral particles per animal.

2.2.2. Adult Tail Vein Injection

1. Mice 3 weeks or older.
2. Rodent restrainer such as model MTI from Braintree Scientific.
3. 3/10 cc Insulin syringe with half in 30 G needle, one per animal.
4. Alcohol wipes.
5. scAAV9 viral solution $\geq 5 \times 10^{11}$ viral particles per animal.

2.3. Retrograde Transport from the Periphery to Target Motor Neurons

1. Ten-microliter Hamilton syringe connected to a beveled 40-mm-long 30 G needle (Hamiton, ref 701SN Pst3).
2. Viral suspension diluted in DPBS (with Ca and Mg, BioWittaker) at the desired titer (usually $> 10^{12}$ viral genomes per milliliter; titers are matched if several viruses are used in the same experiment) and kept on ice during the whole procedure.
3. Anesthetics: ketamine (Ketalar 50 mg/ml, Pfizer); xylaxine (Rompun 2%, Bayer).
4. Laminar flow (biosafety cabinet), individual ventilation cages, masks, gloves, 1 M NaOH.

2.4. Dissection and Processing of Rat Brains

1. Dry ice.
2. Thermometer (down to – 40°C).
3. Methylbutane 99% (Aldrich).

2.4.1. Freshly Frozen Brains

2.4.2. Perfused Paraformaldehyde-Fixed Brains

1. Paraformaldehyde (Sigma).
2. Physiological saline (NaCl 0.9%).
3. Peristaltic pump; 20 G I.V. catheter (Versatus, Terumo, Somerset, NJ, USA).
4. Scissors; Vibratome (e.g., VTS1000, Leica).

2.5. Histological Analysis of Transduction

2.5.1. Evaluation of the Number and Regional Distribution of GFP-Positive Cells

1. Primary antibody: anti-GFP polyclonal rabbit serum (Molecular Probes).
2. Secondary antibody: donkey anti-rabbit IgG conjugated with biotin (Amersham).
3. Staining reagents: Streptavidin conjugated to cyanine 2 (Jackson ImmunoResearch, West Grove), ABC Elite vectastain kit and diaminobenzidine (Vector, NTL Laboratories, Brussels, Belgium), xylene (Merck).
4. Horse serum (HS) (Gibco, Invitrogen).
5. THST 50 mM Tris, 0.5 M NaCl, 0.5% Triton X-100 (Merck), pH 7.6.
6. TBS :Tris 10 mM, NaCl 0.9%, pH 7.6.
7. Mounting fluids: FluorSave (Calbiochem); DPX (Sigma).
8. Disposables:polystyrene multipurpose containers (15 ml) with lids (Greiner #203170); gelatin-coated slides (see Note 3), coverslips.
9. Microscopy: optical fractionator of the Stereoinvestigator software (MBF Bioscience, USA); CCD video camera connected to the microscope (Leica, Germany).

2.5.2. Characterization of GFP-Positive Cells by Co-labeling with Cell Type-Specific Antibodies

1. Primary antibodies: anti-tyrosine hydroxylase mouse monoclonal antibody (Millipore, Chemicon), anti-neuronal nuclei (NeuN) mouse monoclonal antibody (Millipore, Chemicon), anti-glial fibrillary acidic protein (GFAP) mouse monoclonal antibody (Millipore, Chemicon), anti-parvalbumin mouse monoclonal antibody (Sigma), and anti-glutamic acid decarboxylase (GAD) mouse monoclonal antibody (Millipore, Chemicon).
2. Secondary antibodies: rabbit biotinylated anti-goat IgG (Vector), donkey anti-mouse IgG coupled to cyanine 3 (Jackson ImmunoResearch).
3. Confocal microscope with automatic image analysis system (Lasersharp version 3.2, Biorad).
4. Axiovert 100 microscope (Carl Zeiss, Germany).
5. Image J software (NIH, USA).

2.6. Quantitative Analysis of Transduction

2.6.1. Preparation of Samples for DNA, RNA, and Protein Extractions

1. Steel brain matrix (for coronal sections, Alto Rofoz, Gaithesburg, MD).
2. One-edge razor blades.
3. Plastic Petri dishes.
4. 1.5 ml RNAse-free microfuge tubes (Ambion).
5. Forceps.
6. Precision balance.

7. Tissue punch set (Stoelting).
8. Nucleotide and RNAse cleaning solution (RNAse AWAY, Invitrogen).

2.6.2. Viral DNA

1. Lysis buffer: Tris 10 mM, pH 8.0, EDTA 10 mM, SDS 1%.
2. DNase-free RNase 10 mg/ml (Roche Applied Bioscience).
3. Pronase (Roche Applied Bioscience).
4. Proteinase K (Roche Applied Bioscience).
5. Tabletop microcentrifuge.
6. Phenol/chloroform/isoamyl alcohol (25/24/1) (Sigma).
7. Chloroform/isoamyl alcohol (24/1) (Sigma).
8. 100% Ethanol (Sigma).
9. TE buffer.

2.6.3. mRNA Extraction and Reverse Transcription

1. MagNA Pure LC Instrument (Roche Applied Bioscience).
2. MagNA Pure LC mRNA Isolation Kit II (Roche Applied Bioscience).
3. Transcriptor First Strand cDNA Synthesis Kit (Roche Applied Bioscience).
4. Anchored-oligo $(dT)_{18}$ primers.

2.6.4. Real-Time Quantitative PCR of GFP Transgene and cDNA

1. LightCycler FastStart DNA master SYBR Green 1 kit.
2. Real-time SYBRgreen qPCR analysis kit (Roche Applied Bioscience).
3. LightCycler 1.5 apparatus (Roche Applied Bioscience).
4. Reaction capillaries (Roche Applied Science).

2.6.5. Protein Extraction

1. Lysis buffer: PBS 1% NP40, 10% glycerol, protease inhibitors cocktail (Roche; 1 pellet for 50 ml).
2. Sonificator (e.g., Branson sonifier 250).
3. 1 N HCl.

3. Methods

3.1. Direct Intracerebral rAAV Delivery by Stereotaxy

1. Install the stereotaxic frame and instruments in a biosafety class 2 cabinet (see Note 2) in a biosafety class 2 laboratory. Use masks and gloves.
2. Fix the Hamilton syringe in the injector, fill it by immersion of the needle tip in the viral suspension and aspirate using the "Fast reverse" function.

3. Check the absence of bubble by using the "fast forward" function until a drop appears at the needle tip. Remove the drop using a cotton wipe (disposed in 0.1 M NaOH).
4. Anesthetize rats of approximately 250 g by intraperitoneal injection of xylazine (10 mg/kg) and ketamine (100 mg/kg) using a 1 ml syringe with a 25 G needle.
5. Settle the anesthetized rats on the stereotaxic frame by first placing incisor teeth on the tooth bar. Then, place the ear bars in the external auditory meatuses and firmly fix the head. Check that the skull is flat and the two eyes at the same horizontal level. Put a drop of carbomerum in each eye in order to avoid drying during the anesthesia. Position the light source so that it illuminates the head of the animal. Shave the head and clean it with alcohol.
6. Make a antero-posterior cut in the scalp using a blade and maintain it open using forceps. Use cotton buds to remove the blood. Remove the periosteum (membrane that lines the outer surface of the cranial bone) to visualize the bregma.
7. Adjust the vertical position of the tooth bar so that the height of the skull surface at bregma and lambda (point of intersection of the sagittal and lamboïd sutures) are the same. If the sutures are difficult to visualize, allow the skull to dry for 5–10 min.
8. The stereotaxic instrument (see Fig. 1) has an antero-posterior (AP), a dorso-vertical (DV), and a medio-lateral (ML) scale to determine the position inside the brain. It is equipped with manipulators with 0.1 mm vernier scales for coordinates adjustment. Antero-posterior, lateral, and vertical movements are made possible due to screw movements of knobs. Measure the AP and ML coordinates of the bregma by placing the tip of the needle vertical to the bregma. Calculate the AP and ML positions of the targeted site according to the Atlas and move the syringe on the AP and ML axis using the screws. Make a mark on the cranial bone at the desired AP and ML coordinates.
9. Make a hole in the bone using a drill. Pay attention not to damage the dura (outer layer of the meninges).
10. Place the needle at the surface of the dura and measure the DV coordinate of the bregma. Calculate the DV coordinate of the target site.
11. Slowly move the needle manually vertically by using the screw to reach the site of injection and leave it in place for 5 min.
12. Infuse 2 μl of the viral suspension at a speed of 0.2 μl/min using the programmable injector. (It is useful to check the meniscus of the viral suspension before and after infusion to

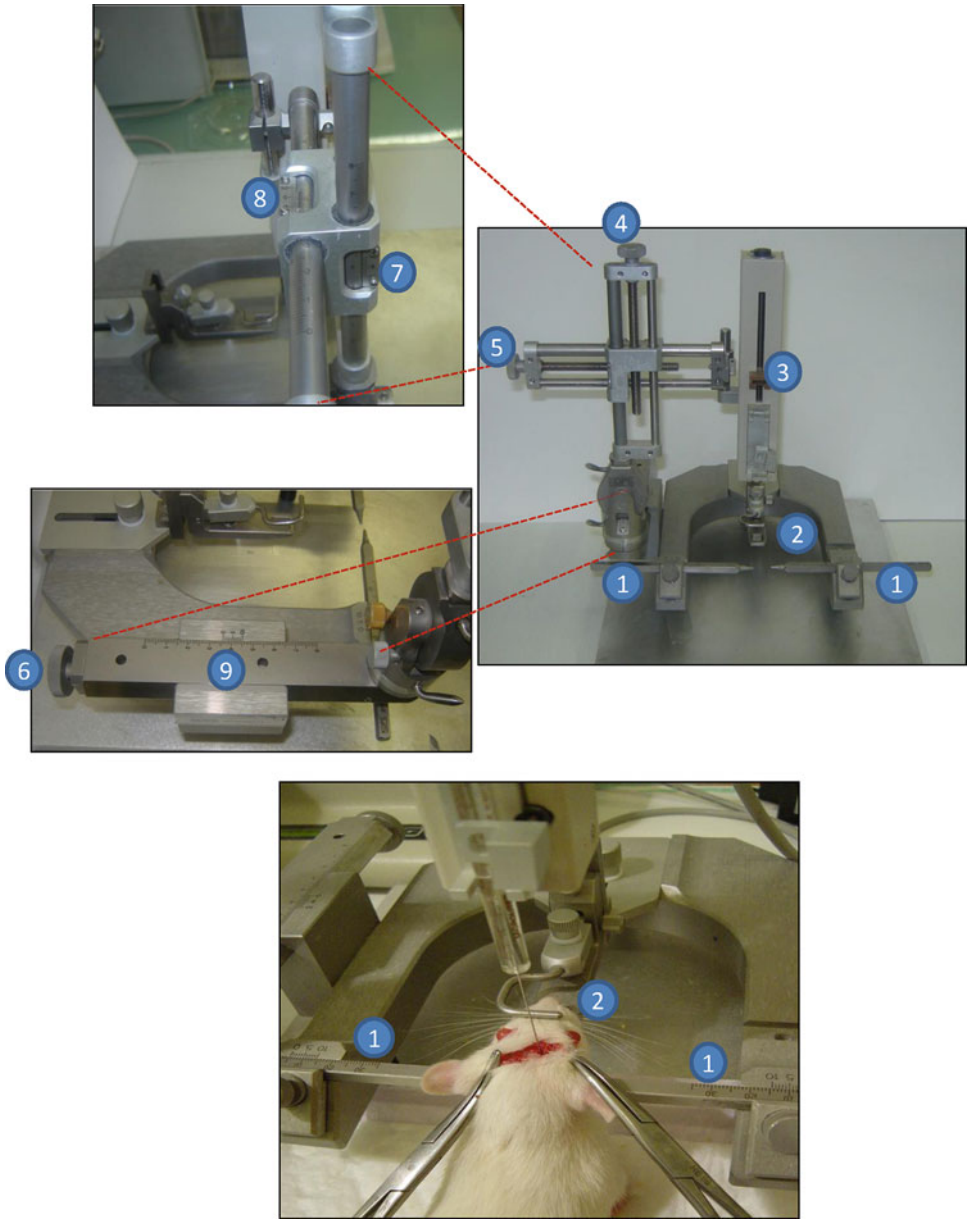

Fig. 1. Stereotaxic frame. The Hamilton syringe is fixed in the injector and filled with the viral suspension. Anesthetized rats of approximately 250 g are settled on the frame by placing incisor teeth on the tooth bar and the ear bars in the external auditory meatuses. An antero-posterior cut is made in the scalp and the periosteum removed in order to visualize the bregma. The needle tip is placed on the bregma, and AP and ML coordinates of the bregma are measured. The AP and ML position of the target site are calculated according to the atlas and the syringe is moved on the AP and ML axis using the corresponding screws. A mark is made on the cranial bone at the desired AP and ML coordinates, and a hole is made in the bone using a drill. The needle is placed at the surface of the dura and the DV coordinate is measured. The DV coordinate of the target site is calculated. The needle is then slowly moved down manually by using the vertical screw to reach the site of injection and left in place for 5 min. Two microliters of the viral suspension are infused at a speed of 0.2 μl/min using the programmable injector. At the end of the infusion, the needle is left in place for 5 min before slowly removing it manually. (1) Ear bars; (2) tooth bar; (3) syringe holder of the programmable injector; (4) screw for setting vertical coordinate; (5) screw for setting lateral coordinate; (6) screw for antero-posterior coordinate; (7) vertical vernier scale; (8) lateral vernier scale; (9) antero-posterior vernier scale.

confirm the volume of virus injected). At the end of the infusion, leave the needle in place for 5 min before slowly removing it manually.

13. Sew the scalp, attach a numbered ear tag to the earlobe and place the rat in a clean cage separate from the other rats until waking up (see Note 4).
14. Keep animals in individual ventilation cages (e.g., Allentown) during the first days postsurgery (see Note 2).
15. Dispose needles and surgical materials properly in biohazardous containers. Clean instruments with 0.1 M NaOH or 10% chlorine bleach and thoroughly rinse with distilled water, then with alcohol.

3.2. Intravenous Injection of AAV9

3.2.1. Neonate Temporal Vein Injection

1. Position the light source so that it illuminates your microscope field. A moderate light intensity is best to visualize the vein.
2. Place one mouse pup directly on the ice to anesthetize the animal for 1–3 min.
3. While the animal is on ice, fill your syringe with virus. The volume should not exceed 100 µl. Volumes between 30 and 100 µl do not influence transduction pattern in our experience.
4. Position the animal in view of the microscope. With your non-injecting hand, place your index finger on the side of the mouse muzzle and your middle finger just caudal to the ear bud. This hand position is important to stretch the skin and visualize the temporal vein.
5. Identify the temporal vein. It should be visible through the skin just anterior to the ear bud and inferior to small peripheral vasculature. The temporal vein appears shadowy, runs dorsal to ventral, and feeds into the jugular.
6. Enter the vein with the bevel up. You should see the needle bevel fill with blood through the skin. Depress the plunger and note the blanching of the vein down the side of the face.

3.2.2. Adult Tail Vein Injection

1. Secure the animal into the restrainer.
2. Clean the tail with the alcohol wipe.
3. Warm the tail with warm water or the trough in the mouse tail illuminator.
4. Load the syringe with the viral solution.
5. Target the vein starting closer to the tip of the tail. Enter the vein. If you miss the vein, move closer to the base of the tail and try again.
6. Inject viral solution in a bolus. Injection volumes range from 100 to 250 µl.
7. Return the animal to its housing.

3.3. Retrograde Transport from the Periphery to Target Motor Neurons

1. Anesthetize rats of approximately 250 g by intraperitoneal injection of xylazine (10 mg/kg) and ketamine (100 mg/kg) using a 1 ml syringe with a 25 G needle.
2. Settle anesthetized rats on a sterile drape. Put a drop of carbomerum in each eye in order to avoid drying during the anesthesia.
3. Shave the muscle region and clean it with alcohol. Make a cut in the skin using a blade and maintain it open using forceps to visualize the muscle.
4. Fill the Hamilton syringe with virus solution obviating air and bubbles.
5. Squeeze the muscle to clearly establish the thickness of the muscle and place the needle in the belly of the muscle.
6. Move the needle slowly manually and leave the needle in place for 1 min before infusing 10–20 μl of the viral suspension at a speed of 10 μl/min.
7. At the end of the infusion, leave the needle in place for 2 min before slowly removing it manually. Multiple injections can be performed.
8. Suture the skin, attach a numbered ear tag to the earlobe, and place the rat in a clean cage separate from the other rats until waking up.
9. Dispose needles and surgical materials properly in sharps and biohazardous containers.

3.4. Processing of Rat Brains

3.4.1. Freshly Frozen Brains

1. Put the brain in a becher containing methylbutane (enough to cover the brain) using a spoon.
2. Add dry ice until the temperature drops to –10°C. Wait for 10 s. Add dry ice until the temperature drops to –20°C. Wait for 20 s.
3. Remove the brain, wrap it in aluminum foil, and keep at –80°C at least one night.

3.4.2. Perfused Paraformaldehyde-Fixed Brains

1. Deeply anesthetize the rats with a twofold excess of ketamine and xylasine.
2. Open the thorax and infuse 0.9% physiological saline at room temperature through the ascending aorta and drain it through the right atrium using a catheter inserted at the basis of the left ventricle with the tip placed into the ascending aorta (see Note 5).
3. Perfuse 200–300 ml at a flow rate of 20 ml/min.
4. Perfuse –300 ml of ice-cold 4% paraformaldehyde (kept on ice during the whole procedure; see Note 6).
5. The body becomes rigid and the paws usually show typical movements in response to PF4.

6. Remove brains and postfix overnight in ice-cold PF4.
7. Rinse brains are rinsed in PBS before sectioning using a Vibratome at 50 μm.
8. Store sections in PBS at 4°C. For long-term storage, add 0.1 M sodium azide (see Note 7).

3.5. Histological Analysis of Transduction

GFP-positive cells can be evidenced microscopically either using the protein native fluorescence (see Note 8) or using antibodies. For immunohistochemical detection (see Note 9),

3.5.1. Evaluation of the Number and Regional Distribution of GFP-Positive Cells

1. Perform the following incubations under agitation in 5 ml of reagents or 1 ml of antibody-containing solutions. Wash three times in TBS for 10 min between each step.
   (a) 3% H_2O_2 in TBS for 30 min at room temperature (RT). This step aims at irreversibly inactivating endogenous peroxidase using a saturating concentration of its natural substrate, H_2O_2.
   (b) THST containing 10% HS for 1 h at RT.
   (c) Polyclonal rabbit anti-GFP (1:3,000) in THST containing 5% HS overnight at 4°C.
   (d) Donkey anti-rabbit IgG conjugated with biotin (1:600) in THST 5% HS, 2 h at RT.
2. Reveal peroxidase staining using the ABC Elite Vectastain kit and diaminobenzidine according to the manufacturer's protocol.
3. Mount sections on gelatin-coated slides, place the slides vertically in racks, dehydrate by sequential 2 min incubations in 70% ethanol, 96% ethanol, 100% ethanol (twice), xylene (twice), and coverslip using DPX.
4. Evaluate the number of GFP-positive cells and the volume of the labeled brain area by stereological procedures based on the Cavalieri principle (31) as follows. For each animal, analyze serial sections with an interval of 500 μm by means of the optical fractionator of the Stereoinvestigator software connected with a CCD video camera to the microscope.

3.5.2. Characterization of GFP-Positive Cells by Co-labeling with Cell Type-Specific Antibodies

Examples of co-labelings of GFP-positive cells with neuronal and glial markers are given below (see also Fig. 2).

1. Incubate vibratome sections (50 μm) obtained from fixed brains sequentially in the following reagents. Three washes in TBS are performed between each step.
   (a) THST containing 10% HS for 2 h.
   (b) Polyclonal rabbit anti-GFP (1:3,000) combined with mouse monoclonal anti-NeuN (1:200), anti-GAD (1:200), anti-parvalbumin (1:2,000), anti-TH (1:500), or anti-GFAP (1:200) in THST 5% HS for 16 h at 4°C.

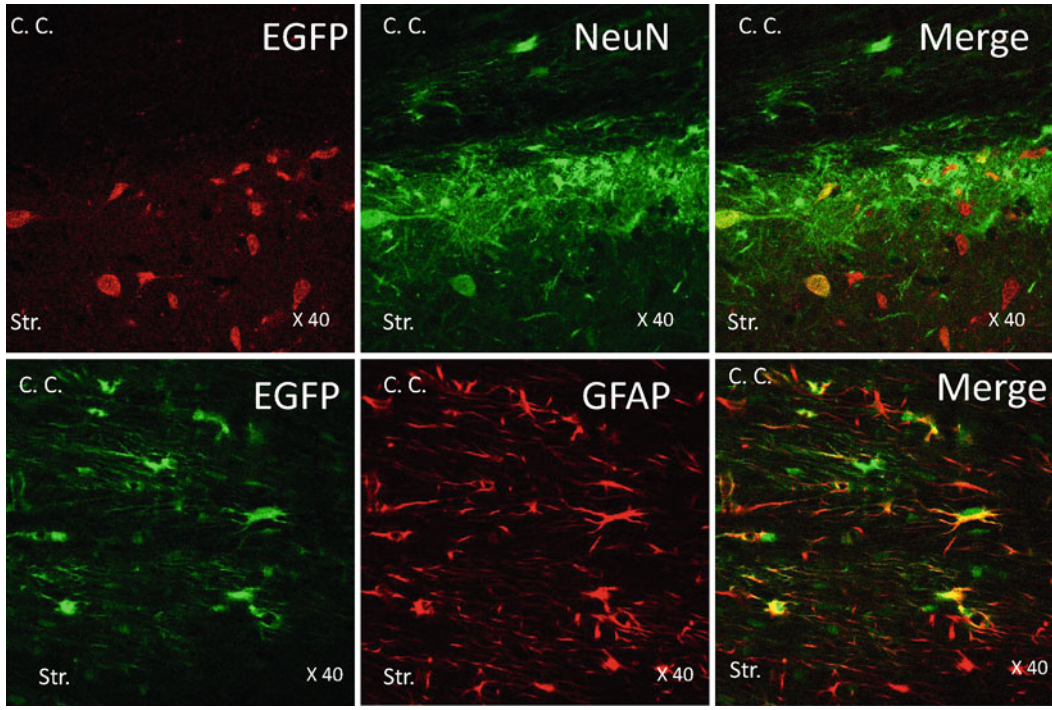

Fig. 2. Dentification of transgene-expressing cells by double immunofluorescence and confocal microscopy. *Upper panels*: 5 weeks after injection of a tetracycline-inducible vector trans-encapsidated into serotype 1 capsids (rAAV2/1-tetON-M2-eGFP) above the substantia nigra of adult rats (coordinates: AP = 5.3 mm posterior, *L* = 2.2 mm lateral to bregma, and *V* = −6.6 mm below the dural surface), 50 μm vibrating blade microtome sections of the midbrain were co-labeled with anti-GFP (*green fluorescence*) and anti-TH (*red fluorescence*) antibodies. Confocal pictures show GFP and TH double-labeled cells (*yellow*) in the substantia nigra pars compacta. *Arrows* indicate examples of double-labeled cells. Scale bar: 50 μm. *Lower panels*: 2 days after injection of rAAV2/1-CMV-eGFP into the medial striatum of adult rats (coordinates: AP = 0 mm, *L* = −2.2 mm relative to bregma, and *V* = −4.2 mm below the dural surface), 50 μm vibrating blade microtome sections of the forebrain were co-labeled with anti-GFP (*green fluorescence*) and anti-GFAP (*red fluorescence*) antibodies. Confocal pictures showing the absence of co-labeled cells in the subventricular zone. *Scale bar*: 50 μm.

(c) Donkey anti-rabbit IgG conjugated with biotin (1:600) in THST 5% HS 2 h at RT.

(d) Cy2-conjugated streptavidin (1:300) combined with cy3-conjugated donkey anti-mouse IgG (1:200) in THST 5% HS, 2 h at RT under aluminum foil.

2. Mount sections using FluorSave and keep in the dark at room temperature at least 1 h before microscopic examination. For storage, keep sections in the dark at 4°C.

3. For optimal results, use a confocal microscope to identify co-labeled cells (see Note 10). Perform co-labeling analysis on pictures taken on at least three different sections within the transduction zone using an automatic image analysis system (Lasersharp version 3.2, Biorad) coupled to Axiovert 100 microscope (Carl Zeiss, Germany). Pictures (e.g., see Fig. 2) are then processed and analyzed with the Image J software (NIH, USA).

3.6. Quantitative Analysis of Transduction

In case of RNA extraction, all the sectioning and punching operations are made in a clean RNAse free –20°C environment in RNAse-free conditions. The section chamber of a cryostat can be used if it has a sufficient horizontal surface.

3.6.1. Preparation of Samples for DNA, RNA, and Protein Extractions

1. Weight carefully each RNAse-free microfuge tubes.
2. Clean all slicing material with RNAse inhibitor solution (e.g., Invitrogen's RNAse Away).
3. Equilibrate frozen brains, slicing material, and collection tubes 1 h at –20°C before being used.
4. Make 1 mm thick sections using a steel brain matrix and one-edge razor blades. Fix the brain first in the matrix by two blades flanking the region of interest. From one edge, introduce two blades in each section groove to make the two first slices. Remove the outer blade in order to expose the first section. Transfer it into a plastic Petri dish. Continue inserting blades and extraction of slices until the end of the desired structure.
5. Collect punches of tissue corresponding to the desired structure from three slices around the injection site for each animal (see Note 11). In order to make reproductive samples, use a tissue punch kit. Take the same number of punches from the same region for each sample. Transfer punches to the pre-weighted tubes (see Note 12). Weight the samples to ensure a good reproducibility of sample size and the adequation between sample weight and extraction protocol.
6. Store samples at –80°C before extraction.

3.6.2. Viral DNA

Extract low-molecular-weight DNA according to the Hirt DNA extraction method (32).

1. Homogenize tissue samples (approximately 10 mg) by repeated pipettings in 300 µl of lysis buffer complemented with 1 µl of DNase-free RNase for 30 min at 37°C.
2. Add pronase and proteinase K to final concentrations of 0.5 and 1 mg/ml, respectively (1.5 µl of 10 mg/ml and 20 mg/ml stock solution, respectively). Incubate at 37°C for 2 h.
3. Add NaCl to a final concentration of 1.1 M (67.3 µl of a stock solution at 5 M) and keep overnight at 4°C.
4. Following overnight precipitation of high molecular weight DNA, samples are spun at 18,600 × *g* for 1 h and supernatant transferred in a clean tube (see Note 13).
5. Low-molecular-weight DNA is purified from the supernatant by phenol/chloroform/isoamyl alcohol extractions (twice) followed by chloroform/isoamyl alcohol extractions (twice).
6. Add 300 µl of absolute ethanol and precipitate overnight at –20°C.
7. Centrifuge samples at 14,000 rpm for 1 h, discard supernatant.

8. Resuspend the final DNA pellet in 50 µl of TE buffer.
9. Further digest with RNase (at a final concentration of 0.2 ng/µl) for 30 min at room temperature.
10. Quantify viral sequences quantitative PCR.

3.6.3. mRNA Extraction and Reverse Transcription

1. Extract RNA with MagNA Pure LC Instrument using the MagNA Pure LC mRNA Isolation Kit II according to the manufacturer's recommendations. Alternatively, Trizol extraction can also be performed.
2. Convert mRNA samples to cDNA using the Transcriptor First Strand cDNA Synthesis Kit according to the manufacturer's recommendations using 3 µl of the RNA sample and anchored-oligo $(dT)_{18}$ primers.
3. Use quantitative PCR to quantify transgene cDNA.

3.6.4. Real-Time Quantitative PCR of gfp Transgene and cDNA

- Quantify gfp sequences using real-time SYBRgreen qPCR analysis and a LightCycler apparatus using the following primers: *forward*: GCA-GAA-GAA-CGG-CAT-CAA-GGT; *reverse*: ACG-AAC-TCC-AGC-AGG-ACC-ATG.
- For normalization of amounts of gfp mRNA, perform qPCRs for house-keeping genes (tyrosine 3-monooxygenase/tryptophan 5-monooxygenase activation protein, zeta polypeptide (YWHAZ), and actin γ2) transcript levels using the following primers: for actin γ2: *forward*: TAC-CCT-ATT-GAG-CAC-GGC-AT; *reverse*: CGC-AGC-TCG-TTG-TAG-AAG-GT; and for YWHAZ: *forward*: CAA-GCA-TAC-CAA-GAA-GCA-TTT-GA; *reverse*: GGG-CCA-GAC-CCA-GTC-TGA.
- For normalization of gfp copy numbers in Hirt DNA samples, establish a standard curve based on serial dilutions of plasmids harboring the recombinant AAV genome containing the GFP sequence in each run.
- Run the cycles with the LightCycler 1.5 apparatus using the LightCycler FastStart DNA master SYBR Green 1 kit following manufacturer's recommendations. In practice:
  - *Standard curve (for quantification of Hirt DNA only)*
    Dilute the vector plasmid harboring the rAAV genome in TE buffer to a concentration of 10^{10} plasmid copies per microliter using the following formula: $6.02 \times 10^{23} \times ((\text{plasmid concentration (ng/µl)}/1{,}000)/(\text{plasmid size (bp)} \times 646)/1{,}000{,}000) = \text{number of plasmid copies per microliter}$.

    Starting from the concentration of 10^{10} plasmid copies per microliter, the plasmid is further submitted to serial 1:10 dilutions in TE down to concentration of 10^2 plasmid copies per microliter.

- *Primers*
  Dilute the primers in PCR water (provided with qPCR kits) to a concentration of 100 μM for the stock solution and 5 μM final.
- *Preparations of samples*
  1. Prepare all reagents necessary for the PCR except the template DNA in a mix in room apart from the PCR room. Perform all steps in a cooler box at 4°C. Keep all reagents and samples at −20°C.
  2. For each reaction, the mix is composed of 8.2 μl of PCR H_2O, 0.8 μl of 25 mM $MgCl_2$, 2 μl of each primer diluted at 10 μm, and 2 μl of the LightCycler FastStart DNA Master SYBR Green 1 (10× concentrated). Distribute the mix (15 μl in each capillary) in the reaction capillaries.
  3. Bring the capillaries to the PCR room and add DNA standard curve, Hirt DNA, and cDNA dilutions into the capillaries (5 μl for each sample),
  4. Close the capillaries, insert them into the reaction carrousel, and centrifuge to bottom the reaction mix.
  5. Load the carrousel into the LightCyler 1.5 apparatus for analysis.
- *Reaction*
  PCR conditions are: 95°C 10 min, 45 cycles of 95°C 10 s, 60°C 30 s, 72°C 20 s.
- Amplification is followed by a melting curve step to assess the specificity of the amplification. Each run comprises samples containing PCR grade water and no DNA as negative control.
- *Analysis of data*
  Data analysis and normalizations are performed using qBase software (Ghent University, Belgium).

  For cDNA sample, normalize expression levels of GFP transcripts relative to actin γ2 and YWHAZ transcript levels.

  For Hirt DNA samples, normalize GFP copy numbers relative to plasmid concentrations in the standard curve.

3.6.5. Protein Extraction

1. Weight the samples. Add lysis buffer up to 1 ml per 50 mg.
2. For some proteins, acidification allows a higher recovery (see Note 14). Acidify to pH < 4.0 with HCl 1 N. Keep tubes on ice.
3. Sonicate (output 2, 30% duty cycle) three times for 10 s. Keeping the tubes on ice to avoid warming due to sonification.

4. Centrifuge (10,000 × *g* for 10 min).
5. Take supernatant. If acidification was performed, neutralize with NaOH 1 N. Keep at –80°C.

4. Notes

1. In order to reduce surgery-related damage and inflammation that could elicit immune rejection of transduced cells, minimally invasive methods should be used: use blunt-end thin (30 G) needles instead of sharp needles, move needle up and down very slowly, infuse virus slowly with a programmable injector (0.2 µl/min), wait 5 min before and after each injection to allow viral suspension to diffuse and tissue to retract.
2. Legal recommendations might differ from one country to the other and should be checked with national regulatory authorities. Ideally, surgery should be performed in a biosafety Class 2 cabinet. However, the manipulation of the stereotaxic frame as well as coordinates reading requires an open access to the head of the animal and is thus difficult in a cabinet with a small opening. We perform stereotaxy in a dual access animal containment workstation (e.g., ESCO VIVA VDA-4A1, Analis, Belgium) which is equipped with a laminar vertical flow and ULPA filters, bearing mask and gloves. Animals are kept in individual ventilation cages until viral particles are considered to be absent in the body fluids, generally after few days. Litter and bottles are treated as required by the P2 containment rules. However, it should be taken into account that AAV viral particles are resistant to acidic conditions, to heat, and to most commercial virucidal detergents.
3. To prepare gelatin-coated slides:
   (a) Prepare racks of slides with rack holders. Wash with detergent and rinse several times with distilled water; fill racks with slides.
   (b) Immerse slides in 1 M HCl for 15 min. Rinse with distilled water (3× 5 min). Let them dry in a dust-free environment (e.g., a laminar flow hood).
   (c) Prepare sibbing solution: heat 1 L of MilliQ water at 50°C in a becher with a magnet; slowly add 5 g of gelatin (Sigma G-2500) (avoid clamping); allow gelatine to completely dissolve (at least 1 h); add chromic potassium sulfate (solution turns light green). Use this solution freshly because it becomes rapidly contaminated.
   (d) Take a dried slide rack with a rack holder and submerge in the sibbing solution, then slowly remove the rack.

Allow the slides to drain in the same position, then incline the rack laterally for more draining.

(e) Place the racks on a clean diaper. Cover with saran wrap to avoid dust. Allow to dry for 1–3 days.

4. Since some of the rats remove their ear tags, they might be impossible to identify at the end of the experiment. It is therefore important to have separate cages for rats belonging to different groups.
5. The tip of the canula can be stained in dark color in order to be visible through the aorta wall.
6. To prepare 1 L of 4% paraformaldehyde (PF4), dissolve 40 g of PF in 500 ml of MilliQ water, add 40 drops of 1 M NaOH, and heat up to 50°C while stirring. Dissolving takes about 20 min (if required, add more NaOH). Filtrate the fixative and add 250 ml of 0.4 M phosphate buffer (for 1 L: 810 ml of 0.4 M Na_2HPO_4 and 190 ml of 0.4 M NaH_2PO_4.).Adjust the pH to 7.4. Add MilliQ water up to 1 L and store at 4°C. PF4 is made up fresh, usually the day before or at least a few days before perfusion. Solutions are discarded if older than 1 week.
7. Sodium azide is a mutagen. Manipulate with gloves. Sodium azide also inhibits peroxidase. Sections kept in sodium azide have to be extensively washed (24 h in several washes of PBS) before peroxidase labelings.
8. The detection of native GFP can be performed using a fluorescence microscope and FITC-filter on vibratome sections (50 μm) from perfused animals. However, the procedure is difficult due to a rapid fading of the green signal. Therefore, immunohistochemistry is usually preferred.
9. While cutting, distribute 50 μm vibratome sections in five sequential Greiner vials (maximum 20 sections per vial) so that five different staining can be performed on each brain.
10. If confocal microscopy is not available, sections can also be examined using a fluorescence microscope (e.g., a Zeiss Axiophot 2 microscope equipped with FITC and TRITC filters as well as a Zeiss AxioCam digital camera). Images can be acquired as jpeg files using, for example, the AxioVision software (Zeiss).
11. If the vector carries a GFP transgene, the injection point can easily be determined by native fluorescence under a fluorescent binocular lens using FITC filters.
12. The same number of punches has to be taken from the same region for each sample. Samples are weighted to ensure a good reproducibility of sample size and the adequation between sample weight and extraction protocol.
13. Genomic DNA tends to detach from the wall of the microfuge tubes. Do not manipulate too many samples at the same time.

Keep the remaining sample turning into the tabletop centrifuge during the transfer.

14. Acidification of samples allows a more efficient release of some factors which bind to receptors (e.g., glial cell line-derived neurotrophic factor) (33). Neutralization is usually required for compatibility with subsequent assays.

Acknowledgments

O.B. was the recipient of a predoctoral fellowship from the Belgian "FRIA" (Fonds pour la Recherche dans l'Industrie et l'Agriculture and FNRS-Télévie). L.T. was the recipient of a "Crédit aux chercheurs" from the Belgian National Research Foundation. This work was also supported by grants from "Fonds National de la Recherche Scientifique Médicale," "Région Bruxelles-Capitale," and "Association Française contre les Myopathies."

The Kaspar Laboratory is funded in part from The National Institute of Health (NIH).

References

1. Ciron C, Desmaris N, Colle MA, Raoul S, Joussemet B, Verot L, et al. (2006) Gene therapy of the brain in the dog model of Hurler's syndrome. *Ann Neurol* **60**, 204–213.
2. Cachon-Gonzalez MB, Wang SZ, Lynch A, Ziegler R, Cheng SH, Cox TM. (2006) Effective gene therapy in an authentic model of Tay-Sachs-related diseases. *Proc Natl Acad Sci USA* **103**, 10373–8.
3. Dodge JC, Clarke J, Song A, Bu J, Yang W, Taksir TV, et al. (2005) Gene transfer of human acid sphingomyelinase corrects neuropathology and motor deficits in a mouse model of Niemann-Pick type A disease. *Proc Natl Acad Sci USA* **102**, 17822–7.
4. Fu H, Samulski RJ, McCown TJ, Picornell YJ, Fletcher D, Muenzer J. (2002) Neurological correction of lysosomal storage in a mucopolysaccharidosis IIIB mouse model by adeno-associated virus-mediated gene delivery. *Mol Ther* **5**, 42–49.
5. Liu G, Chen YH, He X, Martins I, Heth JA, Chiorini JA, et al. (2007) Adeno-associated virus type 5 reduces learning deficits and restores glutamate receptor subunit levels in MPS VII mice CNS. *Mol Ther* **15**, 242–7.
6. Kirik D, Rosenblad C, Bjorklund A, Mandel RJ. Long-term rAAV-mediated gene transfer of GDNF in the rat Parkinson's model: intrastriatal but not intranigral transduction promotes functional regeneration in the lesioned nigrostriatal system. *J Neurosci* 2000 Jun 15;**20**(12): 4686–4700.
7. Mandel RJ, Spratt SK, Snyder RO, Leff SE. (1997) Midbrain injection of recombinant adeno-associated virus encoding rat glial cell line-derived neurotrophic factor protects nigral neurons in a progressive 6-hydroxydopamine-induced degeneration model of Parkinson's disease in rats. *Proc Natl Acad Sci USA* **94**, 14083–8.
8. Yang X, Mertens B, Lehtonen E, Vercammen L, Bockstael O, Chtarto A, et al. (2009) Reversible neurochemical changes mediated by delayed intrastriatal glial cell line-derived neurotrophic factor gene delivery in a partial Parkinson's disease rat model. *J Gene Med* **11**, 899–912.
9. Kells AP, Henry RA, Connor B. (2008) AAV-BDNF mediated attenuation of quinolinic acid-induced neuropathology and motor function impairment. *Gene Ther* **15**, 966–977.
10. Luo J, Kaplitt MG, Fitzsimons HL, Zuzga DS, Liu Y, Oshinsky ML, et al. (2002) Subthalamic GAD gene therapy in a Parkinson's disease rat model. *Science* **298**, 425–9.
11. Haberman RP, Samulski RJ, McCown TJ. (2003) Attenuation of seizures and neuronal

death by adeno-associated virus vector galanin expression and secretion. *Nat Med* **9**, 1076–80.

12. Shen Y, Muramatsu SI, Ikeguchi K, Fujimoto KI, Fan DS, Ogawa M, et al. (2000) Triple transduction with adeno-associated virus vectors expressing tyrosine hydroxylase, aromatic-L-amino-acid decarboxylase, and GTP cyclohydrolase I for gene therapy of Parkinson's disease. *Hum Gene Ther* **11**, 1509–19.
13. Carlsson T, Winkler C, Burger C, Muzyczka N, Mandel RJ, Cenci A, et al. Reversal of dyskinesias in an animal model of Parkinson's disease by continuous L-DOPA delivery using rAAV vectors. (2005) *Brain* **128**, 559–69.
14. Xia H, Mao Q, Eliason SL, Harper SQ, Martins IH, Orr HT, et al. (2004) RNAi suppresses polyglutamine-induced neurodegeneration in a model of spinocerebellar ataxia. *Nat Med* **10**, 816–20.
15. Rodriguez-Lebron E, Denovan-Wright EM, Nash K, Lewin AS, Mandel RJ. (2005) Intrastriatal rAAV-mediated delivery of anti-huntingtin shRNAs induces partial reversal of disease progression in R6/1 Huntington's disease transgenic mice. *Mol Ther* **12**, 618–33.
16. Johnston LC, Su X, Maguire-Zeiss K, Horovitz K, Ankoudinova I, Guschin D, et al. (2008) Human interleukin-10 gene transfer is protective in a rat model of Parkinson's disease. *Mol Ther* **16**, 1392–9.
17. Yin D, Forsayeth J, Bankiewicz KS. (2009) Optimized cannula design and placement for convection-enhanced delivery in rat striatum. *J Neurosci Methods* 187, 46–51.
18. Mastakov MY, Baer K, Kotin RM, During MJ. (2002) Recombinant adeno-associated virus serotypes 2- and 5-mediated gene transfer in the mammalian brain: quantitative analysis of heparin co-infusion. *Mol Ther* **5**, 371–380.
19. Mastakov MY, Baer K, Xu R, Fitzsimons H, During MJ. (2001) Combined injection of rAAV with mannitol enhances gene expression in the rat brain. *Mol Ther* **3**, 225–232.
20. Paxinos, G. and Watson, 1997. "The rat brain in stereotaxic coordinates", 3rd compact edition, Academic Press, Orlando, FLA
21. Paxinos, G. and Franklin, K.B.J., 1997. "The mouse brain in stereotaxic coordinates" 2nd edition, Academic Press
22. Peden CS, Burger C, Muzyczka N, Mandel RJ. (2004) Circulating anti-wild-type adeno-associated virus type 2 (AAV2) antibodies inhibit recombinant AAV2 (rAAV2)-mediated, but not rAAV5-mediated, gene transfer in the brain. *J Virol* **78**, 6344–59.
23. Peden CS, Manfredsson FP, Reimsnider SK, Poirier AE, Burger C, Muzyczka N, et al. (2009) Striatal readministration of rAAV vectors reveals an immune response against AAV2 capsids that can be circumvented. *Mol Ther* **17**, 524–537.
24. Duque S, Joussemet B, Riviere C, Marais T, Dubreil L, Douar AM, et al. (2009) Intravenous administration of self-complementary AAV9 enables transgene delivery to adult motor neurons. *Mol Ther* **17**, 1187–96.
25. Foust KD, Nurre E, Montgomery CL, Hernandez A, Chan CM, Kaspar BK. (2009) Intravascular AAV9 preferentially targets neonatal neurons and adult astrocytes. *Nat Biotechnol* **27**, 59–65.
26. Saunders NR, Joakim EC, Dziegielewska KM. (2009) The neonatal blood-brain barrier is functionally effective, and immaturity does not explain differential targeting of AAV9. *Nat Biotechnol* **27**, 804–5.
27. Towne C, Schneider BL, Kieran D, Redmond DE, Jr., Aebischer P. (2010) Efficient transduction of non-human primate motor neurons after intramuscular delivery of recombinant AAV serotype 6. *Gene Ther* **17**, 141–6.
28. Kaspar BK, Llado J, Sherkat N, Rothstein JD, Gage FH. (2003) Retrograde viral delivery of IGF-1 prolongs survival in a mouse ALS model. *Science* **301**, 839–842.
29. Zheng H, Qiao C, Wang CH, Li J, Li J, Yuan Z, et al. (2010) Efficient retrograde transport of adeno-associated virus type 8 to spinal cord and dorsal root ganglion after vector delivery in muscle. *Hum Gene Ther* **21**, 87–97.
30. Hollis ER, Kadoya K, Hirsch M, Samulski RJ, Tuszynski MH. (2008) Efficient retrograde neuronal transduction utilizing self-complementary AAV1. *Mol Ther* **16**, 296–301.
31. Sterio DC. (1984) The unbiased estimation of number and sizes of arbitrary particles using the disector. *J Microsc* **134**, 127–36.
32. Hirt B. (1967) Selective extraction of polyoma DNA from infected mouse cell cultures. *J Mol Biol* **26**: 365–9.
33. Okragly AJ, Haak-Frendscho M. (1997) An acid-treatment method for the enhanced detection of GDNF in biological samples. *Exp Neurol* **145**, 592–6.

Chapter 8

Adeno-Associated Virus Mediated Gene Therapy for Retinal Degenerative Diseases

Knut Stieger, Therese Cronin, Jean Bennett, and Fabienne Rolling

Abstract

Retinal gene therapy holds great promise for the treatment of inherited and noninherited blinding diseases such as retinitis pigmentosa and age-related macular degeneration. The most widely used vectors for ocular gene delivery are based on adeno-associated virus (AAV) because it mediates long-term transgene expression in a variety of retinal cell types and elicits minimal immune responses. Inherited retinal diseases are nonlethal and have a wide level of genetic heterogeneity. Many of the genes have now been identified and their function elucidated, providing a major step towards the development of gene-based treatments. Extensive preclinical evaluation of gene transfer strategies in small and large animal models is key to the development of successful gene-based therapies for the retina. These preclinical studies have already allowed the field to reach the point where gene therapy to treat inherited blindness has been brought to clinical trial.

In this chapter, we focus on AAV-mediated specific gene therapy for inherited retinal degenerative diseases, describing the disease targets, the preclinical studies in animal models and the recent success of the LCA-RPE65 clinical trials.

Key words: Inherited retinal diseases, Retina, Gene therapy, AAV, AAV serotypes, Animal models, RPE65 clinical trial

1. Introduction

Several human clinical trials are ongoing or in preparation using recombinant Adeno-Associated Virus (rAAV), derived from a non-pathogenic virus, as a vehicle to treat or cure disease. rAAV has proven to be effective for treatments of a variety of eye disorders in preclinical studies (reviewed by refs. 1–3) partly because its ability to transduce nondividing cells has made it especially suitable for the retina. Indeed retinal tissue has distinct advantages for rAAV-mediated therapy: the tissue can be easily imaged and researchers have a contralateral eye as the ideal internal control for an in vivo

Richard O. Snyder and Philippe Moullier (eds.), *Adeno-Associated Virus: Methods and Protocols*,
Methods in Molecular Biology, vol. 807, DOI 10.1007/978-1-61779-370-7_8,

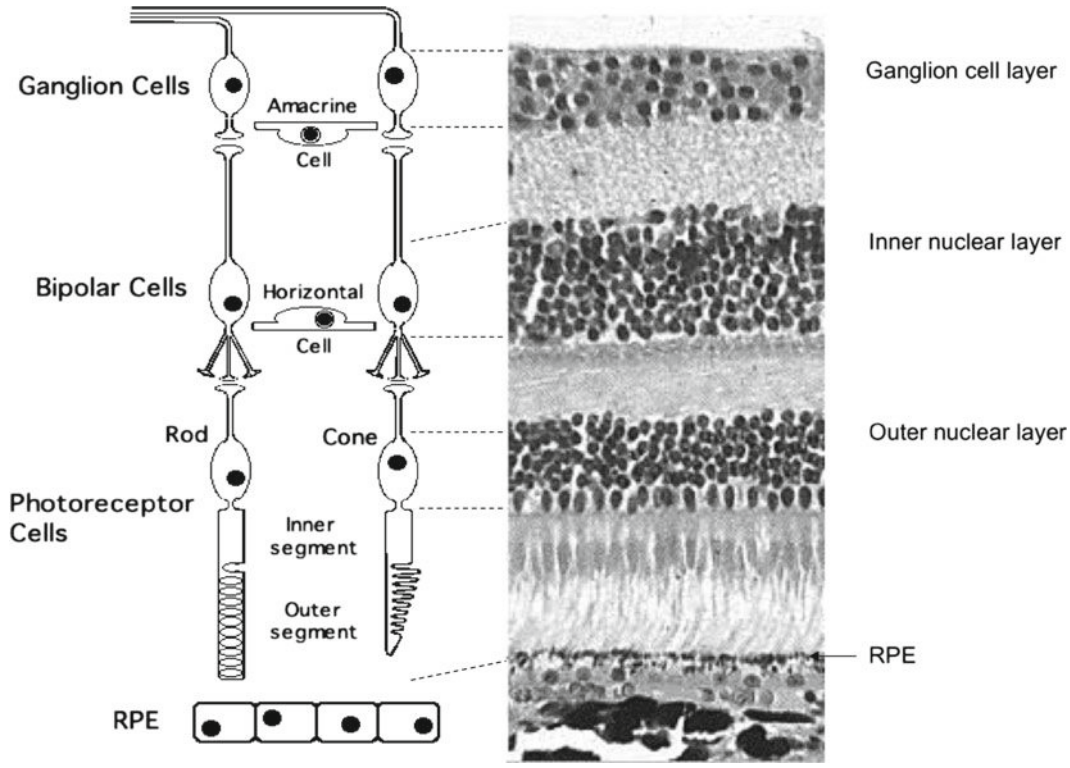

Fig. 1. Schematic and histological overview on the most prominent retinal layers. The different neuronal cell types are connected by different forms of synapses, thus allowing the converted electrical impulses from the photoreceptors to reach the axons of the ganglion cells, which will transport the information into the brain.

experiment. The diverse populations of retinal cells are arranged in discrete layers and their connections are so well mapped that investigators can determine the specific tropism of the injected virus (see Fig. 1 for retinal anatomy). Apart from these practical advantages, a less well understood but potentially critical benefit to retinal gene delivery is the relative naivety of the tissue to the innate and adaptive immune system. Corneal transplantation already takes advantage of the eye's "immune privileged" status. Re-administration studies in mice, dogs, and in nonhuman primates have verified the lack of inflammatory response after delivery and repeated delivery of AAV to the retina (4–6). Thus there are many contributing factors that have motivated investigators to make the retina an early candidate tissue for human gene therapy. Recent successes in this field have shown it to be a judicious choice. In fact AAV's promise in the retina may give renewed validity to gene therapy in general, as it has allowed lessons learned from early clinical trials to ultimately be put into practice.

Retinal diseases are non-lethal and do not in general have a significant adverse effect on fertility or reproduction within a population. This accounts for the wide level of genetic heterogeneity,

which presents the pathologies with an equally broad range of clinical guises; in brief, retinal degeneration (RD) as a disease group is a challenge to categorize. Nonetheless, this mutational complexity has attracted the attention of molecular and clinical geneticists worldwide. Oftentimes their research efforts are supported by highly motivated patient groups. In addition to tireless fund raising, these groups provide information on family genealogy, enabling projects that map linked genes and reveal the identity of many causal mutations. Emerging alongside this gene discovery effort has been the advances in transgenic animal modelling, primarily using mice, frogs and zebrafish. This has helped investigators to elucidate the molecular pathology that leads from a mutant gene to such conditions as choroideremia (7), Stargardt's disease (8), retinitis pigmentosa (9, 10) and X-linked juvenile retinoschisis (11). The molecular genetics behind these diseases will be discussed in greater depth in Subheading 2. In many cases it is the naturally occurring animal models that have been more relevant in discerning the physiopathological bases of the degeneration. While the Royal College of Surgeons (RCS) rat is the first known animal model of inherited RD, the *rd1* mouse is the best characterised, having been studied for well over 80 years (12). Screens for spontaneous mutations in zebrafish have helped in the understanding of retinal development (13) and have been used to test therapeutic agents (14). However, timing therapeutic rescue in the animal models can be complicated, with the pathology being either too severe where it arises early in development, or too mild where it arises late in the lifespan of the animal.

The move to large animal testing marked a critical turning point in the research and accelerated the pace of discovery to clinical application. This was largely due to the many differences in retinal anatomy across species and the reality that direct comparisons cannot be made between a mouse and a man. While dogs do not have the highly pigmented macular region near the center of the retina found in primates, they do have a cone-enriched portion of the area (area centralis). Because of the size, surgical approaches similar to those that would be used in a human can be used (15). Further, canine models of inherited RDs have been very informative with respect to AAV therapies. The rescue of the disease in one such model, the Briard dog, established the therapeutic window available for the successful treatment of a form of retinal degeneration, Leber's congenital amaurosis (LCA), by gene augmentation therapy (16–21). This therapeutic approach has taken advantage of the long-term stability of transgene expression mediated by AAV. Where the dog model has been important in treatment design, the nonhuman primate has been important for preclinical testing of toxicity and immune response to both AAV and the therapeutic transgene it delivers (6, 22).

Furthermore, the work in large animal models has allowed investigators to optimise technical aspects of the injection procedure, retinal function testing, and imaging used to evaluate efficacy. All this has brought the field to the point where gene therapy to treat inherited blindness has been brought to clinical trial (23–25); a point that would not yet have been reached but for the animals with naturally occurring and engineered retinal phenotypes. Although challenges lie ahead, it is only a matter of time before proof-of-concept of gene augmentation therapy for other forms of retinal degeneration brings other blinding diseases to clinical trial.

2. Disease Targets

The retinal diseases can be divided into two groups, the hereditary degenerative disorders, and the neovascular disorders. While the first group of diseases is solely due to mutations in certain genes, the second group has its origins in a more complex mix of genetic and environmental causes.

In the following chapter, the authors will present the hereditary retinal disorders, which have been targeted for gene therapy using AAV vectors (Table 1).

The hereditary degenerative disorders of the retina are primarily divided into three groups, depending on which type of photoreceptor manifests the initial insult, rods, or cones. These three groups include *rod-cone dystrophies* (Retinitis pigmentosa, RP), *cone-rod dystrophies* and *cone dystrophies* (maculopathies). In addition, the wide range of clinical symptoms in these diseases has resulted in the definition of two subgroups, in which the most severe forms of the degenerative disorders are included, LCA and early onset severe retinal dystrophy (EOSRD). However, more hereditary retinal diseases exist that have been subjected to the development of retinal gene therapy strategies. They include the stationary cone dysfunction disorder achromatopsia, retinoschisis, which is due to the separation of retinal layers and subsequent loss of retinal circuits, and albinism.

The visual symptoms in retinal degenerative disorders indicate the gradual loss of the two photoreceptor types: rods, which are present in the periphery and mediate achromatic vision under poor lightning conditions; and cones, which are concentrated in the central area (macula) and are important for color vision and fine visual acuity in daylight.

The different forms of hereditary retinal disorders will be shortly presented with prevalence, clinical symptoms and genetic situation with the aim to provide the reader with some background for the better understanding of the therapeutic applications.

Table 1
Retinal degenerative diseases that have been targeted by AAV-mediated gene therapy

Disease	Prevalence	Inheritance pattern	Target genes for gene therapy	Location of mutated gene
Rod-cone dystrophy	1:4,000	ar, ad, X	*Rho*, *PDE6ß*, ABCA4, RPE65, LRAT, RDS/Peripherin, MERTK, IMPDH1	RPE, PR
Cone-rod dystrophy	1:40,000	ar, ad, X	GUCY2D, RDS/Peripherin, AIPL1, ABCA4, RPGRIP1	RPE, PR
LCA/EOSRD	1:80,000	ar, (ad)	IMPDH1, AIPL1, GUCY2D, LRAT, MERTK, RPGRIP1, RPE65	RPE, PR
Juvenile maculopathy (M. Stargardt)	1:10,000	ar	ABCA4	PR
Stationary cone dystrophy (achromatopsia)	1:30,000	ar	GNAT2, CNGB3	PR
Juvenile retinoschisis	1:15,000–30,000	X	Rs1	PR
Ocular albinism	1:60,000	X	OA1	RPE
Oculocutaneous albinism	Not known	ar	(OCA1) tyrosinase	RPE

ar autosomal recessive, *ad* autosomal dominant, *X* X-linked, *RPE* retinal pigmented epithelium, *PR* photoreceptor, *LCA* Leber congenital amaurosis, *EOSRD* early onset severe retinal dystrophy

2.1. Retintis Pigmentosa (Rod-Cone Dystrophies)

Retintis pigmentosa (RP) has a worldwide prevalence of 1 in 4,000 people, leading to more than one million total affected individuals worldwide (26).

RP is a heterogenous disorder. The onset of the disease can vary significantly: some patients may lose vision very early in life while others remain asymptomatic until midadulthood. Patients develop difficulties with dark adaptation and night blindness in adolescence and loss of mid-peripheral visual field in early adulthood. In a more advanced stage of the disease, patients have only a very limited visual field and will eventually also lose the central vision.

Most cases of RP are monogenic, but the disease itself is very heterogenous. To date, about 200 loci have been associated with retinal dystrophies, and about 45 genes have been identified and characterized causing RP (http://www.sph.uth.tmc.edu/retnet/sum-dis.htm). Interestingly, these 45 genes collectively account for

only a little over half of all patients. The mode of inheritance can be divided into three groups, autosomal recessive (50–60%), autosomal dominant (30–40%), and X-linked (5–15%). Other forms of inheritance exist for RP such as uniparental isodisomy or non-Mendelian inheritance (mitochondrial or digenic), but these occur only very rarely. Most genes cause only a small proportion of cases, but some exceptions are known; the *RHO* gene causes about 25% of autosomal dominant RP cases, the USH2A gene causes 20% of autosomal recessive cases, and RPGR causes 70% of X-linked cases. Mutations in these three genes account for about 30% of all RP cases (26).

2.2. Cone-Rod Dystrophies

The prevalence of this type of photoreceptor degeneration is 1 in 40,000 people worldwide (27).

Because of the initial insult in cones, patients with cone-rod dystrophy rapidly lose central vision and develop abnormalities of color vision associated with a variable degree of nystagmus and photophobia. The clinical course of the disease is often more severe when compared to patients with rod-cone dystrophy, as the central visual field loss severely hampers the vision early in these patients. Over time, the loss of cones and associated rod system abnormalities will lead to impaired peripheral vision as well (28). As with the rod-cone dystrophies, inheritance pattern of autosomal recessive, autosomal dominant and X-linked have been reported. The major genes responsible for autosomal recessive cone-rod dystrophies are ABCA4 (29) (see below), which is also called Stargardt disease, the ion channel subunit CNGA3 (30) that can also be responsible for complete achromatopsia, and the ciliary transport protein RPGRIP-1 (31). The most important genes responsible for the onset of autosomal dominant cone-rod dystrophy are CRX (32) that is involved in the embryogenesis of photoreceptors, GUCY2D (33) that is involved in the Calcium homeostasis of the photoreceptors, peripherin/RDS (28) being an important structural protein in the outer segments and AIPL1 (34), which assists in the assembly of PDE in the photoreceptor membrane. Finally, mutations in the gene RPGR have been reported to be responsible in some rare cases of X-linked cone-rod dystrophy (35).

2.3. LCA–EOSRD

LCA is the most severe form of all hereditary retinal dystrophies and is responsible for congenital blindness. Its prevalence is estimated at about 1:80,000 (36). If the symptoms start in early childhood and legal blindness is diagnosed before the age of 20, the disease should be called as EOSRD (37, 38).

Clinical signs include severe impairments of visual function from birth or with onset in the first months of life (for LCA), or during the first years of life (for EOSRD). In infants, these signs include the inability to visually fix on objects, nystagmus, a diminished photomotor reflex, and the presence of the oculo-digital

Franceschetti sign. The funduscopic image of such patients is normal and the electroretinogram (ERG) nonrecordable (36).

In most cases the inheritance pattern is autosomal recessive, although some autosomal dominant mutations are known. To date, 15 genes have been identified as being involved in the onset of the disease: IMPDH1, AIPL1, CRB1, CEP290, CRX, GUCY2D, LRAT, RD3, RDH12, MERTK, RPGRIP1, TULP1, SPATA5, RPE65 and LCA5 (http://www.sph.uth.tmc.edu/retnet/sum-dis.htm) (39). Only about 50% of all cases are associated with mutations in these genes, indicating that many genes responsible for the onset remain undiscovered.

2.4. Juvenile Maculopathy/ Stargardt Disease

The most common form of juvenile maculopathy is called Stargardt disease and has a prevalence of 1 in 10,000 people in the world.

Onset of symptoms in patients with Stargardt disease starts in the second decade and will deteriorate progressively (40). Typical clinical signs are central scotoma, the bulls eye formed macula in the fundus autofluorescence image and yellow dots dispersed over the entire retina in the fundus examination (fundus flavimaculatus) (41). The gene responsible for Stargardt disease is the ABCA4 gene, the gene product of which is involved in the clearance of all trans-retinol from the photoreceptor cells. If ABCA4 function is impaired, the chromophore is accumulating in the RPE as lipofuscin and hampering the functional correlation of RPE cells and photoreceptors.

Some mutations are also associated with milder forms of the disease and later onset of symptoms, and are therefore often classified as AMD. The inheritance pattern of Stargardt disease is autosomal recessive (42).

2.5. Stationary Cone Dystrophies/ Achromatopsia

For gene therapy studies, the most relevant stationary cone dystrophy is complete achromatopsia, in which function of cones is completely lost. The prevalence of the disease is unknown but is estimated at about 1:30,000 (43).

Patients suffer from reduced visual acuity, photophobia and dayblindness. Residual ERG recordings are measurable in very few patients. Mutations in three different genes are known to cause achromatopsia, CNGB3 (cyclic nucleotide gated channel β-3), CNGA3 (cyclic nucleotide gated channel α-3) and GNAT2 (guanine nucleotide α transducin) (44–46). All three gene products are involved in the phototransduction cascade, with CNGA3 and CNGB3 being subunits of the cone-specific cGMP-gated cation channel, and GNAT2 being the subunit of the cone-specific G-protein transducin.

The inheritance pattern for all three genes is autosomal recessive.

2.6. Juvenile Retinoschisis

Juvenile retinoschisis is the leading cause of juvenile macular degeneration in males and leads to a schisis (splitting) of retinal layers (47). The prevalence is estimated to be between 1:15,000 and 1:30,000.

Clinical symptoms differ greatly among patients and no correlation with underlying mutations has been made. Visual acuity varies between 20/20 and 20/600. The cartwheel like structure of folds radiating out from the fovea is the characteristic sign of juvenile retinoschisis (47). This phenomenon can become less distinct with age. Generally, large bullous lesions that can be observed by OCT imaging in infancy disappear and become invisible in older patients. Visual function can remain stable until midadulthood but can also deteriorate rapidly when complications such as hemorrhage or retinal detachments occur. Affected individuals have a relatively normal a-wave in the ERG, while the b-wave is completely abolished (negative ERG), indicating deficient responses from the inner retina (48). Female carriers of the mutation remain normally asymptomatic.

The underlying cause of the disease is a mutation in the retinoschisis gene RS1, which encodes the retinoshisin gene (49). The inheritance pattern is X-linked.

2.7. Albinism

The onset of albinism with ocular involvement has to be divided into two groups, (1) the pure ocular albinism (OA) and (2) the oculo-cutaneous albinism (OCA). All forms share the typical lack of abnormal production of the pigment melanin, which causes an increased light sensibility in organs that are exposed to light, such as the skin and the eye. There are at least ten forms of OA and four forms of OCA known due to different genes that can be mutated. Patients with OA develop pathologies primarily in the eye, while patients with OCA have also skin and hair abnormalities to a varying degree.

X-linked ocular albinism type 1 (OA1) is the most common form of ocular albinism and is caused by mutations in the *oa1* gene. The prevalence of this disease is reported to be 1 in 60,000 (50). Patients have reduced and abnormal ERG recordings, severely reduced visual acuity and photophobia. The iris is in part translucent, the ocular fundus is hypopigmented and the macula shows foveal hypoplasia. The crossing of optic nerve fibers in the optic chiasm is reduced, which leads to the typical results of ipsilateral visually evoked potentials after unilateral light stimuli in these patients (albino-VEP). The protein encoded by OA1 is responsible for the correct organization of RPE melanosoms, and mutations lead to the occurrence of large pigment granules, the macromelanosoms. Rare forms of ocular albinism that are not X-linked have been reported.

OCA can be caused by mutations in different genes, the most severe form is OCA1 due to mutations in the tyrosinase gene (51).

The protein tyrosinase is involved in early steps of the generation of melanin granula in epithelial cells such as the RPE in the eye. The clinical symptoms are similar to OA1 but the inheritance pattern of the disease is autosomal recessive (52). Clinically, the disease can be divided into OCA1-A with absence of any tyrosinase activity and OCA1-B with reduced tyrosinase activity.

3. Delivery Methods

3.1. Injection Method

Because of the blood/retina barrier, it is not possible to inject AAV intravenously and then obtain transduction of the retina. Instead, the rAAV must be delivered to an area in contact with the target cells (the intravitreal space or the subretinal space) so that those cells can be transduced (see Fig. 2). The serotypes of AAV most widely evaluated do not diffuse across the layers of the retina.

3.1.1. Intravitreal

Intravitreal injection exposes cells lining both the inner surface of the retina and the anterior segment. Thus, depending on the rAAV capsid serotype and the presence of appropriate receptors (see below), retinal ganglion cells and Muller cells can be transduced and in the anterior segment, trabecular meshwork, Schlemm's canal, corneal endothelial cells, lens, iris and ciliary body epithelial cells can be transduced (53–55). Although transduction of anterior segment structures is not desirable in retinal gene augmentation or gene knockdown strategies, it may be useful in the future for delivery

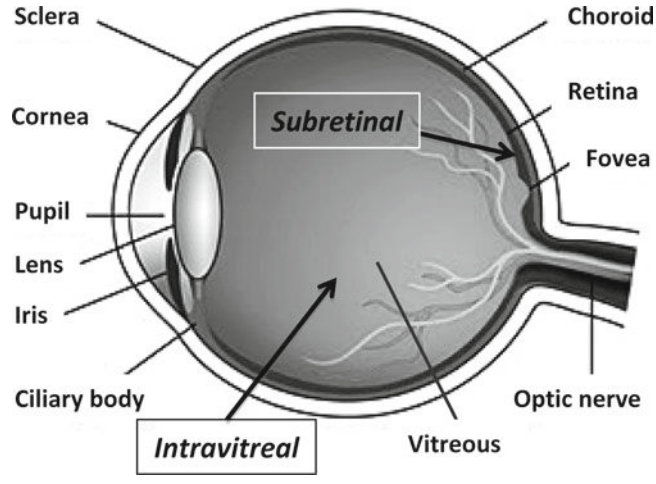

Fig. 2. Anatomical features of the eye and the positions, where intravitreal and subretinal deliveries are performed. For intravitreal injection, the needle is introduced into the vitreous. For subretinal injection, the needle is advanced through the vitreous and positioned in the retina between the photoreceptors and the RPE.

of neurotrophic factors (not discussed further in this review). Retinal ganglion cell transduction, which can be achieved through intravitreal delivery can deliver transgene product to those areas of the brain where ganglion cells synapse (lateral geniculate nucleus, superior colliculus, etc.) (54–56).

3.1.2. Subretinal

Subretinal injection exposes cells lining both the outer surface of the retina and the retinal pigment epithelium (RPE). Thus, retinal photoreceptors, Muller cells and RPE cells can be transduced after subretinal injection (53, 57–59). Because of the different anatomical features of the mouse eye versus the large animal eye, different subretinal injection techniques must be used in the different species. The lens of the mouse eye occupies nearly the entire vitreous cavity. Thus it is difficult to deliver the AAV from an anterior approach in mice due to risk of damage to the lens with a resultant cataract. In contrast, subretinal injections in dogs, monkeys, and men can be carried out under direct visualization through an operating microscope (6, 15, 19, 22–25).

3.2. Tropism of rAAV Vectors

Different AAV serotypes display tissue preference and specific cellular tropism in a variety of organs. The retina contains within its layers many different cell types, some of them unique to the eye. Therefore, cellular tropism of each serotype needs to be tested in the retina of every animal model before starting any gene therapy protocol (Table 2). Over the last decade, serotypes AAV2/1, 2/2, 2/3, 2/4, 2/5, 2/6, 2/8, and 2/9 and 2/rhu10 have been tested for cellular tropism and long-term expression in the retina of rodents, dogs and nonhuman primates. In addition, AAV serotypes isolated from porcine tissue as well as newly engineered AAV capsid variants have been tested for optimized cellular transduction efficacy.

3.2.1. Cellular Tropism Following Intravitreal Injection

Generally, the transduction efficiency of AAV vectors of any serotype following intravitreal delivery is much lower when compared to subretinal injections. However, the best studied AAV serotype, serotype 2, transduces retinal cells after intravitreal injection, mainly retinal Ganglion cells. Efficacy of transduction and level of transgene expression remain low in all species (54, 56, 60–62). Nonetheless, clinical trials based on the intravitreal injection of AAV2 vectors to express anti-VEGF molecules are currently in progress (63, 64). The intravitreal injection of AAV2/2 vectors expressing the transgene under GFAP promoter resulted in detectable transgene expression in Muller cells (60). Due to minor capsid changes, the AAV variant SSH10, closely related to AAV serotype 6, is capable of transducing Muller cells in the retina following intravitreal injection in mice (65).

One of the reasons for the limited capacity of AAV vectors to transduce retinal cells after intravitreal injection is the presence of

Table 2
Cellular tropism of rAAV serotypes following subretinal injection

rAAV serotype	Mouse	Rat	Dog	Primate
rAAV2/1	RPE	–	–	–
rAAV2/2	RPE, PR	RPE, PR	RPE, PR	RPE, PR
rAAV2/3	–	–	n.d.	n.d.
rAAV2/4	–	RPE	RPE	RPE
rAAV2/5	RPE, PR	RPE, PR	RPE, PR	RPE, PR
rAAV5/5	RPE, PR	n.d.	n.d.	RPE, PR
rAAV2/6	RPE	n.d.	n.d.	n.d.
rAAV2/7	RPE, PR	n.d.	n.d.	n.d.
rAAV2/8	RPE, PR	RPE, PR, INL, GC	RPE, PR, INL, GC	n.d.
rAAV2/9	RPE, PR, MC, INL	n.d.	n.d.	n.d.
rAAV2/po1	PR, RPE	n.d.	n.d.	n.d.
rAAV2/SSH13	MC	n.d.	n.d.	n.d.

RPE retinal pigmented epithelium, *PR* photoreceptors, *MC* Muller cells, *INL* inner nuclear layer, *GC* ganglion cells, *n.d.* not determined

the inner limiting membrane (ILM) at the junction of neuroretina and vitreous. Following the digestion of the ILM using a nonspecific protease, AAV serotypes 2/1, 2/2, 2/5, 2/8, and 2/9 transduced retinal cells to a variable degree, with the AAV5 serotype being the most efficient (66).

Interestingly, even though it has been shown several times that the AAV8 serotype is not able to efficiently transduce retinal cells following intravitreal injection, one study by Park and colleagues reported on the successful expression of the retinoschisin (rs1) gene in photoreceptor and other retinal cells of rs1 knockout mice after intravitreal delivery of the vector (67). However, one potential explanation for this discrepancy would be the altered retinal morphology in $rs1^{-/-}$ mice, in which the normal cellular junctions and barriers of the ILM may be less restrictive to the viral passage into the neuroretina.

3.2.2. Cellular Tropism Following Subretinal Injection

Following subretinal injection in the mouse retina, AAV2/2 vector transduces RPE and photoreceptors (53, 57, 68). Similar cellular specificity but more efficient transduction is obtained using the AAV2/5 serotype (69). AAV2/1 serotype transduces only the RPE in the mouse, with rapid onset of transgene expression (3–4 days) (53). AAV2/3 serotype does not transduce retinal cells; rAAV2/6 seems to weakly transduce RPE cells (70). The more recently

developed AAV serotypes AAV7, 8, and 9 were all shown to very efficiently transduce photoreceptors and RPE in mice (55, 58, 71). In addition, AAV serotype 9 also transduces Mueller cells (58) and cells that have synaptic connections in the outer plexiform layer (72). The AAV variant SSH13, developed through minor capsid changes from AAV serotype 6, transduces Mueller cells in the retina following subretinal injection (73). The porcine AAV serotype AAV2/po1 was as efficient in transducing mouse photoreceptors and RPE cells as AAV2/5 following subretinal injection (74).

Subretinal injection of serotypes AAV2/1, 2/2, 2/3, 2/4, and 2/5 in rats resulted in a hierarchy in the level of transgene expression, with AAV2/4 and AAV2/5 being the most efficient (75). The more recently utilized serotype AAV8 transduces very efficiently cells in all retinal layers, including RPE, photoreceptors, cells of the inner nuclear layer (INL) and ganglion cells (76). Interestingly, this serotype transduces cells that are located inside and outside of the injected area, a characteristic that is unique to AAV8, as it has not yet been reported for other serotypes (76). A way to enhance RPE transduction with AAV serotype 2 after subretinal injection is the co-delivery of ultrasound targeted microbubbles, which would temporarily destroy small areas of the cellular membrane to increase the uptake of the vector (77).

Brainbridge and colleagues observed transgene expression in RPE and photoreceptor cells following subretinal injection of AAV2/2 vector in dogs (78). Comparative studies using AAV2/2 and AAV2/5 serotypes showed that transduction efficacy of photoreceptors by AAV2/5 was superior to that of AAV2/2 in rats, dogs and nonhuman primates (59). The same study showed, that AAV2/4 serotype allowed exclusive and stable transduction of RPE cells in all three animal models tested. Subretinal injection of a complete AAV5/5 showed higher transduction efficacy than AAV2/2 in RPE and photoreceptors of mice and nonhuman primates (79). An interesting observation was that self complementary (sc)AAV vectors of the serotype 5 were capable of transducing RPE and photoreceptor cells at a faster rate with higher level of transgene expression when compared to single-stranded (ss)AAV vectors (55, 80).

Similar to the results in rats following subretinal injection, the serotype AAV8 transduces all cells of the retina inside and outside of the injected area in dogs (76). This finding may have important consequences for gene therapy trials, where widespread expression of the transgene in the retina is the objective.

3.3. Specific Versus Nonspecific Promoter

Combining a cell-type specific promoter and a cell-type specific vector would ensure the most specific and efficient transgene regulation in one cell type and at the same time limit widespread distribution of vector and/or transgene products within the host organism.

In vivo gene transfer studies used mostly strong and ubiquitous viral promoters for driving reporter or therapeutic transgene expression, such as the immediate early cytomegalovirus (CMV) promoter (20, 53, 57) or a chimeric chicken beta-actin (CBA)/CMV enhancer promoter (16). Gene regulation studies revealed a number of ocular specific promoters capable of driving transgene expression in one cell type: the human RPE65 specific promoter (81) and the VMD2 specific promoter (82) in the RPE, the mouse GFAP specific promoter in Muller cells (83), the human rhodopsin kinase specific promoter in both types of photoreceptors, rods and cones (84), and different opsin promoters specific for rod or cone photoreceptor subtypes: mouse (85), bovine (86) and human rod opsin specific promoter (87), human blue opsin specific promoter (88) and the human red and green opsin specific promoter (89–91)

3.4. Safety and Biodistribution in the Retina

Evaluation of safety of gene transfer in the eye of large animal models is highly relevant for the development of clinical trials. As direct visualization of GFP expression in the retina can easily be carried out by fluorescence fundus photography, vectors encoding this reporter gene have been used to study the capacity of AAV for long term expression in the retina of rodents and large animal models such as dogs and primates. Subretinal injection of AAV2/2.CMV.gfp in dogs resulted in efficient and stable transgene expression for at least 18 months (78). Using the same vector in the primate retina led to efficient transduction of RPE cells and rod photoreceptors for more than 12 months (6). Another study, using the complete AAV5/5 vector, showed similar cellular tropism in the primate retina and persistent transgene expression for 10 months, the duration of the study (79).

To evaluate the short-term morbidity of subretinal injections and the safety of long-term rAAV-mediated transgene expression, Le Meur and colleagues injected the clinically interesting serotypes AAV2/2, AAV2/4 and AAV2/5 unilaterally in 14 beagle dogs and 9 nonhuman primates. They found that subretinal injection of rAAV vectors in dogs and primates is a safe procedure with no perioperative complications and a high rate of successful retinal gene transfer (95%). As assessed by angiography and electroretinography, retinal anatomy and function remained unchanged, with persistent transgene expression up to now 6 years (92) (Rolling, unpublished data).

A primary requirement for safe and successful ocular gene therapy using rAAV is an accurate evaluation of vector distribution after subretinal or intravitreal delivery. Not only are multiple cell types in the retina exposed to the vector, and some scattering of virus to the systemic circulation is possible, but also the eye is closely connected to the brain via the optic nerve and the presence of vector DNA in the brain needs to be examined. Weber and

colleagues documented vector shedding after subretinal delivery of rAAVs in dogs and nonhuman primates (59). Vector DNA could be detected in the serum of injected animals as early as 15 min after AAV administration and for up to 25 days in some individuals. Viral genome was detected in nasal and lacrimal fluid after 15 min and for up to 4 days. The extent of vector shedding is likely affected by the dose delivered.

Regarding the distribution of vector DNA in the optic nerve and brain, investigators have to distinguish between the presence of transgene product and the actual expression of the transgene in the brain. Early studies showed that after intravitreal injection of AAV2/2.CMV.gfp in mice and dogs, levels of GFP protein persists for 6 months in the brain and optic nerve. However, no vector DNA could be detected outside of the retina (54). Other studies showed the presence of lacZ and GUSB as transgene products in the optic nerve or the brain of mice and guinea pigs, respectively (56, 93). Again, vector DNA could not be detected in the optic nerve or brain in both studies. Griffey and colleagues showed improved enzyme activity along the visual pathway in the brain after intravitreal delivery of an AAV2/2 vector encoding for the missing enzyme in a mouse model of infantile neuronal ceroid lipofuscinosis (94). These data suggest that AAV2/2 mediated intravitreal gene transfer results in the transduction of retinal ganglion cells and transgene products are anterogradely transported along the visual pathway into the brain. However, these data do not show any anterograde transport of vector DNA into the brain via the optic nerve.

In contrast, Provost and colleagues studied the vector DNA distribution in rats, dogs and nonhuman primates after subretinal or intravitreal injection of AAV2/2, 2/4 and 2/5 vectors (95). They detected vector DNA occasionally in peripheral blood mononuclear cells at early time points after injection in all animals. Specifically, vector DNA sequences were present in the optic nerve of dogs and primates that received subretinal injections of AAV2/4 or AAV2/5; intravitreal injection of rAAV2/2 in dogs resulted in the detection of vector DNA along the visual pathway in the brain – the optic nerve, optic chiasm, optic tract, lateral geniculate nucleus and visual cortex. These results suggested for the first time the anterograde transport of rAAV2/2 from the retina to central visual structures.

Jacobson and colleagues studied vector DNA distribution in dogs and primates after subretinal or intravitreal injection of AAV2/2 vector at different time points post injection (22, 96). Vector DNA could not be detected in a dose escalation study of subretinally injected AAV2/2 in dogs (96). In contrast, vector DNA could be temporarily detected in the optic nerve and brain of primates injected subretinally with the AAV2/2 vector at 1 week post injection (22). At 3 months post injection, only one primate had a detectable number of copies in the left geniculate nucleus.

In all cases, even though vector DNA was detected in the brain, no transgene expression was observed in brain structures after subretinal injection. This observation may be due to spreading of nonfunctional vector that does not allow transgene expression, or lack of expression due to particular issues related to the transgene cassette, or because transgene expression was below the detection level. However, a recent study by Stieger et al. reported the presence of vector DNA, GFP mRNA and GFP protein in neurons in the left lateral geniculate nucleus (contralateral to the injected eye) after subretinal delivery in dogs (76). In addition, vector DNA was found in many parts of the brain, but chiefly on the contralateral side. These results demonstrated for the first time that subretinal injection of AAV2/8 vector leads to gene transfer into distal parts of the brain. Because axons of the retinal ganglion cells project to the contralateral geniculate nucleus, the data also suggest transsynaptic transport as the mode of delivery to these neurons; however, due to limitations in the experimental design, this could not be proved.

An unexpected observation was made by the group of Rolling and colleagues when they studied the ultrastructure of the retina in dogs and primates several years after subretinal injections of AAV vectors. They observed persisting particles of the AAV serotypes 2, 4, and 5 in the outer plexiform layer (OPL) and in other retinal layers of dogs and primates up to 6 years following successful gene transfer into the retina (97). This observation opens the concept of in vivo intracellular clearance of vector particles as a potentially critical factor for the design of gene therapy clinical trials, especially in terms of immunological safety.

3.5. Preclinical Studies for Inherited Degenerative Diseases

This chapter focuses on specific gene therapy, which includes gene addition or gene silencing to treat autosomal recessive and autosomal dominant inherited degenerative diseases, respectively (Table 3). Nonspecific gene therapy strategy, which involves expression of neurotrophic factors to promote cell survival in retinal degenerations is not discussed.

3.5.1. Treatment of Autosomal Recessive Diseases

The strategy to treat autosomal recessive diseases, in which the mutated gene product is not existent or does not cause toxic effects, is to provide the cell with a correct allele of the mutated gene by gene addition technology. As it has been mentioned above, choice of vector and promoter for the expression cassette will depend on the targeted cell that is in most of the cases either the RPE or the photoreceptors. Therefore, a general differentiation of the gene therapy approaches has been established into those targeting diseases originating in the RPE and those targeting diseases originating in photoreceptors.

In general, it turned out that diseases originating in the RPE seem to be more amenable to gene therapy treatment than diseases

Table 3
Preclinical studies in animal models of retinal degeneration

Gene therapy		Targeted gene	Animal model	Human disease	References
Gene addition	Targeting RPE	RPE65	RPE65 $^{-/-}$ mouse, RPE65$^{-/-}$ Briard dog	LCA/EOSRD	(16–21, 104–107)
		LRAT	LRAT$^{-/-}$ mouse	LCA/EOSRD	(109)
		Oa 1	Oa1$^{-/-}$ mouse	Ocular albinism	(111)
		OCA 1	OCA mouse	Oculocutaneous albinism	(112)
		Mertk	RCS rat	LCA/EOSRD	(113)
	Targeting PR	PDE6ß	rd1 mouse, rd10 mouse	arRP	(114, 116)
		GNAT2	GNAT2^{cpfl3} mouse	Achromatopsia	(89)
		CNGB3	CNGB3 dog	Achromatopsia	(119)
		GUCY2D	RetGC1$^{-/-}$ mouse	LCA/EOSRD	(120)
		AIPL1	Aipl1$^{-/-}$ mouse, Aipl1$^{h/h}$ mouse	LCA/EOSRD	(121, 122)
		ABCA4	abca4$^{-/-}$ mouse	Morbus Stargardt	(125)
		RPGRIP1	RPGRIP-KO mouse	LCA/EOSRD	(126)
		Peripherin 2	Prph2 $^{rd2/rd2}$ mouse	arRP	(127–130)
		Rs1h	RS1h$^{-/Y}$ mouse	Juvenile retinoschisis	(67, 132–136)
Gene silencing	Ribozyme	*Rho*	*RHO*$^{+/-}$ mouse, P23H rat	adRP	(140–143)
	siRNA	*Rho*	*RHO*$^{+/-}$ mouse, *RHO*-M mouse, *RHO*347$^{-/-}$*Rho*$^{-/-}$mouse, P23H rat	adRP	(144–147, 149, 150)
		IMPDH1	AAVmut IMPDH1 mouse	adRP	(151)

RPE retinal pigmented epithelium, *PR* photoreceptor, *LCA* Leber congenital amaurosis, *EOSRD* early onset severe retinal dystrophy, *adRP* autosomal dominant retinitis pigmentosa, *arRP* autosomal recessive retinitis pigmentosa

from the second group. This is in part due to the single layer characteristic of the RPE, which can be more efficiently targeted by AAV vectors. Another reason is the impact of corrected and functional RPE cells on the adjacent photoreceptors, because up to 40 of these specialized and very sensitive neurons depend on nutritional as well as metabolic support from one RPE cell. On the other hand, diseases originating in the photoreceptor cells often result in rapid induction of apoptosis limiting the extent of therapeutic intervention. The complex expression pattern of some of the genes in photoreceptors (i.e. RPGR, RPGRIP) and the involvement in complex enzymatic cascades (i.e. phototransduction cascade) is likely to require further technologic improvements, such as the ability to confer physiologic transgene expression and the production of cell specific isoforms.

Concerning the RPE cell layer, gene augmentation protocols targeting five different genes have been reported: the all-trans retinylester isomerohydrolase RPE65, the lecithin retinal acyltransferase (*LRAT*), the mer tyrosine kinase (*Mertk*) and the genes *OA1* and tyrosinase (*Tyr*). While the last two genes are involved in the onset of albinism, mutations in *LRAT*, *MERTK* and *RPE65* cause LCA or EOSRD.

Two of the genes targeted in photoreceptors are involved in the visual cycle, the LCA genes *RPE65* and the *LRAT*.

The *RPE65* gene encodes for an RPE specific 65-kDa protein that has been identified as the isomerohydrolase in the visual cycles, which restores the rhodopsin ligand 11-cis retinal (98, 99). Mutations in this gene are responsible for about 6% of LCA cases. In addition to a genetically engineered *rep65* knockout mouse model (100), two naturally occurring models of LCA caused by mutations in *rpe65* exist: the homozygous Swedish Briard dog (101, 102) and the *rd12* mouse (103). Similar to humans, these animals do not develop sufficient amounts of the photopigment rhodopsin, they have poor vision and diminished light and dark adapted ERG responses. Especially the Briard dog model represents a valuable model for the development of a gene replacement therapy for RPE65 deficient patients, as the phenotype of the retinal degeneration is very similar to the one in humans. In these animals, a 4-bp deletion leads to a premature stop codon and the absence of functional protein in the retina (101, 102).

In mice, Lai and colleagues reported successful restoration of vision in *rpe65* knockout animals following rAAV2/2 vector administration that carried the mouse *rpe65* gene under the control of the CMV promoter (104). Pang and colleagues reported the successful restoration of vision in *rd12* mice using a rAAV2/5 vector carrying the human *RPE65* gene driven by the CBA promoter (105). To verify functional vision in these animals, the morris water maze test was modified to test rod function under dim light, and indeed, treated animals behaved like wildtype mice, while untreated

control mice failed this test. Dejneka et al. showed that delivery of human *RPE65* through rAAV2/1 resulted in rescue in adult *rpe65* knockout mice (106). The authors of the last mentioned study showed in addition that in utero administration of rAAV2/1 vector carrying the human *RPE65* gene driven by a CMV promoter could restore visual function in the KO mouse (106). However, there are limitations to this approach that make in utero gene therapy in humans rather unlikely.

In dogs, two groups demonstrated that a single subretinal injection of a rAAV2/2 vector carrying the canine *rpe65* gene under the control of a strong CBA promoter was sufficient to restore visual function in affected dogs, as assessed by ERG, immunochemistry and behavioral testing (16, 20). In an attempt to improve the expression cassette and the vector, the first group injected several different constructs using AAV2/1, 2/2 or 2/5 capsids, the non-specific CBA promoter or the tissue-specific RPE65 promoter to drive either the canine or the human *rpe65* gene and reported long-term restoration of visual function for up to 3 years (17). Finally, improvements to the promoter were done in order to increase specificity of the method (18). The second group studied the long-term outcome of their AAV2/2.CMV.c*rpe65* injected animals and reported a gradual loss of visual function as measured by ERG responses over 3 years, the reason for which is not clear (107). In addition, Le Meur and colleagues have demonstrated the capacity of a rAAV2/4 vector carrying the human *rpe65* gene under control of the human RPE65 promoter to restore vision in the Briard dog model (19). As mentioned above, rAAV2/4 vectors transduce exclusively the RPE and therefore, the use of this serotype increases the specificity and safety of the therapy. In addition, the tissue-specific RPE65 promoter also increases specificity by allowing transgene expression only in RPE cells. In two safety studies on AAV2/2 mediated retinal gene transfer, Jacobson and colleagues and Bennicelli and colleagues reported preclinical safety data on a total of 21 *rpe65*$^{-/-}$dogs and 17 normal nonhuman primates subretinally injected with a rAAV2/2 vector carrying the human *rpe65* gene driven by the CMV/β-actin hybrid promoter (18, 22, 96).

LRAT is an enzyme located in the RPE, which converts all-*trans*-retinol into all-*trans*-retinyl ester, a key step in the restoration of 11-cis retinal during the retinoid cycle. In *lrat*$^{-/-}$ mice, no 11-cis retinal is produced and visual function is severely impaired at 2 months of age, as measured by scotopic and photopic ERG (108). Subretinal injection of a rAAV2/1 vector carrying the mouse *lrat* gene under the control of the human VMD2 promoter restored ERG waves to 50% of wildtype mice (109). Interestingly, oral administration of 9-cis-retinyl succinate and 9-cis-retinyl acetate, which bypass the LRAT function in the retinoid cycle, similarly restored ERG responses to 50% of wildtype mice (109).

Two genes targeted in the RPE are involved in melanin synthesis and mutations in these genes are responsible for OA1 or OCA1.

A mouse model of ocular albinism type 1 has been generated, which mimics the human phenotype (110). Subretinal injection of a rAAV2/1 vector carrying the murine *oa1* gene driven by a CMV promoter in 8 months old mice resulted in an increased number and normal density of melanosomes in the RPE (111). More importantly, ERG recordings in dark adapted *oa1*$^{-/-}$ mice were improved, regardless of the age at which the mice were treated (1 or 8 month of age).

A spontaneous null mouse of OCA1 (Tyr c-2j) that has several retinal function anomalies due to photoreceptor loss beginning at 7 month of age was used to study the effect of AAV-mediated gene therapy in this disease (112). An AAV2/1 vector driving the human tyrosinase gene under the control of the CMV promoter was injected subretinally into 1-month old mice. Animals had detectable levels of melanin at 2 months post injection, indicating that the pathway for the production of the pigment is functional. Similarly, electrophysiological examination revealed increased light sensitivity and improved photoreceptor function.

In the RCS rat, phagocytosis of photoreceptor outer segments by RPE cells is impaired due to a mutation in the receptor tyrosine kinase gene, mertk. This leads to the accumulation of outer segment debris in the subretinal space and subsequently to progressive loss of photoreceptors by apoptosis. Subretinal injection of rAAV2/2 vector carrying the mouse mertk gene driven by either a strong CMV promoter or the cell-specific RPE65 promoter led to prolonged photoreceptor survival for as long as 9 weeks compared to untreated control eyes (113).

Concerning photoreceptor cells, nine different genes have been targeted by AAV-mediated gene therapy, encoding the phosphodiesterase 6 beta subunit (*PDE6B*), alpha transducin subunit (GNAT2), the cyclic nucleotide gated channel subunit beta (CNGB3), the retinal guanylate cyclase 1 (RetGC1, GUCY2D), the aryl hydrocarbon receptor-interacting protein like 1 (AIPL1), the ATP binding cassette transporter (ABCA4), the Retinitis pigmentosa GTPase regulator interacting protein 1 (RPGRIP1), peripherin and retinoschisin (Rsh1).

The *rd1* mouse contains a mutation in the ß subunit of the phosphodiesterase (*pde6b*) gene, which results in a rapid onset of photoreceptor degeneration. At postnatal day 21, only one row of photoreceptors remains in the retina. This mouse model was the first to be used in a gene replacement protocol using AAV vectors. In 1997, Jomary and colleagues injected intravitreally a rAAV vector containing the *PDE6*β gene under the control of a truncated opsin promoter into 8 days old mice (114). At 21 days, treated eyes showed increased numbers of photoreceptor rows

when compared to noninjected control eyes. Unfortunately, functional recovery was not evaluated in vivo, but only in vitro. Treated retinas showed a twofold increase in sensitivity to light. This study provided for the first time evidence that AAV-mediated gene augmentation therapy may rescue photoreceptors morphologically and functionally.

A second mouse (rd10) strain that has a mutation in exon 13 of the *pde6b* gene shows a slightly less rapid degeneration. Loss of photoreceptors starts at 2 weeks of age and highest rates of apoptosis are observed at 5 weeks (115). Subretinal injection of an AAV2/5 vector carrying the mouse *pde6b* gene under the control of the ubiquitous CBA into 2-week-old mice resulted in prolonged survival of photoreceptors until p35 (3 weeks post injection) and substantial scotopic ERG recordings (116). However, long-term examination was not reported.

Gnat2^{cpfl3} homozygous mice have a mutation in the murine *gnat2* gene homolog *cpfl3* (cone photoreceptor function loss 3), and exhibit cone dysfunctioning and progressive loss of cone α-transducin immunolabeling (117). This mouse model of achromatopsia was recently used to study an AAV-mediated gene therapy protocol targeting cones (89). Subretinal injection of a rAAV2/5 vector containing the murine *gnat2* gene under the control of a red/green opsin promoter in 3–4 weeks old *gnat2*^{cpfl3} mice resulted in rescue of cone function and visual acuity for at least 5 months.

Achromatopsia has been associated in dogs with a substitution in exon 6 (D262N) of the CNGB3 gene in German shorthaired pointer dogs and with a nonsense mutation in Alaskan malamute dogs (118). In both canine models of achromatopsia, cone response was abolished at the age of 8 weeks. Affected dogs were injected unilaterally into the subretinal space with an AAV5 vector containing the canine CNGB3 gene under the control of four different promoters (PRO.5, 3LCR-PRO.5, PR2.1, and the human cone arrestin promoter). Four weeks after treatment, successful restoration of cone function was achieved in ten dogs with either CNGB3 null or missense mutation. The best outcome was observed when animals were treated at a young age. While positive results were seen with all four promoters, the most robust restoration of cone function was obtained with the PR2.1 promoter. Two dogs treated with AAV5.PR2.1.CNGB3 were monitored for over 14 months and no deterioration of the rescue effect was observed (91, 119).

In *retgc1* knockout mice, the light-driven translocation of cone arrestin is compromized, which leads to loss of function and photoreceptor cell death within the first 6 month of life. Subretinal injection of a rAAV2/5 vector containing the *retgc1* gene driven by either the cell specific mouse opsin promoter or the strong CBA promoter lead to restoration of light-driven translocation of cone arrestin, but not rescue of function of cones as assessed by ERG (120). Failure to restore function of cones was potentially due to toxic side effects caused by *retgc1* overexpression in these cells.

The AIPL1 is involved in the biosynthesis and correct localisation of PDE in photoreceptors and mutations in this gene lead to the rapid onset of LCA (34). Three different mouse models with four different rates of photoreceptor degeneration have been used to study the effect of gene therapy: the Aipl1$^{-/-}$ knockout mouse with a very rapid loss of photoreceptors (all gone by 3 weeks of age); the hypomorphic Aipl1$^{h/h}$ mouse under low levels of illumination showing a slow degeneration (degeneration starts at 12 weeks and half of all photoreceptors are gone by 6 months of age) and the same hypomorphic Aipl1$^{h/h}$ mouse under increased light condition showing an accelerated retinal degeneration by two- to threefold when compared to the low illuminance condition (121). Finally, a crossbred mouse line called Aipl1hypo that was produced by mating the Aipl1$^{-/-}$ and AIpl1$^{h/h}$ mice and has a slightly faster onset of disease as the original Aipl$^{h/h}$ mouse under low lightning conditions (122). Subretinal injection of an AAV2/2 vector carrying the murine Aipl1 transgene under the control of the CMV promoter was sufficient to preserve morphology and function in the Aipl1$^{h/h}$ mouse under low lightning conditions, and a similarly constructed AAV2/8 vector was even capable to preserve morphology and function in the light accelerated Aipl1$^{h/h}$ mouse and in the Aipl1$^{-/-}$ knockout mouse (121). In a related approach, AAV2/5 and AAV2/8 vectors driving the human Aipl1 gene under the control of the rhodopsin kinase (Rk) promoter were injected subretinally into the Aipl1hpo mouse model at 5 months of age and photoreceptors were still detectable after 23 months (122). In addition, the AAV2/8 vector was also able to preserve morphology and function in the Aipl1$^{-/-}$ when injected at p9 to p13 (122).

An ABCA4$^{-/-}$ knockout mouse model based on pigmented (123) or albino (124) mice, which resembles the phenotype of Stargardt disease has been used for the study of AAV-mediated gene therapy. Subretinal injection of an AAV2/5 vector driving the ABCA4 gene under the control of the CMV promoter into this mouse model resulted in properly localized ABCA4 protein in the photoreceptor layer, normal RPE cell appearance and decreased RPE thickness (125). Functionally, the recovery time from light desensitization was significantly improved.

Retinitis pigmentosa GTPase regulator (RPGR) is a protein connected to the photoreceptor cilium by RPGR interacting protein 1 (RPGRIP1). If RPGRIP1 is nonfunctional due to mutation in its encoding gene, RPGR is delocalized, causing deregulation of protein trafficking across the connecting cilium and subsequently photoreceptor loss. In RPGRIP-1 knockout mice, the degeneration of photoreceptors and subsequently all retinal layers is rapid (126). The subretinal injection of a rAAV2/2 vector containing the *rpgrip1* gene driven by a mouse opsin promoter resulted in the transient morphological and functional protection of photoreceptors as assessed by histology and ERG (126).

Prph$^{Rd2/Rd2}$ mice, formerly known as *rds* (retinal degeneration slow) mice carry a homozygous null mutation in the *Prph2* gene, encoding the structural protein peripherin2, which is essential for outer-segment formation. Due to the failure to develop photoreceptor discs and outer segments, photoreceptor cells undergo progressive apoptosis. ERGs are diminished early after birth and decline to undetectable levels within 2 month. Gene replacement has been tested using an AAV2/2 vector carrying the wildtype *Prph2* gene under the control of a rhodopsin promoter. Subretinal injection of this vector led to improvement of photoreceptor structure and function as shown by electron microscopy and ERG (127, 128). Sarra et al. demonstrated that the potential of morphological improvement depends upon the age at which animals are treated and overexpression of the peripherin 2 protein might be harmful to photoreceptor cells (129). Another study by Schlichtenbrede et al. showed the improvement of higher visual functions after gene replacement therapy in *Prph*$^{Rd2/Rd2}$ mice based on recordings from visually responsive neurons in the superior colliculus (130).

The mouse ortholog of the retinoschisin gene is known as *rs1h* (131). Two knockout mouse models of RS have been generated, both of which exhibit to a certain degree a similar phenotype when compared to the human disease (11, 132). Each mouse model was then used to study the efficacy of gene therapy protocols. The first group of studies used an AAV2/2 vector containing the murine *rs1h* gene under the control of a CMV promoter. In 13 weeks old *rs1h*$^{-/Y}$ mice (132), subretinal injection of this vector leads to the detection of retinoschisin in all retinal cell layers and the restoration of the normal b-wave amplitude (132). However, normal retinal structure could not be restored. Following the initial results, the authors presented the long-term results of the retinal changes following AAV-mediated gene transfer in this mouse model (133). A correlation between functional and morphological changes for up to 14 months post injection was demonstrated. Furthermore, in a different study, the authors demonstrated mislocalization and reduced levels of pre- and postsynaptic markers in photoreceptors in mice (PSD95, mGluR6, synaptophysin) at 4 weeks, which explains the reduced b-wave in ERG recordings and therefore the block in transmitting information from the photoreceptors to ganglion cells and subsequently to higher visual regions in the brain (134). Apparently, the Retinoschisin expression helps at least in part in the preservation of normal synaptic structures and gene addition therapy using the AAV2/2.CMV.rs1 vector partially restored synaptic integrity in these animals. Very recently, the intravitreal injection of an AAV2/8 vector containing the rs1 gene (including a truncated first intron) under the control of a retinoschisin promoter resulted in detectable retinoschisin expression in rs1 knockout mice (67). This successful gene transfer resulted in improved ERG recordings up to 15 weeks post injection.

The second group of studies employed an AAV2/5 vector carrying the human *rs-1* gene driven by a mouse opsin promoter, which was subretinally injected into 2 weeks old *rs1h*$^{-/-}$ mice (135). Using this approach, retinochisin was detected in all cell layers identical to that seen in wild type animals, and normal visual function was restored as observed by the increased b-wave and lasted for at least 1 year. In addition, structural integrity of the retina was improved and photoreceptors were preserved for the duration of the study. The authors explored in a second study the feasibility of subretinal injections of the vector at later time points during the disease (136). They demonstrated that a treatment with the AAV2/5.mopsin.Rs1 vector at later time points (up until 7 months of age) can result in detectable retinoschisin expression, even though morphological or functional rescue remains marginal if treatment is performed later than 2 months of age.

3.5.2. Treatment of Autosomal Dominant Diseases

Autosomal dominant diseases are caused by mutations, which result in a toxic "gain of function" effect of the encoded protein. Mutations of the rhodopsin gene account for the largest proportion of autosomal dominant retinitis pigmentosa (adRP) and affect the folding, stability and intracellular processing of the protein. The presence of only one allele is sufficient for the onset of retinal degeneration. One particular rhodopsin mutation, P23H, is responsible for 12% of all adRP cases in the US (137) and transgenic mice and rats containing this mutation have been developed to study the disease and evaluate potential treatment strategies. Mutations in another gene, the inosine 5 -monophosphate dehydrogenase 1 (IMPDH1) cause the adRP form that is called RP10 (138).

To treat these kinds of disorders, gene augmentation therapy is not suitable, as the mutant allele, mRNA or protein product must be silenced beforehand. To down-regulate the production of toxic proteins in a cell, two strategies have been developed involving either ribozymes or siRNA.

Ribozymes are RNA enzymes capable of cleaving a complementary mRNA sequence and according to their form in the cytoplasm they are called either hammerhead or hairpin ribozymes (139). Naturally occurring ribozymes have been screened to identify molecules, that are capable of cleaving specifically the mutant rhodopsin mRNA and allow the expression of the normal allele. Subretinal injection of a rAAV2/2 containing the allele specific ribozyme (hammerhead or hairpin) driven by an opsin promoter in P23H rats at postnatal day P15 led to preservation of photoreceptors for at least 3 months (140). The ribozymes were able to decrease the mRNA level of the mutant allele by 10–15%. LaVail and colleagues demonstrated that the same treatment strategy slowed photoreceptor degeneration for up to 8 months when animals were treated at either P15 or later (P30 or P45) (141). In addition, compared with

control eyes, the treatment resulted in higher ERG amplitudes up to 6 months after injection.

As more than 200 mutations in the rhodopsin gene have been found to cause adRP, allele specific ribozymes would have to be found for each mutation. An alternative approach is to develop allele independent ribozymes, that digest all endogenous rhodopsin mRNA, mutant or wild type. At the same time, a ribozyme-resistant rhodopsin gene would be introduced into photoreceptors by gene transfer.

One such ribozyme, Rz397, was introduced into an rAAV2/2 vector driven by a mouse opsin promoter, and subretinally injected into rhodopsin knockout hemizygous ($rho^{+/-}$) mice at P6 and P60 (142). The ribozyme was capable of decreasing the amount of rhoposin by 80% in these animals. In a second experiment, the same group developed a ribozyme, Rz525, which is capable of cleaving all dog, mouse, and human, but not rat rhodopsin (143). Subretinal injection of a rAAV2/5 vector containing this ribozyme driven by a mouse opsin promoter into P23H hemizygous rats carrying one rat and one mouse rhodopsin allele resulted in 46% reduction of mouse mRNA but no change in rat mRNA. By diminishing the amount of mouse rhodopsin in these rats, toxic effects were less important and photoreceptor morphology could partially be preserved.

Small interfering RNAs (siRNAs) are double stranded RNA molecules of 20–25 bp length which are capable of cleaving complementary mRNA. These molecules are processed from small hairpin (sh) RNA driven by an RNA polymerase III promoter like U6 or H1, or by a polymerase II promoter like CMV.

Subretinal injection of a rAAV2/5 vector carrying an shRNA specifically targeting the mouse P23H rhodopsin gene under the control of a U6 promoter were injected subretinally into P23H transgenic rats (144). The processed and allele specific siRNA diminished the amount of mouse mutant rhodopsin in these animals but was not sufficient to prevent or block photoreceptor degeneration.

Another study used allele independent siRNA molecules capable of degrading mutant and wild type rhodopsin (145). Subretinal injection of a rAAV2/5 vector carrying a shRNA complementary to mouse rhodopsin driven by a H1 promoter were injected subretinally into heterozygous rhodopsin knockout mice at P16. Endogenous rhodopsin protein could be decrease by 60%, mRNA levels by 30%. Retinal function was diminished due to the reduction of rhodopsin content.

Similarly, the allele independent strategy of nonspecific suppression of all Rhodopsin alleles and replacement with a codon modified allele is the basis of the gene therapy strategy developed by the group of Farrar and colleagues. They developed different strategies to overcome the major hurdles of such an approach,

which is the necessity of complete downregulation of endogenous *Rho* and at the same time a very effective replacement by gene transfer.

To overcome the first hurdle, functional siRNAs were developed, screened for efficiency in vitro and tested in vivo using an AAV2/5 vector (AAV2/5.shBB.EGFP) in mouse model that expresses the human Rhodopsin gene on a mouse Rhodopsin background (NHR$^{+/-}$*Rho*$^{-/-}$) (146). The siRNA expression downregulated the human Rhodopsin mRNA level for up to 90%. In addition, the same vector was shown to be efficient in downregulating the human Rhodopsin allele containing the P347S mutation that was crossbred on a normal mouse line (*RHO*347$^{+/-}$*Rho*$^{+/+}$) (147). As the siRNA is specific for the human Rhodopsin gene, suppression of the mouse Rhodopsin in this mouse model was not observed and retinal function and morphology remained normal following the administration of the vector.

A more challenging point is the second hurdle, which is the sufficient replacement of the Rhodopsin protein, as it makes up to 90% of the outer segment membrane proteins (148). Furthermore, the replaced Rhodopsin gene has to be unspecific for the siRNA mediated downregulation, which can be achieved by modifying the DNA sequence at crucial points (codon modification). In order to study the effect of a codon modified human Rhodopsin gene, a mouse model was generated that expresses such an allele on a mouse rhodopsin background (*Rho*-M) (149). It was shown that the codon modified gene was equivalent to the endogenous Rhodposin gene in producing sufficient protein with the correct function in the retina of these animals. In order to test the capacity of an rAAV-mediated gene transfer of the codon modified Rhodopsin gene into the retina of *Rho*$^{-/-}$ mice, eight different constructs containing the transgene, different promoters and the siRNA cassette were incorporated into the AAV2/5 serotype (150). Subretinal injections, performed as early as p0, resulted in transgene expression of up to 40% of normal levels and the formation of outer segments and significant rod-derived ERG recordings in treated eyes. To summarize the treatment strategies for adRP caused by mutations in the Rhodopsin gene, the combined strategy of downregulation and replacement seems to be a practical and reliable way to circumvent the extensive allelic heterogeneity in the human population.

Downregulating the mutant gene by siRNA was also used as treatment strategy for adRP due to mutations in the IMPDH1 gene (151). AAV-mediated expression of the mutant human or mouse IMPDH1 gene in the retinas of wild type mice was performed and retinal degeneration with complete loss of the ONL was observed in both models 4 weeks after the injection (151). In order to treat the pathologic condition, an AAV2/5 vector was constructed containing the IMPDH1 specific siRNA and was

co-injected with an AAV2/5 vector expressing the mutant IMPDH1 gene in to adult wild type mice. After 4 weeks, the morphology of the retina was conserved in co-injected mice compared to mice injected with the mutant IMPDH1 gene alone, indicating that the down regulation of all endogenous genes, including the toxic allele would be beneficial for patients suffering from this form of retinal degeneration (also known as RP10).

3.6. Human Clinical Trials

This chapter focuses on design and strategy of the first gene therapy human clinical trials for inherited retinal degeneration. These trials were proposed after proof-of-concept of gene augmentation therapy had been demonstrated in dog and mouse models of LCA due to *RPE65* mutations.

3.6.1. Design

Three separate groups near simultaneously initiated open label, dose escalation, unilateral subretinal gene transfer studies in a small number of individuals with LCA due to *RPE65* mutations (Table 4). In all studies, baseline studies of retinal/visual function were carried out and then, after surgery, the studies were repeated as a function of time after injection. All three groups used rAAV2/2 vectors; two of them used the CBA promoter and one used a RPE-cell specific (RPE65) promoter. The doses were 1.5E10 (3 subjects), 4.8E10 (6 subjects) and 1.5E11 vector genomes (vg) (3 subjects), (Children's Hospital of Philadelphia, CHOP), up to 1E11 vg in three subjects (dose was dependant on volume; University College London, UCL) and 5.9E10 vg in three subjects (University of Florida-University of Pennsylvania, UFl). The volumes of injection ranged from 150 μl to 1.0 ml (UCL). Subjects in the UCL and UFl studies were young adults while those in the CHOP study ranged in age from 8 years old to 44 years old (23–25).

Because of the many variables that differed between the three studies (regulatory sequences, method of preparation and purification of the vector, dose, volume, disease-causing mutations, age of subject, location of injection, outcome measures, etc.), it is not possible to compare the data directly from one study to another. However, several important conclusions can be drawn: (1) The procedure was safe. There were no harmful inflammatory responses and immune responses were benign. The procedure was well tolerated by the 18 subjects (total number reported in these three studies). There were no severe adverse events and the few adverse events were mild; (2) The majority of the subjects benefited from the procedure. All 12 of the subjects in the CHOP study showed both improvements in retinal and visual function as assessed by both subjective and objective measures. The level of improvement was most striking in the youngest subjects, as might have been expected based on results from animal studies (152). All four of the children (8–11 years old) and one of the adults (26 years old) in the CHOP study gained the ability to ambulate independently

Table 4
Published human clinical trials for patients with mutations in the RPE65 gene

Study	NCT number	Design	Vector	No. of patients	Age	Dose
UCL (23)	00643747	phase I	AAV2/2.hRPE65p.hRPE65 (hRPE65 promoter)	3	17–23	≤1E11
CHOP (25, 153, 156)	00516477	phase I/II	AAV2-hRPE65v2 (CBA promoter)	12	8–44	1.5E10–1.5E11
Ufl (24, 154, 155, 157)	00481546	phase I	AAV2-CB^{SB}-h*RPE65* (CBA promoter with shortened CMV enhancer)	3	21–24	5.96E10

UCL University College London, *CHOP* Children's Hospital of Philadelphia, *Ufl* University of Florida, *NCT* clinicaltrials.gov registry number, *CBA* chicken beta actin, *CMV* cytomegalovirus

using the injected eye (153). All three of the subjects in the UFL study and one of the subjects in the UCL study showed improvements in subjective measures of visual function (23, 24). The subject in the UCL study who showed improvements in microperimetry and dark-adapted perimetry also became able to navigate independently; and (3) The safety profile persisted and the improvements in retinal/visual function that were reported soon after injection were maintained in at least in two of the three trials. Cideciyan reported that the improvements in visual sensitivity were maintained between 3 and 12 months (154). In addition, this group reported that one of the three patients was able to foveate using the injected portion of her retina (155). The excellent safety and efficacy profile of the CHOP trial was also maintained through the 2-years timepoint (153, 156). All three of the subjects followed the longest continued to show significant improvements in visual acuity and pupillary light reflexes, and the ability to ambulate independently was maintained in the one individual in whom that had been documented at the previous timepoints (156).

3.6.2. General Considerations

The success of the LCA-RPE65 clinical trials to date provides a great incentive to evaluate gene augmentation approaches for other retinal degenerative diseases in future clinical trials. The data from the LCA-RPE65 studies will be useful in preparing for these other targets. The safety data to date using rAAV2/2 in a dose range of 1.5E10–1.5E11 vg will be helpful in designing these follow-up studies. However, additional preclinical safety studies

will need to be carried out using hybrid rAAVs with capsids of other serotypes. Photoreceptors are the primary disease-causing cells in the majority of hereditary retinal degenerations, and more efficient transduction can be achieved in this cell type using other rAAV vectors than AAV2/2 (see above). The dosing strategy will present more of a challenge for these situations because there will not be efficacy if too low a dose is given but too high of a dose could lead to toxicity.

Preclinical data have demonstrated the stability of AAV-mediated retinal gene transfer and, so far, this has been verified at least through a 1–2 years time period in the human clinical trials (153, 154, 156). At present, it is not known how long rAAV-mediated transgene expression will persist in the human retina. However, there are two facts that lend hope to the idea that it will persist long term: (1) Retinal cells are post-mitotic at birth and so even though the transgene cassette is maintained episomally in retinal cells, it is unlikely to be diluted due to cell division; and (2) Given the long follow-up in dogs (6 and 11 years, Rolling and Bennett, personal communication) and the stable expression of transgenes after subretinal injection in these animals, rAAV-mediated transgene expression should persist in other species. Therefore, as long as the gene transfer slows down the degenerative component of the disease, rAAV-mediated transgene expression is expected to be stable.

A real challenge will be an economic one – to develop and test a gene-based treatment for each one of the hundreds of different genes involved in retinal degenerative disease. Preclinical studies can generally be funded through traditional mechanisms, such as government-issued grants and private foundations. Successful proof-of-concept studies then lead to candidates for a clinical trial. There are very few funding sources, however, that will cover the costs of initiating and completing a clinical trial. Following demonstration of proof-of-concept, additional studies aimed at optimizing a vector (selecting the appropriate regulatory sequence, carrying out dose-ranging studies, completing and submitting regulatory documents, etc.) can cost $250,000. The cost of generating a clinical-grade vector is currently about $500,000. Preclinical safety studies will likely require testing in nonhuman primates, since eyes of those animals are most similar anatomically to those of humans (Primates are the only animals with a macula). Those safety studies can easily cost $250,000. One must be absolutely sure that the rAAV vector is optimal prior to generating the clinical vector, because if there is a change thereafter, the entire process starts anew.

Next, clinical trials themselves are costly. The cost of a phase 1 clinical trial involving 12 subjects seen at one site was about $1 million. If there is a second Center, bills are incurred not only for the clinical trial itself but also to monitor regulatory compliance. Thus, it can easily cost $2 million to carry out a phase 1 clinical trial.

Assuming safety and efficacy are identified in the phase 1 study, the subsequent studies (phase 2/3 trials) are even more costly.

For all retinal degenerative diseases, the best chance of success (recovery of vision or of prevention of further deterioration of vision), will be to intervene early in the disease process. Once the photoreceptor cells have died, there is nothing left to treat. In many forms of RP, it is possible that rescue could be achieved in teens or young adults. In choroideremia, it may be desirable to target teens and in Stargardt disease, it may be desirable to target pre-teens. For LCA, the optimal results may be obtained in treating infants as vision deficits are present in that disease early in life. In LCA, not only would it be most desirable to treat the retina before cells are lost to degenerative processes but also because there is a loss in plasticity of the connections between the retina and brain after about age 3. For example, in LCA-CEP290 and LCA-AIPL1, vision is severely abnormal even in infancy and so it would be sensible to treat as early as possible. In contrast, individuals with LCA-RPE65 generally have formed (but poor) vision before age 3 years old and thus the retinal/CNS circuitry is established. Therefore, individuals in their teens, twenties and even as old as 44 years old can benefit from delivery of the wildtype RPE65 cDNA (23, 24, 153).

One question that will need to be addressed, however, is, whether it is safe to re-administer the vector to the contralateral eye at a later timepoint. Although re-administration in animals appears safe, the safety of re-administration in humans is unknown. In young children, a unilateral injection could result in a favoring of one eye versus the other and amblyopia, a condition whereby the brain is incapable of recognizing signal from an eye. If this were to happen because one eye was treated and was seeing better than the other, or if one eye was patched due to a complication from surgery, it would prevent benefit of future surgery on the amblyopic eye.

The ages of inclusion for each clinical trial will be determined through an evaluation of risk:benefit ratios and through consideration of principles of clinical research involving vulnerable (pediatric) subjects. In the USA in the clinical trial run at CHOP, enrollment of pediatric subjects was approved even though there was thought to be slightly greater than minimal risk, classified as code 45 CFR 46.405 in the USA. This code states that research can be carried out which involves greater than minimal risk on vulnerable subjects but there must be a prospect of direct benefit to the individual. In the CHOP study, this code forced the team to use a dose that had been shown to rescue vision in >90% of dogs (instead of a lower, potentially ineffective dose). Finally, the lower age limit may be selected by determining whether a child is able to give assent. It is widely felt that children 8 years old and above are capable of understanding what they are agreeing to as long as the language is appropriate (http://www.webconferences.com/nihoba/13_dec_2005.html).

3.6.3. Outcome

One of the most important details of clinical trial design is selection of the most appropriate outcome measures. The tests should be sensitive, quantitative, and reproducible. Some retinal function/visual function tests are subjective in nature (i.e., the subject tells the examiner the response and the results can be influenced by the subject's levels of wakefulness, cooperation, etc.). It is thus desirable to include objective tests as well. That way, one can be sure that the subject is not simply showing a placebo or learning effect or is too tired to comply. It is important that the tests/test preparation do not overburden the subject. This is particularly a concern in children with short attention spans. Finally, it is desirable to carry out sufficient testing and to repeat the testing as warranted in order to be able to obtain sufficient data for robust statistical analyses.

3.7. Comparison of the Results of rAAV-Mediated Gene Therapy in Human Trials and Animal Models

Interestingly, the data obtained in animal models of LCA-RPE65 were largely predictive of the results in the human clinical trials. First, subretinal delivery was safe in both animals and humans, the vector remained predominantly in the eye (i.e., there was minimal "shedding") and the delivery resulted in stable improvements in vision relating to the area/portion of retina treated. A single unilateral subretinal injection of 1.5E10 (or higher) vg in all of the Briard dogs younger than 2 years old resulted in increased light sensitivity, improvements in the full field ERG and also the ability of the animals to navigate. In dogs, the first suggestion that there was efficacy was an improvement in pupillary light reflexes noted at 2 weeks after injection. PLRs and ERGS were also readily recordable in Rpe65$^{-/-}$ mice treated subretinally up to 4 months of age ("young adult mice"), but were severely reduced in aged mice. An improvement in PLRs was noted soon after injection in human subjects – the earliest timepoint being 8 days (153). A benefit with the humans was that they could also describe their sense if increased brightness in the injected eye at early (and late) timepoints.

A full field ERG has not been recorded to date in any of the 18 individuals age 8 years old or older enrolled to date in any of the three trials. However, multifocal mf ERGs were recorded from two young subjects in the CHOP study (153). Further, all of the youngest subjects (and two older ones – see above) gained the ability to navigate independently in the clinical trials (25, 153, 156). The ability to ambulate reflects a combination of different visual abilities: light sensitivity, visual acuity and visual fields. Visual acuity and visual fields could not be measured in the dogs, but improved in the majority of the humans enrolled in the CHOP trial (153). Like the dogs (17), both rod and cone-mediated responses were recovered in humans tested in the UFl trial (24).

What was not predictive based on the animal experiments was that while there were permanent pigmentary changes in the dog retinas indicating the borders of the original retinal detachments

(17, 18), no such changes were detectable in the injected human retinas (25, 153, 156). It may be that injection-induced changes in the underlying reflective tapetum in dogs contribute to the ophthalmoscopically detectable changes in this species. The other finding that was not predictive based on the animal experiments was that there was improvement in retinal/visual function in a human as old as 44 years old. This individual did not recover normal vision, but did show improved PLRs, and improvements in subjective measures of retinal/visual function. Bilateral PLRS were not measured in the older dogs that were evaluated and so a direct comparison across species cannot be made. However, there has been no clear-cut demonstration of improvement in the older (>2 years old) dogs that have been tested.

4. Conclusion

There has been great progress over the past decade in characterizing and generating animal models for retinal degeneration, developing and testing strategies for ameliorating the disease process and moving the promising proof-of-concept data into clinical trials. Because of these strides, there is great promise for future applications of AAV-mediated gene therapy for blindness. There are a number of technical and economic challenges that must be tackled to be able to successfully ameliorate these inherited conditions. In addition, there are still a number of safety concerns, including issues relating to immune response, stability, and long-term effects of high levels of transgene expression. However, meticulous preclinical safety and efficacy studies combined with a cautious, stepwise translational approach based on a careful evaluation of risk: benefit ratios will lead the way to the ultimate goal of being able to use rAAV to ameliorate or possibly even cure forms of inherited blindness.

References

1. Chung, D. C., Lee, V., and Maguire, A. M. (2009) Recent advances in ocular gene therapy *Curr. Opin. Ophthalmol* ***20***, 377–381.
2. Smith, A. J., Bainbridge, J. W., and Ali, R. R. (2009) Prospects for retinal gene replacement therapy *Trends Genet.* ***25***, 156–165.
3. Surace, E. M. and Auricchio, A. (2008) Versatility of AAV vectors for retinal gene transfer *Vision Res.* ***48***, 353–359.
4. Anand, V., Chirmule, N., Fersh, M., Maguire, A. M., and Bennett, J. (2000) Additional transduction events after subretinal readministration of recombinant adeno-associated virus *Hum Gene Ther* ***11***, 449–457.
5. Barker, S. E., Broderick, C. A., Robbie, S. J., Duran, Y., Natkunarajah, M., Buch, P., Balaggan, K. S., MacLaren, R. E., Bainbridge, J. W., Smith, A. J., and Ali, R. R. (2009) Subretinal delivery of adeno-associated virus serotype 2 results in minimal immune responses that allow repeat vector administration in immunocompetent mice *J. Gene Med.* ***11***, 486–497.
6. Bennett, J., Maguire, A. M., Cideciyan, A. V., Schnell, M., Glover, E., Anand, V., Aleman, T. S., Chirmule, N., Gupta, A. R., Huang, Y., Gao, G. P., Nyberg, W. C., Tazelaar, J., Hughes, J., Wilson, J. M., and Jacobson, S. G.

(1999) Stable transgene expression in rod photoreceptors after recombinant adeno-associated virus-mediated gene transfer to monkey retina *Proc. Natl. Acad. Sci. U. S. A* ***96***, 9920–9925.

7. Moosajee, M., Tulloch, M., Baron, R. A., Gregory-Evans, C. Y., Pereira-Leal, J. B., and Seabra, M. C. (2009) Single choroideremia gene in nonmammalian vertebrates explains early embryonic lethality of the zebrafish model of choroideremia *Invest Ophthalmol Vis. Sci.* ***50***, 3009–3016.
8. Jang, Y. P., Matsuda, H., Itagaki, Y., Nakanishi, K., and Sparrow, J. R. (2005) Characterization of peroxy-A2E and furan-A2E photooxidation products and detection in human and mouse retinal pigment epithelial cell lipofuscin *J. Biol. Chem.* ***280***, 39732–39739.
9. Hagstrom, S. A., Duyao, M., North, M. A., and Li, T. (1999) Retinal degeneration in tulp1−/− mice: vesicular accumulation in the interphotoreceptor matrix *Invest Ophthalmol Vis. Sci.* ***40***, 2795–2802.
10. Tam, B. M. and Moritz, O. L. (2006) Characterization of rhodopsin P23H-induced retinal degeneration in a Xenopus laevis model of retinitis pigmentosa *Invest Ophthalmol Vis. Sci.* ***47***, 3234–3241.
11. Weber, B. H., Schrewe, H., Molday, L. L., Gehrig, A., White, K. L., Seeliger, M. W., Jaissle, G. B., Friedburg, C., Tamm, E., and Molday, R. S. (2002) Inactivation of the murine X-linked juvenile retinoschisis gene, Rs1h, suggests a role of retinoschisin in retinal cell layer organization and synaptic structure *Proc. Natl. Acad. Sci. U. S. A* ***99***, 6222–6227.
12. Keeler, C. (1927) Rodless retina, an ophthalmic mutation in the house mouse, Mus musculus, *Jour Exp Zool* ***46***, 355–407.
13. Fadool, J. M. and Dowling, J. E. (2008) Zebrafish: a model system for the study of eye genetics *Prog. Retin. Eye Res.* ***27***, 89–110.
14. Hong, C. C. (2009) Large-scale small-molecule screen using zebrafish embryos *Methods Mol. Biol.* ***486***, 43–55.
15. Bennett, J., Anand, V., Acland, G. M., and Maguire, A. M. (2000) Cross-species comparison of in vivo reporter gene expression after recombinant adeno-associated virus-mediated retinal transduction *Methods Enzymol.* ***316***, 777–789.
16. Acland, G. M., Aguirre, G. D., Ray, J., Zhang, Q., Aleman, T. S., Cideciyan, A. V., Pearce-Kelling, S. E., Anand, V., Zeng, Y., Maguire, A. M., Jacobson, S. G., Hauswirth, W. W., and Bennett, J. (2001) Gene therapy restores vision in a canine model of childhood blindness *Nat Genet* ***28***, 92–5.
17. Acland, G. M., Aguirre, G. D., Bennett, J., Aleman, T. S., Cideciyan, A. V., Bennicelli, J., Dejneka, N. S., Pearce-Kelling, S. E., Maguire, A. M., Palczewski, K., Hauswirth, W. W., and Jacobson, S. G. (2005) Long-term restoration of rod and cone vision by single dose rAAV-mediated gene transfer to the retina in a canine model of childhood blindness *Mol Ther* ***12***, 1072–82.
18. Bennicelli, J., Wright, J. F., Komaromy, A., Jacobs, J. B., Hauck, B., Zelenaia, O., Mingozzi, F., Hui, D., Chung, D., Rex, T. S., Wei, Z., Qu, G., Zhou, S., Zeiss, C., Arruda, V. R., Acland, G. M., Dell'Osso, L. F., High, K. A., Maguire, A. M., and Bennett, J. (2008) Reversal of blindness in animal models of leber congenital amaurosis using optimized AAV2-mediated gene transfer *Mol. Ther* ***16***, 458–465.
19. Le Meur, G., Stieger, K., Smith, A. J., Weber, M., Deschamps, J. Y., Nivard, D., Mendes-Madeira, A., Provost, N., Pereon, Y., Cherel, Y., Ali, R. R., Hamel, C., Moullier, P., and Rolling, F. (2007) Restoration of vision in RPE65-deficient Briard dogs using an AAV serotype 4 vector that specifically targets the retinal pigmented epithelium *Gene Ther* ***14***, 292–303.
20. Narfstrom, K., Katz, M. L., Bragadottir, R., Seeliger, M., Boulanger, A., Redmond, T. M., Caro, L., Lai, C. M., and Rakoczy, P. E. (2003) Functional and structural recovery of the retina after gene therapy in the RPE65 null mutation dog *Invest Ophthalmol Vis Sci* ***44***, 1663–72.
21. Narfstrom, K., Katz, M. L., Ford, M., Redmond, T. M., Rakoczy, E., and Bragadottir, R. (2003) In vivo gene therapy in young and adult RPE65−/− dogs produces long-term visual improvement *J Hered* ***94***, 31–7.
22. Jacobson, S. G., Boye, S. L., Aleman, T. S., Conlon, T. J., Zeiss, C. J., Roman, A. J., Cideciyan, A. V., Schwartz, S. B., Komaromy, A. M., Doobrajh, M., Cheung, A. Y., Sumaroka, A., Pearce-Kelling, S. E., Aguirre, G. D., Kaushal, S., Maguire, A. M., Flotte, T. R., and Hauswirth, W. W. (2006) Safety in nonhuman primates of ocular AAV2-RPE65, a candidate treatment for blindness in Leber congenital amaurosis *Hum Gene Ther* ***17***, 845–58.
23. Bainbridge, J. W., Smith, A. J., Barker, S. S., Robbie, S., Henderson, R., Balaggan, K., Viswanathan, A., Holder, G. E., Stockman, A., Tyler, N., Petersen-Jones, S., Bhattacharya, S. S., Thrasher, A. J., Fitzke, F. W., Carter, B. J., Rubin, G. S., Moore, A. T., and Ali, R. R. (2008) Effect of gene therapy on visual function in Leber's congenital amaurosis *N. Engl. J. Med.* ***358***, 2231–2239.

24. Cideciyan, A. V., Aleman, T. S., Boye, S. L., Schwartz, S. B., Kaushal, S., Roman, A. J., Pang, J. J., Sumaroka, A., Windsor, E. A., Wilson, J. M., Flotte, T. R., Fishman, G. A., Heon, E., Stone, E. M., Byrne, B. J., Jacobson, S. G., and Hauswirth, W. W. (2008) Human gene therapy for RPE65 isomerase deficiency activates the retinoid cycle of vision but with slow rod kinetics *Proc. Natl. Acad. Sci. U. S. A* ***105***, 15112–15117.

25. Maguire, A. M., Simonelli, F., Pierce, E. A., Pugh, E. N., Jr., Mingozzi, F., Bennicelli, J., Banfi, S., Marshall, K. A., Testa, F., Surace, E. M., Rossi, S., Lyubarsky, A., Arruda, V. R., Konkle, B., Stone, E., Sun, J., Jacobs, J., Dell'osso, L., Hertle, R., Ma, J. X., Redmond, T. M., Zhu, X., Hauck, B., Zelenaia, O., Shindler, K. S., Maguire, M. G., Wright, J. F., Volpe, N. J., McDonnell, J. W., Auricchio, A., High, K. A., and Bennett, J. (2008) Safety and efficacy of gene transfer for Leber's congenital amaurosis *N. Engl. J. Med.* ***358***, 2240–2248.

26. Hartong, D. T., Berson, E. L., and Dryja, T. P. (2006) Retinitis pigmentosa, *Lancet 368*, 1795–809.

27. Hamel, C. P. (2007) Cone rod dystrophies *Orphanet. J. Rare. Dis.* ***2***, 7.

28. Michaelides, M., Hardcastle, A. J., Hunt, D. M., and Moore, A. T. (2006) Progressive cone and cone-rod dystrophies: phenotypes and underlying molecular genetic basis *Surv Ophthalmol* ***51***, 232–58.

29. Cremers, F. P., van de Pol, D. J., van, D. M., den Hollander, A. I., van Haren, F. J., Knoers, N. V., Tijmes, N., Bergen, A. A., Rohrschneider, K., Blankenagel, A., Pinckers, A. J., Deutman, A. F., and Hoyng, C. B. (1998) Autosomal recessive retinitis pigmentosa and cone-rod dystrophy caused by splice site mutations in the Stargardt's disease gene ABCR *Hum Mol. Genet. 7*, 355–362.

30. Wissinger, B., Gamer, D., Jagle, H., Giorda, R., Marx, T., Mayer, S., Tippmann, S., Broghammer, M., Jurklies, B., Rosenberg, T., Jacobson, S. G., Sener, E. C., Tatlipinar, S., Hoyng, C. B., Castellan, C., Bitoun, P., Andreasson, S., Rudolph, G., Kellner, U., Lorenz, B., Wolff, G., Verellen-Dumoulin, C., Schwartz, M., Cremers, F. P., pfelstedt-Sylla, E., Zrenner, E., Salati, R., Sharpe, L. T., and Kohl, S. (2001) CNGA3 mutations in hereditary cone photoreceptor disorders *Am. J. Hum Genet.* ***69***, 722–737.

31. Hameed, A., Abid, A., Aziz, A., Ismail, M., Mehdi, S. Q., and Khaliq, S. (2003) Evidence of RPGRIP1 gene mutations associated with recessive cone-rod dystrophy *J. Med. Genet.* ***40***, 616–619.

32. Freund, C. L., Gregory-Evans, C. Y., Furukawa, T., Papaioannou, M., Looser, J., Ploder, L., Bellingham, J., Ng, D., Herbrick, J. A., Duncan, A., Scherer, S. W., Tsui, L. C., Loutradis-Anagnostou, A., Jacobson, S. G., Cepko, C. L., Bhattacharya, S. S., and McInnes, R. R. (1997) Cone-rod dystrophy due to mutations in a novel photoreceptor-specific homeobox gene (CRX) essential for maintenance of the photoreceptor *Cell* ***91***, 543–553.

33. Kelsell, R. E., Gregory-Evans, K., Payne, A. M., Perrault, I., Kaplan, J., Yang, R. B., Garbers, D. L., Bird, A. C., Moore, A. T., and Hunt, D. M. (1998) Mutations in the retinal guanylate cyclase (RETGC-1) gene in dominant cone-rod dystrophy *Hum Mol. Genet. 7*, 1179–1184.

34. Sohocki, M. M., Perrault, I., Leroy, B. P., Payne, A. M., Dharmaraj, S., Bhattacharya, S. S., Kaplan, J., Maumenee, I. H., Koenekoop, R., Meire, F. M., Birch, D. G., Heckenlively, J. R., and Daiger, S. P. (2000) Prevalence of AIPL1 mutations in inherited retinal degenerative disease *Mol. Genet. Metab* ***70***, 142–150.

35. Demirci, F. Y., Rigatti, B. W., Wen, G., Radak, A. L., Mah, T. S., Baic, C. L., Traboulsi, E. I., Alitalo, T., Ramser, J., and Gorin, M. B. (2002) X-linked cone-rod dystrophy (locus COD1): identification of mutations in RPGR exon ORF15 *Am. J. Hum Genet.* ***70***, 1049–1053.

36. Koenekoop, R. K. (2004) An overview of Leber congenital amaurosis: a model to understand human retinal development *Surv Ophthalmol* ***49***, 379–98.

37. Lorenz, B., Gyurus, P., Preising, M., Bremser, D., Gu, S., Andrassi, M., Gerth, C., and Gal, A. (2000) Early-onset severe rod-cone dystrophy in young children with RPE65 mutations *Invest Ophthalmol Vis Sci* ***41***, 2735–42.

38. Lorenz, B., Wabbels, B., Wegscheider, E., Hamel, C. P., Drexler, W., and Preising, M. N. (2004) Lack of fundus autofluorescence to 488 nanometers from childhood on in patients with early-onset severe retinal dystrophy associated with mutations in RPE65 *Ophthalmology* ***111***, 1585–1594.

39. den Hollander, A. I., Roepman, R., Koenekoop, R. K., and Cremers, F. P. (2008) Leber congenital amaurosis: genes, proteins and disease mechanisms *Prog. Retin. Eye Res. 27*, 391–419.

40. Gerth, C., ndrassi-Darida, M., Bock, M., Preising, M. N., Weber, B. H., and Lorenz, B. (2002) Phenotypes of 16 Stargardt macular dystrophy/fundus flavimaculatus patients with known ABCA4 mutations and evaluation of

genotype-phenotype correlation *Graefes Arch Clin Exp Ophthalmol* ***240***, 628–638.

41. Lorenz, B. and Preising, M. N. (2005) Age matters – thoughts on a grading system for ABCA4 mutations *Graefes Arch. Clin. Exp. Ophthalmol.* ***243***, 87–89.
42. Martinez-Mir, A., Paloma, E., Allikmets, R., Ayuso, C., del, R. T., Dean, M., Vilageliu, L., Gonzalez-Duarte, R., and Balcells, S. (1998) Retinitis pigmentosa caused by a homozygous mutation in the Stargardt disease gene ABCR *Nat. Genet.* ***18***, 11–12.
43. Kohl, S. (2009) (Genetic causes of hereditary cone and cone-rod dystrophies) *Ophthalmologe* ***106***, 109–115.
44. Kohl, S., Marx, T., Giddings, I., Jagle, H., Jacobson, S. G., pfelstedt-Sylla, E., Zrenner, E., Sharpe, L. T., and Wissinger, B. (1998) Total colourblindness is caused by mutations in the gene encoding the alpha-subunit of the cone photoreceptor cGMP-gated cation channel *Nat. Genet.* ***19***, 257–259.
45. Kohl, S., Baumann, B., Broghammer, M., Jagle, H., Sieving, P., Kellner, U., Spegal, R., Anastasi, M., Zrenner, E., Sharpe, L. T., and Wissinger, B. (2000) Mutations in the CNGB3 gene encoding the beta-subunit of the cone photoreceptor cGMP-gated channel are responsible for achromatopsia (ACHM3) linked to chromosome 8q21 *Hum Mol. Genet.* ***9***, 2107–2116.
46. Kohl, S., Baumann, B., Rosenberg, T., Kellner, U., Lorenz, B., Vadala, M., Jacobson, S. G., and Wissinger, B. (2002) Mutations in the cone photoreceptor G-protein alpha-subunit gene GNAT2 in patients with achromatopsia *Am. J. Hum Genet.* ***71***, 422–425.
47. Sikkink, S. K., Biswas, S., Parry, N. R., Stanga, P. E., and Trump, D. (2007) X-linked retinoschisis: an update *J. Med. Genet.* ***44***, 225–232.
48. Khan, N. W., Jamison, J. A., Kemp, J. A., and Sieving, P. A. (2001) Analysis of photoreceptor function and inner retinal activity in juvenile X-linked retinoschisis *Vision Res.* ***41***, 3931–3942.
49. Sauer, C. G., Gehrig, A., Warneke-Wittstock, R., Marquardt, A., Ewing, C. C., Gibson, A., Lorenz, B., Jurklies, B., and Weber, B. H. (1997) Positional cloning of the gene associated with X-linked juvenile retinoschisis *Nat. Genet.* ***17***, 164–170.
50. Rosenberg, T. and Schwartz, M. (1998) X-linked ocular albinism: prevalence and mutations – a national study *Eur. J. Hum Genet.* ***6***, 570–577.
51. Ray, K., Chaki, M., and Sengupta, M. (2007) Tyrosinase and ocular diseases: some novel thoughts on the molecular basis of oculocutaneous albinism type 1 *Prog. Retin. Eye Res.* ***26***, 323–358.
52. King, R. A., Pietsch, J., Fryer, J. P., Savage, S., Brott, M. J., Russell-Eggitt, I., Summers, C. G., and Oetting, W. S. (2003) Tyrosinase gene mutations in oculocutaneous albinism 1 (OCA1): definition of the phenotype *Hum Genet.* ***113***, 502–513.
53. Bennett, J., Duan, D., Engelhardt, J. F., and Maguire, A. M. (1997) Real-time, noninvasive in vivo assessment of adeno-associated virus-mediated retinal transduction *Invest Ophthalmol Vis Sci* ***38***, 2857–63.
54. Dudus, L., Anand, V., Acland, G. M., Chen, S. J., Wilson, J. M., Fisher, K. J., Maguire, A. M., and Bennett, J. (1999) Persistent transgene product in retina, optic nerve and brain after intraocular injection of rAAV *Vision Res* ***39***, 2545–53.
55. Lebherz, C., Maguire, A., Tang, W., Bennett, J., and Wilson, J. M. (2008) Novel AAV serotypes for improved ocular gene transfer *J. Gene Med.* ***10***, 375–382.
56. Guy, J., Qi, X., Muzyczka, N., and Hauswirth, W. W. (1999) Reporter expression persists 1 year after adeno-associated virus-mediated gene transfer to the optic nerve *Arch Ophthalmol* ***117***, 929–37.
57. Ali, R. R., Reichel, M. B., Thrasher, A. J., Levinsky, R. J., Kinnon, C., Kanuga, N., Hunt, D. M., and Bhattacharya, S. S. (1996) Gene transfer into the mouse retina mediated by an adeno-associated viral vector *Hum Mol Genet* ***5***, 591–4.
58. Allocca, M., Mussolino, C., Garcia-Hoyos, M., Sanges, D., Iodice, C., Petrillo, M., Vandenberghe, L. H., Wilson, J. M., Marigo, V., Surace, E. M., and Auricchio, A. (2007) Novel adeno-associated virus serotypes efficiently transduce murine photoreceptors *J Virol* ***81***, 11372–80.
59. Weber, M., Rabinowitz, J., Provost, N., Conrath, H., Folliot, S., Briot, D., Cherel, Y., Chenuaud, P., Samulski, J., Moullier, P., and Rolling, F. (2003) Recombinant adeno-associated virus serotype 4 mediates unique and exclusive long-term transduction of retinal pigmented epithelium in rat, dog, and nonhuman primate after subretinal delivery *Mol Ther 7*, 774–81.
60. Dorrell, M. I., Aguilar, E., Jacobson, R., Yanes, O., Gariano, R., Heckenlively, J., Banin, E., Ramirez, G. A., Gasmi, M., Bird, A., Siuzdak, G., and Friedlander, M. (2009) Antioxidant or neurotrophic factor treatment preserves function in a mouse model of neovascularization-associated oxidative stress *J. Clin Invest.* ***119***,611-623

61. Folliot, S., Briot, D., Conrath, H., Provost, N., Cherel, Y., Moullier, P., and Rolling, F. (2003) Sustained tetracycline-regulated transgene expression in vivo in rat retinal ganglion cells using a single type 2 adeno-associated viral vector *J Gene Med* ***5***, 493–501.
62. Liang, F. Q., Aleman, T. S., Dejneka, N. S., Dudus, L., Fisher, K. J., Maguire, A. M., Jacobson, S. G., and Bennett, J. (2001) Long-term protection of retinal structure but not function using RAAV.CNTF in animal models of retinitis pigmentosa *Mol Ther* ***4***, 461–72.
63. Ciulla, T. A. and Rosenfeld, P. J. (2009) Anti-vascular endothelial growth factor therapy for neovascular ocular diseases other than age-related macular degeneration *Curr. Opin. Ophthalmol* ***20***, 166–174.
64. Ciulla, T. A. and Rosenfeld, P. J. (2009) Antivascular endothelial growth factor therapy for neovascular age-related macular degeneration *Curr. Opin. Ophthalmol* ***20***, 158–165.
65. Klimczak, R. R., Koerber, J. T., Dalkara, D., Flannery, J. G., and Schaffer, D. V. (2009) A novel adeno-associated viral variant for efficient and selective intravitreal transduction of rat Muller cells *PLoS. One.* ***4***, e7467.
66. Dalkara, D., Kolstad, K. D., Caporale, N., Visel, M., Klimczak, R. R., Schaffer, D. V., and Flannery, J. G. (2009) Inner limiting membrane barriers to AAV-mediated retinal transduction from the vitreous *Mol. Ther* ***17***, 2096–2102.
67. Park, T. K., Wu, Z., Kjellstrom, S., Zeng, Y., Bush, R. A., Sieving, P. A., and Colosi, P. (2009) Intravitreal delivery of AAV8 retinoschisin results in cell type-specific gene expression and retinal rescue in the Rs1-KO mouse *Gene Ther* ***16***, 916–926.
68. Ali, R. R., Reichel, M. B., De Alwis, M., Kanuga, N., Kinnon, C., Levinsky, R. J., Hunt, D. M., Bhattacharya, S. S., and Thrasher, A. J. (1998) Adeno-associated virus gene transfer to mouse retina *Hum Gene Ther* ***9***, 81–6.
69. Auricchio, A., Kobinger, G., Anand, V., Hildinger, M., O'Connor, E., Maguire, A. M., Wilson, J. M., and Bennett, J. (2001) Exchange of surface proteins impacts on viral vector cellular specificity and transduction characteristics: the retina as a model *Hum Mol Genet* ***10***, 3075–81.
70. Yang, G. S., Schmidt, M., Yan, Z., Lindbloom, J. D., Harding, T. C., Donahue, B. A., Engelhardt, J. F., Kotin, R., and Davidson, B. L. (2002) Virus-mediated transduction of murine retina with adeno-associated virus: effects of viral capsid and genome size *J Virol* ***76***, 7651–60.
71. Natkunarajah, M., Trittibach, P., McIntosh, J., Duran, Y., Barker, S. E., Smith, A. J., Nathwani, A. C., and Ali, R. R. (2007) Assessment of ocular transduction using single-stranded and self-complementary recombinant adeno-associated virus serotype 2/8 *Gene Ther* ***15***,463-467
72. Lei, B., Zhang, K., Yue, Y., Ghosh, A., and Duan, D. (2009) Adeno-associated virus serotype-9 efficiently transduces the retinal outer plexiform layer *Mol. Vis.* ***15***, 1374–1382.
73. Koerber, J. T., Klimczak, R., Jang, J. H., Dalkara, D., Flannery, J. G., and Schaffer, D. V. (2009) Molecular evolution of adeno-associated virus for enhanced glial gene delivery *Mol. Ther* ***17***, 2088–2095.
74. Bello, A., Tran, K., Chand, A., Doria, M., Allocca, M., Hildinger, M., Beniac, D., Kranendonk, C., Auricchio, A., and Kobinger, G. P. (2009) Isolation and evaluation of novel adeno-associated virus sequences from porcine tissues *Gene Ther* ***16***, 1320–1328.
75. Rabinowitz, J. E., Rolling, F., Li, C., Conrath, H., Xiao, W., Xiao, X., and Samulski, R. J. (2002) Cross-packaging of a single adeno-associated virus (AAV) type 2 vector genome into multiple AAV serotypes enables transduction with broad specificity *J Virol* ***76***, 791–801.
76. Stieger, K., Colle, M. A., Dubreil, L., Mendes-Madeira, A., Weber, M., Le, M. G., Deschamps, J. Y., Provost, N., Nivard, D., Cherel, Y., Moullier, P., and Rolling, F. (2008) Subretinal delivery of recombinant AAV serotype 8 vector in dogs results in gene transfer to neurons in the brain *Mol. Ther.* ***16***, 916–923.
77. Li, H. L., Zheng, X. Z., Wang, H. P., Li, F., Wu, Y., and Du, L. F. (2009) Ultrasound-targeted microbubble destruction enhances AAV-mediated gene transfection in human RPE cells in vitro and rat retina in vivo *Gene Ther* ***16***, 1146–1153.
78. Bainbridge, J. W., Mistry, A., Schlichtenbrede, F. C., Smith, A., Broderick, C., De Alwis, M., Georgiadis, A., Taylor, P. M., Squires, M., Sethi, C., Charteris, D., Thrasher, A. J., Sargan, D., and Ali, R. R. (2003) Stable rAAV-mediated transduction of rod and cone photoreceptors in the canine retina *Gene Ther* ***10***, 1336–44.
79. Lotery, A. J., Yang, G. S., Mullins, R. F., Russell, S. R., Schmidt, M., Stone, E. M., Lindbloom, J. D., Chiorini, J. A., Kotin, R. M., and Davidson, B. L. (2003) Adeno-associated virus type 5: transduction efficiency and cell-type specificity in the primate retina *Hum Gene Ther* ***14***, 1663–71.

80. Petersen-Jones, S. M., Bartoe, J. T., Fischer, A. J., Scott, M., Boye, S. L., Chiodo, V., and Hauswirth, W. W. (2009) AAV retinal transduction in a large animal model species: comparison of a self-complementary AAV2/5 with a single-stranded AAV2/5 vector *Mol. Vis.* ***15***, 1835–1842.
81. Nicoletti, A., Kawase, K., and Thompson, D. A. (1998) Promoter analysis of RPE65, the gene encoding a 61-kDa retinal pigment epithelium-specific protein *Invest Ophthalmol Vis Sci* ***39***, 637–44.
82. Esumi, N., Oshima, Y., Li, Y., Campochiaro, P. A., and Zack, D. J. (2004) Analysis of the VMD2 promoter and implication of E-box binding factors in its regulation *J Biol Chem* ***279***, 19064–73.
83. Kuzmanovic, M., Dudley, V. J., and Sarthy, V. P. (2003) GFAP promoter drives Muller cell-specific expression in transgenic mice *Invest Ophthalmol Vis Sci* ***44***, 3606–13.
84. Young, J. E., Vogt, T., Gross, K. W., and Khani, S. C. (2003) A short, highly active photoreceptor-specific enhancer/promoter region upstream of the human rhodopsin kinase gene *Invest Ophthalmol Vis Sci* ***44***, 4076–85.
85. Lem, J., Applebury, M. L., Falk, J. D., Flannery, J. G., and Simon, M. I. (1991) Tissue-specific and developmental regulation of rod opsin chimeric genes in transgenic mice *Neuron* ***6***, 201–10.
86. Zack, D. J., Bennett, J., Wang, Y., Davenport, C., Klaunberg, B., Gearhart, J., and Nathans, J. (1991) Unusual topography of bovine rhodopsin promoter-lacZ fusion gene expression in transgenic mouse retinas *Neuron* ***6***, 187–99.
87. Bennett, J., Sun, D., and Kariko, K. (1995) Sequence analysis of the 5.34-kb 5 flanking region of the human rhodopsin-encoding gene *Gene* ***167***, 317–20.
88. Chen, J., Tucker, C. L., Woodford, B., Szel, A., Lem, J., Gianella-Borradori, A., Simon, M. I., and Bogenmann, E. (1994) The human blue opsin promoter directs transgene expression in short-wave cones and bipolar cells in the mouse retina *Proc Natl Acad Sci U S A* ***91***, 2611–5.
89. Alexander, J. J., Umino, Y., Everhart, D., Chang, B., Min, S. H., Li, Q., Timmers, A. M., Hawes, N. L., Pang, J. J., Barlow, R. B., and Hauswirth, W. W. (2007) Restoration of cone vision in a mouse model of achromatopsia *Nat Med* ***13***, 685–7.
90. Fei, Y. (2003) Development of the cone photoreceptor mosaic in the mouse retina revealed by fluorescent cones in transgenic mice *Mol Vis* ***9***, 31–42.
91. Komaromy, A. M., Alexander, J. J., Cooper, A. E., Chiodo, V. A., Glushakova, L. G., Acland, G. M., Hauswirth, W. W., and Aguirre, G. D. (2008) Targeting gene expression to cones with human cone opsin promoters in recombinant AAV *Gene Ther.* ***15***, 1049–1055.
92. Le Meur, G., Weber, M., Pereon, Y., Mendes-Madeira, A., Nivard, D., Deschamps, J. Y., Moullier, P., and Rolling, F. (2005) Postsurgical assessment and long-term safety of recombinant adeno-associated virus-mediated gene transfer into the retinas of dogs and primates *Arch Ophthalmol* ***123***, 500–6.
93. Hennig, A. K., Levy, B., Ogilvie, J. M., Vogler, C. A., Galvin, N., Bassnett, S., and Sands, M. S. (2003) Intravitreal gene therapy reduces lysosomal storage in specific areas of the CNS in mucopolysaccharidosis VII mice *J Neurosci* ***23***, 3302–7.
94. Griffey, M., Macauley, S. L., Ogilvie, J. M., and Sands, M. S. (2005) AAV2-mediated ocular gene therapy for infantile neuronal ceroid lipofuscinosis *Mol Ther* ***12***, 413–21.
95. Provost, N., Le Meur, G., Weber, M., Mendes-Madeira, A., Podevin, G., Cherel, Y., Colle, M. A., Deschamps, J. Y., Moullier, P., and Rolling, F. (2005) Biodistribution of rAAV vectors following intraocular administration: evidence for the presence and persistence of vector DNA in the optic nerve and in the brain *Mol Ther* ***11***, 275–83.
96. Jacobson, S. G., Acland, G. M., Aguirre, G. D., Aleman, T. S., Schwartz, S. B., Cideciyan, A. V., Zeiss, C. J., Komaromy, A. M., Kaushal, S., Roman, A. J., Windsor, E. A., Sumaroka, A., Pearce-Kelling, S. E., Conlon, T. J., Chiodo, V. A., Boye, S. L., Flotte, T. R., Maguire, A. M., Bennett, J., and Hauswirth, W. W. (2006) Safety of recombinant adeno-associated virus type 2-RPE65 vector delivered by ocular subretinal injection *Mol Ther* ***13***, 1074–84.
97. Stieger, K., Schroeder, J., Provost, N., Mendes-Madeira, A., Belbellaa, B., Le, M. G., Weber, M., Deschamps, J. Y., Lorenz, B., Moullier, P., and Rolling, F. (2009) Detection of intact rAAV particles up to 6 years after successful gene transfer in the retina of dogs and primates, *Mol. Ther. 17*, 516–523.
98. Jin, M., Li, S., Moghrabi, W. N., Sun, H., and Travis, G. H. (2005) Rpe65 is the retinoid isomerase in bovine retinal pigment epithelium *Cell* ***122***, 449–59.
99. Moiseyev, G., Chen, Y., Takahashi, Y., Wu, B. X., and Ma, J. X. (2005) RPE65 is the isomerohydrolase in the retinoid visual cycle *Proc Natl Acad Sci U S A* ***102***, 12413–8.

100. Redmond, T. M., Yu, S., Lee, E., Bok, D., Hamasaki, D., Chen, N., Goletz, P., Ma, J. X., Crouch, R. K., and Pfeifer, K. (1998) Rpe65 is necessary for production of 11-cis-vitamin A in the retinal visual cycle *Nat Genet* ***20***, 344–51.

101. Aguirre, G. D., Baldwin, V., Pearce-Kelling, S., Narfstrom, K., Ray, K., and Acland, G. M. (1998) Congenital stationary night blindness in the dog: common mutation in the RPE65 gene indicates founder effect *Mol Vis* ***4***, 23.

102. Veske, A., Nilsson, S. E., Narfstrom, K., and Gal, A. (1999) Retinal dystrophy of Swedish briard/briard-beagle dogs is due to a 4-bp deletion in RPE65 *Genomics* ***57***, 57–61.

103. Pang, J. J., Chang, B., Hawes, N. L., Hurd, R. E., Davisson, M. T., Li, J., Noorwez, S. M., Malhotra, R., McDowell, J. H., Kaushal, S., Hauswirth, W. W., Nusinowitz, S., Thompson, D. A., and Heckenlively, J. R. (2005) Retinal degeneration 12 (rd12): a new, spontaneously arising mouse model for human Leber congenital amaurosis (LCA) *Mol Vis* ***11***, 152–62.

104. Lai, C. M., Yu, M. J., Brankov, M., Barnett, N. L., Zhou, X., Redmond, T. M., Narfstrom, K., and Rakoczy, P. E. (2004) Recombinant adeno-associated virus type 2-mediated gene delivery into the Rpe65−/− knockout mouse eye results in limited rescue *Genet Vaccines Ther* ***2***, 3–7.

105. Pang, J. J., Chang, B., Kumar, A., Nusinowitz, S., Noorwez, S. M., Li, J., Rani, A., Foster, T. C., Chiodo, V. A., Doyle, T., Li, H., Malhotra, R., Teusner, J. T., McDowell, J. H., Min, S. H., Li, Q., Kaushal, S., and Hauswirth, W. W. (2006) Gene therapy restores vision-dependent behavior as well as retinal structure and function in a mouse model of RPE65 Leber congenital amaurosis *Mol Ther* ***13***, 565–72.

106. Dejneka, N. S., Surace, E. M., Aleman, T. S., Cideciyan, A. V., Lyubarsky, A., Savchenko, A., Redmond, T. M., Tang, W., Wei, Z., Rex, T. S., Glover, E., Maguire, A. M., Pugh, E. N., Jr., Jacobson, S. G., and Bennett, J. (2004) In utero gene therapy rescues vision in a murine model of congenital blindness *Mol. Ther.* ***9***, 182–188.

107. Narfstrom, K., Vaegan, Katz, M., Bragadottir, R., Rakoczy, E. P., and Seeliger, M. (2005) Assessment of structure and function over a 3-year period after gene transfer in RPE65−/− dogs *Doc Ophthalmol* ***111***, 39–48.

108. Batten, M. L., Imanishi, Y., Maeda, T., Tu, D. C., Moise, A. R., Bronson, D., Possin, D., Van Gelder, R. N., Baehr, W., and Palczewski, K. (2004) Lecithin-retinol acyltransferase is essential for accumulation of all-trans-retinyl esters in the eye and in the liver *J Biol Chem* ***279***, 10422–32.

109. Batten, M. L., Imanishi, Y., Tu, D. C., Doan, T., Zhu, L., Pang, J., Glushakova, L., Moise, A. R., Baehr, W., Van Gelder, R. N., Hauswirth, W. W., Rieke, F., and Palczewski, K. (2005) Pharmacological and rAAV gene therapy rescue of visual functions in a blind mouse model of Leber congenital amaurosis *PLoS Med* ***2***, e333.

110. Incerti, B., Cortese, K., Pizzigoni, A., Surace, E. M., Varani, S., Coppola, M., Jeffery, G., Seeliger, M., Jaissle, G., Bennett, D. C., Marigo, V., Schiaffino, M. V., Tacchetti, C., and Ballabio, A. (2000) Oa1 knock-out: new insights on the pathogenesis of ocular albinism type 1 *Hum Mol Genet* ***9***, 2781–8.

111. Surace, E. M., Domenici, L., Cortese, K., Cotugno, G., Di Vicino, U., Venturi, C., Cellerino, A., Marigo, V., Tacchetti, C., Ballabio, A., and Auricchio, A. (2005) Amelioration of both functional and morphological abnormalities in the retina of a mouse model of ocular albinism following AAV-mediated gene transfer *Mol Ther* ***12***, 652–8.

112. Gargiulo, A., Bonetti, C., Montefusco, S., Neglia, S., Di, V. U., Marrocco, E., Corte, M. D., Domenici, L., Auricchio, A., and Surace, E. M. (2009) AAV-mediated tyrosinase gene transfer restores melanogenesis and retinal function in a model of oculo-cutaneous albinism type I (OCA1) *Mol. Ther* ***17***, 1347–1354.

113. Smith, A. J., Schlichtenbrede, F. C., Tschernutter, M., Bainbridge, J. W., Thrasher, A. J., and Ali, R. R. (2003) AAV-Mediated gene transfer slows photoreceptor loss in the RCS rat model of retinitis pigmentosa *Mol. Ther.* ***8***, 188–195.

114. Jomary, C., Vincent, K. A., Grist, J., Neal, M. J., and Jones, S. E. (1997) Rescue of photoreceptor function by AAV-mediated gene transfer in a mouse model of inherited retinal degeneration *Gene Ther* ***4***, 683–90.

115. Chang, B., Hawes, N. L., Pardue, M. T., German, A. M., Hurd, R. E., Davisson, M. T., Nusinowitz, S., Rengarajan, K., Boyd, A. P., Sidney, S. S., Phillips, M. J., Stewart, R. E., Chaudhury, R., Nickerson, J. M., Heckenlively, J. R., and Boatright, J. H. (2007) Two mouse retinal degenerations caused by missense mutations in the beta-subunit of rod cGMP phosphodiesterase gene *Vision Res.* ***47***, 624–633.

116. Pang, J. J., Boye, S. L., Kumar, A., Dinculescu, A., Deng, W., Li, J., Li, Q., Rani, A., Foster, T. C., Chang, B., Hawes, N. L., Boatright, J. H., and Hauswirth, W. W. (2008) AAV-mediated gene therapy for retinal degeneration in the

rd10 mouse containing a recessive PDEbeta mutation *Invest Ophthalmol. Vis. Sci.* ***49***, 4278–4283.

117. Chang, B., Dacey, M. S., Hawes, N. L., Hitchcock, P. F., Milam, A. H., Atmaca-Sonmez, P., Nusinowitz, S., and Heckenlively, J. R. (2006) Cone photoreceptor function loss-3, a novel mouse model of achromatopsia due to a mutation in Gnat2 *Invest Ophthalmol Vis Sci* ***47***, 5017–21.
118. Seddon, J. M., Hampson, E. C., Smith, R. I., and Hughes, I. P. (2006) Genetic heterogeneity of day blindness in Alaskan Malamutes *Anim Genet.* ***37***, 407–410.
119. Komaromy, A. M., Alexander, J. J., Chiodo, V., Garcia, M. M., Tanaka, J. C., Craft, C. M., Acland, G. M., Hauswirth, W. W., and Aguirre, G. D. (2008) Longterm rescue of cone function in a canine model of achromatopsia by AAV mediated gene therapy ARVO presentation (Association of Research in Vision and Ophthalmology, 2008 annual meeting) April 28th, Fort Lauderdale
120. Haire, S. E., Pang, J., Boye, S. L., Sokal, I., Craft, C. M., Palczewski, K., Hauswirth, W. W., and Semple-Rowland, S. L. (2006) Light-driven cone arrestin translocation in cones of postnatal guanylate cyclase-1 knockout mouse retina treated with AAV-GC1 *Invest Ophthalmol Vis Sci* ***47***, 3745–53.
121. Tan, M. H., Smith, A. J., Pawlyk, B., Xu, X., Liu, X., Bainbridge, J. B., Basche, M., McIntosh, J., Tran, H. V., Nathwani, A., Li, T., and Ali, R. R. (2009) Gene therapy for retinitis pigmentosa and Leber congenital amaurosis caused by defects in AIPL1: effective rescue of mouse models of partial and complete Aipl1 deficiency using AAV2/2 and AAV2/8 vectors *Hum Mol. Genet.* ***18***, 2099–2114.
122. Sun, X., Pawlyk, B., Xu, X., Liu, X., Bulgakov, O. V., Adamian, M., Sandberg, M. A., Khani, S. C., Tan, M. H., Smith, A. J., Ali, R. R., and Li, T. (2011) Gene therapy with a promoter targeting both rods and cones rescues retinal degeneration caused by AIPL1 mutations *Gene Ther 17*, 117–131.
123. Weng, J., Mata, N. L., Azarian, S. M., Tzekov, R. T., Birch, D. G., and Travis, G. H. (1999) Insights into the function of Rim protein in photoreceptors and etiology of Stargardt's disease from the phenotype in abcr knockout mice *Cell* ***98***, 13–23.
124. Radu, R. A., Mata, N. L., Bagla, A., and Travis, G. H. (2004) Light exposure stimulates formation of A2E oxiranes in a mouse model of Stargardt's macular degeneration *Proc. Natl. Acad. Sci. U. S. A* ***101***, 5928–5933.
125. Allocca, M., Doria, M., Petrillo, M., Colella, P., Garcia-Hoyos, M., Gibbs, D., Kim, S. R., Maguire, A., Rex, T. S., Di, V. U., Cutillo, L., Sparrow, J. R., Williams, D. S., Bennett, J., and Auricchio, A. (2008) Serotype-dependent packaging of large genes in adeno-associated viral vectors results in effective gene delivery in mice *J. Clin. Invest* ***118***, 1955–1964.
126. Pawlyk, B. S., Smith, A. J., Buch, P. K., Adamian, M., Hong, D. H., Sandberg, M. A., Ali, R. R., and Li, T. (2005) Gene replacement therapy rescues photoreceptor degeneration in a murine model of Leber congenital amaurosis lacking RPGRIP *Invest Ophthalmol Vis Sci* ***46***, 3039–45.
127. Ali, R. R., Sarra, G. M., Stephens, C., Alwis, M. D., Bainbridge, J. W., Munro, P. M., Fauser, S., Reichel, M. B., Kinnon, C., Hunt, D. M., Bhattacharya, S. S., and Thrasher, A. J. (2000) Restoration of photoreceptor ultrastructure and function in retinal degeneration slow mice by gene therapy *Nat Genet* ***25***, 306–10.
128. Schlichtenbrede, F. C., da, C. L., Stephens, C., Smith, A. J., Georgiadis, A., Thrasher, A. J., Bainbridge, J. W., Seeliger, M. W., and Ali, R. R. (2003) Long-term evaluation of retinal function in Prph2Rd2/Rd2 mice following AAV-mediated gene replacement therapy *J. Gene Med.* ***5***, 757–764.
129. Sarra, G. M., Stephens, C., De, A. M., Bainbridge, J. W., Smith, A. J., Thrasher, A. J., and Ali, R. R. (2001) Gene replacement therapy in the retinal degeneration slow (rds) mouse: the effect on retinal degeneration following partial transduction of the retina *Hum. Mol. Genet.* ***10***, 2353–2361.
130. Schlichtenbrede, F. C., Smith, A. J., Bainbridge, J. W., Thrasher, A. J., Salt, T. E., and Ali, R. R. (2004) Improvement of neuronal visual responses in the superior colliculus in Prph2(Rd2/Rd2) mice following gene therapy *Mol Cell Neurosci* ***25***, 103–10.
131. Gehrig, A. E., Warneke-Wittstock, R., Sauer, C. G., and Weber, B. H. (1999) Isolation and characterization of the murine X-linked juvenile retinoschisis (Rs1h) gene *Mamm. Genome* ***10***, 303–307.
132. Zeng, Y., Takada, Y., Kjellstrom, S., Hiriyanna, K., Tanikawa, A., Wawrousek, E., Smaoui, N., Caruso, R., Bush, R. A., and Sieving, P. A. (2004) RS-1 Gene Delivery to an Adult Rs1h Knockout Mouse Model Restores ERG b-Wave with Reversal of the Electronegative Waveform of X-Linked Retinoschisis *Invest Ophthalmol Vis Sci* ***45***, 3279–85.
133. Kjellstrom, S., Bush, R. A., Zeng, Y., Takada, Y., and Sieving, P. A. (2007) Retinoschisin gene therapy and natural history in the

Rs1h-KO mouse: long-term rescue from retinal degeneration *Invest Ophthalmol Vis Sci* ***48***, 3837–45.

134. Takada, Y., Vijayasarathy, C., Zeng, Y., Kjellstrom, S., Bush, R. A., and Sieving, P. A. (2008) Synaptic pathology in retinoschisis knockout (Rs1-/y) mouse retina and modification by rAAV-Rs1 gene delivery *Invest Ophthalmol Vis. Sci.* ***49***, 3677–3686.
135. Min, S. H., Molday, L. L., Seeliger, M. W., Dinculescu, A., Timmers, A. M., Janssen, A., Tonagel, F., Tanimoto, N., Weber, B. H., Molday, R. S., and Hauswirth, W. W. (2005) Prolonged recovery of retinal structure/function after gene therapy in an Rs1h-deficient mouse model of x-linked juvenile retinoschisis *Mol Ther* ***12***, 644–51.
136. Janssen, A., Min, S. H., Molday, L. L., Tanimoto, N., Seeliger, M. W., Hauswirth, W. W., Molday, R. S., and Weber, B. H. (2008) Effect of late-stage therapy on disease progression in AAV-mediated rescue of photoreceptor cells in the retinoschisin-deficient mouse *Mol. Ther* ***16***, 1010–1017.
137. Dryja, T. P., Hahn, L. B., Cowley, G. S., McGee, T. L., and Berson, E. L. (1991) Mutation spectrum of the rhodopsin gene among patients with autosomal dominant retinitis pigmentosa *Proc Natl Acad Sci U S A* ***88***, 9370–4.
138. Kennan, A., Aherne, A., Palfi, A., Humphries, M., McKee, A., Stitt, A., Simpson, D. A., Demtroder, K., Orntoft, T., Ayuso, C., Kenna, P. F., Farrar, G. J., and Humphries, P. (2002) Identification of an IMPDH1 mutation in autosomal dominant retinitis pigmentosa (RP10) revealed following comparative microarray analysis of transcripts derived from retinas of wild-type and Rho(-/-) mice *Hum Mol. Genet.* ***11***, 547–557.
139. Lewin, A. S. and Hauswirth, W. W. (2001) Ribozyme gene therapy: applications for molecular medicine *Trends Mol Med 7*, 221–8.
140. Lewin, A. S., Drenser, K. A., Hauswirth, W. W., Nishikawa, S., Yasumura, D., Flannery, J. G., and LaVail, M. M. (1998) Ribozyme rescue of photoreceptor cells in a transgenic rat model of autosomal dominant retinitis pigmentosa *Nat Med* ***4***, 967–71.
141. LaVail, M. M., Yasumura, D., Matthes, M. T., Drenser, K. A., Flannery, J. G., Lewin, A. S., and Hauswirth, W. W. (2000) Ribozyme rescue of photoreceptor cells in P23H transgenic rats: long-term survival and late-stage therapy *Proc Natl Acad Sci U S A 97*, 11488–93.
142. Gorbatyuk, M. S., Pang, J. J., Thomas, J., Jr., Hauswirth, W. W., and Lewin, A. S. (2005) Knockdown of wild-type mouse rhodopsin using an AAV vectored ribozyme as part of an RNA replacement approach *Mol Vis* ***11***, 648–56.
143. Gorbatyuk, M., Justilien, V., Liu, J., Hauswirth, W. W., and Lewin, A. S. (2007) Preservation of photoreceptor morphology and function in P23H rats using an allele independent ribozyme *Exp Eye Res* ***84***, 44–52.
144. Tessitore, A., Parisi, F., Denti, M. A., Allocca, M., Di Vicino, U., Domenici, L., Bozzoni, I., and Auricchio, A. (2006) Preferential silencing of a common dominant rhodopsin mutation does not inhibit retinal degeneration in a transgenic model *Mol Ther* ***14***, 692–9.
145. Gorbatyuk, M., Justilien, V., Liu, J., Hauswirth, W. W., and Lewin, A. S. (2007) Suppression of mouse rhodopsin expression in vivo by AAV mediated siRNA delivery *Vision Res* ***47***, 1202–8.
146. O'Reilly, M., Palfi, A., Chadderton, N., Millington-Ward, S., Ader, M., Cronin, T., Tuohy, T., Auricchio, A., Hildinger, M., Tivnan, A., McNally, N., Humphries, M. M., Kiang, A. S., Humphries, P., Kenna, P. F., and Farrar, G. J. (2007) RNA interference-mediated suppression and replacement of human rhodopsin in vivo *Am J Hum Genet* ***81***, 127–35.
147. Chadderton, N., Millington-Ward, S., Palfi, A., O'Reilly, M., Tuohy, G., Humphries, M. M., Li, T., Humphries, P., Kenna, P. F., and Farrar, G. J. (2009) Improved retinal function in a mouse model of dominant retinitis pigmentosa following AAV-delivered gene therapy *Mol. Ther* ***17***, 593–599.
148. Palczewski, K. (2006) G protein-coupled receptor rhodopsin *Annu. Rev. Biochem.* ***75***, 743–767.
149. O'Reilly, M., Millington-Ward, S., Palfi, A., Chadderton, N., Cronin, T., McNally, N., Humphries, M. M., Humphries, P., Kenna, P. F., and Farrar, G. J. (2007) A transgenic mouse model for gene therapy of rhodopsin-linked Retinitis Pigmentosa *Vision Res* ***48***, 386–391.
150. Palfi, A., Millington-Ward, S., Chadderton, N., O'Reilly, M., Goldmann, T., Humphries, M. M., Wolfrum, U., Humphries, P., Kenna, P. F., and Farrar, G. J. (2011) AAV-Mediated Rhodopsin Replacement Provides Therapeutic Benefit in Mice with a Targeted Disruption of the Rhodopsin Gene *Hum Gene Ther 21*, 311–323.
151. Tam, L. C., Kiang, A. S., Kennan, A., Kenna, P. F., Chadderton, N., Ader, M., Palfi, A., Aherne, A., Ayuso, C., Campbell, M., Reynolds, A., McKee, A., Humphries, M. M.,

Farrar, G. J., and Humphries, P. (2008) Therapeutic benefit derived from RNAi-mediated ablation of IMPDH1 transcripts in a murine model of autosomal dominant retinitis pigmentosa (RP10) *Hum. Mol. Genet.* ***17***, 2084–2100.

152. Jacobson, S. G., Aleman, T. S., Cideciyan, A. V., Sumaroka, A., Schwartz, S. B., Windsor, E. A., Traboulsi, E. I., Heon, E., Pittler, S. J., Milam, A. H., Maguire, A. M., Palczewski, K., Stone, E. M., and Bennett, J. (2005) Identifying photoreceptors in blind eyes caused by RPE65 mutations: Prerequisite for human gene therapy success *Proc. Natl. Acad. Sci. U. S. A* ***102***, 6177–6182.
153. Maguire, A. M., High, K. A., Auricchio, A., Wright, J. F., Pierce, E. A., Testa, F., Mingozzi, F., Bennicelli, J. L., Ying, G. S., Rossi, S., Fulton, A., Marshall, K. A., Banfi, S., Chung, D. C., Morgan, J. I., Hauck, B., Zelenaia, O., Zhu, X., Raffini, L., Coppieters, F., De, B. E., Shindler, K. S., Volpe, N. J., Surace, E. M., Acerra, C., Lyubarsky, A., Redmond, T. M., Stone, E., Sun, J., McDonnell, J. W., Leroy, B. P., Simonelli, F., and Bennett, J. (2009) Age-dependent effects of RPE65 gene therapy for Leber's congenital amaurosis: a phase 1 dose-escalation trial *Lancet* ***374***, 1597–1605.
154. Cideciyan, A. V., Hauswirth, W. W., Aleman, T. S., Kaushal, S., Schwartz, S. B., Boye, S. L., Windsor, E. A., Conlon, T. J., Sumaroka, A., Pang, J. J., Roman, A. J., Byrne, B. J., and Jacobson, S. G. (2009) Human RPE65 gene therapy for Leber congenital amaurosis: persistence of early visual improvements and safety at 1 year *Hum Gene Ther* ***20***, 999–1004.
155. Cideciyan, A. V., Hauswirth, W. W., Aleman, T. S., Kaushal, S., Schwartz, S. B., Boye, S. L., Windsor, E. A., Conlon, T. J., Sumaroka, A., Roman, A. J., Byrne, B. J., and Jacobson, S. G. (2009) Vision 1 year after gene therapy for Leber's congenital amaurosis *N. Engl. J. Med.* ***361***, 725–727.
156. Simonelli, F., Maguire, A. M., Testa, F., Pierce, E. A., Mingozzi, F., Bennicelli, J. L., Rossi, S., Marshall, K., Banfi, S., Surace, E. M., Sun, J., Redmond, T. M., Zhu, X., Shindler, K. S., Ying, G. S., Ziviello, C., Acerra, C., Wright, J. F., McDonnell, J. W., High, K. A., Bennett, J., and Auricchio, A. (2010) Gene Therapy for Leber's Congenital Amaurosis is Safe and Effective Through 1.5 Years After Vector Administration *Mol. Ther* *18*, 643–650.
157. Hauswirth, W. W., Aleman, T. S., Kaushal, S., Cideciyan, A. V., Schwartz, S. B., Wang, L., Conlon, T. J., Boye, S. L., Flotte, T. R., Byrne, B. J., and Jacobson, S. G. (2008) Treatment of leber congenital amaurosis due to RPE65 mutations by ocular subretinal injection of adeno-associated virus gene vector: short-term results of a phase I trial *Hum. Gene Ther.* ***19***, 979–990.

Chapter 9

Adeno-Associated Virus Vector Delivery to the Heart

Lawrence T. Bish, H. Lee Sweeney, Oliver J. Müller, and Raffi Bekeredjian

Abstract

Cardiac gene transfer may serve as a novel therapeutic approach in the treatment of heart disease. For it to reach its full potential, methods for highly efficient cardiac gene transfer must be available to investigators so that informative preclinical data can be collected and evaluated. We have recently optimized AAV-mediated cardiac gene transfer protocols in both the mouse and rat. In the mouse, we have developed a procedure for intrapericardial delivery of vector in the neonate and successfully applied intravenous injections in adult animals. In the rat, we have developed a procedure for direct injection of vector into the myocardium in adults and established a protocol for vector delivery into the left ventricular anterior wall by ultrasound-targeted destruction of microbubbles loaded with AAV. Each protocol can be used to achieve safe and efficient cardiac gene transfer in the model of choice.

Key words: Heart, Gene therapy, Adeno-associated virus, AAV, Animal model, Microbubbles, Ultrasound

1. Introduction

The highly efficient and stable gene transfer mediated by AAV makes it ideal for use as a cardiac gene transfer vector since most cardiac diseases follow a chronic course. Indeed, AAV-mediated cardiac gene transfer has been discussed in several recent reviews which highlight its broad application in animal models of heart failure (1–3). The most common application of AAV in heart failure involves modulation of calcium cycling. Investigators have successfully blocked the progression of heart failure using AAV-mediated cardiac gene transfer of the following calcium cycling proteins in various animal models: dominant negative phospholamban (dnPLB) in a delta sarcoglycan knock out hamster model of dilated cardiomyopathy (DCM) (4), in a rat model of ischemic cardiomyopathy via coronary artery ligation (5), and in a sheep model of

Richard O. Snyder and Philippe Moullier (eds.), *Adeno-Associated Virus: Methods and Protocols*,
Methods in Molecular Biology, vol. 807, DOI 10.1007/978-1-61779-370-7_9,

pacing induced cardiomyopathy (6); SERCA2a in a rat model of pressure overload cardiomyopathy via aortic banding (7) and in a porcine model of volume overload failure induced by mitral valve impairment (8); and S100A1 in a rat model of ischemic cardiomyopathy via coronary artery ligation (9). AAV-mediated cardiac gene transfer has also been used successfully to block apoptosis by the overexpression of genes such as TGF-β (10) and heme oxygenase-1 (11, 12) in a rat model of ischemia–reperfusion injury; to induce angiogenesis by the overexpression of VEGF (13) or the combination of VEGF and angiopoietin-1 (14) in a mouse model of ischemic cardiomyopathy, or by the overexpression of IGF-1 in a rat model of ischemic cardiomyopathy (15); and to downregulate coxsackievirus B3 RNA polymerase by RNA interference in a mouse model of viral cardiomyopathy. Finally, AAV-mediated cardiac gene therapy has been successfully used to correct monogenic defects in several mouse models of inherited diseases in which cardiomyopathy is part of the phenotype, including the mdx model of Duchenne muscular dystrophy (16); the delta sarcoglycan knockout model of limb girdle muscular dystrophy (17); the alpha galactosidase A knock-out model of Fabry disease (18); the acid alpha-glucosidase knock out model of Pompe disease (19); and the very long chain acyl Co-A dehydrogenase (VLCAD) knock-out model of VLCAD deficiency (20).

To achieve the successful cardiac gene transfer described above, investigators have employed a variety of delivery methods, each with its own advantages and disadvantages. Direct intramyocardial injection following left thoracotomy has been described in both mouse (13, 14) and rat (21) models. This method allows the investigator to localize gene delivery to the region of the myocardium where expression is desired with minimal systemic vector exposure. Delivery is also independent of coronary flow; therefore, it is especially useful in models of heart failure in which blood flow to the target area is compromised, such as in ischemic cardiomyopathy. Disadvantages include the requirements for invasive surgery and multiple injections. Another common delivery method, described in both the hamster (4) and the rat (5, 7, 9), is intracoronary delivery via aortic root injection. This method allows efficient, global gene transfer, but also requires invasive surgery and the use of potentially dangerous vasodilators. It is also dependent on coronary flow and is associated with high systemic exposure of vector. A final common delivery method is intravenous injection, which has been described almost exclusively in mouse models (22–25). This minimally invasive procedure can be used to achieve efficient global cardiac gene transfer but is dependent on coronary flow and associated with high levels of systemic vector exposure. Methods for cardiac AAV delivery in large animal models have been recently reviewed (26) and described in detail elsewhere (27, 28); therefore, this chapter focuses on AAV vector delivery in the mouse and rat heart.

In this chapter, we describe two methods for vector delivery to the mouse heart and two methods for vector delivery to the rat heart. Since we and others have demonstrated that AAV9 is the most cardiotropic serotype in the mouse and rat (21–23, 25, 29, 30), we recommend the use of AAV9 over serotypes 1–8. This will maximize transgene expression and minimize the likelihood that the potential efficacy of the gene being evaluated will be underestimated or missed altogether.

The first method for cardiac AAV delivery in the mouse involves intrapericardial injection of vector in neonates using a closed-chest, subxiphoid approach (30, 31). Since mice are injected as neonates, this procedure can be used as a simple alternative to the creation of cardiac-specific transgenic or knock-out (using shRNA (32)) lines. This would be especially useful in the case of a gene whose manipulation during embryonic development produces a lethal phenotype. Alternatively, this gene transfer technique could be used to screen potentially therapeutic transgenes in many of the widely available mouse models of cardiac disease to identify candidates for large animal trials. Finally, by using the high vector dose, one could simultaneously treat both the heart and diaphragm, a technique that may prove useful in the mdx mouse model of Duchenne muscular dystrophy (33).

The second method for cardiac AAV delivery in the mouse utilizes intravenous injection into the tail vein of adult mice (17, 34). Due to their high efficiency for myocardial transduction in adult mice upon systemic administration (22, 23, 25, 29), AAV9 vectors allow the evaluation of preclinical gene therapy approaches in mice by a simple intravenous injection. Since systemic transfer of AAV9 vectors also results in a significant transduction of other organs, tissue-specific promoters can be used for transcriptional targeting (9, 34).

The first method for cardiac AAV delivery in the rat involves direct injection of vector into the left ventricular free wall of adult animals following left thoracotomy (30). Use of rat models is important because, as larger animals, rats offer the opportunity to evaluate potentially therapeutic genes in a more clinically relevant model. For example, it is technically more feasible to create models of ischemic cardiomyopathy via coronary artery ligation or models of pressure overload cardiomyopathy via aortic banding in the rat than in the mouse, and these rat models are well established in the literature (7, 9). Use of our technique facilitates highly efficient gene transfer in these models that is independent of coronary flow.

The second method for cardiac AAV delivery in the rat utilizes ultrasound-targeted destruction of intravenously infused microbubbles loaded with AAV. Ultrasound-targeted microbubble destruction (UTMD) has evolved as an additional tool to augment site-specific gene transfer using various target organs or vector types. The first application in the heart was performed using

β-galactosidase encoding adenovirus (35). Further studies demonstrated its applicability for plasmid transfection (36, 37). More recently, we could demonstrate augmentation of cardiac AAV-transduction using UTMD (38).

The effects of UTMD are based upon physical properties of such microbubbles. These consist of a gas filled core and a stabilizing shell (mostly phospholipid or albumin). Microbubbles are traditionally used as ultrasound contrast agents, since they can reflect ultrasound. In addition, microbubbles may oscillate in an ultrasound field when sonified with ultrasound of their resonance frequency. These oscillations may lead to microbubble destruction. Two different mechanisms are mainly responsible for their effectiveness in gene transfer. First, the gene therapy vector loaded on microbubbles can be released by UTMD with high local concentrations in the target organ. Second, the destruction of microbubbles may transiently increase capillary and cell membrane permeability (39, 40), thus augmenting transduction. Their small size (about 2 μm) allows intravenous administration, since they will pass the pulmonary circulation and reach the systemic circulation. Due to the size of the ultrasound probe and the ultrasound focus, this technique is mainly to be used for animals at least of the size of rats. The protocol described below is designed for rat applications (minimum 150 g). (Adapted, in part, from Bish et al. (30).)

2. Materials

2.1. Mouse Protocol #1: Intrapericardial Injection in Neonatal Mice

1. Hamilton Gastight 250 μL glass syringe, series 1725TLL. (Hamilton Company, Reno, Nevada).
2. Hamilton 33-gauge needle. (Hamilton Company, Reno, Nevada).
3. Saint Gobain Tygon microbore tubing, Formula S-54-HL (inner diameter: 0.51 mm, wall thickness: 0.51 mm, outer diameter: 1.53 mm; Saint Gobain Performance Plastics, Akron, OH).
4. Single-stranded adeno-associated virus 9 (ssAAV9) vector. Prior to dilution, vector can be stored at −80°C for >6 months, or at 4°C for up to 6 months.
5. Normal saline (sterile).

2.2. Mouse Protocol #2: Intravenous Injection into Adult Mice

1. Mouse restrainer (e.g. Indulab AG, Gams, Switzerland).
2. 27–30-gauge needle.
3. U-100 insulin syringe.
4. Heating lamp (alternatively warm water for soaking the tail).
5. Sterile gauze with 70% ethanol.
6. AAV9 vector solution (in PBS or Iodixanol (≤40%)).

2.3. Rat Protocol #1: Direct Injection into Myocardium of Left Ventricle

1. Anesthesia and perioperative medications: Preoperative analgesia (buprenorphine 0.05 mg/kg subcutaneous injection), induction (ketamine 50–100 mg/kg, xylazine 5–10 mg/kg (intraperitoneal injection)), maintenance (isoflurane 1%), postoperative analgesia (buprenorphine 0.05 mg/kg subcutaneous injection at 4 and 12 h following surgery), antibiotic prophylaxis (cefazolin 20 mg/kg subcutaneous injection prior to skin incision and at 4 and 12 h following surgery).
2. Suture: 4–0 Maxon (Covidien Syneture, Mansfield, MA), 4–0 Vicryl, 5–0 Vicryl, 7–0 Prolene (Ethicon, Somerville, NJ).
3. Otoscope for intubation.
4. Rodent Work Stand for intubation (Hallowell EMC, Pittsfield, MA).
5. Rat intubation pack containing intubation speculum, endotracheal intubation tubes, an endotracheal tube guide wire, an incisor loop, and a brief video tutorial of how to perform the intubations (Hallowell EMC, Pittsfield, MA).
6. 18-gauge angiocath (1.88 in. length).
7. Rodent Anesthesia Workstation, including rodent ventilator and isoflurane vaporizer (available fully assembled with all necessary accessories from Systems Specialties, Inc, Warminster, PA).
8. Recovery ventilator (optional): Model 141 (NEMI Scientific, Medfield, MA) (see Note 1).
9. Standard surgical instrument pack, sterile drapes, sterile gowns, sterile gloves.
10. Chlorhexidine 2% surgical scrub.
11. 0.5 mL insulin syringe with 28-gauge needle, 0.5 in. length.
12. Single-stranded adeno-associated virus 9 (ssAAV9) vector diluted to a final volume of 250 μL containing 5×10^{11} genome copies (gc) (concentration: 2×10^{12} gc/mL), in sterile normal saline. Prior to dilution, vector can be stored at −80°C for >6 months, or at 4°C for up to 6 months.

2.4. Rat Protocol #2: Ultrasound Targeted Microbubble Destruction for Cardiac AAV Delivery

1. Diagnostic ultrasound machine with the ability to perform myocardial contrast echocardiography in a triggered mode, such as a Sonos 5500, Philips, Eindhoven, The Netherlands.
2. Standard ultrasound gel.
3. Self-adhesive EKG-electrodes that fit to the EKG-cables of the ultrasound machine.
4. Support stand with a clamp to hold the ultrasound transducer.
5. Intraperitoneal anesthesia for rats, e.g., 100 mg/kg body weight ketamine, 5 mg/kg bodyweight xylazine.
6. A perfluorcarbon gas, such as octafluorpropane.

7. Amalgamator (e.g., Capmix; 3M, St. Paul, MN).
8. Phosphate-buffered saline (PBS).
9. DL-α-Phosphatidylcholine, Dipalmitolyl.
10. DL-α-Phosphatidylethanolamine, Dipalmitolyl.
11. Glucose.
12. Sterile gauze.
13. Alcohol spray (for skin).
14. 18-gauge needle.
15. 25-gauge needle.
16. Luer Stub Adapter 23 gauge (alternatively 23-gauge needle).
17. 6–0 silk suture.
18. 4–0 silk suture with needle.
19. Polyethylene tubing PE50 (e.g., BD Intramedic™ Polyethylene Tubing, Becton Dickinson, Franklin Lakes, NJ).
20. Depilation cream.
21. 3 mL sterile syringe.
22. Precision infusion pump (e.g., Genie – Kent Scientific Corporation, Torrington, CT, USA).
23. Small surgical blunt forceps (about 15 cm).
24. Vannas Scissors Curved 80 mm.
25. Needle holder.
26. Surgical scissors.
27. Curved clamp (about 15 cm).
28. AAV6 or AAV9-vector (maximum amount 200 μL vector solution per preparation).

3. Methods

All animal studies must follow National Institute of Health Guidelines (*Guide for the Care and Use of Laboratory Animals*, NIH publication No. 85–23, revised 1996) and be approved by the appropriate Institutional Animal Care and Use Committee.

3.1. Mouse Protocol #1: Intrapericardial Injection in Neonatal Mice

1. Breed mice so that 4–5-day-old pups will be available for injection (see Note 2).
2. On day of injection, prepare AAV vector by diluting AAV vector stock to a final concentration of 5×10^{12} genome copies per mL (gc/mL) with sterile normal saline (see Note 3 for additional information on dosing). Prepare sufficient diluted

vector to allow for a 50-μL injection per pup as well as an additional 100 μL to account for losses during preparation and injection. Keep diluted virus on ice until injection.

3. Thread Tygon tubing over the 33-gauge Hamilton needle to be used for injection. Cut the tubing such that 3 mm of the needle are left exposed (see Note 4).
4. Immediately prior to injection, remove pups from their mother, and place on ice for approximately 2–3 min to induce cryoanesthesia. The pups will become lethargic, but their activity will not completely cease.
5. While the pups are on ice, attach the 25-gauge needle to the Hamilton syringe, and withdraw sufficient vector for injection. Multiple doses can be drawn up at the same time.
6. Remove the 25-gauge needle, and attach the Hamilton 33 gauge needle covered with Tygon tubing (prepared in step 3) to the Hamilton syringe. Gently advance the plunger until vector is expelled to remove any air.
7. To position the animal for injection, grasp the pup by the nape of the neck (dorsally) by pinching that area of the neck between the thumb and index finger of one's nondominant hand. Rotate one's wrist so that the pup's ventral surface, including sternum, ribs, and xiphoid process, can be visualized.
8. Using one's dominant hand, insert the Hamilton 33 gauge needle at the left costo-xiphoid angle of the pup (see Note 5), and advance the needle superiorly until the Tygon tubing contacts the skin (3 mm). As the needle is advanced, it must be maintained parallel to the left sternal border (see Note 6).
9. Once the needle had been advanced 3 mm, slowly inject 50 μL of vector into the pericardial space (see Notes 7 and 8).
10. After injection, return pup to mother, and proceed with subsequent injections.
11. Schedule euthanasia based on specific study protocol (see Note 9).

3.2. Mouse Protocol #2: Intravenous Injection into Adult Mice

1. Dilute vector solution with PBS in order to enable injection of at least 100 μL per animal, maximum volume should not exceed 200–250 μL (see Note 10).
2. Draw it up into the U-100 insulin syringe, add the needle and carefully remove remaining air.
3. Allow dilation of the tail veins by placing a heating lamp above the cage or soaking the mouse tail in warm water.
4. Place the mouse into a mouse restrainer in order to avoid additional anesthesia.
5. Disinfect the tail with a sterile gauze soaked with 70% ethanol.

6. Extend the tail carefully and locate one of the two lateral veins.
7. Insert the needle tip almost parallel to one of the lateral veins and move forward into the tail vein (2–3 mm).
8. Carefully pull the plunger: flow of venous blood into the syringe confirms the location of the needle tip within the vein.
9. Slowly push the plunger, and observe the vein: if there is no resistance and blood is washed out temporarily, injection is successful and should be continued until the target volume has been injected (see Note 11).
10. Remove the needle, and slightly compress the injection site with gauze.
11. Place the mouse back in its cage, and observe it for 5 min to ensure adequate hemostasis (see Note 12).

3.3. Rat Protocol #1: Direct Injection into Myocardium of Left Ventricle

1. On day of injection, prepare AAV vector by diluting AAV vector stock to a final concentration of 2×10^{12} gc/mL with sterile normal saline (see Note 13 for additional information on dosing). Prepare sufficient diluted vector to allow for a 250-μL injection per pup as well as an additional 100 μL to account for losses during preparation and injection. Keep diluted virus on ice until injection.
2. Anesthetize an approximately 300 g adult rat by injection of the medications listed above (see Notes 14 and 15).
3. After induction, secure rat to Rodent Work Stand for intubation using incisor loop and adjustable restraints.
4. Intubate rat by using otoscope with speculum to visualize vocal cords. Use forceps to extend tongue as necessary. Pass guide wire through vocal cords, and then remove otoscope while keeping guide wire in place. Pass endotracheal tube over guide wire and into position in the trachea. Remove guide wire. Use 10 mL syringe to inflate lungs and confirm proper placement. Secure endotracheal tube in position with suture (see Note 16).
5. Connect the rat's endotracheal tube to the Anesthesia Work Station with the rat in left lateral recumbency position (see Note 17). Set O_2 flow to 2 L/min; ventilator rate to 70 beats per minute, and isoflurane to 1%.
6. Shave the surgical site; scrub the site three times with chlorhexidine solution, and drape the rat in a sterile fashion.
7. Make a 2-cm skin incision over the fourth intercostal space; divide the subcutaneous tissue and underlying muscle, and enter the thorax through the fourth intercostal space. Visualize the left phrenic nerve in its course through the pericardium, and open the pericardium without disrupting the nerve to expose the left ventricle (see Note 18).

8. Place a 7–0 Prolene suture through the apex of the left ventricle, and secure the end with a pair of hemostats. This suture will be used to manipulate the heart during injection.
9. Load insulin syringe (0.5 mL with 28 gauge, 0.5 in. needle) with 250 μL vector, and hold in dominant hand.
10. Grasp the 7–0 suture with one's nondominant hand, and manipulate the position of the heart to maximize exposure of the left ventricle for injection (see Note 19).
11. Inject the myocardium of left ventricle in five equally spaced aliquots of 50 μL. Before each injection, withdraw the plunger once the needle is in the myocardium to ensure the needle is not in a blood vessel or within in the left ventricular cavity. (There should be no blood return.) Continue to manipulate the position of the heart with the 7–0 suture as necessary (see Note 20).
12. Once injections are complete, place an 18-gauge angiocath through the skin into the thorax via the fifth or sixth intercostal space, and remove the needle. This will serve as a chest tube to restore negative intrathoracic pressure. Give a manual sigh breath from the ventilator to re-inflate the lungs completely.
13. Reapproximate the ribs with interrupted 4–0 Maxon, muscle with continuous 4–0 Vicryl, subcutaneous tissue with continuous 5–0 Vicryl, and skin with continuous, subcuticular 5–0 Vicryl.
14. Once the skin is closed, attach a 10-mL syringe to the angiocath chest tube; withdraw the plunger of the syringe until resistance is encountered, and remove the angiocath and syringe from the animal, maintaining resistance until it is completely removed.
15. If multiple procedures are being performed the same day, the rat can be moved to the optional recovery ventilator until spontaneous respirations are observed (see Note 21.)
16. Give buprenorpine and cefazolin as directed above at 4 and 12 h postsurgery.

3.4. Rat Protocol #2: Ultrasound Targeted Microbubble Destruction for Cardiac AAV Delivery

3.4.1. Preparation of Lipid Suspension (Stock Solution)

Add to 10 mL PBS

- 200 mg DL-α-Phosphatidylcholine, Dipalmitolyl (Sigma P-5911)
- 50 mg DL-α-Phosphatidylethanolamine, Dipalmitolyl (Sigma P-3275)
- 1 g Glucose

To dissolve ingredients, heat in boiling water-bath (approximately 20–30 min) and pipette up and down every 5 min until no particles are visible. This stock solution can be stored at 4°C.

3.4.2. Preparation of Microbubbles

1. Heat 250 μL of stock solution to room temperature in a 1.5 or 2 mL eppendorf tube.
2. Add 50 μL glycerol.
3. Add AAV-suspension in a total volume of less than 200 μL.
4. Add PBS to make the total volume 500 μL.
5. Replace air with Octafluoropropane gas.
6. Shake in an Amalgamator for 20 s.
7. Before infusion add 0.5 mL PBS and mix carefully.
8. Depending on the availability of suitable antibodies, successful loading of microbubbles might be visualized (see Note 22).

3.4.3. Insertion of a Catheter into the Jugular Vein

1. After anesthetizing the rat, the chest has to be depilated and the neck has to be disinfected with the alcohol spray.
2. An incision will be made (about 5 mm) with scissors anterolateral of the neck (preferably at the right side) where a pulsation is visible.
3. With the curved clamp enlarge the incision and then use the curved clamp to bluntly prepare the jugular vein.
4. Use the clamp to pull a 6–0 silk suture underneath the vein. Be careful not to twist the vein when pulling the suture through. Adding a drop of water can help.
5. Ligate the vein with a cranial suture and prepare a caudal suture to bind over the catheter later.
6. Prepare the catheter by cutting about 30 cm of the polyethylene tubing. By using an oblique position of the scissors the tip of the catheter becomes curved. A 45° angle is favorable.
7. Insert the Luer Stub Adapter 23 gauge (or alternatively 23 gauge needle) in one end and flush the catheter with saline or PBS. Be careful not to leave any air in the catheter, since low volumes of air are sufficient to kill the rat by embolization (see Note 23).
8. Insert the catheter into the jugular vein by holding the vein at the cranial suture and making a careful superficial cut with the Vannas scissors. After the incision is made, insert the catheter into the vein.
9. After insertion, proper catheter position can be verified by aspirating the syringe (blood flows back).
10. Tie the caudal suture tightly around the catheter. Now, the catheter can be connected with the infusion pump.

3.4.4. Ultrasonic Microbubble Destruction

1. After the catheter is inserted, three EKG electrodes will be attached to three paws. A drop of ultrasound gel on each electrode helps to improve EKG signal.

2. A small amount of ultrasound gel is distributed on the chest. This helps to avoid small air bubbles trapped under some hairs.
3. After localizing the heart (feeling the pulse with the finger), a large amount of gel is added on the chest to produce a stand off for the probe. Be careful to avoid air bubbles.
4. Then the S3 ultrasound probe will be clamped on the chest leaving at least 1 cm of gel between the probe and the skin. A mid short axis view is to be acquired. This is mostly possible after the contrast agent has been injected. A good quality image is crucial for efficient transfer of the AAV-microbubble solution. If the image is good, myocardium and cavity are clearly distinguishable. The following ultrasound settings apply to the Sonos 5500 (Philips):
   (a) Ultraharmonic mode (transmit 1.3 MHz)
   (b) Mechanical Index 1.6
   (c) Triggered imaging – every fourth beat – four frames of ultrasound
   (d) Delay 80 ms
   (e) All segmental gains to 0
   (f) Gain 50
   (g) Compress 75
   (h) Postprocess B
5. 1 mL of microbubbles suspension should be infused over a 15–20-min period. It is important to agitate the infusion pump regularly in order to maintain a homogeneous bubble suspension.
6. During infusion, successful infusion and destruction of microbubbles can be followed by watching the left ventricular cavity (see Notes 23 and 24). Also watch the EKG (see Note 25).
7. After finishing the experiment, the catheter is removed and the skin is closed with a 4–0 silk suture. The animal should awake within 30–60 min.
8. Depending on the experimental question, animals can be followed up for several weeks to months (see Note 26).

4. Notes

1. If multiple surgeries are to be performed on the same day, it will be useful to purchase 1–2 ventilators that will be used solely for recovery. This will allow the next surgery to start

immediately following skin closure of the previous surgery, without the need to wait for return of spontaneous respiration. These ventilators are less expensive than the Anesthesia Workstation since they are not equipped with isoflurane vaporizes.

2. It is important to use neonatal mice on days 4–5 of life. The parietal pericardium in neonatal mice is a continuous serous membrane that lacks pericardial pores until day 6 (41). The lack of pericardial pores favors the containment of vector in the pericardial space.
3. We have previously published the dose–response relationship for AAV9-mediated expression of LacZ in the murine heart using this method (30). At a dose of 2.5×10^{11} gc per pup (50 μL of 5×10^{12} gc/mL), high level expression of transgene was observed almost entirely throughout the heart and diaphragm with minimal expression in the liver. At a lower dose of 2.5×10^{10} gc per pup (50 μL of 5×10^{11} gc/mL), high level transgene expression was still observed in the heart, but with only minimal expression in the diaphragm and liver (see Fig. 1).
4. The Tygon tubing will create a hub at 3 mm, which will prevent advancement of the needle into the myocardium or left ventricular cavity and allow the investigator to maintain the needle easily in the pericardial space for injection. It is critical for global cardiac gene transfer that the vector be injected into the pericardial space and not the myocardium or left ventricular cavity.
5. The point at which the most inferior rib meets the xiphoid process of the sternum on the left side (left costoxiphoid angle) can be easily visualized in the neonatal mouse on days 4–5 of life.

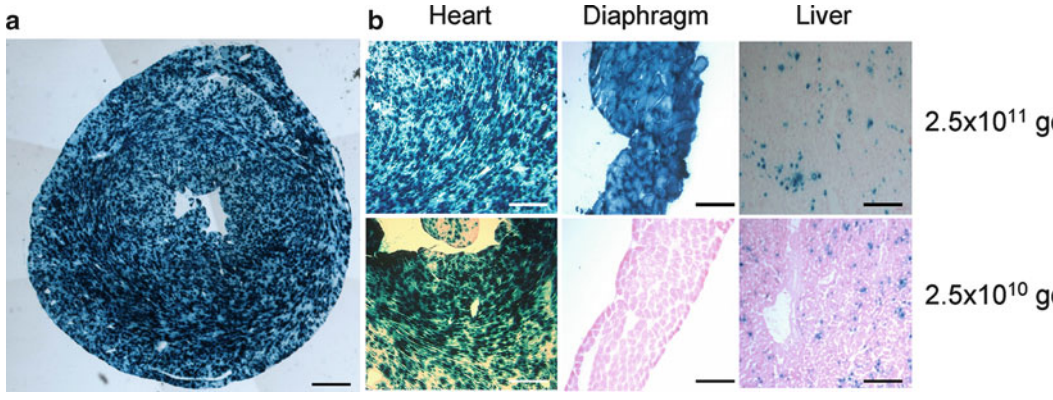

Fig. 1. Representative photomicrographs of sections from mouse heart, diaphragm, and liver 6 weeks following intrapericardial injection of 50 μL AAV9-CB-LacZ. (**a**) Low magnification photomicrograph of the heart depicting global transgene expression after injection of 2.5×10^{11} gc. Scale bar: 1 mm. (**b**) Photomicrographs of heart, diaphragm, and liver after receiving either 2.5×10^{11} or 2.5×10^{10} gc of vector. Scale bar: 200 μm. Sections have been stained with X-gal and counterstained with eosin. CB: chicken beta actin promoter with cytomegalovirus enhancer. Adapted from Bish et al. (30).

6. The murine pericardium is extensively attached to the sternum to form a pericardial cavity rather than a true sac, thus allowing easy access via this subxiphoid approach without a thoracotomy (42). At the time of injection, the needle will be positioned beneath the sternum and anterior to the heart in the pericardial space.
7. It is critical to inject the vector solution slowly as we have frequently experienced a delayed response time when using a Hamilton 33-gauge needle. This will help to avoid overinjection and/or loss of vector. New investigators may consider injecting saline into several control pups to become familiar with the Hamilton needle and syringe prior to working with vector.
8. The injection volume of 50 μL has been optimized previously. Larger volumes have been associated with increased mortality (31). In our experience, mortality is extremely rare with the 50 μL injection.
9. We have observed transgene expression from 1 week to 1 year using this protocol (see Fig. 2).
10. Take care that all experimental groups are injected with the same volume and – in case of vector solutions containing iodixanol – the same concentration of iodixanol (≤40%).
11. Observation of a subcutaneous prominence during injection or immediately thereafter indicates an extravasation and thus an at least incomplete intravenous injection. Therefore, animals should not be further used within the study. This might especially occur when using vectors in 40% iodixanol (high viscosity). Dilution of the vector solution in PBS might help.
12. In case of murine heart failure models, the injected amount of vector should be as small as possible. Furthermore, observation of respiration or activity for an extended period is suggested.
13. We have previously identified the minimum dose required for high level, AAV9-mediated expression of LacZ in the rat heart using this method (30). At a dose of 5×10^{11} gc per rat (250 μL of 2×10^{12} gc/mL), high level expression of transgene was

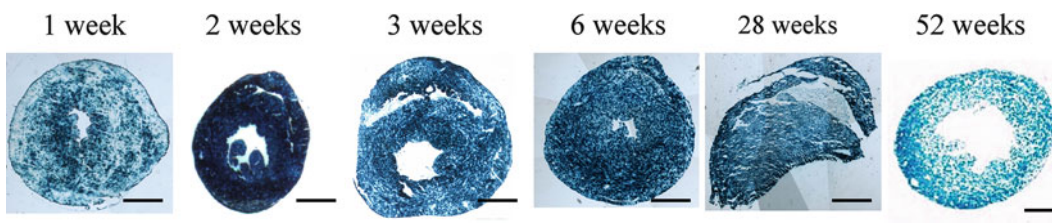

Fig. 2. Time course of LacZ expression following intrapericardial injection of 50 μL containing 2.5×10^{11} gc of AAV9-CB-LacZ. Representative photomicrographs have been stained with X-gal and counterstained with eosin. Scale bar: 1 mm. Adapted from Bish et al. (30).

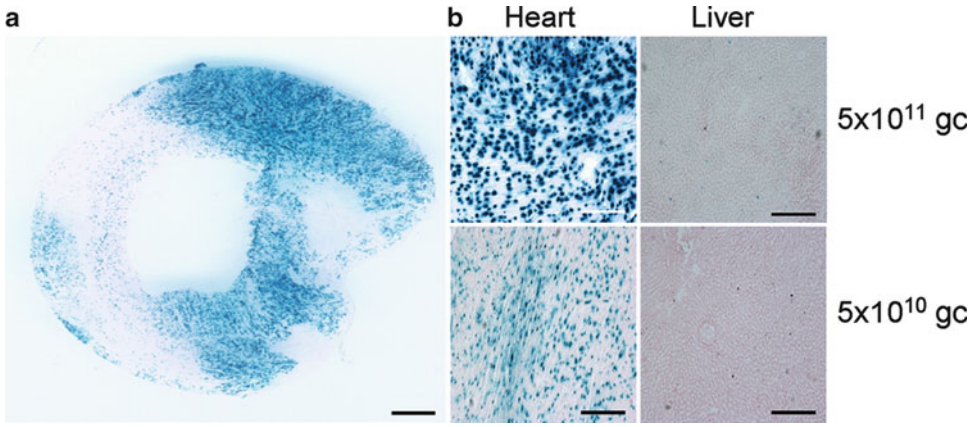

Fig. 3. Representative photomicrographs of sections from rat heart and liver 4 weeks following direct myocardial injection into the left ventricular free wall of 250 μL AAV9-CB-LacZ in five equal aliquots. (**a**) Low magnification photomicrograph of the heart depicting high level transgene expression throughout the left ventricular free wall after injection of 5×10^{11} gc. Scale bar: 2.4 mm. (**b**) Photomicrographs of heart and liver after receiving either 5×10^{11} or 5×10^{10} gc of vector. Scale bar: 200 μm. Sections have been stained with X-gal and counterstained with eosin. Adapted from Bish et al. (30).

observed almost entirely throughout the left ventricular free wall with minimal expression in the liver and other organs. Below this dose, expression was dramatically reduced (see Fig. 3).

14. For induction of anesthesia, we create a ketamine/xylazine cocktail by mixing 1.8 mL of ketamine (100 mg/mL), 0.75 mL of xylazine (20 mg/mL), and 0.45 mL of normal saline. We give an initial injection of 0.15–0.20 mL of this cocktail to a 300-g rat as an initial dose. Additional drug can be given if the rat still responds to pain after 5 min.
15. If rats are to be used in an ischemic cardiomyopathy model, we recommend the use of Lewis inbred rats. It has been previously reported that ligation of the left anterior descending artery in these rats results in a larger and more uniform infarct with lower mortality when compared to Sprague–Dawley rats (43).
16. An instructive video is supplied with the rat intubation pack that first-time users may find helpful. Intubation should proceed as quickly and as smoothly as possible. We have noted that loss of spontaneous respiration can be associated with prolonged and/or traumatic intubations. If this occurs, emergency tracheotomy can be performed.
17. This may require an adapter, which can be provided by the manufacturer and/or supplier of the Anesthesia Work Station.
18. A small self-retaining retractor may be useful to maximize exposure of the heart.
19. Take care not to maintain the heart in a position that will restrict inflow or outflow for prolonged periods of time (maximum 30 s). If cardiac function becomes compromised during

the procedure for any reason, we recommend injecting 0.1 mL of dobutamine (12.5 mg/mL) into the left ventricular cavity. This can be repeated as necessary.

20. Avoid damaging coronary arteries or veins during the injection. (Some investigators may choose to wear loupes during the procedure.) A wheal should appear in the myocardium following each injection. In addition, the needle can be manipulated during each individual injection to maximize the area of injection. If an investigator experiences difficulty distributing vector across the entire left ventricular free wall with five injections, the number of injections can be increased as long as the volume of each individual injection is reduced proportionally to keep the total volume constant at 250 μL. We have noted that increasing the total volume of vector can lead to depressed cardiac function and death. Mortality is extremely rare using the protocol with a volume of 250 μL.
21. We have found that the rate of re-intubation can be greatly reduced by extubating the rat only after spontaneous movement has been observed.
22. We have previously shown successful loading of microbubbles with AAV2 (see Fig. 4) (38). Other serotypes might be visualized depending on the availability of suitable antibodies.
23. Pulmonary embolism occurs if air was injected by mistake or if microbubbles are too large (foamy microbubbles). This event is normally characterized by missing contrast in the left ventricle and a highly opacified large right ventricle. Usually, the rat will stop breathing within a minute and rarely survives.
24. If microbubbles do not develop a sufficient contrast effect after injection or if contrast effect is too short, then the tube most

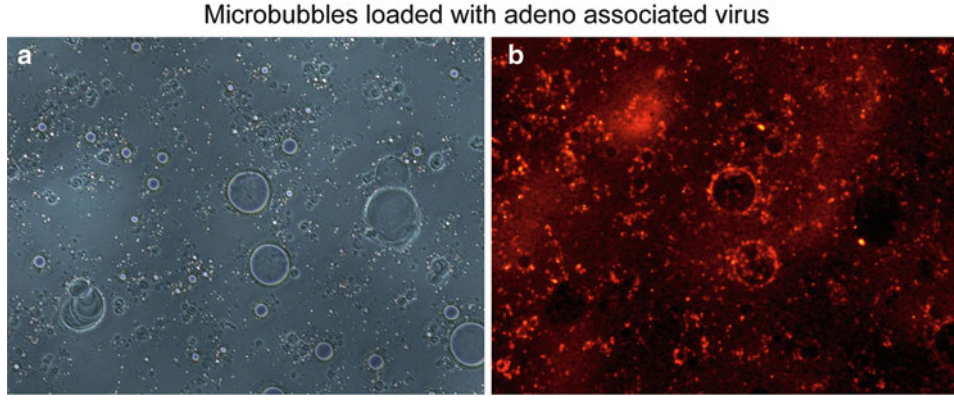

Fig. 4. Localization of intact AAV2 capsids on microbubbles. Efficient loading of AAV2 vectors on microbubbles was shown by immunostaining of the AAV/microbubble-suspension with the A20 primary antibody specifically binding to intact AAV-2 capsids. Microbubbles loaded with AAV-2 show a patchy fluourescence signal on the microbubble surface (**b**). (**a**) Shows the corresponding transmission photograph.

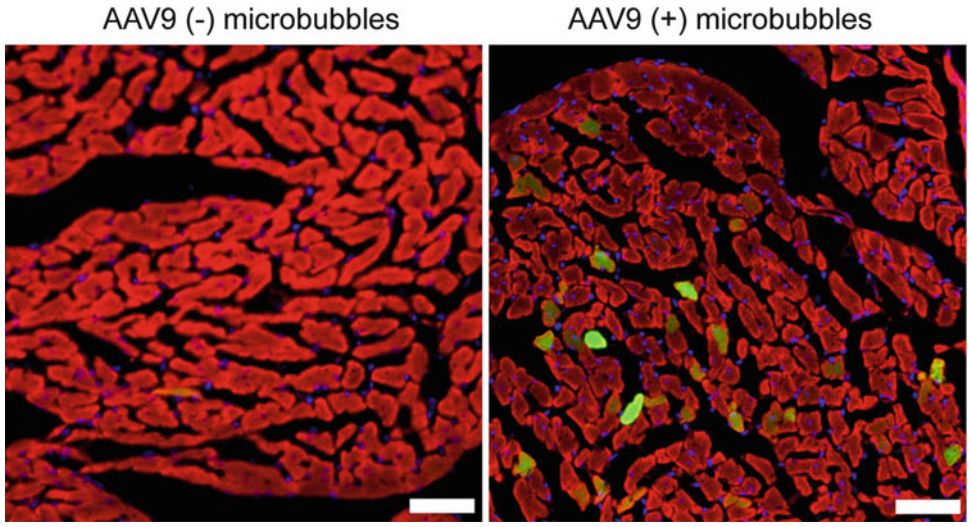

Fig. 5. Localization of gene expression in cardiac cryosections (10 μm) after UTMD of microbubbles loaded with 10^{11} gc of AAV-9/CMV-MLC0.26-EGFP vectors. No fluorescent signals were detectable in control sections after intravenous infusion of the same vector without microbubbles (*left*). In contrast, multiple GFP positive cardiomyocytes are present in the UTMD group (*right*). Photomicrographs were obtained by merging two channels (515–555 and 605–655 nm) after Alexa Fluor 546-Phalloidin staining. Scale bar 50 μm.

likely had lost too much air when bubbles were made (either empty gas cylinder or leaking tubes). Always use high-quality tubes that will close tightly, and make sure enough gas is available. Lower shaking times might cause decreased stability of microbubbles, too.

25. The high-mechanical index (MI) ultrasound may cause premature ventricular beats. As long as these occur rarely they can be tolerated. If, however, they occur with each high MI US and come in doublets and triplets, the mechanical index should be reduced, since the animal will be at risk for ventricular tachycardia or even ventricular fibrillation. Usually, reducing the MI to 1.3 will reduce the arrhythmia and after a few minutes the MI can be gradually increased again. If an animal develops ventricular tachycardia, the probe should be immediately removed.
26. It should be noted that transmural gene transfer occurs predominantly in the anterior wall of the left ventricle (see Fig. 5) (38).

Acknowledgments

This work was supported by a grant from the NHLBI (P01-HL059407 to HLS) and by TG-HL-007748 to LTB. Further support was obtained by a grant of the Deutsche Forschungsgemeinschaft

(MU 1654/3-2) and the Bundesministerium für Bildung und Forschung (01GU0527) to OJM as well as by the BioFuture grant of the Bundesministerium für Bildung und Forschung to RB. We thank Stefanie Schinkel for her help in preparing this manuscript.

References

1. Kaye, D. M., Hoshijima, M., and Chien, K. R. (2008) Reversing advanced heart failure by targeting Ca2+ cycling, *Annu Rev Med* ***59***, 13–28.
2. Lyon, A. R., Sato, M., Hajjar, R. J., Samulski, R. J., and Harding, S. E. (2008) Gene therapy: targeting the myocardium, *Heart* ***94***, 89–99.
3. Vinge, L. E., Raake, P. W., and Koch, W. J. (2008) Gene therapy in heart failure, *Circ Res* ***102***, 1458–1470.
4. Hoshijima, M., Ikeda, Y., Iwanaga, Y., Minamisawa, S., Date, M. O., Gu, Y., Iwatate, M., Li, M., Wang, L., Wilson, J. M., Wang, Y., Ross, J., Jr., and Chien, K. R. (2002) Chronic suppression of heart-failure progression by a pseudophosphorylated mutant of phospholamban via in vivo cardiac rAAV gene delivery, *Nat Med* ***8***, 864–871.
5. Iwanaga, Y., Hoshijima, M., Gu, Y., Iwatate, M., Dieterle, T., Ikeda, Y., Date, M. O., Chrast, J., Matsuzaki, M., Peterson, K. L., Chien, K. R., and Ross, J., Jr. (2004) Chronic phospholamban inhibition prevents progressive cardiac dysfunction and pathological remodeling after infarction in rats, *J Clin Invest* ***113***, 727–736.
6. Kaye, D. M., Preovolos, A., Marshall, T., Byrne, M., Hoshijima, M., Hajjar, R., Mariani, J. A., Pepe, S., Chien, K. R., and Power, J. M. (2007) Percutaneous cardiac recirculation-mediated gene transfer of an inhibitory phospholamban peptide reverses advanced heart failure in large animals, *J Am Coll Cardiol* ***50***, 253–260.
7. Sakata, S., Lebeche, D., Sakata, N., Sakata, Y., Chemaly, E. R., Liang, L. F., Tsuji, T., Takewa, Y., del Monte, F., Peluso, R., Zsebo, K., Jeong, D., Park, W. J., Kawase, Y., and Hajjar, R. J. (2007) Restoration of mechanical and energetic function in failing aortic-banded rat hearts by gene transfer of calcium cycling proteins, *J Mol Cell Cardiol* ***42***, 852–861.
8. Kawase, Y., Ly, H. Q., Prunier, F., Lebeche, D., Shi, Y., Jin, H., Hadri, L., Yoneyama, R., Hoshino, K., Takewa, Y., Sakata, S., Peluso, R., Zsebo, K., Gwathmey, J. K., Tardif, J. C., Tanguay, J. F., and Hajjar, R. J. (2008) Reversal of cardiac dysfunction after long-term expression of SERCA2a by gene transfer in a pre-clinical model of heart failure, *J Am Coll Cardiol* ***51***, 1112–1119.
9. Pleger, S. T., Most, P., Boucher, M., Soltys, S., Chuprun, J. K., Pleger, W., Gao, E., Dasgupta, A., Rengo, G., Remppis, A., Katus, H. A., Eckhart, A. D., Rabinowitz, J. E., and Koch, W. J. (2007) Stable myocardial-specific AAV6-S100A1 gene therapy results in chronic functional heart failure rescue, *Circulation* ***115***, 2506–2515.
10. Dandapat, A., Hu, C. P., Li, D., Liu, Y., Chen, H., Hermonat, P. L., and Mehta, J. L. (2008) Overexpression of TGFbeta1 by adeno-associated virus type-2 vector protects myocardium from ischemia-reperfusion injury, *Gene Ther* ***15***, 415–423.
11. Melo, L. G., Agrawal, R., Zhang, L., Rezvani, M., Mangi, A. A., Ehsan, A., Griese, D. P., Dell'Acqua, G., Mann, M. J., Oyama, J., Yet, S. F., Layne, M. D., Perrella, M. A., and Dzau, V. J. (2002) Gene therapy strategy for long-term myocardial protection using adeno-associated virus-mediated delivery of heme oxygenase gene, *Circulation* ***105***, 602–607.
12. Pachori, A. S., Melo, L. G., Zhang, L., Solomon, S. D., and Dzau, V. J. (2006) Chronic recurrent myocardial ischemic injury is significantly attenuated by pre-emptive adeno-associated virus heme oxygenase-1 gene delivery, *J Am Coll Cardiol* ***47***, 635–643.
13. Su, H., Lu, R., and Kan, Y. W. (2000) Adeno-associated viral vector-mediated vascular endothelial growth factor gene transfer induces neovascular formation in ischemic heart, *Proc Natl Acad Sci U S A* ***97***, 13801–13806.
14. Su, H., Takagawa, J., Huang, Y., Arakawa-Hoyt, J., Pons, J., Grossman, W., and Kan, Y. W. (2009) Additive effect of AAV-mediated angiopoietin-1 and VEGF expression on the therapy of infarcted heart, *Int J Cardiol* ***133***, 191–197.
15. Dobrucki, L. W., Tsutsumi, Y., Kalinowski, L., Dean, J., Gavin, M., Sen, S., Mendizabal, M., Sinusas, A. J., and Aikawa, R. (2009) Analysis of angiogenesis induced by local IGF-1 expression after myocardial infarction using microSPECT-CT imaging, *J Mol Cell Cardiol.*
16. Bostick, B., Yue, Y., Lai, Y., Long, C., Li, D., and Dongsheng, D. (2008) AAV-9 micro-dystrophin gene therapy ameliorates electrocardiographic abnormalities in mdx mice, *Hum Gene Ther.*

17. Goehringer, C., Rutschow, D., Bauer, R., Schinkel, S., Weichenhan, D., Bekeredjian, R., Straub, V., Kleinschmidt, J. A., Katus, H. A., and Muller, O. J. (2009) Prevention of cardiomyopathy in delta-sarcoglycan knockout mice after systemic transfer of targeted adeno-associated viral vectors, *Cardiovasc Res* ***82***, 404–410.
18. Ogawa, K., Hirai, Y., Ishizaki, M., Takahashi, H., Hanawa, H., Fukunaga, Y., and Shimada, T. (2009) Long-term inhibition of glycosphingolipid accumulation in Fabry model mice by a single systemic injection of AAV1 vector in the neonatal period, *Mol Genet Metab* ***96***, 91–96.
19. Sun, B., Young, S. P., Li, P., Di, C., Brown, T., Salva, M. Z., Li, S., Bird, A., Yan, Z., Auten, R., Hauschka, S. D., and Koeberl, D. D. (2008) Correction of multiple striated muscles in murine Pompe disease through adeno-associated virus-mediated gene therapy, *Mol Ther* ***16***, 1366–1371.
20. Merritt, J. L., 2nd, Nguyen, T., Daniels, J., Matern, D., and Schowalter, D. B. (2009) Biochemical correction of very long-chain acyl-CoA dehydrogenase deficiency following adeno-associated virus gene therapy, *Mol Ther* ***17***, 425–429.
21. Palomeque, J., Chemaly, E. R., Colosi, P., Wellman, J. A., Zhou, S., Del Monte, F., and Hajjar, R. J. (2007) Efficiency of eight different AAV serotypes in transducing rat myocardium in vivo, *Gene Ther* ***14***, 989–997.
22. Inagaki, K., Fuess, S., Storm, T. A., Gibson, G. A., McTiernan, C. F., Kay, M. A., and Nakai, H. (2006) Robust systemic transduction with AAV9 vectors in mice: efficient global cardiac gene transfer superior to that of AAV8, *Mol Ther* ***14***, 45–53.
23. Pacak, C. A., Mah, C. S., Thattaliyath, B. D., Conlon, T. J., Lewis, M. A., Cloutier, D. E., Zolotukhin, I., Tarantal, A. F., and Byrne, B. J. (2006) Recombinant adeno-associated virus serotype 9 leads to preferential cardiac transduction in vivo, *Circ Res* ***99***, e3-9.
24. Bostick, B., Ghosh, A., Yue, Y., Long, C., and Duan, D. (2007) Systemic AAV-9 transduction in mice is influenced by animal age but not by the route of administration, *Gene Ther* ***14***, 1605–1609.
25. Zincarelli, C., Soltys, S., Rengo, G., and Rabinowitz, J. E. (2008) Analysis of AAV serotypes 1–9 mediated gene expression and tropism in mice after systemic injection, *Mol Ther* ***16***, 1073–1080.
26. Katz, M. G., Swain, J. D., Low, D., White, J. D., Stedman, H. H., and Bridges, C. R. (2009) Cardiac Gene Therapy: Optimization of Gene Delivery Techniques in Vivo, *Hum Gene Ther*.
27. Bish, L. T., Sleeper, M.M., Sweeney, H.L. (2011) Percutaneous transendocardial delivery of self-complementary adeno-associated virus 6 in the canine, *Methods Mol Biol 709*, 369–78.
28. Raake, P. W., Hinkel, R., Muller, S., Delker, S., Kreuzpointner, R., Kupatt, C., Katus, H. A., Kleinschmidt, J. A., Boekstegers, P., and Muller, O. J. (2008) Cardio-specific long-term gene expression in a porcine model after selective pressure-regulated retroinfusion of adeno-associated viral (AAV) vectors, *Gene Ther* ***15***, 12–17.
29. Vandendriessche, T., Thorrez, L., Acosta-Sanchez, A., Petrus, I., Wang, L., Ma, L., L, D. E. W., Iwasaki, Y., Gillijns, V., Wilson, J. M., Collen, D., and Chuah, M. K. (2007) Efficacy and safety of adeno-associated viral vectors based on serotype 8 and 9 vs. lentiviral vectors for hemophilia B gene therapy, *J Thromb Haemost* ***5***, 16–24.
30. Bish, L. T., Morine, K., Sleeper, M. M., Sanmiguel, J., Wu, D., Gao, G., Wilson, J. M., and Sweeney, H. L. (2008) Adeno-associated virus (AAV) serotype 9 provides global cardiac gene transfer superior to AAV1, AAV6, AAV7, and AAV8 in the mouse and rat, *Hum Gene Ther* ***19***, 1359–1368.
31. Zhang, J. C., Woo, Y. J., Chen, J. A., Swain, J. L., and Sweeney, H. L. (1999) Efficient transmural cardiac gene transfer by intrapericardial injection in neonatal mice, *J Mol Cell Cardiol* ***31***, 721–732.
32. Andino, L. M., Takeda, M., Kasahara, H., Jakymiw, A., Byrne, B. J., and Lewin, A. S. (2008) AAV-mediated knockdown of phospholamban leads to improved contractility and calcium handling in cardiomyocytes, *J Gene Med* ***10***, 132–142.
33. Yue, Y., Li, Z., Harper, S. Q., Davisson, R. L., Chamberlain, J. S., and Duan, D. (2003) Microdystrophin gene therapy of cardiomyopathy restores dystrophin-glycoprotein complex and improves sarcolemma integrity in the mdx mouse heart, *Circulation* ***108***, 1626–1632.
34. Muller, O. J., Leuchs, B., Pleger, S. T., Grimm, D., Franz, W. M., Katus, H. A., and Kleinschmidt, J. A. (2006) Improved cardiac gene transfer by transcriptional and transductional targeting of adeno-associated viral vectors, *Cardiovasc Res* ***70***, 70–78.
35. Shohet, R. V., Chen, S., Zhou, Y. T., Wang, Z., Meidell, R. S., Unger, R. H., and Grayburn, P. A. (2000) Echocardiographic destruction of albumin microbubbles directs gene delivery to the myocardium, *Circulation* ***101***, 2554–2556.

36. Bekeredjian, R., Chen, S., Frenkel, P. A., Grayburn, P. A., and Shohet, R. V. (2003) Ultrasound-targeted microbubble destruction can repeatedly direct highly specific plasmid expression to the heart, *Circulation **108***, 1022–1026.
37. Chen, S., Shohet, R. V., Bekeredjian, R., Frenkel, P., and Grayburn, P. A. (2003) Optimization of ultrasound parameters for cardiac gene delivery of adenoviral or plasmid deoxyribonucleic acid by ultrasound-targeted microbubble destruction, *J Am Coll Cardiol **42***, 301–308.
38. Muller, O. J., Schinkel, S., Kleinschmidt, J. A., Katus, H. A., and Bekeredjian, R. (2008) Augmentation of AAV-mediated cardiac gene transfer after systemic administration in adult rats, *Gene Ther **15***, 1558–1565.
39. Bekeredjian, R., Kroll, R. D., Fein, E., Tinkov, S., Coester, C., Winter, G., Katus, H. A., and Kulaksiz, H. (2007) Ultrasound targeted microbubble destruction increases capillary permeability in hepatomas, *Ultrasound Med Biol **33***, 1592–1598.
40. Geis, N. A., Mayer, C. R., Kroll, R. D., Hardt, S. E., Katus, H. A., and Bekeredjian, R. (2009) Spatial distribution of ultrasound targeted microbubble destruction increases cardiac transgene expression but not capillary permeability, *Ultrasound Med Biol **35***, 1119–1126.
41. Matsuda, T., Fukuo, Y., Shinohara, H., Morisawa, S., and Nakatani, T. (1990) The postnatal development of the mouse pericardium; the time and mechanism of formation of pericardial pores, *Okajimas Folia Anat Jpn **67***, 115–120.
42. Nakatani, T., Shinohara, H., Fukuo, Y., Morisawa, S., and Matsuda, T. (1988) Pericardium of rodents: pores connect the pericardial and pleural cavities, *Anat Rec **220***, 132–137.
43. Liu, Y. H., Yang, X. P., Nass, O., Sabbah, H. N., Peterson, E., and Carretero, O. A. (1997) Chronic heart failure induced by coronary artery ligation in Lewis inbred rats, *Am J Physiol **272***, H722–727.

Chapter 10

Evaluation of the Fate of rAAV Genomes Following In Vivo Administration

K. Reed Clark and Magalie Penaud-Budloo

Abstract

Recombinant adeno-associated virus (rAAV) vectors are capable of mediating long-term gene expression in a wide variety of animals, including primates. The rAAV genome is packaged into the virion as single-stranded DNA devoid of any viral genes. A proportion of the single-stranded genomes are converted into transcriptionally active double-stranded DNA (dsDNA) early after nuclear entry by second-strand synthesis mediated by host repair DNA polymerases or/and by annealing of the rAAV (−) and (+) strands. Second-generation, self-complementary vectors are packaged as single-strand hairpins and rapidly assume a dsDNA conformation independent of the action of polymerases. In both cases, linear dsDNA vector genomes circularize and can undergo concatemerization into higher order forms (McCarty et al. Annu Rev Genet 38: 819–845, 2004; Schultz and Chamberlain Mol Ther 16: 1189–1199, 2008; Duan et al. J Virol 72: 8568–8577, 1998). As a result, rAAV vector genomes are maintained mainly as circular monomeric and concatemeric episomal forms in skeletal muscle and liver (Schnepp et al. J Virol 77: 3495–3504, 2003; Penaud-Budloo et al. J Virol 82: 7875–7885, 2008; Nakai et al. J Virol 75: 6969–6976, 2001). Moreover, in nonhuman primate skeletal muscle, it has been shown that rAAV episomes assimilate into chromatin with a typical nucleosomal pattern that presumably is important for persistence and gene expression in quiescent tissues over a period of several years (Penaud-Budloo et al. J Virol 82: 7875–7885, 2008).

Conversely, although rAAV is not considered as an integrative vector per se, introduction of exogenous DNA into the nuclear compartment can result in low-level vector assimilation into the host genome. One mechanism appears to involve vector insertion at sites of double-strand DNA breaks using cellular DNA repair enzymes. As rAAV gene transfer technology and applications mature, a better characterization of the genetic fate of the rAAV genome is critical to accurately evaluate the risk/benefit ratio for a particular disease indication. In this chapter, two complementary methods are detailed to enable characterization of rAAV molecular structure in a particular target tissue and estimation of its integration frequency.

Key words: Recombinant AAV, rAAV, Adeno-associated virus, Integration, Episome, Plasmid-safe DNase, B1-PCR

1. Introduction

To characterize the molecular structures of diverse recombinant adeno-associated virus (rAAV) vector genomes present in transduced tissues, two complementary techniques are presented. The

Richard O. Snyder and Philippe Moullier (eds.), *Adeno-Associated Virus: Methods and Protocols*,
Methods in Molecular Biology, vol. 807, DOI 10.1007/978-1-61779-370-7_10,

first assay allows direct visualization by Southern blot of episomal rAAV forms through the use of the novel exonuclease Plasmid-Safe DNase. As its name suggests, PS-DNase does not degrade double-stranded circular DNA under defined conditions while readily digesting linear DNA (see Fig. 1) (4, 5, 7). Using this enzyme

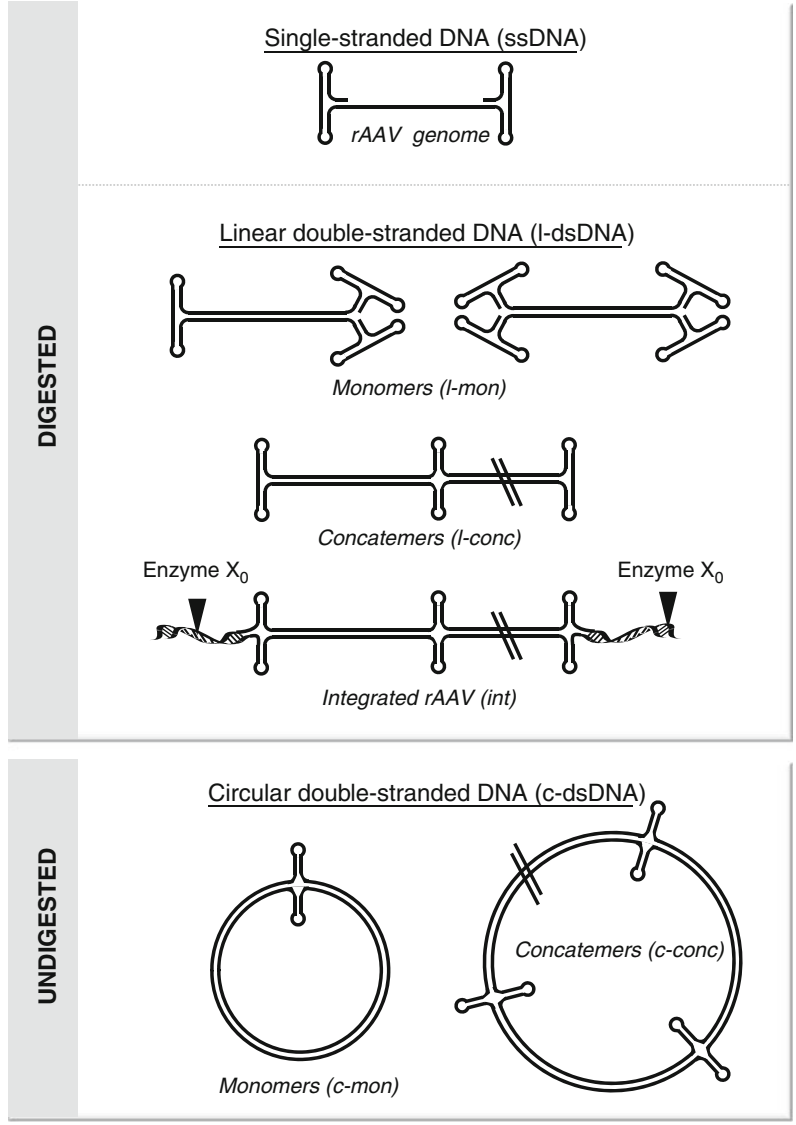

Fig. 1. Plasmid-Safe ATP-dependant DNase cleavage specificity adapted for rAAV molecular structure analysis. Diverse rAAV genomic forms are hydrolyzed after PS-DNase treatment: AAV single-stranded genomes, and linear monomers (l-mon) or concatemers (l-conc). rAAV genomic integrants (int) are removed as a result of digestion with restriction enzyme X_0 that does not cut in the rAAV vector genome but generates numerous breaks within the host genome. Conversely, circular monomers (c-mon) and concatemers (c-conc) are resistant to degradation and remain intact.

followed by Southern blot, one can visualize monomeric and concatemeric forms of rAAV in tissue DNA samples. The second method describes the use of PCR targeting interspersed repetitive sequences to detect and quantify rAAV integration events within mouse tissue (B1-PCR, see Fig. 3). This assay can be adapted to multiple species through the use of appropriate species-specific amplification primers that target highly repetitive Alu-like elements. Using this protocol, we previously showed that rAAV integration frequency in rodent skeletal muscle is less than 0.5% of the total detectable vector genomes (4). Both methods should prove useful in preclinical and clinical studies to characterize the form and integration frequency of persisting rAAV genomes as vector serotype, dose, and route vary from one application to another.

2. Materials

2.1. PS-DNase Southern Blot Detection

1. rAAV-transduced tissue (refer to Subheading 3.1.1, step 1).
2. Plasmid-Safe™ ATP-dependent DNase at 10 U/μl supplied with the (10×) reaction buffer and 25 mM ATP (Epicentre Biotechnologies, Madison, WI).
3. Restriction enzyme X_0 (see Note 1) supplied with the correct buffer (concentration ≥10 U/μl) and 1 mg/mL BSA (if necessary) (New England Biolabs Inc., Ipswich, MA).
4. 10× PBS, pH 7.4: 80.6 mM sodium phosphate, 19.4 mM potassium phosphate, 27 mM KCl, and 1.37 M NaCl.
5. Urea Buffer: 8 M Urea, 1% SDS, 10 mM EDTA, 300 mM NaCl, 10 mM Tris-HCl, pH 7.5.
6. Proteinase K at 10 mg/mL (Qiagen, Valencia, CA).
7. Sterile, single-edge razor blade.
8. Phenol/chloroform, pH 8.0.
9. 3 M sodium acetate, pH 5.2.
10. Glycogen at 20 mg/mL (Roche Applied Science, Indianapolis, IN).
11. 70 and 100% ethanol.
12. TE 10:1: 10 mM Tris-HCl, pH 8.0, and 1 mM EDTA, pH 8.0.
13. RNase A at 10 mg/mL (Sigma–Aldrich, St. Louis, MO).
14. Sterile water (dH_2O).
15. Agarose Seakem LE (Lonza, Basel, Switzerland).
16. 50× TAE, pH 8.0: 2 M Tris base, pH 8.0, 50 mM EDTA, pH 8.0, and 1.56 M acetic acid.
17. Ethidium bromide at 10 mg/mL (Sigma–Aldrich, St. Louis, MO) (☠ mutagen).

18. 0.25 N HCl.
19. 0.4 N NaOH.
20. Biotrans(+) positive charged nylon membrane (MP Biomedicals, Solon, OH).

2.2. B1-PCR

1. B1-mouse repetitive element primer: 5′AGTTCCAGGACA GCGAGGGCTAYACAGA3′.
2. Total cellular DNA (gDNA) isolated from naïve control and rAAV-transduced mouse tissue.
3. C2C12 mouse cells (ATCC, Manassas, VA) and gDNA isolated from cells.
4. rAAV2.CMV.GFP-Zeocin fusion vector (NCH Viral Vector Core, Columbus, OH).
5. rAAV2.CMV.GFP-Zeocin-transduced C2C12 cell pool and gDNA isolated from pools.
6. Lysis buffer: 10 mM Tris-HCl, pH 8.0, 100 mM NaCl, 25 mM EDTA, 0.5% SDS.
7. Proteinase K at 10 mg/mL (Qiagen, Valencia, CA).
8. Sterile, single-edge razor blade.
9. ABI 7000 or 7500 Taqman machine (Applied BioSystems, Carlsbad, CA).
10. 2× TaqMan Master mix (Applied BioSystems, Carlsbad, CA).
11. Peltier thermal cycler with the heated lid option (MJ Research PTC200 Thermo Cycler, Waltham, MA).
12. Blood & Cell Culture DNA Mini Kit (Qiagen, Valencia, CA).
13. pAAV.CMV.eGFP DNA plasmid (NCH Viral Vector Core, Columbus, OH).
14. Pac I restriction enzyme (New England Biolabs Inc., Ipswich, MA).
15. 10 mM dNTP mix (New England Biolabs Inc., Ipswich, MA).
16. Herculase Hot Start DNA polymerase supplied with 10× PCR buffer (Stratagene, La Jolla, CA).
17. Sterile Water, RNA/DNA-free for PCR (Invitrogen, Carlsbad, CA).
18. Sterile 10 mM Tris–HCl, pH 8.0.
19. 2× PCR Master Mix (Applied BioSystems, Carlsbad, CA).
20. CMV forward primer: 5′TGGAAATCCCCGTGAGTCAA3′, 300 nM final concentration.
21. CMV reverse primer: 5′CATGGTGATGCGGTTTTGG3′, 300 nM final concentration.
22. CMV TaqMan probe: 5′[6-FAM]CCGCTATCCACGCCCAT TGATG[TAMRA]3′, 200 nM.

23. Mouse *gus* forward primer: 5′ACCCTGCGGTTGTGAT GTG3′, 50 nM final concentration.
24. Mouse *gus* reverse primer: 5′AATATGCGG CGGGTTT CAG3′, 300 nM final concentration.
25. Mouse *gus* probe: 5′[6-FAM]TGTGGCCAATGAGCCT TCCTCTGC[TAMRA]3′, 200 nM.
26. PCR tubes: 0.2 and 1.5-mL tubes.
27. Optical caps (Applied BioSystems, Carlsbad, CA).
28. 96-well reaction plates (Applied BioSystems, Carlsbad, CA).
29. DNase and RNase-free filter tips.
30. Dulbecco's Modified Eagle Medium (DMEM) high glucose media (Invitrogen, Carlsbad, CA).
31. Zeocin (Invitrogen, Carlsbad, CA).
32. General tissue culture flasks (Corning or equivalent).
33. 1× Hanks Balanced Salt Solution (HBSS) (Invitrogen, Carlsbad, CA).
34. 1× Trypsin–5 mM EDTA. Add 50 mL of 10× Trypsin (Invitrogen, Carlsbad, CA) + 5 mL of 0.5 M EDTA, pH 8.0 (Invitrogen, Carlsbad, CA) to 445 mL of 1× HBSS (Invitrogen, Carlsbad, CA).
35. 100× Penicillin/Streptomycin (P/S) (Invitrogen, Carlsbad, CA).
36. Fetal Bovine Serum (FBS) (Invitrogen, Carlsbad, CA).
37. Dimethyl sulfoxide (DMSO) (Sigma–Aldrich, St. Louis, MO).

3. Methods

3.1. PS-DNase Southern Blot

This assay allows detection and characterization of the predominant AAV molecular structures in vivo (4, 5). PS-DNase exonuclease hydrolyzes double-stranded DNA (dsDNA) at slightly alkaline pH and with lower efficiency single-stranded DNA (ssDNA). This reaction is ATP dependent and does not affect supercoiled or relaxed circular dsDNA. To ensure complete digestion of high-molecular-weight linear gDNA, prior to PS-DNase exonuclease digestion, we treat the extracted total DNA with a restriction enzyme (X_0) that cuts often in the host genome (see Note 1) but does not cut in the rAAV genome. Furthermore, two overnight incubations with the PS-DNase are performed to completely remove gDNA (see Fig. 2a, b). Using the experimental conditions described below, only rAAV molecules that are of a circular double-stranded conformation remain after PS-DNase digestion (see Fig. 1). rAAV integrants are digested in a similar manner

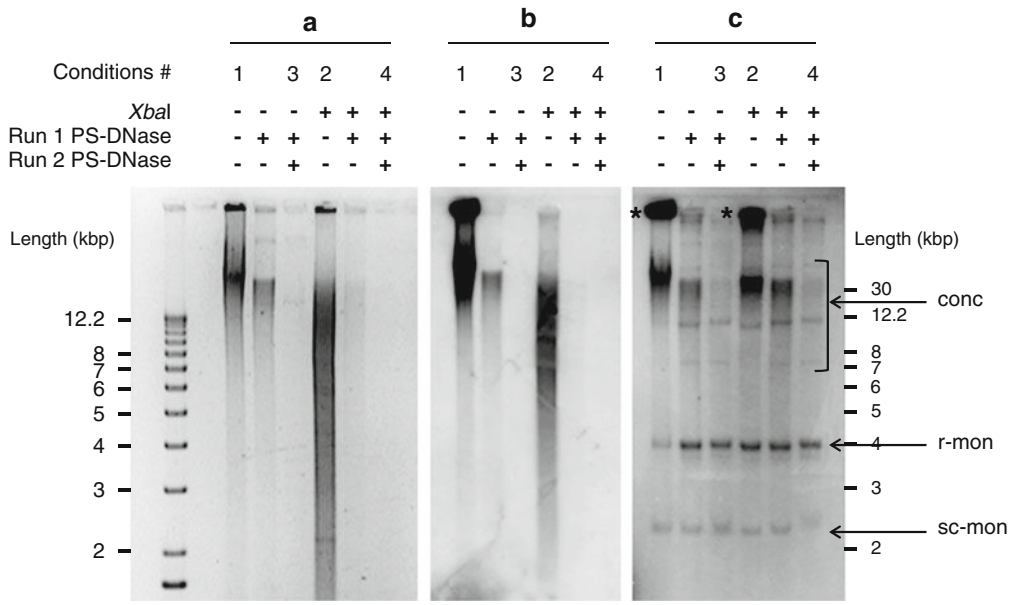

Fig. 2. PS-DNase assay analysis of primate muscle after rAAV2/1 vector administration. A rhesus macaque received 5×10^{12} vg/kg of rAAV2/1-RSV-LEA29Y-wpre by three intramuscular injection into the tibialis anterior muscle. A muscle biopsy was performed at 21 months post injection and gDNA analyzed by Southern blot hybridization. Panel (**a**) represents the gDNA migration on a 0.8% agarose gel after ethidium bromide staining. The four labeled conditions are (1) uncut DNA; (2) enzyme X_0 (Xba I) alone; (3) PS-DNase alone; and (4) enzyme X_0 (Xba I) + PS-DNase. The running profile obtained for Condition #1 validates the fact that the total DNA is high-molecular-weight DNA. Panel (**b**) corresponds to the hybridization with a probe that is specific for an endogenous gene sequence (cynomologus erythropoietin – cmEpo). This blot shows that the assay induces a complete digestion of the host genome. Panel (**c**) is obtained after hybridization with a probe that is specific for the rAAV sequence (woodchuck hepatitis virus posttranscriptional regulatory element followed by the SV40 polyA – wpre-pA). A gDNA trapping phenomenon is observed at the top of the gel and indicated by a (*) (conditions #1 and #2) and could be minimized by preparing a lower % agarose gel. The PS-DNase-resistant forms detected in lane #4 correspond to rAAV molecules present in the primate muscle more than 1.5 years after administration and are double-stranded, circular episomes. Thus, the rAAV genome persists as relaxed (r-mon) (3,928 bp) or supercoiled monomers (sc-mon), and as high-molecular-weight concatemers (conc).

as linear gDNA following restriction enzyme X_0 treatment. The protocol is optimized for 20 μg of initial gDNA.

Calculate the enzyme quantity and the buffer volumes for differing gDNA amounts (see Note 2). Do not use mechanical shearing and avoid vortex mixing or repeated pipetting during the DNA isolation procedure. This can alter the viral DNA and lead to undesired digestion of high-molecular-weight rAAV forms. Four conditions per sample should be included in your assay: (1) uncut DNA control; (2) enzyme X_0 alone; (3) PS-DNase alone; and (4) enzyme X_0 + PS-DNase. The first 2 conditions (1 and 2) confirm that enzyme X_0 does not alter the rAAV genome forms (see Fig. 2c) and that the gDNA is cleaved efficiently to generate a broad smear of DNA fragments (see Fig. 2a). Inclusion of PS-DNase (3 and 4) identifies the resistant dsDNA circular forms (see Fig. 2c).

3.1.1. gDNA Sample Preparation

1. Obtain sufficient tissue to isolate ~100 μg of gDNA for the four separate samples detailed above. Depending on the density of nuclei per gram of tissue, start with less or more material. For example, process ~30 mg of liver or ~200 mg of skeletal muscle. Finely mince the tissue in cold 1× PBS, pH 7.4. Centrifuge at 800 × *g* for 5 min at 4°C to pellet the tissue, and then wash with cold 1× PBS, pH 7.4.
2. Digest washed tissue with 4 mL of urea buffer per gram of tissue and add fresh proteinase K to a final concentration of 2 mg/mL. Incubate at 56°C for 3 h with occasional mixing by gentle inversion.
3. Add an equal volume of urea buffer and proteinase K and repeat digestion overnight.
4. Extract sample two times with phenol/chloroform, pH 8.0, and precipitate DNA with 1/10th volume of 3 M sodium acetate (pH 5.2) and 2.5 volumes of 100% ethanol. Mix by gentle inversion and place at −20°C for a minimum of 30 min.
5. Pellet DNA by centrifuging at ≥12,000 × *g* and gently wash the DNA pellet with 70% ethanol.
6. Centrifuge again at ≥12,000 × *g* for 5 min and discard ethanol wash.
7. Air dry pellet for 15–30 min and then resuspend in 100–200 μl of TE 10:1 with 50 μg/mL of RNase A final concentration.
8. Determine DNA concentration using $OD_{260/280}$, where an OD_{260} of 1 is equal to 50 μg/mL.

3.1.2. Restriction Enzyme X_0 Digestion of gDNA

To facilitate the PS-DNase activity, the gDNA is first digested with restriction enzyme X_0 that does not cut in the rAAV vector genome (see Note 1).

1. Set up the four reactions in labeled microfuge tubes: #1 uncut DNA control; #2 enzyme X_0 alone; #3 PS-DNase alone; and #4 enzyme X_0 + PS-DNase.
2. For reaction conditions #1 and #3, add in the following order to labeled microcentrifuge tubes: 10 μl of the appropriate restriction 10× buffer, 10 μl of 1 mg/mL BSA (if necessary), dH_2O to a final reaction volume of 100 μl, and 20 μg of total genomic DNA in TE 10:1.
3. For reaction conditions #2 and #4, prepare duplicate reaction component mixes as above, and then add 50 units of the selected restriction endonuclease X_0 (see Note 2).
4. Incubate the tubes #1 to #4 for 3 h at the recommended restriction temperature (in general, 37°C).

5. Repeat the X_0 digestion to ensure complete restriction by first adding an additional 10 µl of the appropriate restriction 10× buffer and 10 µl of 1 mg/mL BSA (if necessary).
6. Add dH_2O to a final reaction volume of 200 µl.
7. Add another 50 U of the selected restriction endonuclease X_0 to tubes #2 and #4.
8. Incubate for an additional 3 h at the recommended temperature.
9. Precipitate gDNA adding 1/10th volume of 3 M sodium acetate (pH5.2), 2 µl of glycogen and 2.5 volumes of 100% ethanol to all samples. Mix by gentle inversion and place at −20°C for a minimum of 30 min.
10. Centrifuge at ≥12,000 × *g* for 15 min.
11. Discard the supernatant being careful not to dislodge the DNA pellet on the side of the tube.
12. Gently wash the pellet with 100 µl of 70% ethanol.
13. Centrifuge again at ≥12,000 × *g* for 5 min and discard ethanol wash.
14. Let the pellet dry at room temperature until all ethanol is evaporated (15–30 min).
15. Dissolve the pellet in 20 µl of dH_2O.
16. Allow the pellet to resuspend at least for 1 h at 25°C.

3.1.3. PS-DNase Digestion

1. For reaction conditions #3 and #4, add in the following order to labeled microcentrifuge tubes: 20 µg of resuspended DNA (the entire 20 µl sample from above), dH_2O to a final reaction volume of 250 µl (including PS-DNase volume), 25 µl of the PS-DNase 10× buffer, 10 µl of 25 mM ATP, and 10 µl of PS-DNase (Epicentre Biotechnologies) at 10 U/µl (100 U total). For samples #1 and #2, substitute dH_2O for PS-DNase.
2. Incubate for 16 h at 37°C (see Note 3).
3. Repeat PS-DNase treatment with an additional 250 µl reaction volume (500 µl total).
4. Incubate for another 16 h at 37°C (see Note 3).
5. Transfer 250 µl of the reaction mixture to a second tube and to each tube add 25 µl of 3 M sodium acetate, 2.5 µl of glycogen, and 2.5 volumes of 100% ethanol. Mix carefully and place at −20°C for a minimum of 30 min.
6. Centrifuge at ≥12,000 × *g* for 15 min.
7. Carefully perform 70% ethanol wash and after air drying the pellet (15–30 min), dissolve each pellet in 20 µl of dH_2O.
8. Allow the pellet to resuspend for at least 1 h at 25°C and then pool the two tubes (40 µl final volume).

3.1.4. Southern Blot Conditions

Perform a standard Southern blot (8) with the following modifications:

1. Prepare a 0.8% agarose gel in 1× TAE buffer without ethidium bromide (EtBr) (see Notes 4 and 5). Varying the agarose concentration allows one to better resolve monomeric or concatemeric forms.
2. Electrophoresis conditions are: 16 h at 25°C at 35 V in 1× TAE buffer.
3. After electrophoresis, stain the gel with ethidium bromide for 30 min (EtBr final concentration of 1 μg/mL) and then destains the gel in a water bath for 10 min.
4. Quickly photograph the gel under a low-energy UV light source (see Note 6).
5. Treat the gel with 0.25 N HCl for 30 min to depurinate the DNA and improve transfer efficiency.
6. Blot transfer the DNA onto a positively charged membrane under alkaline conditions using 0.4 N NaOH (see Note 7).
7. Perform DNA hybridization with a probe that is specific of the rAAV sequence (5) (see Note 8 and Fig. 2).
8. Strip the blot, and then rehybridize with a probe that is specific for an endogenous gene sequence (see Fig. 2).

3.1.5. Data Interpretation

The persisting rAAV vector forms are revealed by the condition #4 pattern after hybridization with the rAAV genome-specific probe (see Fig. 2c). Furthermore, experimental interpretation is facilitated by the inclusion of the three additional conditions (#1 to #3). Indeed, the comparison of #1 and #2 profiles after ethidium bromide staining (see Fig. 2a) confirms that the host gDNA is intact after extraction and homogenously digested by the enzyme X_0 contrary to the rAAV genomic DNA (see Fig. 2c). Importantly, the protocol described includes two steps of digestion with the exonuclease. These two steps are necessary to completely hydrolyze the host genome and potential random rAAV integrants (see Fig. 2b, #4).

PS-DNase-resistant forms are double-stranded, circular episomes, but one should note that interpretation is dependent on DNA integrity. Indeed, in our example (see Fig. 2), some high-molecular-weight forms are sensitive to PS-DNase. This is consistent with several possibilities: (1) the occurrence of integration in the host genome, (2) the presence of linear concatemers, or (3) damage to high-molecular-weight episomes during DNA extraction. Based on the signal visualized on the top of the gel (see Fig. 2c, lane #3), these molecules are sensitive to the PS-DNase action even if they are not treated with the enzyme X_0. Consequently, after further investigation, the third hypothesis is the most likely. To assess the rAAV integration frequency, refer to the protocol detailed below.

3.2. B1-PCR

Interspersed repetitive sequence (B1 element) PCR is a technique designed to detect integrated rAAV vector genomes in mouse tissues (4). This method is predicated on the random PCR amplification of mouse gDNA that is flanked by Alu-like interspersed repetitive sequences known as B1 repeats. B1 elements are approximately 135 bp long and are present at 80,000–100,000 copies per haploid genome, spaced on average every 15 kb. Upon genome-wide amplification with a single conserved B1-primer, rAAV vector DNA integrated between two B1elements is concurrently amplified. Amplification of rAAV vector genomes is, therefore, diagnostic for integration and is measured using qPCR targeting the vector genome before and after B1-PCR. Importantly, episomal rAAV DNA is not amplified, although the molecules contribute to the initial input vector genome copy number before the B1-PCR reaction (see Fig. 3 for overview schematic and Schnepp et al. (4)).

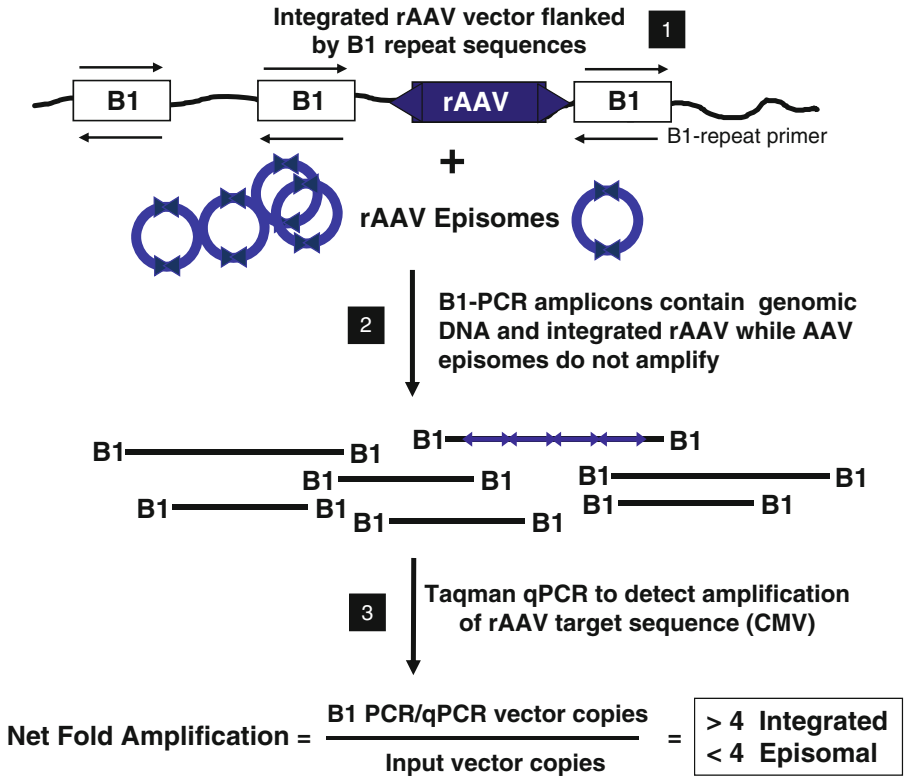

Fig. 3. B1-PCR overview schematic. Flowchart schematic of the B1-PCR analysis showing in Box 1 the possible rAAV genomic forms present in vivo, whereby in addition to episomal forms, integrated vector copies could be present. If present, integrated rAAV sequences would be expected to be flanked by repetitive B1 elements. Upon gDNA isolation, B1-PCR is performed (Box 2) to amplify B1 amplicons. This would be expected to amplify integrated rAAV sequences in addition to host genomic DNA. To then quantify the level of rAAV sequence amplification, a portion of the B1-PCR reaction is analyzed by Taqman qPCR (Box 3) to measure whether rAAV sequences were amplified above input levels. If net amplification is above a threshold level (four- to fivefold), then the sample is scored positive for integration. If the value is below the threshold, then vector genome copies are present almost exclusively as episomal forms.

To obtain meaningful data, the assay requires that (1) assay sensitivity is established and (2) the "background" level of episomal amplification is defined to enable a designation of a threshold above which is defined as significant amplification. (1) Assay sensitivity is determined by preparing a positive control "library" for randomly integrated rAAV vector sequences in cell culture using the C2C12 mouse myoblast cell line. The random integration library is generated by the transduction at a high multiplicity of infection (10^4 to 10^5 vg/cell) with rAAV expressing a selectable marker vector (rAAV2.CMV.eGFP-zeo). Using drug selection, a pool of rAAV integrants is generated and used to define the assay's limit of detection (LOD) to detect random rAAV integration events. This is accomplished by spiking differing amounts of the integrated C2C12 pool DNA into 20 ng of gDNA isolated from various naïve mouse tissues. B1-PCR is performed on the spiked samples and the fold amplification of integrated vector sequences is determined for each sample. Twenty nanograms of gDNA was chosen because this amount of DNA allows robust, genome-wide PCR amplification that demonstrates a broad range of amplified fragment sizes (up to 17 kb). The amplification of the endogenous mouse *gus* gene is used as a DNA integrity control for the assay. (2) A series of circular plasmid dilutions are subjected to B1-PCR to define "background" episomal amplification. This establishes a threshold, whereby fold amplification above this level is diagnostic for vector genome integration. In our experience, the threshold is approximately four- to fivefold over the input vector copy number for a particular tissue gDNA sample.

3.2.1. Generation of an Integrated AAV Cell Pool Using C2C12 Cells

1. Seed approximately 10^7 C2C12 cells into a T-175 flask with DMEM media containing 10% FBS and 1% P/S (growth media).
2. The next day, remove growth media and replace with 15 mL of 2% FBS media containing 10^{12} vector genomes (vg) of rAAV2.CMV.eGFP-zeo (MOI = 10^5). Gently rock flask every 30 min for 2 h (see Note 9).
3. The next day, remove the virus inoculum and refeed with 20 mL of growth media (DMEM + 10% FBS + 1% P/S).
4. Two days post transduction, remove growth media and wash cells with 10 mL of 1× HBSS. Remove HBSS, add 2 mL of 1× trypsin–5 mM EDTA, swirl to cover the cell surface, and then pipette off excess solution.
5. Place the flask in a CO_2 incubator and leave for 10–15 min (or until cells start separating from the flask surface). Cells should appear rounded under the microscope when they are disassociated.

6. Gently tap the flask against the palm of your hands to dislodge the cells and add 18 mL of complete DMEM growth media to neutralize the trypsin–EDTA. Disperse cell clumps by pipetteing cells vigorously against the bottom of flask to obtain a single-cell suspension. Split cells into 6T-175 flasks in complete growth media (3 mL trypsinized cell suspension plus 23 mL growth media per flask).
7. Concurrently, seed two 10-cm tissue culture dishes with 10^3 and 10^4 cells of the above cell suspension in growth media to determine library complexity (see Note 10).
8. After an additional 24 h, replace the media with 20 mL of fresh growth media containing 800 μg/mL of Zeocin and replenish with fresh selective media every 4 days.
9. At 15–20 days following selection, trypsinize the cells and seed into 6T-175 flasks at 3×10^6 cells per flask. Isolate genomic DNA from the remaining cells and label this as passage zero (p0 gDNA).
10. C2C12 gDNA is isolated using the Blood and Cell Culture DNA Mini Kit (Qiagen) according to the manufacturer's instructions and stored at −20°C.
11. Following an additional 7–10 days, split the cells again at 1:10 into six new flasks and isolate gDNA from the remaining cells and label as passage one (p1 gDNA).
12. Following an additional 7–10 days, pool the cells from the six flasks and generate cryopreserved cell stocks by stepwise freezing of harvested cells. Freeze six vials of cells in 90% FBS + 10% DMSO at 5×10^6 cells/mL. Isolate gDNA from the remaining cells and label as passage two (p2 gDNA) (see Note 11). Determine DNA concentration using $OD_{260/280}$, where an OD_{260} of 1 is equal to 50 μg/mL.
13. Determine the number of integrated vector copies (IVCs) per nuclei by using 20 ng of gDNA from each C2C12 passage (p0-2) in a qPCR TaqMan reaction using a vector-specific (CMV) primer and probe set and plasmid DNA standard curve (see Subheading 3.2.4). To confirm that the vector copies are integrated (and not episomal), restrict 400 ng of gDNA with a restriction enzyme (10 units) that does not cut within the vector genome for 2 h. Split the sample into two aliquots and then treat one (200 ng) with 10 units of PS-DNase in a similar manner as described in Subheading 3.1.3 and leave the second aliquot on ice. Perform CMV qPCR reactions on the equivalent of 20 ng from each sample (+/− PS-DNase). The absence of detectable vector signal after PS-DNase treatment confirms that the vast majority of vector sequence is integrated within the C2C12 genome (see Note 12).

14. Calculate IVC by obtaining the CMV copy number in the 20 ng of gDNA sample from extrapolation off the DNA plasmid standard curve and divide this value by 3,333.3 (20,000 pg/6 pg/nuclei). This yields the IVC per nuclei value needed for determining assay sensitivity (Subheading 3.2.2 below). Typically, 2–6 IVCs/nuclei are observed for rAAV-transduced C2C12 gDNA.

3.2.2. Define Assay Sensitivity by Performing Spike Experiments Using the AAV-Integrated C2C12 Cell Pool gDNA

Random rAAV integrants present in the C2C12 pool 2 (p2) gDNA is used to generate a gDNA dilution series to define assay LOD to detect random rAAV IVCs in the presence of naive C2C12 gDNA.

1. Prepare the following C2C12 p2 log dilutional series: 0, 1.5, 15, 50, 150, 1,500, and 15,000 IVC in 5 μl of 10 mM Tris–HCl, pH 8.0. The actual amount of C2C12 p2 gDNA to be added is calculated once the average IVC/nuclei is determined for the p2 gDNA as detailed in Subheading 3.2.1 above.
2. IVCs from the transduced C2C12 pool gDNA are then spiked into 20 ng of naïve mouse gDNA to maintain similar gDNA amounts for all samples in the 50 μl B1-PCR reaction volume.
3. Perform a standard B1-PCR reaction as detailed in Subheading 3.2.5.
4. Transfer 5% of the B1-PCR reaction volume (2.5 μl) and perform Taqman qPCR to measure amplification of the CMV target sequence (Subheading 3.2.4, steps 6–12). Perform at least six replicates and determine assay sensitivity in the absence of competitor episomal DNA.
5. To score this assay, divide the CMV qPCR after B1-PCR amplification by the calculated input amount of IVC. Amplification over input in the range of 100- to 500-fold is direct evidence of IVC detection. Background "amplification" of four- to five-fold over input is observed and is not considered positive based on data defining a baseline amplification level generated in Subheading 3.2.3 below. Typically, an LOD of 50–150 IVC is observed.
6. To define assay sensitivity in the presence of competing episomal rAAV vector DNA, perform a spike mixing experiment as detailed immediately below. This mimics actual muscle samples, where episomal vector DNA is present, and the assay must discriminate between episomal and integrated vector forms.
7. Generate another C2C12 p2 dilutional series (0, 1.5, 15, 50, 150, 1,500, and 15,000 IVC), but spike with 15,000 copies of plasmid DNA (episomal competitor) and add both components into 20 ng of naïve mouse gDNA in a final B1-PCR reaction volume of 50 μl (see Note 13).

8. Repeat the B1-PCR and CMV qPCR reactions and define assay LOD as the lowest IVC dilution that demonstrates clear CMV amplification above the predefined threshold (determined in Subheading 3.2.3 below) in the presence of 1.5×10^4 input plasmid DNA copies. The net effect of increasing input plasmid copies is to reduce the overall fold amplification. However, the assay LOD sensitivity is not significantly affected by inclusion of additional episomal copies. Therefore, the observed assay LOD is typically 75–150 IVC (4).

3.2.3. Define "Background" Amplification to Set Threshold for Integrated Vector DNA Amplification

A plasmid DNA dilution series is made to simulate the presence of episomal rAAV vector DNA and this is subjected to B1-PCR to measure the level of "background" or spurious amplification following a plasmid DNA spike into naïve C2C12 cell gDNA.

1. Prepare the following pAAV.CMV.eGFP supercoiled plasmid (or equivalent) DNA log dilutional series: 0, 1.5, 15, 50, 150, 1,500, and 15,000 plasmid DNA copies in 5 µl of 10 mM Tris–HCl, pH 8.0.
2. Plasmid DNA copies are then spiked into 20 ng of naïve mouse gDNA in a final B1-PCR reaction volume of 50 µl.
3. Perform standard B1-PCR reaction as detailed in Subheading 3.2.5.
4. Transfer 5% of the B1-PCR reaction volume (2.5 µl) and perform qPCR to measure baseline amplification of the CMV target sequence (Subheading 3.2.4, steps 7–13). Perform nine replicates for each dilution and determine the threshold for B1-PCR amplification as two standard deviations above the mean background amplification for all dilutions combined. This analysis typically yields a threshold of four- to fivefold over the input plasmid (B1-PCR CMV copy mean + 2SD/input CMV copies). This threshold value, then, allows the precise discrimination between positive amplification of IVC versus spurious low-level background amplification (4).

3.2.4. DNA Tissue Sample Preparation and Determination of Vector Copies per Nuclei Using Taqman qPCR

The B1-PCR assay is optimized for the 20–40 ng of gDNA and a total vector copy input of 1.5×10^4 vector copies. Therefore, one must first determine how many vector copies per nuclei are present in each mouse tissue sample using Taqman qPCR targeting a unique vector-specific sequence.

1. Genomic DNA from mouse tissues (30–200 mg) is isolated by digesting tissue in lysis buffer and proteinase K (200 µg/mL final concentration) for 12 h at 56°C. Prior to sample digestion, finely mince tissue samples with a sterile blade to promote complete tissue solubilization. Alternatively, extract gDNA according to Subheading 3.1.1, which yields gDNA of similar quality.

2. Perform two sequential phenol/chloroform extractions followed by ethanol precipitation (see Subheading 3.1.1, steps 4–7). Determine DNA concentration using $OD_{260/280}$, where an OD_{260} of 1 is equal to 50 μg/mL.
3. To determine vector genome copies, set up a standard 25 μl Taqman qPCR reaction using a vector-specific primer/probe combination (CMV in this protocol) and quantitate the vector genome copies in a 20 ng sample of gDNA (diluted in a 2.5-μl volume). Depending on the vector, other sequence-specific targets can be readily identified using Taqman ABI selection software.
4. First, digest 1 μg of mouse gDNA with 10 units of Pac I restriction enzyme in a 50-μl reaction volume for 1 h under standard reaction conditions in order to reduce sample viscosity.
5. Following Pac I digestion, incubate sample at 65°C for 20 min to inactivate the Pac I enzyme.
6. For each 25 μl Taqman qPCR reaction, add 12.5 μl of the 2× Taqman Master mix, 1 μl of forward primer, 1 μl of reverse primer, 0.75 μl of probe, and 7.25 μl of dH_2O. These volumes are scaled to generate sufficient complete master mix for all samples and standards.
7. Aliquot 22.5 μl reaction mix per reaction well using a multichannel pipette into a 96-well Taqman qPCR plate. Add 2.5 μl of template (20 ng sample or plasmid DNA standard) per well. All samples are run in duplicate. Also run a no-template control (NTC) in duplicate (add dH_2O in place of sample). *Save remaining unused Pac I-restricted gDNA for B1-PCR analysis in Subheading 3.2.5.*
8. To allow sample quantitation, a plasmid DNA standard dilution is generated and run in triplicate. The plasmid DNA standard is generated by diluting the plasmid in 1× Taqman PCR buffer to yield a concentration of 10^{11} copies/mL and is stored at –20°C in 25-μl aliquots (aliquots are stable for 6–12 months). To generate the standards for the Taqman run, remove 5 μl of the 10^{11} plasmid stock and add to 45 μl of 1× PCR buffer (10 mM Tris–HCl, 50 mM KCl, 5 mM $MgCl_2$, pH 8.0). Serially, dilute the plasmid from 10^{10} copies/mL to 10^4 copies/mL, then use 2.5 μl of each dilution per well, and run in triplicate. This generates a standard curve of 2.5×10^7 to 25 copies.
9. Using an ABI 7000 or 7500 machine, set Taqman qPCR run conditions as follows: 50°C for 2 min, 95°C for 10 min, followed by 40 cycles of 95°C for 15 s and 60°C for 1 min in a 25-μl final reaction volume.
10. After the run, the data are analyzed using the ABI SDS Sequence Detection program. The plasmid DNA standard

curve coefficient of correlation (R^2) should be > 0.995. Make sure that NTC controls are negative ($C_T > 38$) and that C_T values for standards are in the expected range (see Note 14).

11. Calculate vector genome copies per nuclei by taking the actual Taqman software-derived value and dividing by 3,333.3, which is the number of nuclei in 20 ng of gDNA.
12. Since the subsequent B1-PCR assay is optimized for a *total vector copy input of 1.5× 104* (see Subheading 3.2.5), if the calculated vector copy number per nuclei exceeds a value of 4.5 ($4.5 \times 3{,}333.3 = 1.5 \times 10^4$), the sample has to be diluted with naïve gDNA to yield 1.5×10^4 copies in 20 ng of gDNA for the B1-PCR assay. Conversely, if the vector copy number per nuclei is 2.25 or below, add a maximum of 40 ng of the sample gDNA to get as close as possible to the 1.5×10^4 total vector copy input in the B1-PCR reaction.

3.2.5. B1-PCR and Taqman qPCR Reactions

The B1 assay is optimized for an input of 20 ng total gDNA, but a maximum of 40 ng can be used if needed to increase the total vector copy input. This amount of DNA gives the greatest level and size distribution of B1 amplicon amplification. Higher DNA amounts rapidly exhausted the primer and nucleotide pools resulting in PCR products with a smaller size distribution. The assay is also optimized for a maximum input of 1.5×10^4 total vector copies, and if the input copy number exceeds this value it should be diluted to this input with naïve mouse gDNA (see Note 15).

1. On the basis of the results of Subheading 3.2.4, the rAAV vector copy number per nuclei is known. Calculate the amount of sample gDNA needed to bring the total vector input to 1.5×10^4 copies, but do not exceed 40 ng total gDNA. As discussed, if the copy number exceeds 4.5 per nuclei, then add sample gDNA to the 1.5×10^4 input and then add naïve mouse gDNA to reach a total of 20 ng.
2. Obtain the remaining Pac I digested sample gDNA from Subheading 3.2.4 (step 7) and set up samples in replicates of 4.
3. The samples are then amplified in the B1-PCR reaction as follows: Add 20 mM Tris–HCl, pH 8.75, 10 mM KCl, 10 mM $(NH_4)_2SO_4$, 2 mM $MgCl_2$, 400 μM each dNTP, 5 U Herculase Hotstart DNA polymerase (Stratagene), and 2 μg of B1 primer in a 50-μl reaction volume. To facilitate replicates, prepare a B1-PCR master mix by multiplying the reagent volumes above for an individual reaction by the number of total B1-PCR reactions, including a no-template sample. Therefore, for a 50 μl reaction, add 35 μl of dH_2O, 5 μl of 10× Herculase PCR buffer, 2 μl of 10 mM dNTP mixture, 2 μl of B1-PCR primer (1 mg/mL), and 1 μl of Herculase Hot Start DNA Polymerase (5 U/μl).

4. Place 45 μl of the master mix into 0.2-mL PCR tubes and then add 5 μl of the DNA template (20–40 ng). Include an NTC tube that contains 5 μl of water as the template.
5. In addition, a "1.5×10^4 vector copy input" sample is required for each DNA sample dilution that is not subjected to B1-PCR amplification. This is made by simply adding 5 μl containing 1.5×10^4 vector DNA copies from each sample to 45 μl of 10 mM Tris–HCl, pH 8.0. This sample serves as a template in the subsequent qPCR reaction to verify vector copy DNA input. Although this sample is not subjected to B1-PCR amplification, the sample should undergo the cycling conditions given in the next step for completeness.
6. B1-PCR cycling is accomplished using a Peltier thermal cycler with the heated lid option. The cycling conditions are as follows: denaturation at 95°C for 2 min followed by 10 cycles at 95°C, 30 s; 64°C, 30 s; 72°C, 7 min and 30 s, with an additional 20 cycles of 95°C, 30 s; 64°C, 30 s; 72°C, 10 min and 30 s and then 4°C hold.
7. Following B1-PCR, 2.5 μl of the B1 reaction is used as the template for real-time qPCR (TaqMan) detection to quantitate vector sequence-specific amplification in the B1-PCR reaction. Depending on the rAAV vector, select a unique target sequence for amplification that is not present in the host genome. The CMV promoter primer/probe sequence is our vector-specific target for Taqman qPCR and reaction conditions are as stated in Subheading 3.2.4, steps 6–12 (50°C for 2 min, 95°C for 10 min, followed by 40 cycles of 95°C for 15 s and 60°C for 1 min in a 25-μl reaction volume). For sample quantification, generate plasmid DNA standard curve in triplicate using 25 to 2.5×10^6 plasmid DNA copies. Experimental values are obtained by extrapolation of the SDS software from the plasmid DNA standard curve (coefficient of linearity $R^2 \geq 0.995$).
8. In an identical manner as described immediately above in step 7, CMV qPCR is performed on "input" samples that have not undergone B1-PCR-mediated amplification, and should theoretically be close to a value of 750 input copies (1.5×10^4 vector copies × 5%) (see Note 16).
9. Calculate net-fold amplification by dividing the B1-PCR/CMV qPCR sample value (step 7) by the CMV qPCR vector input value (step 8). If the average net amplification value for the four replicates is above the threshold defined in Subheading 3.2.3, then the sample is considered positive for rAAV integration. If the average net amplification is below the threshold cutoff, then the sample is said to contain fewer IVCs than the determined experimental LOD per 1.5×10^4

total vector copies. We have observed less than 75 IVCs per 1.5×10^4 total vector copies or stated in another way, <0.5% of the total vector copies are integrated in mouse muscle gDNA following intramuscular injection.

10. As a positive control for integrated sequence amplification, input and B1-PCR-amplified reaction products are also subjected to a second Taqman qPCR reaction targeting the single-copy endogenous beta-glucuronidase (*gus*) locus using identical conditions as described for the CMV primer/probe pair. We typically observe 500- to 1,000-fold net B1-PCR amplification over input using the *gus* primer/probe pair.

3.2.6. Data Interpretation

By defining assay sensitivity and background amplification parameters, sample interpretation is straightforward. Samples demonstrating net amplification below the threshold as defined in Subheading 3.2.3 are said to contain IVCs less than the assay LOD (defined in Subheading 3.2.2). For example, if the LOD is 50 IVCs and no vector integration is detected, then <50 IVCs per 15,000 total vector copies is present (<0.33% of total copies integrated). To increase the sensitivity of the assay, one can perform additional C2C12 p2 gDNA spike experiments to refine the LOD (Subheading 3.2.2, step 7) to reach maximum assay sensitivity. Conversely, if vector integration is detected, additional titration of rAAV vector inputs can be performed to define the minimum rAAV vector input that still demonstrates significant B1-PCR-mediated gene amplification. From this information, one can estimate the fraction of vector genomes demonstrating vector integration. For example, if positive vector integration was detected at an input of 10,000 vector copies and the LOD is 50 IVCs, then one can state that there are ≥50 IVCs in 10,000 total vector copies. Lastly, the assay is flexible in that multiple tissues, transgenes, and species can be analyzed in a similar manner as described herein once amplification conditions are experimentally defined for the particular system.

4. Notes

1. Ideally, select a restriction enzyme (X_0) that does not cut in the vector but cuts often within the mouse genome so that the average length of the generated genomic fragments is less than 10 kb.
2. Nonspecific cleavage with restriction enzymes can occur under conditions of excess glycerol, which should not be more than 10% in the final reaction mixture. To avoid such "star activity", the restriction enzyme should have a concentration ≥10 U/μl so that the volume added is ≤5 μl in 100-μl final reaction volume.

3. Do not increase the reaction time or heat inactivate the PS-DNase at 70°C. The subsequent ethanol precipitation step stops the reaction and removes the enzyme.
4. Ethidium bromide is an intercalating agent that alters the DNA conformation. Thus, it can modify the viral DNA molecules' mobility during the electrophoresis, so do not include ethidium bromide in the gel. To obtain a maximal resolution, prepare as thin a gel as possible that accommodates the load volume.
5. For resolution of high-molecular-weight rAAV DNA concatemers and to avoid trapping these molecules in the well, a multipurpose 0.5% agarose gel can be prepared (Roche Applied Bioscience) in 1× TAE.
6. Capture the gel image using a "preparative" light mode with a ruler in order to measure the distances and location of the DNA molecular weight ladder after hybridization.
7. Denaturation of the dsDNA in an alkaline environment may improve binding of the negatively charged DNA to a positively charged membrane, and separates it into single DNA strands for efficient hybridization to the probe.
8. ^{32}P radioactive probe labeling is suggested for maximum sensitivity, particularly if samples contain fewer than ten vector genome copies/diploid genome.
9. If the rAAV selection vector is limiting, an MOI of 10^4 has been successfully used to isolate rAAV-integrated pools.
10. Library complexity is estimated by seeding 10-cm plates with 10^3 and 10^4 cells after viral transduction and then applying drug selection pressure. After 10 days, colonies should be visible and can be counted. In our experience, starting with 10^7 total cells, we estimate the pool complexity to be between 2×10^5 and 2×10^6 drug-resistant colonies after 10–14 days of zeocin selection.
11. The Qiagen Blood and Cell Culture DNA Mini Kit can accommodate anywhere from 5×10^6 cells to as many as 1×10^8 cells by simply selecting the properly sized genomic DNA resin assembly.
12. While the p2 cell pool is preferred for the subsequent LOD optimization, the earlier pools are acceptable to use if they are free of detectable episomal vector sequences.
13. At high IVC inputs (1.5×10^4 copies), one may exceed the 20 ng total gDNA limit if the IVCs/nuclei of your p2 pool is on the low end (e.g., 2 IVCs/nuclei). This is acceptable as long as you do not exceed a total input of 40 ng of gDNA that can result in impaired B1-PCR amplification efficiency.
14. In our experience, most plasmid DNA standards with 2.5 to 5×10^6 copies cross the cycle threshold (C_T) between 18 and

20 cycles. In addition, the slope of the standard should be between −3.0 and −3.8, and indicates whether the dilutions were made correctly.

15. For optimal B1-PCR amplification, the amount of gDNA should be kept between 20 and 40 ng. The assay is also optimized for a total vector copy input maximum of 1.5×10^4 vg. Therefore, depending on the vector copy number per nuclei in the tissue sample, one may need to add some naïve mouse gDNA to reach the 20 ng total gDNA (if sample copy number per nuclei is high, >4.5). If the copy number per nuclei is low, add 40 ng of gDNA. If 1.5×10^4 vg input is still not achieved, this is acceptable and simply reduces the overall assay sensitivity since the total vector genomes analyzed are reduced even though the LOD remains the same.
16. Because of the extreme sensitivity of qPCR, a twofold variation between data replicates is often observed. Therefore, some variation is expected and this effect is minimized by the use of multiple experimental replicates.

Acknowledgments

The authors thank Dr. Bruce Schnepp for optimization of the B1-PCR assay conditions and the Nationwide Children's Hospital Viral Vector Core for rAAV vectors and cell lines used in the generation of these methods.

References

1. McCarty, D. M., Young, S. M., Jr., and Samulski, R. J. (2004) Integration of adeno-associated virus (AAV) and recombinant AAV vectors, *Annu Rev Genet* 38, 819–845.
2. Schultz, B. R., and Chamberlain, J. S. (2008) Recombinant adeno-associated virus transduction and integration, *Mol Ther* 16, 1189–1199.
3. Duan, D., Sharma, P., Yang, J., Yue, Y., Dudus, L., Zhang, Y., Fisher, K. J., and Engelhardt, J. F. (1998) Circular intermediates of recombinant adeno-associated virus have defined structural characteristics responsible for long-term episomal persistence in muscle tissue, *J Virol* 72, 8568–8577.
4. Schnepp, B. C., Clark, K. R., Klemanski, D. L., Pacak, C. A., and Johnson, P. R. (2003) Genetic fate of recombinant adeno-associated virus vector genomes in muscle, *J Virol* 77, 3495–3504.
5. Penaud-Budloo, M., Le Guiner, C., Nowrouzi, A., Toromanoff, A., Cherel, Y., Chenuaud, P., Schmidt, M., von Kalle, C., Rolling, F., Moullier, P., and Snyder, R. O. (2008) Adeno-associated virus vector genomes persist as episomal chromatin in primate muscle, *J Virol* 82, 7875–7885.
6. Nakai, H., Yant, S. R., Storm, T. A., Fuess, S., Meuse, L., and Kay, M. A. (2001) Extrachromosomal recombinant adeno-associated virus vector genomes are primarily responsible for stable liver transduction in vivo, *J Virol* 75, 6969–6976.
7. Clark, K. R., Sferra, T. J., Lo, W., Qu, G., Chen, R., and Johnson, P. R. (1999) Gene transfer into the CNS using recombinant adeno-associated virus: analysis of vector DNA forms resulting in sustained expression, *J Drug Target* 7, 269–283.
8. Southern, E. M. (1975) Long range periodicities in mouse satellite DNA, *J Mol Biol* 94, 51–69.

Chapter 11

Measuring Immune Responses to Recombinant AAV Gene Transfer

Ashley T. Martino, Roland W. Herzog, Ignacio Anegon, and Oumeya Adjali

Abstract

Following AAV-based gene transfer, the occurrence of adaptive immune responses specific to the vector or the transgene product is a major roadblock to successful clinical translation. These responses include antibodies against the AAV capsid, which can be neutralizing and therefore prevent the ability to repeatedly administer the vector, and $CD8^+$ cytotoxic T lymphocytes, which can eliminate transduced cells. In addition, humans may have both humoral and cellular preexisting immunity, as a result from natural infection with parent virus or related serotypes. The need for assays to detect and measure these anti-capsid immune responses in humans and in experimental animals is profound. Here, ELISPOT, immunocapture (ELISA), and neutralization assays are explained and provided in detail. Furthermore, such techniques can readily be adapted to monitor and quantify immune responses against therapeutic transgene products encoded by the vector genome.

Key words: AAV, Viral capsid, $CD8^+$ T cells, ELISPOT, IFN-γ, ELISA, Antibody, Neutralization

1. Introduction

Among vector systems that allow efficient in vivo gene transfer, recombinant adeno-associated virus vectors (rAAV) hold great potential. However, untoward immune responses against the viral capsid and/or transgene products have emerged as serious obstacles for successful clinical translation, possibly resulting in prevention or elimination of therapeutic gene expression.

In animal models, rAAV-based gene transfer often resulted in deleterious humoral as well as cellular immune responses towards heterologous and, in some instances, even autologous gene products (1–5). The potential of such responses depends on several

Richard O. Snyder and Philippe Moullier (eds.), *Adeno-Associated Virus: Methods and Protocols*,
Methods in Molecular Biology, vol. 807, DOI 10.1007/978-1-61779-370-7_11,

parameters including vector construct and dose, viral serotype with its ability to transduce antigen-presenting cells (APCs), the purity of viral preparation, and genetic and non-genetic factors in the recipient. Moreover, the route of vector delivery appears to be a key factor, even able to shift the balance from an immunogenic to a tolerogenic response towards the transgene product as shown following intrahepatic rAAV administration (6–11). Aside anti-transgene responses, animal studies have also shown formation of neutralizing antibodies against vector particles following rAAV delivery that prevents re-administration. In humans, high prevalence of anti-AAV preexisting immunity is an additional challenge for rAAV gene transfer. Preformed neutralizing antibodies are present in most individuals with the highest prevalence for AAV2 serotype (12, 13). Low titers of these preexisting antibodies have been shown to neutralize and to abrogate gene transfer efficiency using several AAV serotypes, even when high-dose vector is administered (14–16). Moreover, antibodies against AAV in humans have been shown to be associated to anti-capsid T cell responses including both $CD4^+$ helper and $CD8^+$ cytotoxic T cell (CTL) responses. Importantly, in recent clinical trials using rAAV of serotypes 1 and 2 (17–19), specific capsid CTLs have been detected, and their activation was reported to be dependent on the vector dose (17). In a clinical trial on treatment of hemophilia, these CTLs have been hypothesized to eliminate transduced hepatocytes in vivo. Supportive evidence was recently obtained using an in vitro killing assay (20). Interestingly and for still unclear reasons, this key issue has not been identified in animal studies even when AAV-specific CTLs have been detected.

Therefore, the evaluation of the immune status of potential recipients of AAV vector gene therapy trials prior and after gene transfer is critical and should include monitoring antibodies as well as T cell responses. Specific and sensitive assays for the detection and the quantification of such responses have been developed. This chapter provides protocols used to detect and measure anti-capsid antibodies in the serum of any species using both an enzyme-linked immunosorbent assay (ELISA) technique as well as an AAV neutralizing transduction assay. The ELISA technique allows rapid detection of most anti-AAV antibodies of even low avidity. The neutralizing assay is longer but allows a more relevant functional analysis of the antibodies; in fact both assays are likely complementary and both may have clinical relevance. In terms of cellular responses against capsid, the chapter also describes an enzyme-linked immunospot (ELISPOT) assay for IFN-γ producing cells that utilizes AAV capsid-derived peptides recognized by $CD8^+$ cells from human or mouse origin.

2. Materials

2.1. Isolating White Blood Cells for IFN-γ Secretion (see Note 1)

1. PBS: Sterile phosphate-buffered saline.
2. Hanks Balanced Salt Solution (Invitrogen, Carlsbad, CA).
3. Culture Media: RPMI 1640 Medium [+] L-Glutamine (Invitrogen, Carlsbad, CA) with 25 mM HEPES (Sigma, St. Louis, MO), 10% Heat Inactivated Fetal Bovine Serum (Invitrogen, Carlsbad, CA), and 1% Penicillin–Strepomycin Solution (Mediatech, Manassas, VA).
4. Red Blood Cell Lysis Buffer (ebiosciences, San Diego, CA).
5. 70 μm nylon cell strainer (BD Biosciences, San Jose, CA).
6. Ficoll Paque Plus (GE Healthcare, Piscataway, NJ).
7. Trypan blue (Invitrogen, Carlsbad, CA).

2.2. ELISPOT Detection of IFN-γ Secreting Cells

1. Murine or Human IFN-γ Development Module Kit (R&D Systems, Minneapolis, MN) containing IFN-γ capture and detection antibodies.
2. BCIP/NBT substrate (R&D Systems, Minneapolis, MN): 5-Bromo-4-Chloro-3 Indolylphosphate *p*-Toluidine Salt (BCIP) and Nitro Blue Tertazolium Chloride (NBT) in organic solvent.
3. Streptavidin-AP (R&D Systems, Minneapolis, MN).
4. Specific $CD8^+$ T cell epitope (Anaspec, San Jose, CA).
5. SEB: Staphylococcal enterotoxin B (Sigma, St Louis, MO).
6. PBS: phosphate-buffered saline.
7. Wash buffer: 0.05% Tween 20 in PBS.
8. Blocking buffer: 1% Bovine Serum Albumin (BSA) and 5% Sucrose in PBS.
9. Reagent Diluent Concentration (R&D systems, Minneapolis, MN): filter sterilized PBS with 10% BSA.
10. Tissue culture incubator.
11. dH_2O: Sterile deionized water.
12. 96-well immunospot plate (Millipore, Billerica, MA) (see Note 2).
13. ELISPOT Reader (see Note 3).
14. Optional: multi-channel pipette or automated plate washer.

2.3. Antibody Enzyme-Linked Immunosorbent Assay to rAAV2 Humoral Response

1. Intact (DNA containing or empty) rAAV particles of the same serotype used for gene transfer.
2. Experimental host serum (i.e. from rAAV infected mice or humans).
3. Mouse immunoglobulin standard (IgG2a, Sigma, St. Louis, MO).

4. Anti-mouse IgG2a-HRP (horseradish peroxidase conjugate; Southern Biotech, Birmingham, Alabama) (see Note 4).
5. Coating Buffer: 13 mM Na_2CO, 88 mM $NaHCO_3$.
6. Wash Buffer: 0.05% Tween 20 in PBS.
7. Dilution Buffer: 5% BSA, 0.05% Tween 20 in PBS.
8. dH_2O: Sterile deionized water.
9. OPD (*o*-Phenylenediamine dihydrochloride) Tablets (Sigma, St. Louis, MO).
10. Microtiter Plates (Corning, Lowell, MA); or suitable alternative.
11. Adhesive sealing film (EXCEL Scientific, Victorville, CA).
12. Microplate reader (Biorad, Hercules, CA) or suitable alternative.
13. Optional: Multi-channel pipette or automated plate washer.
14. Optional: Stop solution for HRP development; 3 M HCl or 3 M H_2SO_4.

2.4. Neutralizing Antibody Assay

1. rAAV2-CMV-LacZ particles (see Notes 5 and 6).
2. Wild type adenovirus type 5 (wt Ad5) particles.
3. Experimental host serum (i.e. rAAV2 infected mice, nonhuman primates or humans).
4. HeLa cell line (see Note 6).
5. Sterile trypsin.
6. DMEM: Sterile Dulbecco's Modified Eagle Medium.
7. FCS: Heat inactivated Fetal Calf Serum FCS.
8. PBS: Sterile phosphate-buffer saline PBS.
9. X-Gal staining buffer: 50 ng/mL 5-bromo-4-chloro-3-indolyl-β-D-galactopyranoside (X-Gal) for colorimetric detection of β-galactosidase enzyme activity (Promega), 0.1% $MgCl_2$, 1% potassium ferricyanide, 1% potassium ferrocyanide in PBS (see Note 7).
10. 0.5% Glutaraldehyde in PBS.
11. dH_2O: Sterile deionized water.
12. Sterile 24-well cell culture plates.

3. Methods

3.1. Isolating White Blood Cells for IFN-γ Secretion

3.1.1. Murine Splenocyte Isolation

1. Remove spleen from mouse or rat in a sterile environment and immerse in a container with ice-cold Hanks Media and store on ice.
2. Pulverize spleen on cell strainer, collect cellular content in Hanks Media as it flows through the screen, rinse cell strainer

with Hanks Media and bring volume up to 20–40 mL in a 50-mL tube with Hanks Media.

3. Centrifuge isolated splenocytes and red blood cells at 4°C (350 × *g* for 10 min).
4. Carefully pour off supernatant, break up the cell pellet, resuspend in red blood cell lysis buffer (2–5 mL) and incubate at room temperature for 5 min.
5. Wash with 20–40 mL of Hanks Media and centrifuge white blood cell fraction of bulk splenocytes at 4°C (350 × *g* for 10 min).
6. Carefully pour off supernatant, break up cell pellet and resuspend in complete RPMI 1640 media (containing 2 μg/mL of the peptide antigen that encodes the specific T cell epitope) at a concentration of 1.0×10^7 cells/mL.
7. Determine cell count concentration using a 1:10 dilution of trypan blue to exclude dead cells.

3.1.2. Human PBMC Isolation

1. Pipette 25 mL of human blood collected with anticoagulant onto 12.5 mL of Ficoll-Paque Plus solution.
2. With centrifuge set to "0" acceleration and "0" brake, centrifuge at 500 × *g* for 30 min at room temperature.
3. Isolate the white blood cell fraction (see Note 8), transfer to 50-mL tube and bring volume to 50 mL with PBS and centrifuge at room temperature (350 × *g* for 10 min).
4. Carefully pour off supernatant, break up cell pellet, resuspend in 5–10 mL of red blood cell lysis buffer, and incubate for 5 min at room temperature.
5. Add 25 mL of Hanks buffer and centrifuge PBMCs at room temperature (350 × *g* for 10 min).
6. Carefully pour off supernatant and resuspend in complete RPMI 1640 media (containing 2 μg/mL of the peptide antigen that encodes the specific T cell epitope) at a concentration of 1.0×10^7 cells/mL.
7. Determine cell count concentration using a 1:10 dilution of trypan blue to exclude dead cells.

3.2. ELISPOT Detection of IFN-γ Secreting Cells

3.2.1. Prepare ELISPOT Plate to Culture IFN-γ Secreting White Blood Cells (see Note 9)

1. Pre-wet and coat a 96-well ELISPOT plate 24 h prior to isolating white blood cells from murine splenocytes or human PBMCs.
2. Pre-wet plate with 15 μL/well of 35% ethanol for 15 s and flick out ethanol (DO NOT VACUUM) by inverting plating (see Note 10).
3. To coat plate, prepare 1:60 dilution (see Note 11) of IFN-γ capture antibody in PBS, add 100 μL/well of diluted antibody to 96-well plate and incubate overnight 4°C.

4. Remove capture antibody and wash wells three times with wash buffer using multi-channel pipette or automatic plate washer and remove excess wash buffer by inverting and blotting the plate on a paper towel.
5. Block membrane with 200 µL/well of blocking solution for 2 h at room temperature.
6. Repeat step 3 to remove blocking buffer and wash the plate.
7. After washing, rinse the plate with 200 µL/well of complete RMPI 1640 media and remove the rinse media when IFN-γ secreting cells are ready to be cultured.

3.2.2. Stimulate Activated CD8⁺ rAAV Specific IFN-γ Secreting Cells (see Note 12)

1. Remove rinse media from ELISPOT plate by flicking the plate while inverted and blot remaining rinse media on a paper towel
2. Add 1.0×10^6 cells/well, which is 100 µL of the isolated white blood cells re-suspended at a concentration of 1.0×10^7 cells/mL in the appropriate stimulation media and incubate for 24–36 h (see Note 13) at 37°C in a 5% CO_2 cell culture incubator.
3. Experimental stimulation media consists of the complete RPMI 1640 media with 2 µg/mL of appropriate $CD8^+$ epitope (see Table 1 for examples) to determine the frequency of capsid-specific IFN-γ secreting cells (18, 20–23).
4. Negative control stimulation media consists of complete RMPI 1640 media without epitope to determine background level of IFN-γ secreting cells.
5. A non-specific, positive control stimulation media consists of the complete RMPI 1640 culture media with 10 µg/mL of a highly immunogenic superantigen, Staphylococcal enterotoxin B, to ensure that IFN-γ secreting cells are present and to determine the maximal frequency of IFN-γ secreting T cells.

Table 1
Examples of dominant $CD8^+$ rAAV epitopes

Host	AAV serotype	Peptide sequence	MHC I restriction
Mouse; BALB/c (*H*-2^d)	AAV2 AAV8	VPQYGYLTL IPQYGYLTL	L^d L^d
Mouse; C57BL/6 (*H*-2^b)	AAV2 AAV8	SNYNKSVNV NSLANPGIA	K^b D^b
Human (HLA-A)	AAV2	SADNNNSEY	HLA-A*0101
Human (HLA-B)	AAV2	VPQYGYLTL	HLA-B*0702

6. An internal positive control can be used by the addition of recombinant IFN-γ protein at 2 μg/mL to the culture media alone, without cells, to verify that there are no procedural errors and to ensure the quality of the reagents. This entire well will appear completely bluish-purple after color development.

3.2.3. Detection of IFN-γ Protein Secreted from Stimulated CD8+ rAAV Specific T Cells

1. Remove stimulation media and wash three times with wash buffer as described above.
2. Dilute 10× Reagent Diluent Concentrate in sterile dH_2O and use to prepare a 1:60 dilution of IFN-γ detection antibody, add 100 μL/well of diluted antibody to 96-well plate and incubate overnight at 4°C.
3. Remove detection antibody and wash three times as described above.
4. Dilute 10× Reagent Diluent Concentrate in sterile dH_2O and use to prepare a 1:60 dilution of Streptavidin-AP, add 100 μL/well of diluted Streptavidin-AP and incubate for 2 h at room temperature, and then rinse 1× with dH_2O.
5. Remove Streptavidin-AP and wash plate three times as described above.
6. Add 100 μL/well of BCIP/NBT substrate. Cover and develop the plate in the dark for 10–30 min at room temperature (see Note 14).
7. After development remove BCIP/NBT, rinse THOROUGHLY with dH_2O (see Note 15) and allow plate to air dry at room temperature.
8. The visible spots that have formed can be counted either manually with a dissecting microscope or with an ELISPOT reader (see Fig. 1). Results are typically reported as the average number of spot forming units (SFU) per 10^6 cells plated.

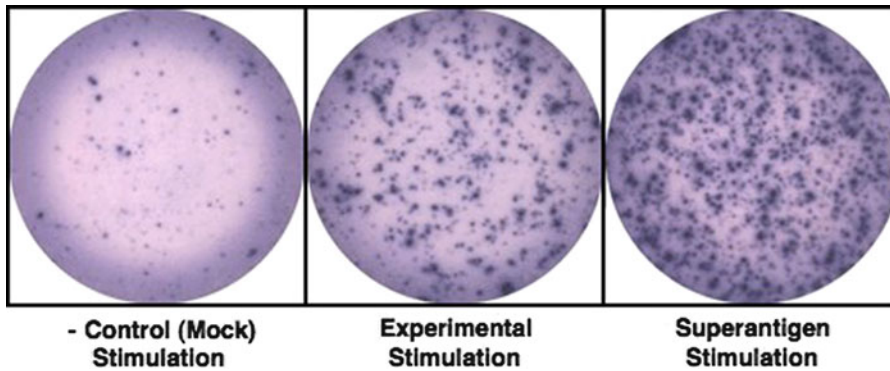

Fig. 1. Examples of ELISPOT wells with SFUs (spot forming units) after color development.

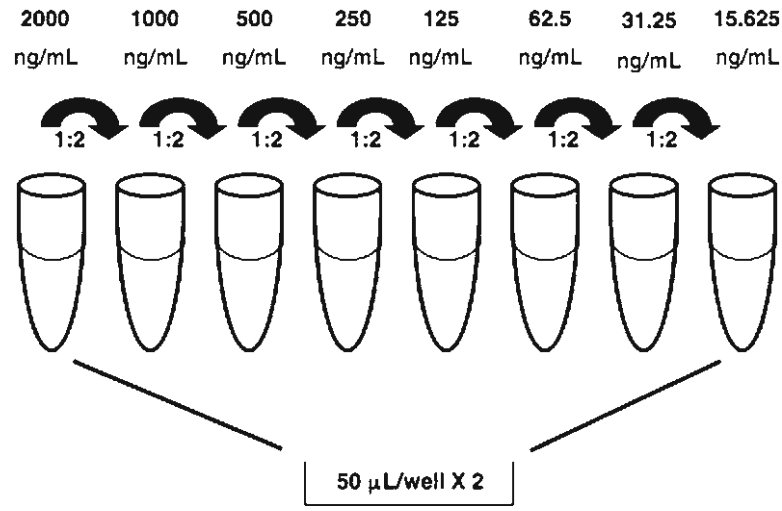

Fig. 2. Schematic to preparing immunoglobulin standard used for ELISA by serial dilution.

3.3. Antibody Enzyme-Linked Immunosorbent Assay to rAAV2 Humoral Response

3.3.1. Preparing Standard Curve for Measuring Antibody Titers

1. Prepare the first point of standard curve using purified mouse IgG2a (Sigma) at a concentration of 2,000 ng/mL in coating buffer and then make 1:2 serial dilutions using coating buffer as diluent to get a total of 8 points with the final point being at a concentration of 15.63 ng/mL (see Note 4 and Fig. 2).
2. Add 50 µL/well of each standard concentration in duplicate to microtiter plate.

3.3.2. Measuring rAAV2 Antibody Titers

1. After the standard curve wells have been added, coat the remaining wells with 4.0×10^9 intact rAAV viral particles of the respective serotype in 50-µL aliquots using coating buffer. Cover the plate with adhesive sealing film and incubate microtiter plate overnight at 4°C.
2. Wash plate three times with 200 µL/well of wash buffer using multi-channel pipette or automated plate washer. Blot inverted microtiter plate on a paper towel after washing to remove residual wash buffer.
3. Block microtiter plate using 200 µL/well of dilution buffer at room temperature for 2 h and then wash plate as previously described.
4. Make a 1:20 dilution (see Note 16) of experimental host serum using dilution buffer. Add 50 µL of diluted experimental host serum in duplicate. Incubate at 37°C for 2 h and then wash plate as previously described. For standard curve wells just add 50 µL of dilution buffer alone. Additionally, blank wells and positive control wells should be used. Dilution buffer alone

should be added to blank wells, and known anti-rAAV positive sera should be used as a positive control to ensure that there have been no procedural errors and to verify that efficient reagents are being used.

5. Make a 1:2,000 dilution (see Note 17) of the rabbit anti-mouse IgG2a-HRP secondary antibody in dilution buffer. Add 100 µL/well of the diluted HRP-labeled secondary antibody to the microtiter plate and incubate at 37°C for 2 h then wash plate as previously described.
6. For HRP-catalyzed color reaction, dissolve OPD tablets in 20 mL of dH_2O and add 200 µL/well to plate.
7. Allow plate to develop for 5–15 min (see Note 18) followed by measurement of absorbance at 450-nm wavelength using a microtiter plate reader. Alternatively, 100 µL/well of stop solution can be added to the plate and the absorbance can be measured later.

3.4. Neutralizing Antibody Assay

1. On day 1, prepare 24-well cell culture plate(s) with 2×10^5 HeLa cells (see Note 19) in 500 µL DMEM 10% FCS per well.
2. On day 2, inactivate experimental, and possibly control, sera (see Note 20) by heating them at 56°C for 30 min.
3. Prior to the assay, remove HeLa adherent cells from three wells using trypsin, count and calculate the average number of cells per well.
4. Aspirate the medium from the wells.
5. Add 500 µL of DMEM 2% FCS containing wt Ad5 preparation at a multiplicity of infection (MOI) of 8 infectious particles/cell
6. Incubate at 37°C for 2 h.
7. During the incubation of the cells with the wt Ad5
   (a) Prepare dilutions of the experimental serum (i.e. 1:5, 1:10, 1:20, 1:50, 1:100, 1:200) in DMEM 2% FCS medium (see Note 21).
   (b) Add to serum dilutions rAAV2-CMV-LacZ viral particles. The number of AAV particles should achieve in the well a MOI of 4,000 particles. The final volume per well of each diluted serum/rAAV should be 500 µL.
   (c) Incubate the serum with rAAV at room temperature for 30 min to allow AAV contact with neutralizing antibodies.
8. Aspirate the wells and add 500 µL of diluted serum/rAAV per well.
9. Incubate the plate at 37°C for 24 h.

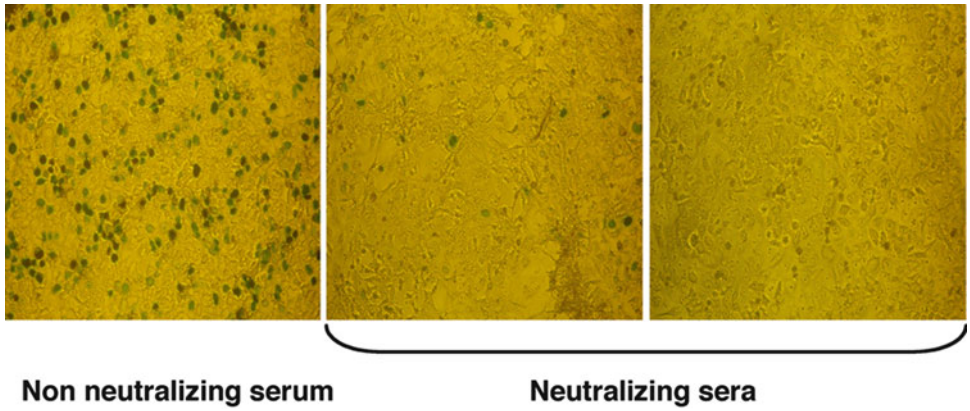

Fig. 3. Examples of X-Gal coloration detected by microscopy. *Left panel*: absence of neutralization. *Blue spots* correspond to transduced cells. *Left* and *middle panels*: neutralizing sera with different amounts of neutralizing antibodies. *Far right panel*, the serum abrogates completely AAV-mediated transduction.

10. Aspirate the wells and fix the cells by adding 500 µL of 0.5% glutaraldehyde in PBS per well.
11. Incubate at room temperature for 5 min.
12. Wash the wells 1× with dH_2O.
13. Add 500 µL of X-Gal staining buffer per well.
14. Incubate at 37°C for 6 h (see Note 22).
15. Wash the wells 1× with dH_2O and read the X-Gal coloration (blue cells) by light microscopy (see Fig. 3 and Notes 23 and 24).

4. Notes

1. Described white blood cell source is from either murine splenocytes or human peripheral blood mononuclear cells (PMBCs).
2. There is a range of immunospot plates with different binding membranes; consult technical support to suit individual needs.
3. In the absence of an ELISPOT reader, a dissecting microscope can be used to count spots.
4. Mice typically produce immunoglobulin of IgG2a subclass against rAAV particles. However, other subclasses, such as IgG3, have also been described and can be tested for and quantified using analogous reagents for the alternate subclass (murine immunoglobulin standards and detecting antibody) (24). In humans, the dominant response is IgG1 (i.e. the human equivalent to IgG2a, reflecting a Th1-driven response),

while IgG2, 3, and 4 may also be found (25). Respective analogous reagents to measure such titers in humans are available. The identical assay can be used to determine antibody titers against the transgene product by coating the microtiter plate with the respective protein instead of with vector particles (8, 26, 27).

5. Other transgenes (i.e. luciferase (13), Green Fluorescent Protein, GFP) can be used for this type of assay and specific detection methods can also be performed (i.e. flow cytometry for GFP+ cells).
6. The assay can be adapted to other rAAV serotypes. Optimal MOI may need to be determined for each serotype. Using Hela or Huh7 hepatoma cell line, a recent study showed that maximal transduction was reached at a MOI of 5,000 vector genomes [Vg]/cell for AAV2, 5 and 6, at MOI of 10,000 Vg/cell for AAV1 and 8, and at a MOI of 100,000 Vg/cell for AAV9 (13).

   Aside MOI, optimal cell line must also be tested for specific serotypes. For instance, even if the assay can be performed with HeLA cell line, it is not optimal for rAAV8 serotype. Boutin et al. showed that HeLA cell were best transduced with recombinant AAV1, 2, 5, 6, and 9, whereas Huh7 cell line was more suitable for serotype 8 (13). In another study, Huh7 cells were used for serotypes 1, 2, 7, and 8 (12).
7. This solution is stable 1 month in dark at 4°C.
8. White blood cell fraction is the white ring below the upper plasma layer.
9. Culture isolated white blood cells the day of isolation for ELISPOT analysis.
10. Pre-wetting plate helps minimize background after detection.
11. A 1:60 dilution is recommended, but optimization of both capture and detection antibodies maybe required.
12. $CD8^+$ T cell responses specific for the transgene product can be assessed with the same assay using the appropriate $CD8^+$ T cell epitope. Similarly, the assay can be used to measure $CD4^+$ T cell responses using peptides encoding the respective epitopes. In this case, frequencies of IFN-γ secreting cells are determined to measure Th1 responses, while for Th2 responses, IL-4 or IL-5 producing cells are typically measured.
13. Begin with a 24-h incubation time but optimization maybe necessary. Optimizing incubation time can be done by using naïve isolated white blood cells and the positive control stimulation media with 5 μg/mL Staphylococcal enterotoxin B. Too short of a time period may result in minimal spot formation and differences in the experimental groups may not be

accurately assessed while excessive incubation time may cause saturation of spot formation.

14. Watch development carefully to prevent overdevelopment, which will lead to high background and make it difficult to accurately count the spots that have formed.
15. If the plate is not thoroughly rinsed, the residual BCIP/NBT can cause overdevelopment of plate while drying. Additionally, the thin plastic sheet on the bottom of the plate that protects the membrane can now be removed manually with pliers so the bottom of the membrane can be rinsed as well.
16. This dilution may need to be optimized depending on antibody titers in sera (i.e. very high levels may need to be diluted more and very low levels may need to be diluted less). Absorbance values should be within the linear range of the standard curve.
17. This dilution may need to be optimized to suit individual needs.
18. Color development should be such to achieve a linear range of immunoglobulin concentration as a function of the absorbance (on a semi-log plot). Therefore, the time of color development has to be optimized. Alternatively, the plate can be measured several times over 5–15-min range in order to identify an optimal readout.
19. Huh7 and 2V6.11 embryonic kidney cell lines have also been described for neutralizing assays for AAV2 serotype (12, 25).
20. Several controls are recommended to validate the assay: (C1) cells alone; (C2) cells + wt Ad5; (C3) cells + rAAV2; (C4) cells + wt Ad5 + rAAV2 (X-Gal positive control); and if possible (C5) cells + wt Ad5 + rAAV2 + control neutralizing negative serum (also X-Gal positive control) and (C6) cells + wt Ad5 + rAAV2 + control neutralizing positive serum (X-Gal negative coloration control). In animal experimental studies, internal neutralizing negative serum can be obtained before rAAV immunization.
21. This is the recommended serum dilution but it may need to be adapted to suit individual needs and depending on levels of rAAV2 antibodies (i.e. very high levels may need to be diluted more, up to 1:5,000).
22. Other variants of incubation with X-Gal are 2 h at 42°C or overnight at 30°C.
23. The plate can be stored at 4°C for further reading.
24. This assay is semi-quantitative (blue cell count using miscroscope) and does not allow precise determination of neutralizing antibody titers. For more precise quantification, the colorimetric detection of β-galactosidase may be assessed by

bioluminiscence after cell lysis and measurement in a microplate luminometer as described elsewhere (12, 25). In assays using luciferase transgene, similar luminescent quantification is described (13).

References

1. Ross, C. J., Twisk, J., Bakker, A. C., Miao, F., Verbart, D., Rip, J., Godbey, T., Dijkhuizen, P., Hermens, W. T., Kastelein, J. J., Kuivenhoven, J. A., Meulenberg, J. M., and Hayden, M. R. (2006) Correction of feline lipoprotein lipase deficiency with adeno-associated virus serotype 1-mediated gene transfer of the lipoprotein lipase S447X beneficial mutation, *Hum Gene Ther 17*, 487–499.
2. Herzog, R. W., Mount, J. D., Arruda, V. R., High, K. A., and Lothrop, C. D., Jr. (2001) Muscle-directed gene transfer and transient immune suppression result in sustained partial correction of canine hemophilia B caused by a null mutation, *Mol Ther 4*, 192–200.
3. Gao, G., Lebherz, C., Weiner, D. J., Grant, R., Calcedo, R., McCullough, B., Bagg, A., Zhang, Y., and Wilson, J. M. (2004) Erythropoietin gene therapy leads to autoimmune anemia in macaques, *Blood 103*, 3300–3302.
4. Favre, D., Blouin, V., Provost, N., Spisek, R., Porrot, F., Bohl, D., Marme, F., Cherel, Y., Salvetti, A., Hurtrel, B., Heard, J. M., Riviere, Y., and Moullier, P. (2002) Lack of an immune response against the tetracycline-dependent transactivator correlates with long-term doxycycline-regulated transgene expression in nonhuman primates after intramuscular injection of recombinant adeno-associated virus, *J Virol 76*, 11605–11611.
5. Chenuaud, P., Larcher, T., Rabinowitz, J. E., Provost, N., Cherel, Y., Casadevall, N., Samulski, R. J., and Moullier, P. (2004) Autoimmune anemia in macaques following erythropoietin gene therapy, *Blood 103*, 3303–3304.
6. Niemeyer, G. P., Herzog, R. W., Mount, J., Arruda, V. R., Tillson, D. M., Hathcock, J., van Ginkel, F. W., High, K. A., and Lothrop, C. D., Jr. (2009) Long-term correction of inhibitor-prone hemophilia B dogs treated with liver-directed AAV2-mediated factor IX gene therapy, *Blood 113*, 797–806.
7. Mount, J. D., Herzog, R. W., Tillson, D. M., Goodman, S. A., Robinson, N., McCleland, M. L., Bellinger, D., Nichols, T. C., Arruda, V. R., Lothrop, C. D., Jr., and High, K. A. (2002) Sustained phenotypic correction of hemophilia B dogs with a factor IX null mutation by liver-directed gene therapy, *Blood 99*, 2670–2676.
8. Mingozzi, F., Liu, Y. L., Dobrzynski, E., Kaufhold, A., Liu, J. H., Wang, Y., Arruda, V. R., High, K. A., and Herzog, R. W. (2003) Induction of immune tolerance to coagulation factor IX antigen by in vivo hepatic gene transfer, *J Clin Invest 111*, 1347–1356.
9. Mingozzi, F., Hasbrouck, N. C., Basner-Tschakarjan, E., Edmonson, S. A., Hui, D. J., Sabatino, D. E., Zhou, S., Wright, J. F., Jiang, H., Pierce, G. F., Arruda, V. R., and High, K. A. (2007) Modulation of tolerance to the transgene product in a nonhuman primate model of AAV-mediated gene transfer to liver, *Blood 110*, 2334–2341.
10. Dobrzynski, E., Mingozzi, F., Liu, Y. L., Bendo, E., Cao, O., Wang, L., and Herzog, R. W. (2004) Induction of antigen-specific CD4+ T-cell anergy and deletion by in vivo viral gene transfer, *Blood 104*, 969–977.
11. Dobrzynski, E., Fitzgerald, J. C., Cao, O., Mingozzi, F., Wang, L., and Herzog, R. W. (2006) Prevention of cytotoxic T lymphocyte responses to factor IX-expressing hepatocytes by gene transfer-induced regulatory T cells, *Proc Natl Acad Sci U S A 103*, 4592–4597.
12. Calcedo, R., Vandenberghe, L. H., Gao, G., Lin, J., and Wilson, J. M. (2009) Worldwide epidemiology of neutralizing antibodies to adeno-associated viruses, *J Infect Dis 199*, 381–390.
13. Boutin, S., Monteilhet, V., Veron, P., Leborgne, C., Benveniste, O., Montus, M. F., and Masurier, C. Prevalence of serum IgG and neutralizing factors against adeno-associated virus types 1, 2, 5, 6, 8 and 9 in the healthy population: implications for gene therapy using AAV vectors, *Hum Gene Ther*.
14. Scallan, C. D., Jiang, H., Liu, T., Patarroyo-White, S., Sommer, J. M., Zhou, S., Couto, L. B., and Pierce, G. F. (2006) Human immunoglobulin inhibits liver transduction by AAV vectors at low AAV2 neutralizing titers in SCID mice, *Blood 107*, 1810–1817.
15. Manno, C. S., Pierce, G. F., Arruda, V. R., Glader, B., Ragni, M., Rasko, J. J., Ozelo, M. C., Hoots, K., Blatt, P., Konkle, B., Dake, M., Kaye, R., Razavi, M., Zajko, A., Zehnder, J., Rustagi, P. K., Nakai, H., Chew, A., Leonard, D., Wright, J. F., Lessard, R. R., Sommer, J. M.,

Tigges, M., Sabatino, D., Luk, A., Jiang, H., Mingozzi, F., Couto, L., Ertl, H. C., High, K. A., and Kay, M. A. (2006) Successful transduction of liver in hemophilia by AAV-Factor IX and limitations imposed by the host immune response, *Nat Med* **12**, 342–347.

16. Jiang, H., Couto, L. B., Patarroyo-White, S., Liu, T., Nagy, D., Vargas, J. A., Zhou, S., Scallan, C. D., Sommer, J., Vijay, S., Mingozzi, F., High, K. A., and Pierce, G. F. (2006) Effects of transient immunosuppression on adenoassociated, virus-mediated, liver-directed gene transfer in rhesus macaques and implications for human gene therapy, *Blood* **108**, 3321–3328.
17. Mingozzi, F., Meulenberg, J. J., Hui, D. J., Basner-Tschakarjan, E., Hasbrouck, N. C., Edmonson, S. A., Hutnick, N. A., Betts, M. R., Kastelein, J. J., Stroes, E. S., and High, K. A. (2009) AAV-1-mediated gene transfer to skeletal muscle in humans results in dose-dependent activation of capsid-specific T cells, *Blood* **114**, 2077–2086.
18. Mingozzi, F., Maus, M. V., Hui, D. J., Sabatino, D. E., Murphy, S. L., Rasko, J. E., Ragni, M. V., Manno, C. S., Sommer, J., Jiang, H., Pierce, G. F., Ertl, H. C., and High, K. A. (2007) CD8(+) T-cell responses to adeno-associated virus capsid in humans, *Nat Med* **13**, 419–422.
19. Brantly, M. L., Chulay, J. D., Wang, L., Mueller, C., Humphries, M., Spencer, L. T., Rouhani, F., Conlon, T. J., Calcedo, R., Betts, M. R., Spencer, C., Byrne, B. J., Wilson, J. M., and Flotte, T. R. (2009) Sustained transgene expression despite T lymphocyte responses in a clinical trial of rAAV1-AAT gene therapy, *Proc Natl Acad Sci U S A* **106**, 16363–16368.
20. Pien, G. C., Basner-Tschakarjan, E., Hui, D. J., Mentlik, A. N., Finn, J. D., Hasbrouck, N. C., Zhou, S., Murphy, S. L., Maus, M. V., Mingozzi, F., Orange, J. S., and High, K. A. (2009) Capsid antigen presentation flags human hepatocytes for destruction after transduction by adeno-associated viral vectors, *J Clin Invest* **119**, 1688–1695.
21. Wang, L., Figueredo, J., Calcedo, R., Lin, J., and Wilson, J. M. (2007) Cross-presentation of adeno-associated virus serotype 2 capsids activates cytotoxic T cells but does not render hepatocytes effective cytolytic targets, *Hum Gene Ther* **18**, 185–194.
22. Sabatino, D. E., Mingozzi, F., Hui, D. J., Chen, H., Colosi, P., Ertl, H. C., and High, K. A. (2005) Identification of mouse AAV capsid-specific CD8+ T cell epitopes, *Mol Ther* **12**, 1023–1033.
23. Chen, J., Wu, Q., Yang, P., Hsu, H. C., and Mountz, J. D. (2006) Determination of specific CD4 and CD8 T cell epitopes after AAV2- and AAV8-hF.IX gene therapy, *Mol Ther* **13**, 260–269.
24. Xiao, W., Chirmule, N., Schnell, M. A., Tazelaar, J., Hughes, J. V., and Wilson, J. M. (2000) Route of administration determines induction of T-cell-independent humoral responses to adeno-associated virus vectors, *Mol Ther* **1**, 323–329.
25. Murphy, S. L., Li, H., Mingozzi, F., Sabatino, D. E., Hui, D. J., Edmonson, S. A., and High, K. A. (2009) Diverse IgG subclass responses to adeno-associated virus infection and vector administration, *J Med Virol* **81**, 65–74.
26. Herzog, R. W., Fields, P. A., Arruda, V. R., Brubaker, J. O., Armstrong, E., McClintock, D., Bellinger, D. A., Couto, L. B., Nichols, T. C., and High, K. A. (2002) Influence of vector dose on factor IX-specific T and B cell responses in muscle-directed gene therapy, *Hum Gene Ther* **13**, 1281–1291.
27. Fields, P. A., Kowalczyk, D. W., Arruda, V. R., Armstrong, E., McCleland, M. L., Hagstrom, J. N., Pasi, K. J., Ertl, H. C., Herzog, R. W., and High, K. A. (2000) Role of vector in activation of T cell subsets in immune responses against the secreted transgene product factor IX, *Mol Ther* **1**, 225–235.

Chapter 12

Modification and Labeling of AAV Vector Particles

Hildegard Büning, Chelsea M. Bolyard, Michael Hallek, and Jeffrey S. Bartlett

Abstract

Adeno-associated virus (AAV) has become a versatile vector platform. In recent years, powerful techniques for the generation of tropism-modified vectors (rAAV-targeting vectors) and for investigation of virus–cell interaction were developed. The following chapter describes strategies for insertion of peptide ligands into the viral capsid and the subsequent characterization of capsid mutants, for producing mosaic capsids and for labeling the viral capsid chemically or genetically.

Key words: Labeling, Capsid particles, Ligands, Chemical modification, Mosaic

1. Introduction

Adeno-associated virus (AAV) has a number of attributes that make it an attractive platform for the development of viral gene transfer vectors Traditionally, serotype 2 vectors (rAAV-2) have been used, which can be produced to high titer and purity. These vectors are very stable, mediate long-term transgene expression in vivo and elicit only mild immune responses compared to other viral vectors. However, many clinically relevant cell types are refractory to rAAV-2 transduction. For this reason, serotypes others than rAAV-2 have been engineered as vectors and their potential have more recently been evaluated in both preclinical and clinical studies. However, one shortcoming of natural occurring serotypes, including rAAV-2 is a lack of specificity. Thus, after local application, tissues in the vicinity of the target can be transduced inadvertently. On the other hand, systemically applied AAV vectors accumulate in liver

Richard O. Snyder and Philippe Moullier (eds.), *Adeno-Associated Virus: Methods and Protocols*,
Methods in Molecular Biology, vol. 807, DOI 10.1007/978-1-61779-370-7_12,

and spleen and are thus not available for transduction of other organs. One strategy to overcome such limitations is to generate receptor/tissue-specific vectors by genetic modification of the viral capsid (targeting). Besides an improved selectivity of cell transduction, lower vector doses are needed, thereby contributing to vector safety. Targeting may also be employed to generate vectors able to transduce cell types that are refractory to infection with natural occurring AAVs.

Most often, targeting is accomplished using site-directed mutagenesis to introduce DNA oligonucleotides encoding small exogenous peptides with receptor-binding specificity into the AAV capsid (*cap*) open reading frame (ORF). When inserted into appropriate sites, these epitopes are displayed on the capsid surface and can mediate novel cellular interactions. Sites within the capsid protein(s) that accept peptide insertions have been defined by a number of laboratories and include the N-terminal region of VP1 and of VP2, and the loop III and IV regions of VP3 (see Table 1). Importantly, AAV packaging constructs have been generated containing restriction sites in many of these locations (1–3). This greatly simplifies the generation of modified packaging constructs, since double-stranded DNA oligonucleotides can simply be inserted into these pre-engineered sites. Alternatively, PCR primers need to be designed, and the exogenous DNA sequences inserted by PCR-based site-directed mutagenesis. Both methods are described here. Generally, most sites can tolerate insertions of up to about 15 amino acids while maintaining wild-type levels of vector assembly and DNA packaging. See Note 1 for suggestions on selecting appropriate insertion sites.

In most instances, small flexible linker sequences flanking the inserted epitopes have proven essential in maintaining titer and efficient display of the targeting epitope on the surface of AAV particles. Although there is not one linker sequence that is best for displaying all peptides in all sites, successful epitope display has been demonstrated using: TG-*peptide insert*-GLS, TG-*peptide insert*-ALS, TG-*peptide insert*-LLA, AS-*peptide insert*-A, and AAA-*peptide insert*-AA (1–6) (see Note 2).

Another approach used to generate AAV vectors with novel characteristics is to mix AAV helper plasmids encoding different serotype capsids during vector preparation. This tactic generates mosaic AAV particles. These mosaic particles usually have properties similar to the serotypes from which they were generated, but in some instances these particles can display novel and unexpected behaviors that may be beneficial for some gene transfer applications (7, 8).

The labeling of AAV capsids has been useful for investigating the process of AAV infection. Green fluorescent protein (GFP) is

Table 1
List of sites that tolerate peptide insertion within the AAV capsid

Serotype	Site (between indicated residues)	Location	Used for targeting	References
AAV1	D590_P591	VP1, VP2, VP3		(1)
AAV2	P34_A35	VP1	x	(25)
	G115_R116	VP1		(3)
	T138_A139	VP1, VP2	x[a]	(25)
	T138_A139	VP2	x	(26)
	A139_P140	VP1, VP2	x	(3)
	K161_A162	VP1, VP2		(3)
	S261_S262	VP1, VP2		(22)
	N381_N382	VP1, VP2, VP3		(22)
	R447_T448	VP1, VP2, VP3		(22)
	T448_N449	VP1, VP2, VP3		(27)
	G453_T454	VP1, VP2, VP3	x	(28)
	R459_L460	VP1, VP2, VP3		(3)
	F534_P535	VP1, VP2, VP3		(22)
	T573_E574	VP1, VP2, VP3		(22)
	Q584_R585	VP1, VP2, VP3		(3)
	N587_R588	VP1, VP2, VP3	x	(22)
	R588_Q589	VP1, VP2, VP3	x	(5)
	A591_T592	VP1, VP2, VP3		(25)
	A664_K665	VP1, VP2, VP3		(25)
AAV3	S586_S587	VP1, VP2, VP3		(1)
AAV4	S584_N585	VP1, VP2, VP3		(1)
AAV5	S575_S576	VP1, VP2, VP3		(1)
AAV6	D590_P591	VP1, VP2, VP3		(1)

[a]Insertion within cap ORF, i.e., within VP1 and at the N′-terminus of VP2

an attractive label because of its high labeling specificity and ease of use. GFP has been fused to the amino-terminus of AAV-2 VP2, and particles incorporating this fusion have been proven extremely useful (9, 10). However, the low valency of VP2 display significantly lessens the signal intensity obtained with this approach. Other protein-based tags that either react covalently or form high affinity complexes with small-molecule probes have yet to be introduced into AAV particles (11, 12). Alternative labeling approaches rely on direct fluorophore conjugation, and although somewhat inefficient have been widely applied and have yielded valuable information regarding intracellular AAV particle trafficking (13–17) and AAV distribution within tissues (18). Both approaches are described here.

2. Materials

2.1. Genetic Modification of AAV Capsids via Peptide Insertion into Surface-Exposed Loops of AAV Capsids

1. QuikChange® Site-Directed Mutagenesis kit (Agilent Technologies, Stratagene Products), or comparable kit.
   (a) *PfuTurbo* DNA Polymerase (2.5 U/µl).
   (b) 10× reaction buffer: 100 mM KCl, 100 mM $(NH_4)_2SO_4$, 200 mM Tris–HCl (pH 8.8), 20 mM $MgSO_4$, 1% Triton®-X 100, 1 mg/ml nuclease-free bovine serum albumin (BSA).
   (c) *Dpn*I restriction enzyme (10 U/µl).
   (d) Oligonucleotide control primers, each a 34-mer (100 ng/µl) – see manual for sequence.
   (e) pWhitescript 4.5-kb control plasmid (5 ng/µl).
   (f) dNTP mix.
   (g) XL1-Blue supercompetent cells.
   (h) pUC18 control plasmid (0.1 ng/µl in TE buffer).
2. DNA oligonucleotides for PCR-based mutagenesis (see Note 3), or complementary DNA oligonucleotides for epitope cloning.
3. AAV helper plasmid: pACG2 (19), pAAV-RC (Stratagene, Agilent Technologies) or similar (see Note 4).
4. 14-ml BD Falcon polypropylene round-bottom tubes (BD Biosciences).
5. NZY+ Broth. Prepared by combining 10 g NZ amine (Sigma Aldrich), 5 g yeast extract, and 5 g NaCl in a total volume of 1 L deionized dH_2O. Adjust the pH to 7.0 with NaOH, autoclave, and then add the following filter-sterilized supplements prior to use: 12.5 ml 1 M $MgCl_2$, 12.5 ml $MgSO_4$, and 10 ml 2 M glucose.
6. LB agar plates containing antibiotic selection (100 µg/ml ampicillin). LB plates are prepared by combining 10 g NaCl, 10 g tryptone, 5 g yeast extract, and 20 g agar (Fisher Bioreagents) in 1 L deionized dH_2O. Adjust pH to 7.0 with 5 N NaOH, autoclave to sterilize, cool to 55°C, add 10 ml filter-sterilized ampicillin (10 mg/ml), and pour into Petri dishes.
7. LB media containing ampicillin (100 µg/ml). LB media is prepared by combining 10 g NaCl, 10 g tryptone, and 5 g yeast extract in deionized dH_2O to a final volume of 1 L. Adjust pH to 7.0 with 5 N NaOH, autoclave, cool to 55°C, and add 10 ml of filter-sterilized ampicillin (10 mg/ml).
8. QIAprep Spin MiniPrep kit (QIAGEN, USA), or comparable mini-prep kit.
9. Equipment and buffer solutions for DNA agarose gel electrophoresis.

2.2. Generation of Mosaic AAV Vector Particles

1. Low passage (<30) human embryonic kidney (HEK) 293 cells (ATCC® number CRL-1573) grown in Dulbecco's modified Eagle's medium (DMEM, Invitrogen) supplemented with 10% fetal bovine serum (FBS) or cosmic calf serum (Hyclone, Thermo Scientific), and 1% penicillin/streptomycin (10,000 U/ml; Hyclone, Thermo Scientific).
2. Two different AAV helper plasmids encoding different AAV serotype capsids (see Note 4).
3. AAV vector plasmid DNA containing the transgene of interest (e.g., pAAV-hrGFP, Stratagene, Agilent Technologies).
4. Adenovirus helper plasmid DNA, such as pXX6-80 (20), pDG (21), or pHelper vector (Stratagene, Agilent Technologies).
5. Calcium phosphate ($CaPO_4$) transfection system (Invitrogen), or
   (a) tissue culture sterile water.
   (b) 2× Hepes-buffered saline (HBS), pH 7.12: 50 mM HEPES, 280 mM NaCl, 1.5 mM Na_2HPO_4 (see Note 5).
   (c) 2 M $CaCl_2$.
6. 100 mM sodium citrate (NaCitrate).
7. Dry ice bath: dry ice and 95% ethanol.
8. Benzonase (Sigma).
9. Iodixanol solution for gradient purification:
   (a) 10× TMSC: 1 M NaCitrate, 100 mM Tris, 25 mM $MgCl_2$, pH 8.0–8.3.
   (b) 15% Iodixanol: 50 ml 60% iodixanol (OptiPrep Density Gradient Medium, Sigma-Aldrich), 20 ml 10× TMSC, 130 ml dH_2O; filter sterilize; store at 4°C and protect from light.
   (c) 25% Iodixanol: 41.7 ml 60% iodixanol, 10 ml 10× TMSC, 49.3 ml dH_2O, neutral red (see Note 6); filter sterilize; store at 4°C and protect from light.
   (d) 40% Iodixanol: 66.7 ml 60% iodixanol, 10 ml 10× TMSC, 23.3 ml dH_2O; filter sterilize; store at 4°C and protect from light.
   (e) 60% Iodixanol: 200 ml 60% iodixanol, 5.822 g NaCitrate, 0.888 g Tris–HCl, 0.570 g Tris Base, 0.102 g $MgCl_2$, neutral red; filter sterilize; store at 4°C and protect from light.
10. Opti-seal™ 30 ml centrifuge tube and protective caps (Beckman-Coulter).
11. Ultracentrifuge and rotor (e.g., Beckman Optima ™ LE-80K Ultracentrifuge with Beckman Type 70.1 Ti Rotor).

2.3. Characterization of Modified Capsids

2.3.1. Assess Genomic Particle Titer of Vector Preparations by Real-Time qPCR

1. DNeasy Blood & Tissue kit (Qiagen, Hilden, Germany), or comparable kit.
2. LightCycler FastStart DNA Master Plus SYBR I kit (Roche Diagnostics GmbH, Mannheim, Germany), or comparable kit.
3. AAV vector plasmid encoding for the vector genome that was packaged.
4. Oligonucleotide Real-Time PCR primers:
   (a) Example of primer pair for the detection of eGFP:
   eGFP-forward: 5′-CACAACGTCTATATCATGGC-3′
   eGFP-backward: 5′-TGTGATCGCGCTTCTC-3′
   (b) Example of primer pair for the detection of β-galactosidase:
   β-Galactosidase-forward: 5′-ATCCTCTGCATGGTCAG GTC-3′
   β-Galactosidase-backward: 5′-CTGGGCCTGATTCAT TCC-3′
5. PBS (Invitrogen, Karlsruhe, Germany).

2.3.2. Assess Capsid Titer of AAV Preparations by ELISA

1. AAV capsid standard.
2. Nunc-Immuno-Plate (Thermo Fisher Scientific, Rochester, USA).
3. PBS (Invitrogen, Karlsruhe, Germany).
4. Washing buffer: 0.05% Tween20 in PBS.
5. Blocking buffer: 3% BSA, 5% sucrose, and 0.05% Tween20 in PBS.
6. Capsid-specific antibody (see Note 7).
7. Biotin-conjugated secondary antibody, for example biotin-conjugated rabbit anti-mouse antibody (Dianova, Hamburg, Germany).
8. Horseradish peroxidase conjugated streptavidin (Dianova, Hamburg, Germany).
9. Start Solution: 1 mg tetramethylbenzidine (TMB) in 10 ml 0.1 M NaOAc (pH 6.2) and 100 µl dimethyl sulfoxide (DMSO). Add 1 µl of 30% H_2O_2 before use.
10. 1 M H_2SO_4.
11. *Alternatively*: AAV capsid ELISA (Progen, Heidelberg, Germany), or comparable kit.

2.3.3. Determine Transduction Efficiency of AAV Vectors by Flow Cytometry

1. Cell line or primary cells.
2. Cell culture multiwell plates.
3. Culture medium including supplements.
4. PBS (Invitrogen, Karlsruhe, Germany).

5. *Optional*: trypsin (0.05% with EDTA) to harvest adherent cells.
6. *Optional*: heparin (Braun Melsungen AG, Melsungen, Germany), or comparable product to assay for pseudotransduction by rAAV-2 preparations.

2.4. Tropism and Specificity of Modified AAV Vectors

2.4.1. Monitoring Cell Entry by Real-Time qPCR

1. Cell lines/primary cells expressing targeted receptor.
2. Control (nontarget) cell lines.
3. Cell culture multiwell plates.
4. Culture medium including supplements.
5. Trypsin (0.05% with EDTA).
6. PBS (Invitrogen, Karlsruhe, Germany).
7. DNeasy Blood & Tissue kit (Qiagen, Hilden, Germany), or comparable kit.
8. LightCycler FastStart DNA Master Plus SYBR I kit (Roche Diagnostics GmbH, Mannheim, Germany), or comparable kit.
9. AAV vector plasmid encoding for the vector genome that was packaged.
10. Oligonucleotide Real-Time PCR primer pair (vector genome).
11. Oligonucleotide Real-Time PCR primer pair (reference gene).
12. LightCycler Relative Quantification Software (Roche Diagnostics GmbH, Mannheim, Germany), or comparable program.

2.4.2. Determining Cell Transduction Efficiency by Flow Cytometry

1. Cell lines/primary cells expressing targeted receptor.
2. Control (nontarget) cell lines.
3. Cell culture multiwell plates.
4. Culture medium including supplements.
5. *Optional*: trypsin (0.05% with EDTA) to harvest adherent cells.
6. PBS (Invitrogen, Karlsruhe, Germany).
7. Competing and noncompeting peptides, proteins, or anti-receptor antibodies to assay for ligand-receptor interaction of modified vectors.
8. Heparin (Braun Melsungen AG, Melsungen, Germany), or comparable product to assay for HSPG/heparin binding ability of modified rAAV-2 vectors.

2.5. Chemical Labeling of the Capsid

1. Highly purified stock of AAV or rAAV vector (see Note 8).
2. The following reagents have been successfully used to fluorescently label AAV particles:
   (a) Cy-Dye labeling reagents (GE Health Care, CyDye FluoroLink reactive dye).

(b) Alexa Fluor labeling reagents (Invitrogen, Alexa Fluor protein labeling kit).

(c) DyLight labeling reagents (Pierce, Thermo Fisher Scientific, DyLight Fluor antibody labeling kit).

(d) LI-COR labeling reagents (LI-COR, IRDye protein labeling kit).

3. Appropriate buffer specified by the labeling reagent:
   (a) CyDye FluorLink; 1.0 M sodium carbonate buffer, pH 9.3.
   (b) Alexa Fluor protein labeling kit; 0.5 M sodium bicarbonate buffer, pH 8.3.
   (c) DyLight Fluor antibody labeling kit; 50 mM sodium borate, pH 8.5.
   (d) IRDye protein labeling kit; 50 mM phosphate buffer, pH 8.5.
4. G-50 (Sephadex) spin columns.
5. TMSC Buffer.

2.6. Genetic Labeling

1. Competent *E. coli* cells or comparable cells for plasmid transformation.
2. Plasmid encoding for *cap* ORF as template for VP2 modification and isolation.
3. peGFP-C3 (BD Bioscience, Heidelberg, Germany) or comparable plasmid.
4. Oligonucleotide PCR primer pair to amplify VP2 and simultaneously mutate the VP2 start codon. For example:
   (a) AAV2-VP2-forward: 5′-GAA GCG CGA TCA CAT GGT CC-3′
   (b) AAV2-VP2-backward: 5′-TCA GCG TGG AGA TCG AGT GG-3′
5. AAV helper plasmid encoding the *rep* ORF and *cap* ORF, e.g., pRC (22), pACG2 (19), pAAV-RC (Stratagene, Agilent Technologies) or similar (see Note 4).
6. Oligonucleotide PCR primer for site-directed mutagenesis of VP2 start codon in AAV helper plasmid. For example:
   (a) AAV2-VP2k.o.-forward: 5′-GTTAAGACCGCTCCG GG-3′
   (b) AAV2-VP2k.o.-back: 5′-CCCGGAGCGGTCTTAAC-3′
   (c) AAV2-ligation primer-forward: 5′-AAATCAGGTATGGC TGCCGA-3′
   (d) AAV2-ligation primer-back: 5′-GTTGCCTCTCTGGAG GTT-3′.

7. T4 polynucleotide kinase.
8. Calf intestine phosphatase.
9. Restriction endonucleases and buffer (e.g., *Bgl*II to linearize peGFP-C3, and *Bst*WI and *Eco*NI to isolate *cap* fragment).
10. T4 DNA ligase and buffer.
11. *Pfu Turbo* DNA polymerase for PCR amplification of VP2 and for site directed mutagenesis.
12. QiaQuick Gel Extraction Kit (Qiagen, Hilden, Germany).
13. LB agar plates containing antibiotic selection (kanamycin at 50 μg/ml or amplicilin at 50–100 μg/ml).
14. LB media.
15. LB media containing ampicillin at 50–100 μg/ml or kanamycin 50 μg/ml.
16. Qiagen MiniPrep kit (Qiagen, Hilden, Germany), or comparable kit.
17. HEK293 cells for AAV vector packaging.
18. $CaCl_2$ solution (2 M stock solution) and HBS buffer for plasmid transfection into HEK293 cells.
19. peGFP-AAV2-VP2 encodes for the eGFP-VP2 fusion protein (Subheading 3.6.1).
20. pRC-VP2.k.o. encodes for *rep* ORF of AAV-2, and VP1 and VP3 of AAV-2 (Subheading 3.6.2).
21. AAV vector plasmid containing AAV ITRs and transgene of choice.
22. Adenoviral helper plasmid, e.g., pXX6-80 (20) or similar.
23. Lysis buffer: 150 mM NaCl and 50 mM Tris/HCl (pH 8.5).
24. Benzonase (Merk, Darmstadt, Germany).

3. Methods

3.1. Genetic Modification of AAV Capsids via Peptide Insertion into Surface-Exposed Loops of AAV Capsids

Several AAV packaging constructs have been generated containing unique restriction sites engineered into the *cap* ORF (1–3). Use of these constructs as starting reagents greatly simplifies the process of epitope insertion, since two 5' phosphorylated complementary DNA oligonucleotides need only be synthesized with compatible cohesive ends and cloned into these pre-engineered sites. Alternatively, site-directed mutagenesis is used to insert DNA oligonucleotides encoding the desired epitopes into the AAV *cap* ORF. Use of a kit, such as the QuikChange Site-Directed Mutagenesis Kit (Agilent, Stratagene, La Jolla, CA) is recommended. Mutagenesis is performed using a thermostable DNA polymerase

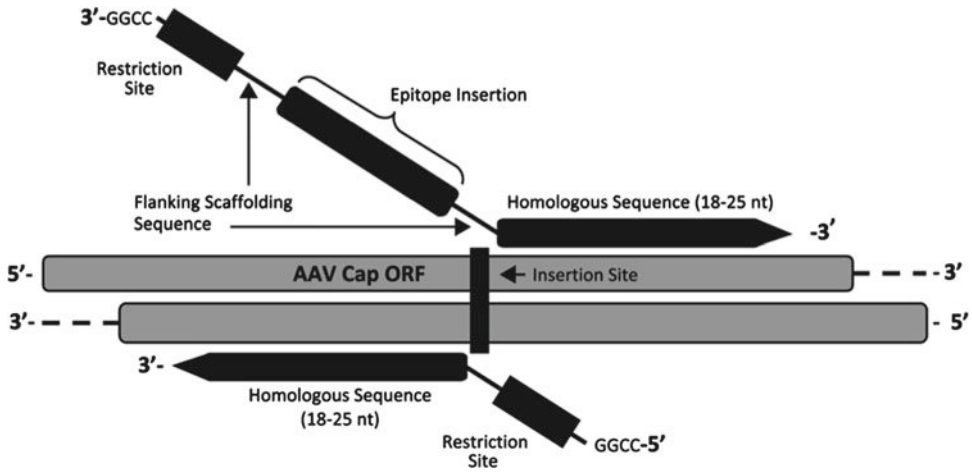

Fig. 1. Design of oligonucleotides for PCR-based site-directed mutagenesis.

(see Note 9) and a temperature cycler. The basic procedure utilizes a supercoiled double-stranded DNA plasmid containing the AAV *cap* ORF and two synthetic oligonucleotide primers containing the desired insertion (see Fig. 1). The oligonucleotide primers, each complementary to opposite strands of the vector, are extended during temperature cycling by the thermostable DNA polymerase. Incorporation of the oligonucleotide primers generates a mutated packaging construct containing staggered nicks. Following temperature cycling, the product is treated with *Dpn*I. The *Dpn*I endonuclease (target sequence: 5′-Gm6ATC-3′) is specific for methylated and hemimethylated DNA and is used to digest the parental DNA template and to select for the modified DNA. The nicked DNA containing the desired insertion is then transformed into *E. coli* (e.g., XL1-Blue supercompetent cells). The small amount of starting DNA template required to perform this method, the high fidelity of DNA polymerase, and the low number of thermal cycles all contribute to high efficiency and decreased potential for generating random mutations during the reaction.

3.1.1. Mutagenic Primer Design

For cloning into an AAV helper plasmid containing a pre-engineered restriction site, two complementary DNA oligonucleotides encoding the chosen epitope need to be designed. It may be appropriate to flank the desired epitope with scaffolding sequences, although these may also be encoded by the in-frame restriction site (see Note 10). In addition, nucleotide overhangs to the restriction site need to be added to the 5′ and 3′ end of the DNA oligonucleotides, respectively. Primers should be 5′ phosphorylated and purified either by fast polynucleotide liquid chromatography (FPLC) or by polyacrylamide gel electrophoresis (PAGE). Skip to Subheading 3.1.3 for cloning reactions.

3.1.2. Site-Directed Mutagenesis

For site-directed mutagenesis, primers must be designed according to the desired mutation and site of insertion (see Note 3). The 5′ ends of each primer should contain complementary versions of a unique restriction site not present in the parental plasmid. Primers need not be 5′ phosphorylated but must be purified either by FPLC or by PAGE. Failure to purify the primers results in a significant decrease in mutation efficiency.

1. If using the QuikChange® Site Directed Mutagenesis kit (Agilent Technologies, Statagene Products), set up sample and control reactions in thin-walled PCR tubes as follows:

   Control reaction

   (a) 5 µl 10× reaction buffer.

   (b) 2 µl (10 ng) dsDNA template (e.g., pWhitescript control plasmid (5 ng/µl)).

   (c) 1.25 µl (125 ng) of oligonucleotide primer, forward (e.g., oligonucleotide control primer #1).

   (d) 1.25 µl (125 ng) of oligonucleotide primer, reverse (e.g., oligonucleotide control primer #2).

   (e) 1 µl dNTP mix (see Note 11).

   (f) 40.5 µl ddH_2O (to a final volume of 50 µl).

   (g) 1 µl *PfuTurbo* DNA polymerase
   (Total volume 51 µl)

   Sample reaction

   (a) 5 µl 10× reaction buffer.

   (b) 2 µl (10 ng) dsDNA template, e.g., AAV packaging plasmid (5 ng/µl) (see Note 12).

   (c) 1.25 µl (125 ng) of oligonucleotide primer, forward (e.g., mutant forward primer).

   (d) 1.25 µl (125 ng) of oligonucleotide primer, reverse (e.g., mutant reverse primer).

   (e) 1 µl dNTP mix (see Note 11).

   (f) 40.5 µl ddH_2O (to a final volume of 50 µl).

   (g) 1 µl *PfuTurbo* DNA polymerase
   (Total volume 51 µl)

2. Overlay each reaction with mineral oil (~30 µl) if the thermal cycler to be used does not have a hot-top assembly.

3. Cycle each reaction using the following cycling parameters:

   (a) Denature at 95°C for 30°s.

   (b) Three-step amplification cycle (Run 18 cycles): Denature at 95°C for 30 s, anneal at 55°C for 1 min, and then extend at 68°C for 1 min/kb of plasmid length.

   (c) Maintain the reaction at 4°C after cycling.

4. Add 1 µl of *DpnI* endonuclease (10 U/µl) directly to amplification reaction. Be sure to add enzyme below mineral oil overlay, if used. Mix gently and thoroughly by pipetting solution up and down several times.
5. Incubate at 37°C for 1 h to eliminate nonmutated parental plasmid template (see Note 13). Skip to Subheading 3.1.4 for transformation of XL1-Blue supercompetent cells.

3.1.3. Cloning of DNA Oligonucleotides

1. Resuspend each oligonucleotide at ~100 µg/ml in TE buffer containing 150 mM NaCl. Mix equimolar amounts of each strand and heat 10 min at 65°C.
2. Cool slowly to room temperature by placing the tube at room temperature for 20 min. Check the OD_{260} to determine final concentration, and check to be sure that the oligonucleotides have completely annealed by running aliquots of each complementary strand, as well as the annealed double-stranded oligonucleotide, on a 4% sieving agarose gel.
3. Digest the AAV helper plasmid with the restriction enzyme that recognizes the unique site, engineered for epitope insertion, within the AAV *cap* ORF, dephosphorylate, gel purify, and determine the final concentration of the linearized DNA.
4. Assemble the ligation reaction, as exemplified by the following. Mix the linearized AAV helper plasmid DNA with a 50-fold molar excess of the hybridized oligonucleotides; use ~400 ng total DNA in 10 µl, for a final concentration of 40 µg/ml. Add 0.4 µl (160 cohesive-end units) T4 DNA ligase and incubate 2 h at 15°C.
5. Dilute the ligation mixture fourfold to a concentration of 10 µg/ml.

3.1.4. Transformation of Competent Cells

1. Transform 2 µl of the ligation mixture (Subheading 3.1.3), or 1 µl of the *Dpn* I-treated DNA from each control and sample site-directed mutagenesis reactions (Subheading 3.1.2) into the XL1-Blue supercompetent cells (see Note 14).
2. Plate transformation reactions on LB agar plates containing the appropriate antibiotic selection (ampicillin). For mutagenesis and transduction controls using the QuikChange® site directed mutagenesis kit, plate cells on LB-ampicillin plates containing 80 µg/µl X-gal and 20 mM IPTG.
3. Incubate the plates overnight (>16 h) at 37°C (see Note 15).
4. Select three to five mutant colonies, and incubate them in 3 ml LB broth with ampicillin overnight at 37°C with shaking.
5. Extract DNA using QIAprep Spin MiniPrep kit.
6. Screen for sequence insertion by restriction endonuclease digestion (see Note 10) and sequence mutant construct to confirm epitope insertion and lack of second site mutations.

3.1.5. Production of Capsid-Modified AAV Vectors

1. To produce AAV vectors comprised of modified capsid proteins, use the modified AAV helper plasmid (generated by site-directed mutagenesis, Subheading 3.1.2, or oligonucleotide cloning, Subheading 3.1.3), in place of standard AAV helper plasmid in the triple transfection protocol for AAV vector production (described elsewhere).
2. Characterize modified vectors as described below (Subheading 3.3).

3.2. Generation of Mosaic AAV Vector Particles

To produce mosaic AAV vectors, transfect low passage HEK293 cells following calcium phosphate transfection protocol. HEK293 cells should be approximately 80% confluent on a 15 cm tissue culture plate.

1. Change media on HEK293 cells 4 h prior to transfection. Add 18 ml of fresh media.
2. Add the following DNAs (47 μg total) to $CaCl_2$-buffered dH_2O (250 mM final concentration).
   (a) Adenovirus helper plasmid containing VA, E2A, and E4 genes.
   (b) AAV vector plasmid containing AAV ITRs and transgene of choice.
   (c) The two different AAV helper plasmids (encoding different serotype AAV capsids) at varying ratios (for example, 1:19, 1:3, 1:1, 3:1, 19:1). Assessment of different ratios of one capsid component to another permits appraisal of the importance of each (see Table 2 for example).
3. Prepare the DNA-$CaCl_2$ and HBS solutions according to Table 3. Volumes can be scaled based on the number of plates to be used in transfection.
4. Using a pipette, slowly add solution from Tube A dropwise to Tube B while bubbling air through 2× HBS solution (Tube B) with another pipette. This is a slow process which should be done over several minutes.
5. A fine precipitate should form. Add the precipitate dropwise to the media, 2 ml per 15 cm plate.
6. Incubate overnight at 37°C in a humidified CO_2 incubator.
7. Change the media after 24 h.
8. Sixty hours after transfection, harvest cells. Using a cell scraper, dislodge cells, and collect both the media and cells in a 250 ml conical tube. Harvest cells by centrifugation at 500×*g* for 10 min.
9. Resuspend cell pellet in 2 ml of 100 mM NaCitrate per plate. Transfer to a 50 ml Falcon tube (see Note 16).

Table 2
Relative amounts of DNA used to produce mosaic virions

Plasmid	Composition	Amount (µg)/plate
Adenovirus helper plasmid (e.g., pXX6-80)		27 µg
Vector plasmid (e.g., AAV-hrGFP)		10 µg
Serotype A/serotype B helper plasmid	100% A 5% B/95% A 33% B/67% 50% B/50% A 67% B/33% A 95% B/5% A	10 µg A 0.5 µg B:9.5 µg A 2.5 µg B:7.5 µg A 5.0 µg B:5.0 µg A 7.5 µg B:2.5 µg A 9.5 µg B:0.5 µg A

Table 3
Components of transfection mixture

Tube A	Volume/plate	Tube B	Volume/plate
DNA (47 µg)	*x*µl	2× HBS	1,000 µl
2.5 M $CaCl_2$	100 µl		
Sterile dH_2O	(900 – *x*)µl		
Total	1,000 µl	*Total*	1,000 µl

10. Release intracellular viral particles by inducing cell lysis via three consecutive freeze-thaw cycles, consisting of shuttling cell suspension between dry ice/ethanol bath and 37°C water bath (tubes should be vortexed vigorously after each thawing step).
11. Clarify the crude lysate by centrifugation at 500 × *g* for 10 min, and reduce viscosity by treating with benzonase (50 U/ml of cell lysate) for 30 min at 37°C, with occasional mixing.
12. Pellet cell debris by centrifuging at 5,000 × *g* for 25 min at 18°C.
13. Purify viral particles from cell debris via iodixanol density-gradient purification. Prepare an iodixanol step gradient in an Opti-seal 30 ml centrifuge tube.
    (a) Bring viral vector lysate to 15 ml with NaCitrate if necessary.
    (b) Add the viral vector lysate to an Opti-seal 30 ml centrifuge tube. Underlay the crude viral vector preparation with 6 ml of a 15% iodixanol solution, then 4 ml of a 25%

iodixanol solution, 3 ml of 40% iodixanol solution, and 2 ml of 60% iodixanol solution.

14. Balance centrifuge tubes and ensure that they are full. Bubbles in the tube lead to tube collapse during centrifugation. Cap and seal tubes.
15. Centrifuge in a fixed angle rotor (e.g., Beckman 70Ti) with protective caps at 68 K for 1 h at 18°C.
16. Remove protective caps and seal. Using an 18 gauge needle, puncture the bottom of the tube and allow the iodixanol fractions to drain; collect the 40% fraction containing AAV.
17. Characterize iodixanol-purified vector as described below (Subheading 3.3).
18. Further purify AAV vectors as needed and store vectors at –20°C.

3.3. Characterization of Modified Capsids

Viral/vector genomes are packaged into preformed capsids. Viral/vector preparations therefore contain both empty and DNA-containing capsids. While the capsid titer (amount of capsids per ml) can be determined by ELISA using anticapsid antibodies, real-time qPCR is commonly used to determine the genomic titer (DNA containing particles per ml) of a preparation. Comparison of the capsid-to-genomic particle ratio of capsid-modified and unmodified vectors reveals whether a capsid modification interferes with packaging.

Furthermore, by assessing the cell entry and transduction efficiencies of capsid-modified vectors on target and nontarget cells conclusions on the tropism can be drawn. Tropism can be further analyzed by conducting cell transductions in the presence and absence of substances interfering with target receptor binding.

3.3.1. Assess Genomic Particle Titer of Vector Preparations by Real-Time qPCR

1. Dissolve 10 µl of AAV vector preparation in 190 µl PBS.
2. Isolate vector DNA by DNeasy Blood & Tissue Kit according to the protocol "Purification of total DNA from cells."
3. Elute vector DNA in 200 µl 10 mM Tris–HCL pH 8.0.
4. Store DNA at –20°C or proceed to real-time qPCR analysis.
5. Prepare at least four PCR standards (10^6 to 10^9 AAV vector plasmids per µl).
6. If using the LightCycler FastStart DNA MasterPLUS SYBR I kit, set up sample reaction in LightCycler capillary, containing the following reagents:
   (a) 4 µl SYBR Green PCR Master Mix
   (b) 1 µl oligonucleotide PCR primer #1 (20 µM)
   (c) 1 µl oligonucleotide PCR primer #2 (20 µM)
   (d) 12 µl ddH_2O

7. Run real-time PCR; e.g., for quantification of vector genomes coding for eGFP on a LightCycler platform use the following cycling parameters:
   (a) Denature at 95°C for 5 min.
   (b) Three-step amplification cycle (run 40 cycles): Denature at 95°C for 15 s, anneal at 60°C for 10 s, and then extend at 72°C for 30 s.
   (c) The temperature transition rate should be 20°C/s.
8. Confirm the specificity of target amplification by melting curve analysis and agarose gel electrophoresis.

3.3.2. Assess Capsid Titer of rAAV-2 Vector Preparations by ELISA

1. Prepare a serial dilution of the vector preparation in PBS. The assumed concentration should be between 2×10^5 and 2×10^7 capsids per µl (see Note 17).
2. Prepare a serial dilution of the capsid standard in PBS.
3. Coat the Nunc-Immuno plate with 100 µl of vector dilutions (and standard) per well.
4. Incubate overnight at 4°C.
5. Perform three washing steps with washing buffer (200 µl per well).
6. Add blocking buffer to the wells (200 µl per well).
7. Incubate for 2 h at room temperature.
8. Remove the blocking buffer.
9. Add A20 (anti-AAV2) antibody dilution (1:4 in blocking buffer; 100 µl per well).
10. Incubate for 1 h at room temperature.
11. Perform three washing steps with washing buffer (200 µl per well).
12. Add biotin-conjugated anti-mouse antibody dilution (1:25,000 in blocking buffer; 100 µl per well).
13. Incubate for 1 h at room temperature.
14. Perform three washing steps with washing buffer (200 µl per well).
15. Add horseradish peroxidase-conjugated streptavidin (1:500 in blocking buffer; 100 µl per well).
16. Incubate for 1 h at room temperature.
17. Perform three washing steps with washing buffer (200 µl per well).
18. Perform two washing steps with water (200 µl per well).
19. Add Start Solution to the well (100 µl per well).
20. Stop color reaction by adding 1 M H_2SO_4 (50 µl per well).
21. Measure the intensity of color reaction (450 nm).

3.3.3. Determine Transduction Efficiency of AAV Vectors by Flow Cytometry

1. *Suspension cells*: Seed the desired number of cells in fresh medium (containing all the required supplements) into a cell culture multiwell plate.

   Adherent cells: Seed cells in fresh medium (containing all the required supplements) into a cell culture multiwell plate. Incubate the cells at 37°C in a humidified CO_2 (5%) incubator for 24 h. Prior to transduction, determine the amount of cells per well in one of the wells and change the media in the remaining wells (see Note 18).
2. Calculate the amount of vector solution that is needed per well based on the number of cells per well, the genomic particle titer of the rAAV preparation and the desired particle-to-cell ratio.
3. Thaw the vector solution on ice.
4. Add vector solution to the wells and mix. Do not forget to prepare a negative control (no vector).
5. Incubate the cells for 48 h at 37°C in a humidified CO_2 (5%) incubator.
6. Harvest the cell and wash the cell pellet twice with PBS.
7. Resuspend pellet in 500 µl PBS.
8. *Optional*: Incubate cell pellet with antibodies specific for your transgene product according to the manufacturer's instructions (see Note 19).
9. Perform flow cytometry measurements according to manufacturer's instructions. Negative control should be set as 1%. Count a minimum of 5,000 cells for each sample.

3.3.4. Determine Transducing Titer of Vector Preparation

1. Seed permissive cells (see Note 20) in a 12-well cell culture plate (4 cm^2) and incubate the cells for 24 h at 37°C in a humidified CO_2 (5%) incubator (see Note 18).
2. Prepare a serial dilution of vector preparation in medium containing all required supplements (see Note 21).
3. Remove the medium from the wells.
4. Add 1 ml medium to cells of the negative control.
5. Add 500 µl medium to the remaining wells and add 500 µl of each dilution.
6. *Optional*: In order to assay for pseudotransduction by rAAV-2 vector preparations add 425 IU of heparin to the medium of one well (final volume 1 ml) and add 1 µl of the vector preparation to this well.
7. Incubate the cell culture plate for 48 h at 37°C in a humidified CO_2 (5%) incubator.
8. Determine the amount of cells per well by counting the cells of the negative control.

9. Measure the percentage of transgene expressing cells by flow cytometry (see above).
10. Calculate the transducing titer of the vector solution from the dilution that led to ~10% transgene expressing cells as shown in the following example:
    (a) Cells per well: 8×10^4
    (b) Percentage of transgene expressing cells: 9.5%
    (c) Negative control: 1%
    (d) Vector solution: 0.0003 µl
    (e) $[(8 \times 10^4 \times (9.5 - 1)]/100)/0.0003 = \text{transducing particles}/\mu\text{l}$.

3.4. Tropism and Specificity of Modified rAAV Vectors

Post-entry barriers may limit successful cell transduction even though vectors are capable of binding and entering target cells. Hence, both cell entry and cell transduction should be determined in order to fully assess the tropism and specificity of a modified vector.

3.4.1. Monitoring of Cell Entry by Real-Time qPCR

1. Seed target and control cells as described above (see Note 18).
2. Thaw the vector solutions (different serotypes or modified and unmodified vector) on ice.
3. Transduce the cells with equal genomic particle-per-cell ratios of the vectors you would like to compare. Do not forget to prepare a negative control (no vector).
4. Incubate the cells for 4 h at 37°C in a humidified CO_2 (5%) incubator.
5. Harvest the cells and wash the cell pellet twice with PBS (see Note 22).
6. Resuspend cell pellet (a maximum 5×10^6 cells) in 200 µl PBS.
7. Isolate vector DNA by DNeasy Blood & Tissue Kit according to the protocol "Purification of total DNA from cells."
8. Elute vector DNA in 200 µl 10 mM Tris–HCl pH 8.0.
9. Store at –20°C or proceed to real-time qPCR analysis.
10. Prepare at least four PCR standards (10^6 to 10^9 AAV vector plasmids per µl).
11. If using the LightCylcer FastStart DNA MasterPLUS SYBR I kit, set up sample reaction in LightCycler capillary, containing the following reagents:
    (a) 4 µl SYBR Green PCR Master Mix
    (b) 1 µl oligonucleotide primer #1 (20 µM)
    (c) 1 µl oligonucleotide primer #2 (20 µM)
    (d) 18 µl ddH_2O.

12. Run real-time qPCR according to requirements of PCR reaction.
13. Confirm the specificity of target amplification by melting curve analysis and agarose gel electrophoresis.
14. Repeat steps 11–13 with oligonucleotide PCR primer pair amplifying a reference (housekeeping) gene.
15. Use the LightCycler Relative Quantification Software (Roche Diagnostics GmbH, Mannheim, Germany), or a comparable program to normalize the values obtained for the vector/viral genomes.

3.4.2. Determining Cell Transduction Efficiency by Flow Cytometry

1. Seed target and control cells as described above (see Note 18).
2. Thaw the vector solutions (different serotypes or modified and unmodified vector) on ice.
3. Transduce the cells with equal genomic particle-per-cell ratios of the vectors you would like to compare. Assay at least three different particle-to-cell ratios per cell line. Do not forget to prepare a negative control (no vector).
4. *Optional*: To assess the use of HSPG as cellular receptor, perform cell transductions in the presence of 425 IU of heparin.
5. To assess the use of target receptor, perform cell transductions in the presence and absence of competing and noncompeting peptides, proteins, or antireceptor antibodies (see Note 23).
6. Add competitor (e.g., heparin or peptides) to the cells prior to vector transduction.
7. Incubate the cells for 48 h at 37°C in a humidified CO_2 (5%) incubator.
8. Harvest the cells and determine the percentage of transgene expressing cells, e.g., by flow cytometry.

3.5. Chemical Labeling of the Capsid

1. Buffer exchange. Adjust AAV stock to a concentration of 1.33×10^{14} particles/ml (1 mg/ml) in the appropriate buffer. Buffer exchange can be accomplished by passing the vector through a desalting column equilibrated with reaction buffer. Alternatively, the vector solution can be dialyzed against the reaction buffer in a small dialysis cassette. If the vector is in a simple PBS buffer free of ammonium ions or primary amines, the pH of the solution can be raised by adding the concentrated buffer (e.g., 1 M potassium phosphate, pH 9 for IRDye labeling). However, the time the virus/vector is maintained at pH 9 should be kept to an absolute minimum.
2. Reconstitute the labeling reagent with the diluted AAV stock in 1-ml of reaction buffer. Make sure *all* of the dye is dissolved. Undissolved dye will retain reactivity and may co-purify with the labeled virus and hamper further characterization.

3. Incubate at room temperature for 60 min.
4. Purify labeled AAV from unreacted dye by either dialysis against 3 L TMSC buffer using a dialysis chamber (Slide-a-Lyser, 6,000–8,000 MW cutoff, Pierce, Thermo Fisher Scientific), or gel filtration on a G-50 (Sephadex) column equilibrated with TMSC buffer. The benefit of this technique is that purification can be monitored visually.
5. Characterize labeled AAV as described above (Subheadings 3.3 and 3.4). The titer of the labeled virus should not have significantly changed. Preparations that show a decrease in titer of more than 50% should be used with caution. Decreases in titer usually come from too high a labeling ratio (dye:particle) or failure to rapidly adjust pH following coupling. To determine the conjugation efficiency, read the absorbance spectrum of the labeled AAV and determine the dye concentration (per recalculated particle number) using the extinction coefficient for the fluorophore (provided by the manufacturer). AAV labeling ratios should be approximately 2 dye molecules per virion/vector for the greatest sensitivity with the least effect on AAV biology.

3.6. Genetic Labeling of the Capsid

The N-terminus of VP2 tolerates the insertion of fluorescent proteins. In order to generate AAV capsids that do not contain wild-type VP2, the VP2 start codon has to be deleted in the *cap* ORF of AAV helper plasmid and in the ORF encoding for the fusion protein.

3.6.1. Cloning of Fluorescent Protein-VP2 N-Terminal Fusion Protein Using peGFP-AAV2-VP2 as Example

1. Perform site directed mutagenesis of the VP2 start codon by PCR. For serotype 2, set up the following sample reaction:
   (a) Plasmid coding for AAV-2 *cap* ORF (100 ng)
   (b) Oligonucleotide PCR primer: AAV2-VP2-forward (30 pmol)
   (c) Oligonucleotide PCR primer: AAV2-VP2-backward (30 pmol)
   (d) dNTP mix (see Note 11)
   (e) *Pfu Turbo* DNA polymerase (1.25 U)
   (f) ddH_2O to a final volume of 50 µl
   (g) PCR cycling parameters:
   - Denaturation at 95°C for 5 min.
   - Three-step amplification cycle (run 30 cycles): Denature at 95°C for 1 min, anneal at 53°C for 1 min, and then extend at 72°C for 2 min.
   - Final extension at 72°C for 10 min.
2. Purify PCR fragment by agarose gel electrophoresis and QiaQuick Gel Extraction Kit, or a comparable kit.

3. Phosphorylate the PCR fragment using T4 polynucleotide kinase according to standard protocols.
4. Prepare the plasmid backbone using peGFP-C3 as example:
   (a) Linearize peGFP-C3 (10 µg) with 20 U *Bgl*II in 1× reaction buffer in a final volume of 20 µl for 3 h at 37°C.
   (b) Isolate the linearized backbone by agarose gel electrophoreses and QiaQuick Gel Extraction Kit.
   (c) Modify the backbone by DNA polymerase I (Large Klenow Fragment) using 1 U per µg template, 33 µM dNTP (each), and 1× reaction buffer in a final volume of 50 µl.
   (d) Stop the reaction after a 15-min incubation at 25°C by addition of EDTA (final concentration of 10 mM) and a 20-min incubation at 75°C.
   (e) Dephosphorylate the backbone using calf intestine phosphatase (CIAP) according to standard protocols.
   (f) Purify the backbone by QiaQuick Gel Extraction kit.
5. Ligate PCR fragment and backbone using T4 DNA ligase.
6. Transform bacteria according to standard protocols.
7. Incubate bacterial suspension in LB medium for 1 h at 37°C.
8. Plate transformation reaction on LB agar plates containing the appropriate antibiotic selection.
9. Incubate the plates overnight (>16 h) at 37°C.
10. Select three to five colonies and incubate them in 3 ml LB with appropriate antibiotic overnight at 37°C with shaking.
11. Extract plasmid DNA using Qiagen MiniPrep kit or a comparable kit.
12. Screen for in frame VP2 insertion by restriction endonuclease digest and sequencing to confirm insertion and lack of second-site mutation.

3.6.2. Site Directed Mutagenesis of VP2 Start Codon of Cap ORF (Cloning of pRC-VP2.k.o.)

1. Perform site directed mutagenesis of the AAV-2 VP2 start codon, followed by PCR-mediated ligation of the fragment. For site-directed mutagenesis, prepare the following two PCR reactions:

   Fragment #1

   (a) *Cap* ORF encoding plasmid (100 ng)
   (b) Oligonucleotide PCR primer: AAV2-VP2k.o.-forward (30 pmol).
   (c) Oligonucleotide PCR primer: AAV2-ligation primer-backward (30 pmol)
   (d) dNTP mix (see Note 11)
   (e) *Pfu Turbo* DNA polymerase (2.5 U)
   (f) ddH_2O to a final volume of 50 µl.

(g) PCR cycling parameters:
- Denaturation at 95°C for 5 min.
- Three-step amplification cycle (run 35 cycles): Denature at 95°C for 30 s, anneal at 50°C for 1 min, and then extend at 72°C for 2 min.
- Final extension at 72°C for 10 min.

(h) Purify PCR fragment, e.g., by agarose gel electrophoreses and QiaQuick Gel Extraction according to manufacturer's instruction.

Fragment #2

(a) *Cap* ORF encoding plasmid (100 ng)

(b) Oligonucleotide PCR primer: AAV2-ligation primer-forward (30 pmol)

(c) Oligonucleotide PCR primer: AAV2-VP2k.o.-backward (30 pmol)

(d) dNTP mix (see Note 11)

(e) *Pfu Turbo* DNA polymerase (2.5 U)

(f) ddH_2O to a final volume of 50 µl

(g) PCR cycling parameters:
- Denaturation at 95°C for 5 min.
- Three-step amplification cycle (run 35 cycles): Denature at 95°C for 30 s, anneal at 50°C for 1 min, and then extend at 72°C for 2 min.
- Final extension at 72°C for 10 min

(h) Purify PCR fragment, e.g., by agarose gel electrophoreses and QiaQuick Gel Extraction according to manufacturer's instruction.

Ligation of fragment #1 and fragment #2

(a) Fragment #1 and fragment #2 in ratio of 4:1 (~100 ng)

(b) Oligonucleotide PCR primer: AAV2-VP2k.o.-forward (30 pmol)

(c) Oligonucleotide PCR primer: AAV2-VP2k.o.-backward (30 pmol)

(d) dNTP mix (see Note 11)

(e) *Pfu Turbo* DNA polymerase (2.5 U)

(f) ddH_2O to a final volume of 50 µl

(g) PCR cycling parameters:
- Denaturation at 95°C for 5 min
- Three-step amplification cycle (run 35 cycles): Denature at 95°C for 30 s, anneal at 50°C for 1 min, and then extend at 72°C for 3 min.
- Final extension at 72°C for 10 min

(h) Purify PCR fragment, e.g., by agarose gel electrophoreses and QiaQuick Gel Extraction according to manufacturer's instruction.

2. Linearize plasmid backbone (*rep* and *cap* ORF encoding AAV helper plasmid, e.g., pRC (22)) by adding 10 U of restriction endonuclease *Bsi*WI to 10 µg of plasmid in 1× reaction buffer adjusted to a final volume of 30 µl.
3. Following 3 h of incubation at 55°C, add restriction endonuclease *Eco*NI (15 U) and incubate for further 3 h at 37°C.
4. Dephosphorylate the backbone by CIAP using standard protocols.
5. Purify backbone by agarose gel electrophoresis and QiaQuick Gel Extraction Kit according to standard protocols.
6. Modify the PCR fragment with *Bsi*WI and *Eco*NI as described for plasmid backbone with exception of step 4.
7. Ligation of backbone and PCR fragment by T4 DNA Ligase
8. Transform bacteria, followed by incubation in LB medium for 1 h at 37°C.
9. Plate bacterial suspension on LB agar plates containing ampicillin (50–100 µg/ml).
10. Incubate the plates overnight (>16 h) at 37°C.
11. Select three to five colonies, incubate them in 3 ml LB with ampicillin (final concentration: 50–100 µg/ml) overnight at 37°C with shaking.
12. Extract plasmid DNA using Qiagen MiniPrep kit or a comparable kit.
13. Screen for fragment insertion by restriction endonuclease digestion.
14. Sequence modified plasmid to confirm insertion, mutation of VP2 start codon, and lack of second-site mutations.

3.6.3. Generation of eGFP-Tagged rAAV-2 Vector Particles

1. To produce eGFP-tagged rAAV-2 vector particles, transfect low passage HEK293 cells following calcium phosphate transfection protocol (see Note 18).
2. Change media 4 h prior to transfection. Adding 18 ml of fresh media.
3. Add the following plasmids (1:1:1:1 M ratio; 47 µg total) to $CaCl_2$-buffered dH_2O (250 mM final concentration).
   (a) Adenovirus helper plasmid containing VA, E2A, and E4 genes
   (b) AAV vector plasmid containing AAV ITRs and transgene of choice

(c) The two different AAV helper plasmids (pRC-VP2-k.o. and peGFP-AAV2-VP2)

4. Proceed with AAV vector preparation as described above (Subheading 3.2).

4. Notes

1. While there are a number of permissive insertion sites within the AAV-2 capsid, we recommend starting with inserting novel targeting ligands following amino acid 587 or 588. Insertions at amino acid 587 block heparan sulfate binding. Insertions at 588 can be engineered to maintain heparan sulfate binding when appropriate linker sequences are incorporated. This is an important consideration when endogenous receptor binding is desired, or for heparin-based purification.
2. A major factor in maintaining infectivity following peptide insertion is accurate capsid assembly. Including appropriate linker/scaffolding sequences flanking the inserted epitope can be critical for this process. It has been shown that different linker sequences can greatly influence both assembly and stability of modified AAV capsids.
3. It is suggested that a primer design program (e.g., QuikChange® Primer Design Program; available online at http://www.stratagene.com/qcprimerdesign) be utilized to design the two primers for PCR-based site-directed mutagenesis. The primers should encode the desired targeting epitope flanked by 15 or 20 homologous base pairs on each side of the insertion (see Fig. 1).
   (a) The targeting epitope should be less than 16 amino acids long, epitopes of 9–12 amino acids are typical. However, an upper limit for epitope length has not been rigorously defined and will depend on insertion site and primary amino acid sequence.
   (b) Only one of the mutagenic primers should contain sequences encoding the desired insertion.
   (c) The primers should anneal to contiguous sequences flanking the insertion site on opposite strands of the plasmid template (AAV helper plasmid containing the AAV *cap* ORF).
   (d) The 5' end of each primer should contain a restriction site not present in the plasmid template, and a GC cap of at least 3 nt.
   (e) Primers should contain about 18–25 bases complementary to the plasmid template, with a melting temperature (T_m) of ≥78°C.

(f) Primers should have a minimum GC content of 40%, and should terminate in one or more G or C bases.

(g) Primers must maintain appropriate reading frame of AAV *cap* ORF.

4. Several different AAV helper plasmids have been described in the literature as for example (19, 23). There is not a single preferred construct. The serotype of encoded AAV *cap* ORF should be chosen based on the application at hand. The plasmid should only encode the AAV *rep* and *cap* ORF, and should not contain adenovirus sequences or AAV terminal repeats.
5. $CaPO_4$-DNA transfection is primarily based on pH, thus it is very important for the HBS to be maintained at the proper pH. This may require using several pH meters to ensure accuracy.
6. Adding neutral red to the 25% and 60% iodixanol layers allows easier discrimination of the layers. This aids in the isolation of the 40% iodixanol layer in which virus is distributed.
7. AAV serotypes differ in the amino acid composition of their capsid and therefore differ in epitopes recognized by the immune system. The antibody A20, e.g., recognizes AAV-2 and AAV-3 capsids (24). A20 supernatant as well as anticapsid antibodies for AAV-1 and AAV-5 are, e.g., available from Progen (Heidelberg, Germany).
8. The concentration and purity of the initial AAV stock are of critical importance. If purifying via CsCl gradient, at least 3 successive CsCl gradients are required. Protease digestion during the isolation of AAV should be kept to a minimum. The titer of the AAV stock must be above 1.33×10^{14} particles/ml for effective labeling. The purity of the final AAV stock must be greater than 99.9% since contaminants will be preferentially labeled with the fluorescent labeling reagents. There should be no cellular proteins or viral proteins other than full-size VP1, VP2, and VP3 evident on overloaded silver-stained SDS-polyacrylamide gels.
9. Platinum *Pfx* DNA polymerase (Stratagene, La Jolla, CA) is preferred due to its high fidelity, and better efficiency and stability when replicating large templates. Several other thermostable DNA polymerases are also available and are acceptable.
10. The nonhomologous sequences that flank the insert serve a dual purpose to both encode the critical scaffolding sequences, and contain restriction sites for confirmation of epitope insertion. Designing an *Age*I or *Ngo*MIV restriction site can be easily done and these are convenient sites for enzymatic digestion screening, and are absent from commonly used AAV helper plasmids.

11. Do not subject the dNTP mixture to repeated freeze/thaw cycles. Thaw the dNTP mixture once, prepare single-use aliquots, and store the aliquots at −20°C. Nucleotide solutions are often optimized for specific buffers and thermostable DNA polymerases; do not substitute dNTP mixtures from different PCR-based site-directed mutagenesis kits.
12. For the sample reactions, it is best to set up a series of reactions using increasing amounts of template double-stranded DNA (e.g., 5, 10, 15, 20, 50 ng) while maintaining excess primer concentration.
13. Digestion of parental DNA template by *Dpn*I is dependent on methylation. Thus, plasmid expression in dam+ *E. coli* strains is critical. DNA isolated from dam(−) *E. coli* strains, such as JM110 and SCS 110 is not suitable for this protocol.
14. If using the XL1-Blue supercompetent cells for transformation, make sure to use the specified 14-ml BD Falcon polypropylene tubes. The heat pulse protocol has been optimized for transformation in these tubes according to their thickness and shape.
15. The expected number of colonies from the pWhitescript control mutagenesis reaction is between 50 and 800, 80% of which should contain the mutation and appear as blue colonies on the X-gal/IPTG plates. The transformation control (pUC18) should have >250 colonies, with >98% maintaining the blue phenotype.
16. Using sodium citrate for cell suspension at this step is preferred because this buffer has been shown to reduce viral particle aggregation.
17. The capsid titer is commonly tenfold higher than the genomic titer.
18. Cells should be approximately 70% confluent.
19. For detection of nonfluorescent intracellular transgene products, cells have to be fixed and permeabilized prior to incubation with antibodies.
20. The human carcinoma cell line HeLa (ATCC® number CCL2) is highly permissive for AAV-2 and can therefore be used for determining the transducing titer of rAAV-2 vector preparations. If HeLa cells are used, seed 7×10^4 cells/well into a 12-well plate.
21. Example of serial dilution:
    (a) Add 2 µl of vector preparation to 1 ml medium (sample A) and mix
    (b) Add 70 µl of sample A to 630 µl medium (sample C) and mix

(c) Add 70 µl of sample C to 630 µl medium (sample E) and mix

(d) Add 70 µl of sample E to 630 µl medium (sample G) and mix

(e) Add 210 µl of sample A to 490 µl medium (sample B) and mix

(f) Add 70 µl of sample B to 630 µl medium (sample D) and mix

(g) Add 70 µl of sample D to 630 µl medium (sample F) and mix

(h) Add 70 µl of sample F to 630 µl medium (sample H) and mix.

22. In order to remove membrane bound particles treat the vector transduced (adherent as well as suspension) cells with trypsin prior to cell lysis.

23. It is suggested that at least three different concentrations of the competitor is used.

References

1. Arnold, G. S., Sasser, A. K., Stachler, M. D., and Bartlett, J. S. (2006) Metabolic biotinylation provides a unique platform for the purification and targeting of multiple AAV vector serotypes, *Mol Ther* ***14***, 97–106.
2. Nicklin, S. A., Buening, H., Dishart, K. L., de Alwis, M., Girod, A., Hacker, U., Thrasher, A. J., Ali, R. R., Hallek, M., and Baker, A. H. (2001) Efficient and selective AAV2-mediated gene transfer directed to human vascular endothelial cells, *Mol Ther* ***4***, 174–181.
3. Shi, W., Arnold, G. S., and Bartlett, J. S. (2001) Insertional mutagenesis of the adeno-associated virus type 2 (AAV2) capsid gene and generation of AAV2 vectors targeted to alternative cell-surface receptors, *Hum Gene Ther* ***12***, 1697–1711.
4. Perabo, L., Buning, H., Kofler, D. M., Ried, M. U., Girod, A., Wendtner, C. M., Enssle, J., and Hallek, M. (2003) In vitro selection of viral vectors with modified tropism: the adeno-associated virus display, *Mol Ther* ***8***, 151–157.
5. Shi, W., and Bartlett, J. S. (2003) RGD inclusion in VP3 provides adeno-associated virus type 2 (AAV2)-based vectors with a heparan sulfate-independent cell entry mechanism, *Mol Ther 7*, 515–525.
6. Stachler, M. D., Chen, I., Ting, A. Y., and Bartlett, J. S. (2008) Site-specific modification of AAV vector particles with biophysical probes and targeting ligands using biotin ligase, *Mol Ther* ***16***, 1467–1473.
7. Hauck, B., Chen, L., and Xiao, W. (2003) Generation and characterization of chimeric recombinant AAV vectors, *Mol Ther 7*, 419–425.
8. Rabinowitz, J. E., Bowles, D. E., Faust, S. M., Ledford, J. G., Cunningham, S. E., and Samulski, R. J. (2004) Cross-dressing the virion: the transcapsidation of adeno-associated virus serotypes functionally defines subgroups, *J Virol 78*, 4421–4432.
9. Lux, K., Goerlitz, N., Schlemminger, S., Perabo, L., Goldnau, D., Endell, J., Leike, K., Kofler, D. M., Finke, S., Hallek, M., and Buning, H. (2005) Green fluorescent protein-tagged adeno-associated virus particles allow the study of cytosolic and nuclear trafficking, *J Virol 79*, 11776–11787.
10. Warrington, K. H., Jr., Gorbatyuk, O. S., Harrison, J. K., Opie, S. R., Zolotukhin, S., and Muzyczka, N. (2004) Adeno-associated virus type 2 VP2 capsid protein is nonessential and can tolerate large peptide insertions at its N terminus, *J Virol 78*, 6595–6609.
11. Keppler, A., Pick, H., Arrivoli, C., Vogel, H., and Johnsson, K. (2004) Labeling of fusion proteins with synthetic fluorophores in live

cells, *Proc Natl Acad Sci U S A* ***101***, 9955–9959.

12. Miller, L. W., Sable, J., Goelet, P., Sheetz, M. P., and Cornish, V. W. (2004) Methotrexate conjugates: a molecular in vivo protein tag, *Angew Chem Int Ed Engl* ***43***, 1672–1675.
13. Bartlett, J. S., and Samulski, R. J. (1998) Fluorescent viral vectors: a new technique for the pharmacological analysis of gene therapy, *Nat Med* ***4***, 635–637.
14. Bartlett, J. S., Wilcher, R., and Samulski, R. J. (2000) Infectious entry pathway of adeno-associated virus and adeno-associated virus vectors, *J Virol* ***74***, 2777–2785.
15. Ren, C., White, A. F., and Ponnazhagan, S. (2007) Notch1 augments intracellular trafficking of adeno-associated virus type 2, *J Virol* ***81***, 2069–2073.
16. Sanlioglu, S., Benson, P. K., Yang, J., Atkinson, E. M., Reynolds, T., and Engelhardt, J. F. (2000) Endocytosis and nuclear trafficking of adeno-associated virus type 2 are controlled by rac1 and phosphatidylinositol-3 kinase activation, *J Virol* ***74***, 9184–9196.
17. Seisenberger, G., Ried, M. U., Endress, T., Buning, H., Hallek, M., and Brauchle, C. (2001) Real-time single-molecule imaging of the infection pathway of an adeno-associated virus, *Science* ***294***, 1929–1932.
18. Bartlett, J. S., Samulski, R. J., and McCown, T. J. (1998) Selective and rapid uptake of adeno-associated virus type 2 in brain, *Hum Gene Ther* ***9***, 1181–1186.
19. Li, J., Samulski, R. J., and Xiao, X. (1997) Role for highly regulated rep gene expression in adeno-associated virus vector production, *J Virol* ***71***, 5236–5243.
20. Xiao, X., Li, J., and Samulski, R. J. (1998) Production of high-titer recombinant adeno-associated virus vectors in the absence of helper adenovirus, *J Virol* ***72***, 2224–2232.
21. Grimm, D., Kern, A., Rittner, K., and Kleinschmidt, J. A. (1998) Novel tools for production and purification of recombinant adenoassociated virus vectors, *Hum Gene Ther* ***9***, 2745–2760.
22. Girod, A., Ried, M., Wobus, C., Lahm, H., Leike, K., Kleinschmidt, J., Deleage, G., and Hallek, M. (1999) Genetic capsid modifications allow efficient re-targeting of adeno-associated virus type 2, *Nat Med* ***5***, 1052–1056.
23. Rabinowitz, J. E., Rolling, F., Li, C., Conrath, H., Xiao, W., Xiao, X., and Samulski, R. J. (2002) Cross-packaging of a single adeno-associated virus (AAV) type 2 vector genome into multiple AAV serotypes enables transduction with broad specificity, *J Virol* ***76***, 791–801.
24. Wobus, C. E., Hugle-Dorr, B., Girod, A., Petersen, G., Hallek, M., and Kleinschmidt, J. A. (2000) Monoclonal antibodies against the adeno-associated virus type 2 (AAV-2) capsid: epitope mapping and identification of capsid domains involved in AAV-2-cell interaction and neutralization of AAV-2 infection, *J Virol* ***74***, 9281–9293.
25. Wu, P., Xiao, W., Conlon, T., Hughes, J., Agbandje-McKenna, M., Ferkol, T., Flotte, T., and Muzyczka, N. (2000) Mutational analysis of the adeno-associated virus type 2 (AAV2) capsid gene and construction of AAV2 vectors with altered tropism, *J Virol* ***74***, 8635–8647.
26. Yang, Q., Mamounas, M., Yu, G., Kennedy, S., Leaker, B., Merson, J., Wong-Staal, F., Yu, M., and Barber, J. R. (1998) Development of novel cell surface CD34-targeted recombinant adenoassociated virus vectors for gene therapy, *Hum Gene Ther* ***9***, 1929–1937.
27. Grifman, M., Trepel, M., Speece, P., Gilbert, L. B., Arap, W., Pasqualini, R., and Weitzman, M. D. (2001) Incorporation of tumor-targeting peptides into recombinant adeno-associated virus capsids, *Mol Ther* ***3***, 964–975.
28. Boucas, J., Lux, K., Huber, A., Schievenbusch, S., von Freyend, M. J., Perabo, L., Quadt-Humme, S., Odenthal, M., Hallek, M., and Buning, H. (2009) Engineering adeno-associated virus serotype 2-based targeting vectors using a new insertion site-position 453-and single point mutations, *J Gene Med* ***11***, 1103–1113.

Chapter 13

AAV-Mediated Gene Targeting

Daniel G. Miller

Abstract

The precise alteration of sequences by homologous recombination is an important strategy for gene therapies as well as investigating gene function and cellular DNA repair pathways. Inefficient delivery of template DNA to the nucleus using transfection or electroporation methods is one limitation of the frequency of homologous recombination in primary cells. AAV vectors can be used to efficiently deliver single stranded DNA recombination templates to the nucleus of primary cells and the AAV genome structure with single DNA strands stabilized by inverted terminal repeat sequences is likely one reason for the increase in recombination frequencies observed. Thus, an AAV-mediated gene targeting approach allows cells from normal or disease-affected individuals to be modified for careful study. When clones of primary cells can be expanded, autologous transplantation of phenotypically corrected cells is also feasible. Here we describe a basic approach to gene targeting using an AAV-mediated strategy. Vector design strategies are discussed, and protocols for altering expressed and non-expressed loci in primary somatic cells, and stem cells are reviewed.

Key words: Homologous recombination, Gene targeting, Gene editing, Genome engineering, Targeted repair, Targeted gene disruption, AAV-mediated

1. Introduction

AAV-mediated gene targeting strategies have both experimental and therapeutic applications including the study of disease mechanisms, or the generation of modified primary cells for transplantation and disease treatment. AAV vectors have a number of features that likely result in increased transduction frequencies through homologous recombination pathways. A large number of distinct serotypes have now been identified that allow efficient transduction of most cultured cells (1, 2). The ability to transduce a wide variety of cell types, as well as the ability to generate vector preparations with titers close to 1×10^{13} genome containing particles per milliliter, allows the introduction of multiple vector genome copies per cell. These genomes are efficiently uncoated and transported to

Richard O. Snyder and Philippe Moullier (eds.), *Adeno-Associated Virus: Methods and Protocols*,
Methods in Molecular Biology, vol. 807, DOI 10.1007/978-1-61779-370-7_13,

the nucleus where single stranded forms are available for pairing with homologous genomic sequence. The combination of high multiplicity of infection (MOI), the single stranded DNA topology, and efficient delivery of vector genomes to the nucleus likely allows homologous recombination to occur at higher frequencies than are observed with conventional approaches, or delivery of nucleic acid sequences using other vector systems.

Homologous recombination between vector and chromosomal sequences is one of several AAV vector transduction pathways. Other pathways include pairing of plus and minus vector strands allowing transcription from double stranded hybrid molecules (3), transcription from single molecules that have undergone second strand DNA synthesis primed by ITR sequences (4) or included in the vector genome design (5–7). AAV vectors also form concatemers of multiple genomes in linear and circular configurations (3, 8, 9), and single genomes or concatemers of genomes integrate during the repair of DNA breaks transiently present in all cells (10–14). While alternate transduction pathways cannot be eliminated, careful vector design can shift the balance of detection towards events that occur by homologous recombination. The most important design consideration is to include homology between vector and chromosomal target site with nucleotide changes located in the center of the homology region so that vector genomes can pair with chromosomal sequence and form structures that are resolved by cellular homologous recombination pathways (7, 15–17). Additional strategies include vector designs that trap the transcriptional activity of promoters at target sites (18, 19), or increasing the frequency of recombination-mediated transduction by producing DNA breaks within target sites using specifically designed endonucleases (20–24).

AAV-mediated gene targeting frequencies have been quantified at multiple chromosomal locations so that effects due to target site location are averaged over multiple sites in the same cells. AAV vectors can undergo recombination with chromosomal target sites in 0.1–1.0% of total cells without selection for transduction events. The largest determinants of recombination frequency are MOI, and the capsid serotype (7, 15, 17, 19). The frequencies of homologous recombination occurring using conventional gene targeting approaches varies depending on the homology length of targeting templates (25), and the target site location (26–28). Similar variations are expected when recombination templates are delivered using AAV vectors and additional sources of variation have been identified including MOI (17, 29), time between infection and assaying for transduction events (29), the type of target-site modification (30), and the percentage of cells traversing S-phase of the cell cycle (31). Here we discuss the design and construction of AAV gene targeting vectors, a typical gene targeting assay performed in normal primary human cells, and the detection of recombinants by Southern blotting.

2. Materials

2.1. Design and Construction of Gene Targeting Vectors

1. DNA oligonucleotides.
2. Primer design (Primer 3, http://sourceforge.net/projects/primer3).
3. Taq DNA polymerase.
4. Big Dye terminator sequencing reaction mix.
5. dNTP mix.

2.2. Fibroblast Cell Culture and Transduction by AAV Vectors

1. Dulbecco's Modified Eagle's Medium (DMEM) (Invitrogen, Carlsbad, CA), 10% fetal bovine serum (FBS), penicillin streptomycin solution.
2. Trypsin solution: 0.25% Trypsin, and 1 mM ethylenediamine tetraacetic acid (Sigma-Aldrich, St. Louis, MO) in phosphate buffered saline, pH 7.4 (PBS).
3. Six well dishes, 6 cm diameter culture dishes, 10 cm diameter culture dishes.
4. Cells HT-1080, (#CCL-121, American Type Culture Collection, Manassas, VA), normal human fibroblasts (Coriell Cell Repository, Camden, NJ).
5. Glass cloning rings for clonal isolation of cells. (Corning Life Sciences, Lowell, MA).

2.3. Screening Transduced Cells for Recombinants by Southern Blot Technique

1. Genomic DNA purification from cultured cells (Gentra DNA Purification Kit, Qiagen, Valencia, CA).
2. Phosphate buffer (for Church buffer). Mix 342 ml of 1 M Na_2HPO_4 with 158 ml of 1 M NaH_2PO_4 and 500 ml of H_2O to give 1 L of phosphate buffer (Sigma-Aldrich, St. Louis, MO).
3. Church Buffer. For preparation of 1 L dissolve 10 g bovine serum albumin ((BSA), Sigma-Aldrich, St. Louis, MO) in small 1 g increments in 50 ml of H_2O (do not heat). Dissolve 70 g sodium dodecyl sulfate (SDS) by small increments in 400 ml of H_2O (stir and gently heat; this should be done under a fume hood). Mix 500 ml of phosphate buffer with the BSA and SDS solutions, add 2 ml of 0.5 M EDTA, and bring to a total volume of 1 L. Filter using vacuum filtration and store in 50ml aliquots at room temperature.
4. 20× sodium chloride, sodium citrate solution (SSC): 175.3 g sodium chloride, 88.2 g sodium citrate in 800 ml of distilled water, adjust pH to 7.0 with HCL or NaOH, bring to 1 L total volume and sterilize.
5. Salmon sperm DNA solution (Invitrogen, Carlsbad, CA).
6. Amersham Rediprime II DNA labeling system (GE Healthcare, Piscataway, NJ).

7. Hybond-N+ nylon membrane (GE Healthcare, Piscataway, NJ).
8. Blotting paper (3MM Chr, GB005, Whatman, GE Healthcare, Piscataway, NJ).
9. Sodium hydroxide pellets.
10. Ethidium bromide.
11. Sephadex G50 spin column (Roche Applied Science, Indianapolis, IN).
12. dCTP, [alpha^{32}P]-800 Ci/mmol 10 mCi/ml, 500 μCi (PerkinElmer, Waltham, MA).

3. Methods

The utility of a gene targeting strategy depends on the ability to target genomic sequences. AAV vectors transduce cells through a variety of mechanisms but stable transduction of dividing cells occurs by integration during the repair of double strand breaks (10, 12–14), or by homologous recombination with target site sequences (15, 17). The frequency of these events, and the implication for AAV-mediated gene targeting is discussed in Note 1. Transcriptionally active genes can be targeted using promoter trap strategies, greatly reducing the detection of transduction events that occur due to vector integration at random genomic locations. Promoterless expression cassettes are constructed so that integration within a transcribed sequence is necessary for their detection (Fig. 1). In the context of disease-causing mutations, a promoter trap strategy can be an effective approach for gene knockout in cases where the effect of the absence of a gene product is being studied, or where therapeutic approaches require the disruption of transcription from mutated alleles at autosomal loci. Knockout of both alleles can be achieved by using different selectable markers (Fig. 2), or by screening for crossover events that result in loss of heterozygosity at the target locus (32, 33). Promoterless vectors can also be used to target introns, and produce corrective changes in a small number of nucleotides, or mutations in adjacent exon sequence (Fig. 3).

Targeted manipulation of non-transcribed sequences requires the incorporation of a selection cassette that is expressed at most loci, or efficient high throughput screening techniques so that the targeted modification can be identified from pools of cells exposed to the targeting vector. Disruption of *HPRT* gene expression by the mutagenic incorporation of a neomycin expression cassette allows gene targeting rates to be measured by the frequency of 6-thio-guanine (6TG) resistance without pre-selection

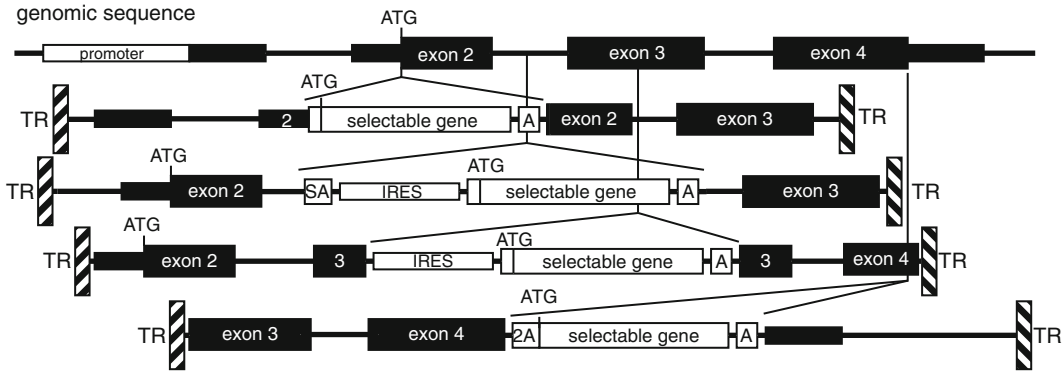

Fig. 1. Promoterless gene targeting vectors. Four examples of promoterless targeting vectors are shown below a hypothetical genomic sequence. The first targeting vector is designed to insert a selectable marker gene at the genomic ATG start codon, or just upstream of this sequence making the first ATG in the resulting transcript that of the selectable gene. The second design example utilizes a splice acceptor (SA) and internal ribosomal entry site (IRES) to produce a synthetic exon that is translated by ribosomes loading on to the IRES sequence. Point mutations located in adjacent exons can be introduced or corrected using this type of vector. The third vector utilizes an internal ribosome entry site (IRES) sequence to initiate translation of the selectable gene and can be targeted to any exon sequence that will disrupt gene function. The Fourth vector utilizes a self cleaving peptide (2A) from Foot and Mouth Disease Virus (FMDV) for separation of the selectable enzyme or fluorescent protein from a larger fusion protein and is useful for making point mutations in the 3′ end of genes. The genetic elements shown are: TR, AAV terminal repeat; A, polyadenylation sequence; SA, splice acceptor site; UTR, untranslated region; ATG, translation start; 2A, Foot and Mouth Disease Virus (FMDV) self cleaving peptide cleavage sequence.

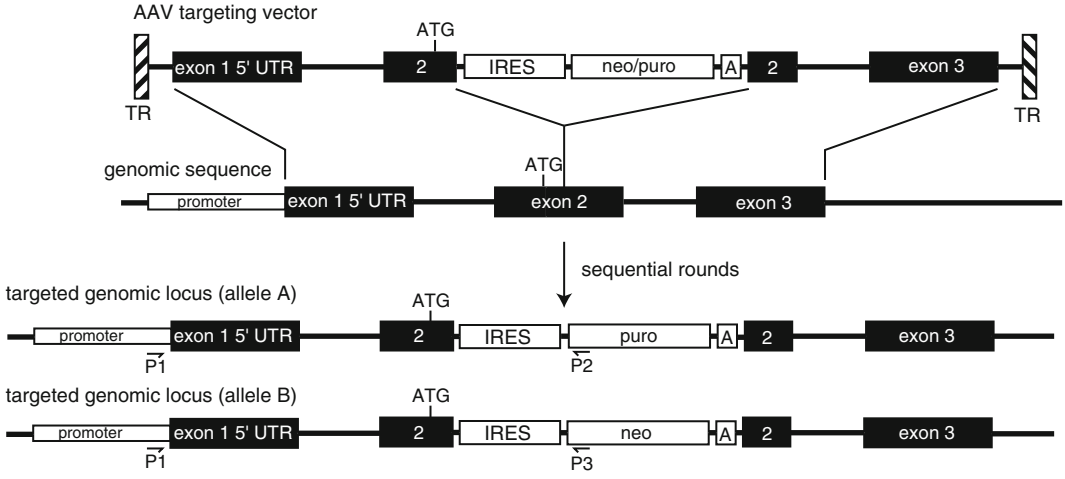

Fig. 2. Targeted disruption of transcription. The AAV targeting vector contains genomic sequence with a selectable gene inserted in the open reading frame of the gene, just downstream of the ATG start codon, which in the example shown lies in the second exon (the first exon contains an untranslated region or 5′ UTR). Clones resistant to the selectable gene are screened by PCR and confirmed using Southern analysis. A repeat of this procedure with a different selectable marker allows for disruption of both alleles of autosomal target loci. The genetic elements shown are: TR, AAV terminal repeat; IRES, internal ribosomal entry site; *neo*, neomycin phosphotransferase gene; *puro*, puromycin *N*-acetyl transferase gene; A, polyadenylation signal. p1, p2 and p3 indicate the positions of PCR primers that can be used to identify targeted alleles.

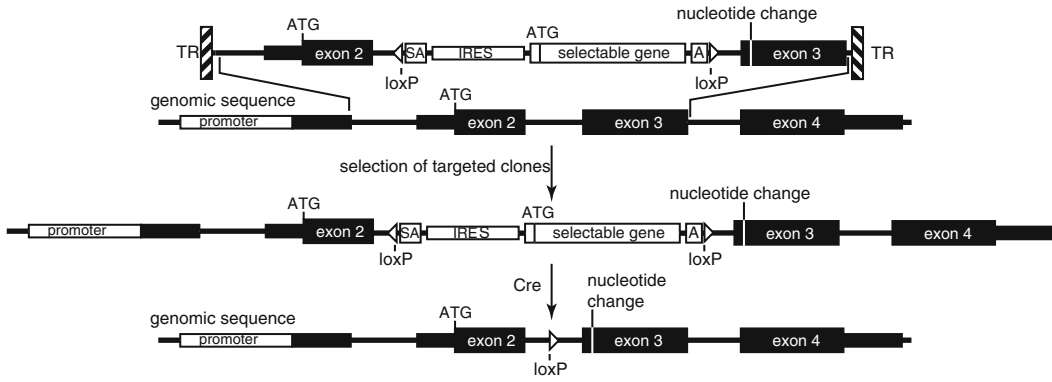

Fig. 3. Introduction of single base changes at transcribed loci. The promoterless AAV vector containing a point mutation within exon 3 is designed to target an intron of a transcriptionally active gene. Areas of homology are indicated by *thin adjoining lines* between the vector and chromosomal target. Selection for AAV vector transduction will generate a population of cells mostly containing recombinants with the gene of interest because transduction will not be detected if integration occurs at transcriptionally inactive sites. The polyclonal cell population can be transiently exposed to CRE recombinase using helper-dependent Adenovirus vectors or a non-integrating retrovirus vector and clones of cells isolated and screened for evidence of the nucleotide change. The genetic elements shown are: TR, AAV terminal repeat; ATG, translational start sites; IRES, internal ribosomal entry site; loxP, loxP attachment sites for CRE recombinase (indicated by *small triangles*); selectable gene, the gene for a drug resistance enzyme such as neomycin phosphotransferase, or the gene for a fluorescent protein such as *GFP*.

for transduction events, and vector transduction frequencies can be measured independently by scoring G418 resistant colony formation. Using this assay, the percent of transduction events that result from gene targeting can be easily determined. The frequency of 6TG resistance was approximately 1 in 10 G418-resistant clones when this assay was used to quantify AAV-mediated gene targeting frequencies in human cells, and recombination frequencies were observed to occur more efficiently when vectors were designed to introduce relatively large insertions of selection cassettes (15). AAV-mediated gene targeting at a number of autosomal loci has now been performed and again rates range between 0.1% and 1% and include introduction of specific mutations without selection (34) or gene knockout using expression cassettes (15, 18, 19, 35, 36). It is difficult to predict the number of clones that will need to be screened to identify a sufficient number of recombinants at a specific target locus as different loci may exhibit large differences in recombination frequencies. However, as a starting point, around 5% of infected cells should contain vector integrants, and between 0.1 and 1.0% should contain recombinants. Thus one will need to screen a minimum of 100 clonal isolates but likely closer to 1,000 clones should be analyzed when selection is not applied.

Here we describe a protocol for the construction of a gene targeting vector designed to trap promoter activity at the target site (Figs. 1 and 2). Most transduction by this type of vector will

result from homologous recombination with the target site, minimizing the number of clones needed to be screened to identify recombinants, and in some cases allowing studies to be performed on transduced cell populations without isolating clones.

3.1. Design and Construction of Gene Targeting Vectors

1. The location of the expression cassette insertion at the target site is an important factor in the success of this approach. Care must be taken to omit promoter sequences within the homology arms of the targeting vector as this may allow transduction of cells in the absence of targeting.
2. When using promoter trap strategies, it is important to select exons within the 5′ end of a gene so that recombinants result in complete disruption of transcription from that allele.
3. The reading frame of the target exon is also an important consideration and an exon where putative exon-skipping events do not maintain the reading frame should be chosen when possible.
4. Targeting vectors should include homology arms of maximal size such that right arm, left arm, and expression cassette total size is roughly 4.4 kb. The combination of targeting vector sequence and the two inverted terminal repeats should result in a final vector size of ~4.7 kb.
5. The expression cassette should be placed in the center of the homology region for optimal gene targeting frequencies. Vector construction strategies are discussed in Note 2.
6. Several examples of promoter trap vector designs are illustrated in Figs. 1–3. In each case transcription from the target locus results in expression of a selection cassette inserted at the target site. Since these cassettes lack promoter sequences, integration events that occur at random genomic locations will not be detected.
7. A strategy for altering a small number of nucleotides within an exon is described in Note 3, and illustrated in Fig. 3.
8. The generation of AAV vector preparations and determining their titer is briefly described in Note 4, and described in more detail in Chapters 2 and 16.

3.2. Gene Targeting Assay

1. Typically a small number of target cells are seeded to a 6-well dish at 50% confluence. This number can vary depending on cell size but for primary fibroblasts we usually seed 5×10^4 cells/well. (see Note 5 for choice of cells)
2. Sixteen to twenty hours later, vector preparations are added so that the MOI varies from 500 to 50,000 genome-containing particles per cell over five separate wells. (see Note 6 for calculating MOI). Untreated cells, or cells treated with an unrelated vector preparation are always included as a control.

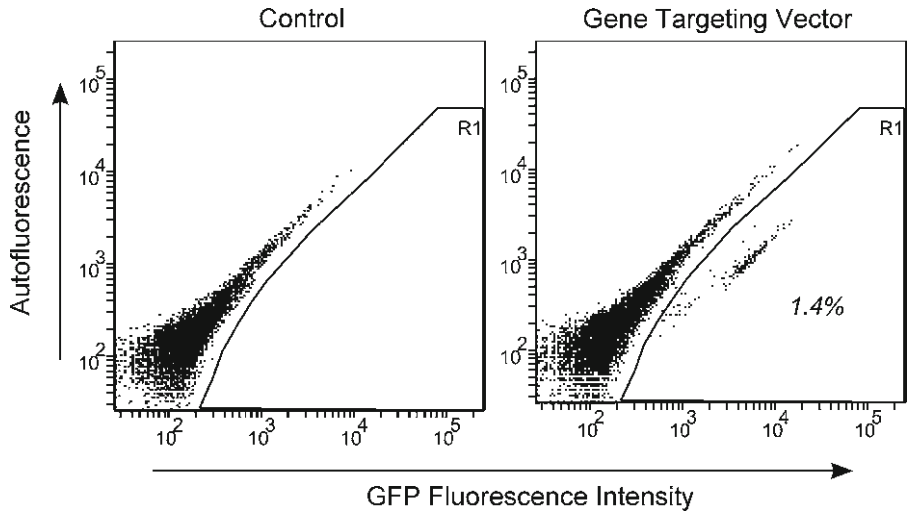

Fig. 4. *GFP* fluorescence resulting from transduction by a gene targeting vector in normal Human keratinocytes. *GFP* fluorescence is shown after transduction of normal human keratinocytes with an AAV vector designed to target exon 3 of the *KRT-14* gene (see the third IRES-containing vector in Fig. 1 for an illustration of this vector). The multiplicity of infection (MOI) was 5×10^5 genome-containing particles per cell and *GFP* fluorescence was measured approximately 1 week after infection using flow cytometry. The *GFP*(+) population (gate R1) was collected using a fluorescence activated cell sorter and colonies were cloned as described in Subheading 3.2, steps 6 and 7. Genomic DNA from individual clones was probed on Southern blots and all clones contained a targeted insertion of the expression cassette in exon 3 of the *KRT-14* gene.

3. Cells are detached with trypsin the following day and seeded to 10-cm diameter dishes for expansion.
4. Five to seven days later, cells are detached with trypsin from confluent dishes and assayed for *GFP* fluorescence using a flow cytometer (Fig. 4). (see Note 7).
5. Because of the promoter trap design, most transduction events should be a consequence of recombination between vector and chromosomal target so polyclonal populations of transduced cells can be sorted or selected to determine if target sequences have been modified. *GFP* positive cells can also be sorted and seeded at limiting dilution for analysis of individual clones. We usually seed 5×10^3 sorted cells to a 10-cm diameter dish, anticipating that there will be cell death caused by the cell sorter and generally obtain 20–50 colonies per 10-cm diameter dish allowing for clear isolation of clones.
6. One to two weeks later, isolated *GFP* positive colonies are circled with a marker, and cloned using small glass rings that have been prepared by sterilization on a layer of vacuum grease in glass Petri dishes. The medium is removed from culture dishes containing colonies and washed with PBS. Cloning rings are lifted from the grease-covered dishes with sterile forceps and placed over the colony using the marked circle as a guide. 50 µl of trypsin solution is added to the ring, and after 5 min, the

cells are transferred to a well of a 6-well dish containing 2 ml of pre-warmed DMEM-10% FBS for expansion and analysis of genomic DNA by Southern blot techniques.

7. After expansion, cells are again detached with trypsin and seeded to two 6-cm diameter dishes, one for preparation of genomic DNA, and one to freeze cells for storage.

3.3. Screening Transduced Cells for Recombinants by Southern Blot Technique

Although detection of vector:chromosome junctions using PCR primers is a tempting approach, we find that Southern blots are more informative and require about the same amount of time to optimize.

1. Genomic DNA purified from cell clones or polyclonal transduced cell populations is digested with a restriction endonuclease that cuts once within the target vector and has genomic sites that flank the targeted region but are located outside of vector homology arms. The size of the fragment originating from the non-targeted locus should be 10–15 kb, with a smaller fragment generated from targeted loci such that clear separation of size can be demonstrated on a 0.8% agarose gel.
2. An approximately 500-bp DNA probe adjacent to one of these sites and again located outside of vector homology arms is amplified from genomic DNA and a portion is sequenced to confirm its identity (see Note 8).
3. Five to ten micrograms of genomic DNA is digested with the appropriate restriction endonuclease. While a 4 h digestion period using 2–4 U of enzyme per microgram of DNA is usually sufficient. These incubations are sometimes allowed to continue overnight to ensure complete digestion.
4. Genomic DNA fragments are diluted to a volume of 500 μl, and extracted twice with a 1:1 mixture of phenol and chloroform, and once with a 23:1 mixture of chloroform and isoamyl alcohol. DNA fragments are concentrated by ethanol precipitation and resuspended in 10–20 μl final volume of 10 mM Tris pH 8.0, 1 mM EDTA (pH 8.0).
5. The DNA concentration is again determined on these digested samples and an equal amount of DNA loaded to each lane of a 0.8% agarose gel to separate fragments based on size.
6. Agarose gels are soaked in a 0.5 μg/ml ethidium bromide solution to stain DNA fragments and allow visualization under ultraviolet light to confirm complete digestion of samples. It is also useful to photograph the gel next to a ruler so that the position of size markers can be transferred to blotting membranes and autoradiography film at a later step.
7. Hydrochloric acid-mediated depurination is performed to facilitate efficient transfer of large DNA fragments from the gel

matrix to the membrane. Transfer the agarose gel to a clean plastic container and add 500 ml of 0.25 M HCl. Incubate at room temperature on a rocking platform for 10–15 min and then remove the HCl and add 500 ml fresh 0.25 M HCl and incubate for an additional 15 min.

8. Remove HCl and add 500 ml 0.4 M NaOH. Incubate at room temperature for 15–20 min and replace with 500 ml of fresh 0.4 M NaOH. Allow the gel to equilibrate for another 15–20 min and proceed to alkaline transfer.
9. The DNA fragments are transferred from the gel to a positively charged nylon membrane by wicking a buffer solution (0.4 M NaOH) from a reservoir through the gel to wicks located above the nylon membrane. Diagrams of this setup can be found in general laboratory manuals (37) (see Note 9).
10. When alkaline buffer is used to transfer DNA to a positively charged nylon membrane as described here, no additional crosslinking is necessary.
11. Add 15 ml Church buffer to the hybridization cylinder plus Salmon Sperm (SS) DNA at a final concentration of 150 μg/ml (SS DNA is boiled 5–10 min then iced). Rotate the cylinder containing the buffer and SS DNA in the 65°C oven until the membrane is ready.
12. Add the membrane to the cylinder by rolling it into a tube, and try to remove all bubbles between the membrane and the cylinder (if you are starting with a dry membrane wet in 2× SSC). The prehybridization period can be anywhere from 1 h to overnight without a significant change in signal quality.
13. DNA probes are generally labeled with rediprime and alpha^{32}P-dCTP and unincorporated nucleotides removed by centrifugation through a sephadex G50 spin column. Labeled probes can be added directly to the prehybridization solution and membranes are incubated at 65°C overnight
14. The hybridization solution is discarded in the radioactive waste container, and the membrane is rinsed with 20 ml of 2× SSC, 0.1% SDS solution which is also discarded in an appropriate radioactive waste container. This rinse is repeated with 50 ml of 2× SSC, 0.1% SDS and the solution is discarded. Membranes are washed sequentially in 2× SSC, 0.1% SDS for 15 min at 65°C twice, then in 0.2× SSC, 0.1% SDS at 65°C for 30 min.
15. The membrane is sandwiched in plastic wrap and placed on autoradiography film with an intensifying screen at −80°C for 3–5 days and developed to observe probe hybridization signals.
16. The same blot can be stripped of the target site probe by three sequential washes in water heated to 100°C. We

generally use a 500 ml volume, heat it to boiling, and add the membrane in a plastic container allowing it to rock until the water cools to room temperature and repeat. The blot can then be probed with a DNA fragment from the insertion cassette to determine the percentage of clones that also contain targeting vector sequences at random genomic locations. (Begin again at step 11).

4. Notes

1. The frequency of transduction through homologous recombination pathways ranges from 0.1 to 1.0% of total cells (15, 17). AAV vector integration occurs in most cell populations at frequencies of around 3–5% of infected cells. Recombination and integration frequencies occur independently of each other so one can expect that 3–5% of recombinants will also contain a vector integrated at a random genomic location. Conversely, if all integration results in transduction, the number of cells transduced by homologous recombination will vary between 1 in 20 and 1 in 200 clones. The ratio of the number of transduced cells that have undergone homologous recombination to the total number of transduced cells can be improved by using vectors without transcriptional promoters to target transcribed gene sequences. This vector design allows selection or detection of transduction only when the vector has trapped an active promoter and effectively reduces the detection of vector integration at random locations. In specialized cell types, this strategy can effectively eliminate detection of vector integration at random genomic locations due to a limited number of transcribed genes.
2. AAV vectors designed for gene targeting are constructed using a panel of available expression cassettes and production of homology arms by PCR amplification of genomic DNA from the target cells to minimize polymorphic differences in sequence. Left and right homology arms are amplified in independent reactions and unique enzyme sites are incorporated within oligonucleotides used to prime the reaction. Alternatively, seamless cloning strategies can also be used to facilitate construction of targeting vectors (18). Amplified DNA fragments are assembled and sequenced in standard cloning vector backbones, and then transferred to a vector containing AAV ITR's as the final step. This order of construction is preferable because AAV vector ITR's are unstable in most bacterial strains resulting in deletion of ITR sequences at

fairly high frequency. Thus, in the final cloning step, several plasmids are chosen and ITR sequence is checked for integrity by digestion with enzymes that cleave within the ITR's. We typically use *Ahd*I, *Sma*I, and *Bgl*I for these diagnostic digests on ITR sequence from AAV2 vectors.

3. When the desired outcome is to produce point mutations, or correct endogenous mutations at target loci, introns can be targeted as well. This approach allows promoter activity to be trapped without disrupting exon sequence. Synthetic exons are constructed such that a splicing event results in their inclusion in mRNAs produced from target loci. Small nucleotide changes in adjacent exon sequence can be engineered by including the changes within vector homology arms. Recombination events that result from crossovers outside of the engineered changes will incorporate the exon change at the genomic site. Genomic DNA from transduced clones and polyclonal populations can be screened for recombinants by Southern blot, and normal splicing restored upon Cre-mediated removal of the expression cassette from the intron (Fig. 3). Transient expression of Cre in recombinant cells can be accomplished by expression of the protein from non-integrating vectors such as adenovirus (38) or modified forms of lentivirus vectors (39) and treated cell populations again screened by Southern to identify clones, or cell populations showing evidence of loss of expression cassette sequences (*GFP* negative cells) can be collected by cell sorting.
4. Vector preparations are produced by transfection of HEK-293 cells with a packaging plasmid such as pDG (40) and the targeting vector plasmid. After a transient expression period, cell lysates are generated by several freeze thaw cycles, and vector particles purified by isopycnic density gradient centrifugation and affinity chromatography with heparin columns when serotypes 2, 3b, or 6 are used (41). Vector containing particles produced using packaging plasmids from other serotypes can be bound to Q or S sepharose columns (42), or simply dialyzed after concentration and purification over $CsCl_2$ gradients (43). The titer of AAV vector preparations is always determined and expressed as genome containing particles per milliliter. Genomes in vector preparations can be quantified using real time PCR, or by analysis of the DNA from vector preparations on alkaline Southern blots and quantification by comparing hybridization signals of vector containing lanes to known quantities of plasmid controls in adjacent lanes using a phosphorimager. The latter approach is preferred because vector preparations contain a substantial fraction of DNA fragments that will likely be inactive in targeting assays and

Southern blot analysis allows an assessment of the percentage of full length vector genomes in the preparation.

5. Normal human fibroblast cells have been used for the majority of our studies. These cells are appropriate for gene targeting, as they are diploid and useful for studying gene function in a normal human cell. Cells from males are used for targeting the *HPRT* locus on the X chromosome because the 6-thioguanine (6-TG) resistant phenotype is recessive and requires a single copy locus. Human keratinocytes, or diploid, human HT-1080 fibrosarcoma cells are useful when significant expansion of targeted cells is necessary. When the target loci being studied are introduced by retroviral vectors, aneuploid cells can also be used.
6. Depending on the cell type it is usually assumed that the seeding efficiency is around 50%, and the cells divide once in a 16 h period so MOI's are calculated using the original number of cells placed in the well.
7. Gene targeting vectors with promoter trap design should have relatively low transduction frequencies when compared to vectors containing endogenous promoters. Transduction rates typically range from 0.1 to 1.0% of total cells and correlate directly with the MOI.
8. The genomic location and sequence of the probe for Southern blot analysis is critical if clear results are to be obtained. A general rule is to keep probes small to maintain their specificity. Usually a 500-bp fragment is sufficient to generate high specific during labeling activity and high specificity during probing. In addition, once a probe sequence is selected, alternate homologies within the target cell genome should be determined using the BLAT tool on the University of California, Santa Cruz, genome browser (http://genome.ucsc.edu/). If the sequence matches to multiple genomic sites because it contains repetitive DNA sequence, or because pseudogenes or similar gene families exist, alternate probe sequences should be chosen.
9. After placing the membrane on the gel, the location of the wells and the lower right corner of the gel are marked with a graphite pencil so that the position of size markers can be transferred with a ruler, and the orientation of the membrane relative to the gel can be determined. Efficient wicking of buffer through the gel is critical for efficient transfer of the DNA fragments from the gel to the membrane, so care must be taken to ensure that this process is occurring efficiently. Some protocols suggest putting weight on the towels above the gel but our experience indicates this compresses the wick and the gel below and impedes transfer.

References

1. Gao, G., Vandenberghe, L.H., Alvira, M.R., Lu, Y., Calcedo, R., Zhou, X. and Wilson, J. M. (2004) Clades of adeno-associated viruses are widely disseminated in human tissues. *J. Virol.* **78**, 6381–6388.
2. Gao, G., Alvira, M.R., Wang, L., Calcedo, R., Johnston, J. and Wilson, J. M. (2002) Novel adeno-associated viruses from rhesus monkeys as vectors for human gene therapy. *Proc. Natl. Acad. Sci. U.S.A.* **99**, 11854–11859.
3. Nakai, H., Storm, T. and Kay, M. (2000) Recruitment of single-stranded recombinant adeno-associated virus vector genomes and intermolecular recombination are responsible for stable transduction of liver in vivo. *J. Virol.* **74**, 9451–9463.
4. Ferrari, F., Samulski, T., Shenk, T. and Samulski, R. (1996) Second-strand synthesis is a rate-limiting step for efficient transduction by recombinant adeno-associated virus vectors. *J. Virol.* **70**, 3227–3234.
5. McCarty, D. M. (2008) Self-complementary aav vectors; advances and applications. *Mol. Ther.* **16**, 1648–1656.
6. McCarty, D. M., Fu, H., Monahan, P.E., Toulson, C.E., Naik, P. and Samulski, R. J. (2003) Adeno-associated virus terminal repeat (tr) mutant generates self-complementary vectors to overcome the rate-limiting step to transduction in vivo. *Gene Ther.* **10**, 2112–2118.
7. Hirata, R. and Russell, D. (2000) Design and packaging of adeno-associated virus gene targeting vectors. *J. Virol.* **74**, 4612–4620.
8. Chen, Z., Yant, S., He, C., Meuse, L., Shen, S. and Kay, M. (2001) Linear dnas concatemerize in vivo and result in sustained transgene expression in mouse liver. *Mol. Ther.* **3**, 403–410.
9. Nakai, H., Yant, S., Storm, T., Fuess, S., Meuse, L. and Kay, M. (2001) Extrachromosomal recombinant adeno-associated virus vector genomes are primarily responsible for stable liver transduction in vivo. *J. Virol.* **75**, 6969–6976.
10. Nakai, H., Wu, X., Fuess, S., Storm, T., Munroe, D., Montini, E., Burgess, S., Grompe, M. and Kay, M. (2005) Large-scale molecular characterization of adeno-associated virus vector integration in mouse liver. *J. Virol.* **79**, 3606–3614.
11. Nakai, H., Montini, E., Fuess, S., Storm, T., Grompe, M. and Kay, M. (2003) Aav serotype 2 vectors preferentially integrate into active genes in mice. *Nat. Genet.* **34**, 297–302.
12. Miller, D., Trobridge, G., Petek, L., Jacobs, M., Kaul, R. and Russell, D. (2005) Large-scale analysis of adeno-associated virus vector integration sites in normal human cells. *J. Virol.* **79**, 11434–11442.
13. Miller, D., Rutledge, E. and Russell, D. (2002) Chromosomal effects of adeno-associated virus vector integration. *Nat. Genet.* **30**, 147–148.
14. Miller, D., Petek, L. and Russell, D. (2004) Adeno-associated virus vectors integrate at chromosome breakage sites. *Nat. Genet.* **36**, 767–773.
15. Hirata, R., Chamberlain, J., Dong, R. and Russell, D. (2002) Targeted transgene insertion into human chromosomes by adeno-associated virus vectors. *Nat. Biotechmol.* **20**, 735–738.
16. Inoue, N., Dong, R., Hirata, R. and Russell, D. (2001) Introduction of single base substitutions at homologous chromosomal sequences by adeno-associated virus vectors. *Mol. Ther.* **3**, 526–530.
17. Russell, D. and Hirata, R. (1998) Human gene targeting by viral vectors. *Nat. Genet.* **18**, 325–330.
18. Kohli, M., Rago, C., Lengauer, C., Kinzler, K.W. and Vogelstein, B. (2004) Facile methods for generating human somatic cell gene knockouts using recombinant adeno-associated viruses. *Nucleic Acids Res.* **32**, e3.
19. Chamberlain, J., Schwarze, U., Wang, P., Hirata, R., Hankenson, K., Pace, J., Underwood, R., Song, K., Sussman, M., Byers, P. and Russell, D. (2004) Gene targeting in stem cells from individuals with osteogenesis imperfecta. *Science* **303**, 1198–1201.
20. Miller, D., Petek, L. and Russell, D. (2003) Human gene targeting by adeno-associated virus vectors is enhanced by dna double-strand breaks. *Mol. Cell. Biol.* **23**, 3550–3557.
21. Porteus, M., Cathomen, T., Weitzman, M. and Baltimore, D. (2003) Efficient gene targeting mediated by adeno-associated virus and dna double-strand breaks. *Mol. Cell. Biol.* **23**, 3558–3565.
22. Porteus, M. H. and Carroll, D. (2005) Gene targeting using zinc finger nucleases. *Nat. Biotechnol.* **23**, 967–973.
23. Durai, S., Mani, M., Kandavelou, K., Wu, J., Porteus, M.H. and Chandrasegaran, S. (2005) Zinc finger nucleases: custom-designed molecular scissors for genome engineering of plant and mammalian cells. *Nucleic Acids Res.* **33**, 5978–5990.
24. Bibikova, M., Beumer, K., Trautman, J.K. and Carroll, D. (2003) Enhancing gene targeting with designed zinc finger nucleases. *Science* **300**, 764.

25. Deng, C. and Capecchi, M. R. (1992) Reexamination of gene targeting frequency as a function of the extent of homology between the targeting vector and the target locus. *Mol. Cell. Biol.* **12**, 3365–3371.
26. Thomas, K. R., Folger, K.R. and Capecchi, M. R. (1986) High frequency targeting of genes to specific sites in the mammalian genome. *Cell* **44**, 419–428.
27. Lin, F., Sperle, K. and Sternberg, N. (1985) Recombination in mouse l cells between dna introduced into cells and homologous chromosomal sequences. *Proc. Natl. Acad. Sci. U.S.A.* **82**, 1391–1395.
28. Yáñez, R. J. and Porter, A. C. G. (2002) A chromosomal position effect on gene targeting in human cells. *Nucleic Acids Res.* **30**, 4892–4901.
29. Inoue, N., Hirata, R. and Russell, D. (1999) High-fidelity correction of mutations at multiple chromosomal positions by adeno-associated virus vectors. *J. Virol.* **73**, 7376–7380.
30. Russell, D. W. and Hirata, R. K. (2008) Human gene targeting favors insertions over deletions. *Hum. Gene Ther.* **19**, 907–914.
31. Trobridge, G., Hirata, R. and Russell, D. (2005) Gene targeting by adeno-associated virus vectors is cell-cycle dependent. *Hum. Gene Ther.* **16**, 522–526.
32. te Riele, H., Maandag, E.R., Clarke, A., Hooper, M. and Berns, A. (1990) Consecutive inactivation of both alleles of the pim-1 proto-oncogene by homologous recombination in embryonic stem cells. *Nature* **348**, 649–651.
33. Mortensen, R. M. (1993) Double knockouts. production of mutant cell lines in cardiovascular research. *Hypertension* **22**, 646–651.
34. Grim, J. E., Gustafson, M.P., Hirata, R.K., Hagar, A.C., Swanger, J., Welcker, M., Hwang, H.C., Ericsson, J., Russell, D.W. and Clurman, B. E. (2008) Isoform- and cell cycle-dependent substrate degradation by the fbw7 ubiquitin ligase. *J. Cell Biol.* **181**, 913–920.
35. Bunz, F., Fauth, C., Speicher, M.R., Dutriaux, A., Sedivy, J.M., Kinzler, K.W., Vogelstein, B. and Lengauer, C. (2002) Targeted inactivation of p53 in human cells does not result in aneuploidy. *Cancer Res.* **62**, 1129–1133.
36. Petek, L.M., Fleckman, P., Miller, D.G. (2010) Efficient KRT14 Targeting and Functional characterization of transplantal human keratinocytes for the treatment of epidermolysis Bullosa Simplex Mol. Ther. **18**, 1624–1632.
37. Maniatis, T, Fritsch, EF, Sambrook, J. Molecular cloning, a laboratory manual. Cold Spring Harbor, New York, 1982.
38. Wang, P., Anton, M., Graham, F.L. and Bacchetti, S. (1995) High frequency recombination between loxp sites in human chromosomes mediated by an adenovirus vector expressing cre recombinase. *Somat. Cell Mol. Genet.* **21**, 429–441.
39. Vargas, J. J., Gusella, G.L., Najfeld, V., Klotman, M.E. and Cara, A. (2004) Novel integrase-defective lentiviral episomal vectors for gene transfer. *Hum. Gene Ther.* **15**, 361–372.
40. Grimm, D., Kern, A., Rittner, K. and Kleinschmidt, J. (1998) Novel tools for production and purification of recombinant adeno-associated virus vectors. *Hum. Gene Ther.* **9**, 2745–2760.
41. Clark, K., Liu, X., McGrath, J. and Johnson, P. (1999) Highly purified recombinant adeno-associated virus vectors are biologically active and free of detectable helper and wild-type viruses. *Hum. Gene Ther.* **10**, 1031–1039.
42. Kaludov, N., Handelman, B. and Chiorini, J. A. (2002) Scalable purification of adeno-associated virus type 2, 4, or 5 using ion-exchange chromatography. *Hum. Gene Ther.* **13**, 1235–1243.
43. Zhou, X. and Muzyczka, N. (1998) In vitro packaging of adeno-associated virus dna. *J. Virol.* **72**, 3241–3247.

Chapter 14

Preclinical Study Design for rAAV

Terence R. Flotte, Thomas J. Conlon, and Christian Mueller

Abstract

The process of moving a novel drug such as an adeno-associated viral vector from the bench top to bedside is an arduous process requiring coordination and skill from multiple laboratories and regulatory agencies. Proceeding to a phase I safety trial in humans after most of the proof-of-concept data have been acquired may take several years. During this time, agencies including the FDA, NIH Office of Biotechnology Activities (OBA), and Recombinant DNA Advisory Committee (RAC) along with the investigator's team will develop a series of preclinical toxicology and biodistribution studies in order to develop a safety profile for the intended novel drug. In this chapter, key features of the pharm–tox study design and conduct will be discussed. Highlighted features include choosing a sufficient animal number and species to use in testing, dose determination, typical toxicological assays performed, the use of Standard Operating Procedures in respect to good laboratory practices compliancy, and role of the Quality Assurance Unit.

Key words: AAV gene therapy, Preclinical testing, AAV toxicology, Vector biodistribution, Good laboratory practices

1. Introduction

The ultimate goal of all gene therapy research is to develop novel therapies for human disease based on the introduction of genetic material. As with all therapies, genetic therapies must meet the standard of being "safe and effective" in humans, in order to be licensed for human use in the USA and other countries (1–3). Preclinical studies are, therefore, designed to predict human safety and efficacy. The progress of translational research has generally developed in a manner that separates early "proof-of-concept" preclinical studies from later stage more formalized pharmacology–toxicology (pharm–tox) studies. In the proof-of-concept stage, investigators may demonstrate the ability to express a potentially therapeutic transgene product, evaluate the level and duration of expression, demonstrate important functional activities of the transgene product, or even demonstrate the reversal of a disease

Richard O. Snyder and Philippe Moullier (eds.), *Adeno-Associated Virus: Methods and Protocols*,
Methods in Molecular Biology, vol. 807, DOI 10.1007/978-1-61779-370-7_14,

phenotype in an animal model. If that animal model is a close mimic of a human disease state, such studies often generate considerable excitement in the field. At that point, one may anticipate a rapid translation to clinical application. Unfortunately, the time, effort, funding, and energy that stand between "curing the mouse" and initiating the first-in-human trial for a given therapy are often formidable, creating the so-called "Valley of Death" for promising new therapeutics.

In the formal pharm–tox stage, one must begin to consider issues such as dose-ranging, a more complete kinetic profile, remote biodistribution of vector DNA, and potential toxicities that are either relatively infrequent or related to long-term exposure to the vector (4–10). For example, if a potentially serious side effect of vector administration leads to death in 10% of recipients, one might easily miss it in a proof-of-concept study performed with 5–6 experimental animals and an equal number of controls, even though such samples sizes provide the adequate statistical power to demonstrate a phenotypic cure. Likewise, a toxicity of vector administration that frequently occurs 6 months after vector injection could easily be missed in a 3-month proof-of-concept experiment.

All of these factors lead to important differences in the emphasis between proof-of-concept and pharm–tox studies (Table 1). Nonetheless, there are features of the study design for both proof-of-concept preclinical work and for formal preclinical pharm–tox studies, which can enhance the chances of success at each stage and smooth the transitions between proof-of-concept, pharm–tox, and clinical studies. Furthermore, in addition to the issues discussed above, there are important features of the biology of AAV itself and of rAAV vectors which can influence study design at each stage which are discussed below.

1.1. Biological Features of rAAV Relevant to Preclinical Studies

The design of any preclinical gene therapy study must take into account a number of key parameters, such as the biodistribution of vector DNA, the timing of onset of gene expression, the duration of expression, dose-range, the cellular tropism of the vector, and the tendency of the vector to elicit innate and acquired immune responses. Various aspects of rAAV biology affect these parameters quite significantly. Several of these are listed in Table 2. One important example is the fact that rAAV vector DNA is present in single-stranded form within the virion, and must undergo conversion to a double-stranded DNA template prior to transcription (11–14). Self-complementary vectors can facilitate this process by allowing such a conversion to occur via a simple intramolecular refolding and hybridization (15–19). However, this design can only be approached in cases where the expression cassette is of a size less than half of the packaging limit of the vector. Otherwise, with typical single-stranded rAAV vectors, the delay in time to peak transgene expression may last from several days to several weeks, depending on the tissue type, dose, and capsid serotype.

Table 1
Differences in design emphasis between proof-of-concept and pharmacology–toxicology studies

Study element	Proof-of-concept	Pharmacology–toxicology
Vector design	Well-suited for robust transgene expression	Taking into account safety and scalable production in addition to robust expression
Vector identity relative to the one proposed for human use	Generally similar to the proposed product	Most studies performed with vector identical to the proposed product
Methods and conditions of vector preparation	Research grade and scale	Matching methods and conditions for proposed initial human uses
Quality control assays on vector preparations	A few directed characterizations: lack of replication-competent virus, accurate titer assay	More extensive quality control assays, including some of those proposed for clinical lot release
Dose of vector	May include only one or two dosage levels, chosen to optimize the chances of demonstrating a transgene effect	Must include a range of doses, typically ranging from the no-effect dose to the maximal tolerated dose
Animal model	Preference for animal model of the disease, often a knock-out model of a genetic deficiency	Generally includes two species, often a rodent and a larger animal; may or may not include deficient animals
Study endpoints	Most focused on delivery, expression, and functional effects of the transgene; premium on reversal of pathology in a deficient model	Most focused on safety at site of administration and a broad-ranging panel of distant sites; should include molecular biodistribution and immune response profiles
Study timepoints	Chosen to maximize opportunity to demonstrate a therapeutic-like effect	Must include a broad range of time points; include some very long-term time points that might detect long-term risks, such as the risk of carcinogenesis

Table 2
Unique aspects of rAAV biology and the implications for preclinical study design

Biological property of rAAV	Implication for preclinical study design
Single-stranded AAV genome is not transcriptionally active until converted to ds-DNA	Must either allow sufficient time for leading strand synthesis or employ self-complementary vector design
Vector DNA is primarily episomal	Use of rAAV is optimal in terminally differentiated (G_0 phase) cells
Packaging capacity is limited to 4.5 kb in most cases	May need to use minigenes (as with dystrophin or CFTR) or dual vector approaches

Table 3
AAV receptors by serotype

AAV serotype	Known receptors
AAV1	α2-3 and α2-6-N-linked sialic acid
AAV2	Heparan sulfate proteoglycan, $\alpha_V\beta_5$ integrin, FGF-R
AAV4	α2-3-O-linked sialic acid
AAV5	α2-3-N-linked sialic acid
AAV6	Heparan sulfate proteoglycan and sialic acid

AAV is a nonenveloped icosahedral parvovirus, which typically begins its interaction with a permissive cell by binding to a cell surface receptor (20). The initial binding receptor varies by serotype. Several such receptors have been identified as listed in Table 3 (21–25). There is an additional internalization step, which is also receptor-dependent in many cases, and involves an endosomal pathway (26). Subsequent steps include endosomal escape, nuclear trafficking, and nuclear entry (27). Between endosomal escape and nuclear entry, certain AAV capsids are known to undergone ubiquitination and may be susceptible to proteasomal degradation (28, 29). In most cases, uncoating of vector DNA occurs either concomitantly with or after nuclear entry. Within the nucleus, there appear to be microenvironments within which both wild-type or recombinant AAV DNA reside (30). These environments may be conducive to conversion to double-stranded DNA. In a typical single-stranded rAAV genome, hairpin self-priming can provide a template for leading strand synthesis, most likely through a DNA repair mechanism. There is strong evidence to indicate a role for the phosphorylation state of a ss-DNA binding protein in the FKBP family for regulating this conversion (31, 32). In other circumstances, it has been argued that separate positive and negative polarity strands from two different rAAV virions anneal after nuclear entry. The fact that both AAV and rAAV packaging result in packaging of both positive and negative strands makes either explanation feasible.

Once a double-stranded template is in place, transcription can commence. However, the duration of gene expression may then depend upon further processing of the genomes. Under most circumstances, the predominant fate of the rAAV genomes appears to undergo some form of intermolecular recombination, perhaps through nonhomologous end-joining, to form a higher molecular weight concatemer that remains extrachromosomal (33–41). These larger episomes appear to be quite stable in nondividing cells, but are rapidly lost in dividing cells. In tissues which are nondividing

but can regenerate after injury (such as liver or muscle), the duration of gene expression is typically quite long unless the organ is severely injured, as can be induced in the liver by a partial hepatectomy (37, 39).

Finally, once gene expression has been established, the duration of gene expression may also be influenced by the development of host responses to the manipulation. Over time, it has become clear that rAAV-mediated transduction will reproducibly induce the production of serotype-specific antibody responses. In most cases, these responses will limit the ability to successfully repeat dosing of the same serotype (42–44). There is also some evidence of cross-serotype antibody formation as well, but this is not nearly as common and may be peculiar to certain situations (45). In general, however, rAAV-mediated transduction of nondividing cells is life-long and so may not require repeated dosing.

Injection of a rAAV vector in most organs will also elicit an effector T-cell response to the capsid antigen, which can include both CD4+ and CD8+ as well as possible cytotoxic T-cell responses (46). Interestingly, such responses may be weak in wt-AAV infections unless a helper virus is present to allow for productive replication (47). Nonetheless, effector T-cell responses after rAAV-mediated transduction have been hypothesized to present a limitation to both preclinical and clinical studies. The hypothesis more fully stated is that cross-presentation of AAV capsid epitopes is present on transduced cells after vector administration and that these epitopes continue to be displayed for weeks after the initial injection of vector, so that effector T cells may identify the transduced cells and eliminate them. This mechanism was invoked in the interpretation of one liver-directed trial of rAAV2-factor IX in hemophilia B patients (46, 48). One must keep in mind that such cross-presentation would involve residual capsid protein from the initial injection, since the capsid genes are not present within the therapeutic vector, unless they are there as contaminants.

Data from other recent clinical trials with a different route of delivery have yielded different results (45). In a study of intramuscular injection of rAAV1-alpha1 antitrypsin vector, the subjects were given doses as high as 6×10^{13} vector genomes of rAAV. At that dose, each subject developed effector T-cell responses, including gamma interferon-expressing and perforin expressing cells, thereby indicating a cytotoxic T-cell response. There was no indication that there was any loss of transduced cells in these individuals, however. Transgene expression persisted at a consistent plateau level (albeit subtherapeutic) for a full year, even in the face of the T-cell responses. It is important to note that these findings occurred in the absence of any immune suppression, which has been adopted by some clinical investigators as a study design feature after the hemophilia B experience. It is also worthy of note that one of the

three rAAV2-rpe65 trials that reported clinical efficacy in Leber congenital amaurosis (LCA) after intraretinal injection has also demonstrated continued transgene expression at 1 year after injection, without immune suppression (49, 50).

2. Proof-of-Concept Study Design

Clearly, understanding these elements of the biology will dictate when and how rAAV may be useful in proof-of-concept type studies and which serotype or variant may be best suited for a particular indication. If the cell target for gene expression is rapidly proliferating, it may be difficult to achieve high level or sustained expression with rAAV, and a retrovirus or lentivirus vector may be more appropriate.

If a particular experiment calls for a vector that will express very rapidly after injection, it may be difficult to get optimal results with a standard ssAAV vector, so a self-complementary AAV (scAAV) may be preferred. Alternatively, one may choose to use a ssAAV vector because of the size of the expression cassette or for other reasons, and consequently have to time the vector injection to allow sufficient time for transgene expression to be activated prior to measuring the key endpoint in question in the experiment.

Providing a comprehensive list of optimal choices of rAAV serotype for any given cell type of choice is a somewhat challenging and risky proposition, since the number of available serotypes is rapidly expanding, as is the published experience with several of these serotypes. Nonetheless, such a listing is provided in Table 4.

Table 4
Optimal rAAV capsid serotype choices for various mouse tissues

Tissue	Optimal serotype	Other choices
Brain	rAAV2	rAAV9, rAAV5
Retina	rAAV2	rAAV5
Airway epithelium	rAAV1	rAAV5, rAAV6, rAAV-rh10
Liver	rAAV8	rAAV9, rAAV1
Skeletal muscle	rAAV1	rAAV9
Spinal cord	rAAV9	
Pancreas	rAAV8	

There are a number of important considerations beyond the cell type question, the chief of which is a consideration of the species of interest. There are a growing number of examples in which the optimal serotype of choice for mouse studies is not the same as that serotype for use in larger animals or humans. One such example is illustrated in the recent publication by Flotte et al., which sought to address the following discrepancy. rAAV5 vectors have consistently performed very well in mouse bronchial epithelial cells in vivo. However, in comparative studies in a well-differentiated airway cell culture model, rAAV1 vectors were superior in human cells. Importantly, the rAAV5 vector was also superior when either mouse or lower primate bronchial epithelial cells were put into the culture system. In the study, a chimpanzee model was used in an attempt to closely mimic human cells in vivo. Chimpanzees are much more closely related to humans than are lower primates, and are much better predictors of human virus tropism (such as with respiratory syncytial virus or hepatitis C virus). In the paper in question, a dual luciferase reporter system was used to compare the in vivo efficiency of gene transfer between rAAV1 and rAAV5 vectors. The results clearly indicated a closer correlation between chimpanzee in vivo and human culture results, with a 20-fold advantage for rAAV1 in the chimpanzees, which was sustained for 3 months in vivo (51).

Such studies clearly point to the fact that the matching of vector and cell type for preclinical studies must also take into account the matching of species to the purpose at hand. There may be a number of instances in which studies in a well-defined mouse model may be extremely valuable. For example, with the airway epithelium case, one might readily prefer to use the rAAV5 system for such studies. However, if the question to be addressed in the preclinical study relates more to anatomy and vector tropism, a better choice may be to use rAAV1 and a higher primate.

The choice of species may also have an important effect on the predictive value of immune response experiments. For instance, the use of rAAV8 vectors in the liver of mice has been shown to induce immune tolerance, even postnatally, in some situations. In contrast, rAAV vector delivery to the liver in humans has been shown to be quite immunogenic, as described earlier. Furthermore, no manipulation has yet shown to the induction of true postnatal tolerance in humans, so the likelihood of that being observed with rAAV transduction seems very remote.

2.1. Pharmacology–Toxicology Study Design

There are a number of features of the study design and procedural framework that one must consider when moving toward submission of an Investigative New Drug (IND) application to the FDA. At this stage, one must prove the vector in question to be a well-defined biological therapeutic agent, prepared and characterized in a consistent manner that is suitable for human use. One must

also consider a set of preclinical data that can define the behavior of the vector over a fairly wide range of dosages and time points. This should be based upon animal model and cell culture data appropriate for the safety and efficacy considerations that will be important for the intended clinical use, and particularly for the intended first human trial.

These considerations would hold true for all new drugs. There are additional specific considerations for gene therapy agents, which relate to the potential for inadvertent germ line transmission of genetic material. This is generally considered to be ethically undesirable and has the potential for insertional mutagenesis leading to cancer, which could be a long-delayed toxicity only apparent years after vector administration. On the basis of these considerations, the design of pharm–tox studies will include molecular biodistribution type studies (i.e., DNA detection in a wide-ranging panel of distant organs), and long-term time points.

Viral gene transfer vectors also share certain properties with live virus vaccines. As such, one must consider an appropriate set of immune response assays in the context of the pharm–tox studies. Interestingly, this may mandate the use of a vector for some of the studies that is not identical to the clinical product, but rather encodes an isogenic (same species) version of the transgene. For instance, the use of a human factor IX vector in a mouse may lead to a greater risk of antitransgene antibody production within the mice than would actually exist in the patients, simply because of the cross-species nature of the transgene. In such circumstances, a portion of the preclinical work may be performed with a murine transgene.

There are also special considerations for the preparation of the material for the formal pharm–tox studies and for the conduct of the studies themselves. First, the production method must be the same as that to be used for the clinical grade material. This may be an issue if the production method used for the earlier proof-of-concept work is not well-suited for clinical grade production. One may have to embark on a rather prolonged phase of *process development*.

The range of considerations in developing a clinical grade process is quite broad and a few instances are provided in Table 5. For instance, if the production of a recombinant virus (such as rAAV or a lentivirus vector) requires transfection of a plasmid, it has become an accepted standard that such plasmids should not contain an Ampicillin-resistance cassette, but rather should use kanamycin resistance or some other antibiotic resistance for which there is no history of human exposure and possible prior sensitization. Another example is the desire for the use of containers and processes that are completely closed to the external environment. While the use of open flasks or dishes within a biosafety cabinet may be very acceptable in the context of research grade material, such conditions are not generally appropriate for clinical use.

Table 5
Considerations for clinical grade production processes

Production process feature	Research grade	Clinical grade
Upstream production options	Proviral plasmid transfection, cell lines, infectious helpers	Prefer to avoid transfection in favor of scalable cell lines and/or infectious helpers; avoid serum-containing medium if possible (due to Transmissible Spongiform Encephalopathies)
Properties of proviral plasmids (if used)	May use standard plasmid preparations if purity allows for efficient transfection; may use Amp^R plasmids	Plasmid production under controlled conditions with minimal endotoxin level; avoid Amp^R gene containing plasmids
Downstream production features	Moderate purity and concentration of final product is adequate; emphasis on reliability of method at small scale	Priority on purity; higher concentration of final product preferred; orthagonal purification methods; closed system for routing of material between purifications (often in automated column chromatography format)

In a broader context, there is generally a greater desire for a scalable process in the context of clinical grade product, since most animal experiments call for lower absolute doses of vector than one would use in a human. The scalability of a process usually entails moving to some form of bioreactor, typically meaning that one moves to a well-characterized producer cell line and away from transfection-based methods. There are exceptions to this, but there are clearly advantages to moving in this direction when one approaches clinical trials.

If such a movement is contemplated, then one must consider having at least some of the formal pharm–tox work performed with material that is prepared with the process to be used for the clinical trial. This may cause added expense and delay. Some elements of the preclinical pharm–tox package could be done with material made under conditions similar to the research grade material if the property being assessed is not likely to be affected by the production method. For instance, the immune response profiles might be done with material in which the upstream production process is not the final process, so long as the downstream purification is quite similar and the ultimate product is characterized to be the same, with defined strength and impurity limits.

2.2. Key Variables in Pharm–Tox Study Design

The key variables to be explored in the design of pharm–tox studies include the dose of vector to be administered and the duration of exposure of the recipient to the vector. In all of these studies, the

dosing and timing relate to the ultimate desired clinical use of the vector, which should be reflected in the design of the first phase I clinical trial. In projecting the doses required for the pharm–tox study, one may consider a dosage per body weight anticipated as the highest dose in the clinical trial. One can then project that back to the weight of the experimental animal (or the approximate weight of that species). Finally, one should consider a safety margin of 10- to 100-fold on a per body weight basis, meaning that the dose per kilogram in the animal would exceed the highest anticipated human dose by 10- to 100-fold. In addition, it may be more desirable to express the dose in an organ or compartment-specific manner, such as in the retina or isolated muscle mass during a perfusion administration. Most dosing is based on vector genome titer since the infectious titer is cell-type dependent and in most instances will not reflect the in vivo target. Internal standards that are calibrated to a recognized reference standard, such as the AAV2 reference standard, are important so that comparisons between studies can be made.

For persistent viral vectors (rAAV, lentivirus, and retrovirus), the duration of exposure is equivalent to the time elapsed after vector delivery. The timing of assessments is generally designed to include time points that will detect early (within the first hours or days after vector administration), mid-range, and long-term toxicities. There are some limitations to the practicality of performing truly long-term toxicology studies prior to the first human use. For integrating or persistent vectors, such studies would span the life time of the animal, which would be at least 18–30 months for mice and many years for larger animals. The impracticality of such long intervals must be balanced against the imperative to move forward with developing better therapies for patients. Further consideration must be given to the fact that the version of a vector entering the first phase 1 trials may not correspond to the ultimate version that will be licensed for general use. Thus, many potential vectors are moved forward into the clinic with pharm–tox data in the 3- to 6-month range. At some point later in the clinical development of a vector, additional longer-term studies may be needed.

One must also consider the number of animals required. If one considers idiosyncratic toxicities that occur in a limited percentage of animals, one must include sufficient numbers to detect relatively low-frequency events. For instance, one could not reliably anticipate detecting an adverse reaction with an actual prevalence of 5% if one only administers the vector to three animals in each group. The sample size is also critical with regard to statistical confidence regarding outcomes that are measureable on a continuous scale, such as the dose-related level of transgene expression or reproducible dose-related toxicities. In both cases, one must consider the desired statistical power of the study, defined as 1.0 minus the probability of a type 2 error (missing the occurrence of a real

difference as compared to control conditions). For most purposes, a statistical power of 0.80 is acceptable.

When considering statistical power for a continuous outcome, the three variables contributing to statistical power are the magnitude of the difference between the two groups, the variation in the measurements, and the sample size. The magnitude of the difference between the two groups is generally related to the real biological effect, the variability of the measurements includes both biological components and technical variability of the test, and the sample size is the one element that the designer controls deliberately to reach the desired power.

When considering sample size relative to idiosyncratic toxicities, there is general agreement that it is acceptable to perform studies with approximately 20 rodents per dose level, with numbers split evenly between males and females. This would allow for the detection of sex-independent toxicities occurring in about 5% of animals and sex-specific toxicities occurring in about 10% of animals. As this discussion implies, a study design must take into account the species of animal to be used and the potential effects of the sex and age of the experimental animals. It is often desirable to include within the entire preclinical package studies in both rodents and larger animals. Rodents are generally a practical model for allowing larger samples sizes and higher doses per body weight and their short life spans provide an opportunity for a better representation of near life-long exposure. Finally, there may be cases where a portion of the pharm–tox work might be performed within a knock-out mouse model, such as when an immune response to the transgene product might be a contributing factor to the biological characterization of the vector.

There are a number of factors involved in the potential choice of a larger animal model. In some cases, the larger animal models will allow for a better approximation of the technical or surgical procedure for injection of the vector that will be used in humans. Examples of this would be the use of a particular vascular intervention for isolated limb perfusion or a specific neurosurgical technique for injecting a vector within a desired region of the brain. The rodent model may make such an approximation impractical either because of a lack of anatomical similarity or because of the limitations imposed by their small size. In some cases, biological differences are important in choosing larger animals as well. For instance, the human-like profile of certain receptors for viral vectors may only be reproduced in nonhuman primates. In other cases, there may be a useful large animal model for the disease process, as with canine models of LCA or hemophilia.

2.3. Outcome Assessments in Pharm–Tox Studies

As mentioned above, outcome assessments for pharm–tox studies in gene therapy will include both those outcomes that one would monitor with any novel therapeutic as well as certain outcomes

that are specific to gene therapy. In the former category, one would include serum chemistries, blood counts, and histopathologic analysis of multiple organs. A basic serum chemistry panel for animals in such a study would include electrolytes (sodium, potassium, chloride, and bicarbonate) and measures of renal toxicity (blood urea nitrogen and creatinine) and hepatic toxicity (transaminases and alkaline phosphatase). Blood counts would include a measurement of hematocrit and/or hemoglobin concentration, total white blood counts, and platelet counts. The histopathologic analysis will include detailed sampling of the organ exposed to the greatest dose of vector (e.g., the site of direct injection and the draining lymph nodes) and a general examination of other critical organs that might be exposed to vector that is disseminated systemically, such as lungs, heart, liver, kidneys, brain, pancreas, small bowel, and potentially other sites. The primary abnormalities screened for at these sites include acute and chronic inflammation, tumor formation, necrotic changes, and apoptosis.

In considering gene therapy specific outcomes, the primary concerns will be biodistribution analysis and longer-term examinations for evidence of tumor formation. The latter will easily be detected on histopathologic analysis, but the former generally require specific DNA detection assays of both blood and peripheral organs, with special attention to gonads, as the spread of vector DNA to gonads could indicate a risk for inadvertent germline transmission. A number of assays could be used for the detection of vector DNA sequences, but the general consideration is that the limit of detection should be at least 100 vector genome copies per microgram of cellular DNA. For a mouse, 1 μg of cellular DNA would represent approximately 3×10^5 diploid genomes, so the presence of 100 copies would be the equivalent of 1 positive host cell out of 3,000. It is important to note that the sensitivity of the assay must be demonstrated to be operative in the presence of the cellular DNA extract to be used in the assay. The customary method of doing this is to have a known quantity of vector genomes "spiked in" to one of the replicates of the specific sample. In some instances, one organ extract might contain substances that inhibit the detection assay (such as quantitative PCR) while others do not, matrix effects should also be taken into consideration. For example, there is a major interest in detecting the presence of vector genomes in the blood, since this presence if often time- and dose-dependent and may correspond with the risk for hematogenous dissemination to other organs. However, some versions of Taq polymerase may be partially inhibited by the presence of heme in blood extracts, requiring optimization of the assay conditions. Finally, it is essential that the primers and probe designed are specific to the vector sequence target and will not anneal nonspecifically to endogenous species sequences. General guidelines for performing real-time PCR for vector genomes are found in Appendix 1.

2.4. General Considerations of Conducting Pharm–Tox Studies

Finally, one must consider that at least a portion of the pharm–tox package must be performed in compliance with FDA-prescribed good laboratory practices (GLP). While one may have personnel formally trained in GLP within the academic setting, such studies are often performed at contract research organizations (CROs). In addition to GLP compliance, there is generally a desire for animal handling and housing to be maintained under conditions that eliminate variability to as great an extent as possible. Specific-pathogen free (SPF) conditions are usually warranted, as the time and expense of repeating a study or investigating spurious findings caused by a coincident pathogenic infection are highly undesirable. Other factors, such as the ambient temperature, humidity, and light cycling of the animals in the study could also affect outcome variables. Thus, these factors must be kept as consistent as possible. Finally, the conditions for necropsy should be designed to avoid contamination of organ samples with vector DNA as outlined in Appendix 2. Thus, one would ideally harvest organs from control animals prior to lower dosage animals, and then perform necropsies on the highest dosage animals last. Within a given necropsy, one might consider harvesting the gonads prior to other organs, and then harvesting the injection site last. Additional benefit may be gained from changing instruments between the harvest of each of the organs or body cavities, and certainly between individual animals, so that vector genomes present in one animal will not be inadvertently carried over into samples from the next.

3. Summary

In summary, preclinical gene therapy studies must be based upon well-defined scientific questions in order to be effective. In general, the differences between proof-of-concept studies and pharmacology–toxicology studies reflect the differences in these questions, which emphasize potential for efficacy in the former and safety in the latter. Proof-of-concept studies are best performed in animal models of a disease and the conditions are optimized for the vector to exert the desired transgene effect. Pharmacology–toxicology studies may be performed in a number of different species (usually one rodent species and one larger animal species). Pharm–tox studies for gene therapy may include additional studies to address the potential for inadvertent germline transmission and the potential for long-term carcinogenesis from integrating vector DNA. Pharm–tox studies may also have an emphasis on immune responses to the transgene product and to other vector components. Proof-of-concept studies are often performed with vector constructs that are similar in all biologically relevant aspects to the eventual vector intended for human use but may not be identical to that clinical

vector. By contrast, the pharm–tox studies must include at least some work with the vector identical to that to be used in the first clinical trials. Both types of studies are indispensible in the attempt to predict whether or not a proposed gene therapy agent will be safe and effective in humans. Properly performed, the entire preclinical data package will allow for a better estimation of the starting dose for a clinical trial, a more focused set of safety studies, a better understanding of the anticipated kinetics of any functional responses, and a generally more successful clinical study campaign. As such, a well-done set of preclinical studies may be incredibly valuable during the long and arduous course of gene therapy product development.

Appendix 1. General Guidelines for Real-Time PCR Standard Operating Procedure

Procedure Setup

1. Document on Form Real-Time PCR Procedure Record all information requested.
2. Wipe down entire work surface, 1.5 mL tube racks, and pipettes with 10% bleach.
3. Wipe down work surface area, 1.5 mL tube racks, and pipettes with DNA away.
4. Follow with an ethanol wipe down of work area, 1.5 mL tube racks, and pipettes

   Note: A separate set of pipettes are used for PCR preparation. The pipettes used for gDNA extractions must not be used.
5. Place a clean absorbent pad down on work area and lay all cleaned racks and pipettes on the pad.

   Note: Place and label all tubes in the rack to be used. Make sure to place the tubes used for preparing the standard curves in a separate rack.
6. Document the lot number and expiration date of the universal master mix.

Preliminary Run Set Up

1. Wipe down pipettes with DNA Away.
2. Based on the calculations, pipette water volumes required for gDNA sample wells.
3. Pipette water into the FAM standard wells.
4. Pipette water into a well indicated for FAM no template control (NTC) wells.
5. Prepare the master mix for the FAM-labeled probe.

   Note: Do not pipette master mix to plate at this time.

6. Prepare gDNA samples based on gDNA needed for sample type.

   Note: All genomic DNA dilutions should be made on the day the PCR assay is run. They should not be made in advance.

   Note: Do not pipette gDNA samples at this time.
7. Vortex briefly and pipette master mix Cocktail to FAM standard and NTC wells.
8. Vortex briefly and pipette master mix Cocktail to sample wells.
9. Vortex briefly and pipette diluted gDNA samples to designated wells.
10. Vortex briefly and pipette the required amount of each standard dilution into the appropriate well based on vector length.
11. Vortex briefly and pipette Spike in to designated wells.

    Note: Spike in is calculated to keep a 100 copy/μg genomic DNA ratio. If less than 0.1 μg DNA is loaded, a ten-copy spike in is always used. Example: If 0.7 μg is loaded, then a 70-copy spike in will be used.
12. Cover plate with optical cover according to instructions. The optical cover should not be touched.
13. Settle the samples in the plate by tapping on side. This gets out any bubbles that are sitting at the bottom of the wells.
14. Transfer to isolated room housing the real-time PCR machine and run.

Analysis

1. When the run is complete, analyze the run using the appropriate software.
2. Remove outliers on the standard curve if necessary. GLP standards require at least six standard curve points; therefore up to three outliers may be removed. Reanalyze run if outliers are removed.
3. Start baseline (red flag) should be set at a standard predetermine value or default to be considered acceptable.
4. Stop baseline (red flag) should be set 1 cycle before amplification of the 10E8 standard point begins (rounded to a whole number).
5. After setting the baselines section, the threshold should be set to maximize the R2 using the following criteria:
   - The threshold should be set above the background
   - Below the plateaued and linear regions of the amplification curve
   - Within the geometric phase of the amplification curve

6. The acceptable range for the slope should be between ±0.3 of the study mean. The R2 should be equal or greater than 0.97 for the run to be acceptable.
7. The acceptable range for the efficiency should be 95–105%.

$$\text{Efficiency} = -1 + 10^{(-1/\text{slope})}$$

8. Observe the copy count (Ct) for the NTC. The acceptable range for the NTC is less than or equal to 15 copies/μg gDNA.
9. Complete the SOP associated form to determine if the run is acceptable.
10. If the run is unacceptable, discuss with laboratory director before attempting the run again.

Appendix 2. General Guidelines for Necropsy Standard Operating Procedure

Gross Necropsy

1. A complete necropsy will be conducted on all animals dying spontaneously, euthanized in extremis or at the scheduled necropsy dates. Necropsy will include examination of:
   - The external body surface
   - All orifices
   - The cranial, thoracic, abdominal, and pelvic cavities and their contents.
2. Prior to sampling, the pathologist will perform a gross necropsy.
3. All body surfaces and orifices are observed carefully and external surfaces palpated gently. All abnormalities will be recorded in the appropriate sections of the necropsy forms.
4. After dissection and sampling, carefully examine all body cavities. The condition of the blood should be noted.
5. The remainder of the esophagus and GI tract should be opened and the mucosa and contents examined.
6. If required by protocol, a licensed pathologist will then examine the previously removed organ tissues in wet tissue containers for abnormalities and lesions found will be fixed in NBF for further examination.
7. If required by protocol, a licensed pathologist will verify the identification of the animal, verify tissue accountability, assess

lesions, and check for completeness and accuracy of the entries on the necropsy form and sign and date the necropsy form.

8. An audio recording may be taken during necropsy and the audio file will be sent to the Study Director for archiving. At the end of the study, this audio file will be copied to CD for archiving.
9. Depending on the analyses that need to be performed on these tissues (e.g., histopathology, PCR, or both), multiple samples may be required.
10. *Pathologist* refers to the person ultimately responsible for the necropsy.
11. Depending on the tissues to be collected employ specific teams (e.g., one team will remove the head and harvest the brain, a second team will harvest the heart and lungs, and a third team will collect the remaining organs).
12. During the course of the dissection, change gloves and instruments between each organ. Instruments used for obtaining study samples should not have been used previously for any other tissue (e.g., use a separate set of instruments for cutting away connective tissue to free an organ and cutting the actual sample from that organ). All cutting boards, containers, and necropsy surfaces will be either disposable or washed with DNA Away, 10% bleach, and 70% ethanol between animals to prevent contamination of DNA/mRNA. Individuals handling the tissue should not touch bare human skin while handling the tissues in order to prevent contamination with RNAase. Razor blades should be discarded between organs to prevent contamination.
13. All gross macroscopic lesions should be recorded on a necropsy form, using the approved terminology and format, and preserved in 10% neutral buffered formalin until consultation with the Study Director or Sponsor for possible histopathologic evaluation. If any questions regarding the identification or description of an organ/lesion arise, the pathologist should be immediately consulted. At each of the steps outlined, it is understood that careful visual observation and gentle palpation (as needed) are essential. Lesion descriptions will include organ, morphology, and where appropriate, color, site, size in millimeters or milliliters, and distribution.
14. Take note of the condition of the blood (e.g., normal, thin, thick, and clotted). In anemic animals, blood can look thin while in lipemic animals it can appear a homogenous pale pink color with a thick consistency.

15. If a bone marrow smear is required, it should be prepared using a portion of the rib (or the bone specified in the protocol). The rib or bone specified for bone marrow smear should be submitted as early in the necropsy procedure as possible.

Organ and Tissue Collection

1. After removing the organs from the body, as much extraneous tissue as possible is removed and the organ is rinsed in a container with iced saline to remove blood and debris.
2. Required organs are weighed and the weight is recorded on the study-specific necropsy form.
3. Clean the weighing pan by brushing with a soft brush, or wiping the pan with a clean, lint-free cloth or Kimwipe®.
4. Place a disposable bench pad in the weighing pan and tare the scale.
5. Place the sample on the disposable bench pad and weigh them together in the weighing pan. Record the results on the study-specific necropsy form.
6. Pat the organ dry with the disposable bench pad, remove the organ, and weigh only the pad. Record the pad weight on the study-specific necropsy form.
7. Paired organs will be weighed together. Each organ may be placed back into the container containing ice-cold saline before the tissue area to be collected is harvested and cut into small blocks with dedicated cutting boards and instruments. The tissues may be rinsed in containers (appropriate tubs, buckets, pans, etc.) and saline squeeze bottles should also be available. Saline will be chilled overnight and dispensed immediately before use. It may be kept cold, for example, by refrigeration, using frozen bags of saline or saline ice cubes, or setting the saline container in ice.
8. After trimming, the remaining organ will be examined by the necropsy team for gross abnormalities and samples obtained for fixation if required.
9. If a quick frozen sample is needed for analyses such as PCR, place tissue into the appropriate prelabeled cryogenic containers, snap freeze in liquid nitrogen, and transfer to a –70°C freezer. The sample size should be no more than two thirds of the vial in order to allow for expansion of the tissue during freezing. If trimming occurs on a dissection board, use a separate dissection board for each organ.
10. Tissues for histopathology are generally fixed in neutral buffered formalin (NBF). Tissues will be fixed at a thickness not to exceed 5 mm except as stated.

References

1. Barker, L. F. (1975) Food and Drug Administration regulations and licensure. Fed Proc **34**, 1522–1524.
2. Snyder, R. O., and Francis, J. (2005) Adeno-associated viral vectors for clinical gene transfer studies. Curr Gene Ther **5**, 311–321.
3. Francis, J. D., and Snyder, R. O. (2005) Production of Research and Clinical Grade Recombinant Adeno-associated Virus Vectors, in Laboratory Techniques in Biochemistry and Molecular Biology (Berns, K. I., and Flotte, T. R., Eds.) pp 19–56, Elsevier, Amsterdam.
4. Conrad, C. K., Allen, S. S., Afione, S. A., Reynolds, T. C., Beck, S. E., Fee-Maki, M., Barrazza-Ortiz, X., Adams, R., Askin, F. B., Carter, B. J., Guggino, W. B., and Flotte, T. R. (1996) Safety of single-dose administration of an adeno-associated virus (AAV)- CFTR vector in the primate lung. Gene Ther **3**, 658–668.
5. Song, S., Scott-Jorgensen, M., Wang, J., Poirier, A., Crawford, J., Campbell-Thompson, M., and Flotte, T. R. (2002) Intramuscular administration of recombinant adeno-associated virus 2 alpha-1 antitrypsin (rAAV-SERPINA1) vectors in a nonhuman primate model: safety and immunologic aspects. Mol Ther **6**, 329–335.
6. Poirier, A., Campbell-Thompson, M., Tang, Q., Scott-Jorgensen, M., Combee, L., Loiler, S., Crawford, J., Song, S., and Flotte, T. R. (2004) Toxicology and biodistribution studies of a recombinant adeno-associated virus 2-alpha-1 antitrypsin vector. Preclinica **2**, 43–51.
7. Flotte, T. R., Conlon, T. J., Poirier, A., Campbell-Thompson, M., and Byrne, B. J. (2007) Preclinical characterization of a recombinant adeno-associated virus type 1-pseudotyped vector demonstrates dose-dependent injection site inflammation and dissemination of vector genomes to distant sites. Hum Gene Ther **18**, 245–256.
8. Jacobson, S. G., Boye, S. L., Aleman, T. S., Conlon, T. J., Zeiss, C. J., Roman, A. J., Cideciyan, A. V., Schwartz, S. B., Komaromy, A. M., Doobrajh, M., Cheung, A. Y., Sumaroka, A., Pearce-Kelling, S. E., Aguirre, G. D., Kaushal, S., Maguire, A. M., Flotte, T. R., and Hauswirth, W. W. (2006) Safety in nonhuman primates of ocular AAV2-RPE65, a candidate treatment for blindness in Leber congenital amaurosis. Hum Gene Ther **17**, 845–858.
9. Jacobson, S. G., Acland, G. M., Aguirre, G. D., Aleman, T. S., Schwartz, S. B., Cideciyan, A. V., Zeiss, C. J., Komaromy, A. M., Kaushal, S., Roman, A. J., Windsor, E. A., Sumaroka, A., Pearce-Kelling, S. E., Conlon, T. J., Chiodo, V. A., Boye, S. L., Flotte, T. R., Maguire, A. M., Bennett, J., and Hauswirth, W. W. (2006) Safety of recombinant adeno-associated virus type 2-RPE65 vector delivered by ocular subretinal injection. Mol Ther **13**, 1074–1084.
10. Goldman, M. J., Litzky, L. A., Engelhardt, J. F., and Wilson, J. M. (1995) Transfer of the CFTR gene to the lung of nonhuman primates with E1- deleted, E2a-defective recombinant adenoviruses: a preclinical toxicology study. Hum Gene Ther 6, 839–51.
11. Ferrari, F. K., Samulski, T., Shenk, T., and Samulski, R. J. (1996) Second-strand synthesis is a rate-limiting step for efficient transduction by recombinant adeno-associated virus vectors. J Virol **70**, 3227–3334.
12. Fisher, K. J., Gao, G. P., Weitzman, M. D., DeMatteo, R., Burda, J. F., and Wilson, J. M. (1996) Transduction with recombinant adeno-associated virus for gene therapy is limited by leading-strand synthesis. J Virol **70**, 520–532.
13. Afione, S. A., Wang, J., Walsh, S., Guggino, W. B., and Flotte, T. R. (1999) Delayed expression of adeno-associated virus vector DNA. Intervirology **42**, 213–220.
14. Song, S., Morgan, M., Ellis, T., Poirier, A., Chesnut, K., Wang, J., Brantly, M., Muzyczka, N., Byrne, B. J., Atkinson, M., and Flotte, T. R. (1998) Sustained secretion of human alpha-1-antitrypsin from murine muscle transduced with adeno-associated virus vectors. Proc Natl Acad Sci U S A **95**, 14384–14388.
15. McCarty, D. M., Monahan, P. E., and Samulski, R. J. (2001) Self-complementary recombinant adeno-associated virus (scAAV) vectors promote efficient transduction independently of DNA synthesis. Gene Ther **8**, 1248–1254.
16. McCarty, D. M., Fu, H., Monahan, P. E., Toulson, C. E., Naik, P., and Samulski, R. J. (2003) Adeno-associated virus terminal repeat (TR) mutant generates self-complementary vectors to overcome the rate-limiting step to transduction in vivo. Gene Ther **10**, 2112–2118.
17. Fu, H., Muenzer, J., Samulski, R. J., Breese, G., Sifford, J., Zeng, X., and McCarty, D. M. (2003) Self-complementary adeno-associated virus serotype 2 vector: global distribution and broad dispersion of AAV-mediated transgene expression in mouse brain. Mol Ther **8**, 911–917.
18. Zhong, L., Chen, L., Li, Y., Qing, K., Weigel-Kelley, K. A., Chan, R. J., Yoder, M. C., and Srivastava, A. (2004) Self-complementary adeno-associated virus 2 (AAV)-T cell protein tyrosine phoshatase vectors as helper viruses to improve transduction efficiency of conventional single-stranded AAV vectors in vitro and in vivo. Mol Ther **10**, 950–957.

19. Vandenberghe, L. H., Wang, L., Somanathan, S., Zhi, Y., Figueredo, J., Calcedo, R., Sanmiguel, J., Desai, R. A., Chen, C. S., Johnston, J., Grant, R. L., Gao, G., and Wilson, J. M. (2006) Heparin binding directs activation of T cells against adeno-associated virus serotype 2 capsid. Nat Med **12**, 967–971.
20. Flotte, T. R., and Berns, K. I. (2005) Adeno-associated virus: a ubiquitous commensal of mammals. Hum Gene Ther **16**, 401–407.
21. Summerford, C., and Samulski, R. J. (1998) Membrane-associated heparan sulfate proteoglycan is a receptor for adeno-associated virus type 2 virions. J Virol **72**, 1438–1445.
22. Summerford, C., Bartlett, J. S., and Samulski, R. J. (1999) AlphaVbeta5 integrin: a co-receptor for adeno-associated virus type 2 infection. Nat Med **5**, 78–82.
23. Walters, R. W., Yi, S. M., Keshavjee, S., Brown, K. E., Welsh, M. J., Chiorini, J. A., and Zabner, J. (2001) Binding of adeno-associated virus type 5 to 2,3-linked sialic acid is required for gene transfer. J Biol Chem **276**, 20610–20616.
24. Qing, K., Mah, C., Hansen, J., Zhou, S., Dwarki, V., and Srivastava, A. (1999) Human fibroblast growth factor receptor 1 is a co-receptor for infection by adeno-associated virus 2. Nat Med **5**, 71–77.
25. Chen, S., Kapturczak, M., Loiler, S. A., Zolotukhin, S., Glushakova, O. Y., Madsen, K. M., Samulski, R. J., Hauswirth, W. W., Campbell-Thompson, M., Berns, K. I., Flotte, T. R., Atkinson, M. A., Tisher, C. C., and Agarwal, A. (2005) Efficient transduction of vascular endothelial cells with recombinant adeno-associated virus serotype 1 and 5 vectors. Hum Gene Ther **16**, 235–247.
26. Duan, D., Yue, Y., Yan, Z., Yang, J., and Engelhardt, J. F. (2000) Endosomal processing limits gene transfer to polarized airway epithelia by adeno-associated virus. J Clin Invest **105**, 1573–1587.
27. Sanlioglu, S., Benson, P. K., Yang, J., Atkinson, E. M., Reynolds, T., and Engelhardt, J. F. (2000) Endocytosis and nuclear trafficking of adeno-associated virus type 2 are controlled by rac1 and phosphatidylinositol-3 kinase activation. J Virol **74**, 9184–9196.
28. Yan, Z., Zak, R., Luxton, G. W., Ritchie, T. C., Bantel-Schaal, U., and Engelhardt, J. F. (2002) Ubiquitination of both adeno-associated virus type 2 and 5 capsid proteins affects the transduction efficiency of recombinant vectors. J Virol **76**, 2043–2053.
29. Yan, Z., Zak, R., Zhang, Y., Ding, W., Godwin, S., Munson, K., Peluso, R., and Engelhardt, J. F. (2004) Distinct classes of proteasome-modulating agents cooperatively augment recombinant adeno-associated virus type 2 and type 5-mediated transduction from the apical surfaces of human airway epithelia. J Virol **78**, 2863–74.
30. Weitzman, M. D., Fisher, K. J., and Wilson, J. M. (1996) Recruitment of wild-type and recombinant adeno-associated virus into adenovirus replication centers. J Virol 70, 1845–1854.
31. Qing, K., Wang, X. S., Kube, D. M., Ponnazhagan, S., Bajpai, A., and Srivastava, A. (1997) Role of tyrosine phosphorylation of a cellular protein in adeno- associated virus 2-mediated transgene expression. Proc Natl Acad Sci U S A 94, 10879–10884.
32. Qing, K., Hansen, J., Weigel-Kelley, K. A., Tan, M., Zhou, S., and Srivastava, A. (2001) Adeno-associated virus type 2-mediated gene transfer: role of cellular FKBP52 protein in transgene expression. J Virol **75**, 8968–8976.
33. Flotte, T. R., Afione, S. A., and Zeitlin, P. L. (1994) Adeno-associated virus vector gene expression occurs in nondividing cells in the absence of vector DNA integration. Am J Respir Cell Mol Biol **11**, 517–521.
34. Afione, S. A., Conrad, C. K., Kearns, W. G., Chunduru, S., Adams, R., Reynolds, T. C., Guggino, W. B., Cutting, G. R., Carter, B. J., and Flotte, T. R. (1996) In vivo model of adeno-associated virus vector persistence and rescue. J Virol **70**, 3235–3241.
35. Kearns, W. G., Afione, S. A., Fulmer, S. B., Pang, M. C., Erikson, D., Egan, M., Landrum, M. J., Flotte, T. R., and Cutting, G. R. (1996) Recombinant adeno-associated virus (AAV-CFTR) vectors do not integrate in a site-specific fashion in an immortalized epithelial cell line. Gene Ther **3**, 748–755.
36. Song, S., Laipis, P. J., Berns, K. I., and Flotte, T. R. (2001) Effect of DNA-dependent protein kinase on the molecular fate of the rAAV2 genome in skeletal muscle. Proceedings of the National Academy of Sciences USA **98**, 4084–4088.
37. Nakai, H., Yant, S. R., Storm, T. A., Fuess, S., Meuse, L., and Kay, M. A. (2001) Extrachromosomal recombinant adeno-associated virus vector genomes are primarily responsible for stable liver transduction in vivo. J Virol **75**, 6969–76.
38. Chen, Z. Y., Yant, S. R., He, C. Y., Meuse, L., Shen, S., and Kay, M. A. (2001) Linear DNAs concatemerize in vivo and result in sustained transgene expression in mouse liver. Mol Ther **3**, 403–410.
39. Song, S., Lu, Y., Choi, Y. K., Han, Y., Tang, Q., Zhao, G., Berns, K. I., and Flotte, T. R. (2004) DNA-dependent PK inhibits adeno-associated virus DNA integration. Proc Natl Acad Sci USA **101**, 2112–2116.

40. Duan, D., Yue, Y., and Engelhardt, J. F. (2003) Consequences of DNA-dependent protein kinase catalytic subunit deficiency on recombinant adeno-associated virus genome circularization and heterodimerization in muscle tissue. J Virol **77**, 4751–4759.
41. Yan, Z., Zhang, Y., Duan, D., and Engelhardt, J. F. (2000) Trans-splicing vectors expand the utility of adeno-associated virus for gene therapy. Proc Natl Acad Sci USA **97**, 6716–6721.
42. Moss, R. B., Rodman, D., Spencer, L. T., Aitken, M. L., Zeitlin, P. L., Waltz, D., Milla, C., Brody, A. S., Clancy, J. P., Ramsey, B., Hamblett, N., and Heald, A. E. (2004) Repeated adeno-associated virus serotype 2 aerosol-mediated cystic fibrosis transmembrane regulator gene transfer to the lungs of patients with cystic fibrosis: a multicenter, double-blind, placebo-controlled trial. Chest **125**, 509–521.
43. Beck, S. E., Jones, L. A., Chesnut, K., Walsh, S. M., Reynolds, T. C., Carter, B. J., Askin, F. B., Flotte, T. R., and Guggino, W. B. (1999) Repeated delivery of adeno-associated virus vectors to the rabbit airway. J Virol **73**, 9446–9455.
44. Halbert, C. L., Rutledge, E. A., Allen, J. M., Russell, D. W., and Miller, A. D. (2000) Repeat transduction in the mouse lung by using adeno-associated virus vectors with different serotypes. J Virol **74**, 1524–1532.
45. Brantly, M. L., Chulay, J. D., Wang, L., Mueller, C., Humphries, M., Spencer, L. T., Rouhani, F., Conlon, T. J., Calcedo, R., Betts, M. R., Spencer, C., Byrne, B. J., Wilson, J. M., and Flotte, T. R. (2009) Sustained transgene expression despite T lymphocyte responses in a clinical trial of rAAV1-AAT gene therapy. Proc Natl Acad Sci U S A **106**, 16363–16368.
46. Mingozzi, F., Maus, M. V., Hui, D. J., Sabatino, D. E., Murphy, S. L., Rasko, J. E., Ragni, M. V., Manno, C. S., Sommer, J., Jiang, H., Pierce, G. F., Ertl, H. C., and High, K. A. (2007) CD8(+) T-cell responses to adeno-associated virus capsid in humans. Nat Med **13**, 419–422.
47. Hernandez, Y. J., Wang, J., Kearns, W. G., Loiler, S., Poirier, A., and Flotte, T. R. (1999) Latent adeno-associated virus infection elicits humoral but not cell- mediated immune responses in a nonhuman primate model. J Virol **73**, 8549–8558.
48. Manno, C. S., Pierce, G. F., Arruda, V. R., Glader, B., Ragni, M., Rasko, J. J., Ozelo, M. C., Hoots, K., Blatt, P., Konkle, B., Dake, M., Kaye, R., Razavi, M., Zajko, A., Zehnder, J., Rustagi, P. K., Nakai, H., Chew, A., Leonard, D., Wright, J. F., Lessard, R. R., Sommer, J. M., Tigges, M., Sabatino, D., Luk, A., Jiang, H., Mingozzi, F., Couto, L., Ertl, H. C., High, K. A., and Kay, M. A. (2006) Successful transduction of liver in hemophilia by AAV-Factor IX and limitations imposed by the host immune response. Nat Med **12**, 342–347.
49. Hauswirth, W. W., Aleman, T. S., Kaushal, S., Cideciyan, A. V., Schwartz, S. B., Wang, L., Conlon, T. J., Boye, S. L., Flotte, T. R., Byrne, B. J., and Jacobson, S. G. (2008) Treatment of leber congenital amaurosis due to RPE65 mutations by ocular subretinal injection of adeno-associated virus gene vector: short-term results of a phase I trial. Hum Gene Ther **19**, 979–990.
50. Cideciyan, A. V., Aleman, T. S., Boye, S. L., Schwartz, S. B., Kaushal, S., Roman, A. J., Pang, J. J., Sumaroka, A., Windsor, E. A., Wilson, J. M., Flotte, T. R., Fishman, G. A., Heon, E., Stone, E. M., Byrne, B. J., Jacobson, S. G., and Hauswirth, W. W. (2008) Human gene therapy for RPE65 isomerase deficiency activates the retinoid cycle of vision but with slow rod kinetics. Proc Natl Acad Sci U S A **105**, 15112–15117.
51. Flotte, T. R., Fischer, A. C., Goetzmann, J., Mueller, C., Cebotaru, L., Yan, Z., Wang, L., Wilson, J. M., Guggino, W. B., and Engelhardt, J. F. (2009) Dual reporter comparative indexing of rAAV pseudotyped vectors in chimpanzee airway. Mol Ther **18**, 594–600.

Chapter 15

Biodistribution and Shedding of AAV Vectors

Caroline Le Guiner, Phillipe Moullier, and Valder R. Arruda

Abstract

Determining the AAV vector biodistribution and shedding is central for the safety assessment of proposed early-phase clinical trials. It is especially crucial in the case of AAV vectors since they are injected directly in situ with no possibility of an intermediate ex vivo step, such as in retroviral-mediated approaches. This sole administration mode, the high capsid diversity (natural and chimeric), the various routes of delivery (e.g., intramuscular, intravenous, intra-arterial, and intracranial) make biodistribution and shedding studies a major investigational field for several years ahead. Indeed, the ideal scenario whereby they become generic is less likely to occur as long as the engineered capsid, the therapeutic strategies (expression of cDNA versus oligonucleotides for exon skipping), and the mode of delivery continue to evolve quickly to clinical translational strategies.

An important aspect of biodistribution and shedding studies is that they practically should not be performed on a "research" mode but rather within the frame of the regulatory animal pharmacology and toxicology studies in order to directly implement the Investigational New Drug (IND) application. Yet, if biodistribution and shedding in animal models are explored at an early research stage, i.e., to investigate whether a given AAV serotype administered in a given way transduces certain immunocompetent cells (how does the vector distribute itself in the immune system and with what kinetic?), it is advisable to use an AAV vector manufactured and quality controlled similarly to what will be done ultimately at the clinical stage.

This chapter provides protocols and recommendations to study how an AAV vector distributes and sheds after administration. We discuss (1) the requirements for a rigorous methodology; (2) avoiding nucleic acid cross contamination; (3) systematically assessing the assay sensitivity, specificity, and reproducibility because milieus can be drastically different, i.e., feces versus urine; and (4) choosing the appropriate animal model(s) when anticipating the regulatory pharmacological/toxicological studies.

Key words: AAV vector, Biodistribution, Shedding, Germ line transmission, DNA extraction, PCR analysis, Infectious particles detection

Richard O. Snyder and Philippe Moullier (eds.), *Adeno-Associated Virus: Methods and Protocols*,
Methods in Molecular Biology, vol. 807, DOI 10.1007/978-1-61779-370-7_15, © Springer Science+Business Media, LLC 2011

1. Introduction

Shedding is defined as the dissemination of the AAV vector through secretions and/or excreta from the animal model or patient, whereas biodistribution relates to the spreading of the AAV vector within the animal model and the patient's body from the site of administration (1). The design of nonclinical studies to test the safety of biotechnology-derived pharmaceutical products is addressed in guidelines developed by the International Conference on Harmonisation (ICH) S6 (2, 3). Although gene therapy vectors are specifically excluded from the scope of ICH S6, it is commonly accepted that general principles described in these guidelines can be considered relevant to this product class.

One of the challenges in preclinical and clinical safety evaluation studies is the fact that biodistribution and shedding features of viral vectors have been evolving with the advent of newer gene therapy technologies that have resulted in vectors with higher titers, increased transduction efficiencies, and often broader tissue/organ tropism, adding to the existing concerns regarding the risk of germ line transmission.

The ICH on technical requirements for registration of pharmaceuticals for human use published a concept paper in July 2009 regarding general principles to address virus and vector shedding (1). This document provides recommendations for designing nonclinical and clinical shedding studies. For both situations, emphasis is put on the analytical assays used for detection, and considerations are given for the sampling profiles and schedules. The assessment of shedding can be utilized to estimate the likelihood of transmission of vectors to third parties, such as healthcare workers and family members. Although AAV vectors are designed and produced to avoid the presence of replication-competent virus in the therapeutic product, this topic remains important because: (1) gene therapy clinical research has become global and (2) AAV vectors are exclusively administered directly to patients. There are examples that demonstrate that viral vectors can be shed in patient excreta and in some cases, shedding occurs for extended periods of time (4). In addition, the recent finding that the AAV vector can persist for several years as intact particles in the subretinal space of dogs and nonhuman primates (5) raises the possibility of low levels of replication, which has never been formally excluded in vivo. An alternative explanation is the ability for AAV vector particles to resist clearance when aggregated in sheltered areas after local administration at high concentration in virtual spaces, i.e., subretinal space. In any case, in vivo persistence of AAV vectors – at least documented so far for certain serotypes (AAV2, AAV4, and AAV5) – expands the requirement for comprehensive shedding investigations. Surprisingly, the route of administration of the AAV vector does not appear to have

a significant impact on hematogenous shedding patterns both in large animal models and patients. Indeed, whether the AAV vector is injected via the hepatic artery (6), intramuscularly (7) or directly in the putamen (8), vector DNA can be detected for several weeks in the serum. One priority for the near future is to develop standardized practices especially in optimization of analytical methods used to detect shed vectors, i.e., sensitivity, specificity, addressing sample interference, and quality of samples. Quantitative assays are preferred as these will aid in quantifying the probability of transmission to third parties and the potential risk to the environment. Assessment of interference from the biological sample matrix is important and it might be appropriate to dilute the sample prior to analysis to avoid extensive interference (9). The quantification of AAV vector of single-stranded or self-complementary genomes may differ in terms of the assay used (10).

PCR and infectivity are the two assays used for the detection of shed vector. Use of quantitative polymerase chain reaction (Q-PCR) is recommended despite its inability to distinguish between intact virion and noninfectious or degraded AAV. If the infectivity assay is the only way to test the potential for transmission, the sensitivity of the test article is usually low for several reasons, such as the lack of a highly permissive in vivo cell line transduction for a given AAV serotype, the interference mediated by the milieu, i.e., urine, the usual high physical particle versus infectious particle ratio. A general rule is that if the amount of AAV vector detected by Q-PCR is below the limit of detection of the infectivity assay, one might not choose to further characterize the shed AAV vector by infectivity assays due to the constraints of assay sensitivity.

The ICH Steering Committee in November 2006 provided a concept paper regarding the risk of inadvertent germ line integration of gene therapy vectors (11). This document stresses the requirement to have biodistribution studies conducted with the product that is intended for use in clinical trials. Tissue distribution studies of the AAV vector identify tissue/organ systems in addition to the desired target site, where the vector might concentrate and are thus useful for the identification of potential target organs of toxicity. In vivo distribution of an AAV vector includes analyses of gonads (testes or ovaries) because detection of the vector in gonad tissue indicates the potential for germ line integration and propagation to the descendants. Using an assay for nucleic acid sequences is appropriate for the detection of vector dissemination. It is also recommended that testing for the presence of vector sequences be done by at least one sensitive assay, such as (Q-PCR). An important aspect provided in ICH is that previous biodistribution studies of the vector containing other transgenes could be used to support early phase clinical development. An important aspect of biodistribution studies is organ sampling (12) and it is described below.

This paper identifies general principles for monitoring biodistribution and shedding of AAV vectors as well as a special emphasis addressing inadvertent germ line transmission.

The risk of germ line transmission of vector sequences in humans is a major safety concern, since the enrollment of subjects of reproductive age in early-phase clinical trials of gene transfer continues to increase. Intramuscular injection of AAV2 vector was not associated with vector shedding to the semen of experimental animals or adult men with hemophilia B (13, 14). However, the delivery of AAV2 to the liver via the hepatic artery resulted in unexpected transient vector dissemination to the semen that eventually disappears in all patients (6). In rabbit models, intravenous injection of AAV2, AAV5, AAV6, or AAV8 demonstrated dose-dependent and time-dependent vector dissemination to the semen (15–17). Interestingly, the kinetics of clearance was remarkably faster for AAV-5 (3–5 weeks) compared to the other serotypes AAV (10–13 weeks) (17). No late recurrence of AAV vector sequences was found in semen samples collected over hundred of consecutive cycles of spermatogenesis of rabbits, a similar found observed in humans. The frequency of renewal of the ejaculate also influences the kinetics of vector clearance from the semen (16). Moreover, AAV2 or AAV8 sequences were detected in the semen of vasectomized animals that lack germ cells (15). Therefore, structures of the genitourinary tract, as well as the testis, contribute significantly to vector shedding in the semen, and this risk is also dependent on the route of vector administration.

2. Materials

2.1. Tissue Sampling

- Disposable or sterile DNA-free sets of materials and containers.
- Phosphate-buffered saline.
- Cryovial tubes.
- Liquid nitrogen.

2.2. Fluid and Feces Sampling

- 15 mL tubes.
- 1.5 mL tubes.
- Swabs.
- Urinary catheter.
- 0.22 μm filters.
- DMEM medium supplemented with 10% heat-inactivated fetal calf serum and 1% penicillin/streptomycin.

2.3. Collection and Fractionation of Semen Specimens

- Sterile plastic specimen container.

2.4. Purification of Motile Sperm, Seminal Fluid, and Seminal Fluid Cells

- 15 mL tubes.
- Sterile transfer pipettes.
- Centrifuge.
- PureSperm (Nidacon International AB, Gothemberg, Sweden).
- Enhance WG wash media (Nicadon International AB).

2.5. DNA Extraction from Tissue Samples

- Plastic pipettes, micropipettes, and sterile pipette tips.
- Microcentrifuge.
- Petri dishes.
- Balance.
- Nanospectrophotometer.
- Sterile scalpel blades.
- 1.5 mL tubes.
- Oven or water bath at 56 °C and at 37 °C.
- Dry ice.
- Wet ice.
- Gentra® Puregene® kit (Qiagen).
- Proteinase K at 10 mg/mL.
- Isopropanol.
- 70% ethanol.
- Glycogen at 20 mg/mL.

2.6. DNA Extraction from Fluid and Feces Samples

- Plastic pipettes, micropipettes, and sterile pipette tips.
- Microcentrifuge.
- Vortex.
- 1.5 mL tubes.
- QIAamp RNA viral mini kit (Qiagen).
- 100% ethanol.

2.7. DNA Extraction from Semen Specimen

- Plastic pipettes, micropipettes, and sterile pipette tips.
- Pasteur pipettes.
- Centrifuge.
- Nanospectrophotometer.
- 15 mL tubes.
- 1.5 mL tubes.
- Oven or water bath at 55 °C.

- Gentra® Puregene® kit (Qiagen).
- 1 M dithiothreitol.
- Proteinase K at 14.4 mg/mL.
- Isopropanol.
- 70% ethanol.

2.8. PCR +/– Southern-Blot Analysis

- Plastic pipettes, micropipettes and sterile pipette tips.
- Plasmid DNA purification kit.
- 1.5 mL tubes.
- 50 mL tubes.
- PCR tubes or plates.
- Hybridization tube.
- Microcentrifuge.
- Vortex.
- Nanospectrophotometer.
- ABI Prism 7900 HT Sequence Detection System or other equivalent instrument.
- Oven or water bath at 37 °C.
- Hybridization oven at 55 °C.
- Boiling water bath.
- Electrophoresis system.
- UV Imager.
- Vacuum apparatus for Southern blot.
- Autoradiography films and cassette, and development system.
- Nylon positively charged membrane.
- Wet ice.
- Restriction enzymes.
- PCR primers.
- PCR mix and enzyme.
- Agarose.
- Ethidium bromide.
- Sterile water.
- 0.4 N NaOH.
- 2× SSC.
- Alkphos® labeling and detection kits (GE Healthcare).
- Glycerol.
- *Hybridization buffer*: Hybridization buffer (Alkphos® kit) + 0.5 M NaCl + 4% (w/v) Blocking reagent (Alkphos® kit).

- *Primary wash buffer*: 2 M Urea + 0.1% (w/v) SDS + 50 mM Na phosphate pH 7.0 + 150 mM NaCl + 1 mM $MgCl_2$ + 0.2% (w/v) Blocking reagent (Alkphos® kit).
- *Secondary wash buffer (20× stock)*: 1 M Tris base + 2 M NaCl.
- *Secondary wash buffer (working solution)*: 1/20 dilution of the stock + 2 mM $MgCl_2$.

2.9. Q-PCR Analysis

- Plastic pipettes, micropipettes and sterile pipette tips.
- Plasmid DNA purification kit.
- 1.5 mL tubes.
- PCR tubes or plates.
- Microcentrifuge.
- Vortex.
- Nanospectrophotometer.
- Applied Biosystem StepOne Plus® Real-Time PCR system or other equivalent instrument.
- Electrophoresis system.
- UV imager.
- Wet ice.
- Restriction enzymes.
- PCR primers.
- Taqman® probe.
- Q-PCR mix and enzyme.
- Sterile water.

2.10. Detection of AAV Infectious Particles from Fluid and Feces Samples

- Plastic pipettes, micropipettes and sterile pipette tips.
- Sterile culture plates.
- 1.5 mL tubes.
- 50 mL tubes.
- Hybridization tube.
- Microcentrifuge.
- Vortex.
- Nanospectrophotometer.
- Oven or water bath at 37 °C.
- Hybridization oven at 55 °C.
- Boiling water bath.
- Autoradiography films and cassette, and development system.
- Nylon positively charged membrane.
- Wet ice.

- HeLaRC32 cells (ATCC CRL-2972™).
- Adenovirus type 5.
- DMEM medium supplemented with 10% heat inactivated fetal calf serum and 1% penicillin/streptomycin.
- Trypsine.
- Sterile water.
- 0.5 M NaOH, 1.5 M NaCl.
- 1 M Tris–HCl pH 7.0, 2× SSC.
- Alkphos® labeling and detection kits (GE Healthcare).
- Glycerol.
- *Hybridization buffer*: Hybridization buffer (Alkphos® kit) + 0.5 M NaCl + 4% (w/v) Blocking reagent (Alkphos® kit).
- *Primary wash buffer*: 2 M urea + 0.1% (w/v) SDS + 50 mM Na phosphate pH 7.0 + 150 mM NaCl + 1 mM $MgCl_2$ + 0.2% (w/v) Blocking reagent (Alkphos® kit).
- *Secondary wash buffer (20× stock)*: 1 M Tris base + 2 M NaCl.
- *Secondary wash buffer (working solution)*: 1/20 dilution of the stock + 2 mM $MgCl_2$.

2.11. Detection of AAV Infectious Particles in the Semen

- Plastic pipettes, micropipettes and sterile pipette tips.
- Sterile culture plates.
- 1.5 mL tubes.
- PCR tubes or plates.
- Microcentrifuge.
- Vortex.
- Nanospectrophotometer.
- Applied Biosystem StepOne Plus Real-Time PCR system or other equivalent instrument.
- Oven or water bath at 37 °C.
- HeLaRC32 cells (ATCC CRL-2972™).
- Adenovirus type 5.
- DMEM medium supplemented with 10% heat inactivated fetal calf serum and 1% penicillin/streptomycin.
- Trypsine.
- Sterile water.
- DNA isolation kit.
- PCR primers.
- Q-PCR mix and enzyme.

3. Methods

3.1. Tissue Sampling

Tissue sampling must be performed using disposable or sterile DNA-free sets of material and containers to minimize cross contamination. The order of organ sampling is also critical. The injected targeted organ need to be harvested at the end of the procedure, while the organs that are less likely to contain vector DNA, i.e., gonads, need to be sampled at the beginning of the procedure. Since the liver is a powerful "filter" due to the large liver endothelial cell gaps permissible to small and large viral vectors often resulting in significant transduction, it should be among the last organs sampled even if the AAV vector has been administered at a distant site (7). Perfusion or washing the organs (with phosphate-buffered saline), when feasible, reduces contamination with transduced circulating blood cells especially peripheral blood mononuclear cells (PBMC) (6, 7, 9). After sampling, each organ must be sliced in small fragments using disposable stainless steel blades that must be changed often and at least between different organs. Tissue samples are distributed in several tubes and immediately frozen in liquid nitrogen. After that, tissue samplings are kept at −80 °C in a monitored freezer and physically separated from other samples originating from other studies to avoid cross contamination (tubes, nucleic acids, etc.).

3.2. Fluid and Feces Sampling

3.2.1. Saliva, Lacrimal and Nasal Fluids

1. Collect saliva, lacrimal and nasal fluids using a swab.
2. Immediately place the swab in a 15 mL conical tube-containing 2 mL of DMEM medium supplemented with 10% heat inactivated fetal calf serum and 1% penicillin/streptomycin. Mix by gentle agitation.
3. Aliquot the supernatant and freeze at −80 °C.

3.2.2. Urine

1. Collect the urine either using a sterile condition or urethral catheter is clinically indicated for female subjects (see Note 1). Avoid collecting urine indirectly on the ground of the cage unless the recipient is maintained as "clean" as possible.
2. If the urine is collected indirectly, filter it through a 0.22 μm disposable filter.
3. Aliquot the urine and freeze at −80 °C.

3.2.3. Feces

1. Collect the feces in the cage of the animal.
2. Place it in a 15 mL conical tube containing 2 mL of DMEM medium supplemented with 10% heat inactivated fetal calf serum and 1% penicillin/streptomycin. Mix by gentle agitation.
3. Aliquot the supernatant and freeze at −80 °C.

3.3. Collection and Fractionation of Semen Specimens

1. Collect semen sample by masturbation after 5 days of sexual abstinence (see Note 2). Collect the sample in a sterile plastic specimen container.
2. Freeze the sample at –80 °C or keep it at room temperature if further semen fractionation is required.
3. Examine the samples (minimum of 10 μL) by routine analysis according to World Health Organization standards.
4. If necessary (see Note 3), fractionate the total semen sample upon receipt (minimum volume of 1 mL): allow liquefying for 15–30 min at room temperature. If liquefaction is not complete after this time, allow sample to set for an additional 30 min.

3.4. Purification of Motile Sperm, Seminal Fluid, and Seminal Fluid Cells

1. Aliquot 1 mL of prepared PureSperm (Nidacon International AB-90% Gradient: 900 μL PureSperm and 100 μL Enhance WG wash media) into a 15 mL conical tube.
2. Layer 1 mL of semen onto the PureSperm gradient: using a sterile transfer pipette, gently place semen over the PureSperm layer, being careful not to cause any mixing. Centrifuge for 20 min at 500 × *g*.
3. Remove the top layer of seminal fluid and cells to a new 15 mL conical tube. Remove the PureSperm layer from above the motile sperm pellet and discard, being careful not to disturb the pellet. Transfer the motile sperm pellet to a new 15 mL conical tube to obtain the motile sperm fraction. (Note if there is no pellet after centrifugation only total semen will be analyzed.)
4. Add 2 mL Enhance WG Wash Media to the motile sperm pellet and centrifuge the motile sperm at 400 × *g* for 5 min. Repeat this procedure for total of 3–4 washes to obtain the "motile sperm fraction".
5. Centrifuge the total seminal fluid at 400 × *g* for 5 min. Transfer the upper fluid layer that is the "seminal fluid fraction" to a new 15 mL conical tube and add 1–2 mL Enhance WG Wash Media to the seminal fluid cell pellet. Centrifuge the seminal fluid cells at 400 × *g* for 5 min. This procedure should be repeated at least two times to obtained the final "seminal fluid cells fraction". Freeze at –80 °C.
6. Save the seminal fluid, which will contain few if any cells and freeze at –80 °C.

3.5. DNA Extraction from Tissue Samples (see Note 4)

1. Place a small 50–150 mg fragment of tissue in a Petri dish standing on dry ice.
2. Using sterile scalpel blades grind the tissue in small fragments and transfer them in a 1.5 mL tube.
3. Add 300 μL of Cell Lysis Solution (Gentra® Puregene®) and 30 μL of proteinase K at 10 mg/mL, and incubate at 56 °C

under rotation for 1 h to overnight, until the tissue is completely lysed.

4. Allow the sample to stand for about 1 min at room temperature and add 1.5 μL of RNAse A Solution (Gentra® Puregene®). Mix the sample by inverting the tube back and forth and incubate at 37 °C for 15 min.
5. Incubate for 1 min on ice to quickly cool the sample and add 100 μL of Protein Precipitation Solution (Gentra® Puregene®). Mix the sample by repeated pipetting and centrifuge for 3 min at 16,000 × *g*.
6. Collect the supernatant containing the DNA, leaving behind the precipitated protein pellet, and transfer it into a clean 1.5 mL tube. Add 1 μL of glycogen at 20 mg/mL and 300 μL of isopropanol to precipitate the DNA. Mix the sample by inverting the tube back and forth at least 20 times and centrifuge for 3 min at 16,000 × *g*.
7. Carefully discard the supernatant, taking care that the pellet remains in the tube. Wash the pellet with 300 μL of 70% ethanol and centrifuge it again for 3 min at 16,000 × *g*.
8. Carefully discard the supernatant, taking care that the pellet remains in the tube, and air-dry the pellet.
9. Add 20–100 μL of DNA Hydratation Solution, depending on the size of the pellet. Incubate 5 min at room temperature and resuspend the DNA by repeated gentle pipetting.
10. Incubate the DNA overnight at 4 °C, gently pipetting it again and determine its concentration using a nanospectrophotometer. For long-term storage, keep the DNA at –20 °C.

3.6. DNA Extraction from Fluid and Feces Samples (see Note 5)

1. Into a 1.5 mL tube, mix 560 μL of Buffer AVL (QIAamp viral RNA mini kit) containing 0.56 μL of carrier RNA (QIAamp viral RNA kit) and 140 μL of the fluid or feces sample. Vortex the mix during 15 s and incubate at room temperature during 10 min.
2. Briefly centrifuge the tube to remove drops from the inside of the lid and add 560 μL of 100% ethanol. Vortex the mix during 15 s and briefly centrifuge the tube to remove drops from the inside of the lid.
3. Apply 630 μL of the mix to a QIAamp mini column (QIAamp viral RNA mini kit), put on a 2 mL tube. Centrifuge at 6,000 × *g* for 1 min.
4. Place the column into a clean 2 mL tube and add the rest of the mix (630 μL) to the column. Centrifuge at 6,000 × *g* for 1 min.

5. Place the column into a clean 2 mL tube and add 500 µL of Buffer AW1 (QIAamp viral RNA mini kit) to the column. Centrifuge at 6,000 × *g* for 1 min.
6. Place the column into a clean 2 mL tube and add 500 µL of Buffer AW2 (QIAamp viral RNA mini kit) to the column. Centrifuge at 20,000 × *g* for 3 min.
7. Place the column into a clean 2 mL tube and centrifuge again at 20,000 × *g* for 1 min to eliminate all the Buffer AW2.
8. Place the column into a clean 1.5 mL tube and add 40 µL of Buffer AVE (QIAamp viral RNA mini kit). Incubate 1 min at room temperature and centrifuge at 6,000 × *g* for 1 min.
9. To increase the elution yield, add again 40 µL of Buffer AVE, incubate 1 min at room temperature and centrifuge at 6,000 × *g* for 1 min.
10. Store the DNA at –20 °C.

3.7. DNA Extraction from Semen Specimens

1. Incubate 500 µL of the semen specimen with 3 mL Cell Lysis Solution (Gentra® Puregene®) and add 120 µL of a 1 M dithiothreitol solution to the sample and 20 µL Proteinase K (14.4 mg/ml). Incubate at 55 °C for 1 h to overnight, until cells have completely lysed.
2. Add 1 mL Protein Precipitation Solution (Gentra® Puregene®) and vortex the sample vigorously at a high speed. Centrifuge at maximum speed for 10 min.
3. Pour the supernatant containing the DNA (or upper phase), leaving behind the precipitated protein pellet, into a 15 mL centrifuge tube containing 3 mL isopropanol to precipitate the DNA. Using a Pasteur pipette, transfer the DNA to a microcentrifuge tube for 1 min. Wash the pellet with 500 µL of 70% ethanol, and centrifuge it again for 1 min. Remove the supernatant and air-dry the pellet.
4. Add 100 µL of warmed AE buffer (Gentra® Puregene®) and shake the sample overnight to dissolve the pellet. Obtain an OD reading using Nanospectrophotometer to determine its concentration. Record this number on the extraction worksheet and the requisition form (see Note 6).

3.8. PCR +/– Southern-Blot Analysis

For the preparation of the internal control, we favor the use of linearized DNA, as supercoiled DNA can interfere with PCR efficiency.

3.8.1. Preparation of DNA Plasmid for Internal Control

1. Linearize 15 µg of a DNA plasmid containing one copy of the sequence to analyze, and purify the digestion product using a plasmid DNA purification kit.
2. Measure the concentration of the linearized DNA, using a nanospectrophotometer.

3. Prepare a dilution at 10^{11} copies of plasmid in a final volume of 5 µL. The weight of one copy of the plasmid is calculated using the following formula:

$$\text{Weight of one copy of the plasmid} = \frac{\text{weight of 1bp(g/mol)} \times \text{size of the plasmid (bp)}}{\text{Avogadro's number(molecules/mol)}} = \frac{660 \times \text{size of the plasmid (bp)}}{6,022^{E}23}.$$

4. Confirm the concentration of this dilution, using a nanospectrophotometer. If necessary, adjust it to precisely obtain 10^{11} copies of plasmid in a final volume of 5 µL. Kept this stock solution at –20 °C, and use it for further preparation of plasmid ranges. Just ensure that its concentration remains stable, by regular checking on a nanospectrophotometer.
5. Prepare serial dilutions of this DNA plasmid to finally obtain a range from 10^8 or 10^5 copies to 0.01 copy of transgene in a final volume of 5 µL. Aliquot these dilutions and keep them at –20 °C for 1 month max.

3.8.2. Design of the PCR Assay

- A PCR assay specific for AAV vector can be used for screening samples for the presence of vector DNA. The desired sensitivity is ≤100 copies per reaction in the presence of 100–750 ng of DNA (see Note 7), or in the presence of 10 µL of extraction product from fluid or feces samples. In order to enhance the sensitivity of vector genomes detection, PCR amplicons can be further processed by Southern blot. The sensitivity can then increased to 0.1 copy.
- PCR primers for AAV-specific sequences are based on the design of a forward primer and a reverse primer located specifically in the vector genome. Avoid primer sequences that could match with endogenous sequences, as it could interfere with the efficiency and specificity of the reaction (see Note 8).
- To evaluate the sensitivity of the assay, run the analysis on serial dilutions of a DNA plasmid containing the sequence to be amplified. Test a plasmid range from 10^5 copies to 0.1 copy of transgene, spiked in water, or in 100–750 ng of DNA extracted from a noninjected subject, or in 10 µL of extraction product from fluid or feces from a noninjected subject (or prior AAV vector administration). As PCR inhibition by DNA can differ between tissues and fluid samples, perform this analysis for each type of DNA.
- To validate the specificity of the assay and exclude false positive results, run also the analysis on the tissue or fluid DNA alone.
- To validate the quality of DNA and extraction, exclude false negative results if the control experiment shows no PCR product, run also a PCR specific for an endogenous gene (see Note 9). Indeed, the tissue samples contain several

components that may inhibit the PCR reaction, and therefore the internal control experiment is required. As no DNA can be dosed in the extraction product from fluids or feces samples, no PCR specific for an endogenous gene will be run on these samples.

- Analysis of the PCR results is done by migration of the amplicons (entire or half PCR reaction volume) on an agarose gel and visualization by ethidium bromide staining (see Note 10).
- The overall strategy for semen samples is given in Note 11.
- If necessary (low detection level), the samples can be further processed by Southern blot.

3.8.3. Southern Blot: Transfer of the PCR Amplicons on a Membrane

1. After migration on an agarose gel, transfer the PCR amplicons under alkaline conditions (NaOH 0.4 N) on a nylon positively charged membrane, during 2 h if the transfer is done using a vacuum apparatus, or during one night if the transfer is done by capillarity.
2. Rinse the membrane with 2× SSC and store it at 4 °C until hybridization.

3.8.4. Southern Blot: Probe Labeling, Hybridization, and Revelation

Usually, a nonradioactive probe can be used for such Southern blot. An example of probe labeling, hybridization, and revelation using the AlkPhos® system from GE Healthcare is given below.

1. Using a PCR amplification or enzymatic digestion, prepare a DNA probe, specific for the vector genome. Purify this DNA probe, and adjust its concentration to 10 ng/μL.
2. Denature 10 μL of this DNA probe by heating for 5 min in a boiling water bath, and immediately cool it on ice for 5 min. Spin briefly in a microcentrifuge to collect the contents at the bottom of the tube.
3. Dilute 2 μL of cross-linker solution (AlkPhos® kit) with 8 μL of water.
4. On ice, add 10 μL of reaction buffer (AlkPhos® kit), 2 μL of labeling reagent (AlkPhos® kit) and 10 μL of the diluted cross-linker to the denatured DNA probe. Mix by vortexing and spin briefly in a microcentrifuge to collect the contents at the bottom of the tube.
5. Incubate at 37 °C for 30 min. The probe can be used immediately or kept on ice for up to 2 h. For long-term storage, store it at –20 °C in 50% (v/v) glycerol.
6. Preheat the required volume (0.25 mL/cm^2 of membrane) of AlkPhos® hybridization buffer to 55 °C.
7. Place the membrane to hybridized into the hybridization buffer (in a hybridization glass tube) and prehybridize for at least 15 min at 55 °C under agitation in a hybridization oven.

8. Add the labeled probe to the hybridization buffer (typically half of a probe for 30 mL of hybridization buffer). Hybridize at 55 °C overnight under agitation in a hybridization oven.
9. Preheat the required volume (2–5 mL/cm² of membrane) of primary wash buffer (AlkPhos® kit) to 55 °C.
10. Discard the hybridization solution and replace it by the primary wash buffer. Wash for 10 min at 55 °C under agitation in a hybridization oven.
11. Perform an additional wash in primary wash buffer at 55 °C for 10 min.
12. Discard the wash buffer and replace it by the secondary wash buffer (2–5 mL/cm² of membrane). Wash for 5 min at room temperature, under agitation.
13. Perform an additional wash in secondary wash buffer at room temperature for 5 min.
14. Remove the membrane of the hybridization tube and drain the excess of the secondary wash buffer.
15. With the sample side of the membrane up (inward), add 30–40 μL of detection reagent (AlkPhos® kit)/cm² of membrane, and incubate at room temperature for 5 min.
16. Expose the membrane to an autoradiography film.

A typical example of results obtained after PCR and Southern-blot analysis of DNA from tissues of AAV8-injected mice is presented in Fig. 1.

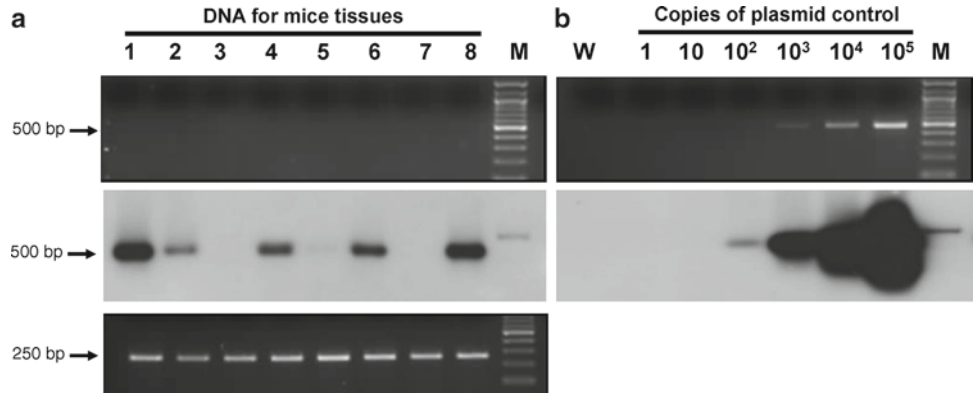

Fig. 1. Detection of AAV8 sequences in DNA from mice tissues 15 days post-intramuscular injection. DNA was extracted from each tissue at the time of the sacrifice of the animals. (**a**) The 500 bp fragment corresponds to vector amplicons. PCR products were separated on an agarose gel (*upper panel*), and then transferred to a nylon membrane and hybridized with a vector-specific probe (*middle panel*). Each sample was also subjected to amplification of a 250 bp hypoxanthine-guanine phosphoribosyl transferase endogenous DNA fragment (*lower panel*). (**b**) Amplification from different dilutions of a DNA control plasmid. *Upper panel* corresponds to PCR products and *lower panel* corresponds to the same PCR products hybridized with the vector-specific probe. Note that the sensitivity of the assay is higher after Southern blot. *M* molecular weight, *W* water.

3.9. Q-PCR Analysis (see Note 12)

Vector DNA copy numbers are determined using primers and probe designed to amplify and match: (1) the vector genome and (2) an endogenous gene. For each sample, Ct values are compared to those obtained with different dilutions of standard plasmids (containing either the vector genome, either the endogenous gene). Final results are expressed in vector genome per diploid genome (vg/dg).

3.9.1. General Considerations for Q-PCR Analysis of Tissue or Semen Samples

- Depending on the amplified sequences, the sensitivity of such assay is often between 0.001 and 0.05 vg/dg.
- When designing primers and probe(s), avoid sequences that could match with endogenous sequences, as it could interfere with the efficiency and specificity of the reaction.
- Perform Q-PCR analysis using 10–500 ng of tissue or semen DNA.

3.9.2. General Considerations for Q-PCR Analysis of Fluid or Feces Samples

- As no DNA can be dosed in the extraction product from fluids or feces samples, no PCR specific for an endogenous gene will be run. Express the final results in vg/mL of fluid or feces sample.
- Perform Q-PCR analysis using 10 μL of the extraction product.

3.9.3. Design and Validation of the Q-PCR Assay

- Run all samples in triplicate.
- Prepare linearized DNA plasmid control dilutions as described above for PCR analysis. The analysis by Q-PCR of triplicates of these serial dilutions of DNA plasmid control will allow the generation of a standard curve (Ct values correlated to the copy number of vector genomes).
- To be reliable, the linearity of the standard curve has to be checked ($r^2 \geq 0.99$).
- To be robust, the efficiency of the amplification reaction has to be between 95 and 105%. If this criterion is not reached in the first experiments, adjust the conditions of the reaction (amplification conditions, primers and/or probe concentrations).
- The sensitivity of each Q-PCR will be defined by the lower copy number for which Ct value is above the background of the reaction.
- As PCR inhibition can occur in tissue, semen, fluid, or feces DNA, the sensitivity of the assay has to be determined by analyzing serial dilutions of DNA plasmid control in water or in an noninjected sample DNA. Ten to five hundred nanogram of tissue or semen DNA, or 10 μL or fluid or feces extract, can be evaluated. Same sensitivity, same efficiency and same Ct values of plasmid dilutions in the presence or absence of a noninjected sample DNA confirm the absence of Q-PCR inhibition on the experimental conditions. As PCR inhibition by DNA can differ between samples, perform this analysis for each type of sample DNA.

- To validate the specificity of the assay and exclude false positive results, run the Q-PCR analysis on each noninjected sample DNA alone, and against water alone.

3.10. Detection of AAV Infectious Particles from Fluid and Feces Samples

To determine whether the physical presence of AAV sequences correlates with infectious activity, a replication center assay reported earlier (18) was adapted for fluid or feces samples.

1. Collect fluid or feces samples before and at different timings post-AAV administration.
2. Add adenovirus type 5 at an MOI of 200 in the culture medium of 10^6 subconfluent HeLaRC32 cells (ATCC # CRL-2972™), an AAV2 Rep/Cap-expressing cells.
3. After 2 h, add 200 µL of fluid or feces sample.
4. After 48 h, trypsin the cells and wash them with phosphate-buffered saline. Filter them through a nylon positively charged.
5. Soak the filters in 0.5 M NaOH, 1.5 M NaCl for 5 min, and then neutralize in a 1 M Tris–HCl pH 7.0, 2× SSC solution.
6. Hybridize the filters overnight to a fluorescein-labeled probe corresponding to the transgene included in the rAAV vector, and process the filters as described above for Southern-blot analysis, and expose them to an autoradiography film.

The sensitivity of the assay is determined by mixing fluid or feces sample collected before injection (or collected in a noninjected subject) in culture medium with serial dilution of the rAAV vector (ranging from 0 to 5^E6 vg). The sensitivity of the assay is usually about 500 infectious particles/mL of fluid sample.

3.11. Detection of AAV Infectious Particles in the Semen

To determine whether the physical presence of AAV sequences correlates with infectious activity, a replication center assay reported earlier (19) was adapted for semen testing.

1. Collect semen samples before and at days 4, 7, and 14 post-AAV administration.
2. Mix 100 µL of semen in the culture medium of an HeLa-derived AAV2 Rep/Cap-expressing cell line grown in 96-well plates in the presence of adenovirus serotype 5 (100 particles per cell).
3. Harvest the cells after 48 h and extract DNA.
4. Determine the replication of AAV in each well by Q-PCR with primers and probes specific for the transgene.

The sensitivity of the assay is determined by mixing semen sample from an untreated human subject in culture medium with serial dilution of AAV2 (ranging from 0 to 5^E6 vg). The sensitivity of the assay is usually about 100–500 infectious particles/well.

4. Notes

1. Weekly urethral catheterization is likely to be rejected for both men and women and in the former the risk of infection is even higher.
2. Sperm constitutes only 5% of the ejaculate, whereas 60–75% of the semen is produced in the seminal vesicles and 20% produced in the prostate gland and bulbourethral and urethral glands (20). Moreover, cells other than germ cells are commonly found in semen and include epithelial cells, white blood cells, and occasionally uncharacterized cells. Semen samples collected by masturbation after 5 days of sexual abstinence ensure that sperm count, motility, and viability are maximized in the analyzed samples.
3. The goal is to fractionate the total semen samples of subjects who have undergone a gene transfer procedure into motile sperm, nonmotile sperm, and seminal fluid factors (16). Samples containing urine, gel, and other contaminants should not be fractionated and only the total semen fraction tested. The purpose of this procedure is to collect a motile sperm fraction that is free of contamination by other cellular or fluid elements of semen. DNA is extracted from this motile sperm fraction for analysis in a sensitive PCR assay. Therefore, extreme care must be taken to avoid contamination of the motile sperm fraction.
4. For DNA extraction from tissue samples of AAV-injected subjects, we exclude kits that rely on columns or resins because we are concerned about competition between genomic DNA and AAV episomes (21) at the binding step. We validated efficient extraction of AAV genomes using the Gentra® Puregene® kit from Qiagen (22).
5. The goal of DNA extraction from fluid and feces samples is to analyze the presence of AAV genomes (in intact, noninfectious, or degraded virions). We validated efficient extraction of virions using the QIAamp viral RNA mini kit from Qiagen. However, depending on the fluid sample, the extraction yield can vary from 10 to 100% (C. Le Guiner et al., unpublished data). Therefore, we advise to always perform a validation of the extraction protocol by: (1) spiking different dilutions of AAV vector stock in the fluid sample of interest, (2) doing the extraction, and (3) analyzing the recovery of the spiked vector in the final extraction product.
6. It is important to certify that cells other than germ cells are present or not in the final sample to confirm the purity of the motile sperm fraction.

7. In optimized PCR assays, vector DNA sequences are detected as few as one (13, 16) or eight copies per $3^{E}5$ haploid genomes (15) for AAV2 and AAV8, respectively. The sensitivity of these assays allow the detection of vector sequences below the rates of endogenous mutation that arise from retrotransposon elements in the human genome, which occurs at rates of 1 in 100 sperm cells (23) or even more frequent (24).
8. PCR primers for AAV-specific sequences can be based on the design of a forward primer located at the promoter/enhancer region and a reverse primer in an intronic region of the cassette containing the therapeutic gene.
9. To validate the sample extraction and PCR efficiencies, spiked controls can also be carried out using a template that results in a shorter or longer amplicon than AAV vector under the same PCR conditions.
10. An example of semen samples is presented on Fig. 2. This PCR protocol resulted in PCR product of 647 bp. An internal control experiment consisted of a deleted plasmid derived from the AAV template that results in PCR product of 550 bp (Fig. 2). All samples are tested in triplicate or quadruplicate. In addition, one well is spiked with 100 copies of vector and another one with ten copies of the vector containing 1 μg of DNA. A control with water alone is also analyzed. The optimal PCR conditions for these experiments were 50 °C (2 min, one cycle), 95 °C (10 min, one cycle), 95 °C (15 s, 50 cycles), and 60 °C (1 min). PCR products are separated by agarose gel electrophoresis and visualized by ethidium bromide staining. In Fig. 2, the deleted plasmid is derived from the original AAV-hF.IX16 but has a deletion of 97 bp, yielding an amplicon of 550 bp, which could be easily distinguished from vector-derived sequences of 647 bp.
11. Overall strategy for semen analysis: All specimens other than semen fractions containing motile or nonmotile sperm are

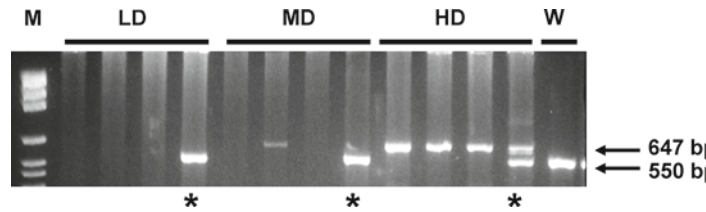

Fig. 2. Detection of AAV2 sequences in DNA from total semen from rabbits following 1-week post-intravenous injection. AAV2 was delivered at dose doses of $1^{E}11$ vg/kg (low dose *LD*), $1^{E}12$ vg/kg (mid dose *MD*), or $1^{E}13$ vg/kg (high-dose *HD*). PCR analysis for AAV sequences resulted in a fragment of 647 bp (AAV-FIX16). *Asterisk* denotes PCR assay in which ten copies of the 97-deleted control phFIX16 was spiked into the test sample. *M* molecular weight, *W* water.

tested with the spiked and the unspiked master mix, one reaction for each master mix containing 10 µL seminal fluid DNA per reaction. Controls are one 100 copies spiked reaction without DNA, one 10 copies spiked reaction without DNA, and one water control. For semen specimens, run 4–6 unspiked reactions with 500 ng DNA per reaction, one 100 copies spiked reaction with 500 ng DNA, one 10 copies spiked reaction with 500 ng DNA, one 100 copies spiked reaction without DNA, one 10 copies spiked reaction without DNA, and one water control. If the amount of DNA for a semen specimen is low, reduce the number of unspiked reactions to 2 or 1, and request a repeat specimen, or extract the remainder of the specimen, if there is more. If there is not sufficient DNA for one spiked and one unspiked reaction, or if the DNA concentration is not high enough to use 500 ng of DNA per reaction, the test will not appropriate. The copy quantity of the 10 and 100 copies determined from the standard curve are reported for each semen fraction in order to validate the experimental sample results. Samples are considered negative if no PCR is detected in the unspiked test and if both 10 and 100 copies are ready detected. Positive samples are considered vector-containing sequences if the PCR product is detected in both unspiked and control spiked samples. Typically, PCR amplification efficiency is the rate at which PCR amplification is generated and expressed as a percentage value. These parameters should be established for each apparatus, samples, and specific protocol requirements.

12. As a general point of view, we favor the use of a real-time Q-PCR with a Taqman® probe (in contrast to real-time Q-PCR using Sybr-Green), which will be more specific, especially when the analysis of several different tissues is required.

References

1. EMEA. (2009) General principles to address virus and vector shedding, in *ICH Considerations*, EMEA/CHMP/ICH/449035/442009.
2. EMEA. (1997) Preclinical safety evaluation of biotechnologicy-derived pharmaceuticals S6, in *ICH harmonised tripartite guideline*.
3. EMEA. (2009) Addenedum to ICH S6: Preclinical safety evaluation of biotechnologicy-derived pharmaceuticals S6(R1), in *ICH draft consensus guideline*.
4. Schenk-Braat, E. A., van Mierlo, M. M., Wagemaker, G., Bangma, C. H., and Kaptein, L. C. (2007) An inventory of shedding data from clinical gene therapy trials, *J Gene Med* 9, 910–921.
5. Stieger, K., Schroeder, J., Provost, N., Mendes-Madeira, A., Belbellaa, B., Le Meur, G., Weber, M., Deschamps, J. Y., Lorenz, B., Moullier, P., and Rolling, F. (2009) Detection of intact rAAV particles up to 6 years after successful gene transfer in the retina of dogs and primates, *Mol Ther* 17, 516–523.
6. Manno, C. S., Pierce, G. F., Arruda, V. R., Glader, B., Ragni, M., Rasko, J. J., Ozelo, M. C., Hoots, K., Blatt, P., Konkle, B., Dake, M., Kaye, R., Razavi, M., Zajko, A., Zehnder, J., Rustagi, P. K., Nakai, H., Chew, A., Leonard, D., Wright, J. F., Lessard, R. R., Sommer, J. M., Tigges, M., Sabatino, D., Luk, A., Jiang, H., Mingozzi, F., Couto, L., Ertl, H. C., High, K. A.,

and Kay, M. A. (2006) Successful transduction of liver in hemophilia by AAV-Factor IX and limitations imposed by the host immune response, *Nat Med* 12, 342–347.

7. Toromanoff, A., Cherel, Y., Guilbaud, M., Penaud-Budloo, M., Snyder, R. O., Haskins, M. E., Deschamps, J. Y., Guigand, L., Podevin, G., Arruda, V. R., High, K. A., Stedman, H. H., Rolling, F., Anegon, I., Moullier, P., and Le Guiner, C. (2008) Safety and efficacy of regional intravenous (r.i.) versus intramuscular (i.m.) delivery of rAAV1 and rAAV8 to nonhuman primate skeletal muscle, *Mol Ther* 16, 1291–1299.
8. Ciron, C., Cressant, A., Roux, F., Raoul, S., Cherel, Y., Hantraye, P., Deglon, N., Schwartz, B., Barkats, M., Heard, J. M., Tardieu, M., Moullier, P., and Colle, M. A. (2009) AAV1-, AAV2- and AAV5-Mediated human alpha-Iduronidase Gene Transfer In The Brain of Nonhuman Primate: Vector Diffusion and Bio Distribution, *Hum Gene Ther 20*, 350–360.
9. Favre, D., Provost, N., Blouin, V., Blancho, G., Cherel, Y., Salvetti, A., and Moullier, P. (2001) Immediate and long-term safety of recombinant adeno-associated virus injection into the nonhuman primate muscle, *Mol Ther* 4, 559–566.
10. Nathwani, A. C., Rosales, C., McIntosh, J., Rastegarlari, G., Nathwani, D., Raj, D., Nawathe, S., Waddington, S. N., Bronson, R., Jackson, S., Donahue, R. E., High, K. A., Mingozzi, F., Ng, C. Y., Zhou, J., Spence, Y., McCarville, M. B., Valentine, M., Allay, J., Coleman, J., Sleep, S., Gray, J. T., Nienhuis, A. W., and Davidoff, A. M. (2011) Long-term Safety and Efficacy Following Systemic Administration of a Self-complementary AAV Vector Encoding Human FIX Pseudotyped With Serotype 5 and 8 Capsid Proteins, *Mol Ther 19*, 876–885.
11. EMEA. (2006) General principles to address the risk of inadvertent germline integration of gene therapy vectors, in *ICH Considerations*, PEMEA/CHMP/ICH/469991/462006.
12. Gonin, P., and Gaillard, C. (2004) Gene transfer vector biodistribution: pivotal safety studies in clinical gene therapy development, *Gene Ther* 11 Suppl 1, S98–S108.
13. Arruda, V. R., Fields, P. A., Milner, R., Wainwright, L., De Miguel, M. P., Donovan, P. J., Herzog, R. W., Nichols, T. C., Biegel, J. A., Razavi, M., Dake, M., Huff, D., Flake, A. W., Couto, L., Kay, M. A., and High, K. A. (2001) Lack of germline transmission of vector sequences following systemic administration of recombinant AAV-2 vector in males, *Mol Ther* 4, 586–592.
14. Manno, C. S., Chew, A. J., Hutchison, S., Larson, P. J., Herzog, R. W., Arruda, V. R., Tai, S. J., Ragni, M. V., Thompson, A., Ozelo, M., Couto, L. B., Leonard, D. G., Johnson, F. A., McClelland, A., Scallan, C., Skarsgard, E., Flake, A. W., Kay, M. A., High, K. A., and Glader, B. (2003) AAV-mediated factor IX gene transfer to skeletal muscle in patients with severe hemophilia B, *Blood* 101, 2963–2972.
15. Favaro, P., Downey, H. D., Zhou, J. S., Wright, J. F., Hauck, B., Mingozzi, F., High, K. A., and Arruda, V. R. (2009) Host and vector-dependent effects on the risk of germline transmission of AAV vectors, *Mol Ther* 17, 1022–1030.
16. Schuettrumpf, J., Liu, J. H., Couto, L. B., Addya, K., Leonard, D. G., Zhen, Z., Sommer, J., and Arruda, V. R. (2006) Inadvertent germline transmission of AAV2 vector: findings in a rabbit model correlate with those in a human clinical trial, *Mol Ther* 13, 1064–1073.
17. Favaro, P., Finn, J. D., Siner, J. I., Wright, J. F., High, K. A., and Arruda, V. R. (2011) Safety of liver gene transfer following peripheral intravascular delivery of AAV-5 and AAV-6 in a large animal model, *Hum Gene Ther 22*, 843–852.
18. Salvetti, A., Oreve, S., Chadeuf, G., Favre, D., Cherel, Y., Champion-Arnaud, P., David-Ameline, J., and Moullier, P. (1998) Factors influencing recombinant adeno-associated virus production, *Hum Gene Ther* 9, 695–706.
19. Zen, Z., Espinoza, Y., Bleu, T., Sommer, J. M., and Wright, J. F. (2004) Infectious titer assay for adeno-associated virus vectors with sensitivity sufficient to detect single infectious events, *Hum Gene Ther* 15, 709–715.
20. Sharpe, R. (1994) Regulation of spermatogenesis., in *The physiology of reproduction*. (Knobil E, N. J., eds., Ed.), pp 1363–1419, Raven Press, Ltd, New York.
21. Penaud-Budloo, M., Le Guiner, C., Nowrouzi, A., Toromanoff, A., Cherel, Y., Chenuaud, P., Schmidt, M., von Kalle, C., Rolling, F., Moullier, P., and Snyder, R. O. (2008) Adeno-associated virus vector genomes persist as episomal chromatin in primate muscle, *J Virol* 82, 7875–7885.
22. Ni, W., Le Guiner, C., Gernoux, G., Penaud-Budloo, M., Moullier, P., and Snyder, R.O. (2011) Longevity of rAAV vector and plasmid DNA in blood after intramuscular injection in nonhuman primates: implications for gene doping, *Gene Ther 18*, 709–718.
23. Kazazian, H. H., Jr. (1999) An estimated frequency of endogenous insertional mutations in humans, *Nat Genet* 22, 130.
24. Goodier, J. L., and Kazazian, H. H., Jr. (2008) Retrotransposons revisited: the restraint and rehabilitation of parasites, *Cell* 135, 23–35.

Chapter 16

Production and Purification of Recombinant Adeno-Associated Vectors

Lijun Wang, Véronique Blouin, Nicole Brument, Mahajoub Bello-Roufai, and Achille Francois

Abstract

The use of recombinant adeno-associated virus (rAAV) vectors in gene therapy for preclinical studies in animal models and human clinical trials is increasing, as these vectors have been shown to be safe and to mediate persistent transgene expression in vivo. Constant improvement in rAAV manufacturing processes (upstream production and downstream purification) has paralleled this evolution to meet the needs for larger vector batches, higher vector titer, and improved vector quality and safety. This chapter provides an overview of existing production and purification systems used for adeno-associated virus (AAV) vectors, and the advantages and disadvantages of each system are outlined. Regulatory guidelines that apply to the use of these systems for clinical trials are also presented. The methods described are examples of protocols that have been utilized for establishing rAAV packaging cell lines, production of rAAV vectors using recombinant HSV infection, and for chromatographic purification of various AAV vector serotypes. A protocol for the production of clinical-grade rAAV type 2 vectors using transient transfection and centrifugation-based purification is also described.

Key words: Adeno-associated virus, rAAV, Vector, Production, Purification, Gene therapy, Clinical trial, cGMP

1. Introduction

1.1. Production of Recombinant Adeno-Associated Virus Vectors

The assembly of recombinant adeno-associated virus (rAAV) vector virions is achieved in cultured cells to which three components have been supplied: (1) the rAAV vector composed of the transgene expression cassette flanked by the adeno-associated virus (AAV) terminal repeats, (2) the AAV *rep* and *cap* coding sequences, and (3) the helper virus functions (1, 2). Various methods and cell culture systems have been developed on the basis of this principle

Richard O. Snyder and Philippe Moullier (eds.), *Adeno-Associated Virus: Methods and Protocols*,
Methods in Molecular Biology, vol. 807, DOI 10.1007/978-1-61779-370-7_16,

to produce AAV vectors. The most commonly used method consists of a two (or three) plasmid transfection of adherent HEK293 cells, a human embryonic kidney derived cell line. Although this method is rapid, efficient, and has the advantage of avoiding the use of a helper virus, it is laborious and time-consuming when large quantities of vector are needed, especially when tissues such as liver, heart, or skeletal muscle are targeted. Alternative methods that use suspension cell culture systems and allow for larger-scale production have been developed. The two major alternative methods are based on either (1) insect cells to which all three components are provided through recombinant baculovirus infection or (2) stable mammalian packaging (i.e., containing *rep* and *cap*) or producer (i.e., also containing the rAAV) cell lines to which certain components are provided through adenovirus infection. Another system, also based on mammalian cells, uses recombinant HSV-1 to provide *rep–cap*, rAAV vector and helper functions. Recently, stable insect packaging cell lines (containing *rep* and *cap*) have also been developed. Table 1 references the main described production systems for AAV vectors (see refs. 3 and 4 for detailed review).

Each of the rAAV vector production systems offer some advantages and disadvantages that have to be considered relative to the amount of vector needed for preclinical studies, the human clinical trial, and product stability studies prior to the establishment of a manufacturing process. Tables 2 and 3 list the advantages and disadvantages of the components used in each AAV production system, i.e., cells and helper functions.

Table 4 provides indications about the suitability of each production system according to the amount of vector needed, i.e., the production scale. The largest production scale reported for each system is also indicated.

Protocols for rAAV production using these four systems are continuously evolving and improving. Whatever the system used, the amount of vector particles generated is in the range of 10^4–10^5 DNase-resistant particles (DRP) per cell (4), which is approximately one log less than wild-type AAV, but the ratio of full-to-empty particles and infectious-to-full particles is different from one system to another (4), and still remains much lower than that of wild-type AAV, as described for AAV serotype-2 (31).

Production using transfection of HEK293 cells, the most widely used system, has been continuously improved and large vectors batches of rAAV vectors have been produced this way in multitray cell factories or in roller bottles (32, 33). Transfection in suspension culture has also been reported (28). Although this system is easier and faster to set up, avoids the use of helper virus, and is sufficient for preclinical and early phase clinical trials, it may not be suitable for the production of phase III or commercial vector lots.

Table 1
Overview of the main production systems for AAV vectors

Host cell type	Cell line	AAV functions	Helper functions	rAAV vector	References
Insect cells	Sf9	Bac-Rep + Bac-VP	*Provided by the Bac vectors*	Bac-rAAV	(5)
	Sf9	Bac-RepCap	*Provided by the Bac vectors*	Bac-rAAV	(6)
	Sf9/RepCap	*Provided by the cells*	*Provided by the Bac vectors*	Bac-rAAV	(7)
Mammalian cells	HEK293	pRepCap	pAd	pAAV	(8, 9)
	HEK293	pRepCap/Ad		pAAV	(10–12)
	HeLa/RepCap	*Provided by the cells*	Ad5	Ad/rAAV	(13–15)
	HeLa/RepCap/rAAV	*Provided by the cells*	Ad5	*Provided by the cells*	(16–18)
	HeLa/RepCap/rAAV	*Provided by the cells*	HSV-1	*Provided by the cells*	(19)
	A549/RepCap	*Provided by the cells*	Ad5	Ad/rAAV	(20)
	A549/RepCap/rAAV	*Provided by the cells*	Ad5	*Provided by the cells*	(21)
	293/rAAV	HSV-RepCap	*Provided by the HSV vectors*	*Provided by the cells*	(22)
	HEK293	HSV-RepCap	*Provided by the HSV vectors*	HSV-rAAV	(23)
	BHK21	HSV-RepCap	*Provided by the HSV vectors*	HSV-rAAV	(24)

Table 2
Cells used for AAV production

	Advantages	Disadvantages
Sf9 cells	• Suspension-adapted cells available • Specific SFM commercially available • Culture to high density • High production efficiency	• Culture at 30°C maximum • Low infectivity/PLA2 activity for some AAV serotype • High empty-to-full particles ratio
HEK293	• Human origin • Suspension-adapted cells available • Specific SFM commercially available • High transfection efficiency	• Contains Adenovirus ITR and E1 gene • Cannot – to date – be used as a stable packaging cell line
HeLa-based cell lines	• Human origin • Suspension-adapted cells available • Specific SFM commercially available	• Contains HPV genes • Need for selection of stable packaging and/or producing cell clones
A549-based cell lines	• Human origin • Nontransformed cell line	• Adaptation to suspension culture needed • Need for selection of stable packaging and/or producing cell clones
BHK21 cells	• Mammalian origin • Nontransformed cell line • Suspension-adapted cells available	• Nonhuman • Possible contamination with endogenous retrovirus (as found in many cell lines from murine origin)

Table 3
Systems used to provide AAV vector and helper functions to the cells

	Advantages	Disadvantages
Baculovirus	• Used at low MOI • Suitable for production in suspension culture (for both BEV and AAV) • Production in animal-free conditions • Ability to carry Rep expression	• Large genome size/laborious to fully characterize • Genome instability (deletions) • Enveloped virus (fragile) • Long lead time: need to produce and qualify master viral banks • Helper functions not fully characterized • Lack of published data on packaging of BEV DNA into AAV and generation of rcAAV

(continued)

Table 3 (continued)

	Advantages	Disadvantages
Plasmid transfection	• Plasmid easy to produce and characterize • *Escherichia coli* MCB easy to generate • No virus needed • Production in animal-free conditions	• Needs cells to be adherent (time-consuming handling) • Difficult to adapt to suspension • Bacterial culture needed for plasmid production • Large quantity of plasmid needed • Long production time for large vector lots • Packaging of plasmid DNA into AAV • Generation of rcAAV
Adenovirus	• Used at low to medium MOI • Suitable for production in suspension culture (for both Ad and AAV) • Production in animal-free conditions • Easy to produce at high yield • Well-established purification process • Capsid stability • Medium-sized genome • Genome stability • Helper functions fully characterized • No or little rcAAV generated • Ad DNA not packaged into AAV	• Cytotoxic/Immunogenic • Cannot carry Rep expression/needs Rep to be provided by the cells • Long lead time: need to produce and qualify master viral bank
HSV-1	• Used at low MOI • Suitable for production in suspension culture (AAV only) • Ability to carry Rep expression • Can be used with various cell lines	• Large genome size/laborious to fully characterize • Pathogenic/immunogenic • Enveloped virus (capsid fragility) • Long lead time: need to produce and qualify master viral banks • Helper functions not fully characterized • Production is not entirely animal-free (entire serum-free process not documented) and Vero cells for HSV production are adherent • HSV DNA and protein contaminants difficult to remove • Lack of published data on packaging of HSV DNA into AAV and generation of rcAAV

Table 4
Feasibility and capacity of AAV manufacturing systems

Production system	Production scale			Largest scale reported for AAV production	References
	Small	Medium	Large		
Sf9 and baculovirus	+	+++	++++	40 L 90–125 L	(25–27)
HEK293 and plasmids	++++	++	–	3 L 100 Roller bottles	(28, 29)
Mammalian cells and HSV-1	+	+++	++++	10 L	(30)
Packaging/producer cells and Ad	+	++	++++	250 L	(18)

One possible alternative to transfection is the use of HSV-1 vectors, which provide AAV helper functions and are able to carry both the AAV vector and the *rep–cap* genes, as the plasmid does. This system uses mammalian cells such as HEK293 or BHK21 that can be adapted to suspension culture and thus is more suitable for large-scale production. However, there is a long lead time to clone and produce the master viral banks needed for rAAV vector production. Also, HSV is a large enveloped virus that is somewhat fragile, and its large DNA genome (152 kb) makes it difficult to fully characterize. Moreover, propagation of ICP27-deleted HSV-1 vectors currently used for AAV production uses an adherent Vero cell line (34), rendering difficult the use of HSV for an AAV production of phase III or commercial scale vector batches. A protocol for the production of rAAV vectors using dual rHSV-1 vectors infection is described in Subheading 3.4.

In the insect cells/baculovirus system, recent advances involving codon optimization have improved the expression of Rep and Cap proteins, and seem to have resolved the issue of the expression ratio of VP1/VP2/VP3 in the insect cells system (6, 35). The use of low baculovirus MOI, as well as the improvement of the stability of the Bac vectors, make this system more favorable for the production scale-up. However, there is a long lead time to clone and produce the master viral banks needed for rAAV vector production. Also, the issue of baculovirus vectors instability still remains unresolved, due to its large genome (134 kb) and to the inherent generation of deleted and/or defective vectors during viral replication (36). The development of insect packaging cell lines is one possible way to partially address this issue, as only one baculovirus is needed for rAAV production instead of two or three viruses (7). Another drawback of the BEV/insect cells system is the production

of large amount of contaminating empty AAV particles, due to either over expression of capsid proteins or inefficient AAV genome packaging.

To date, the most scalable process for rAAV production resides in the use of packaging or producer cell lines infected with adenovirus (15, 17, 18). This system requires significant effort to generate and select packaging cell lines, and possibly adaptation to suspension culture. But once an efficient and stable packaging cell line is established, the potential for production scale-up can compensate for the time spent on the selection process. The production process requires the use of wild-type or replication-competent Ad5 virus, but handling and characterization of such viruses is now standardized as Ad5 vectors are currently the most widely used vectors in various clinical trials, including gene therapy, cancer therapy, and vaccine clinical trials (37), and efficient process for the removal of infectious Ad5 virus and Ad viral DNA from AAV products has already been validated (18). A protocol for the generation of stable packaging cell lines is described in Subheading 3.1, as a basis for establishing such a scalable rAAV production process.

1.2. Recombinant AAV Vector Purification

High-yielding, scalable rAAV vector purification processes are needed to support clinical trials and commercial applications.

Traditionally, the modes of purification applicable to AAV viruses include gradient centrifugation, ion exchange, gel filtration, and hydrophobic interaction. A series of optimized chromatographic steps typically are required to obtain vector in high yield and purity. Receptor-specific purification has been used successfully to generate AAV2 and AAV5 vectors. Recently a custom ligand that binds multiple serotypes has been commercialized and used in GMP-compliant, large-scale manufacturing. This affinity chromatography resin is specific and results in reasonable recovery and high purity. A recently developed, fully scalable process combining novel ion-exchange (IEX) media and affinity purification allows significant reduction in processing time due to high capture step dynamic binding capacity, flow rates, and resolution.

Table 5 provide a comprehensive summary of the published AAV purification processes. Below, three primary purification modalities and their applications are discussed.

1.2.1. Ion-Exchange Chromatography

Purification by IEX chromatography of AAV is based on the net charge of proteins of the viral capsid. The net charge of AAV particles depends on the pH of the exposed amino-acid groups in solution. Each serotype has distinct net charges under a certain pH; therefore, IEX chromatography permits development of purification protocols that can be used for different AAV serotypes.

Both anion and cation exchange chromatography have been used to prepare different serotypes of vectors with high purity and potency (17, 38–43, 45, 46). IEX chromatography has also been paired with other orthogonal methods, such as gradient

Table 5
Summary of AAV purification methods

Method	AAV serotype	Purification step	Column type	AAV purity	Yield (%)	References
Ion exchange	AAV2	Cation exchange/anion exchange	POROS 20 HE POROS 50 PI	++	90–95 60–70	(38)
	AAV2	Three-step ion exchange	Ceramic hydroxyapatite DEAE Macroprep Cellufine sulfate	++	n/a	(39)
	AAV2 AAV5	Cation exchange/anion exchange	SP Sepharose HP/Source 15Q	++	44 33	(40)
	AAV2	Anion exchange	POROS PI	++	9	(41)
	AAV4	Anion exchange	POROS PI		15	
	AAV5	Anion exchange	POROS-HQ		11	
	AAV8	Cation exchange/anion exchange	Mustang S/Mustang Q	++	n/a	(42)
	AAV2 AAV5	Cation exchange/anion exchange	SP Sepharose HP/Source 15Q	++	n/a n/a	(17)
	AAV5	Anion exchange/ gel filtration	Mono Q HR/Superdex200	++	37	(43)
	AAV1	Cation exchange/HIC	Fractogel SO3-/Butyp-650M	++	75	(44)
	AAV2	Cation exchange/anion exchange	POROS 50HS/Q-Sepharose XL	++	74	(45)
	AAV1	Anion exchange	POROS HQ	++	n/a	(46)
	AAV2	Sulfonated cellulose	Cellulofine sulfate	+	~100	(47)
	AAV2	Affinity/HIC/cation exchange	Heparin agarose Phenyl sepharose SP sepharose	+++	33	(48)
	AAV1 AAV8	Anion exchange/cation exchange	Cation exchange/anion exchange	++	n/a	(49)

Receptor-specific affinity	AAV2	Heparin affinity	Heparin agarose	++	n/a	(50)
	AAV2	Heparin affinity/HIC/heparin affinity	Streamline heparin/HIC/POROSHe/M	++	n/a	(51)
	AAV2	HPLC heparin affinity	POROS HE/M		73	(52)
	AAV2	Heparin affinity	POROS HE/P		35	(53)
	AAV5	Mucin affinity	Mucin sepharose	+	n/a	(54)
	AAV2	A20 antibody affinity	A20 coupled resin(s)	++	n/a	(10)
AVB sepharose affinity and combination of other separation methods	Multiple serotypes	Affinity	AVB sepharose	++	>90%	(55)
	Multiple serotypes	Affinity	AVB sepharose	++	49.9	(6)
	AAV1	Affinity	AVB sepharose	++	n/a	(56)
	AAV1	Affinity/anion exchange	AVB sepharose, Mustang Q	++	n/a	(57)
	AAV1	Affinity/anion exchange	AVB sepharose, CIM Q	++	n/a	(58)
Avidin affinity chromatograph	AAV2	Avidin affinity chromatography capture RGD-modified capsid protein	Monomeric avidin affinity column	++	n/a	(59, 60)
	AAV3			++	n/a	
	AAV4			++	n/a	
	AAV5			++	n/a	
HIS-tag affiinity chromatography	Multiple serotypes	Affinity	Ni-NTA agarose	++	>90	(61)
Multimode purification	AAV1	Polyethylene glycol precipitation	n/a	++	n/a	(62)
		Anion exchange	n/a	++	n/a	
		Gel filtration	n/a	++	n/a	

centrifugation (63), precipitation and gel filtration (62), affinity purification (55–58), and hydrophobic interaction chromatography (HIC) (44). Salt concentration and pH adjustments are necessary for optimization of binding of the viral particles to both IEX resins, and these adjustments are serotype dependent owing to differences in overall net charge. IEX chromatography is fast, reproducible, scalable, and nonserotype-specific; furthermore, this method yields highly purified rAAV and is suitable for large-scale production of clinical-grade vector using classical chromatographic resins and newer monolith and membrane-based supports. The drawback in IEX chromatography is that multiple steps are usually needed to make highly purified rAAV vectors. A protocol for IEX purification of AAV serotypes 2 and 5 is described in Subheading 3.2.

1.2.2. Receptor-Specific Affinity Purification

Although IEX chromatography is robust and flexible, unique resins and conditions must be developed and tailored for specific AAV serotypes. Affinity chromatography is a well-established method for purifying biological molecules from complex source material. The most commonly used application of large-scale affinity chromatography is based on antibody–antigen interaction. Receptor-specific affinity purification has played a vital role in AAV purification.

Heparan sulfate proteoglycan (HSPG) has been identified as a cellular receptor for AAV2, which is essential in the binding stage of viral infection (64–66). Heparin affinity chromatography takes advantage of the stable interaction between AAV2 and the cellular receptor. Several methods that exploit this receptor-specific affinity have been developed and used for AAV2 purification (9, 10, 50–53). High-titer, high-purity AAV2 stocks purified by these receptor-specific affinity methods have been used to make AAV2 for clinical trials (48) and have dramatically increased our understanding of this virus and its utility as a gene transfer vector. Heparin sulfate-based affinity chromatography, however, only works for rAAV2 because other serotypes lack heparin-binding activity. Alpha 2–3 sialic acid has been reported as either a receptor for AAV5 or as a necessary component of a receptor complex for AAV5 binding and transduction (67). Whereas binding of AAV4 requires alpha 2–3 O-linked sialic acid, binding of AAV5 requires N-linked sialic acid due to differences in tropism (67). A sialic-acid-rich protein called mucin has been used as an affinity ligand to purify AAV5 (54). Other purification protocols for AAV2 were developed. The monoclonal antibody A20, which is highly specific for AAV-2 capsid was crosslinked to Sepharose (10). Avidin affinity chromatography was used to purify RGD-engineered capsids, and nickel chromatography was used to purify His-tagged capsids (59, 61).

These ligand affinity chromatography applications led to a significant improvement in recombinant AAV vector production and purification, but they are probably not suitable for use in the clinic.

1.2.3. AVB Sepharose Affinity Chromatography

Receptor-specific affinity purification only works if one or more receptors are known for a specific AAV serotype. A universal antibody for purifying multiple AAV serotypes is desired to support development of rAAV therapeutics. The commercially available AAV affinity ligand provides a one-step affinity chromatography purification method for multiple AAV vectors. The immunoaffinity-based resin AVB Sepharose, which consists of a 14 kDa fragment from a single chain antibody expressed in yeast and conjugated to the Sepharose, is specific for a highly conserved epitope on the AAV capsid, permitting purification of multiple AAV serotypes. The AVB affinity resin is highly specific, has high binding capacity, and is scalable. These characteristics provide a one-column process for producing near homogenous preparations of rAAV from complex crude lysates. The immunoaffinity capture method is likely to replace other liquid column chromatography methods if cost is not a concern. Purification processes using this resin (6, 62) or in conjunction with IEX chromatography have been reported (56–58). For example, a two-step purification process (Q-AVB) allows significant reduction in processing time and cost. The AVB ligand has been shown to have affinity to AAV1, 2, 3, 5, and 8 (although the affinity to, e.g., AAV1 is very different than AAV8). A protocol for the purification of AAV1 using Q-AVB chromatography is described in Subheading 3.3.

1.3. Current Good Manufacturing Practice Production of rAAV for Human Clinical Trials

Like any other biotherapeutic candidate for human clinical trials, rAAV clinical lots are manufactured in compliance with current good manufacturing practices (cGMPs) to ensure that safe, pure, potent, and stable vector lots are being used in clinical trials. Although these principles are country specific, they should be in compliance with US Code of Federal Regulations (21CFR) (http://www.gpoaccess.gov/cfr/index.html), Food and Drug Administration (FDA) guidelines (http://www.fda.gov/cber/guidelines.htm), European Commission Directive (2003/94/EC), (http://www/ec.europa.eu/enterprise/pharmaceuticals/eudralex/vol-1/dir_2003_94/dir_2003_94_en.pdf), International Conference on Harmonization guidelines (ICH Q7A) (http://www.ich.org/), and World Health Organization guidelines (http://www.who.int/medicines/en/).

In general, rAAV vectors are manufactured in facilities with appropriate and qualified or validated equipment and building systems. Personnel involved in product manufacturing, from raw materials reception to the final product shipping, must have appropriate education and job-specific training. The overall operation of

such a facility has been described by Snyder and Francis in 2005 (68) and recently by Mandel et al. (69).

Raw materials such as cell culture vessels and other plasticware are specifically chosen and tested based upon the process and preset specifications. Plasticware should be of USP (United States Pharmacopoeia) class VI quality, traceable, and readily available. Acceptability criteria and specifications should be established for each item. Reagents and chemicals should be cGMP manufactured and tested according to USP criteria or multicompendial grade whenever possible. Water for injection (WFI) should be used to prepare all solutions and buffers.

Solutions and buffers made in-house should be sterile filtered and quarantined until appropriate quality control (QC) tests are completed before use. When reagents are manufactured by an outside vendor, release testing should be reviewed by quality control and quality assurance personnel to ensure they are suitable for use. As much as possible animal origin-free raw materials should be used. Animal derived raw materials should be accompanied by certificates of origin (COO).

Critical substrates and biological material such as cells, plasmids, and viral seeds must originate or derive from fully tested and well-characterized master or working banks.

Specifications for viral seeds may vary with the helper virus used, but depending on the bank (master or working bank), tests should include bioburden, sterility, viral titer, identity (restriction analysis, and partial or complete sequencing), functional testing. Banks should be tested for the absence of mycoplasma, adventitious agents, bovine viruses, porcine viruses, retrovirus-like particles, endotoxin when applicable, and specified human pathogens (AAV, HIV 1, and HIV 2, HTLV I and HTLV II, HBV, HCV, CMV, EBV, Hepatitis B, Hepatitis C, parvovirus B19) (68). Testing must be performed under cGMP according to FDA's Guidance of Industry (http://www.fda.gov/BiologicsBloodVaccines/GuidanceComplianceRegulatoryInformation/Guidances/default.htm). Master and working cell banks must be appropriately stored in liquid nitrogen vapor and master and working viral seeds must be stored at ≤−70°C in a fully monitored and validated cGMP facility. *Escherichia coli* master and working cell banks used to produce plasmids must be appropriately stored in a freezer (<−70°C) within a monitored and qualified/validated cGMP facility (68) and should be tested for host cell identity, phage contamination, plasmid identity, and sequence and functionality. Once produced, plasmids used to transfect cells must be tested for identity, homogeneity, purity, sterility, and for the presence of genomic DNA, RNA, protein, and endotoxin (68). A protocol for the production of clinical-grade AAV2 vector by using transient transfection of HEK293 cells followed by iodixanol ultracentrifugation gradient purification is described in Subheading 3.4.

2. Materials

All protocols described in this chapter require at least standard equipment for cell culture (e.g., TypeII A/B biological safety cabinets, CO_2 incubator, centrifuge, and inverted microscope) and low temperature storage (4°C, –20°C, –80°C, and liquid nitrogen).

2.1. Generation and Selection of Stable Packaging Cell Lines for rAAV Production

1. Equipments and supplies:
   (a) 10-cm and 15-cm cell culture dishes, 48-wells and 6-wells cell culture plates.
   (b) Microcentrifuge and microcentrifuge tubes.
   (c) PCR thermocycler, e.g., PE 9700 (Applied Biosystems, Courtaboeuf, France).
   (d) 37°C and 56°C Water baths.
   (e) Horizontal (for agarose gels) and vertical (for polyacrylamide gels) electrophoresis systems with power supply.
   (f) Whatman 3 M filter paper.
   (g) Positively charged nylon membrane (for Southern blot and dot blot hybridization).
   (h) Hybridization oven.
   (i) Nitrocellulose membrane (for Western blot).
   (j) Semidry gel transfer system, e.g., Trans-Blot SD (Bio-Rad, Marnes-la-Coquette, France).
   (k) 96-Wells dot blot system.
   (l) X-ray films and photography developing reagents.
2. Reagents:
   (a) HeLa (ATCC CCL-2) or A549 (ATCC CCL-185) cells.
   (b) Plasmids: pRC (containing AAV rep–cap genes), pPGK-Neo (Neomycine phosphotransferase expressed from the murine phosphoglycerate kinase promoter), pAAV-CMV-GFP (vector plasmid containing an enhanced Green Fluorescent Protein expression cassette flanked by AAV2 ITR).
   (c) HEK293 (ATCC CRL-1573) and HeRC32 (ATCC CRL-2972) cells.
   (d) Human adenovirus type 5 (ATCC VR-5 or VR-1516).
   (e) Dulbecco's modified Eagle's medium (DMEM) with 4.5 mg/L glucose and fetal bovine serum (FBS).
   (f) Phosphate buffer saline (PBS) and trypsin-EDTA.
   (g) Dimethyl sulfoxide (DMSO).

(h) Tranfection reagents: 2.5 M $CaCl_2$ and 2× HEPES-buffered saline (50 mM HEPES, pH 7.0, 280 mM NaCl, 1.5 mM Na_2HPO_4).

(i) G418-sulfate, i.e., Geneticin (Invitrogen, Cergy-Pontoise, France).

(j) NucleoSpin Blood kit (Macherey-Nagel, Hoerdt, France).

(k) Taq DNA polymerase, e.g., GoTaq polymerase (Promega, Charbonnières-les-Bains, France) and dNTPs.

(l) Agarose and Tris-acetate-EDTA (TAE) buffer.

(m) Proteinase K and 2× proteinase K buffer (20 mM Tris–HCl, pH 7.5, 2 mM EDTA, 200 mM NaCl, 2% SDS).

(n) Phenol pH 8.0, chloroform, isopropanol, ethanol, TE buffer (10 mM Tris, pH 8.0, 1 mM EDTA).

(o) 0.25 M HCl, 0.5 M NaOH, 20× SSC buffer (3 M NaCl, 0.3 M sodium citrate, pH 7.0), and 10% SDS stock solution.

(p) AlkPhos Direct labeling kit, hybridization buffer, and CDP-Star detection reagent (GE HealthCare, Orsay, France).

(q) RIPA buffer: 20 mM Tris–HCl, pH 7.4, 50 mM NaCl, 1 mM EDTA, 0.5% NP-40, 0.5% deoxycholate, 0.5% SDS.

(r) 5× Laemmli sample buffer: 300 mM Tris–HCl, pH 6.8, 50% glycerol, 25% β-mercapto-ethanol, 0.05% bromophenol blue.

(s) 10% Polyacrylamide Tris–Glycine gels (e.g., Novex 10% Tris–Glycine, Invitrogen, Cergy-Pontoise, France) and 10× Tris–Glycine–SDS running buffer (250 mM Tris-HCl, pH 8.3, 1.92 M glycine, 1% SDS).

(t) Anti-Rep 303.9 and Anti-Cap B1 monoclonal antibodies (Progen Biotechnik, Heidelberg, Germany), anti-mouse HRP antibody, antibody dilution buffer (PBS, pH 7.4, 0.1% Tween 20, 5% milk), Pierce ECL Western blotting substrate (ThermoFisher Scientific, Brebières, France).

(u) Cell lysis buffer for AAV harvest: 50 mM HEPES, pH 7.5, 150 mM NaCl.

2.2. Purification of AAV Serotype 2 and 5 by IEX Chromatography

1. Equipments and supplies:

(a) 37°C and 56°C Water baths.

(b) GR-412 centrifuge rotor (Jouan, Saint-Herblain, France).

(c) JA-17 centrifuge rotor (Beckman Coulter, Villepinte, France).

(d) 5 + 0.45 μm PVDF filters.

(e) SP Sepharose HP resin (GE Healthcare, Orsay, France), HR 5/10, HR 10/10, or XK16/10 for 2, 8, and 20 mL of matrix, bed height of 10 cm.

(f) Source 15Q resin (GE Healthcare, Orsay, France), Resource Q 1 mL or HR 5/10.

(g) AKTA Explorer controlled by Unicorn software (GE Healthcare, Orsay, France).

2. Reagents:

(a) Lysis buffer: 25 mM $NaHPO_4$, 20 mM NaCl, 2 mM $MgCl_2$, pH 7.0.

(b) SP Sepharose HP loading buffers:

AAV2: 25 mM $NaHPO_4$, 150 mM NaCl, 2 mM $MgCl_2$, pH 6.5.

AAV5: 25 mM $NaHPO_4$, 100 mM NaCl, 2 mM $MgCl_2$, pH 6.5.

(c) Source 15Q loading buffer:

AAV2: 20 mM Tris, 50 mM NaCl, 2 mM $MgCl_2$, 1 mM $CaCl_2$, pH 8.2.

AAV5: 20 mM Tris, 20 mM NaCl, 2 mM $MgCl_2$, 1 mM $CaCl_2$, pH 8.2.

2.3. Production and Purification of AAV Serotype 1 Using Dual rHSV Infection and IEX/Affinity Chromatography

1. Equipments and supplies:

(a) CIM Q 80 mL monolithic (BIA separation, Ljubljana, Slovenia).

(b) AVB Sepharose HP (GE Healthcare, Piscataway, NJ).

(c) Sartocon Slice 1000 flat sheet: 100-kDa MWCO Hydrosart membranes (Sartorius, Bohemia, NY).

(d) Sartorius 1.2 μm depth filter and 0.8/0.45 μm dead end filter (Sartorius, Bohemia, NY).

(e) 0.22 μm Sterile filter (Sartorius, Bohemia, NY).

(f) 0.45 μm nominal pore size Hydrosart membranes for medium exchange (Sartorius, Bohema, NY).

(g) Bioreactor: BIOSTAT Cultibag RM 20/50 basic control unit and platform (Sartorius Stedim Systems, Springfield, MO).

(h) AKTA Purifier (GE Healthcare, Piscataway, NJ).

(i) Guava EasyCyte mini system (Guava Technologies/Millipore, Hayward, CA).

(j) 300-kDa MWCO hollow fiber cartridge, cat. no. UFP-300-E-MM01A (GE Healthcare Life Sciences, Piscataway, NJ).

2. Reagents:

(a) Suspension-adapted baby hamster Kidney (BHK21) cells (ECACC 85011433).

(b) Cell culture media: Hyclone DEME containing 10% FBS (Thermo Scientific, Rockford, IL).

(c) rHSV-rep2/Cap1 and rHSV-GOI vector stocks, $>1.5\times10^9$ pfu/mL (see production method below) (see Subheading 3.3, step 1).

(d) V27 cells (a Vero-derived ICP27 complementing cell line).

(e) Benzonase (EMD Biosciences, San Diego, CA).

2.4. Production of Clinical-Grade AAV Vector by Transient Transfection

1. Equipments and supplies:
   (a) Biosafety cabinet within an ISO class 7 clean room.
   (b) Incubators at 37 ± 1°C, 5 ± 3% CO_2, 85% relative humidity (Thermo Scientific, Asheville, NC).
   (c) Centrifuge, Jouan GR4i (Thermo Scientific, Asheville, NC) or equivalent.
   (d) Ultracentrifuge, Optima L-90 with T70i rotor (Beckman Coulter Inc., Brea, CA).
   (e) Flasks vented cap, T-75 cm^2, T-225 cm^2. Cell factory ten-layer with vented caps, serological pipettes, polystyrene bottles, 50 mL conical tubes (Corning, Lowell, MA).
   (f) PETG bottles, graduated cylinders (Nalgene, Rochester, NY).
   (g) Sterikap Filter 0.22 μm PES membrane (Millipore, Billerica, MA).
2. Reagents:
   (a) HEK293 cells (ATCC CRL-1573).
   (b) Helper plasmid at 1.0 mg/mL and AAV vector plasmid at 1.0 mg/mL.
   (c) DMEM with 4.5 g/L D-glucose, with L-glutamine, without sodium pyruvate (DMEM), gentamicin reagent solution, 50 mg/mL, Dulbecco's phosphate-buffered saline, without calcium chloride and magnesium chloride (PBS-CMF), Trypan Blue stain, 0.4% (Invitrogen, Carlsbad, CA).
   (d) New Zealand FBS (Hyclone, Logan, UT).
   (e) Calcium chloride dehydrate ($CaCl_2 \cdot 2H_2O$), powder, USP grade (JT Baker, Phillipsburg, NJ).
   (f) HEPES, free acid, powder, Ultrapure grade (JT Baker, Phillipsburg, NJ).
   (g) EDTA disodium salt, USP grade (JT Baker, Phillipsburg, NJ).
   (h) Dextrose, monohydrate, USP grade (JT Baker, Phillipsburg, NJ).
   (i) Potassium chloride (KCl), USP grade (JT Baker, Phillipsburg, NJ).
   (j) Sodium phosphate dibasic (Na_2HPO_4), USP grade.
   (k) Sodium chloride (NaCl), USP grade (JT Baker, Phillipsburg, NJ).
   (l) Sodium hydroxyde 5N (5 N NaOH) (JT Baker, Phillipsburg, NJ).
   (m) Hydrochloric acid 37% (HCl), NF grade (JT Baker, Phillipsburg, NJ).

(n) Iodixanol, OptiPrep® Density Gradient solution 60% in water, Ultrapure Bioreagent (Sigma-Aldrich, St. Louis, MO).

(o) Magnesium chloride, USP grade (JT Baker, Phillipsburg, NJ).

(p) Phenol Red Ultrapure Bioreagent grade (JT Baker, Phillipsburg, NJ).

(q) SP Sepharose HP resin (GE Healthcare, Piscataway, NJ).

(r) WFI (Hyclone, Logan, UT).

3. Preparation of culture medium, buffers, and solutions.

(a) DMEM complete (described for 1,000 mL batch).

- Remove 50 mL of DMEM from a bottle of 1,000 mL.
- Add 50 mL of New Zealand FBS.
- Add 8 mL of gentamicin reagent solution 50 mg/mL.
- Sterile filter the mixture and aliquot in appropriate sizes.
- Store DMEM complete at 2–8°C until use.

(b) PBS with 5 mM EDTA (pH 7.3 ± 0.2) (described for 1,000 mL batch).

- Prepare 500 mM EDTA, pH 7.4, in WFI using 5N NaOH to titrate/dissolve EDTA.
- Add 10 mL of the 500 mM EDTA to 990 mL of PBS.
- Mix the solution for >10 min.
- Sterile filter the solution and aliquot in appropriate sizes.
- Store aliquots at 2–8°C until use.

(c) 2.5 M Calcium chloride (2.5 M CaCl2) (described for 100 mL).

- Add 60 mL of WFI to a graduate cylinder.
- Add 36.75 g of CaCl2 to the cylinder.
- QS solution to 100 mL.
- Mix the solution for >10 min.
- Sterile filter the solution and aliquot in appropriate sizes.
- Store aliquots at −20°C until use.

(d) 2× HEPES buffer saline (2× HBS: 274 mM NaCl, 9.9 mM KCl, 1.5 mM Na_2HPO_4, 11.1 mM dextrose, 42 mM HEPES, 7.05 ± 0.02) (described for 1,000 mL batch).

- Add 700 mL of WFI to a graduate cylinder.
- Add 16.012 g of NaCl, 0.738 g of KCl, 0.215 g of Na_2HPO_4 to the cylinder.
- Add 2.20 g of dextrose, 10.0 g of HEPES to the cylinder.
- Adjust pH to 7.05 ± 0.02 using 5N NaOH (see Note 1).
- QS solution to 1,000 mL and mix the solution for >10 min.

- Sterile filter the solution and aliquot in appropriate sizes.
- Store aliquots at −20°C until use.

(e) Crude lysate buffer (50 mM Tris-Base, 150 mM NaCl, pH 8.5 ± 0.1) (described for 1,000 mL batch).

- Add 700 mL of WFI to a graduate cylinder.
- Add 8.766 g of NaCl, 6.055 g of Tris-base to the cylinder.
- Adjust pH to 8.5 ± 0.1 using HCl.
- Increase volume to 1,000 mL with WFI and mix the solution for >10 min.
- Sterile filter the solution and aliquot in appropriate sizes.
- Store aliquots at 2–8°C until use.

(f) 5× PBS with magnesium and potassium, 5× PBS-MK (5× PBS, 5 mM $MgCl_2$, 12.5 mM KCl) (described for 1,000 mL batch).

- Add 300 mL of WFI to a graduate cylinder.
- Add 500 mL 10× PBS to cylinder.
- Add 1.0165 g of $MgCl_2$, 0.932 g of KCl to the cylinder.
- Mix the solution for >10 min.
- QS solution to 1,000 mL and mix the solution for >10 min.
- Sterile filter the solution and aliquot in appropriate sizes.
- Store aliquots at 2–8°C until use.

(g) 5 M Sodium chloride (5 M NaCl, described for 1,000 mL batch).

- Add 600 mL of WFI to a graduate cylinder.
- Add 292.2 of NaCl to the cylinder.
- Mix the solution and gradually add WFI until complete dissolution.
- QS solution to 1,000 mL and mix the solution for >10 min.
- Sterile filter the solution and aliquot in appropriate sizes.
- Store aliquots at 2–8°C until use.

(h) Iodixanol 15% – 1 M NaCl, density = 1.117–1.130 g/cm^3 (described for 100 mL batch).

- Add 25 mL of iodixanol to a formulation container.
- Add 20 mL of 5 M NaCl, 20 mL of 5× PBS-MK, and 35 mL of WFI to the container.

- Mix the solution by inverting of swirling multiple time.
- Sterile filter the solution and aliquot in appropriate sizes.
- Store aliquots protected from direct light exposure at 12–25°C until use.

(i) Iodixanol 25% – phenol red, density = 1.117–1.130 g/cm^3 (described for 100 mL batch).

- Add 42 mL of iodixanol to a formulation container.
- Add 20 mL of 5× PBS-MK, 3 mL phenol red, and 35 mL of WFI to the container.
- Mix the solution by inverting of swirling multiple time (see Note 2).
- Sterile filter the solution and aliquot in appropriate sizes.
- Store aliquots protected from direct light exposure at 12–25°C until use.

(j) Iodixanol 40%, density = 1.212–1.225 g/cm^3 (described for 100 mL batch).

- Add 67 mL of iodixanol to a formulation container.
- Add 20 mL of 5× PBS-MK, 13 mL of WFI to the container.
- Mix the solution by inverting of swirling multiple time.
- Sterile filter the solution and aliquot in appropriate sizes.
- Store aliquots protected from direct light exposure at 12–25°C until use.

(k) Iodixanol 60% – phenol red, density = 1.307–1.325 g/cm^3 (described for 100 mL batch).

- Add 59.6 mL of iodixanol to a formulation container.
- Add 0.650 mL of phenol red to the container.
- Mix the solution by inverting of swirling multiple time (see Note 3).
- Sterile filter the solution and aliquot in appropriate sizes.
- Store aliquots protected from direct light exposure at 12–25°C until use.
- SP Sepharose buffers (see Subheading 2.2).

3. Methods

It is important to note that execution of these protocols must carefully follow the regulatory requirements for manipulation of viral vectors and genetically modified organisms.

3.1. Generation and Selection of Stable Packaging Cell Lines for rAAV Production

This procedure was originally described by Chadeuf and colleagues, and was used for the generation of the HeLa-derived AAV-2 packaging cell line HeRC32 (70, 71). It has also been used for the generation of other HeLa and A549-derived packaging cell lines for various AAV serotypes (Blouin et al., unpublished data). The critical point for efficient rAAV production from packaging cell lines is the required induced amplification of the *rep–cap* sequences upon helper virus (e.g., wild-type adenovirus type 5) infection (Fig. 1), which relies on the presence of a replication element within the *rep* promoter (72, 73). Although such a replication element is likely to exist in most of the AAV serotypes, the use of *rep–cap* hybrid constructs (i.e., containing *rep* from AAV-2 and *cap* from another serotype) might be preferred, since a large majority

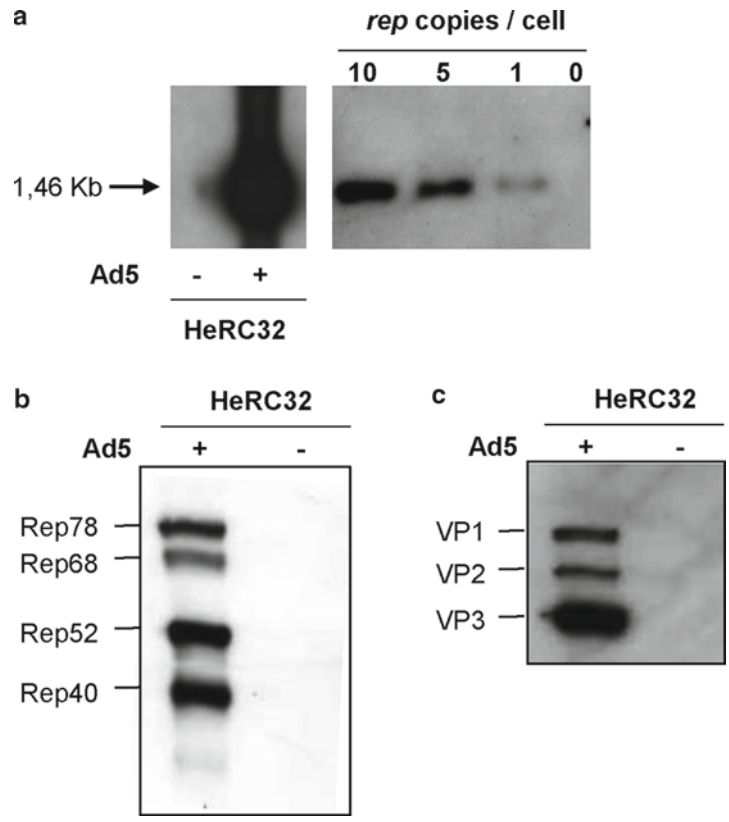

Fig. 1. Analysis of adenovirus-induced *rep–cap* gene amplification and protein expression in HeLa-derived packaging cell line HeRC32. HeRC32 cells were infected (+) or uninfected (–) with wild-type adenovirus type 5 (Ad5) and harvested after 48 h. (**a**) Total cellular DNA was digested with *Pst*I restriction endonuclease and analyzed by Southern blot hybridization with a 509 bp *rep* probe generated through *Sfi*I-*Bam*HI digestion of plasmid pRC. A standard curve was generated using *Pst*I-digested plasmid pRC to assess *rep* copy number per cell. (**b, c**) Cellular proteins were analyzed by Western blot using anti-Rep 303.9 (**b**) and anti-Cap B1 (**c**) monoclonal antibodies (Progen).

of rAAV vectors uses ITR sequences from AAV serotype 2 (and are pseudotyped with the capsids of different AAV serotypes) (17).

The following protocol has been optimized as a continuous process, for screening of critical parameters required to select packaging cell clones, from initial cell transfection to production and stability study, as well as for conservative use of reagents and supplies.

1. Generation of cell clones.
   (a) Seed HeLa or A549 cells in 10-cm dishes and grow cells until 70–80% confluence.
   (b) Day 1: Co-transfect cells with two plasmids, pRC containing the AAV rep–cap genes (without ITR) and pPGK-Neo containing a Neomycin resistance expression cassette, at a 10:1 ratio (10 μg of pRC and 1 μg of pPGK-Neo).
   Cells can be transfected following standard calcium–phosphate precipitation protocol (using 2.5 M $CaCl_2$ and 2× HEPES-buffered saline) or other commercially available transfection reagents.
   (c) Day 2: Dissociate the cells with trypsin-EDTA, resuspend cells in culture medium, and seed four to ten 10-cm dishes with various cell densities (cell suspension diluted 1:5 to 1:15).
   (d) Day 3: Add selection medium to the cells, i.e., DMEM supplemented with 10% FBS containing 1 mg/mL Geneticin (see Note 4).
   (e) Day 5–30: Change selection medium every 2 days to maintain selection pressure until appearance of isolated cell clones, and continue until completion of clone isolation (step 1g).
   (f) Localize cell clones using an inverted microscope, and pick up isolated cell colonies (containing 10–100 cells) using a 200-μL micropipette (see Note 5).
   (g) Expand picked clones in 48-well plates in culture medium with Geneticin.
   (h) Continue cell clones expansion in 6-well plates until 80–100% confluence, in culture medium without Geneticin (see Note 6).
2. PCR screening and expansion of rep–cap positive clones.
   (a) Harvest ~3/4 of cells from each well of 6-well plates for DNA isolation and let the remaining cells grow in the well with fresh medium.
   (b) Perform cell DNA isolation, using NucleoSpin Blood kit or equivalent.

(c) Screen clones by standard PCR for the presence of (1) rep and (2) cap sequences. Run PCR products in agarose gels stained with ethidium bromide or other DNA staining reagent (see Note 7).

(d) Expand PCR positive clones (for both rep and cap) in one 10-cm dish, then in two 10-cm dishes, until 80–90% confluence.

(e) Use one 10-cm dish to prepare two vials for cell freezing, in medium containing 10% DMSO; freeze cells at –80°C or liquid nitrogen.

3. Screening of clones for their ability to amplify rep–cap sequences in the presence of adenovirus by Southern blot hybridization.

(a) Use the other 10-cm dish to seed three wells of a 6-well plate; grow cells until they reach 80–90% confluence.

(b) Harvest one well of the 6-well plate and count cells; calculate the volume of adenovirus (wild-type human Ad5) to get a MOI of 100 ip/cell. Use the harvest cells to seed a 10-cm dish to keep the cells growing.

(c) Dilute the calculated volume of Ad5 in 2 mL of medium (containing 5% maximum of FBS) and replace medium from the second well with this Ad5-containing medium. Change medium from the third well. Incubate both wells for 48 h.

(d) Harvest cells from both wells of 6-well plate, and use 3/4 of the cells for standard DNA isolation using over-night proteinase K digestion, phenol–chloroform extraction and isopropanol precipitation (see Note 8). Wash the remaining 1/4 of the cells with 1× PBS and freeze as a dry pellet for Western blot analysis (step 4a).

(e) Digest 10 μg of DNA from infected and uninfected cells with appropriate restriction enzyme and separate digestion products by overnight electrophoresis in 1% agarose gel in 1× TAE. Use serial dilutions of known amount of the rep–cap plasmid, digested with the same enzyme, as a control for size and copy number (see Note 9).

(f) Transfer DNA from gel to positive nylon membrane in 10× SSC using standard Southern blot protocol, and hybridize the membrane with an alkaline phosphatase-labeled rep probe matching with a single digestion product (labeling performed using AlkPhos Direct kit) overnight at +55°C.

(g) Wash the membrane according to the AlkPhos Direct protocol and perform chemiluminescence detection of hybridization product using CDP-Star substrate.

Positive cell clones should show a rep signal equivalent to 1–10 copies of the rep–cap plasmid per cell genome in the absence of adenovirus. At least 100-fold signal amplifi-

cation (100–1,000 rep copies per cell genome) should be induced upon adenovirus infection. A previously characterized packaging cell line (e.g., HeRC32 cells) can be used as a control (see Fig. 1a).

4. Screening of clones for their ability to express Rep and Cap proteins in the presence of adenovirus by Western blot.
   (a) Thaw the dry cell pellets prepared from the 1/4 of harvested wells of 6-well plate, with and without adenovirus (step 3d), and perform standard protein extraction in RIPA buffer (see Note 10).
   (b) Load 10–20 μg of total proteins per well, from Ad-infected and uninfected cells, into two 10% SDS-PAGE gels. Run the gels for 1–2 h at 100 V in Tris–Glycine–SDS buffer.
   (c) Transfer proteins from gels onto Nitrocellulose membranes. Probe one membrane with anti-AAV2 Rep 303.9 antibody and the other membrane with anti-Cap B1 antibody, diluted in PBS – 0.1% Tween 20 – 5% milk.
   (d) Incubate membranes with HRP-conjugated anti-mouse antibody in the same buffer, and perform chemiluminescence detection of hybridization product using ECL substrate (Pierce).

   Positive cell clones should show no Rep or Cap expression in the absence of adenovirus. A strong expression of all four Rep and all three Cap proteins (VP1, VP2, and VP3) should be induced upon adenovirus infection. A previously characterized packaging cell line (e.g., HeRC32 cells) can be used as a control (see Fig. 1a, b).

5. Screening of clones for their ability to produce recombinant AAV in the presence of adenovirus.
   (a) Recombinant AAV production:
      i. Seed the cell clones into two 15-cm dishes and grow cells until 80–90% confluence.
      ii. Harvest one 15-cm dish and count the cells; calculate the volume of adenovirus (wild-type human Ad5) to get a MOI of 10 ip/cell.
      iii. Transfect the cells in the other dish with plasmid pAAV-CMV-GFP (recombinant AAV-2 vector plasmid containing an eGFP expression cassette), or another plasmid containing a reporter gene under the control of a ubiquitous promoter (e.g., CMV). Use 12.5 μg of vector plasmid DNA per 15-cm dish.
      iv. 6 h Posttransfection, dilute the calculated volume of Ad5 (from step 5a-ii) in 20 mL of medium containing 5% maximum of FBS, and replace medium used for transfection with this Ad5-containing medium. Incubate cells for 48–72 h.

v. Harvest cells in medium by pipetting up and down (using a cell scraper if necessary), pellet cells by centrifugation at 800 × *g* for 5 min, and resuspend cell pellet in 1 mL 50 mM HEPES–150 mM NaCl buffer.

vi. Perform cell lyses by three freeze–thaw cycles, and inactivate adenovirus by 30 min incubation at +56°C (see Note 11).

vii. Centrifuge cell lysate at 3,000 × *g* for 15 min at +4°C and transfer supernatant into a new tube. Use this rAAV crude lysate immediately or store at −80°C.

(b) rAAV genome titer determination:

i. Digest 10 or 20 μL of the crude lysate with DNaseI, in DMEM without FBS, for 30 min at 37°C to remove unpackaged vector DNA (see Note 12).

ii. Extract AAV DNA using proteinase K digestion, phenol–chloroform extraction, and ethanol precipitation, or using NucleoSpin Blood kit or equivalent.

iii. Prepare serial dilutions of the purified AAV DNA and determine the titer by either dot blot hybridization with an alkaline phosphatase-labeled GFP probe (see Subheading 3) (see steps 3f and 3g) or quantitative PCR. Prepare the standard curve with the rAAV-2 vector plasmid used for production.

The calculated GFP copy number in the sample reflects the rAAV genome titer, expressed as viral genomes (vg) or DRP.

(c) rAAV transducing titer determination:

i. Seed HEK293 cells in 6-well plates and grow cells until 90–100% confluence. Prepare at least six wells per crude lysate to be titrated, plus one additional well.

ii. Harvest one well and count the cells; calculate the volume of adenovirus (wild-type human Ad5 or E1-deleted Ad5, e.g., mutant dl324) to get a MOI of 4 ip/cell in each well to be infected.

iii. Dilute the calculated volume of Ad5 in sufficient volume of medium to get 2 mL per well, and replace medium in each well with this Ad-containing medium.

iv. Add different volumes of the rAAV crude lysate (e.g., 0.5, 1, 5, and 10 μL) to the Ad-containing medium in the wells. Test each volume in duplicate.

v. After 24 h incubation, count the cells expressing GFP in each well using an inverted fluorescent microscope. Calculate the number of rAAV vectors expressing GFP in the crude lysate by taking into consideration the dilution factor.

The calculated quantity of AAV expressing GFP, or GFP forming units (GFU), reflects the AAV transducing titer, expressed in transducing units (TU). Determination of the TU titer, when possible (e.g., when using GFP as the transgene) reflects the number of infectious particles efficiently expressing the transgene (see Note 13).

From the packaging cell clones first selected by Southern blot and Western blot assays, the best clones are selected from the results of the rAAV-GFP production assay. The stability and reproducibility of rAAV-GFP production for up to 30 cell passages is then tested on the selected clones. Further characterization is then performed on the stable clones, such as stability of the integrated rep–cap copy number, stability of AAV protein expression, and production of rAAV vectors carrying different transgenes and at different scales.

3.2. Purification of AAV Serotype 2 and 5 by IEX Chromatography

In 2002, an original and versatile procedure for AAV2 and AAV5 purification was described, which was entirely based on two IEX chromatography steps. This process could be applied directly using a crude cellular lysate without any treatment with detergents or nucleases, and resulted in rAAV stocks that were pure as determined by silver staining and had the same biological characteristics as particles purified following other traditional methods like CsCl gradients or iodixanol/heparin purification. The average recovery of transducing particles was evaluated at 44% for AAV2 and 33% for AAV5 (40).

Briefly the rAAV is extracted from the cell pellet by three freeze–thaw cycles. The crude lysate is centrifuged, heated at +56°C to inactivate helper virus, centrifuged again, and the supernatant is filtered. rAAV is then purified by two successive chromatography steps: (1) cation exchange (SP Sepharose HP, GE Healthcare), and (2) anion exchange (Source 15Q, GE Healthcare). This method was demonstrated to be successful for recombinant AAV produced either following transient transfection of HEK293 cells or using a stable packaging cell line infected with either adenovirus type 5 (40) or HSV-1 (19). The method is scalable and applicable to different AAV serotypes by adjusting salt concentrations during the chromatography steps.

1. Cell lysate preparation:
   (a) Harvest cells and centrifuged for 15 min at 800 × *g*.
   (b) Resuspend cell pellet in lysis buffer (25 mM $NaHPO_4$, 20 mM NaCl, 2 mM $MgCl_2$, pH 7.0).
   (c) Perform cell lysis by three freeze–thaw cycles (see Note 14).
   (d) Centrifuged the crude lysate at 10,000 × *g* for 15 min at 4°C.
   (e) Heat the crude lysate at +56°C for 30 min and centrifuge again at 3,000 × *g* for 10 min at +4°C (see Note 15).
   (f) Collect the supernatant and filter through 5 + 0.45 μm PVDF filters.

2. rAAV purification:
   (a) Dilute the filtered supernatant in 25 mM $NaHPO_4$, 150 mM NaCl (for rAAV2), or 100 mM NaCl (for rAAV5) plus 2 mM $MgCl_2$, pH 6.5.
   (b) Inject the diluted supernatant into a SP Sepharose HP column.
   (c) Wash with 25 mM $NaHPO_4$, 150 mM NaCl (for rAAV2), or 100 mM NaCl (for rAAV5) plus 2 mM $MgCl_2$, pH 6.5.
   (d) Elute rAAV using a linear NaCl gradient, up to 500 mM NaCl (see Note 16).
   (e) Dilute the rAAV eluted from first column to 20 mM Tris, 50 (for AAV2), or 20 (for AAV5) mM NaCl, 2 mM $MgCl_2$, 1 mM $CaCl_2$, pH 8.2.
   (f) Inject the diluted rAAV into a Source 15Q column.
   (g) Wash with 20 mM Tris, 50 (for AAV2) or 20 (for AAV5) mM NaCl, 2 mM $MgCl_2$, 1 mM $CaCl_2$, pH 8.2.
   (h) Elute rAAV using a linear NaCl gradient, up to 500 mM NaCl (see Note 17).

3.3. Production and Purification of AAV Serotype 1 Using Dual rHSV Infection and Anion Exchange/Affinity Chromatography

In this protocol, originally developed in 2009 (30), recombinant AAV1 is produced by rHSV co-infection of suspension BHK cells, using two ICP27-deficient rHSV vectors, one harboring the rAAV vector and a second harboring the AAV rep2 and cap1 genes. 10 L of rAAV1 production is done in disposable Wave bioreactors, and volumetric productivities as high as 2.4×10^{15} DRP per 10 L of culture can be achieved. Cell culture is in situ lysed, harvested, depth filtered, and sterile filtered, concentrated and buffer exchanged before column chromatographic steps. A fully scalable two-column chromatography process using anion exchange as a capture step followed by an affinity column is carried out to generate clinical-grade rAAV vectors; details are described by Wang and colleagues (56–58).

1. Recombinant HSV production rHSV-rep2/Cap1 and rHSV-rAAV vectors are propagated on the ICP-27 complementing V27 cell line (74), in a 3.5-L packed-bed bioreactors, supernatant is depth filtered and concentrated by tangential flow filtration (TFF), formulated at $>1.5 \times 10^9$ pfu/mL. This procedure was described in detail by Knop and colleague (34).
2. AAV production:
   (a) Seed BHK cells in 25 mL spinner flask.
   (b) Grow seed train in spinner flasks.
   (c) Seed 4 L volume in a 10 L Wave bag at $2.5–3.5 \times 10^5$ cell/mL.
   (d) Dilute to 10 L at 24 h postseeding. Culture pH is maintained at pH 7.2 (see Note 18). Agitation is maintained at 20 rocks/min at an angle of 6.8°. Temperature is main-

tained at 37°C. A total headspace gas flow rate of 0.1 volume gas/volume culture/min (vvm) is used.

(e) Co-infect 24 h later with two rHSV vectors using optimized MOI 4:2 (rHSV-rAAV vector: rHSV-rep2/cap1) when cell density reaches $1.4–2.2 \times 10^6$ cell/mL (see Note 19).

(f) At 2–4 h postinfection (hpi) medium is exchanged with serum-free DMEM (see Note 20). This is accomplished with flat sheet TFF using 0.45 μm nominal pore size Hydrosart membranes. Volume is reduced five- to tenfold and culture is diluted back to the preinfection volume with DMEM lacking FBS.

(g) Harvest the culture at 24 hpi following the steps:

- Add 10% Triton X-100 to the Wave bag to a final concentration of 1% (v/v).
- Add benzonase (see Note 21).
- Rock the mixture at 37°C for 2–4 h.
- Filter the lysate using a filter train: depth filter (1.2 mm) and dead end filter (0.8/0.45 μm).
- Store filtered harvest at 2–8°C until ready for downstream purification.

3. TFF: 10 L of clarified lysate is concentrated and buffer exchanged using 100 kDa MWCO hydrosart membranes (see Note 22).

4. Two-step chromatography (Q-AVB):

(a) Preequilibrate Q column with 20 mM Tris, 70 mM NaCl, pH 8.0 (buffer A).

(b) Dilute rAAV1 lysate with Tris buffer so that the conductivity of the feed is lower than that of the equilibration buffer, filter through 0.22 μm sterile filter.

(c) Load diluted lysate onto Q column.

(d) Wash unbound molecules off the column with buffer A.

(e) Use 20 mM Tris, 260 mM NaCl, pH 8.0 to step elute rAAV1; collect peak.

(f) Preequilibrate AVB column with 100 mM Tris–HCL, pH 8.5 (buffer B).

(g) Load the Q eluent onto AVB column.

(h) Wash unbound molecules off the AVB column with buffer B.

(i) Step elute rAAV1 with 100 mM sodium citrate containing 100 mM NaCl, pH 3.5 (see Note 23). The affinity column eluent is neutralized to pH 7.0–8.0 (see Note 24).

(j) Formulate rAAV1 to target concentration in desired buffer via TFF (see Note 25).

3.4. Production and Purification of Clinical-Grade AAV Vector by Transient Transfection and Iodixanol Gradient Centrifugation

Similar to the protocol developed by Zolotukhin et al. (63), following transfection of HEK293 cells, rAAV is purified in three steps. First, the crude cell lysate containing rAAV virions (Partial Crude Lysate, PCL) is generated by lysing the transfected cells. The PCL is then purified using centrifugal and chromatographic methods. The purified bulk is formulated, filtered, and filled. The three production steps are executed under cGMP standards using approved production batch records and standard operating procedures. All activities during production must be properly documented.

1. Production of PCL: An example of production process flow chart for rAAV type 2 using transient transfection of ten 10-layer cell factories (CF-10) seeded with HEK293 cells is presented in Fig. 2. Typically, vials of HEK293 (WCB) are thawed and seeded into two T-75 cm^2 flasks containing DMEM without sodium pyruvate supplemented with 5% FBS and 40 μg/mL Gentamicin. Flasks are incubated at 37 ± 1°C in a 5 ± 3% CO_2 humidified incubator. After reaching 80–90% confluence, cells are detached from the flasks using 1× trypsin. The cells are collected and used to seed more flasks and larger vessels. This process continues until ten 10-layer cell factories (CF-10) have been seeded with 8×10^8 cells each. At 70–90% confluence, each CF-10 is co-transfected with 1.8 mg/CF-10 of helper plasmid and 0.6 mg/CF-10 of plasmid containing the gene of interest using the calcium–phosphate mediated transient transfection method. Transfected cells are harvested at 60–72 h posttransfection and samples are prepared with cell resuspended in spent media (Table 6). Remaining cells are pooled and processed to generate a PCL by two cycles of freeze and thaw that is then stored at ≤–70°C until purification. Purification procedures are described below.
   (a) 1× Trypsin preparation (described for 20 mL of 1× trypsin).
      - Add 18 mL of PBS-CMF to one sterile bottle.
      - Add 2 mL of 10× trypsin to the bottle.
      - Swirl the bottle several times to mix.
   (b) Cell passage (see Note 26).
      - Aspirate or discard media from flasks of CF-10s into a waste container. Carefully rinse the cell monolayer with 5, 15, or 500 mL of PBS-CMF for T-75, T-225, or CF-10, respectively.
      - Gently rock flasks or CF-10 back and forth two to four times.
      - Aspirate or discard the PBS-CMF from flasks or CF-10s in a waste container.
      - Add 2, 5, or 200 mL of 1× trypsin to each T-75, T-225, or CF-10, respectively, and incubate at room temperature until cells start to detach (1–1.5 min) (see Note 27).

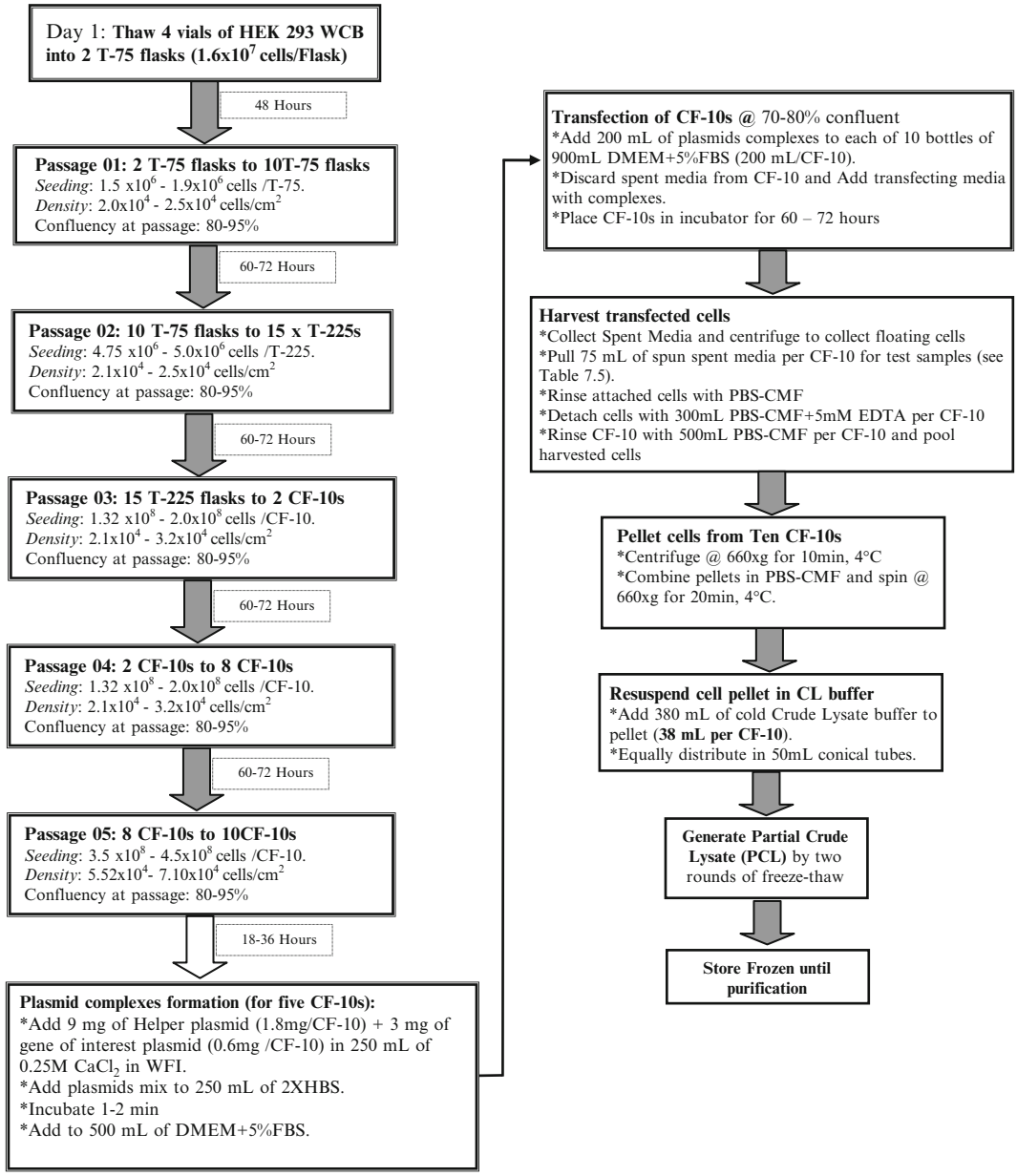

Fig. 2. Process flow chart for rAAV type 2 production in HEK293 cells using transient transfection of ten 10-layer cell factories (CF-10).

Use caution that the 1× Trypsin is not delivered directly onto the cell layer.

- Lightly tap flasks or CF-10s to loosen cells and add 18, 45, or 400 mL of DMEM complete to each flask or CF-10 to stop trypsin action.
- Pool cells in a new sterile container and disperse clumps by pipetting up and down.

Table 6
Partial Crude Lysate harvest test samples

Sample quantity (mL)	Cells	Test	Storage temperature (°C)
2 × 5	5×10^7	Bioburden	2–8 or ≤–70
2 × 15	1.5×10^8	Mycoplasma	≤–70
2 × 6	6×10^7	In vitro contaminants	≤–70
10 × 2	2×10^7	QC Retains	≤–70

- Pipette approximately 0.3 mL of the cell suspension into a sterile microcentrifuge tube.
- Determine viable cells concentration and calculate the volume of cell suspension necessary to seed at the appropriate seeding density and the volume of DMEM complete needed per flask or CF-10 (Fig. 2).
- Place each vessel horizontally in the BSC and move back and forth and side to side to evenly distribute cells.
- Incubate cells in a 37 ± 1°C, 5 ± 3% CO_2 humidified incubator.

(c) Plasmid Complex Formation and transfection (for transfection of five CF-10) (see Note 28).

- Prepare plasmid DNA mixture in 0.25 mM $CaCl_2$.
  - Prepare one 1,000 mL polystyrene bottle containing 500 mL of DMEM complete. Label the bottle "Transfection Mixture."
  - Label one 500 mL polystyrene bottle "DNA Mixture."
  - Add 213 mL of WFI to the bottle.
  - Mix the 2.5 M $CaCl_2$ solution and add 25 mL to the bottle.
  - Swirl the bottle to thoroughly mix the $CaCl_2$/WFI mixture.
  - Mix the Helper plasmid and transfer 9 mL into the bottle.
  - Mix the vector plasmid and transfer 3 mL into the bottle.
  - Swirl the bottle again to thoroughly mix.
- Prepare transfection mixtures (see Note 29).
  - Label a second 500 mL polystyrene bottle "Complexes."

- Transfer 250 mL of 2× HBS to the bottle.
- Swirl the "DNA Mixture" bottle and pour the entire mixture into the bottle containing 2× HBS.
- Quickly swirl the bottle two to three times and allow the complexes to form at room temperature without further mixing.
- Visually monitor the precipitate formation until it becomes slightly hazy (precipitate formation should take 1–2 min).
- When a fine precipitate has formed, immediately add the 500 mL of the precipitate to the 500 mL of media in the "Transfection Mixture" bottle prepared above.
- Swirl the bottle two to three times to mix.
- Transfer approximately 200 mL of "Transfection Mixture" into each of 5 × 900 mL of DMEM complete bottles.

• Remove the culture media from the CF-10 and use a bottle of media containing the DNA precipitate to transfect a CF-10 and incubate for 60–72 h at 37°C, 5% CO_2 (Fig. 2).

(d) Cell harvest.

• Pour spent media from each CF-10 into a sterile bottle. Label "Spent media."

• Add 500 mL of PBS-CMF to the CF-10. Evenly distribute PBS-CMF in the CF-10 and hold.

• Pipette 100 mL from each CF-10 of spent media from each "Spent media" bottle and transfer into the "Spent Media Pool" bottle.

• Gently rock the CF-10 containing 500 mL of PBS-CMF to wash the cells and discard the PBS-CMF wash.

• Add approximately 300 mL of PBS-5 mM EDTA to each CF-10 and evenly distribute in the CF-10. Allow the CF-10 to sit in the BSC for 5–15 min and observe that cell layers start to detach.

• Rock the CF-10 until the cells are completely detached from the CF-10. Examine the CF-10 to ensure that cells have detached from all levels. Transfer the entire CF-10 cell suspension into a 1,000 mL bottle.

• Add 500 mL PBS-CMF to the CF-10 and evenly distribute to harvest remaining cells from the CF-10. Transfer the PBS-CMF wash into the previous 1,000 mL bottle containing harvest cells.

• Swirl bottles containing the cells, transfer 60 mL of cell suspensions to a new bottle labeled "Samples."

(e) Collect test samples.

- Mix thoroughly the "Samples" bottle and equally distribute into two new 500 mL centrifuge bottles.
- Pellet the cells at 660 × *g* for 20 min at 4°C.
- Resuspend each pellet in 25 mL of spent media from the "Spent Media Pool" bottle.
- Transfer and combine the cell suspension from the two centrifuge bottles.
- Rinse the empty bottle with an additional 25 mL of spent media from the "Spent Media Pool" bottle and combine the 25 mL spent media wash with the 50 mL cell suspension.
- Testing samples may be prepared from the obtained cell suspension as outlined in Table 6.

(f) Preparation of PCL.

- Progressively swirl each harvest cell suspension bottle and equally distribute in 500 mL centrifuge bottles. Centrifuge cells at 660 × *g* for 20 min at 4°C to pellet the cells and discard the supernatant.
- Repeat the operation until all cells have been centrifuged.
- Wash each empty centrifuge bottle with 100 mL of PBS-CMF and equally distribute the PBS-CMF wash in the centrifuge bottles and repeat centrifugation.
- Resuspend each pellet in 25 mL of PBS-CMF. Transfer and combine all cell suspension in one of the 500 mL centrifuge bottle.
- Add an additional 25 mL of PBS-CMF to each 500 mL centrifuge bottle to rinse and centrifuge cells at 660 × *g* in a GR4i centrifuge for 20 min at 4°C.
- Prepare a dry ice–ethanol bath in a bath tray outside the BSC by combining 1 part dry ice and 2 parts ethanol.
- Without disturbing the cell pellet aspirate all of the supernatant from the cell pellet.
- Thoroughly resuspend the pellet in 250 mL of cold crude lysate buffer.
- Equally distribute the cell suspension in 20 new 50 mL conical tubes (two conical tubes per CF-10).
- Add an additional 70 mL of cold crude lysate buffer to 500 mL centrifuge bottle to rinse.
- Equally distribute the 70 mL of crude lysate buffer wash into the twenty 50 mL conical tubes.

- Swirl each 50 mL conical tube and snap-freeze the cell suspension by placing the 50 mL conical tubes into the dry ice–ethanol bath. Incubate until lysate is completely frozen.
- Thaw the frozen cell suspension by placing the tubes into a 37°C water bath. Mix by swirling every 5 min. Remove from the 37°C water bath when only a small amount of ice remains and complete thaw at room temperature by swirling.
- Repeat freeze and thaw steps one more time.

2. Production of purified bulk by iodixanol gradient centrifugation: Cell lysate is purified chromatographically, using centrifugal or filtration methods. When using chromatography media, appropriate sanitization is required prior to use. It is preferred that purification steps are carried out using closed systems. Single use disposable containers such as flexible bioprocess bags are recommended. Following purification, all process equipment undergoes cleaning and sanitization using appropriate agents such as NaOH or steam according to established standard operating procedures. Many purification methods have been successfully used to purify rAAV vector. Depending on the amount of vector needed for the study, a simple centrifugation method such as iodixanol gradient (see Table 5 for references) can be used in cGMP production. Iodixanol purified vector can be further purified by using heparin affinity column or sulfo-propyl (SP) cation exchange column.

   The procedure described below allows for rAAV vector purification from PCL using ultracentrifugation generated iodixanol gradient purification.

   (a) Thaw the rAAV2 Vector PCL.

   - Immerse lower half of 50 mL conical PCL tubes into a 37°C water bath to thaw. Swirl tubes every 5 min.
   - Remove tubes from the water when only a small amount of ice remains and complete thaw at RT.

   (b) Treat Crude Lysate with benzonase.

   - Inside the BSC, individually measure the thawed CL in each 50-mL conical tube using an appropriate sized pipette.
   - Calculate the amount of benzonase needed for each measured volume of CL to incubate at 50 U/mL of enzyme.
   - Add the calculated amount of benzonase to each tube of CL, respectively, and recap. Swirl each of the CL tubes briefly after the addition of benzonase.

- Place the CL tubes in the 37°C incubator for 30 min. Swirl each tube for every 5 min.

(c) Clarify the benzonase-treated crude lysate.

- Centrifuge the tubes at 2,500 × *g* for 20 min at 20–25°C.
- When the centrifuge has stopped, carefully remove CL tubes from the centrifuge. Wipe all tubes with disinfectant and place into the BSC.

(d) Prepare the iodixanol ultracentrifugation tubes. If needed, multiple sets of tubes can be prepared for ultracentrifugation to obtain required total number of particles before chromatography. This protocol uses a set of eight tubes per T70i rotor.

- Place eight autoclaved Optiseal centrifuge tubes in one tube rack.
- Pipette 10 mL of clarified CL into each tube by tilting the rack at approximately 45° angle to avoid bubbles.
- Attach a 20 mL syringe to a blunt end needle. Fill the syringe with the 15% iodixanol–1 M NaCl solution approximately 1 mL above the 20 mL line. Invert the syringe-needle assembly and aspirate the solution from the needle.
- Remove air bubbles from the syringe and adjust the solution level to the 20 mL line.
- Insert the assembly into the first centrifuge tube containing the CL. The needle tip should rest on the bottom of the tube, slightly off perpendicular to allow for liquid flow. Slowly underlay the CL by injecting 2.5 mL of the 15% iodixanol–1 M NaCl solution at the bottom of the tube (see Note 30).
- Successively transfer the assembly into the remaining centrifuge tubes and underlay the CL as described above.
- Attach a new 20 mL syringe to a new blunt end needle. Fill the syringe with the 25% iodixanol–phenol red solution approximately 1 mL above the 20 mL line. Invert the syringe-needle assembly and aspirate the solution from the needle.
- Following the same steps described above, insert the assembly into the tube containing the CL + 15% iodixanol–1 M NaCl. Slowly underlay the 15% iodixanol–1 M NaCl solution by injecting 5 mL of the 25% iodixanol–phenol red solution at the bottom of the tube.

- Attach a new 20 mL syringe to a new blunt end needle. Fill the syringe with the 40% iodixanol solution approximately 1 mL above the 15 mL line. Invert the syringe-needle assembly and aspirate the solution from the needle.
- Following the same steps described above, insert the assembly into the first centrifuge tube containing the CL + 15% Iodixanol–1 M NaCl + 25% iodixanol–phenol red. Slowly underlay the 25% iodixanol–phenol red solution by injecting 7.5 mL of the 40% iodixanol solution at the bottom of the tube.
- Attach a new 20 mL syringe to a new blunt end needle. Fill the syringe with the 60% iodixanol–phenol red solution approximately 1 mL above the 20 mL line. Invert the syringe-needle assembly and aspirate the solution from the needle.
- Following the same steps described above, insert the assembly into the eighth centrifuge tube containing the CL + 15% iodixanol–1 M NaCl + 25% iodixanol–phenol red + 40% iodixanol. Slowly underlay the 40% iodixanol solution by injecting 5 mL of the 60% iodixanol–phenol red solution to the bottom of the tube.

(e) Top off the centrifuge tubes, cap, and centrifuge.

- With a 1 mL pipettor, top off the centrifuge tubes to the neck with clarified crude lysate. Make sure to equally fill all the tubes.
- Cap the "Clarified CL" bottle (see Note 31).
- Close each tube with a dry sanitized centrifuge tube plug. Apply the special top of the rack and press to obtain complete closure of the tubes.
- Remove the top of the rack. Pair the plugged tubes using an analytical balance and carefully transfer the tubes into the 70Ti rotor. Cover each tube with an amber spacer and close the rotor.
- Carefully transfer the rotor to the ultracentrifuge.
- Centrifuge tubes at 69,000 rpm for 1 h at 18 ± 1°C. Set for maximal acceleration and slow deceleration.

(f) Collect vector from tubes postultracentrifugation.

- Wipe down two ring stands and two clamps with disinfectant and place them in the BSC.
- Using the empty centrifuge tube rack, preadjust the gap between both ring stands and the height of the clamps to secure the rack and have the 60–40% iodixanol interface at a comfortable height to collect vector.

- Upon completion of the ultracentrifugation, remove the 70Ti rotor from the ultracentrifuge and slightly loosen the lid. Wipe down the rotor with disinfectant and place in the BSC.
- Unscrew the 70Ti rotor lid and remove the spacers. Remove each tube from the rotor using tweezers and transfer the tube to the second empty centrifuge tube rack.
- Cover the rack containing tubes with the holed rack top, allowing the plugs of the tubes to appear. Remove the plugs of the tubes with tweezers and replug them immediately.
- Carefully secure the centrifuge tube rack with the holed rack top between both ring stands. Make sure the clamps are tight and the rack is horizontal. Place a 1 L beaker underneath the tube rack.
- Wipe the appearing side of the tube to be punctured with a 70% IPA wipe.
- Use a sharpie to mark the 60–40% iodixanol interface (yellow – colorless interface) on each tube with a straight fine line.
- Attach a 5 mL syringe to an 18 G, 1.5 in. needle. Pull and push the plunger of the syringe once to make it easier to move the plunger when extracting the vector.
- Steady the tube by holding the rack and gently insert the needle into the side of the first tube, about 2.5 mm below the sharpie mark, with the bevel of the needle pointed upward.
- Steady the syringe, remove the plug of the centrifuge tube with the tweezers, and save it to stop liquid flow after vector has been collected.
- Extract carefully 3 mL (~1 mL from the yellow 60% iodixanol phase and ~2 mL from the colorless 40% iodixanol) of the vector by pulling the plunger of the syringe slowly, keeping the bevel of the needle at the same position.
- When 3 mL are extracted, recap the tube by reinserting the plug.
- Carefully remove the needle from the tube.
- Slowly transfer the recovered volume into a 150-mL polystyrene bottle.

Table 7
Purified bulk test samples

Test	Storage temperature (°C)
Bioburden (after purification or before formulation, filtration, and fill)	2–8 or ≤−70
Infectious titer Vector genome titer Purity pH Conductivity and/or osmolarity Residual host cell DNA Process residuals	≤−70

- Extract the vector from each of the remaining tubes by repeating the steps above and the same 150-mL polystyrene bottle. Change the needle if necessary.
- Iodixanol purified vector bulk can be stored at 2–8°C until further purification by cation exchange chromatography (SP Sepharose HP) as described in Subheading 3.2.

(g) Sampling the final purified bulk.

Following cation exchange or heparin affinity purification of the iodixanol purified vector sample listed in Table 7, unless otherwise preset. Osmolarity sample can be necessary to ensure that the final formulation step is appropriately made to the desired product osmolarity. When the purification involved multiple steps, in-process samples can be taken at major steps especially important during engineering production. These samples might be useful should an investigation has to be conducted.

3. Formulation and filling of final product: Purified bulk is tested based upon specifications required to formulate the final product (i.e., vector genome concentration, infectious titer, and osmolarity). The purified bulk is then thawed and formulated with the appropriate buffer at the proper concentration, and sterile filtered. The filtered bulk is filtered again and filled at the targeted volume into vials to generate the clinical lot. Vials are appropriately labeled and stored at the proper temperature. Samples are taken from the clinical lot to perform release testing (Table 8).

Table 8
Final product test samples

Sample quantity	Test	Storage temperature (°C)
Batch size: less than 100 vials: Four vials if >1 mL/vial Eight vials if <1 mL/vial	Sterility	≤–70
Batch size: less than 500 vials: Four vials if >1 mL/vial Eight vials if <1 mL/vial		
Batch size: more than 500 vials: 2% or 20 vials whichever is less		
One vial	Infectious titer	
One vial	Vector genome titer	
One vial	Capsid titer	
One vial	Transgene expression	
One vial	rcAAV	
One vial	Identity	
One vial	General safety	
One vial	Endotoxin	
One vial	Appearance	
One vial	pH	
One vial	Osmolarity	
Two vials per time point	Stability	
One vial	Aggregation	
One vial	Vector genome sequencing	

4. Notes

1. If pH of 2× HBS solution increases above 7.07 during NaOH addition, do not back titrate with HCl. Discard solution and make a new batch.
2. Solution of 25% iodixanol should turn red as pH solution is neutral.
3. Solution of 60% iodixanol should turn yellow since iodixanol pH is acidic.
4. In DMEM supplemented with 10% FBS, optimal Geneticin concentration for HeLa or A549 cells was determined to be 0.8–1 mg/mL. Different Geneticin concentration may have to be defined when using different serum concentration or medium type.
5. Use a pen to mark clone localization at the bottom of the culture dish, then remove culture medium, wash cells once

with 1× PBS, and recover cells with fresh 1× PBS. Isolated clones can be picked up directly by aspirating with a 200-µL micropipette. Alternatively, cloning cylinders can be used if the use of trypsin-EDTA to detached clones is preferred.

6. Integration of the rep–cap sequences within the cell genome should have been achieved at this stage. Thus, selection pressure is not required anymore.
7. Use 5 µL of total cellular DNA (from 100 µL eluted from the NucleoSpin column) in a 50 µL standard PCR. Load 20–25 µL of the PCR on agarose gel. PCR primers should be designed to amplify a 0.5–1.0 kb fragment specific for the rep and cap sequences; rep and cap PCRs should be performed separately.
8. Pellet cells by centrifugation, resuspend cell pellet in 1× PBS, and perform proteinase K digestion over night at +55°C in 1 mL final volume. After DNA precipitation with isopropanol, wash DNA pellet with 70% ethanol and dissolve DNA in 20 µL TE pH 8.0. Determine DNA concentration through OD_{260} measurement.
9. Perform restriction enzyme digestion in a 20–30 µL final volume. Use a suitable restriction endonuclease such as *Pst*I, which generates a 1,460 bp fragment within the AAV-2 rep sequence and digests efficiently mammalian genomic DNA. Prepare a rep–cap plasmid standard curve ranging from 0 to 100 copies/cell genome (10 µg of human DNA contains approximately 3×10^6 cell genome) in HeLa or A549 genomic DNA, and digest the standard curve together with the samples. After gel electrophoresis, check the gel under UV light to verify digestion efficiency: uninfected cells DNA should appear as a smear, whereas additional multiple bands corresponding to adenovirus DNA digestion products should be visible in Ad-infected cells.
10. As a control for protein extraction and Western blot, use a previously characterized packaging cell line (e.g., HeRC32 cells) or cells transfected with the rep–cap plasmid, infected or not with adenovirus. Use untransfected HeLa or A549 cells as a negative control.
11. For freeze–thaw cycles, use ice-cold ethanol (prepared with dry ice) and a +37°C water bath. Inactivate adenovirus in a +56°C water bath.
12. DNase digestion should not exceed 30 min to avoid degradation of encapsidated vector DNA.
13. The TU titer is dependent on the ability of the vector capsid to interact with the indicator cells and to properly deliver the rAAV genome into the cell nucleus. Thus, for a given quantity of DNA-resistant particles (as calculated by dot blot hybridization), the TU titer determined on HEK293 cells can greatly

differ from one capsid serotype to another and does not account for the efficiency of gene transfer in the target tissue in vivo.

14. Three freeze–thaw cycles are usually performed but we observed that AAV extraction was complete after only one cycle.
15. The temperature of the water bath has to be accurately adjusted at +56°C; at lower temperature, adenovirus inactivation may not be efficient, and a higher temperature may be deleterious for AAV. For example, we have observed a loss of AAV infectivity at +58°C. Also, note that the incubation time may have to be adjusted depending on the volume (i.e., large volumes may require longer incubation times).
16. At this step, a sharp peak of absorbance could not be visualized: the eluted fractions have to be screened for the presence of AAV.
17. At this step, a sharp peak of absorbance (at 280 and 260 nm) corresponding to the presence of AAV could be visualized.
18. The pH is maintained by headspace CO_2 addition. Dissolved oxygen (DO) is monitored until <50% saturation, and then headspace oxygen enrichment is used to maintain the DO at 50%.
19. The optimized rHSV MOI was determined experimentally. For different capsid serotype and length of gene of interest, this ratio may vary. For optimum results, this ratio is to be determined experimentally for each AAV vector.
20. The recirculation rates of 350–500 mL/min and the TMP is maintained at approximately 0.5 psig
21. A final concentration of 25–50 U/mL is commonly used. For optimum Benzonase activity, 2 mM of Mg^{2+} is required (Mg^{2+} concentration may be adjusted by the addition of $MgCl_2$ if needed). Benzonase concentration may be lowered to 1–10 U/mL to reduce the cost.
22. A recirculation rate of 0.5–1.5 L/min is used and the TMP maintains at 8.5 ± 1.5 psig.
23. To minimize the time rAAV is exposed in low pH elution buffer, collect peak into a tube that contains 1 M Tris, pH 8.5, as neutralization buffer. Volume of the neutralization buffer may vary depending on the column dimension and eluent volume.
24. If the pH of the eluent is out of 7.0–8.0 range, use 1 M Tris, pH 8.5, and 100 mM sodium citrate, 100 mM NaCl, pH 3.5, to adjust the final pH.
25. Buffer was exchanged to lactated Ringer's solution, using a 300-kDa MWCO hollowfiber cartridge.
26. It is critical to passage cells within 90% confluency throughout the seed train as overgrowing (>90%) cells may impair the

transfection efficiency. One needs to make sure that flasks and CF-10 are appropriately leveled in the incubator to obtain an evenly distributed cell monolayer.

27. Adherent HEK293 cells are known for being weakly attached to culture vessel. One needs to make sure not to prolong trypsin action. Depending on the trypsin used, this may result in cell damage including pronounced clumping in the suspension. Observing cells monolayer detaching from the vessel is a key element for the duration of trypsin action.
28. Ensure that both $CaCl_2$ and 2× HBS solutions are at equivalent temperature before use. It is recommended to equilibrate $CaCl_2$, 2× HBS and WFI containers at room temperature overnight.
29. Prepare the 500 mL of media to stop complex formation before the addition of 2× HBS. To monitor the complex formation, an equivalent volume of WFI can be added to the same type container and be used to evidence precipitation. Complex formation kinetic is temperature dependent.
30. Avoid fast injection of the 15% iodixanol–1 M NaCl solution. Fast injection will mix the CL with the iodixanol solution.
31. Handle centrifuge tubes with great care so as not to disturb the gradient steps during subsequent manipulations.

References

1. McLaughlin, S. K., Collis, P., Hermonat, P. L., and Muzyczka, N. (1988) Adeno-associated virus general transduction vectors: analysis of proviral structures, *J Virol* ***62***, 1963–1973.
2. Salvetti, A., Oreve, S., Chadeuf, G., Favre, D., Cherel, Y., Champion-Arnaud, P., David-Ameline, J., and Moullier, P. (1998) Factors influencing recombinant adeno-associated virus production, *Hum Gene Ther* ***9***, 695–706.
3. Merten, O. W., Geny-Fiamma, C., and Douar, A. M. (2005) Current issues in adeno-associated viral vector production, *Gene Ther* ***12***Suppl 1, S51-61.
4. Aucoin, M. G., Perrier, M., and Kamen, A. A. (2008) Critical assessment of current adeno-associated viral vector production and quantification methods, *Biotechnol Adv* ***26***, 73–88.
5. Urabe, M., Ding, C., and Kotin, R. M. (2002) Insect cells as a factory to produce adeno-associated virus type 2 vectors, *Hum Gene Ther* ***13***, 1935–1943.
6. Smith, R. H., Levy, J. R., and Kotin, R. M. (2009) A simplified baculovirus-AAV expression vector system coupled with one-step affinity purification yields high-titer rAAV stocks from insect cells, *Mol Ther* ***17***, 1888–1896.
7. Aslanidi, G., Lamb, K., and Zolotukhin, S. (2009) An inducible system for highly efficient production of recombinant adeno-associated virus (rAAV) vectors in insect Sf9 cells, *Proc Natl Acad Sci U S A* ***106***, 5059–5064.
8. Xiao, X., Li, J., and Samulski, R. J. (1998) Production of high-titer recombinant adeno-associated virus vectors in the absence of helper adenovirus, *J Virol 72*, 2224–2232.
9. Rabinowitz, J. E., Rolling, F., Li, C., Conrath, H., Xiao, W., Xiao, X., and Samulski, R. J. (2002) Cross-packaging of a single adeno-associated virus (AAV) type 2 vector genome into multiple AAV serotypes enables transduction with broad specificity, *J Virol 76*, 791–801.
10. Grimm, D., Kern, A., Rittner, K., and Kleinschmidt, J. A. (1998) Novel tools for production and purification of recombinant adenoassociated virus vectors, *Hum Gene Ther* ***9***, 2745–2760.
11. Collaco, R. F., Cao, X., and Trempe, J. P. (1999) A helper virus-free packaging system for recombinant adeno-associated virus vectors, *Gene* ***238***, 397–405.
12. Grimm, D., Kay, M. A., and Kleinschmidt, J. A. (2003) Helper virus-free, optically controllable,

and two-plasmid-based production of adeno-associated virus vectors of serotypes 1 to 6, *Mol Ther 7*, 839–850.

13. Gao, G. P., Qu, G., Faust, L. Z., Engdahl, R. K., Xiao, W., Hughes, J. V., Zoltick, P. W., and Wilson, J. M. (1998) High-titer adeno-associated viral vectors from a Rep/Cap cell line and hybrid shuttle virus, *Hum Gene Ther* ***9***, 2353–2362.
14. Liu, X. L., Clark, K. R., and Johnson, P. R. (1999) Production of recombinant adeno-associated virus vectors using a packaging cell line and a hybrid recombinant adenovirus, *Gene Ther* ***6***, 293–299.
15. Zhang, H., Xie, J., Xie, Q., Wilson, J. M., and Gao, G. (2009) Adenovirus-adeno-associated virus hybrid for large-scale recombinant adeno-associated virus production, *Hum Gene Ther* ***20***, 922–929.
16. Clark, K. R., Voulgaropoulou, F., Fraley, D. M., and Johnson, P. R. (1995) Cell lines for the production of recombinant adeno-associated virus, *Hum Gene Ther* ***6***, 1329–1341.
17. Blouin, V., Brument, N., Toublanc, E., Raimbaud, I., Moullier, P., and Salvetti, A. (2004) Improving rAAV production and purification: towards the definition of a scaleable process, *J Gene Med* ***6 Suppl 1***, S223-228.
18. Thorne, B. A., Takeya, R. K., and Peluso, R. W. (2009) Manufacturing recombinant adeno-associated viral vectors from producer cell clones, *Hum Gene Ther* ***20***, 707–714.
19. Toublanc, E., Benraiss, A., Bonnin, D., Blouin, V., Brument, N., Cartier, N., Epstein, A. L., Moullier, P., and Salvetti, A. (2004) Identification of a replication-defective herpes simplex virus for recombinant adeno-associated virus type 2 (rAAV2) particle assembly using stable producer cell lines, *J Gene Med* ***6***, 555–564.
20. Gao, G. P., Lu, F., Sanmiguel, J. C., Tran, P. T., Abbas, Z., Lynd, K. S., Marsh, J., Spinner, N. B., and Wilson, J. M. (2002) Rep/Cap gene amplification and high-yield production of AAV in an A549 cell line expressing Rep/Cap, *Mol Ther* ***5***, 644–649.
21. Farson, D., Harding, T. C., Tao, L., Liu, J., Powell, S., Vimal, V., Yendluri, S., Koprivnikar, K., Ho, K., Twitty, C., Husak, P., Lin, A., Snyder, R. O., and Donahue, B. A. (2004) Development and characterization of a cell line for large-scale, serum-free production of recombinant adeno-associated viral vectors, *J Gene Med* ***6***, 1369–1381.
22. Conway, J. E., Rhys, C. M., Zolotukhin, I., Zolotukhin, S., Muzyczka, N., Hayward, G. S., and Byrne, B. J. (1999) High-titer recombinant adeno-associated virus production utilizing a recombinant herpes simplex virus type I vector expressing AAV-2 Rep and Cap, *Gene Ther* ***6***, 986–993.
23. Kang, W., Wang, L., Harrell, H., Liu, J., Thomas, D. L., Mayfield, T. L., Scotti, M. M., Ye, G. J., Veres, G., and Knop, D. R. (2009) An efficient rHSV-based complementation system for the production of multiple rAAV vector serotypes, *Gene Ther* ***16***, 229–239.
24. Booth, M. J., Mistry, A., Li, X., Thrasher, A., and Coffin, R. S. (2004) Transfection-free and scalable recombinant AAV vector production using HSV/AAV hybrids, *Gene Ther* ***11***, 829–837.
25. Negrete, A., and Kotin, R. M. (2008) Large-scale production of recombinant adeno-associated viral vectors, *Methods Mol Biol* ***433***, 79–96.
26. Negrete, A., and Kotin, R. M. (2007) Production of recombinant adeno-associated vectors using two bioreactor configurations at different scales, *J Virol Methods* ***145***, 155–161.
27. Cecchini, S., Virag, T., Negrete, A., and Kotin, R. M. (2009) Production and Processing of rAAVU7smOPT in 100L Bioreactors for Canine Models of Duchenne Muscular Dystrophy, *Mol Ther* ***17***, 17.
28. Durocher, Y., Pham, P. L., St-Laurent, G., Jacob, D., Cass, B., Chahal, P., Lau, C. J., Nalbantoglu, J., and Kamen, A. (2007) Scalable serum-free production of recombinant adeno-associated virus type 2 by transfection of 293 suspension cells, *J Virol Methods* ***144***, 32–40.
29. Hauck, B., Qu, G., Zelenaia, O., Zhou, J., Liu, X., Africa, L., High, K. A., and Wright, J. F. (2009) A Scalable Manufacturing Platform for Purification of AAV Serotypes 2, 5, 6 and 8 for IND-Supporting Pre-Clinical Studies and Clinical Trials, *Mol Ther* ***17***, S17.
30. Thomas, D. L., Wang, L., Niamke, J., Liu, J., Kang, W., Scotti, M. M., Ye, G. J., Veres, G., and Knop, D. R. (2009) Scalable recombinant adeno-associated virus production using recombinant herpes simplex virus type 1 coinfection of suspension-adapted mammalian cells, *Hum Gene Ther* ***20***, 861–870.
31. Zeltner, N., Kohlbrenner, E., Clément, N., Weber, T., and Linden, R. M. (2010) Near-perfect infectivity of wild-type AAV as benchmark for infectivity of recombinant AAV vectors., *Gene Ther* ***17***.
32. Ayuso, E., Mingozzi, F., Montane, J., Leon, X., Anguela, X. M., Haurigot, V., Edmonson, S. A., Africa, L., Zhou, S., High, K. A., Bosch, F., and Wright, J. F. (2009) High AAV vector purity results in serotype- and tissue-independent enhancement of transduction efficiency, *Gene Ther*.

33. Wright, J. F. (2009) Transient transfection methods for clinical adeno-associated viral vector production, *Hum Gene Ther* ***20***, 698–706.
34. Knop, D. R., and Harrell, H. (2007) Bioreactor production of recombinant herpes simplex virus vectors, *Biotechnol Prog* ***23***, 715–721.
35. Virag, T., Cecchini, S., and Kotin, R. M. (2009) Producing recombinant adeno-associated virus in foster cells: overcoming production limitations using a baculovirus-insect cell expression strategy, *Hum Gene Ther* ***20***, 807–817.
36. Pijlman, G. P., van Schijndel, J. E., and Vlak, J. M. (2003) Spontaneous excision of BAC vector sequences from bacmid-derived baculovirus expression vectors upon passage in insect cells, *J Gen Virol* ***84***, 2669–2678.
37. Edelstein, M. L., Abedi, M. R., and Wixon, J. (2007) Gene therapy clinical trials worldwide to 2007--an update, *J Gene Med* ***9***, 833–842.
38. Gao, G., Qu, G., Burnham, M. S., Huang, J., Chirmule, N., Joshi, B., Yu, Q. C., Marsh, J. A., Conceicao, C. M., and Wilson, J. M. (2000) Purification of recombinant adeno-associated virus vectors by column chromatography and its performance in vivo, *Hum Gene Ther* ***11***, 2079–2091.
39. O'Riordan, C. R., Lachapelle, A. L., Vincent, K. A., and Wadsworth, S. C. (2000) Scaleable chromatographic purification process for recombinant adeno-associated virus (rAAV), *J Gene Med* ***2***, 444–454.
40. Brument, N., Morenweiser, R., Blouin, V., Toublanc, E., Raimbaud, I., Cherel, Y., Folliot, S., Gaden, F., Boulanger, P., Kroner-Lux, G., Moullier, P., Rolling, F., and Salvetti, A. (2002) A versatile and scalable two-step ion-exchange chromatography process for the purification of recombinant adeno-associated virus serotypes-2 and –5, *Mol Ther* ***6***, 678–686.
41. Kaludov, N., Handelman, B., and Chiorini, J. A. (2002) Scalable purification of adeno-associated virus type 2, 4, or 5 using ion-exchange chromatography, *Hum Gene Ther* ***13***, 1235–1243.
42. Davidoff, A. M., Ng, C. Y., Sleep, S., Gray, J., Azam, S., Zhao, Y., McIntosh, J. H., Karimipoor, M., and Nathwani, A. C. (2004) Purification of recombinant adeno-associated virus type 8 vectors by ion exchange chromatography generates clinical grade vector stock, *J Virol Methods* ***121***, 209–215.
43. Smith, R. H., Ding, C., and Kotin, R. M. (2003) Serum-free production and column purification of adeno-associated virus type 5, *J Virol Methods* ***114***, 115–124.
44. Chahal, P. S., Aucoin, M. G., and Kamen, A. (2007) Primary recovery and chromatographic purification of adeno-associated virus type 2 produced by baculovirus/insect cell system, *J Virol Methods* ***139***, 61–70.
45. Qu, G., Bahr-Davidson, J., Prado, J., Tai, A., Cataniag, F., McDonnell, J., Zhou, J., Hauck, B., Luna, J., Sommer, J. M., Smith, P., Zhou, S., Colosi, P., High, K. A., Pierce, G. F., and Wright, J. F. (2007) Separation of adeno-associated virus type 2 empty particles from genome containing vectors by anion-exchange column chromatography, *J Virol Methods* ***140***, 183–192.
46. Urabe, M., Xin, K. Q., Obara, Y., Nakakura, T., Mizukami, H., Kume, A., Okuda, K., and Ozawa, K. (2006) Removal of empty capsids from type 1 adeno-associated virus vector stocks by anion-exchange chromatography potentiates transgene expression, *Mol Ther* ***13***, 823–828.
47. Tamayose, K., Hirai, Y., and Shimada, T. (1996) A new strategy for large-scale preparation of high-titer recombinant adeno-associated virus vectors by using packaging cell lines and sulfonated cellulose column chromatography, *Hum Gene Ther 7*, 507–513.
48. Francis, J. D. a. S., R.O. (2005) *Production of Research and Clinical Grade Recombinant Adeno-associated Viral Vectors.*, Vol. **31**, Elsevier, Amsterdam.
49. Okada, T., Nonaka-Sarukawa, M., Uchibori, R., Kinoshita, K., Hayashita-Kinoh, H., Nitahara-Kasahara, Y., Takeda, S., and Ozawa, K. (2009) Scalable purification of adeno-associated virus serotype 1 (AAV1) and AAV8 vectors, using dual ion-exchange adsorptive membranes, *Hum Gene Ther* ***20***, 1013–1021.
50. Auricchio, A., Hildinger, M., O'Connor, E., Gao, G. P., and Wilson, J. M. (2001) Isolation of highly infectious and pure adeno-associated virus type 2 vectors with a single-step gravity-flow column, *Hum Gene Ther* ***12***, 71–76.
51. Snyder, R. O., and Flotte, T. R. (2002) Production of clinical-grade recombinant adeno-associated virus vectors, *Curr Opin Biotechnol* ***13***, 418–423.
52. Clark, K. R., Liu, X., McGrath, J. P., and Johnson, P. R. (1999) Highly purified recombinant adeno-associated virus vectors are biologically active and free of detectable helper and wild-type viruses, *Hum Gene Ther* ***10***, 1031–1039.
53. Anderson, R., Macdonald, I., Corbett, T., Whiteway, A., and Prentice, H. G. (2000) A method for the preparation of highly purified adeno-associated virus using affinity column chromatography, protease digestion and solvent extraction, *J Virol Methods* ***85***, 23–34.

54. Auricchio, A., O'Connor, E., Hildinger, M., and Wilson, J. M. (2001) A single-step affinity column for purification of serotype-5 based adeno-associated viral vectors, *Mol Ther* ***4***, 372–374.
55. Cecchini, S., Negrete, A., and Kotin, R. M. (2008) Toward exascale production of recombinant adeno-associated virus for gene transfer applications, *Gene Ther* ***15***, 823–830.
56. Wang, L., and Knop, D. R. (2007) Affinity Chromatography Purification of rAAV Vectors Produced by Transfection or rHSV Co-infection Using CaptureSelect AAV ligand, *Mol Ther* ***15***.
57. Wang, L., Niamke, J., Veres, G., and Knop, D. (2008) Two-Step Scalable Purification Process of rAAV1 Vectors Produced by rHSV Co-Infection in Suspension BHK Cells, *Mol Ther* ***16***, 291.
58. Wang, L., Veres, G., and Knop, D. R. (2009) Two-step Chromatography Purification of rAAV1 Vectors produced by Suspension BHK Cells rHSV Co-infection, *Mol Ther* ***17***, 715.
59. Arnold, G. S., Sasser, A. K., Stachler, M. D., and Bartlett, J. S. (2006) Metabolic biotinylation provides a unique platform for the purification and targeting of multiple AAV vector serotypes, *Mol Ther* ***14***, 97–106.
60. Stachler, M. D., and Bartlett, J. S. (2006) Mosaic vectors comprised of modified AAV1 capsid proteins for efficient vector purification and targeting to vascular endothelial cells, *Gene Ther* ***13***, 926–931.
61. Koerber, J. T., Jang, J. H., Yu, J. H., Kane, R. S., and Schaffer, D. V. (2007) Engineering adeno-associated virus for one-step purification via immobilized metal affinity chromatography, *Hum Gene Ther* ***18***, 367–378.
62. Smith, R. H., Yang, L., and Kotin, R. M. (2008) Chromatography-based purification of adeno-associated virus, *Methods Mol Biol* ***434***, 37–54.
63. Zolotukhin, S., Byrne, B. J., Mason, E., Zolotukhin, I., Potter, M., Chesnut, K., Summerford, C., Samulski, R. J., and Muzyczka, N. (1999) Recombinant adeno-associated virus purification using novel methods improves infectious titer and yield, *Gene Ther* ***6***, 973–985.
64. Summerford, C., and Samulski, R. J. (1998) Membrane-associated heparan sulfate proteoglycan is a receptor for adeno-associated virus type 2 virions, *J Virol 72*, 1438–1445.
65. Mizukami, H., Young, N. S., and Brown, K. E. (1996) Adeno-associated virus type 2 binds to a 150-kilodalton cell membrane glycoprotein, *Virology 217*, 124–130.
66. Qiu, J., Handa, A., Kirby, M., and Brown, K. E. (2000) The interaction of heparin sulfate and adeno-associated virus 2, *Virology* ***269***, 137–147.
67. Kaludov, N., Brown, K. E., Walters, R. W., Zabner, J., and Chiorini, J. A. (2001) Adeno-associated virus serotype 4 (AAV4) and AAV5 both require sialic acid binding for hemagglutination and efficient transduction but differ in sialic acid linkage specificity, *J Virol 75*, 6884–6893.
68. Snyder, R. O., and Francis, J. (2005) Adeno-associated viral vectors for clinical gene transfer studies, *Curr Gene Ther* ***5***, 311–321.
69. Mandel, R. J., Burger, C., and Snyder, R. O. (2008) Viral vectors for in vivo gene transfer in Parkinson's disease: properties and clinical grade production, *Exp Neurol* ***209***, 58–71.
70. Chadeuf, G., Favre, D., Tessier, J., Provost, N., Nony, P., Kleinschmidt, J., Moullier, P., and Salvetti, A. (2000) Efficient recombinant adeno-associated virus production by a stable rep-cap HeLa cell line correlates with adenovirus-induced amplification of the integrated rep-cap genome, *J Gene Med* ***2***, 260–268.
71. Mathews, L. C., Gray, J.T., Gallagher, M.R., and Snyder, R.O. (2002) Recombinant Adeno-associated Viral Vector Production Using Stable Packaging and Producer Cell Lines., in *Methods in Enzymology*, pp 393–413.
72. Nony, P., Chadeuf, G., Tessier, J., Moullier, P., and Salvetti, A. (2003) Evidence for packaging of rep-cap sequences into adeno-associated virus (AAV) type 2 capsids in the absence of inverted terminal repeats: a model for generation of rep-positive AAV particles, *J Virol 77*, 776–781.
73. Francois, A., Guilbaud, M., Awedikian, R., Chadeuf, G., Moullier, P., and Salvetti, A. (2005) The cellular TATA binding protein is required for rep-dependent replication of a minimal adeno-associated virus type 2 p5 element, *J Virol 79*, 11082–11094.
74. Rice, S. A., and Knipe, D. M. (1990) Genetic evidence for two distinct transactivation functions of the herpes simplex virus alpha protein ICP27, *J Virol* ***64***, 1704–1715.

Chapter 17

rAAV Vector Product Characterization and Stability Studies

Richard O. Snyder, Muriel Audit, and Joyce D. Francis

Abstract

Recombinant adeno-associated viral (rAAV) vectors mediate the safe and long-term correction of genetic diseases following a single administration. Preclinical studies in animal models and human trials have shown rAAV vector persistence and safety. In some trials, sustained or transient transgene expression has been demonstrated in humans treated for alpha-1 antitrypsin deficiency, LPL deficiency, hemophilia B and cystic fibrosis, and sustained correction of inherited blindness has been reported by three groups. For human use, rAAV vectors are manufactured and tested in compliance with current Good Manufacturing Practices as outlined in the Code of Federal Regulations (21CFR) or European Good Manufacturing Practices (Eudralex, Volume 4, GMP Guidelines, 2003/94/CE and 91/356/EEC). Manufacturing control, as well as product quality is evaluated by quality control testing and all manufacturing, facilities, and testing activities are reviewed by the quality assurance department. In-process specifications are set and in-process testing is conducted to confirm that the manufacturing process is controlled, aseptic, and performs consistently. Final product is tested to ensure release specifications are met for identity, safety, purity, potency, and stability.

Key words: Adeno-associated virus, Gene therapy, Assay, Testing, Quality control, Quality assurance

1. Introduction

As AAV vector technology has improved, the safety and efficacy of AAV-mediated gene transfer in animal models have been demonstrated, and the vectors have been shown to persist and to be safe in humans (1–10). Transient correction of hemophilia B following hepatic artery administration of a rAAV2-hFIX vector (10, 11) and regional infusion (12) has been reported, and transient transgene expression was detected in patients treated for LPL deficiency (13). Long-term improvements have been reported for the inherited blindness Leber's congenital amaurosis (14–16).

Richard O. Snyder and Philippe Moullier (eds.), *Adeno-Associated Virus: Methods and Protocols*,
Methods in Molecular Biology, vol. 807, DOI 10.1007/978-1-61779-370-7_17,

As described in Chapter 16 of this volume, the physicochemical properties of recombinant adeno-associated viral (rAAV) vector virions are amenable to standard industry manufacturing methodologies, long-term storage, and direct in vivo administration. rAAV vectors are manufactured and tested in compliance with current Good Manufacturing Practices (cGMPs) as outlined in the Code of Federal Regulations (21CFR, http://www.gpoaccess.gov/cfr/index.html) and European Good Manufacturing Practices (Eudralex, Volume 4, GMP Guidelines, 2003/94/CE and 91/356/EEC, http://www.emea.europa.eu and http://ec.europa.eu/enterprise/pharmaceuticals). To meet these requirements, manufacturing controls are established, and quality systems including quality control (QC) and quality assurance (QA) are implemented. Quality control personnel have the responsibility to (1) conduct environmental monitoring of the facility for microbial and particulate contaminants to determine if it is within the specifications for cleanliness, both "at rest" and when personnel are present, (2) monitor manufacturing personnel aseptic processing techniques and hygiene, during the manufacturing process, (3) sample and test raw materials to ensure adherence to specifications, (4) evaluate the manufacturing process by sampling and testing intermediates, (5) develop and qualify new assays, (6) characterize the product, and (7) perform product safety and stability testing. Data generated by QC is provided to manufacturing and QA for their timely responses to process, facility, and testing results.

To eliminate conflict of interest, QA and QC are independent from the manufacturing unit and ensure that production activities are in compliance with cGMPs. QA personnel (1) approve, issue, and maintain documents (standard operating procedures (SOPs), validation protocols and reports, cleaning and use logs, batch records, test records, training records, release specifications, etc.), (2) inspect performance of procedures and processes for compliance with SOPs, (3) audit all manufacturing documents and QC data, and (4) release the facility and raw materials for manufacturing use, and final product lots for use in the clinic. These manufacturing procedures and quality systems ensure that a safe, pure, potent, and stable product is produced.

This chapter focuses on the characterization and stability testing of rAAV vector products used in preclinical and clinical studies.

1.1. Assay Development

Although protocols for AAV characterization may have been used in research and are available, additional assay development for each AAV vector product and assay evaluation is required to support clinical trials. Once the actual methods are established and reagents are sourced, then the documents (reagent preparation records, test records, SOPs, etc.) and specifications need to be written, and qualifications conducted. In parallel, new and existing assays are developed and qualified to characterize intermediates and final product.

1.2. Facilities and Equipment

A dedicated quality control (QC) laboratory is ideal to conduct testing. This laboratory is equipped with modern analytical equipment necessary to perform the in-house reagent, intermediate product, final product, and environmental testing. Additional support space houses an autoclave(s), refrigerators, –20°C and –80°C freezers, liquid nitrogen freezers, stability chambers, secure storage for standards and additional space for materials and reagents stored at room temperature. A central computerized monitoring system monitors temperature and/or humidity in incubators, refrigerators, and freezers, and ensures they function in the specified operating range. This system also automatically initiates staff notification when operating limits are exceeded. The correct operation of all equipment is verified on a daily basis. All QC equipment is validated (Installation Qualification and Operational Qualification) and then calibrated and maintained (cleaning and preventive maintenance) according to a procedurally defined schedule.

Cell and virus manipulations during testing are performed exclusively in ISO 5 (EU class A) BSCs during open steps to protect the QC operator and maintain asepsis. Also, BSCs must be available to prepare qualified QC cell banks and helper virus banks (e.g., adenovirus) that are used in infectious titering and rcAAV assays, and rAAV product testing.

Cleaning procedures, equipment calibration, and preventative maintenance procedure documents are written, and then approved, controlled, and maintained by QA. Frequencies of cleaning and maintenance may vary according to frequency and type of use and manufacturer's recommendations. Calibration of equipment is performed as frequently as with each use for certain equipment (e.g., a pH meter) or up to an annual calibration period. These frequencies must be justified and detailed in the corresponding written procedures. For equipment cleaning, two different filtered germicidal detergents are rotated monthly, and all surfaces and equipment are cleaned periodically according to set schedules.

1.3. Organization and Personnel

Personnel need to have appropriate education and experience prior to working in the testing environment. An organization and reporting structure for QC and QA operations is necessary, and each person is assigned specific responsibilities as indicated in their respective job description. A technician and a supervisor engaged in testing activities is the minimal number required for a QC laboratory. The QC supervisor coordinates environmental and personnel monitoring based on manufacturing activities and testing of raw materials, in-process and product samples. In addition, the supervisor reviews data generated, as well as the performance standards and controls included in each assay. QA maintains appropriate quality systems to assure that the testing performed also supports the quality and safety of the clinical materials. QA's independent oversight of the testing activities, including periodic

inspections of assay performance and other activities to ensure compliance with SOPs, and especially for review of assay acceptability (validity), product release and disposition, is key to the quality systems.

1.3.1. Training

Training is performed according to an issued SOP(s). General training sessions regarding current Good Manufacturing Practices regulations, documentation practices, and other general procedures, are held for new employees with GMP training repeated on an annual basis for all employees. Supervisors, QC analysts, QC technicians, QA reviewers, and support personnel are given initial and refresher training on specific job functions and procedures. Other support groups outside of QC and QA (such as information technology and building maintenance personnel) are also trained on the cGMPs and specific notification and documentation procedures. The supervisor or other trained individual can perform individual training in job-specific responsibilities. To familiarize themselves, individuals are provided the SOP or other issued controlled document covering a particular procedure before the training session. The individual reads the controlled document and receives hands-on training, the amount of which is based on the individual's education and experience. When an individual can complete the tasks in the procedure competently, they have completed training and then are allowed to perform the tasks independently. All training and relevant education records are archived by QA.

1.4. Quality Assurance

Quality assurance performs audits, release of raw materials, and reagents for use in testing, change control, document control, release of clinical lots, and validation support.

1.4.1. Internal and Vendor Audits

Internal inspections are performed according to an issued SOP specifying their frequency. These inspections cover all areas including QC and QA, and review compliance with issued procedures. Findings are reported to unit supervisors, and management. A response and follow-up on completion of corrective activities are required to close the audit. The vendor management program includes on-site audits for compliance with cGMPs or other quality systems (e.g., ISO), and implementation of corrective actions prior to the production of components used in the testing of rAAV vector in-process and product samples. A review of QC recipes and an agreement on release specifications is performed for reagents manufactured under contract.

1.4.2. Raw Materials and Lot Release

The QA director or designated QA staff member is responsible for review and release of all materials and reagents used in manufacturing and testing, and final product lots prior to shipment to clinical sites. The release process includes manufacturing batch record review, environmental monitoring review, review of each QC assay

performed (review of test record), and an evaluation of test results in comparison to release specifications. Other release activities related to raw materials, reagents produced internally, and in-process intermediates and production banks are also the responsibility of QA. All release activities are described in issued SOPs.

1.4.3. Variances and Change Control

A system for the documentation, investigation, and correction/prevention of variances is covered in issued SOPs. Test failures are assigned numbers when they occur and are investigated and tracked by QA until completion of corrective actions or retesting, if appropriate. Retesting is usually allowable if a test procedure is invalid (i.e., the controls did not perform) or an operator error was identified. Planned variances to controlled procedures can be allowed (for phase 1 or 2 materials) for documented controlled changes to procedures for evaluation purposes. Planned Variances are also assigned numbers by QA and tracked until implementation (by revision to the appropriate procedure) or terminated (due to nonutility). The notification and review of planned changes made to equipment, process, raw materials, or specifications as detailed in SOPs or batch records or other controlled documents is required by a change control system. This system allows for the evaluation and review of the effect the change will have on the product or test procedure.

1.4.4. Document Development and Control

QC personnel develop the protocols and procedures used in testing. These written procedures must be approved by QA. These include SOPs for operation, use and maintenance of equipment and the QC facility, testing records, reagent specifications, standards and controls handling, and product release specifications. QA is responsible for document issuance and control. All SOPs, test records, reagent preparation records, and controlled forms used by QC and QA are numbered, reviewed, and issued by QA. All revisions to existing controlled documents are also handled by QA where document change history is tracked, either on the document itself (for SOPs) or on a controlled form used for the revision process. An historical archive of all versions of each controlled document is maintained by QA and all executed records related to any activity performed according to SOPs, or related to the production and release of clinical materials are archived in fire-proof cabinets or other storage located on-site and/or at off-site secured storage facilities. Digitization and electronic storage of completed records, forms, and other documents is also a suitable redundant approach.

1.4.5. Validation Support

Prior to execution, QA reviews and approves the validation master plan, and all assay validation protocols, including acceptance criteria, specifications, and operating limits. Following the execution of the validation studies, QA reviews all reports to ensure completeness and accuracy, and that all acceptance criteria have been met and, if applicable, all deviations have been acceptably resolved.

1.5. Quality Control

QC activities include assay development, assay qualification, environmental and personnel monitoring, and testing of raw materials, reagents, product intermediates, and final product. Data generated by QC are provided to manufacturing and QA for their timely responses to process, facility, and testing results.

1.6. Reagents and Raw Materials

Suitable reagents and raw materials should be chosen, and acceptability criteria and specifications established for each item used in QC testing. United States Pharmacopeia, European Pharmacopeia (EP) or multicompendial grade chemicals and water for injection (WFI) should be used whenever possible. Animal-derived materials, if needed for testing, are accompanied by Certificates of Origin (COO) to ensure the safety of these materials. Upon receipt from the vendor, these materials are inspected (by warehouse personnel), placed in quarantine storage (in the warehouse), and the Certificate of Analysis (COA) is compared to preset specifications by QA. In some cases, samples of purchased reagents need to be taken and analyzed prior to use. Once the verification of the specifications is complete, then the materials are released by QA and moved to the designated released storage area for subsequent use in the testing process. Reagents (cell substrates, buffers, etc.) used in testing that are made on-site in the QC laboratory use controlled records, issued by QA. Testing of these batches is reviewed by QA and released for use in QC.

1.6.1. Cell Banks

QC Cell Banks (QCCBs) are made according to written procedures. These cell banks should be large enough to meet current and future testing needs, and periodically tested for viability and sterility. Typical cell lines that are used include HeLa cells that harbor the AAV *rep* and *cap* genes (17, 18) for infectious titering (see below), and naive HeLa or HEK 293 cells for transduction and rcAAV testing (see below). The components and reagents used during the manufacture of cell banks, should be sourced such that appropriate quality standards can be met. The cell bank is stored in designated monitored equipment below −135°C under liquid nitrogen vapor to reduce the possibility of cross contamination between vials. The QCCB is stored under quarantine while it is being tested (Table 1), and is released for use by QA once qualification is complete.

1.6.2. Plasmids

For plasmid standards used in testing, plasmid DNA and *E. coli* cell banks are needed, and are usually derived from the *E. coli* cell banks used to produce plasmids for vector manufacturing. The vector plasmid harbors the rAAV vector cassette flanked on each end by inverted terminal repeats, and is used as a standard for vector genome titering (see below). Vector plasmid *E. coli* cell banking is performed by transforming *E. coli* strains that are deficient in recombination enzymes and screening subclones for ITR stability

Table 1
Suggested QC cell bank specifications

Test	Method	Specification
In vitro viruses	Indicator cells – cytopathic effect Indicator cells – hemadsorption	Viral contaminants not detected Viral contaminants not detected
Mycoplasma	Agar/broth cultivation Hoechst stain	Mycoplasma not detected Mycoplasma not detected
Viability	Trypan blue stain	>80%
Sterility test	Direct inoculation	No growth
Total viable cells/vial	Trypan blue stain	5×10^6–2×10^7
Identity	Isoenzyme analysis	Match species used

Table 2
Suggested plasmid QC master cell bank specifications

Test	Method	Specification
Antibiotic resistance	LB plate culture	Ampicillin-sensitive Kanamycin resistant
Morphology	Phase contrast microscopy	*E. coli* rods: pass
Restriction enzyme digest with 3 enzymes	Restriction enzyme pattern analysis	Expected pattern according to map
Phage contamination	LB plate culture	Negative
DNA sequencing	Double-stranded primer walking	Conforms to reference sequence

and yield. Glycerol-stabilized master cell banks are produced and plasmid DNA preparations derived from these MCBs are sequenced and analyzed as part of qualification and release (Table 2). In some cases, plasmids harboring the wild-type AAV genome may be needed for rcAAV testing (see below).

1.6.3. Cell Culture and Infection Reagents

High-purity water or water for injection, trypsin, and phosphate-buffered saline (PBS) of suitable quality are available from commercial sources, and tissue culture media can be preformulated, tested, and released. If a helper virus is used in the testing procedures, then a QC Viral Bank (QCVB) should be produced using controlled written procedures, tested and characterized (including genetic integrity and titer), and released by QA for use.

1.6.4. Storage, Shipping, and Testing

Product vials are stored in inventoried locked storage at –70°C to –90°C, and test samples are stored at their appropriate temperature. Samples are packaged with dry ice or freezer packs in an insulated container when shipped to third-party testing sites. The shipping container holds a temperature data logger to ensure the appropriate temperature is maintained during shipment. Upon receipt, the items are removed from the shipping container and again stored at their appropriate temperature until testing is initiated. The data logger is reviewed to confirm that the proper shipping temperature was maintained. The QC unit should establish a sample receipt and tracking system used for in-house and contract laboratory testing. Contract laboratory testing protocols or procedures should be obtained by QC, and reviewed, and approved. When completed the protocols and the final testing reports are reviewed and maintained by QA in their archives.

1.7. Assays

Although several assays are employed to evaluate AAV vectors used for research, additional assay development is required to achieve the appropriate level of assay performance for each phase of product development and ultimately product licensure. It might be sufficient to have preliminary validated assays applicable for products entering Phase I clinical trials, but a full validation package is recommended for all assays used in the quality control analyses of the products entering Phase II/III clinical trials as well as for the assays used in Good Clinical Practice (GCP) studies. The QC assay development activity involves generating standards and controls, writing test records and reagent preparation logs, and training laboratory analysts to perform these procedures. In some cases, internal standards can be calibrated to external reference standard materials that are available to the community. Once the methods are established, then the assays are qualified to demonstrate that they perform appropriately based on their intended use. According to ICH Q2(R1) "Validation of Analytical Procedures," the validation characteristics that should be considered are, according to the type/use of analytical procedure, accuracy, precision (repeatability and intermediate precision), specificity, detection limit, quantification limit, linearity, and range for eventual assay validation. Appropriate in-process and final product sampling and testing will depend on the specific manufacturing process, and some tests may need to be conducted repeatedly throughout the process. Furthermore, sampling and testing may be different for US or EU compliance (Tables 3 and 4).

Requirements, including GMP-related issues, should be upgraded as the clinical study phase progresses. Before the development of a product reaches the market phase, the implementation of guidelines should proceed on a case-by-case basis, according to the phase of the clinical study. Appropriate tests to be performed on vector batches are defined for each product (Table 5).

Table 3
AAV clinical batch sampling and testing based on FDA guidelines

Harvest	Purified bulk	Vialed final product
Sterility or bioburden	Sterility or bioburden	Sterility including bacteriostasis/fungistasis
Mycoplasma	Purity: silver staining/Coomassie blue	Potency: infectious unit titer
In vitro adventitious viral contaminants	Potency: infectious unit titer	Strength: vector genome titer
In vivo adventitious viral contaminants, if needed	Strength: vector genome titer	Strength: particle titer
	Identity	Transgene expression
	Residual host cell DNA	rcAAV
	Process residuals	Endotoxin
	pH	General safety
	Conductivity or osmolality	Aggregation
		Appearance
		Identity
		Stability
		pH
		Osmolality

Depending on the production process, residual biological components used during production (e.g., plasmids, viruses, cell line), will be quantified in the final product. For a production process using a stable cell line it will be necessary to define the number of copies of viral genes and expression cassette per cell as well as integrity and genetic stability. Transient transfection processes will require the quantification of residuals plasmids. The use of viruses also requires their detection in the final product (19). Production with a baculoviruses/insect cells system may require the detection of nodaviruses (20).

1.8. Intermediate and Final Product Testing, and Lot Release

Once produced and purified, the vector batch is characterized using qualified assays to ensure that it meets preset specifications for safety, identity, purity, potency, and stability. These tests can be expensive and consume a significant amount of vector that approaches the amount of vector needed for the clinical doses. Testing and characterization of each lot of the rAAV vector is performed under cGMPs prior to product release. Release documentation (a COA) for each lot is submitted to the US Food and Drug Administration (FDA), European (EMEA) or national regulatory

Table 4
AAV clinical batch sampling and testing based on the European Pharmacopoeia

Harvest	Purified harvest	Vialed final product
Vector identity	Vector identity	Vector identity
Vector concentration (vector genomes and infectious vector)	Vector concentration (vector genomes and infectious vector)	Vector concentration (vector genomes and infectious vector)
Extraneous agents	Genetic characterization	Osmolarity
Producer cells identity + extraneous agents	Residual viruses (if used during the production process)	pH
	Residual host-cells and/or virus proteins	BSA
	Residual DNA from producer cells and production intermediates such as plasmids or viruses	rcAAV
	Residual reagents	Vector aggregates
	Residual antibiotics	Sterility
		Bacterial endotoxins
		Expression of the genetic insert product
		Biological activity

Table 5
Assays utilized for vector characterization

Assay type	Method	Purpose
Titer		
Infectious	Infectious center assay (ICA) Serial dilution replication assay (dRA)	Determine titer of infectious particles produced
Vector genome	Dot-blot hybridization PCR	Determine genome-containing vector concentration
Capsid	ELISA Bradford Western Electron microscopy Optical density (OD)	Determine total capsid protein concentration – enables a determination of empty particles in the prep
Purity		
Protein	SDS-PAGE, HPLC	Determine the presence or absence of contaminating proteins
Cellular DNA	DNA hybridization or PCR	Determine the presence or absence of cellular DNA

(continued)

Table 5 (continued)

Assay type	Method	Purpose
Identity		
Transgene cassette	DNA sequencing or restriction enzyme digestion	Verification of the transgene
Capsid	SDS-PAGE with silver and Coomassie stain	Expected AAV banding pattern
	Limited proteolysis or MS	Serotype identification
Potency		
Transgene expression	Transduction assay in cells or animals	Ensure that the active transgene product is expressed
Safety		
Adventitious agents	Cytopathic effect and qPCR based assays to detect infectious adventitious viral agents	Detect contaminating infectious viral agents of human or animal origin (serum, trypsin)
Mycoplasma	Growth assays on cells in antibiotic-free conditions, followed by dye or PCR to detect mycoplasma	Determine the presence or absence of mycoplasma
	Growth assay in appropriate agar media	
Endotoxin	Rabbit pyrogen assays	Determine the presence or absence of endotoxin
	LAL	
Sterility	Bacteriostasis/fungistasis	Determine the presence or absence of microbial contaminants
Stability		
Physicochemical	SDS-PAGE	Demonstrate that the product is not degrading over time
Infectious titer	TCID50 + qPCR	Demonstrate that infectivity is maintained over time
Sterility	Bacteriostasis/fungistasis	Demonstrate the integrity of final product container over time

authorities as part of the IND or other regulatory filing. To date, the implementation of clinical trials of gene therapy in Europe is being regulated at two distinct levels. Early phases are being reviewed at the national level and marketing authorization is being covered by a centralized procedure through the European Medicines Evaluation Agency (EMEA). Tests and specifications for product release are presented in Table 6. In some cases, no test specification is set so that data can be collected to monitor the manufacturing process or to establish a specification for products in later phases of development; these results obtained are reported on the COA. Having reliable, specific, and sensitive assays is crucial during the development of production and purification

Table 6
Release specification examples for a rAAV final product

Test	Method	Specification
Sterility	Direct inoculation	No growth
Endotoxin	LAL	<50 EU/mL[a]
Titer		
Infectious titer	$TCID_{50}$ with qPCR	≥5 × 10E10 $TCID_{50}$/mL
Vector genome titer	PCR	≥5 × 10E12 vector genomes/mL[b]
Capsid titer	ELISA	Report results
Infectivity ratio	Calculation	Report results
Purity		
Protein purity	PAGE and Coomassie blue stain for protein	>90% pure
293 Cell contaminating DNA	qPCR	Report results
Benzonase residual	ELISA	Report results
rcAAV	Serial infection and qPCR	<1 in 1 × 10E8 vg rAAV
Identity	PAGE with silver and Coomassie blue stains or mass spectroscopy	Expected AAV banding pattern Correct fragment(s) mass
Activity	ELISA following in vitro transduction[b]	Report results
Appearance	Visual inspection	Clear to slightly hazy, colorless, free of foreign materials
pH		pH 6–8
Osmolaltiy	Freezing point depression	Report results

[a]Endotoxin limit is based on route of administration, dosage, and time
[b]Varies based on specific vector

methods. Once produced and purified, the rAAV vector is characterized using a variety of techniques to ensure it is safe, pure, potent, and stable.

1.8.1. Assays for Protein Purity and Identity

Batches are analyzed by silver, fluorescent dye (SYPRO ruby), or Coomassie blue staining of capsid proteins separated on reduced and nonreduced SDS polyacrylamide gels. Three capsid proteins (VP1, 2, and 3) should be visible in the correct stoichiometry of approximately 1:1:10 and have the correct molecular weights (87, 72, 62 kDa), and should be free of non-AAV proteins (Sections 2.1, 3.1,and 4). Identification of protein impurities using specific antibodies, mass spectrometry (MS), or by protein

sequencing can help trace the source (cellular, serum protein, etc.) in order to modify the manufacturing process to eliminate the impurity.

Prior to use in the clinic, an important product release test is the confirmation of product identity to comply with current cGMP regulations. Identity release testing involves not only confirmation by DNA sequencing of the unrearranged vector genome that is packaged, but also the serotype of the capsid. Since immunologic reagents generated to one serotype have the potential to cross react with other serotypes, screening different proteases on different AAV serotypes generates a capsid fingerprint that can distinguish different AAV serotypes isolated (21). Furthermore, mass spectrometry (MS) can be used to confirm the capsid serotype identity of rAAV vectors based on different proteolytic fragment masses (22).

1.8.2. Assay for Infectious rAAV

To obtain an infectious titer, an end-point dilution based on a $TCID_{50}$ format is paired with real-time PCR. Rep/cap cells in a 96-well plate format are infected with adenovirus helper, and serial dilutions of rAAV are made in replicates. Following infection, the wells are evaluated by real-time PCR and the Karber method is used to calculate the infectious titer (23). Since an accurate titer is desired, it is important that the assay is analyzed prior to a second round of infection that could inflate the titer values. The assay measures the ability of the virus to infect *rep/cap* expressing cells (17, 24), unpackage, and replicate to give an accurate measurement of infectious virus regardless of the transgene or promoter used. The method, however, provides no information as to the functional status of the expression cassette delivered by the viral particle. In an alternative strategy, a herpesvirus carrying the AAV *rep/cap* genes can provide all of the helper functions necessary to determine infectious titers of different AAV serotypes on a variety of cell types (25). The switch to *rep/cap* expressing cells or helperviruses also allows the elimination of wtAAV to supply *rep* and *cap* in the RCA (26). This removes a potential source of contamination for production materials.

For the AAV2 serotype vectors, HeLa cell-based rep/cap cell lines have been used. However, other AAV serotypes and helperviruses infect HeLa, 293, and other cell lines inefficiently. Identifying cell lines that can be infected with different AAV serotypes and helper viruses efficiently is greatly needed, as this affects not only the infectious titer values, but also the particle to infectious ratio, transgene expression assays, and the detection of replication-competent AAV (rcAAV) (please see below).

1.8.3. Assay for Replication Competent AAV

Dilutions of the rAAV preparation are used to infect 293 cells (or other suitable cell type that lacks AAV genes) in the presence of adenovirus (or other suitable helper virus) for 48 or 72 h. Since no

additional wild-type AAV is added, only particles in the rAAV preparation that have packaged a wild-type or pseudo-wt AAV genome are capable of replication. A freeze/thaw lysate is generated and used to infect 293 cells along with adenovirus helper; this cycle is repeated two more times. SYBR green or Taqman real-time PCR is conducted using primers in the AAV ITR and *rep* gene. Wild-type virus may contaminate vector preparations, and RCV may be formed during production due to recombination between the vector and the helper sequences found in complementary cell lines or plasmids (27). The presence of wild-type virus or RCV may affect vector expression and mobilization. In order to assess a potential interference between the vector batch to be controlled and the rcAAV detection, it is recommended to test the rcAAV internal control in the presence and in the absence of the vector batch. Indeed, as shown by Gao et al. (28) a high concentration of AAV vector may inhibit the rcAAV detection.

1.8.4. ELISA for Determination of Intact AAV Capsids

The AAV2 capsid ELISA assay is used to quantify total (infectious, noninfectious, and empty) viral particles. Grimm et al. (29) reported that some preparations of rAAV may have a significant amount of empty particles. The A20 antibody recognizes assembled empty and full capsids, but not disrupted or partially assembled capsids (30). This assay can be used to determine what fraction of the rAAV2 particles are empty, but the use of the A20 antibody may be limited to AAV2 and AAV3 (31). Recently, antibodies that recognize intact capsids of other AAV serotypes have been described (31). Alternatively, the optical density can be measured to calculate a total capsid titer (32).

1.8.5. Assay for Transgene Expression

The assay for transgene expression involves the harvesting of the supernatant (for secreted proteins) or cells (for intracellular proteins) from the infectious titer assay (described above) and testing for the presence of the transgene protein product by ELISA, immunoblot, Western, or activity assay (for enzymes or shRNA). This titer determination is also frequently performed on naïve cells (cells without *rep* and *cap*) transduced with serial dilutions of the vector to be controlled in the presence of a helper virus.

1.8.6. Assays for rAAV Genome Titer and the Particle to Infectivity Ratio

The dot blot assay has been historically used to determine the titer of rAAV virions that contain vector genomes. However, real-time PCR-based assays are becoming the accepted standard to determine the vector genome titer (23, 33–35). Plasmid and unpackaged vector DNA is digested for 1 h with nuclease, and the nuclease is inactivated by heat. Treated virus is added directly to the PCR reaction or encapsidated rAAV vector genomes are liberated by protease digestion, phenol extraction, and ethanol precipitation. A dilution series of the vector plasmid DNA that was packaged is prepared as a standard. The PCR primers and probe detect the viral

vector DNA and plasmid standard curve. The vector DNA signal is compared to the signal generated from the plasmid DNA standard curve, and extrapolated to determine a vector genome titer Sections 2.2, 3.2,and 4. Lastly, the optical density (A_{260}) can be measured to calculate a particle titer (32).

A comparison of the vector genome titer to the infectious titer produces the particle:infectious (P:I) ratio. In some cases, when the rAAV vector serotype has difficulty infecting cell lines in vitro to generate an infectious titer, the P:I ratio can be extremely high (25). However, as long as the ratio is consistent enough to show lot to lot product similarity, and correlated to in vivo performance, then the vector lot can be considered suitable for the clinic.

1.8.7. Appearance, pH, and Osmolality

Vials of final product are thawed and visually inspected against a white and a black background. Inspectors look for discoloration of the liquid and presence of particulates. Aggregation can be evaluated by dynamic light scattering. Purified bulk or vials of the final product are tested for pH, and osmolality using calibrated testing equipment as signatures of proper formulation.

1.9. Safety Testing

Safety testing is conducted to ensure that process intermediates or final product is free of detectable contaminating agents or process residuals that can pose risks to patients. These assays can be developed for on-site testing, but there are several commercial vendors who offer testing services. These services should be GMP compliant with appropriate controls and validity criteria, and the vendor will indicate the amount and type of sample required for their tests. However, it is still the responsibility of QC and QA to review the vendor test report for validity and accuracy. The primary safety tests include *Adventitious agents* (in vitro and in vivo): These assays are designed to detect the presence of infectious viral agents of human or animal origin. A choice of cell lines (e.g., human, murine, bovine, porcine, etc.) is available for the in vitro assay where as rodents and embryonated hen's eggs are commonly used for the in vivo assay. *Mycoplasma*: The test for the presence of mycoplasma relies on the growth of mycoplasma during the expansion of indicator cells in antibiotic-free conditions and detection of the organism using dye or PCR, as well as growth of mycoplasma in broth or on appropriate agar media. *Endotoxin*: Endotoxin can be detected using the Limulus Amebocyte Lysate Assay or by using a rabbit pyrogen test. *Sterility*: This assay determines the absence of bacterial or fungal organisms and must also include the performance of bacteriastasis and fungistasis analysis. *General safety*: This assay is designed to determine if there are toxins (chemical or biological) present that induce an acute toxicity in animals.

1.9.1. Stability Study

A stability study should be designed to generate data for a purified rAAV viral vector at the proper storage temperature, formulation, and fill volume, and in the storage container used for patient doses.

The study is designed to demonstrate genetic and physicochemical stability, and container integrity for at least the duration of the clinical trial. A portion of the clinical batch is used to monitor its stability. Stability samples are titered using the infectious titer assay to determine maintenance of the infectivity of the product. Identity and protein purity testing is performed to ensure the chemical stability of the vector (absence of capsid protein degradation). Sterility testing is also performed to ensure that final product container integrity is maintained with storage over time. A typical testing schedule will occur at 1, 3, 6, 9, 12, 18, and 24 months after filling. The length of stability study is dependent on length of clinical trial with at least one testing point that must follow administration to last clinical subject.

1.10. Reference Standards

AAV reference standard efforts were established to address the lack of normalization of doses administered to animals and humans (36). Today, an AAV2 RSM (reference standard material) has been produced and characterized by several laboratories (23), and an AAV8 RSM is being produced and will be made available to all members of the research community (37). The RSMs are used primarily to calibrate the internal standards and analytical methods used by individual laboratories to then inter-relate the doses used in different nonclinical and clinical studies. When reporting titers in the literature or to the regulatory authorities, the relationship to an RSM can be included. The RSMs are available in a form suitable for nonclinical and clinical data support, together with the profile and information regarding the development of each RSM.

1.11. Conclusion

The QC systems and procedures described here can support Phase I clinical trials, however product specifications, manufacturing methodology, facilities, etc. will vary, so these descriptions are based on our experience and may not be applicable to other situations. Compliance requires continued review of federal and international regulations, guidances that are more frequently issued and modified, and other regulatory information sources to ensure that processes and procedures are adapted to meet these requirements. In addition, as the product is evaluated in Phase II, Phase III trials and after licensure (Phase IV), the manufacture and testing of the product require more stringent controls. Referring to FDA (http://www.fda.gov/cber/guidelines.htm) and ICH (http://www.ich.org/) guidances, the United States Pharmacopeoia, and the Code of Federal Regulations (http://www.gpoaccess.gov/cfr/index.html) or European counterparts (http://www.emea.europa.eu and http://ec.europa.eu/enterprise/pharmaceuticals) is essential when developing compliant processes, test methods, and procedures.

2. Materials

2.1. Assay for the Determination of Viral Identity and Purity

1. 10% Tris–HCl Polyacrylamide Gels (Bio-Rad, Hercules, CA).
2. 10× Tris–Glycine SDS Running Buffer (Bio-Rad, Hercules, CA).
3. 5× Laemmli Loading Buffer (10% SDS, 50% Glycerol, 0.25% Bromophenol Blue, 250 mM Tris–HCl pH 6.8).
4. 5× Laemmli Loading Buffer with DTT (10% SDS, 50% Glycerol, 0.25% Bromophenol Blue, 250 mM Tris–HCl pH 6.8, with 500 mM DTT).
5. Protein Ladder (Bio-Rad, Hercules, CA).
6. Silver Stain kit (Bio-Rad, Hercules, CA).
7. GelCode Blue or Imperial Stain Reagent (Pierce, Rockford, IL).

2.2. Vector Genome Titer Determination

1. 10× Benzonase Digestion Buffer (250 mM Tris–HCl pH 7.4, 10 mM $MgCl_2$).
2. Benzonase (EMD Chemicals, Gibbstown, NJ).
3. TaqMan® Universal PCR Master Mix (Applied Biosystems, Foster City, CA).
4. PCR Primers.
5. Taqman® Probe (Applied Biosystems, Foster City, CA).
6. Linearized vector plasmid.

3. Methods

3.1. Assay for the Determination of Viral Identity and Purity

Under fully reduced conditions, combination of the strongly anionic detergent sodium dodecyl sulfate (SDS), the reducing agent DL-dithiothreitol (DTT), and heat are used to dissociate the proteins of the AAV capsid before the sample is loaded onto the gel. The denatured proteins bind SDS and become negatively charged. By comparing the migration of the polypeptides to a protein marker of known molecular weight, it is possible to determine the molecular weight of each polypeptide. Under nonreduced conditions, the samples are mixed with a loading dye containing SDS (and no DTT), but are not boiled. The SDS coats the AAV virion so that it will migrate towards the cathode and enters the stacking portion of the gel, but not the resolving portion since it is too large. Any proteins not associated with the virion should enter the resolving portion of the gel.

After PAGE, the gels are stained to allow the visualization of separated proteins. Silver staining is capable of detecting as little as 0.1–1.0 ng of polypeptide in a single band. The high sensitivity of silver staining allows detection of trace proteins (possible impurities in the sample) and other molecules (DNA, carbohydrates, and lipids) even in relatively dilute samples. The colloidal properties of Coomassie G-250 for protein staining are capable of detecting protein quantities as low as 3 ng of polypeptide in a single band. Coomassie blue binds nonspecifically to proteins, allowing visualization of the proteins as discreet blue bands within the gel. Samples are analyzed in duplicate on two gels (A stained with silver and B stained with Coomassie blue).

1. Thaw sample(s) and positive control
   (a) Remove the sample(s) to be tested and the appropriate positive control from storage.
   (b) Thaw on ice and keep the sample(s) and the positive control on ice.
2. Prepare four 1.5 mL *siliconized* microcentrifuge tubes for each sample to be tested.
   (a) Label two tubes with sample number, "Fully Reduced," date and initials. One tube will be used for gel A and one tube will be used for gel B.
   (b) Label two tubes with sample number, "Nonreduced," date and initials. One tube will be used for gel A and one tube will be used for gel B.
   (c) Mix the sample by finger flicking the tube. DO NOT VORTEX.
   (d) Transfer the vector using a micropipettor, to each labeled sample tube.
   (e) Add 8 μL of 5× Laemmli buffer with DTT to tubes labeled "Reduced."
   (f) Add 8 μL of 5× Laemmli buffer to the tube labeled "Nonreduced."
   (g) Calculate the volume of Ultrapure Water, Distilled Water, or WFI needed to bring the volume in each tube to a total of 40 μL. Briefly spin all tubes to collect all liquid at the bottom.
3. Prepare the negative controls containing 1× Laemmli buffer or 1× Laemmli buffer with DTT.
4. Prepare the positive controls containing a known rAAV vector with the same serotype and either 1× Laemmli buffer or 1× Laemmli buffer with DTT.
5. Prepare the molecular weight protein ladders with either 1× Laemmli buffer or 1× Laemmli buffer with DTT.

6. Heat the "Fully Reduced" Sample(s), the "Fully Reduced" Ladder, the "Fully Reduced" Positive Control, and the "Fully Reduced" Negative Control/Buffer Control at 95–100°C for 10 min.
7. Remove the tubes from the heating block and allow them to cool to room temperature, approximately 5–10 min.
8. Pulse spin the tubes in a microcentrifuge.
9. Two gels will be loaded with sample(s), ladders and controls and run simultaneously: gel A to be stained with Silver Stain and gel B to be stained with Coomassie blue.
10. Allow the gels to run until dye fronts have reached the base of the gels.
11. Separate the plates and transfer the gels into separate trays for staining.
12. Stain gels with silver or Coomassie blue.
13. Capture the gel image for the Coomassie stained gel on a digital or CCD camera apparatus.
    (a) Using the densitometry features of the gel imaging system, measure the background and intensity of all bands for each gel lane.
    (b) Subtract from each band's intensity the bacground level for that gel lane.
    (c) Determine the percentage of intensity for VP1, VP2, VP3, and contaminating bands.
    (d) Sample purity is expressed as the combined intensity of VP1, VP2, and VP3 as a percentage of the intensity of all bands.
14. Criteria for a valid assay
    (a) For the viral identity assay – *fully reduced* samples, the protein ladder standard, the positive control, and the negative control to be considered valid if all of the following criteria are met:
        - The fully reduced protein ladder standard must stain to show at least 12 bands at apparent molecular weights of 220, 160, 120, 100, 90, 80, 70, 60, 50, 40, 30, 25 kDa, respectively.
        - The fully reduced negative control must show no stained bands.
        - The fully reduced positive control must stain to show bands representative of AAV VP1, VP2, and VP3, based on comparison to the protein ladder standard.
        - The fully reduced positive control must stain such that the band representative of VP3 is darker than the VP1 and VP2 bands.

(b) For the viral identity assay – *nonreduced* samples, protein ladder standard, positive control and negative control to be considered valid all of the following conditions must be met.

- The nonreduced protein ladder standard must stain to show at least 12 bands at apparent molecular weights of 220, 160, 120, 100, 90, 80, 70, 60, 50, 40, 30, 25 kDa, respectively.
- The nonreduced negative control must show no stained bands.
- The nonreduced positive control must stain to show the absence of bands representative of VP1, VP2, and VP3 (see note 1 in Section 4).

3.2. Vector Genome Titer Determination

1. Digest unencapsidated DNA
   (a) Label one 1.5 mL microcentrifuge tube for each sample with sample identity, initial and date.
   (b) Label one 1.5 mL microcentrifuge tube for positive control, initial and date.
   (c) Transfer 5 μL of sample and positive control in respective 1.5 mL microcentrifuge tube.
   (d) To each sample and the positive control, add 5 μL of Benzonase digestion buffer (10×), Benzonase enzyme (to 100 U/mL), and nuclease-free water to a final volume of 50 μl. Mix by pipeting up and down two times. Centrifuge the tube briefly.
   (e) Incubate tubes for 30 min at 37°C water bath.
   (f) After incubation briefly centrifuge tubes and place on ice.
2. Prepare 10-point serial fivefold dilutions of digested test samples in duplicate.
3. Prepare 10-point serial fivefold dilutions of the digested positive control in duplicate.
4. Prepare a tenfold serial dilution of linearized vector plasmid DNA to be used for the copy number standard curve.
5. Prepare a negative control containing water.
6. Prepare the PCR master mix for two reactions of each sample, the standard curve, positive control sample, and negative control. The master mix contains primers and probe specific to the sequences targeted in the vector genome along with nucleotides, polymerase, and buffer (see notes 2, 3, and 4 in Section 4).
   (a) Add master mix to each well utilized on the 96-well PCR plate

7. Add each sample, the standard curve, positive control sample, and negative control in duplicate to the corresponding wells of the plate for a total reaction volume of 25 μL.
8. Load the PCR plate into the real-time PCR machine (e.g., ABI 7500 Real Time PCR system).
   (a) Run an appropriate protocol (95°C for 10 min followed by 40 cycles of 95°C for 15 s and 60°C for 1 min). The system software processes the raw fluorescence data to produce threshold cycle (Ct) values for each sample.
9. Criteria of a valid assay (see notes 5, 6 and 7 in Section 4).
   (a) The slope of the standard curve should be between −3.0 and −3.5. The threshold between duplicates should be within 0.5 Ct.
   (b) The Ct values of the negative control should be >30.
   (c) The standard curve should have:
      - Linearity correlation coefficient ≥0.98
      - Efficiency of amplification >85%
10. Determine the number of copies per PCR reaction for each dilution of test article by comparing to the standard curve.
11. Calculate the number of vector copies per milliliter (vg/mL) with respect to the dilution and volume of sample analyzed.
12. Calculate the average of the titers obtained for each dilution.

4. Notes

1. For the nonreduced samples, a stained protein band just below the well is expected and represents intact AAV virions.
2. When designing the real-time PCR assay, the primers and probe should not anneal to themselves or each other, or have significant secondary structure.
3. The T_m of the probe should be 10°C higher than the T_m of the primers.
4. The distance between the primers should be less than 200 bp and target vector sequences located between the AAV ITRs.
5. Reduced PCR sensitivity is experienced when the primers and/or probe is placed within AAV ITR sequences, likely due to the unimolecular annealing reaction of the AAV ITR hairpin.
6. The PCR assay should have a sensitivity of at least 100 copies.

7. The digested positive control should give little or no PCR signal, since the plasmid is digested with Benzonase to show that DNA external to the capsid could be digested.

Acknowledgments

We acknowledge Mahuya Bose and Weiyi Ni for insightful discussions. ROS is an inventor on patents related to recombinant AAV technology and owns equity in a gene therapy company that is commercializing AAV for gene therapy applications. To the extent that the work in this manuscript increases the value of these commercial holdings ROS has a conflict of interest.

References

1. Wagner, J. A., Messner, A. H., Moran, M. L., Daifuku, R., Kouyama, K., Desch, J. K., Manley, S., Norbash, A. M., Conrad, C. K., Friborg, S., Reynolds, T., Guggino, W. B., Moss, R. B., Carter, B. J., Wine, J. J., Flotte, T. R., and Gardner, P. (1999) Safety and biological efficacy of an adeno-associated virus vector-cystic fibrosis transmembrane regulator (AAV-CFTR) in the cystic fibrosis maxillary sinus, *Laryngoscope 109*, 266–274.
2. Flotte, T. R., Zeitlin, P. L., Reynolds, T. C., Heald, A. E., Pedersen, P., Beck, S., Conrad, C. K., Brass-Ernst, L., Humphries, M., Sullivan, K., Wetzel, R., Taylor, G., Carter, B. J., and Guggino, W. B. (2003) Phase I trial of intranasal and endobronchial administration of a recombinant adeno-associated virus serotype 2 (rAAV2)-CFTR vector in adult cystic fibrosis patients: a two-part clinical study, *Hum Gene Ther 14*, 1079–1088.
3. Stedman, H., Wilson, J. M., Finke, R., Kleckner, A. L., and Mendell, J. (2000) Phase I clinical trial utilizing gene therapy for limb girdle muscular dystrophy: alpha-, beta-, gamma-, or delta-sarcoglycan gene delivered with intramuscular instillations of adeno-associated vectors, *Hum Gene Ther 11*, 777–790.
4. Manno, C. S., Chew, A. J., Hutchison, S., Larson, P. J., Herzog, R. W., Arruda, V. R., Tai, S. J., Ragni, M. V., Thompson, A., Ozelo, M., Couto, L. B., Leonard, D. G., Johnson, F. A., McClelland, A., Scallan, C., Skarsgard, E., Flake, A. W., Kay, M. A., High, K. A., and Glader, B. (2003) AAV-mediated factor IX gene transfer to skeletal muscle in patients with severe hemophilia B, *Blood 101*, 2963–2972.
5. Janson, C., McPhee, S., Bilaniuk, L., Haselgrove, J., Testaiuti, M., Freese, A., Wang, D. J., Shera, D., Hurh, P., Rupin, J., Saslow, E., Goldfarb, O., Goldberg, M., Larijani, G., Sharrar, W., Liouterman, L., Camp, A., Kolodny, E., Samulski, J., and Leone, P. (2002) Clinical protocol. Gene therapy of Canavan disease: AAV-2 vector for neurosurgical delivery of aspartoacylase gene (ASPA) to the human brain, *Hum Gene Ther 13*, 1391–1412.
6. During, M. J., Kaplitt, M. G., Stern, M. B., and Eidelberg, D. (2001) Subthalamic GAD gene transfer in Parkinson disease patients who are candidates for deep brain stimulation, *Hum Gene Ther 12*, 1589–1591.
7. Flotte, T. R., Brantly, M. L., Spencer, L. T., Byrne, B. J., Spencer, C. T., Baker, D. J., and Humphries, M. (2004) Phase I trial of intramuscular injection of a recombinant adeno-associated virus alpha 1-antitrypsin (rAAV2-CB-hAAT) gene vector to AAT-deficient adults, *Hum Gene Ther 15*, 93–128.
8. Crystal, R. G., Sondhi, D., Hackett, N. R., Kaminsky, S. M., Worgall, S., Stieg, P., Souweidane, M., Hosain, S., Heier, L., Ballon, D., Dinner, M., Wisniewski, K., Kaplitt, M., Greenwald, B. M., Howell, J. D., Strybing, K., Dyke, J., and Voss, H. (2004) Clinical protocol. Administration of a replication-deficient adeno-associated virus gene transfer vector expressing the human CLN2 cDNA to the brain of children with late infantile neuronal ceroid lipofuscinosis, *Hum Gene Ther 15*, 1131–1154.
9. Brantly, M. L., Chulay, J. D., Wang, L., Mueller, C., Humphries, M., Spencer, L. T., Rouhani, F., Conlon, T. J., Calcedo, R., Betts, M. R., Spencer, C., Byrne, B. J., Wilson, J. M., and Flotte, T. R. (2009) Sustained transgene expression despite T lymphocyte responses in a

clinical trial of rAAV1-AAT gene therapy, *Proc Natl Acad Sci U S A 106*, 16363–16368.

10. Manno, C. S., Pierce, G. F., Arruda, V. R., Glader, B., Ragni, M., Rasko, J. J., Ozelo, M. C., Hoots, K., Blatt, P., Konkle, B., Dake, M., Kaye, R., Razavi, M., Zajko, A., Zehnder, J., Rustagi, P. K., Nakai, H., Chew, A., Leonard, D., Wright, J. F., Lessard, R. R., Sommer, J. M., Tigges, M., Sabatino, D., Luk, A., Jiang, H., Mingozzi, F., Couto, L., Ertl, H. C., High, K. A., and Kay, M. A. (2006) Successful transduction of liver in hemophilia by AAV-Factor IX and limitations imposed by the host immune response, *Nat Med 12*, 342–347.
11. High, K. A. (2007) Update on progress and hurdles in novel genetic therapies for hemophilia, *Hematology Am Soc Hematol Educ Program*, 466–472.
12. Ponder, K. P. (2011) Hemophilia gene therapy: a holy grail found, *Mol Ther 19*, 427–428.
13. Mingozzi, F., Meulenberg, J. J., Hui, D. J., Basner-Tschakarjan, E., Hasbrouck, N. C., Edmonson, S. A., Hutnick, N. A., Betts, M. R., Kastelein, J. J., Stroes, E. S., and High, K. A. (2009) AAV-1-mediated gene transfer to skeletal muscle in humans results in dose-dependent activation of capsid-specific T cells, *Blood 114*, 2077–2086.
14. Bainbridge, J. W., Smith, A. J., Barker, S. S., Robbie, S., Henderson, R., Balaggan, K., Viswanathan, A., Holder, G. E., Stockman, A., Tyler, N., Petersen-Jones, S., Bhattacharya, S. S., Thrasher, A. J., Fitzke, F. W., Carter, B. J., Rubin, G. S., Moore, A. T., and Ali, R. R. (2008) Effect of gene therapy on visual function in Leber's congenital amaurosis, *N Engl J Med 358*, 2231–2239.
15. Maguire, A. M., Simonelli, F., Pierce, E. A., Pugh, E. N., Jr., Mingozzi, F., Bennicelli, J., Banfi, S., Marshall, K. A., Testa, F., Surace, E. M., Rossi, S., Lyubarsky, A., Arruda, V. R., Konkle, B., Stone, E., Sun, J., Jacobs, J., Dell'Osso, L., Hertle, R., Ma, J. X., Redmond, T. M., Zhu, X., Hauck, B., Zelenaia, O., Shindler, K. S., Maguire, M. G., Wright, J. F., Volpe, N. J., McDonnell, J. W., Auricchio, A., High, K. A., and Bennett, J. (2008) Safety and efficacy of gene transfer for Leber's congenital amaurosis, *N Engl J Med 358*, 2240–2248.
16. Cideciyan, A. V., Hauswirth, W. W., Aleman, T. S., Kaushal, S., Schwartz, S. B., Boye, S. L., Windsor, E. A., Conlon, T. J., Sumaroka, A., Pang, J. J., Roman, A. J., Byrne, B. J., and Jacobson, S. G. (2009) Human RPE65 gene therapy for Leber congenital amaurosis: persistence of early visual improvements and safety at 1 year, *Hum Gene Ther 20*, 999–1004.
17. Clark, K. R., Voulgaropoulou, F., and Johnson, P. R. (1996) A stable cell line carrying adenovirus-inducible rep and cap genes allows for infectivity titration of adeno-associated virus vectors, *Gene Ther 3*, 1124–1132.
18. Chadeuf, G., Favre, D., Tessier, J., Provost, N., Nony, P., Kleinschmidt, J., Moullier, P., and Salvetti, A. (2000) Efficient recombinant adeno-associated virus production by a stable rep- cap HeLa cell line correlates with adenovirus-induced amplification of the integrated rep-cap genome, *J Gene Med 2*, 260–268.
19. Knop, D. R., and Harrell, H. (2007) Bioreactor production of recombinant herpes simplex virus vectors, *Biotechnol Prog 23*, 715–721.
20. Merten, O. W. (2007) Attention with virus contaminated cell lines, *Cytotechnology 55*, 1–2.
21. Van Vliet, K., Blouin, V., Agbandje-McKenna, M., and Snyder, R. O. (2006) Proteolytic mapping of the adeno-associated virus capsid, *Mol Ther 14*, 809–821.
22. Van Vliet, K., Mohiuddin, Y., McClung, S., Blouin, V., Rolling, F., Moullier, P., Agbandje-McKenna, M., and Snyder, R. O. (2009) Adeno-associated virus capsid serotype identification: Analytical methods development and application, *J Virol Methods 159*, 167–177.
23. Lock, M., McGorray, S., Auricchio, A., Ayuso, E., Beecham, E. J., Blouin-Tavel, V., Bosch, F., Bose, M., Byrne, B. J., Caton, T., Chiorini, J. A., Chtarto, A., Clark, K. R., Conlon, T., Darmon, C., Doria, M., Douar, A., Flotte, T. R., Francis, J. D., Francois, A., Giacca, M., Korn, M. T., Korytov, I., Leon, X., Leuchs, B., Lux, G., Melas, C., Mizukami, H., Moullier, P., Muller, M., Ozawa, K., Philipsberg, T., Poulard, K., Raupp, C., Riviere, C., Roosendaal, S. D., Samulski, R. J., Soltys, S. M., Surosky, R., Tenenbaum, L., Thomas, D. L., van Montfort, B., Veres, G., Wright, J. F., Xu, Y., Zelenaia, O., Zentilin, L., and Snyder, R. O. (2010) Characterization of a recombinant adeno-associated virus type 2 Reference Standard Material, *Hum Gene Ther 21*, 1273–1285.
24. Zhen, Z., Espinoza, Y., Bleu, T., Sommer, J. M., and Wright, J. F. (2004) Infectious titer assay for adeno-associated virus vectors with sensitivity sufficient to detect single infectious events, *Hum Gene Ther 15*, 709–715.
25. Mohiuddin, I., Loiler, S., Zolotukhin, I., Byrne, B. J., Flotte, T. R., and Snyder, R. O. (2005) Herpesvirus-based infectious titering of recombinant adeno-associated viral vectors, *Mol Ther 11*, 320–326.
26. Snyder, R. O., Xiao, X., and Samulski, R. J. (1996) Production of Recombinant Adeno-Associated Viral Vectors, in *Current Protocols in Human Genetics* (Dracopoli, N., Haines, J., Krof, B., Moir, D., Morton, C., Seidman, C.,

Seidman, J., and Smith, D., Eds.), pp 12.11.11-24, John Wiley and Sons, New York.

27. Nony, P., Chadeuf, G., Tessier, J., Moullier, P., and Salvetti, A. (2003) Evidence for packaging of rep-cap sequences into adeno-associated virus (AAV) type 2 capsids in the absence of inverted terminal repeats: a model for generation of rep-positive AAV particles, *J Virol 77*, 776–781.
28. Gao, G. P., Qu, G., Faust, L. Z., Engdahl, R. K., Xiao, W., Hughes, J. V., Zoltick, P. W., and Wilson, J. M. (1998) High-titer adeno-associated viral vectors from a Rep/Cap cell line and hybrid shuttle virus (In Process Citation), *Hum Gene Ther 9*, 2353–2362.
29. Grimm, D., Kern, A., Pawlita, M., Ferrari, F., Samulski, R., and Kleinschmidt, J. (1999) Titration of AAV-2 particles via a novel capsid ELISA: packaging of genomes can limit production of recombinant AAV-2, *Gene Ther 6*, 1322–1330.
30. Wistuba, A., Kern, A., Weger, S., Grimm, D., and Kleinschmidt, J. A. (1997) Subcellular compartmentalization of adeno-associated virus type 2 assembly, *J Virol 71*, 1341–1352.
31. Grimm, D., Kay, M. A., and Kleinschmidt, J. A. (2003) Helper virus-free, optically controllable, and two-plasmid-based production of adeno-associated virus vectors of serotypes 1 to 6, *Mol Ther 7*, 839–850.
32. Sommer, J. J., Smith, P. H., Parthasarathy, S., Isaacs, J., Vijay, S., Kieran, J., Powell, S. K., McClelland, A., and Wright, J. F. (2003) Quantification of adeno-associated virus particles and empty capsids by optical density measurement, *Mol Ther 7*, 122–128.
33. Clark, K. R., Liu, X., McGrath, J. P., and Johnson, P. R. (1999) Highly purified recombinant adeno-associated virus vectors are biologically active and free of detectable helper and wild-type viruses, *Hum Gene Ther 10*, 1031–1039.
34. Drittanti, L., Rivet, C., Manceau, P., Danos, O., and Vega, M. (2000) High throughput production, screening and analysis of adeno-associated viral vectors, *Gene Ther 7*, 924–929.
35. Veldwijk, M. R., Topaly, J., Laufs, S., Hengge, U. R., Wenz, F., Zeller, W. J., and Fruehauf, S. (2002) Development and optimization of a real-time quantitative PCR-based method for the titration of AAV-2 vector stocks, *Mol Ther 6*, 272–278.
36. Flotte, T. R., Burd, P., and Snyder, R. O. (2002) Utility of a Recombinant Adeno-Associated Viral Vector Reference Standard, *BioProcessing 1*, 75–77.
37. Moullier, P., and Snyder, R. O. (2008) International efforts for recombinant adeno-associated viral vector reference standards, *Mol Ther 16*, 1185–1188.

Chapter 18

rAAV Human Trial Experience

Katherine A. High and Patrick Aubourg

Abstract

Recombinant AAV vectors have been used in clinical trials since the mid-1990s, with over 300 subjects enrolled in studies. Although there are not yet licensed AAV products, there are several clear examples of clinical efficacy, and recombinant AAV vectors have a strong safety record after administration both locally and systemically. This chapter provides a review of two types of studies that have shown efficacy, including studies for Leber's congenital amaurosis, a hereditary retinal degenerative disorder in which subretinal administration of AAV has shown efficacy in terms of improvement in multiple measures of visual/retinal function; and of Parkinson's disease which has also shown improvement in clinical and imaging studies after gene transfer to the CNS. The chapter also provides a detailed review of the results of studies of gene therapy for hemophilia, in which short-term efficacy was achieved, but expression of the donated gene failed to persist, likely due to an immune response to the vector. Safety issues relating to AAV-mediated gene transfer are discussed, including a detailed review of the single death to have occurred in an AAV gene therapy trial (likely unrelated to the AAV vector), and of issues related to integration and insertional mutagenesis, risk of germline transmission, and risks related to immune responses to either vector or transgene product. Finally, protocols for determining the presence of vector DNA in body fluids using real-time quantitative PCR, and for isolating, cryopreserving, and testing peripheral blood mononuclear cells for interferon-γ (IFN-γ) responses to capsid are described in detail.

Key words: AAV, Hemophilia B, Leber's congenital amaurosis, Parkinson's disease, Rheumatoid arthritis, Disseminated histoplasmosis, Hepatocellular carcinoma, IFN-γ ELISpot, PBMCs

1. Introduction

As is clear from the foregoing chapters, recombinant AAV vectors have proven extraordinarily safe in human clinical trials, with over 300 human subjects injected and no serious adverse events related to the vector product (Table 1). The evidence for efficacy is more limited but is quite clear in a few instances, primarily in studies for Leber's congenital amaurosis (1–4) and for Parkinson's disease

Richard O. Snyder and Philippe Moullier (eds.), *Adeno-Associated Virus: Methods and Protocols*,
Methods in Molecular Biology, vol. 807, DOI 10.1007/978-1-61779-370-7_18,

Table 1
Summary of clinical trials by AAV gene transfer[a]

Disease (number of patients)	Transgene	Serotype	Route of administration	Clinical trial	References
α1-Antitrypsin def. (21)	α1-Antitrypsin	AAV-2, AAV-1	IM	Phase I/II	(45, 49)
Age-related macular degeneration (recruiting subjects)	sFLT01	AAV-2	Intravitreal injection	Phase I	
Alzheimer's disease (8)	NGF	AAV-2	Intracranial	Phase I/II	(50)
Arthritis R. (127)	TNFR-Fc	AAV-2	Intraarticular	Phase I	(51, 52)
Batten disease (estimated 10)	CLN2	AAV-2	Direct intracranial administration	Phase I	(53)
Canavan's disease (10)	Aspartoacylase	AAV-2	Intracranial	Phase I	(5)
Cystic fibrosis (>130)[b]	CFTR	AAV-2	Direct instillation to maxillary sinus, bronchoscopy to right lower lobe, aerosol to whole lung	Phase I/II	(54)
Severe heart failure (9)	SERCA2a	AAV-1	Antegrade epicardial coronary artery infusion	Phase I/II	(55)
Hemophilia B (8+8)	Factor IX	AAV-2	IM and hepatic	Phase I/II	(9, 56)
HIV vaccine	HIV gag	AAV-2	IM	Phase I/II	

LPL deficiency (8)	LPL	AAV-1	IM	Phase I/II	(40, 41)
LCA (blindness) (12 + 3 + 3)	RPE65	AAV-2	Subretinal	Phase I/II	(1–4)
Muscular dystrophy: Duchenne (3)	Microdystrophin	AAV-1/2 hybrid	IM	Phase I	
Muscular dystrophy: Limb Girdle (estimated 6)	alpha-Sarcoglycan	AAV-1	2–6 Separate injections into the selected muscle	Phase I	(44)
Parkinson's disease (~22)	AA decarboxylase, GA decarboxylase, Neutrophin	AAV-2	Intracranial	Phase I/II	(5, 7)
Pompe's disease (recruiting subjects)	Alpha-glucosidase (GAA)	AAV-1	Series of intradiaphragmatic injections	Phase I/II	

[a]Includes only published data
[b]Does not include subjects who received placebo only

(5–7). Other studies have yielded encouraging data and at least one biological licensing application has been filed (AAV vector expressing lipoprotein lipase (LPL) for individuals with hypertriglyceridemia due to deficiency of that enzyme) (8). This chapter provides a short overview of the most convincing efficacy results and highlights safety concerns that need to be addressed in informed consent documents and also in trial design.

1.1. Clinical Gene Therapy in the CNS Including Retina

A wealth of animal data has provided convincing evidence of cure of a wide range of genetic and acquired diseases in small and large animal models using AAV vectors. One could argue that these results have translated nearly seamlessly to success in humans for congenital blindness and for Parkinson's disease. In the case of the former, three independent groups have shown improvement in outcome measures of visual and retinal function in nearly all treated subjects affected by this hitherto untreatable condition. In the largest series published to date (2), all 12 subjects, ranging in age from 8 to 44 years, showed improvement in visual acuity, visual fields, pupillary light reflex, full field light sensitivity, or ability to navigate an obstacle course, with most showing improvement in several of these endpoints. Results followed closely those seen in animal models in terms of safety, doses required for efficacy, and observation of greatest improvement in youngest subjects, presumably due to better preservation of photoreceptors, and thus greater potential for restoration of visual function, in younger individuals. That multiple research teams all reported similar observations attests to the robustness of the findings. Subretinal injection of an AAV vector is likely a generalizable platform for the treatment of other retinal degenerative diseases, with the caveat that the gene of interest must fit into an AAV vector (<~5 kb). Plans are currently proceeding to conduct trials for X-linked retinoschesis, Leber's hereditary optic neuropathy, and choroideremia. Ability to assess outcome of the therapy may vary widely among these diseases, with some requiring prolonged follow-up to detect improvement relative to the untreated state. As is always the case for the development of therapeutics for previously untreatable conditions, it will be critical to compile accurate databases of the natural history of the untreated disease, using the same endpoints that will be assessed for product licensing. An advantage for initial studies is the ability to use the uninjected eye as a control; however, since the long-term goal in most of these diseases is to inject both eyes, it will be important to develop means to compare the injected eyes to the subject's own baseline. Overall, the discussion of efficacy endpoints in the context of diseases that have no treatment should take into consideration that improvement in even some percentage of cases represents important progress, particularly if vector administration is demonstrated to be safe, so that the risk is low.

Similarly, studies in subjects with Parkinson's disease, using as endpoints functional imaging studies and clinical improvement as measured on the Uniform Parkinson's Disease Rating Scale, reported improvement in the majority of 22 subjects published to date (5, 7). This is of interest since the trials used two different therapeutic strategies (and transgenes), promotion of dopamine synthesis through transfer of human aromatic L-amino acid decarboxylase on the one hand, and conversion of the subthalamic nucleus into an inhibitory rather than an excitatory structure through gene transfer of glutamic acid decarboxylase (to promote inhibitory GABAergic input) in another trial. Improved outcomes were observed over periods of 6–12 months, with observation ongoing. These trials also appeared generally safe despite the need for localized delivery of vector to the CNS through a neurosurgical procedure.

1.2. Clinical Gene Therapy for Hemophilia

In addition to these two disease entities in which AAV2 vectors were introduced into the subretinal space or the central nervous system, efficacy was also demonstrated in an AAV-mediated trial for hemophilia B in which vector was infused into the liver via the hepatic artery (9). However, in contrast to the findings in the LCA and Parkinson's trials, efficacy in the setting of hemophilia B lasted for only a period of several weeks, rather than for years as has been observed in hemophilic dogs and in nonhuman primates (10–13). The reason(s) for the short duration of expression after vector administration to liver in human subjects are not entirely clear. The gradual decline in Factor IX levels, from a high of ~11% at 2 weeks postvector injection to the baseline of <1% by ~12 weeks after injection, was accompanied by a marked increase in serum transaminases which first appeared at approximately 4 weeks after vector injection, reached a maximum at about 5 weeks, and gradually resolved without medical intervention in a time frame similar to the decline in circulating levels of Factor IX. This study thus identified the therapeutic dose of vector (2×10^{12} vg/kg), which was accurately predicted by studies in dogs, but also focused attention on differences between animal models and humans which might account for the difference in duration of expression in humans vs. other animals. Two obvious factors were the prior exposure to wild-type AAV in humans which are the only natural hosts for AAV2 infection, resulting in the existence of memory immune responses to the vector capsid, and possible differences in the hepatic microenvironment between animals with normal livers, and adults with hemophilia, many of whom have been infected with hepatitis B and C from older plasma-derived clotting factor concentrates. To reduce confounding variables, the next subject studied was one who had never been exposed to hepatitis viruses, since he had been treated exclusively with recombinant concentrates. Studies of circulating lymphocytes from this subject, who

was treated at a fivefold lower dose but still manifested a transaminase rise with the same kinetics as the previous subject, showed T-cell responses, both CD4+ and CD8+, to epitopes in the AAV capsid, but not to epitopes in Factor IX. Using the identified epitopes and high-resolution HLA typing on this subject, it was possible to prepare a MHC class I pentamer that could be used to assay the population of capsid-specific CD8+ T cells directly. This demonstrated an expansion of this population of cells that peaked at about 5 weeks after vector infusion, then contracted, in a time course colinear with the rise and fall in liver enzymes. This has led to the hypothesis that reactivation of a memory T-cell response to capsid may have resulted in immune-mediated destruction of the transduced hepatocytes. Subsequent studies have confirmed that preformed capsid antigen can be presented via MHC Class I on the surface of transduced hepatocytes (14), and that presentation of capsid antigen flags hepatocytes for CTL-mediated destruction by HLA-matched capsid-primed CD8+ T cells. Subsequent studies have shown that T-cell activation in this setting is dose-dependent, with less activation occurring at lower multiplicities of infection (15), and moreover that capsid antigen presentation on hepatocytes is reduced in the presence of the proteosomal inhibitor bortezomib. Thus, the most likely scenario is that, after escape of AAV particles from the endosome, uncoating, and DNA entry into the nucleus, at least some capsid is left behind in the cytosol. This undergoes proteasomal processing, and is then transported via TAP into the ER, where it is loaded onto MHC Class I molecules and presented on the surface of the transduced hepatocyte, making it a target for destruction by capsid-specific memory CD8+ T cells, which are more easily activated than naïve T cells, explaining the difference between humans and other animal species (Fig. 1). Other hypotheses that have been advanced to explain this series of events include contamination of the vector preparation with packaged rep/cap plasmid which is then expressed in the transduced cells (http://oba.od.nih.gov/oba/RAC/meetings/jun2009/RAC_Minutes_06-09.pdf); although it is known that AAV preparations contain variable amounts of DNA impurities, including the plasmid encoding rep/cap genes (16), there is no evidence that these sequences are expressed (17). Expression of alternate open reading frames from the wild-type Factor IX sequence, which are then presented and recognized as neoepitopes has also been proposed (18); however, studies in humans undergoing AAV gene transfer for F.IX and experimental animal models do not support this theory (Hui and Mingozzi, unpublished observation).

The important conclusion from all of this is that AAV can clearly transduce human hepatocytes, as predicted by animal models, but that there is likely some immune-mediated event that prevents long-term expression in humans as compared to animals. The available data would suggest that this limitation is dose-related,

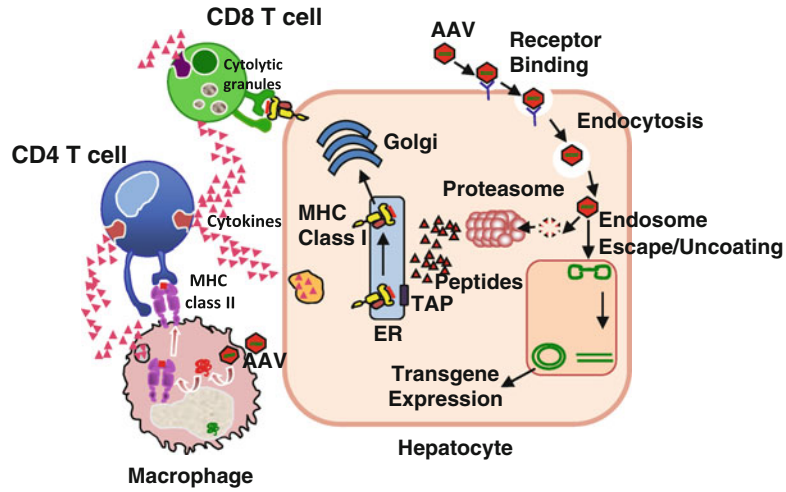

Fig. 1. Model of intracellular trafficking of AAV in hepatocyte. Vector binds to cell surface receptor, enters through clathrin-coated pits, and undergoes endosomal processing critical for transduction. Precise sequence of events surrounding endosomal escape, viral uncoating, and nuclear transport not well-understood. AAV-2 capsid proteins undergo ubiquitination. AAV capsid-derived peptides complexed to MHC class I molecules on surface of AAV-transduced hepatocytes are recognized by capsid-specific CD8+ T cells, which can lyse the target cells.

since the transaminase elevation was more marked at higher doses, and was not evident at all at a dose of 8×10^{10} vg/kg. It will be important to find a solution to this problem if the benefits of liver transduction are to be realized. Clearly a long list of plasma protein deficiencies and metabolic disorders can be approached using AAV therapeutics if a solution is found. Two ongoing trials for hemophilia B are testing two possible solutions: in the first, a more efficient expression cassette that takes advantage of codon optimization and self-complementary design is being infused in an AAV8 capsid, on the supposition that if adequate levels of expression can be achieved at lower vector doses, the immune response will be avoided. The data from in vitro studies in which T-cell activation by AAV-transduced hepatocytes is tracked supports this concept (15). Four subjects have now been enrolled in this study, at doses of 2×10^{11} and 6×10^{11} vg/kg, and have shown detectable levels of circulating F.IX (19). The second study, in which the same AAV2 vector is administered with short-term immunosuppression, tests the hypothesis that the immune response can be blocked or mitigated using drugs that block T-cell proliferation.

1.3. Overall Safety of AAV Vector Administration

As noted at the beginning of this chapter, administration of AAV has proven remarkably safe in a range of clinical settings, from localized to systemic administration. In 2007, a 36-year old woman died while participating in a clinical trial of AAV for rheumatoid arthritis (20). The trial was designed to test the hypothesis that

intraarticular delivery of an AAV vector expressing a TNF-α inhibitor could reduce destructive synovitis in the injected joints. The subject's baseline medical regimen included systemic therapy with a monoclonal antibody to TNF-α, as well as therapy with methotrexate, low-dose prednisone, and cortisone injections of the joint. She underwent uneventful injection of vector in the right knee in February 2007; as specified in the protocol, she underwent a second injection to the same joint in July 2007. The patient was noted to have a low-grade fever (37.6°C) prior to the second injection but otherwise showed normal vital signs. Beginning on the evening of the injection, the patient began to experience nausea, vomiting, fever, and chills; she sought medical attention on several occasions in the ensuing week, and was admitted to hospital 10 days following the injection with a high fever (40°C), elevated white blood cell count, and elevated liver function tests. A diagnostic work-up failed to reveal the cause of the high fever and elevated white count, and the patient was begun on broad-spectrum antibiotics. Clinical and laboratory evidence of a consumptive coagulopathy, acute renal failure, and worsening liver function prompted transfer to a university medical center, but the patient's condition continued to deteriorate and she died 22 days following the injection. Blood cultures had been repeatedly negative during the illness, but cultures drawn on the day of death grew out *Histoplasma capsulatum*, and autopsy findings were consistent with a diagnosis of disseminated histoplasmosis, with organisms present in the liver and the kidney. An expert panel convened by the NIH Recombinant DNA Advisory Committee concluded that the most likely cause of death was the disseminated fungal infection, for which the patient was at risk due to systemic therapy with the monoclonal antibody to TNF-α, and residence in an area where histoplasmosis was endemic (21). Although it is impossible to rule out a relationship to the intraarticular injection of AAV, the experts assembled on the panel noted that the clinical presentation was most consistent with that of disseminated histoplasmosis in an immunocompromised host, a clinical scenario that had been encountered frequently in patients with AIDS living in that part of the USA prior to the availability of highly active antiretroviral therapy. The careful public review of the case by experts, and the availability of extensive laboratory and autopsy data, lend credence to this assessment. Moreover, administration of AAV even systemically has failed to reveal findings similar to those reported here, so that it is difficult to formulate a hypothesis to explain how administration of a recombinant AAV vector to the joint could result in this series of events. The expert panel did point out that it would be useful to develop an assay that would allow investigators to quantify the transgene product as distinct from other biological agents administered in this disease. The consensus of most experts remains that administration of AAV has proven remarkably safe.

1.4. Risks Related to AAV Vector Administration

At the time of this writing, there are no licensed AAV gene therapy products in the USA or Europe. An important consideration for those participating in clinical trials of AAV vectors is a clear understanding of the risks involved in trial participation. These are discussed briefly below.

1.4.1. Risk of Integration and Insertional Mutagenesis

AAV has been classified by the US FDA as a nonintegrating vector (22) and a wealth of published data supports the notion that most of the vector DNA is indeed episomal. However, studies by a number of groups have established that AAV vector DNA can also integrate into the host cell genome, with a preference for integration at existing chromosomal breaks, which favors actively transcribed genes and palindromic sequences (23, 24). There have been two published reports of tumors associated with AAV vector administration (25, 26); these came from the same laboratory and involved the administration of an AAV vector expressing β-glucuronidase to newborn mice, either normal or mice with mucopolysaccharidosis type VII (β-glucuronidase-deficient). In both instances, mice developed hepatocellular carcinoma at higher than expected rates; these occurred at late time points and thus might have escaped notice in other studies in which mice were not followed for prolonged periods. Analysis of integration sites in the normal newborn mice (26) revealed integration within the same 6-kb region on mouse chromosome 12 in four different tumors from four different mice. These specific integration sites were not detected in normal adjacent tissue, and they were associated with a 10- to 100-fold upregulation of expression of miRNAs encoded in regions adjacent to the integration site. Weighing against this is a subsequent study in which high doses of AAV were administered to the livers of young adult mice, which were followed for 18 months, but showed no significant increase in incidence of hepatocellular carcinoma compared to controls at the time of sacrifice (although the study was not powered to detect small differences). Analysis of 1,029 integrants from liver tumors in this study showed no major differences in integration patterns in tumor tissue vs. normal adjacent tissue. These data are in good agreement with data from the hemophilia B dog colony, where >30 animals have been followed for periods of up to 10 years with no evidence of tumor formation on periodic liver ultrasounds (27, 28). At this point, prudence dictates that the informed consent document include a description of the findings in the first mouse study noted above, and acknowledge that it is possible that AAV vector might cause cancer in the liver or in other cells that are exposed to vector. Sample language describing these findings is included below in Subheading 3.1.

1.4.2. Biodistribution/Risk of Germline Transmission

The goal of biodistribution studies is to determine persistence and levels of vector DNA in both the target and other tissues following administration of vector. Given the variation in tropisms for distinct

serotypes, it is likely that new studies must be carried out for each different serotype introduced into clinical trials. Obviously biodistribution differs based on route of administration so that novel methods of administering vector would also require a biodistribution study.

For both preclinical and clinical studies, the level of sensitivity required for the PCR assay is specified by the US regulatory agencies as ≤50 copies vector/μg genomic DNA (22). Typically of greatest concern is distribution to the brain and/or gonads.

While most routes of administration of AAV vectors that have been tested are not associated with detectable distribution of vector to the gonads, delivery of AAV vectors through the systemic circulation in humans has resulted in contamination of semen DNA with vector sequences as detected by a sensitive PCR assay (50 copies/μg genomic DNA). The risk in this setting is that, if the vector integrates into the germ cell, the integration event may disrupt the highly ordered sequence of gene expression and repression events that characterize normal embryonic and fetal development, resulting in fetal malformation or death. A series of studies in a rabbit model has shown that administration of vector into the systemic circulation results in the presence of vector DNA in the semen and that this disappears in a time- and dose-dependent fashion (29, 30). Other studies showed that more frequent ejaculation results in more rapid clearing of the semen in animal models (30) and that the semen is similarly contaminated even in vasectomized rabbits (31), suggesting that structures in the GU tract, as well as the testis, contribute to vector shedding in the semen. Findings have been the same for all serotypes tested in the rabbit model thus far (31). A possibility that is more difficult to address in animal models is that vector could conceivably transduce early spermatocyte precursors (A0 spermatogonia) and that these could eventually begin to cycle and give rise to germ cells that are positive for vector sequences long after the semen had appeared to be negative for vector sequences. Two types of evidence argue against this. First, rabbits receiving vector have been followed through multiple cycles of spermatogenesis after the semen turns negative without evidence of recurrence of positivity (30). Second, at least in the murine model, the spermatogonial precursors are resistant to direct transduction by AAV vectors (29).

To insure that men who wish to father children after the gene transfer procedure have an uncontaminated source of semen for fertilization, individuals are encouraged to bank sperm prior to vector administration. In the ongoing AAV2-F.IX liver trial, the expense of this is borne by the trial. After the administration of vector to the liver, if the semen clears of vector sequences (which has been the case for every subject studied thus far), these samples can be discarded. We advise the use of barrier birth control for these subjects until three consecutive semen samples, drawn 1 month apart, have tested negative in the PCR assay.

Subheading 3.2 provides typical language in an informed consent document to describe the risks of inadvertent germline transmission of vector sequences, and an approach to mitigating risk. Subheading 3.3 provides a sample protocol for detecting vector sequences in DNA extracted from body fluids.

It should be noted here that much of the experimental and clinical database examines risks related to inadvertent germline gene transmission in males rather than females, as a consequence of the fact that assessment of female germ cells is considerably more difficult and invasive. These risks are therefore more difficult to present to research subjects and to provide informed counseling about.

1.4.3. Risks Related to Immune Responses to Vector and/or to Transgene Product

A complexity of in vivo gene therapy in general and of AAV vectors in particular is that therapy may be complicated or thwarted by immune responses to either the transgene product or to the vector capsid. When these arise, it is critical to determine which part of the multicomponent therapeutic, the vector or the transgene product, has given rise to the response, since otherwise it is impossible to know how to move forward. As a general rule, animal models have more accurately predicted clinical immune responses to the transgene product than to the vector capsid. A number of variables influence immune responses to the transgene product; some of these are well-known based on studies of protein therapeutics. Thus, the presence of local inflammation in the target tissue and the degree of tolerance to the transgene product conferred by the underlying mutation responsible for the genetic disease are well-recognized factors in determining immune responses to (protein) enzyme replacement therapies. These have been verified as risk factors in the gene therapy setting using animal models and gene transfer vectors that encode a species-specific transgene, a crucial requirement for generating interpretable data (the single exception to this is the use of human transgenes in nonhuman primates, due to the high degree of conservation between species) (12, 32–34). In terms of factors that are specific to the gene transfer setting, the route of administration may affect the immune response, with target tissues such as skeletal muscle and skin being associated with a higher risk of immune response to the transgene product (32, 35), and liver being associated with a lower risk, in fact with a tendency to promote tolerance to the transgene product (36, 37).

The implications of these observations are that it is prudent to carry out preclinical studies in animal models that are also deficient in the transgene product if these exist, and that these should be done with a species-specific transgene. It should also be borne in mind that some inbred mouse strains are probably less likely to mount immune responses than humans, and thus when possible data from outbred large animal strains is to be preferred. A conservative approach when information is lacking is to include in initial

clinical trials only those subjects with underlying genetic mutations that are likely to confer some degree of tolerance to the transgene product, i.e., those with missense mutations, and to exclude individuals with, e.g., large gene deletions.

Immune responses to AAV capsid have proven more difficult to dissect, partly because, until quite recently, they have not been analyzed in a systematic fashion. We have chosen to screen for these using interferon-γ (IFN-γ) ELISPOT, which is useful as a screening tool because it is sensitive enough to detect even low-frequency cells (as low as 1 in 10^5), does not require in vitro expansion of cells, which can bias results, and uses small volumes of primary cells. Data that have emerged over the past year have tended to confirm our initial observations, i.e., that T-cell responses against the AAV capsid are detected in a dose-dependent fashion after the delivery of AAV vector to nonimmunoprivileged compartments in humans (vide infra). Whether or not these result in any clinical manifestations will depend on a number of factors including the level of MHC Class I expression of the target tissue, and whether the transgene product itself is an immunomodulatory molecule, such as α_1-antitrypsin, a serine protease inhibitor which blocks the activity of enzymes released by CD8+ T cells that are required for cellular lytic function (38, 39).

Evidence that T-cell responses are triggered against the AAV capsid in a dose-dependent fashion comes from experience with intramuscular (IM) delivery of AAV vectors in humans. As shown in Table 2, increasing doses of AAV1 vectors delivered IM result in an increased frequency of detection of capsid-directed T cells, with 100% of subjects having detectable capsid T cells in peripheral blood at doses $>2 \times 10^{13}$ vg total. Similarly, an increase in the magnitude of the response in terms of higher numbers of reactive T cells circulating in peripheral blood, or faster kinetics of detection of T cells in the periphery, is also associated with higher vector doses administered IM.

Table 2
Immune response to capsid after IM injection of AAV vectors is dose-dependent

Serotype	Transgene	Dose (vg)	IFN-γ ELISPOT	Magnitude SFU/10^6 cells	References
AAV 1	Sarcoglycan	3.25×10^{11}	1/3	60–70	(44)
AAV 1	LPL	7.0×10^{12}	2/4	~300	(41)
	LPL	2.1×10^{13}	3/6	~300 Different kinetics	(41)
AAV 1	α1-Antitrypsin	2.2×10^{13}	2/2 tested	~100	(45)
	α1-Antitrypsin	6.0×10^{13}	3/3 tested	<200–428	(45)

Vector dose-dependent activation of capsid T-cell responses has been described in a clinical study of AAV1 intramuscular gene transfer for LPL deficiency. LPL deficiency is a rare inherited diseased associated with high triglyceride (TG) levels in serum and recurrent bouts of pancreatitis. (40).

T-cell monitoring in the subjects from the LPL study showed a dose-dependent activation of T-cell responses in terms of kinetics of detection, with earlier detection at higher vector doses. In addition, while at lower vector doses (1×10^{11} vg/kg), mainly CD4+ T-cell response was documented, higher vector doses resulted in the activation of both CD4+ and CD8+ capsid T cells (41). The significance of detection of capsid T cells in terms of therapeutic efficacy is still the subject of debate. Studies by several groups in mice have shown that transgene-specific CD8+ T cells undergo apoptosis-mediated silencing after trafficking to injected muscle (42, 43). Whether a similar fate occurs with capsid-specific CD8+ T cells in humans is unknown. Moreover, the clinical consequences of activation of capsid-specific T cells on transgene expression are likely influenced by several other factors, including the levels of expression of MHC class I in the target tissue (44) and the immunomodulatory properties (or the immunogenicity) of the therapeutic transgene product itself (45, 46). At this point, it is probably useful to monitor T-cell responses to both capsid and transgene product in human subjects undergoing AAV-mediated gene transfer. These data will help to determine whether immune responses are interfering with optimal expression of the donated gene. Protocols for isolation and preservation of peripheral blood mononuclear cells (PBMCs) (Subheading 3.4) and for screening of these cells for immune responses to capsid or transgene product by ELISpot (Subheading 3.5) are provided.

2. Materials

2.1. Analysis of Viral Vector Shedding by Real-Time Quantitative PCR

1. Puregene DNA isolation kit (Gentra Systems, Minneapolis, MN cat. no. D5500A).
2. Tissue culture grade water (Sigma Chemical Company, St. Louis, MO).
3. Universal Master Mix.
4. Primers (forward and reverse) and probes stored at –20°C.
5. ABI Prism 7900 HT Sequence Detection System (Applied Biosystems).
6. 384-Well plates with barcode (Applied Biosystems).
7. Powder-free gloves.

2.2. Isolation and Cryopreservation of PBMCs

1. PBS, sterile, Ca^{2+}, Mg^{2+} free, Invitrogen 14190–136 or equivalent.
2. Heat-inactivated fetal bovine serum (FBS), Hyclone, or equivalent.
3. DMSO, Tissue culture grade (Sigma D2650).
4. 2-Propanol, Sigma, or equivalent.
5. 500 mL Filtering system, 0.22 μm, Millipore SCGPU05RE.
6. Trypan Blue (Sigma T8154 or equivalent) for viable cell counts.
7. Vials, cryogenic, 1.8 mL, sterile Nalgene/Nunc #368632.
8. Human AB serum (filtered and heat-inactivated).

   Heat-inactivate the serum at 56°C for 30 min.

   Let cool to room temperature and filter through 0.22 μM filter.

   Store in 10 mL aliquots at –20°C, maintain sterile.
9. PBS 1% HuAB.

   Work under biological safety cabinet, maintain reagents sterility.

   Thaw an aliquot of Human AB serum in a 37°C waterbath.

   Add 1 part of Human AB serum in 99 parts of 1× PBS (1% volume Human AB) in a 50-mL centrifuge tube.
10. Freezing Medium A.

    Work under biological safety cabinet, maintain reagents sterility.

    Freezing Medium A consists of 100% Human AB serum.

    Thaw the amount needed in 37°C waterbath, make sure to equilibrate to room temperature before use.
11. Freezing Medium B.

    Work under biological safety cabinet, maintain reagents sterility.

    Freezing Medium B consists of 20% DMSO in Human AB serum.

    Thaw the amount needed in 37°C waterbath, make sure to equilibrate to room temperature before use.

    Add one part of DMSO in four parts of human AB serum (20% volume DMSO) in a 15-mL centrifuge tube.

    Gently invert the tube several times to mix the content, avoid formation of bubbles.

    Prepare fresh, discard leftover, equilibrate to room temperature after mixing.

2.3. Analyzing Immune Responses to Capsid by IFN-γ ELISpot

1. Dulbecco's PBS, sterile.
2. AIM-V lymphocyte medium.
3. FBS, heat-inactivated and filtered.
4. Bovine serum albumin (BSA).

5. Phorbol 12-myristate 13-acetate (PMA).
6. Ionomycin Calcium Salt.
7. CEF (CMV, EBV, Flu peptide pool).
8. Anti-human IFN-γ purified, coating antibody.
9. Anti-human IFN-γ biotin-conjugated, detecting antibody.
10. Streptavidin-ALP.
11. BCIP/NBT phosphate substrate.
12. Benzonase.
13. MultiScreen HTS-IP Filter Plate, Millipore.
14. Microplate washer.
15. ELISpot reader.

3. Methods

3.1. Sample Language on Risk of Insertional Mutagenesis

This is taken from the informed consent document used in the AAV2-Factor IX liver trial sponsored by the Center for Cellular and Molecular Therapeutics at the Children's Hospital of Philadelphia (47). This language has thus been reviewed and approved by both local and federal regulatory authorities in Philadelphia and the USA, respectively. The language used attempts to explain the findings on insertional mutagenesis in a manner easily understood by someone without a scientific background.

"It is possible that AAV vectors could cause cancer in the liver or other cells that are exposed to AAV2-hFIX

- The FDA, which oversees clinical studies of new drugs, became aware of studies of mice with a rare genetic disease who received an AAV vector shortly after birth. Some of these mice developed tumors (liver, blood vessel tumors) many months later.
- In another study by the same investigators, normal mice injected with an AAV vector in the newborn period also developed tumors.
- Studies with adult mice, as well as dogs and monkeys (normal and with other genetic diseases), infused with AAV vectors have not shown more tumors than in control groups regardless of the disease, and whether AAV was given directly into the general circulation, into muscle, lung, or into the liver directly.
- There have been no cancers reported in human subjects enrolled in the earlier AAV hemophilia studies. The first subjects were injected with vector in the muscle in 1999 and in the liver in 2001."

3.2. Sample Language on Risk of Inadvertent Germline Transmission of Vector Sequences

As above in Subheading 3.1, this language is taken from the informed consent document used in the AAV2-F.IX liver trial (vide supra). Since hemophilia B is an X-linked disorder, and all candidates for this trial are males, the language deals only with risks of germline transmission in males.

Study subjects shall be adult males who are 18 years of age or older. Subjects infused with vector in the earlier version of the liver study were shown by very sensitive techniques to have vector in the semen for as long as 16 weeks after administration, after which point vector was no longer detectable.

- All subjects are strongly urged to use barrier birth control devices (condoms) until the subject is informed that semen has been clear of vector for at least 2 months.
- The investigators will notify you when it is safe to stop barrier methods of birth control.
- The consequences of gene transfer to germline cells (sperm cells) are unknown but could potentially result in serious birth defects or fetal death or other unanticipated health consequences (such as cancer) in the offspring due to the disruption of normal genes by the transferred DNA.
- If you are considering having children in the future, it is recommended that you bank sperm prior to beginning the procedure to ensure a source of sperm that is free of contamination with the vector. The reason for storing the semen is that it is possible that if the sperm cells do take up the vector during the procedure, it may or may not result in lifelong changes to the sperm.
- This has not occurred in the previous subjects studied with this procedure, but the investigators need to continue to monitor for this possibility.
- The investigators will provide you with information on sperm banking. This opportunity will be provided to you at no additional expense.

3.3. Analysis of Viral Vector Shedding by Real-Time Quantitative PCR

Monitoring of vector shedding is performed on DNA extracted from blood and various body fluids by measuring vector genome copy number using real-time quantitative PCR.

Depending on the route of vector administration, and the results from the preclinical biodistribution studies, in addition to blood components (serum and PBMC), a variety of body fluids may be analyzed, including saliva, semen, urine, tear swabs, etc.

DNA extraction should be optimized, as DNA and protein contaminants will be present in variable amounts depending on the nature of the specimens (see Note 1).

An inhibition control (vide infra) should always be included in the PCR and cross-contamination must also be scrupulously

avoided in the preanalytic stage, i.e., during sample collection and handling (see Note 2).

A reference sample with known gene copy number should be prepared by digesting a plasmid (see Note 3) containing the sequence of the AAV expression cassette with a restriction enzyme that cuts only once within the plasmid backbone (outside the ITR).

3.3.1. DNA Extraction

Extract DNA from source materials according to established protocols. Measure OD and determine OD 260/280 ratio, repeat DNA extraction or perform DNA precipitation if the ratio is too low (e.g., <1.8).

3.3.2. Preparation of Linearized Plasmid DNA for Sample Spiking and Standard Curve

1. Any plasmid bearing the specific target sequence (the expression cassette flanked by the viral ITRs) can be used to prepare the linearized material for the real-time PCR.
2. Select a single cutting restriction enzyme located outside the target sequence used for real-time PCR.
3. Set up a digest of a large quantity of plasmid, 10–30 μg, making sure that the reaction conditions will allow optimal cutting.
4. Verify complete digestion by running a small aliquot of digested plasmid on an agarose gel. If digestion is not complete, add more enzyme to the reaction and incubate longer.
5. Heat-inactivate the restriction enzyme at 65°C for 20 min. Note that some restriction enzymes will require higher temperatures for heat inactivation. Store at –20°C.
6. Perform phenol–chloroform extraction of DNA. As an alternative to heat inactivation, one can proceed directly to phenol–chloroform extraction after restriction digest.
7. After phenol–chloroform extraction, precipitate DNA.
8. Resuspend DNA and run an aliquot on an agarose gel.
9. Measure DNA concentration with a spectrophotometer; perform several dilutions to obtain an accurate measurement.
10. Calculate the number of molecules in the solution assuming that 1 mg of a 1 Kb of double-stranded DNA is equivalent to 9.1×10^{11} molecules (copies). Therefore, the copies per milliliter of solution of the linearized plasmid can be obtained with the following equation:

$$\text{Concentration}\left(\text{copies} / \text{mL}\right) = [\text{DNA concentration}(\mu\text{g} / \text{mL}) \times 9.1 \times 10^{11} \ (\text{copies} / \mu\text{g})] / [\text{Plasmid size } (\text{kb}) / 1 \text{ kb}]$$

11. Dilute to the appropriate copy number/mL and store at –20°C in aliquots (see Note 4).

3.3.3. Preparation of the Standard

1. If stored for a prolonged period, verify integrity of the linearized plasmid DNA by agarose electrophoresis and absorbance at 260 nm.
2. Prepare eight serial dilutions of the linearized plasmid in a large volume (see Note 5), like 5,000 µL (dilutions can be stored at −80°C in 20 µL aliquots and used multiple times).

3.3.4. Preparation of Real-Time Quantitative PCR Amplification Mix

The following is an example of a real-time quantitative PCR mix. For standards, no test DNA should be included; for spiking controls 10 or 100 copies of linearized plasmid should be mixed with the test DNA (see Notes 6–11).

Reagents[a]	1× (µL)	Final concentration
Universal master mix (2×)	10.0	1×
Forward primer (50 µM)	0.36	900 nM
Reverse primer (50 µM)	0.36	900 nM
Probe (100 µM)	0.05	250 nM
Water	1.23	
Test DNA (125 ng/µL)	8.0	1 µg
Total volume	20.0	

[a] TaqMan™ technology

3.3.5. Interpretation of Results

1. The water control should not give any amplification signal.
2. The gene copy number of the 10-copy and 100-copy spiking controls will be reported for each specimen. These values will be used as a reference to validate the assay (see Note 12).
3. A specimen is interpreted as negative if there is no amplification in the wells with the unspiked specimens or if the signal is lower than that of the spiked 10-copy vector control.
4. Amplification must be detected in the spiked 100-copy vector control, otherwise the assay should be rejected.
5. A specimen is interpreted as inhibited if no amplification is detected in the 100-copy or the 10-copy controls, as well as the unspiked experimental samples. Any specimen reported as inhibited should be column-purified or re-extracted and re-tested to try to eliminate inhibition.
6. A specimen is interpreted as positive for vector if there is amplification detected in both the spiked and unspiked reactions.
7. If identical replicate samples have a threshold cycle (CT) standard deviation >0.3 and/or the standard curve has a correlation coefficient (R^2 value) <0.99, the accuracy of the data is questionable.

8. PCR amplification efficiency is the rate at which PCR amplicons are generated, commonly expressed as a percentage value. If a particular PCR amplicon doubles in quantity during the geometric phase of the PCR amplification, the PCR assay has 100% efficiency. The slope of a standard curve is commonly used to estimate the PCR amplification efficiency of a real-time PCR. A real-time PCR standard curve is graphically represented as semi-log regression line plots of CT value vs. log of input nucleic acid. A standard curve slope of −3.32 indicates a PCR with 100% efficiency. Slopes more negative than −3.32 (e.g., −3.9) indicate reactions that are less than 100% efficient. Slopes more positive than −3.32 (e.g., −2.5) may indicate sample quality or pipetting problems.

3.4. Isolation and Cryopreservation of PBMCs

Isolation and cryopreservation of PBMC from whole blood is the most critical step in immunomonitoring. The quality of PBMC preparations will influence cell viability and thus the outcome of the downstream assays (ELISpot assay and other T-cell assays).

The classic protocols for PBMC isolation from whole blood are based on ficoll gradient centrifugation, which are very effective but require trained personnel and are time-consuming. Alternative techniques or devices can be used for PBMC separation, for example, the cell preparation tube (CPT) vacutainers, which allow for separation of PBMC directly within the blood collection tube with a simple centrifugation step. In the first part of this section both methods will be reviewed.

3.4.1. Isolation of PBMC Using Ficoll Gradient

1. Whole blood should be obtained by venipuncture into properly labeled blood collection tubes containing an anticoagulant such as heparin, EDTA, or sodium citrate.
2. Keep samples at room temperature; proceed to PBMC isolation within 12–24 h of blood collection. If shipping the samples to a centralized laboratory for further processing, protect the specimens from extreme temperatures with proper insulation; never freeze blood.
3. Pool blood from all collection tubes into a 50-mL conical tube.
4. Add an equal volume of Ca-free sterile PBS at room temperature to blood and mix gently by inverting the tube.
5. In a separate 50 mL tube, add a volume of room temperature ficoll equal to one-third that of the diluted blood, divide into multiple 50 mL tubes if necessary.
6. Gently overlay the ficoll with the diluted blood, minimize mixing of the two phases.
7. Centrifuge at 740 × *g* for 30 min at room temperature with *brake off* to preserve the density gradient.

8. When the centrifuge comes to a complete stop, collect the PBMC layer that will be visible at the interface between plasma and ficoll and place the cells into a fresh, sterile 50 mL tube. Try to avoid collecting ficoll while collecting the PBMCs.
9. Add at least two volumes of room temperature Ca-free PBS to the PBMC, if necessary split the cells into multiple tubes.
10. Centrifuge the PBMC at 330×*g* for 10 min at room temperature (brake on).
11. At the end of the centrifuge spin, *immediately* decant supernatant and resuspend the cell pellet(s) by tapping the tube until no clumps are visible. Do not pipette or vortex.
12. Resuspend in 5 mL PBS. To help prevent cell clumping at this step, use PBS with 2% heat-inactivated FBS and 25 U/mL benzonase.
13. Count PBMC with an automated cell counter or using a hemocytometer.
14. Wash PBMC a second time by spinning the cells at 330×*g* for 10 min at room temperature.
15. At the end of the centrifuge spin, *immediately* decant supernatant and resuspend the cell pellet(s) by tapping the tube until no clumps are visible.
16. Proceed to cell freezing.

3.4.2. Isolation of PBMC Using CPTs

1. CPT vacutainer tubes (Becton Dickinson) with the appropriate anticoagulant should be kept at room temperature and properly labeled with visit date, visit name, and subject identification (unique subject ID).
2. Collect blood into the tubes using standard venipuncture techniques. Invert tubes approximately ten times.
3. After collection, store the tube upright at room temperature until centrifugation. For best results, do not store the tube for more than 2 h after blood collection without spinning.
4. Before centrifugation, mix the blood by gently inverting the CPT an additional eight to ten times. Use a temperature-controlled horizontal rotor (swinging bucket) centrifuge and set the temperature to 18–25°C. Centrifuge tube with blood sample at 1,800×*g* for 30 min at room temperature.
5. After centrifugation you should be able to see the PBMC band above the gel barrier retaining all red cells at the bottom of the tube.
6. Continue if proceeding for freezing. (If shipping to a central sample processing location, see Note 13).
7. Using a serological pipette carefully remove and discard the top half of plasma layer in the tube. Do not disturb the PBMC

layer. From an individual CPT, collect remaining plasma with the PBMC with a serological pipette. Transfer the contents of one CPT into one 15 mL tube. Add PBS to bring the volume in the tube up to 14 mL.

8. Cap 15 mL tube and invert to mix cell solution. Centrifuge at $330 \times g$ for 10 min at room temperature (brake on).
9. At the end of the centrifuge spin, *immediately* decant supernatant and resuspend the cell pellet(s) by tapping the tube until no clumps are visible. Do not pipette or vortex.
10. Resuspend in 5 mL PBS. To help prevent cell clumping at this step, use PBS with 2% heat-inactivated FBS and 25 U/mL benzonase.
11. Count PBMC with an automated cell counter or using a hemocytometer.
12. Wash PBMC a second time by spinning the cells at $330 \times g$ for 10 min at room temperature.
13. At the end of the centrifuge spin, *immediately* decant supernatant and resuspend the cell pellet(s) by tapping the tube until no clumps are visible.
14. Proceed to cell freezing (Subheading 3.4.3).

3.4.3. Cryopreservation of PBMC

1. After re-suspending the cell pellet by tapping the tube, add the appropriate amount of FBS to adjust the cell concentration to 2×10^7/mL.
2. Mix cells by gently tapping the tube.
3. Add dropwise to the side of the tube an equal volume of FBS with 20% DMSO to the cells resuspended in FBS only.
4. Mix the cells gently, and *promptly* aliquot the PBMC suspension into the prelabeled cryovials (~10 million cells per vial).
5. Place the cryovials with the cells in a cryofreezing container filled with 2-propanol and place the container in a −70°C freezer for a minimum of 12 h.
6. For long-term storage, place the cryovials in the vapor phase of a liquid nitrogen cryostat. Ship in dry ice and do not refreeze cells after thawing.

3.5. Analyzing Immune Responses to Capsid by IFN-γ ELISpot

Analysis of cellular immune responses to a specific antigen such as vector capsid can be conveniently monitored over time and among different subjects using the ELISpot assay. A range of different cytokines or other T-cell activation markers may be assayed for, however, IFN-γ is typically used as a screen since it is a general marker of activation and effector activity of T cells. The ELISpot is attractive as a screening assay since it is sensitive enough to detect even low-frequency cells (as low as 1 in 10^5), does not require

in vitro expansion of cells, which can bias results, and uses small volumes of primary cells. Disadvantages are that it cannot distinguish CD4+ from CD8+ T-cell responses without additional cell selection, and cannot distinguish memory from effector responses.

The ELISpot technique is adapted from the ELISA. Cells are placed over antibodies coated to a membrane in a tissue culture plate (see Notes 14 and 15). Upon stimulation with an antigen of interest, in this case either whole capsid or capsid-derived peptides, cells secrete cytokines which are trapped by the antibodies coated to the well and which can be detected by a secondary antibody conjugated to an enzyme such as alkaline phosphatase. Cleavage of a colorless substrate by the enzyme is used to make localized colored spots where the reactive T cell was present. Counting each spot, and knowing the number of cells added to the well, allows an estimation of the frequency of antigen-specific cells within a population of cells. Monitoring of these over time can allow tracking of a response after vector infusion. Results can be compared in terms of magnitude and kinetics of response.

Although ELISpots are frequently considered one of the most straightforward immune assays to standardize, there can still be considerable variability from one laboratory to another. A recent study used proficiency panels, frozen PBMCs on which results of IFN-γ ELISpot had already been determined, to survey ELISpot assays in 36 laboratories considered expert at the procedure, and still recorded substantial variations in results. Factors such as careful attention to cell viability and the use of conditions that result in low background were crucial for a reliable and accurate assay (48).

3.5.1. Coating the Plate: Day 1 of the Assay

1. Coat each well with 100 μL of anti-IFN-γ primary antibody in sterile PBS.
2. Wrap each plate in plastic wrap and incubate overnight at 4°C.

3.5.2. Plating the Cells: Day 2 of the Assay

1. Decant primary antibody.
2. Wash each well 3× with 200 μL of sterile PBS.
3. Block membrane with 3% FBS in sterile PBS. Incubate at room temperature for about 2 h.
4. Thaw cells to be assayed quickly in a 37°C waterbath; make sure that the cryovial containing the sample is well sealed, wipe the vial with 70% ethanol before opening it under a tissue culture hood.
5. Transfer the thawed cells with a pipette to a sterile 15 mL tube containing 10 mL of AIM-V medium with 3% FBS (or equivalent) and 10 U/mL of benzonase.
6. Spin at 450×*g* for 5 min in a swinging-bucket centrifuge.
7. Decant supernatant and quickly resuspend the pellet by tipping the tube.

8. Add 10 mL of AIM-V with 3% FBS and 10 U/mL of benzonase. Mix gently by inverting the tube.
9. Spin at 450×*g* for 5 min.
10. Decant supernatant and resuspend the pellet by tipping the tube.
11. Add to 1 mL AIM-V with 3% FBS without benzonase.
12. Count the cells.
13. Dilute cells to $1–3 \times 10^6$ cells/mL (depending on cell yield) using AIM-V with 3% FBS.
14. Prepare antigens (whole protein or peptides), positive controls (CEF peptide pool, anti-CD3 antibody, PMA, etc.), and negative controls (medium only, solvent only, irrelevant antigen, etc.) by diluting them in assay medium at a 2× concentration.
15. Decant the PBS 3% FBS blocking solution and wash the plate twice with the test medium (AIM-V 3% FBS).
16. Add 100 µL of antigens and controls in triplicate to the appropriate wells on the plate.
17. Add 100 µL of cells to each well dropwise with a multichannel pipette, making sure to change tips each time.
18. Incubate overnight at 37°C 5% CO_2. (see Note 16).

3.5.3. Washing and Developing the Assay Plate: Day 3 of the Assay

1. Remove media from plate by decanting contents.
2. Wash each well with wash buffer (0.05% Tween 20 in PBS) by pipetting up and down several times from different angles.
3. Decant, repeat once.
4. Wash 4× using a plate washer.
5. Rinse the plate one time with PBS. Decant.
6. Add 100 µL of biotin-conjugated secondary antibody diluted in PBS 1% BSA.
7. Incubate at room temperature for 2 h.
8. Decant secondary antibody.
9. Wash six times with wash buffer using a plate washer.
10. Wash one time with PBS, decant.
11. Add 100 µL of streptavidin-ALP in PBS 1% BSA.
12. Incubate at room temperature for 1 h (Meanwhile remove the substrate from the refrigerator to let it warm up to room temperature).
13. Decant, wash four times with wash buffer using the plate washer.
14. Wash with PBS.
15. Dry plate by blotting on paper towels.

16. Add 100 μL per well of substrate.
17. Wait for color development, approximately 10 min.
18. Wash carefully with water, blot plate on paper towels, and remove protective film from the bottom of the plate.
19. Dry overnight protected from light.

3.5.4. Reading the Results

1. Read the plate on an ELISpot reader.
2. Transfer results to an Excel spreadsheet and express results in spot forming units (SFUs) per million cells plated (e.g., if 2.5×10^5 cells were plated in each well, the spot count in each well will be multiplied ×4 to obtain the SFU/10^6 PBMC count).
3. Archive results properly.

3.5.5. Data Interpretation

The cutoff for positivity generally accepted in the ELISpot assay is threefold the SFU/10^6 PBMC of the negative control and greater than 50 SFU/10^6 PBMC absolute count (see Note 17).

4. Notes

1. For the accuracy of the assay, it is very important to obtain DNA free of contaminants that may interfere with the efficiency the PCR by inhibiting the DNA polymerase (like heme from whole blood or chemical residues from the DNA extraction). The 260/280 OD ratio should reflect a low protein content.
2. Contamination of one sample by another is always an important concern when using a PCR-based method for the detection of viral genomes. Always practice standard methods to avoid PCR contaminations (e.g., changing filter tips, insuring clean working surfaces, using small reagent aliquots, etc.); additionally, extreme care should be used when handling the reaction standard and when spiking samples with plasmid DNA (vide infra) as the risk of contamination is very high.
3. It is important to use only linearized DNA fragments because supercoiled plasmid DNA may result in low amplification efficiency in the PCR.
4. Each new stock of linearized plasmid for real-time PCR use should be validated against the previous one to insure consistency of results.
5. When preparing the dilutions, make sure to cover a range from ~10 copies to ~10^8 copies.

6. For some specimens, e.g., tear swab, the DNA recovery at extraction may be very low, thus necessitating that the PCR be run with <1 μg starting material.
7. All specimens should be tested in quadruplicate.
8. Inhibition controls should be included in the assay by spiking test DNA with 100 and 10 copies of linearized vector.
9. Include a no amplification (water only) control.
10. Standards should be included in each test with 1, 10, 100, 1,000, and 100,000 copies of vector in water.
11. Cycle settings of the amplification reaction will vary depending on the technology and thermocycler used for the real-time quantitative PCR.
12. For example, if the gene copy number of the 10-copy control is 2.43 copies, some level of inhibition is present. In that case, the gene copy number of the unspiked test sample could be adjusted for the inhibition, or the test DNA could be column-purified or re-extracted and re-tested to try to eliminate inhibition.
13. If shipping CPTs to a central sample processing location, invert the CPTs several times to mix the PBMC layer with the plasma. Ship at room temperature in an insulated container to avoid extreme temperatures. Do not freeze. Process cells to frozen within 12–24 h of blood collection.
14. Use sterile reagents and techniques for Days 1 and 2 of the ELISpot assay. *No sterile techniques are required beginning with Day 3; however, human samples should be considered potentially infectious at all times.*
15. When using cryopreserved PBMC it is advisable to introduce a 20-h rest period between thawing and plating of the cells. This helps ensure that a more homogeneous and viable population of cells is plated in the ELISpot assay by excluding cells that are not apoptotic at the time of counting and trypan blue exclusion. If resting cells, thawing should be done on Day 1 of the assay and plating on Day 2.
16. Depending on the cytokine/analyte assayed with the ELISpot assay, more than an overnight incubation may be required.
17. Cell viability will greatly influence the outcome of the ELISpot assay, thus it is important to either introduce an overnight resting period for the cells (when using cryopreserved PBMC) or otherwise carefully evaluate cell viability. Positive controls may help to determine a sample's cell viability. CEF, which is a pool of reactive peptides from common viruses, may be particularly helpful. However, depending on the HLA type, some subjects may not react to CEF.

References

1. Bainbridge, J. W., Smith, A. J., Barker, S. S., Robbie, S., Henderson, R., Balaggan, K., Viswanathan, A., Holder, G. E., Stockman, A., Tyler, N., Petersen-Jones, S., Bhattacharya, S. S., Thrasher, A. J., Fitzke, F. W., Carter, B. J., Rubin, G. S., Moore, A. T., and Ali, R. R. (2008) Effect of gene therapy on visual function in Leber's congenital amaurosis, *N Engl J Med* ***358***, 2231–2239.
2. Maguire, A. M., High, K. A., Auricchio, A., Wright, J. F., Pierce, E. A., Testa, F., Mingozzi, F., Bennicelli, J. L., Ying, G. S., Rossi, S., Fulton, A., Marshall, K. A., Banfi, S., Chung, D. C., Morgan, J. I., Hauck, B., Zelenaia, O., Zhu, X., Raffini, L., Coppieters, F., De Baere, E., Shindler, K. S., Volpe, N. J., Surace, E. M., Acerra, C., Lyubarsky, A., Redmond, T. M., Stone, E., Sun, J., McDonnell, J. W., Leroy, B. P., Simonelli, F., and Bennett, J. (2009) Age-dependent effects of RPE65 gene therapy for Leber's congenital amaurosis: a phase 1 dose-escalation trial, *Lancet* ***374***, 1597–1605.
3. Maguire, A. M., Simonelli, F., Pierce, E. A., Pugh, E. N., Jr., Mingozzi, F., Bennicelli, J., Banfi, S., Marshall, K. A., Testa, F., Surace, E. M., Rossi, S., Lyubarsky, A., Arruda, V. R., Konkle, B., Stone, E., Sun, J., Jacobs, J., Dell'Osso, L., Hertle, R., Ma, J. X., Redmond, T. M., Zhu, X., Hauck, B., Zelenaia, O., Shindler, K. S., Maguire, M. G., Wright, J. F., Volpe, N. J., McDonnell, J. W., Auricchio, A., High, K. A., and Bennett, J. (2008) Safety and efficacy of gene transfer for Leber's congenital amaurosis, *N Engl J Med* ***358***, 2240–2248.
4. Hauswirth, W. W., Aleman, T. S., Kaushal, S., Cideciyan, A. V., Schwartz, S. B., Wang, L., Conlon, T. J., Boye, S. L., Flotte, T. R., Byrne, B. J., and Jacobson, S. G. (2008) Treatment of leber congenital amaurosis due to RPE65 mutations by ocular subretinal injection of adeno-associated virus gene vector: short-term results of a phase I trial, *Hum Gene Ther* ***19***, 979–990.
5. Christine, C. W., Starr, P. A., Larson, P. S., Eberling, J. L., Jagust, W. J., Hawkins, R. A., VanBrocklin, H. F., Wright, J. F., Bankiewicz, K. S., and Aminoff, M. J. (2009) Safety and tolerability of putaminal AADC gene therapy for Parkinson disease, *Neurology* ***73***, 1662–1669.
6. Eberling, J. L., Jagust, W. J., Christine, C. W., Starr, P., Larson, P., Bankiewicz, K. S., and Aminoff, M. J. (2008) Results from a phase I safety trial of hAADC gene therapy for Parkinson disease, *Neurology* ***70***, 1980–1983.
7. Kaplitt, M. G., Feigin, A., Tang, C., Fitzsimons, H. L., Mattis, P., Lawlor, P. A., Bland, R. J., Young, D., Strybing, K., Eidelberg, D., and During, M. J. (2007) Safety and tolerability of gene therapy with an adeno-associated virus (AAV) borne GAD gene for Parkinson's disease: an open label, phase I trial, *Lancet* ***369***, 2097–2105.
8. (2010) AMT submits its lead product Glybera® application for marketing authorisation to EMA. Available at: http://investors.amtpharma.com/phoenix.zhtml?c=212989&p=irolmediaArticle&ID=1373195&highlight=. Accessed on: 1/23/2011.
9. Manno, C. S., Pierce, G. F., Arruda, V. R., Glader, B., Ragni, M., Rasko, J. J., Ozelo, M. C., Hoots, K., Blatt, P., Konkle, B., Dake, M., Kaye, R., Razavi, M., Zajko, A., Zehnder, J., Rustagi, P. K., Nakai, H., Chew, A., Leonard, D., Wright, J. F., Lessard, R. R., Sommer, J. M., Tigges, M., Sabatino, D., Luk, A., Jiang, H., Mingozzi, F., Couto, L., Ertl, H. C., High, K. A., and Kay, M. A. (2006) Successful transduction of liver in hemophilia by AAV-Factor IX and limitations imposed by the host immune response, *Nat Med* ***12***, 342–347.
10. Mount, J. D., Herzog, R. W., Tillson, D. M., Goodman, S. A., Robinson, N., McCleland, M. L., Bellinger, D., Nichols, T. C., Arruda, V. R., Lothrop, C. D., Jr., and High, K. A. (2002) Sustained phenotypic correction of hemophilia B dogs with a factor IX null mutation by liver-directed gene therapy, *Blood* ***99***, 2670–2676.
11. Niemeyer, G. P., Herzog, R. W., Mount, J., Arruda, V. R., Tillson, D. M., Hathcock, J., van Ginkel, F. W., High, K. A., and Lothrop, C. D., Jr. (2009) Long-term correction of inhibitor-prone hemophilia B dogs treated with liver-directed AAV2-mediated factor IX gene therapy, *Blood* ***113***, 797–806.
12. Nathwani, A. C., Gray, J. T., McIntosh, J., Ng, C. Y., Zhou, J., Spence, Y., Cochrane, M., Gray, E., Tuddenham, E. G., and Davidoff, A. M. (2007) Safe and efficient transduction of the liver after peripheral vein infusion of self-complementary AAV vector results in stable therapeutic expression of human FIX in non-human primates, *Blood* ***109***, 1414–1421.
13. Nathwani, A. C., Gray, J. T., Ng, C. Y., Zhou, J., Spence, Y., Waddington, S. N., Tuddenham, E. G., Kemball-Cook, G., McIntosh, J., Boon-Spijker, M., Mertens, K., and Davidoff, A. M. (2006) Self-complementary adeno-associated virus vectors containing a novel liver-specific human factor IX expression cassette enable

highly efficient transduction of murine and nonhuman primate liver, *Blood* ***107***, 2653–2661.

14. Pien, G. C., Basner-Tschakarjan, E., Hui, D. J., Mentlik, A. N., Finn, J. D., Hasbrouck, N. C., Zhou, S., Murphy, S. L., Maus, M. V., Mingozzi, F., Orange, J. S., and High, K. A. (2009) Capsid antigen presentation flags human hepatocytes for destruction after transduction by adeno-associated viral vectors, *J Clin Invest* ***119***, 1688–1695.
15. Finn, J. D., Hui, D., Downey, H. D., Dunn, D., Pien, G. C., Mingozzi, F., Zhou, S., and High, K. A. Proteasome inhibitors decrease AAV2 capsid derived peptide epitope presentation on MHC class I following transduction, *Mol Ther* ***18***, 135–142.
16. Nony, P., Chadeuf, G., Tessier, J., Moullier, P., and Salvetti, A. (2003) Evidence for packaging of rep-cap sequences into adeno-associated virus (AAV) type 2 capsids in the absence of inverted terminal repeats: a model for generation of rep-positive AAV particles, *J Virol 77*, 776–781.
17. Hauck, B., Murphy, S. L., Smith, P. H., Qu, G., Liu, X., Zelenaia, O., Mingozzi, F., Sommer, J. M., High, K. A., and Wright, J. F. (2009) Undetectable transcription of cap in a clinical AAV vector: implications for preformed capsid in immune responses, *Mol Ther* ***17***, 144–152.
18. Li, C., Goudy, K., Hirsch, M., Asokan, A., Fan, Y., Alexander, J., Sun, J., Monahan, P., Seiber, D., Sidney, J., Sette, A., Tisch, R., Frelinger, J., and Samulski, R. J. (2009) Cellular immune response to cryptic epitopes during therapeutic gene transfer, *Proc Natl Acad Sci U S A* ***106***, 10770–10774.
19. Nathwani, A. C., Tuddenham, E., Rosales, C., McIntosh, J., Riddell, A., Rustagi, P., Glader, B., Kay, M., Allay, J., Coleman, J., Sleep, S., High, K. A., Mingozzi, F., Gray, J. T., Reiss, U. M., Nienhuis, A. W., and Davidoff, A. (2010) Early clinical trial results following administration of a low dose of a novel self complementary adeno-associated viral vector encoding human Factor IX in two subjects with severe hemophilia B., in *52nd ASH Annual Meeting*, Orlando, FL.
20. Frank, K. M., Hogarth, D. K., Miller, J. L., Mandal, S., Mease, P. J., Samulski, R. J., Weisgerber, G. A., and Hart, J. (2009) Investigation of the cause of death in a gene-therapy trial, *N Engl J Med* ***361***, 161–169.
21. Meetings of the NIH Recombinant DNA Advisory Committee, September 2007 and January 2008. Available at: http://oba.od.nih.gov/rdna_rac/rac_past_meetings_2000.html. Accessed on: 1/23/2011.
22. (2006) Guidance for Industry: Gene Therapy Clinical Trials--Observing Subjects for Delayed Adverse Events. Available at: http://www.fda.gov/BiologicsBloodVaccines/GuidanceComplianceRegulatoryInformation/Guidances/CellularandGeneTherapy/ucm072957.htm. Accessed on: 1/23/2011.
23. Miller, D. G., Petek, L. M., and Russell, D. W. (2004) Adeno-associated virus vectors integrate at chromosome breakage sites, *Nat Genet* ***36***, 767–773.
24. Lin, Y., and Waldman, A. S. (2001) Capture of DNA sequences at double-strand breaks in mammalian chromosomes, *Genetics* ***158***, 1665–1674.
25. Donsante, A., Vogler, C., Muzyczka, N., Crawford, J. M., Barker, J., Flotte, T., Campbell-Thompson, M., Daly, T., and Sands, M. S. (2001) Observed incidence of tumorigenesis in long-term rodent studies of rAAV vectors, *Gene Ther* ***8***, 1343–1346.
26. Donsante, A., Miller, D. G., Li, Y., Vogler, C., Brunt, E. M., Russell, D. W., and Sands, M. S. (2007) AAV vector integration sites in mouse hepatocellular carcinoma, *Science* ***317***, 477.
27. Li, H., Malani, N., Hamilton, S. R., Schlachterman, A., Bussadori, G., Edmonson, S. E., Shah, R., Arruda, V. R., Mingozzi, F., Wright, J. F., Bushman, F. D., and High, K. A. (2011) Assessing the potential for AAV vector genotoxicity in a murine model, *Blood* **117**, 3311–3319.
28. Nichols, T. C., Dillow, A. M., Franck, H. W., Merricks, E. P., Raymer, R. A., Bellinger, D. A., Arruda, V. R., and High, K. A. (2009) Protein replacement therapy and gene transfer in canine models of hemophilia A, hemophilia B, von willebrand disease, and factor VII deficiency, *ILAR J* ***50***, 144–167.
29. Arruda, V. R., Fields, P. A., Milner, R., Wainwright, L., De Miguel, M. P., Donovan, P. J., Herzog, R. W., Nichols, T. C., Biegel, J. A., Razavi, M., Dake, M., Huff, D., Flake, A. W., Couto, L., Kay, M. A., and High, K. A. (2001) Lack of germline transmission of vector sequences following systemic administration of recombinant AAV-2 vector in males, *Mol Ther* ***4***, 586–592.
30. Schuettrumpf, J., Liu, J. H., Couto, L. B., Addya, K., Leonard, D. G., Zhen, Z., Sommer, J., and Arruda, V. R. (2006) Inadvertent germline transmission of AAV2 vector: findings in a rabbit model correlate with those in a human clinical trial, *Mol Ther* ***13***, 1064–1073.

31. Favaro, P., Downey, H. D., Zhou, J. S., Wright, J. F., Hauck, B., Mingozzi, F., High, K. A., and Arruda, V. R. (2009) Host and vector-dependent effects on the risk of germline transmission of AAV vectors, *Mol Ther* ***17***, 1022–1030.
32. Herzog, R. W., Mount, J. D., Arruda, V. R., High, K. A., and Lothrop, C. D., Jr. (2001) Muscle-directed gene transfer and transient immune suppression result in sustained partial correction of canine hemophilia B caused by a null mutation, *Mol Ther* ***4***, 192–200.
33. Wang, Z., Kuhr, C. S., Allen, J. M., Blankinship, M., Gregorevic, P., Chamberlain, J. S., Tapscott, S. J., and Storb, R. (2007) Sustained AAV-mediated dystrophin expression in a canine model of Duchenne muscular dystrophy with a brief course of immunosuppression, *Mol Ther* ***15***, 1160–1166.
34. Mingozzi, F., Hasbrouck, N. C., Basner-Tschakarjan, E., Edmonson, S. A., Hui, D. J., Sabatino, D. E., Zhou, S., Wright, J. F., Jiang, H., Pierce, G. F., Arruda, V. R., and High, K. A. (2007) Modulation of tolerance to the transgene product in a nonhuman primate model of AAV-mediated gene transfer to liver, *Blood* ***110***, 2334–2341.
35. Mavilio, F., Pellegrini, G., Ferrari, S., Di Nunzio, F., Di Iorio, E., Recchia, A., Maruggi, G., Ferrari, G., Provasi, E., Bonini, C., Capurro, S., Conti, A., Magnoni, C., Giannetti, A., and De Luca, M. (2006) Correction of junctional epidermolysis bullosa by transplantation of genetically modified epidermal stem cells, *Nat Med* ***12***, 1397–1402.
36. Mingozzi, F., Liu, Y. L., Dobrzynski, E., Kaufhold, A., Liu, J. H., Wang, Y., Arruda, V. R., High, K. A., and Herzog, R. W. (2003) Induction of immune tolerance to coagulation factor IX antigen by in vivo hepatic gene transfer, *J Clin Invest* ***111***, 1347–1356.
37. Ziegler, R. J., Lonning, S. M., Armentano, D., Li, C., Souza, D. W., Cherry, M., Ford, C., Barbon, C. M., Desnick, R. J., Gao, G., Wilson, J. M., Peluso, R., Godwin, S., Carter, B. J., Gregory, R. J., Wadsworth, S. C., and Cheng, S. H. (2004) AAV2 vector harboring a liver-restricted promoter facilitates sustained expression of therapeutic levels of alpha-galactosidase A and the induction of immune tolerance in Fabry mice, *Mol Ther* ***9***, 231–240.
38. Hudig, D., Greee, N. J., C-M., K., and Powers, J. C. (1987) Lymphocyte granule-mediated cytolysis requires serine protease activity., *Biochem Biophys Res Commun* ***149***, 882–888.
39. Chang, T. W., and Eisen, H. N. (1980) Effects of N alpha-tosyl-L-lysyl-chloromethylketone on the activity of cytotoxic T lymphocytes, *J Immunol* ***124***, 1028–1033.
40. Stroes, E. S., Nierman, M. C., Meulenberg, J. J., Franssen, R., Twisk, J., Henny, C. P., Maas, M. M., Zwinderman, A. H., Ross, C., Aronica, E., High, K. A., Levi, M. M., Hayden, M. R., Kastelein, J. J., and Kuivenhoven, J. A. (2008) Intramuscular administration of AAV1-lipoprotein lipase S447X lowers triglycerides in lipoprotein lipase-deficient patients, *Arterioscler Thromb Vasc Biol* ***28***, 2303–2304.
41. Mingozzi, F., Meulenberg, J. J., Hui, D. J., Basner-Tschakarjan, E., Hasbrouck, N. C., Edmonson, S. A., Hutnick, N. A., Betts, M. R., Kastelein, J. J., Stroes, E. S., and High, K. A. (2009) AAV-1-mediated gene transfer to skeletal muscle in humans results in dose-dependent activation of capsid-specific T cells, *Blood* ***114***, 2077–2086.
42. Velazquez, V. M., Bowen, D. G., and Walker, C. M. (2009) Silencing of T lymphocytes by antigen-driven programmed death in recombinant adeno-associated virus vector-mediated gene therapy, *Blood* ***113***, 538–545.
43. Lin, S. W., Hensley, S. E., Tatsis, N., Lasaro, M. O., and Ertl, H. C. (2007) Recombinant adeno-associated virus vectors induce functionally impaired transgene product-specific CD8+ T cells in mice, *J Clin Invest* ***117***, 3958–3970.
44. Mendell, J. R., Rodino-Klapac, L. R., Rosales-Quintero, X., Kota, J., Coley, B. D., Galloway, G., Craenen, J. M., Lewis, S., Malik, V., Shilling, C., Byrne, B. J., Conlon, T., Campbell, K. J., Bremer, W. G., Viollet, L., Walker, C. M., Sahenk, Z., and Clark, K. R. (2009) Limb-girdle muscular dystrophy type 2D gene therapy restores alpha-sarcoglycan and associated proteins, *Ann Neurol* ***66***, 290–297.
45. Brantly, M. L., Chulay, J. D., Wang, L., Mueller, C., Humphries, M., Spencer, L. T., Rouhani, F., Conlon, T. J., Calcedo, R., Betts, M. R., Spencer, C., Byrne, B. J., Wilson, J. M., and Flotte, T. R. (2009) Sustained transgene expression despite T lymphocyte responses in a clinical trial of rAAV1-AAT gene therapy, *Proc Natl Acad Sci U S A* ***106***, 16363–16368.
46. Hudig, D., Haverty, T., Fulcher, C., Redelman, D., and Mendelsohn, J. (1981) Inhibition of human natural cytotoxicity by macromolecular antiproteases, *J Immunol* ***126***, 1569–1574.
47. Gene Transfer for Subjects with Hemophilia B Factor IX Deficiency. In: ClinicalTrials.gov. Available at: http://clinicaltrials.gov/ct2/show/NCT00515710?term=Hemophilia+B&rank=7. Accessed on: 1/23/2011.
48. Janetzki, S., Panageas, K. S., Ben-Porat, L., Boyer, J., Britten, C. M., Clay, T. M., Kalos, M., Maecker, H. T., Romero, P., Yuan, J., Kast, W. M., and Hoos, A. (2008) Results and harmonization guidelines from two large-scale international Elispot proficiency panels con-

ducted by the Cancer Vaccine Consortium (CVC/SVI), *Cancer Immunol Immunother* **57**, 303–315.

49. Brantly, M. L., Spencer, L. T., Humphries, M., Conlon, T. J., Spencer, C. T., Poirier, A., Garlington, W., Baker, D., Song, S., Berns, K. I., Muzyczka, N., Snyder, R. O., Byrne, B. J., and Flotte, T. R. (2006) Phase I trial of intramuscular injection of a recombinant adeno-associated virus serotype 2 alphal-antitrypsin (AAT) vector in AAT-deficient adults, *Hum Gene Ther* **17**, 1177–1186.
50. Tuszynski, M. H., Thal, L., Pay, M., Salmon, D. P., U, H. S., Bakay, R., Patel, P., Blesch, A., Vahlsing, H. L., Ho, G., Tong, G., Potkin, S. G., Fallon, J., Hansen, L., Mufson, E. J., Kordower, J. H., Gall, C., and Conner, J. (2005) A phase 1 clinical trial of nerve growth factor gene therapy for Alzheimer disease, *Nat Med* **11**, 551–555.
51. Mease, P. J., Wei, N., Fudman, E. J., Kivitz, A. J., Schechtman, J., Trapp, R. G., Hobbs, K. F., Greenwald, M., Hou, A., Bookbinder, S. A., Graham, G. E., Wiesenhutter, C. W., Willis, L., Ruderman, E. M., Forstot, J. Z., Maricic, M. J., Dao, K. H., Pritchard, C. H., Fiske, D. N., Burch, F. X., Prupas, H. M., Anklesaria, P., and Heald, A. E. (2009) Safety, Tolerability, and Clinical Outcomes after Intraarticular Injection of a Recombinant Adeno-associated Vector Containing a Tumor Necrosis Factor Antagonist Gene: Results of a Phase 1/2 Study, *J Rheumatol*, Epub 2009/2012/2025.
52. Frank, M. B., Wang, S., Aggarwal, A., Knowlton, N., Jiang, K., Chen, Y., McKee, R., Chaser, B., McGhee, T., Osban, J., and Jarvis, J. N. (2009) Disease-associated pathophysiologic structures in pediatric rheumatic diseases show characteristics of scale-free networks seen in physiologic systems: implications for pathogenesis and treatment, *BMC Med Genomics* **2**, 9.
53. Worgall, S., Sondhi, D., Hackett, N. R., Kosofsky, B., Kekatpure, M. V., Neyzi, N., Dyke, J. P., Ballon, D., Heier, L., Greenwald, B. M., Christos, P., Mazumdar, M., Souweidane, M. M., Kaplitt, M. G., and Crystal, R. G. (2008) Treatment of late infantile neuronal ceroid lipofuscinosis by CNS administration of a serotype 2 adeno-associated virus expressing CLN2 cDNA, *Hum Gene Ther* **19**, 463–474.
54. Moss, R. B., Milla, C., Colombo, J., Accurso, F., Zeitlin, P. L., Clancy, J. P., Spencer, L. T., Pilewski, J., Waltz, D. A., Dorkin, H. L., Ferkol, T., Pian, M., Ramsey, B., Carter, B. J., Martin, D. B., and Heald, A. E. (2007) Repeated aerosolized AAV-CFTR for treatment of cystic fibrosis: a randomized placebo-controlled phase 2B trial, *Hum Gene Ther* **18**, 726–732.
55. Jaski, B. E., Jessup, M. L., Mancini, D. M., Cappola, T. P., Pauly, D. F., Greenberg, B., Borow, K., Dittrich, H., Zsebo, K. M., and Hajjar, R. J. (2009) Calcium upregulation by percutaneous administration of gene therapy in cardiac disease (CUPID Trial), a first-in-human phase 1/2 clinical trial, *J Card Fail* **15**, 171–181.
56. Manno, C. S., Chew, A. J., Hutchison, S., Larson, P. J., Herzog, R. W., Arruda, V. R., Tai, S. J., Ragni, M. V., Thompson, A., Ozelo, M., Couto, L. B., Leonard, D. G., Johnson, F. A., McClelland, A., Scallan, C., Skarsgard, E., Flake, A. W., Kay, M. A., High, K. A., and Glader, B. (2003) AAV-mediated factor IX gene transfer to skeletal muscle in patients with severe hemophilia B, *Blood* **101**, 2963–2972.

Index

Richard O. Snyder and Philippe Moullier (eds.), *Adeno-Associated Virus: Methods and Protocols*,
Methods in Molecular Biology, vol. 807, DOI 10.1007/978-1-61779-370-7, © Springer Science+Business Media, LLC 2011

E

F

G

H

I

L

M

N

P

Q

R

S

T

U

V